Roles and regulation of a *Bdellovibrio bacteriovorus* diguanylate cyclase, phosphodiesterase and a PilZ domain receptor.

Thesis submitted to the University of Nottingham for the degree of Doctor of Philosophy

Ruth Nottingham B.Sc. (Hons)

September 2016

Abstract

Cyclic-di-GMP is a ubiquitous second messenger regulating lifestyles across a wide range of bacteria, most notably motility and virulence. The components of c-di-GMP signalling networks are made up of: diguanylate cyclases (DGCs) that contain a GGDEF domain and make c-di-GMP, phosphodiesterases (PDEs) that contain an EAL or HD-GYP domain and break-down c-di-GMP and PilZ domains (or degenerate DGCs/PDEs) which are receptors for c-di-GMP.

Bdellovibrio bacteriovorus HD100 is a predatory Gram-negative bacterium that preys upon other Gram-negative bacteria. *B. bacteriovorus* HD100 has a complex c-di-GMP signalling network, including four DGCs; one EAL domain protein, six HD-GYP proteins, 19 PilZ domain-proteins, a degenerate DGC and a proposed riboswitch all of which can act as c-di-GMP receptors. Bd0367, a DGC, regulates gliding motility and prey cell exit in *B. bacteriovorus*. Bd0367 has a GGDEF domain but also a response regulator domain, which suggests that c-di-GMP production by Bd0367 may be regulated by a phosphorylation event by a cognate sensor kinase.

This thesis investigated the Bd0367 signalling pathway through analysis of Bd0367 protein interaction networks, Bd0367 DGC c-di-GMP production and searched for the cognate histidine kinase for Bd0367. This study confirmed that a conserved aspartate residue is required for Bd0367 to be an active DGC via mutational studies and cellular c-di-GMP extractions. It also demonstrated that Bd0367 enzymatic activity is essential for prey cell exit, but is less important for gliding motility, this was tested by a Bd0367D63A mutation. Which suggests that localised protein interactions formed by Bd0367 (independent of its enzymatic role) may be more important for gliding motility than the Bd0367 specific c-di-GMP generation.

This concept was supported by other data as deletion of a gene encoding a PilZ domain-protein that interacted with Bd0367 by bacterial two hybrid analysis, caused hyper-reversals during gliding motility. Future work is needed to dissect the exact mechanism by which the PilZ domain protein influences the gliding machinery.

A PDE protein Bd1971 interacts by bacterial two hybrid assay with Bd0367. This study found that Δ*bd1971* resulted in impaired gliding motility, suggesting that a high global

level of c-di-GMP in *B. bacteriovorus* cells can negatively affect motility as seen in many other bacteria. The molecular reason for impaired gliding at high c-di-GMP levels in *B. bacteriovorus* is yet to be determined and requires further study.

Acknowledgements

Firstly, I would like to thank my supervisor Liz Sockett for the opportunity of working in her lab and continual support during my PhD.

Secondly I would like to thank Dr Steven Porter and Dr Vanessa Francis from the University of Exeter for giving up their time to share their phosphotransfer expertise and equipment. These experiments would not have been possible without your support. Additionally I would like to acknowledge the expertise provided by Dr Lijun Chen in carrying out the c-di-GMP quantification and Dr Lovering for amino acid mutation suggestions.

To everyone in C15 and C27 past and present thank you for all your advice and for livening up my time in Nottingham. Also a big thanks to Julie and the A-team, who have kept the lab running and me smiling.

I would like to extend a special thank you to Rob for his help in constructing the final few constructs used in this study and to Rebecca for being great company throughout all our joint trouble shooting this last year.

I thank my family for supporting me despite having to listening to me talk about a very niche area for four years; I promise a change of topic is around the corner. A special thanks to Nic for keeping me going.

Abbreviations

3’ 3 prime (hydroxyl) end of DNA/RNA molecule

5’ 5 prime (phosphate) end of DNA/RNA molecule

A-motility Adventurous motility

Amp Ampicillin

AP Attack Phase

B2H Bacterial adenylate cyclase Two Hybrid

BLAST basic local alignment search tool

ATP Adenosine triphosphate

bp base pairs

BSA Bovine serum albumin

c-di-GMP Cyclic di-GMP

CFU Colony forming units

DGC diguanylate cyclase

DNA deoxyribonucleic acid

dNTP deoxynucleotide triphosphate

EDTA ethylene diamine tetraacetic acid

EPS Exopolysaccharide

FOV field of view

FAC focal adhesion complex/clusters

g gram

g gravitational acceleration force

glt gliding transducer complex

hr hour

HD Host-dependent

HEPES N-(2-Hydroxyethyl) piperazine-N'-(2-ethanesulphonic acid)

HI Host–independent

HK Histidine kinase

IPTG isopropyl β -D-1-thiogalactopyranosidase

kb Kilobases

kDa Kilodalton

Kan Kanamycin

L litre

LPS lipopolysaccharide

M Molar

Mb megabases

mCherry monomeric cherry fluorescent protein

MCP

mins minutes

mRNA messenger Ribonucleic acid

NCBI National Centre for Biotechnology Information XXI

NEB New England Biolabs

OD optical density

ONPG ortho-nitrophenol β -D-galactopyranoside

ORF Open Reading Frame

oriC origin of replication

PBS Phosphate buffered saline

PCR polymerase chain reaction

PDE Phosphodiesterase enzyme

PFU Plaque forming units

pH negative log 10 of the hydrogen ion activity

pGpG 5′-phosphoguanylyl-(3′,5′)-guanosine

PSORTdb subcellular localisation prediction tool

RC Reverse complement

RNA ribonucleic acid

rRNA ribosomal Ribonucleic acid

rpm revolutions per minute

RT-PCR Reverse transcription polymerase chain reaction

RR response regulator domain

SDS Sodium dodecyl sulphate

SDS-PAGE Sodium dodecyl sulphate polyacrylamide gel electrophoresis

SDW sterile distilled water

secs seconds

SignalP signal peptide prediction tool

S-motility Social motility

TF transcription factor

V volts

WT Wild type – Bdellovibrio bacteriovorus HD100

X-gal 5-bromo-4-chloro-3-indolyl-β -D-galactopyranoside

Δ Delta, signifying gene deletion

Table of Contents

Table of Figures

Table of Tables

Chapter 1. Introduction

This chapter starts with a review of the current progress in cyclic-di-GMP (c-di-GMP) signalling research. This is followed by a general overview of *Bdellovibrio bacteriovorus*, a novel predatory bacterium with a distinct c-di-GMP network. This chapter then explains in more detail what is known of the regulatory networks of *B. bacteriovorus* focusing on c-di-GMP signalling. Finally this chapter gives an oversight of the state of research into bacterial gliding motility with a focus on *B. bacteriovorus* surface motility.

1.1. Cyclic-di-GMP

1.1.1. Overview

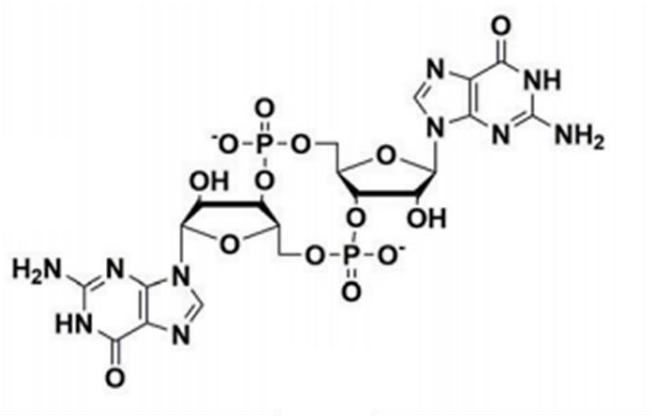

Figure 1.1 Chemical structure of c-di-GMP. C-di-GMP is synthesized from two molecules of GTP.

C-di-GMP (bis-(3'-5')-cyclic di-guanosine monophosphate) (Figure 1.1) was originally discovered in 1987 as a allosteric activator of cellulose synthase in the proteobacterium *Acetobacter xylinum* (Ross et al, 1987). C-di-GMP synthesis and degradation enzymes have been identified in all major bacterial phyla (Bordeleau et al, 2011; den Hengst et al, 2010; Sudarsan et al, 2008) showing that it is a ubiquitous bacterial secondary messenger. The number of c-di-GMP components identified across bacterial phyla shows that bacteria with complex lifestyles carry more c-di-GMP metabolising enzymes than obligate parasites (Galperin, 2005). For an up to date analysis of c-di-GMP components across multiple bacterial genomes see the c-di-GMP census at http://ncbi.nlm.nih.gov/Complete_Genomes/c-di-GMP.html (Romling et al, 2013).

C-di-GMP signalling has been shown by deletion studies to be important in multiple phenotypes, especially in motility, the formation of biofilms, the regulation of virulence and the shift from axenic to predatory growth (Hobley et al, 2012; Jenal, 2004; Paul et al, 2004; Romling et al, 2005; Slater et al, 2000; Tamayo et al, 2007).

The 3D structure of c-di-GMP has been shown to be diverse; it can oligomerise and be bound to proteins as a monomer, dimer or tetramer (Gentner et al, 2012; Tschowri et al, 2014). The dimer of c-di-GMP can also have multiple forms varying in the degree of stacking (Chou & Galperin, 2016). Taken together this indicates the flexibility of c-di-GMP as a signalling molecule and has implications on the diversity of downstream signalling targets.

1.1.2. Protein domains involved in c-di-GMP signalling

C-di-GMP is generated by diguanylate cyclases (DGCs) that contain GGDEF domains, and is degraded by c-di-GMP phosphodiesterases (PDEs) that contain EAL or HD-GYP domains (Figure 1.2) (Galperin et al, 1999; Hecht & Newton, 1995; Paul et al, 2004; Tal et al, 1998). GG(D/E)EF, EAL, and HD-GYP domains are named such to denote the conserved active site amino acids involved in catalysis. PilZ domain proteins are the most common c-di-GMP receptor domain but other types of receptor also exist and more are being discovered (Amikam & Galperin, 2006).

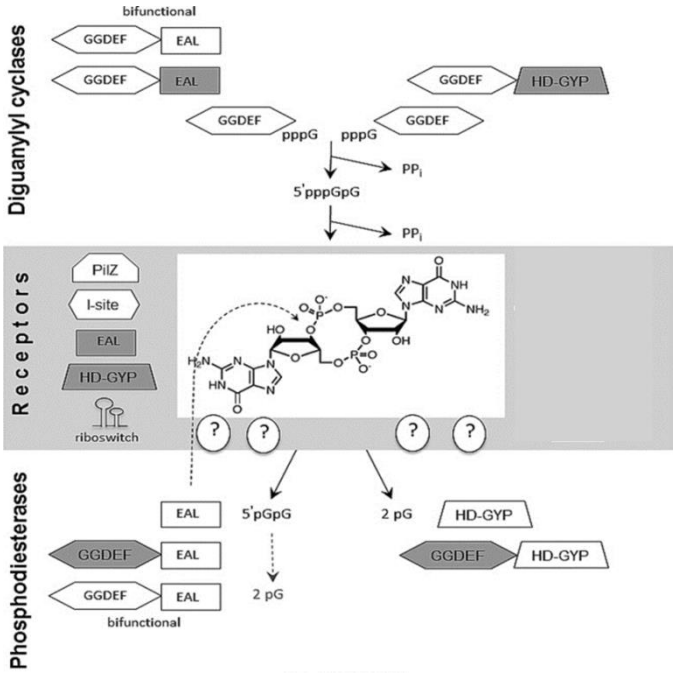

Figure 1.2 Figure of protein domains used in c-di-GMP signalling. Reproduced from (Romling et al, 2013). Shows the simplified architecture of the process and protein domains involved in of c-di-GMP metabolism and signal transduction. Enzymatically active GGDEF, EAL, and HD-GYP domains are shown on a white background. Enzymatically inactive domains involved in substrate binding are shown in light grey.

1.1.2.1. C-di-GMP metabolism

DGC enzymes produce c-di-GMP from two molecules of GTP. The c-di-GMP is synthesized by DGCs with an intact GG(D/E)EF motif from two molecules of GTP in a Mg^{2+} dependent manner. During catalysis, one molecule of GTP binds to the GGDEF domain, which then forms a homodimer with another GTP bound GGDEF domain (Chan et al, 2004).

In addition, many DGCs display product-inhibition by the binding of c-di-GMP to an inhibitory I-site. This binding then alters the conformation of the enzyme so that catalysis is prevented (Christen et al, 2006). The I-site consists of an RxxD motif approximately 5 amino acids from the GGDEF motif, the I site makes direct contact with c-di-GMP. Product inhibition occurs at a c-di-GMP concentration that is defined by the affinity of the I-site for this molecule and varies between DGCs and allows allosteric regulation (Chan et al, 2004).

PDEs degrade c-di-GMP by breaking phosphodiester bonds, by the hydrolytic actions of EAL or HD-GYP domains of PDEs. These enzymes degrade c-di-GMP, HD-GYP domains degrade c-di-GMP directly to two molecules of GMP, whereas EAL domain

proteins degrade c-di-GMP to 5′-phosphoguanylyl-(3′,5′)-guanosine (pGpG) to be further degraded by cellular hydrolases (Christen et al, 2005; Ryan et al, 2006; Schmidt et al, 2005).

PDEs retain some activity as monomers however many form dimers and higher order oligomers (Schmidt et al, 2005; Tarutina et al, 2006). It has been suggested that the dimer is the most used oligomeric state for c-di-GMP hydrolysis *in vivo* (Romling et al, 2013). The degradation reaction requires the presence of Mg^{2+} or Mn^{2+}, and is inhibited by Ca^{2+} (Christen et al, 2005; Ross et al, 1986). The structure of the enzymatically inactive HD-GYP Bd1817 from *Bdellovibrio* was solved by Dr Lovering at The Univrsity of Birmingham and proposed a catalytic mechanism involving water attacking the phosphoester bond of c-di-GMP (Lovering et al, 2011).

Bioinformatics analysis shows that many c-di-GMP synthesis and degradation domains are found conjoined as part of multi-domain proteins (however GGDEF-HD-GYP fusion proteins are less common than GGDEF-EAL combinations)(Romling et al, 2013). In some cases both domains have retained enzymatic ability; in this scenario it suggests that each domain can be differentially regulated by intracellular signals so one enzymatic activity is dominant under particular conditions (Tarutina et al, 2006). However commonly one domain has lost the enzymatic ability and is utilised to bind GTP/c-di-GMP but not process it, or the role of the domain is to be involved in protein-protein interactions. (Christen et al, 2005; Schmidt et al, 2005).

1.1.2.2. C-di-GMP receptors

C-di-GMP binds to diverse downstream receptor molecules in order to exert its effects. These effector proteins are commonly PilZ domain proteins and enzymatically inactive DGC and PDEs.

PilZ domains are receptors for c-di-GMP and can be thought of as c-di-GMP adaptor proteins that transduce c-di-GMP levels to modulate cellular outputs (Amikam & Galperin, 2006). PilZ domain proteins were named after the PilZ protein, PA2960 of *P. aeruginosa* which is involved in pilus formation (Alm et al, 1996). The PilZ domain was first identified as a possible c-di-GMP receptor through bioinformatics analysis, as it has a similar distribution to that of c-di-GMP-metabolizing enzymes (Amikam & Galperin, 2006). C-di-GMP binding to the PilZ domain was subsequently confirmed through biochemical analyses (Christen et al, 2007; Merighi et al, 2007; Ryjenkov et al, 2006).

Hundreds of PilZ domain proteins have since been identified (Amikam & Galperin, 2006) , and many of these are involved in processes known to be regulated by c-di-GMP such as alginate biosynthesis, biofilm formation, motility and virulence (Christen et al, 2007; Pratt et al, 2007) (Merighi et al, 2007) (Ryjenkov et al, 2006).

Many PilZ domain proteins are fused to other domains furthering the potential of c-di-GMP mediated signal transduction (Amikam & Galperin, 2006). Only a small number of residues are required to facilitate sub micromolar binding affinities (Paul et al, 2004; Simm et al, 2004; Weinhouse et al, 1997) of c-di-GMP, this makes the family of PilZ domains a compact and versatile c-di-GMP molecular switch (Benach et al, 2007). In the first PilZ domain protein studied, the key N terminal (Q/E)RRxxxR motif was found to be the binding loop which wraps around c-di-GMP and brings it into proximity with other conserved residues D/NXSXXG (Benach et al, 2007; Ko et al, 2010).

PilZ domains with this full motif are known as type I, other PilZ domain without the full motif (lacking RxxxR) are considered type II and cannot bind c-di-GMP directly, however can use an accessory protein to indirectly respond to c-di-GMP signalling for example FimX (Chou & Galperin, 2016; Guzzo et al, 2013).

Type I PilZ domain proteins can bind c-di-GMP in multiple ways, separate PilZ domain proteins have been seen to bind c-di-GMP as a monomer for example PlzD from *V. cholerae* (Benach et al, 2007) and others as a dimer such as YcgR from *P. putida* or BcsA (Morgan et al, 2014). The fact that structural studies are identifying that PilZ domain proteins have different c-di-GMP binding stoichiometries suggests the differential binding properties of PilZ domains aids in regulating diverse c-di-GMP-mediated processes (Gentner et al, 2012; Habazettl et al, 2011; Ko et al, 2010; Li et al, 2011). The binding of c-di-GMP to the PilZ domain can result in small structural rearrangements which may allow new protein-protein interactions (Benach et al, 2007).

C-di-GMP receptors can also be degenerate c-di-GMP metabolising enzymes, so GGDEF proteins and EAL proteins (Amikam & Galperin, 2006) which have lost catalytic function but can still bind to c-di-GMP through the I-site (Chan et al, 2004; Christen et al, 2006) or the degenerate active site (Newell et al, 2011; Newell et al, 2009). Additionally novel c-di-GMP binding proteins continue to be discovered through c-di-GMP capture compound and differential radial capillary action of ligand assays such as the proteins PgaC/D (Chou & Galperin, 2016; Steiner et al, 2013).

1.1.2.3. Riboswitches that bind c-di-GMP

Riboswitches are RNA aptamers, non-coding segments of mRNA that have a secondary structure that can bind small molecular ligands. It has been discovered that c-di-GMP binds specifically to GEMM riboswitches (Sudarsan et al, 2008) and another riboswitch type that is involved in RNA splicing (Lee et al, 2010). When the ligand binds to the mRNA the structure alters, which can change the transcription, translation or mRNA stability of the downstream genes (Barrick & Breaker, 2007). The riboswitches discovered to date bind c-di-GMP *in vitro* with very high affinities (K_d in the nanomolar range) and are found upstream of a diverse range of genes suggesting more functions in bacteria than currently examined (Sudarsan et al, 2008).

1.1.2.4. Transcription factors that bind c-di-GMP

Several transcription factors (TF) that bind c-di-GMP have been discovered, such as FleQ in *Pseudomonas* and VpsR in *Vibrio cholerae* (Hickman & Harwood, 2008) (Srivastava et al, 2011). C-di-GMP binding to TFs can relieve repression of genes for example c-di-GMP binding reduces FleQ affinity to *pel* promoter allowing EPS biosynthesis transcription or c-di-GMP binding a TF can aid in activating transcription. Interestingly an intact Walker A motif is necessary for the binding of c-di-GMP to FleQ, and the Walker A motif of FleQ is a conserved feature in other AAA+ ATPases suggesting more proteins of this type may bind and respond to c-di-GMP (Baraquet & Harwood, 2013).

1.1.3. Signalling specificity in c-di-GMP networks or global signalling

There are multiple DGC, PDE and c-di-GMP receptor proteins in many bacteria. This duplication of enzymes and receptors leads to questions about the mechanisms used to ensure specificity of c-di-GMP signalling pathways and to reduce undesired cross talk.

There are a few theories about how cells manage to regulate specific c-di-GMP pathways and these strategies can be used in combination. Firstly regulation of gene expression of c-di-GMP components through transcriptional regulation helps manage c-di-GMP signalling networks (Romling et al, 2013).

Secondly spatial organisation can manage specificity in the c-di-GMP network by regulating enzyme activity of DGC or PDEs, for example PleD DGC in *Caulobacter* is only active once dimerization causes sequestration of PleD to the cell pole (Paul et al, 2007). Spatial organisation can also be used to reduce cross talk by the co-localisation of specific DGCs with a specific c-di-GMP receptor.

This co-localisation effect suggests that physical protein interactions between specific DGC and c-di-GMP receptors (or other c-di-GMP components) are important in retaining specific signal transduction (Lindenberg et al, 2013). Further work in this area has shown that effector LapD and DGC GcbC interact by bacterial two hybrid analysis and that GcbC localises to the inner membrane to interact with LapD (Dahlstrom et al, 2015). Collectively this work suggests that physical proximity and protein complexes are an integral mechanism in facilitating specific c-di-GMP signalling.

Thirdly PDEs prevent 'overflow' to protect the local and specific c-di-GMP targets, a loss of a PDE can open up a c-di-GMP receptor to the effects of c-di-GMP production from a non-specific DGC, that was previously 'kept in check' by the PDE (Romling et al, 2013).

Fourthly the c-di-GMP receptor proteins have intrinsic properties that affect the K_d at which they bind c-di-GMP, this differential binding affinity amongst receptors can aid in specificity of c-di-GMP signalling by only some receptors binding c-di-GMP at specific cellular levels. A good example of this is in *S. enterica* (Pultz et al, 2012) where PilZ YcgR binds c-di-GMP and is active binding to the flagellar motor but the PilZ protein BscA is not active and does not stimulate cellulose synthase as BscA has an affinity 40 fold lower than YcgR for c-di-GMP. This level of c-di-GMP allows motility to be inhibited but is not sufficient to stimulate cellulose production and start biofilm formation.

Finally allosteric regulation of the c-di-GMP metabolising proteins can control the rate of c-di-GMP production to reduce the possibility of cross talk. This allosteric regulation is achieved by possession of a negative feedback system via an I site or addition of sensory domains which can influence the enzymes conformation and hence activity (Christen et al, 2006).

1.1.4. Post translational mechanisms of diguanylate cyclase enzymatic regulation

As discussed above, controlling the activity of c-di-GMP metabolising proteins is important for controlling the specificity of c-di-GMP signalling and in mediating correct cellular output. There are a variety of mechanisms used to control the activity of DGC proteins briefly detailed below.

1.1.4.1. GGDEF proteins and response regulator domains

A common mechanism of DGC regulation is via the fusion of a response regulator RR domain to a GGDEF domain. These proteins account for ~2.3% of all RRs found in bacterial genomes, a substantial proportion, the addition of a response regulator domain enables regulation to be mediated by phosphorylation (Galperin, 2010).

1.1.4.2. Phosphorylation dependent regulation

The role of phosphorylation of the RR domain on the activity of the protein can vary. Often phosphorylation leads to activating a proteins enzyme activity, however this is not always the case as phosphorylation of a protein can also cause a protein to be in its 'off' or inactive conformation (Posas et al, 1998). Phosphorylation can promote dimerization, higher order oligomerisation or interactions with other proteins which can further affect enzyme activity (Stock et al, 2000). Interestingly phosphorylation of a tandem GGDEF-EAL protein Lp10329 in *Legionella* can act as a switch decreasing DGC activity and retaining PDE activity (Levet-Paulo et al, 2011).

1.1.4.3. Oligomerisation

Dimerization often induced by phosphorylation is seen to activate PleD DGC activity in *Caulobacter* and add spatial control by sequestering the active DGC to the cell pole (Paul et al, 2007). Higher order oligomerisation is also shown to occur through phosphorylation or a high concentration of the DGC WspR from *Pseudomonas aeruginosa*, this causes subcellular clustering of WspR (into multiple tetramers oligomers) which stimulates its DGC activity (De et al, 2009; De et al, 2008; Huangyutitham et al, 2013).

1.1.4.4. Product feedback inhibition

The conserved I site allows a negative feedback mechanism that provides a system for rapid regulation of DGC enzymatic ability and therefore tight control over the rate of c-di-GMP production. This regulation allows control over the cellular concentration of c-di-GMP which impacts on the response of c-di-GMP receptor proteins and overall signalling outputs (Christen et al, 2006).

1.2. ***Bdellovibrio bacteriovorus***

Bdellovibrio bacteriovorus is a small gram negative predatory δ proteobacterium (Stolp & Petzold, 1962) which preys on other Gram negative bacteria. *Bdellovibrio bacteriovorus* can exist in two different lifestyles: host dependent (HD), where replication can only occur when *B. bacteriovorus* has entered a prey cell (Jurkevitch et al, 2000) and the host independent (HI) lifestyle where the cell can replicate outside of prey. However this is a rare event with a conversion of 1 in 10 million cells becoming HI from HD (Barel & Jurkevitch, 2001).

1.2.1. Host Dependent (HD) *B. bacteriovorus* HD100

Predatory Host Dependent *Bdellovibrio bacteriovorus* are 0.25 μm x 1.25 μm and highly motile in liquid using a unipolar flagellum. These cells can also move on solid surfaces after a period of contact by gliding motility (section 1.5.2). The predatory nature of *Bdellovibrio bacteriovorus* is of interest due to the ability to reduce Gram negative bacterial populations. This property once further investigated could be applied therapeutically in future in the advent of multi-antibiotic resistant gram negative pathogens.

The process of *Bdellovibrio* predation is as follows and depicted in Figure 1.3. The starting point for the HD life cycle is at prey location, at this point *Bdellovibrio* are in attack phase, actively seeking prey, using motility and chemotaxis to collide with prey (Straley & Conti, 1977). Once this collision has occurred attachment of the predatory pole of *Bdellovibrio* to the prey cell outer membrane happens (Abram et al, 1974). At the invasion point the *Bdellovibrio* cell enters the prey periplasm (Shilo, 1969) this entry process is facilitated by the type IV pilus(Evans et al, 2007) and uses enzymes to modify the prey cell wall, this leads to the formation of a rounded cell called a 'bdelloplast' (Lerner et al, 2012; Thomashow & Rittenberg, 1978). Once established in the prey periplasm the *Bdellovibrio* cell quickly kills the prey cell (S.c & Shilo, 1970). A controlled process is then used to degrade proteins, DNA and RNA in the prey cell using a range of specialised degrading enzymes, the resulting breakdown products are then used for *Bdellovibrio* growth and replication (Hespell et al, 1975; Rittenberg & Hespell, 1975). At this stage the *Bdellovibrio* grow and replicate until the prey cell is exhausted of nutrients and predator division occurs by synchronous septation resulting in an average of 3-5 progeny cells (Shilo, 1969). The *Bdellovibrio* then adopt the appropriate motility for the external enivronment

and the bdelloplast undergoes lysis, allowing the new progeny *Bdellovibrio* to repeat the cycle and locate more prey.

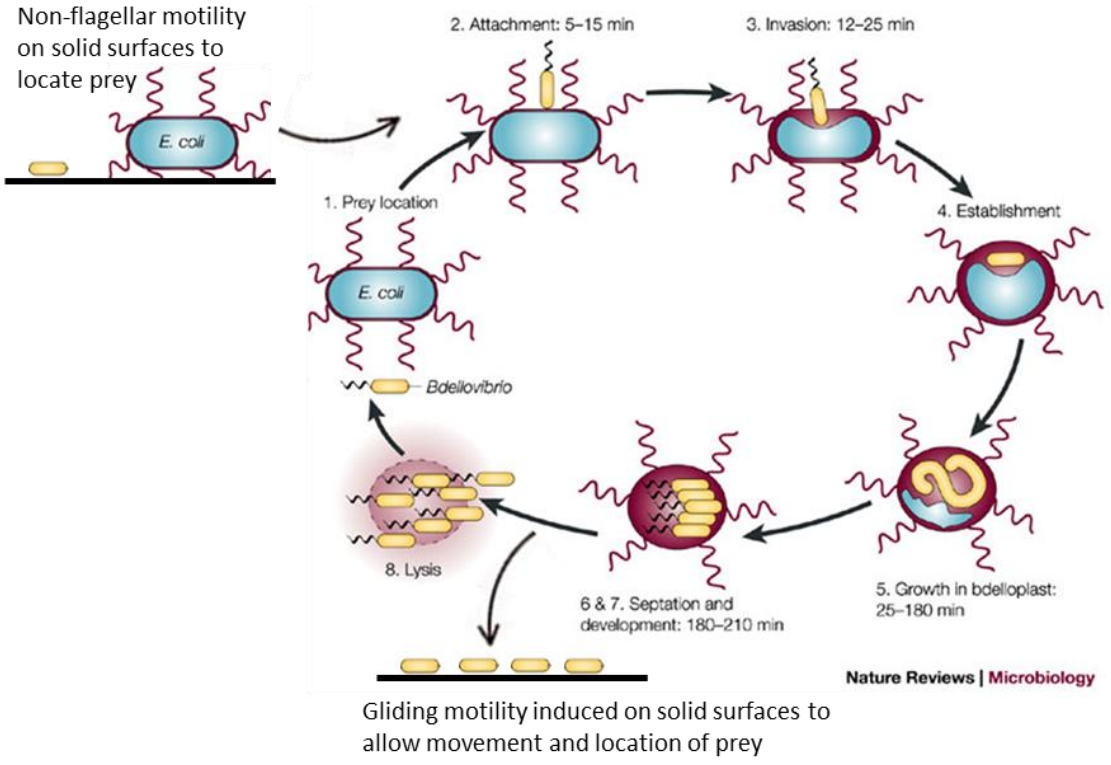

Figure 1.3 Predatory cycle of *Bdellovibrio bacteriovorus*. Figure adapted from (Sockett & Lambert, 2004) Predatory *B. bacteriovorus* HD100 use flagella or gliding motility to come into contact with prey cell, the *Bdellovibrio* attach to these cells and invade them, this process rounds the prey cell into a bdelloplast structure. Once inside, B. bacteriovorus utilise host cell contents to facilitate their own growth, replication and division before lysing the bdellopast structure and using motility to exit so progeny cells can repeat the cycle.

1.2.2. Internal environment of the bdelloplast

The creation of the dead, but intact prey cell structures, called bdelloplasts, enables the invading *Bdellovibrio* cell to benefit from the nutrient rich environment of the prey cell without sharing this resource. Research has been conducted on the hydrolytic *Bdellovibrio* enzymes that are important in creating, maintaining and lysing this structure however there is still little known about the conditions/stresses that the *Bdellovibrio* encounters when degrading the prey cell content. An unknown signal stimulates the synchronous septation, similarly an unknown signal stimulates the *Bdellovibrio* cells to use its lytic enzymes to lyse the bdelloplast at the end of the cycle, and the signal that causes *Bdellovibrio* progeny to exit the bdelloplast by gliding or flagella motility is also still unknown. However the lack of bdelloplast exit in Δ*bd0367* DGC mutant strain suggests

c-di-GMP may play a role in coordinating the leaving process for progeny *Bdellovibrio* (Hobley et al, 2012). It is possible that the initial signal sensed is involved with relaying the redox conditions within the bdelloplast possibly in addition to nutrient limitation, or a yet to be identified signal.

1.2.3. Host Independent (HI) *B. bacteriovorus* HD100

The alternative life cycle for *Bdellovibrio* is the HI life cycle shown in Figure 1.4 this is where 1 in 10^{-7} HD *Bdellovibrio* make the switch into HI growth. In HI growth there are many varied morphologies and increased cell aggregation, along with the ability to grow and divide in the absence of a prey cell when in nutrient rich media (Seidler & Starr, 1969). However when prey cells are introduced many of this HI *Bdellovibrio* can switch to the HD lifecycle again, unless there is a particular mutation that impairs *Bdellovibrio bacteriovorus* predation (Barel & Jurkevitch, 2001).

The axenic growth is thought to be due to a mutation in the *hit* locus (host-interaction), potentially the most common mutation is in *bd0108* which controls the Type IV pili. Recent studies have shown that deletion of *bd0108* greatly reduced the extrusion of pili (Capeness et al, 2013; Roschanski et al, 2011). Pili are essential for prey entry (Evans et al, 2007), it was proposed that Bd0108/Bd0109 regulates pilus production and that the presence of pili is used as a signal that can alter the growth state of *Bdellovibrio* (Capeness et al, 2013; Cotter & Thomashow, 1992; Roschanski et al, 2011).

Additionally biofilm formation of HI cells can occur when cells are incubated in a amino acid rich nutrient environment. The nuclease Bd1244 has been shown to be important in biofilm formation, with biofilm formation impaired on its deletion. It is hypothesised that this nuclease is involved in the regulating the eDNA in the biofilm and that without this regulation less planktonic cells can join the biofilm (Lambert & Sockett, 2013; Medina & Kadouri, 2009). To date the role of c-di-GMP in biofilm formation in *Bdellovibrio* is unknown.

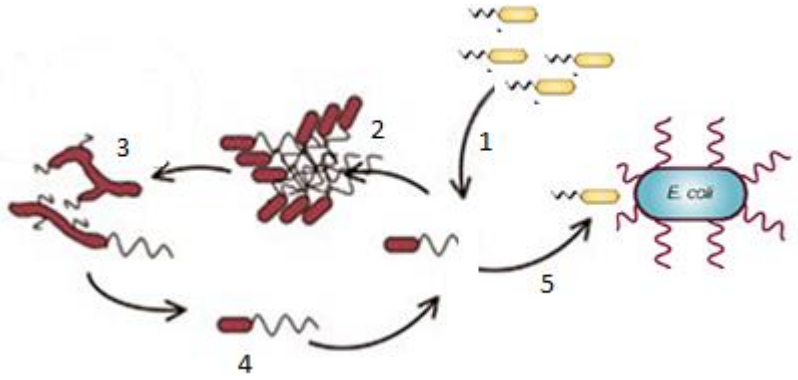

Figure 1.4 Schematic of the Host-independent (HI) growth cycle. Figure adapted from (Sockett & Lambert, 2004). 1) Once cells have reached a critical population density, HD *B. bacteriovorus* HD100 are capable of undergoing the switch to the HI growth mode. 2) HI cells initially thrive in dense cell populations 3) HI cells can have varied morphologies including filamentous and branched 4) HI cells can replicate outside of prey cells and in rich media can continue to grow as HI cells or 5) Most HI cells will revert to the HD lifestyle, if prey becomes available.

1.3. Regulatory cascades in *B. bacteriovorus*

1.3.1. Regulation of processes in *Bdellovibrio* by phosphorylation

To date there has been no research into the role of two component systems (TCS) in *B. bacteriovorus*. However the Mist2.2 database identifies many TCS components in the *Bdellovibrio* genome (Ulrich & Zhulin, 2010). This suggests TCS are important in *B. bacteriovorus* to relay signals such as nutrients levels, osmotic conditions and temperature. TCS may be important in the c-di-GMP signalling network as DGC Bd0367 has a response regulator domain (RR) suggesting synthesis of c-di-GMP could be regulated by phosphorylation. This potential TCS is investigated in Chapters 4 and 5 of this study.

1.3.2. Regulation of processes in *Bdellovibrio* by multi-protein complexes

Work by Dr Milner found that MglA interacted with tetratricopeptide repeat (TPR) protein Bd2492, by bacterial two hybrid and his tag pull down analyses (Milner et al, 2014). Further study found a multiprotein complex of protein interactions occurring at the predatory pole of *Bdellovibrio*. This formed a predatory regulatory hub of proteins, including c-di-GMP associated proteins, which suggests that protein interactions are influential in regulating the prey invasion process in *Bdellovibrio* and suggests protein interactions may be important in regulating other key processes in *Bdellovibrio*.

1.4. Cyclic nucleotide signalling in *B. bacteriovorus*

1.4.1. Overview

From analysis of the *B. bacteriovorus* genome it seems, cAMP, (p)ppGpp, c-di-GMP and cyclic AMP-GMP signalling are all possible (Hallberg et al, 2016). Little is currently known about these signalling systems in *Bdellovibrio*, however cAMP signalling may influence the c-di-GMP signalling network as an EAL protein Bd1971 has a cNMP domain predicted to bind cAMP (Basford, 2015). This link between cAMP and c-di-GMP networks is seen in other bacteria, for example in *V. cholerae*, where cAMP bound to Crp represses expression of CdgA, a c-di-GMP synthesis protein, meaning that c-di-GMP levels cannot rise to trigger biofilm formation (Fong & Yildiz, 2008). The role for cAMP signalling on c-di-GMP levels in *Bdellovibrio* is still unknown and can be only speculated on.

1.4.2. C-di-GMP signalling network in *B. bacteriovorus*

Initial examination of *Bdellovibrio bacteriovorus* HD100 identified five DGCs, four of which are active; one EAL domain protein; six HD-GYP proteins, 2 of which are predicted to be active and 15 PilZ domain proteins (Hobley et al, 2012). The number of PilZ domain proteins is greater than seen previously in bacteria and has recently been increased to 19, indicating the importance of c-di-GMP signalling networks in *Bdellovibrio bacteriovorus* (Galperin, 2005). There has also been the discovery of a noncoding RNA containing a c-di-GMP riboswitch which is highly expressed in attack phase and is proposed to be functioning as an intracellular store for c-di-GMP, potentially sequestering it (Karunker et al, 2013).

Additionally the recent use of the c-di-GMP capture compound on *Bdellovibrio* cell lysate extractions identified 84 putative c-di-GMP binding proteins, 62 of which specifically bound c-di-GMP, of which 17 were predicted c-di-GMP binding proteins (Rotem et al, 2016). This study has demonstrated that there may be more c-di-GMP binding proteins in *Bdellovibrio* than previously thought. These novel c-di-GMP binding protein were found to have a diverse range of cellular functions, such as energy metabolism, regulatory circuits, a TF with Walker A motif (like FleQ) and motility. Three of these putative c-di-GMP binding proteins were confirmed by microscale thermophoresis, to quantify the c-di-GMP binding strength of these proteins.

The Table 1.1 outlines the bioinformtically identified c-di-GMP components in *Bdellovibrio* and includes a selection of the newly identified c-di-GMP binding proteins identified by the c-di-GMP capture compound. The predicted or confirmed function column indicates if the protein was found in the capture compound study or only identified bioinformatically. The absence of a protein from the capture compound study does not mean that it does not bind c-di-GMP as the protein may be absent in the conditions in which the cell lysate was obtained.

Table 1.1 C-di-GMP components in *Bdellovibrio*

Gene number	Domains	Predicted/ confirmed Function	References
GGDEF Domain Proteins			
Bd0367	Response regulator and GGDEF domain	DGC activity confirmed and c-di-GMP binding ability confirmed	(Hobley et al, 2012) (Rotem et al, 2016)
Bd0742	Fork head domain and GGDEF domain	DGC activity confirmed c-di-GMP binding not significant in capture compound study	(Hobley et al, 2012) (Rotem et al, 2016)
Bd1434	N terminal region of unknown function and GGDEF domain	DGC activity confirmed c-di-GMP binding not significant in capture compound study	(Hobley et al, 2012) (Rotem et al, 2016)
Bd3766	Predicted periplasmic N terminal domain with 4 tetratricopeptide repeats and GGDEF domain	DGC activity predicted and c-di-GMP binding ability confirmed	(Hobley et al, 2012) (Rotem et al, 2016)
EAL Domain Protein			
Bd1971	cNMP domain and EAL domain	PDE activity confirmed and c-di-GMP binding ability confirmed	This study and (Rotem et al, 2016)
HD-GYP domain Proteins			
Bd2325	HD-GYP domain and N terminal domain of unknown function	PDE activity confirmed by elevated c-di-GMP level in deletion strain. Predicted c-di-GMP binding ability	(White, 2012)
Bd2421	HD-GYP domain	PDE activity confirmed elevated c-di-GMP level in deletion strain. c-di-GMP binding ability confirmed	(White, 2012) and (Rotem et al, 2016)

C-di-GMP Receptor Proteins			
PilZ Domain Proteins			
Bd0064	PilZ domain	Predicted c-di-GMP binding ability	(Hobley et al, 2012)
Bd0378	PilZ domain	C-di-GMP binding ability confirmed	Predicted (Hobley et al, 2012) Confirmed (Rotem et al, 2016)
Bd0642	PilZ domain (hemolysin)	C-di-GMP binding ability confirmed	Predicted (Hobley et al, 2012) Confirmed (Rotem et al, 2016)
Bd1007	PilZ domain Transmembrane domain	C-di-GMP binding ability confirmed	Predicted (Hobley et al, 2012) Confirmed (Rotem et al, 2016)
Bd1482	PilZ domain Low complexity region Duf4339	C-di-GMP binding ability confirmed	Predicted (Hobley et al, 2012) Confirmed (Rotem et al, 2016)
Bd1996	PilZ domain Duf4339	C-di-GMP binding ability confirmed	Predicted (Hobley et al, 2012) Confirmed (Rotem et al,

			2016)
Bd2059	PilZ domain 4 Transmembrane domains Signal sequence	C-di-GMP binding ability confirmed	Predicted (Hobley et al, 2012) Confirmed (Rotem et al, 2016)
Bd2524	PilZ domain 4 Transmembrane domains	C-di-GMP binding ability confirmed	Predicted (Hobley et al, 2012) Confirmed (Rotem et al, 2016)
Bd2545	Subtilisin like serine protease domain PilZ domain 1 transmembrane 2 low complexity regions	Predicted c-di-GMP binding ability	(Hobley et al, 2012)
Bd2717	PilZ domain	C-di-GMP binding ability confirmed K_d 0.176μM	Predicted (Hobley et al, 2012) Confirmed (Rotem et al, 2016)
Bd2880	PilZ domain	C-di-GMP binding ability confirmed	Predicted (Hobley et al, 2012) Confirmed (Rotem et al, 2016)
Bd3100	PilZ domain 2x Duf4339	C-di-GMP binding ability partially confirmed however was not significantly enriched in 3 out of 5	Predicted (Hobley et al,

		experiments.	2012) Confirmed (Rotem et al, 2016)
Bd3138	PilZ domain 4 transmembrane domains, signal peptide	C-di-GMP binding ability confirmed	Predicted (Hobley et al, 2012) Confirmed (Rotem et al, 2016)
Bd3232	PilZ domain	Predicted c-di-GMP	(Hobley et al, 2012)
Bd3527	PilZ domain	Predicted c-di-GMP binding ability	(Hobley et al, 2012)
Bd0760	PilZ domain	C-di-GMP binding ability confirmed	Confirmed (Rotem et al, 2016)
Bd1616	PilZ domain	not isolated in capture compound study	Predicted (Rotem et al, 2016)
Bd1466	PilZ domain	not isolated in capture compound study	Predicted (Rotem et al, 2016)
Bd2147	No conserved domains Hypotheticall piz domain	not isolated in capture compound study	Predicted (Rotem et al, 2016)
Degenerate enzymatic proteins acting as c-di-GMP receptors			
Bd3125	Degenerate GGDEF domain	C-di-GMP binding ability confirmed	Confirmed (Hobley et al, 2012) Confirmed (Rotem et al, 2016)

Bd1762	Degenerate HD-GYP domain	Predicted c-di-GMP binding ability	(Hobley et al, 2012)
Bd1817	Degenerate HD-GYP domain	Predicted c-di-GMP binding ability	(Hobley et al, 2012)
Bd1822	Degenerate HD-GYP domain	Predicted c-di-GMP binding ability	(Hobley et al, 2012)
Bd3880	Degenerate HD-GYP domain	Predicted c-di-GMP binding ability	(Hobley et al, 2012)
Selection of interesting c-di-GMP receptor proteins identified by c-di-GMP capture compound			
Transcription factor			
Bd0156	NifA like transcription factor, AAA+ domain with Walker A motif	C-di-GMP binding ability confirmed	(Rotem et al, 2016)
Miscellaneous			
Bd1551	Polyribonucleotide nucleotidyltransferase PNPase- RNA turnover regulated by c-di-GMP in ecoli	C-di-GMP binding ability confirmed	(Rotem et al, 2016)
Bd2402	Two component response regulator , DUF4388 domain	C-di-GMP binding ability confirmed and quantified K_d 0.399 μM	(Rotem et al, 2016)
Bd2590	CRP cAMP receptor protein	C-di-GMP binding ability confirmed	(Rotem et al, 2016)
Bd2924	Acyl-CoA dehydrogenase	C-di-GMP binding ability confirmed, K_d 7.67 μM	(Rotem et al, 2016)
Gliding motility			
Bd0179	AglW TolB homologue (Nan et al,	C-di-GMP binding ability confirmed	(Rotem et al, 2016)

	2010)		
Bd0182	AglX potentially part of gliding motor TolQ homologue Identification of genes (Luciano et al, 2011)	C-di-GMP binding ability confirmed	(Rotem et al, 2016)
Bd0836	AglR TolQ homologue (Luciano et al, 2011)	C-di-GMP binding ability confirmed	(Rotem et al, 2016)
Flagellar motility			
Bd0604	Flagellin	C-di-GMP binding ability confirmed	(Rotem et al, 2016)
Bd3395	Flagella hook protein	C-di-GMP binding ability confirmed	(Rotem et al, 2016)
Bd3404	Flagellar M ring protein	C-di-GMP binding ability confirmed	(Rotem et al, 2016)

1.4.3. Studies to date on c-di-GMP signalling in *Bdellovibrio*

The study of c-di-GMP signalling in *Bdellovibrio* is currently limited to five published papers. These studies have analysed: the structure of an un-conventional *Bdellovibrio* HD-GYP protein (Lovering et al, 2011); the phenotypic effect of individual *Bdellovibrio* DGC gene deletions (Hobley et al, 2012); discovery of a *Bdellovibrio* c-di-GMP riboswitch (Karunker et al, 2013); a c-di-GMP receptor in a polar protein hub that allows c-di-GMP signalling input into the *Bdellovibrio* predation process (Milner et al, 2014), and a study using the c-di-GMP capture compound to identify 62 putative c-di-GMP binding proteins in *Bdellovibrio* (Rotem et al, 2016).

1.4.4. Distinct phenotypes arise from deletion of individual diguanylate cyclases in *B. bacteriovorus*

One of biggest insights into c-di-GMP signalling in *Bdellovibrio* was provided by a study conducted by Hobley and co-workers who separately deleted the genes encoding the five GGDEF domain proteins in *Bdellovibrio* and the majority of these deletions resulted in distinct phenotypes detailed in the following text (Hobley et al, 2012). The distinct phenotypes provided by the deletions suggests there are specific c-di-GMP pathways acting in *Bdellovibrio* and that systems are in place to insulate specific pathways from general global c-di-GMP signalling.

Deletion of Bd0367 abolished gliding motility and prey cell exit, this is thought to be the first instance where c-di-GMP synthesis has been shown to specifically control gliding motility (Hobley et al., 2012). Due to the prey exit defect Δ*bd0367* HI *Bdellovibrio* were-not able to sustain a replicative predatory life cycle, as after entering the prey cell, replicating and progeny cells septating there was no induction of gliding motility and the *Bdellovibrio* progeny remained still inside the lysed prey bdelloplast. Whereas a WT *Bdellovibrio* would have sensed a cue to exit and would also be able to induce gliding or flagellar motility dependent on the external environment. The overall effect of the Bd0367 deletion impairs the predatory nature of the *Bdellovibrio* for two reasons. Firstly the deletion strain is unable to hunt for prey on surfaces that require gliding motility and secondly when a *Bdellovibrio* cell manages to encounter prey the cycling through prey is prevented by progeny cells not leaving the empty bdelloplast due to the prey exit defect (Hobley et al., 2012). My study begins to investigate if motility defects prevent bdelloplast exit or if inability to exit the bdelloplast is a separate phenotype.

Bd0742 is implicated in functional predation. Deletion of Bd0742 resulted in the abolition of predation, this strain could only grow axenically in the HI growth state and could not enter prey.

Bd1434 is required for axenic HI growth. The Bd1434 deletion strain had a lower conversion rate from predatory to HI growth, it took $4.5x10^{-11}$ cells in a nutrient rich environment to result in one HI *Bdellovibrio* compared to 1 in 10^{-7} for wild type (Hobley et al., 2012). This result implies that Bd1434 controls the transition between the non-replicative hunting phase and the replicative HI growth phase of *Bdellovibrio*. The effect of this deletion mutation is interesting as it creates an obligatory predatory *Bdellovibrio* which has more potential for therapeutic use (Hobley et al., 2012).

Potential DGC Bd3766 did not inhibit motility on swim plate assay when expressed in *E.coli*. This could mean that the protein is an inactive GGDEF protein or it was potentially not activated in *E.coli*. The lack of detectable phenotype on deletion suggests that that Bd3766 is not an active GGDEF in *Bdellovibrio*, however to conclude this would require c-di-GMP extractions of the gene deletion strain to see if there is a detectable difference in the cellular c-di-GMP level.

1.4.5. Recent developments in cyclic AMP-GMP (3', 3' cGAMP) research

A study in early 2016 by Hallberg et al has revealed that a subfamily of GGDEF proteins can produce an asymmetric signalling molecule cyclic AMP-GMP), shortened to cAG (Hallberg et al, 2016). They demonstrated that the switching of cyclic dinucleotide production between c-di-GMP and cAG was probably based on ATP:GTP ratios for a Hypr GGDEF identified in δ proteobacterium *Geobacter sulfurreducens*, ATP is usually found in excess to GTP, this skews production to cAG at high ATP to GTP ratios, the physiological ranges for *Bdellovibrio* is unknown.

The cAG synthase enzyme in *Geobacter* was identified as GGDEF protein GSU1658 and was found using fluorescent riboswitch based sensors specific to c-di-GMP or cAG, through differences in signal profile. The over expression of DGC GSU1658 led to higher cAG levels.

Examination of GSU1658 compared to PleD crystal revealed a key residue, S347 in place of the D344 in PleD. The mutation of GSU1658 S347D resulted in c-di-GMP

production only, demonstrating the importance of this residue in cAG production and recognition of ATP or GTP. From this GGDEF proteins were bioinformatically screened and 99% of them have the conserved D, however there is a distinct subfamily of enzymes in the GGDEF family that are described as hybrid promiscuous GGDEFs (Hypr GGDEF), they potentially comprise 0.17% of all GGDEF domains. From this bioinformatics analysis Hypr GGDEF proteins were predicted in *Myxococcus xanthus* (MXAN_4463, MXAN_2643) and in *Bdellovibrio* as Bd0367.

When Bd0367 was expressed in *E.coli* and analysed by LC-MS/MS cAG production was identified. Collaborative studies are underway with Dr Hammond and in our lab (by Dr Lowry) to determine the level of cAG produced in vivo in native WT *Bdellovibrio* cells verus the levels in Δ*bd0367* mutant and in a predicted cAG negative mutant.

To date cAG is thought to be important in surface sensing, intestinal colonisation in *V. cholerae*, extracellular electron transfer for *Geobacter sulfurreducens* and it has been shown that cAG levels increase when *Myxococcus* is grown on solid surfaces (Hallberg et al, 2016). The currently known cAG pathway is shown in Figure 1.5.

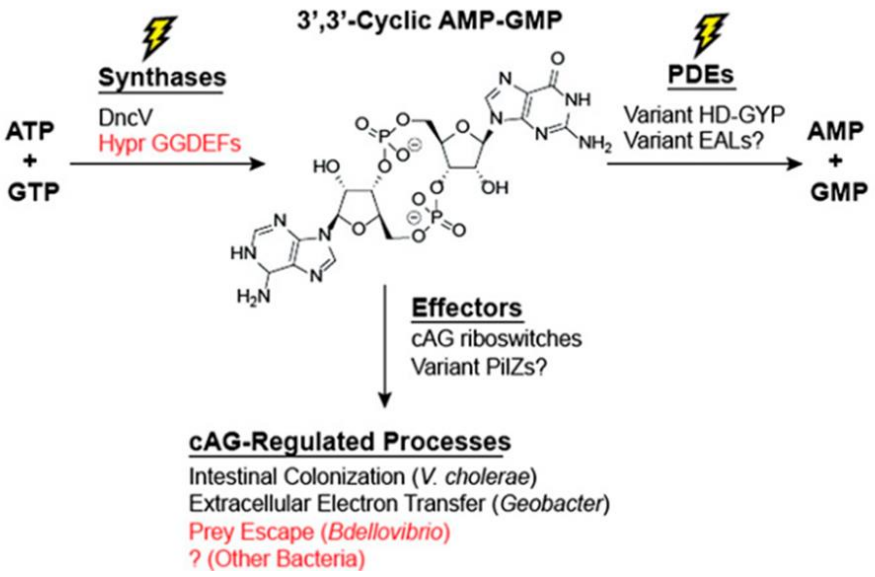

Figure 1.5 cAG pathway adapted from (Hallberg et al, 2016) Hallberg et al predict that a variant of PilZ domains and potential other effector modules for cAG will be found in cAG producing bacteria.

These new data suggest that the DGC Bd0367 is a bifunctional enzyme with the ability to produce c-di-GMP and cAG. To date we know from the work of Hobley 2012 that c-di-GMP level extracted from HID13 wild type is higher than that extracted from the Δ*bd0367* HI strain, suggesting Bd0367 produces c-di-GMP in the conditions tested. To

date the level of cAG in the HID13 wild type versus the Δ*bd0367* strain is unknown however it is under investigation by Dr Lowry. Additionally the relationship between high cAG level and surface behaviours is to be investigated in *Bdellovibrio* strains in the future to see if surface incubation elevates cAG levels. The multifunctional nature of Bd0367 may explain the potentially two separate phenotypes on deletion, loss of gliding ability and inability to exit the prey bdelloplast.

1.5. Gliding motility

Gliding motility is an important phenotype in this study and motility is a phenotype commonly affected by c-di-GMP signalling. Gliding motility is the process of bacterial movement along a surface without aid of flagella or pili. It is not flagellate swimming, flagellar swarming or pilus mediated twitching motility (Jarrell & McBride, 2008).

1.5.1. Deltaproteobacteria gliding motility as seen in *Myxococcus*

The mechanisms behind gliding motility vary across clades and is still relatively poorly understood, however advances have been made in some bacterial genera recently especially in delta proteobacterium *Myxococcus xanthus* by Mignot, Zusman, Sogaard, Anderson and Kaiser labs .

Myxococcus is in the same class as *Bdellovibrio* (δ proteobacteria) this shared ancestry makes the mechanism of *Myxcococcus* gliding motility of particular interest, but it is possible that there has been some diverse evolution of gliding mechanisms between them. *Myxococcus* uses two types of gliding motility one is called S motility and the other A motility. S motility stands for social motility and involves Type IV pili and extracellular polysaccharide matrix (EPS) to move in large cell groups. A motility on the other hand stands for adventurous gliding motility and is defined as the movement of individual cells on a surface (without use of pili) this occurs at 1-4 μm/min in *Myxococcus* and cells reverse direction every 8-10 minute (Spormann & Kaiser, 1995). A motility allows individual *Myxococcus* to explore new locations and leave trails of EPS which can be followed by other cells (Burchard, 1982).

1.5.1.1. Energetics of *Myxococcus* gliding motility

A motility is powered by proton motive force, this is channelled by the AglRQS motor that was shown to be essential for gliding in *Myxococcus*. The proteins that make up the

motor complex AglR/S/Q/X/V have sequence similarity to other bacterial inner-membrane proteins that assemble a proton-conducting channel to energize processes such as TolQR for outer membrane stability (Agrebi et al, 2015; Zhang et al, 2011) and MotA/MotB for the flagellar motor. The ion movement through the motor complex is coupled to motion via the gliding transducer complex (glt) (Figure 1.6) which comprises, cytoplasmic, inner membrane and periplasmic components known from mutagenesis screens to be important in A motility.

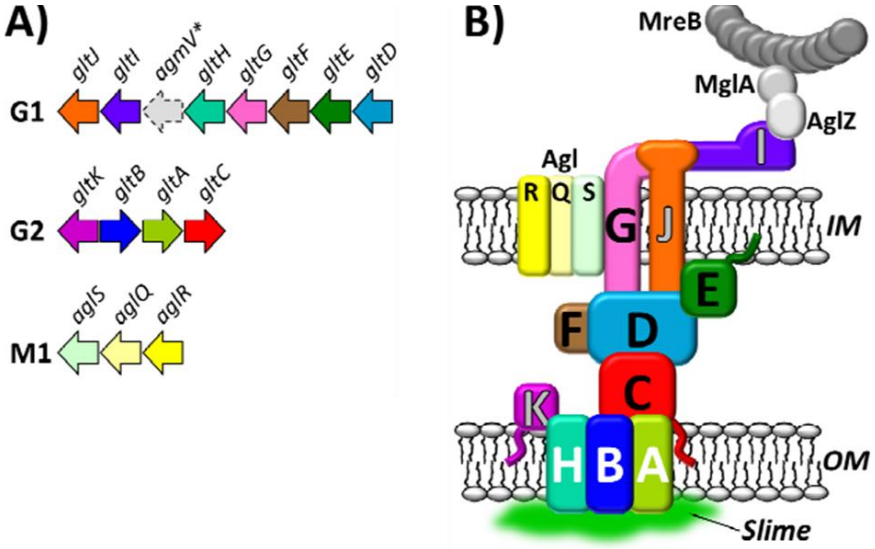

Figure 1.6 The genes and proteins of the gliding transducer complex *Myxococcus* and Agl motor complex. Diagram adapted from (Islam & Mignot, 2015). (A) Shows the chromosomal organization of the known components of the Agl–Glt gliding motility apparatus. (B) Is a schematic of the Agl–Glt complex architecture with the colours for the proteins match their corresponding genes in A. This diagram is slightly more representative of the focal adhesion model from bacterial gliding motility.

1.5.1.2. Two models of adventurous gliding motility

The precise mechanism of A motility is not yet known (Munoz-Dorado et al, 2016), however there are two theories describing how movement occurs, these theories are the focal adhesion model or helical rotor model shown in Figure 1.7.

The AglRQS motor complex that drives bacterial gliding is untethered so free to move within the cell membrane (Nan et al, 2013). Microscopy suggests that AglRQS complexes move in helical trajectories and when incubated on a surface the cell surface contact points (ventral sides) become sites at which AglRQS complexes collect with an even distribution along the cell. When the cell moves forward the motor clusters did not also move but remained at a fixed position in respect to the surface.

From these data two models have been proposed. The focal adhesions model suggest that because the motor clusters remain fixed as the cell moves that this suggest the presence of a larger complex called the 'focal adhesion clusters' (FAC) these in theory span the cell envelop and anchor the cell to the solid surface (containing proteins from the gliding transducer complex (glt)) (Mignot et al, 2007). This model suggests that the gliding motor complexes push against the FAC to move them to the posterior of the cell. The backward motion of the FAC causes the cell to be pushed forward. The limitation with this model is the breaching of the cell wall barrier as the focal adhesion clusters would be moved back through peptidoglycan (Nan & Zusman, 2016).

The alternative model is the helical rotor model; this model suggests the motor complexes cluster on contact with the surface due to the motor complexes slowing down because of increased resistance presented by the solid surface. This has been investigated by studying the appearance of motor complex clusters on agar of differing hardness (Nan et al, 2013; Nan et al, 2010). The clustering of the motor complexes is suggested to create a force that deforms the cell envelope, which creates a backwards wave which would generate enough thrust to propel the cells forward (Nan et al, 2011). This theory does not rely on a breach in the cell wall but still requires an adhesive aspect and suggests 'slime' as this factor (Nan et al, 2014).

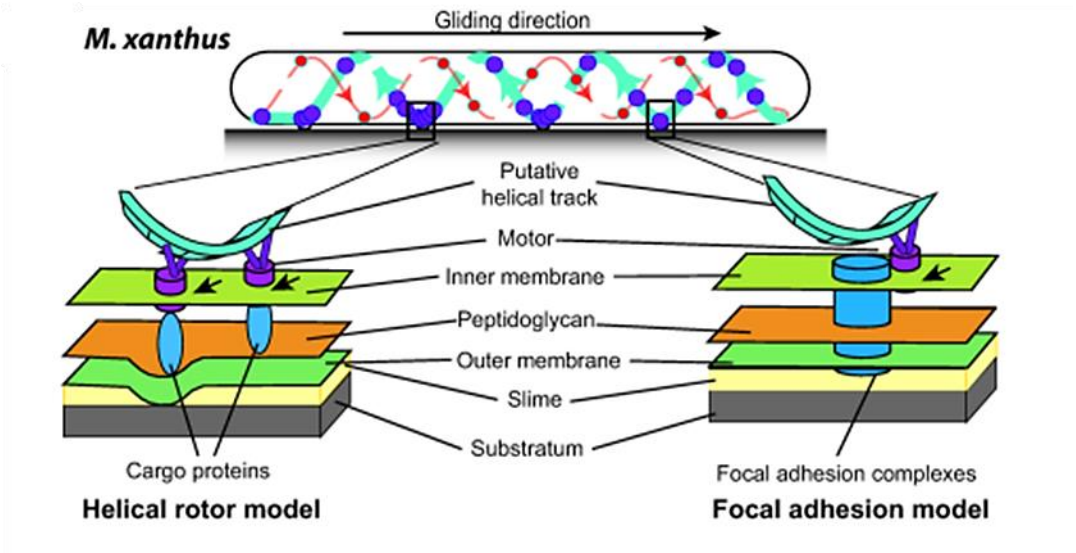

Figure 1.7 Two theories of gliding motility in *M. xanthus*. Figure reproduced from (Nan & Zusman, 2016). Gliding is powered by proton motive force generate by AglRQS complexes that move along helical tracks in the inner membrane. Two models propose different mechanisms by which cells use the proton motive force to propel the cell forward. The helical rotor model proposes that due to the increased resistance from the surface, the speed of motor complexes within the membrane slows down at the sites

where cells contact the surface. The motor complexes accumulate and cause deformation in the cell envelope which pushes against the surface, and creates a backward surface wave that propels cells forward. The other proposed mechanism is the focal adhesion model that suggests focal adhesion complexes (FACs) penetrate the cell envelope and anchor cells to the gliding surface. The motor complexes propel cells forward by pushing the FACs backward towards the end of the cell. It is inferred that *Bdellovibrio* have a similar apparatus.

1.5.1.3. Regulation of direction of travel in *Myxococcus*

The regulation of the direction of motion is complex, especially the process of cellular reversals, this is organised by a collection of envelope spanning proteins known as the FrZ chemosensory system and also utilises RomR and MglABC in *Myxococcus* (McLoon et al, 2016). These components enable regulation of the localisation of gliding engine components (covered in more detail in chapter 6).

1.5.2. Gliding motility in *Bdellovibrio*

Although flagella motility in liquids is most widely reported in *Bdellovibrio*, it can also use adventurous gliding motility to encounter potential prey bacteria on solid surfaces (Lambert et al, 2011). This is a motile behaviour of single cells without flagellar or pili being used. HD *Bdellovibrio* in attack phase (actively seeking prey) were visualised gliding bidirectionally on a 1% agarose /CaHEPES pad, the average speed of gliding was 16 μm hr^{-1}, slower than the previously described *Myxococcus*. This speed increased when they encountered prey bacteria, rising to 35 μm/hr^{-1}. The induction of gliding motility frequently occurred approximately 1 hour after of incubation on solid surface, suggesting that the gliding apparatus may be induced when a surface is sensed. *Bdellovibrio* can also use gliding motility to emerge from lysed bdelloplasts on agarose pads and enables progeny *Bdellovibrio* to scout for more prey bacteria via gliding motility when colonising non-liquid environments. (Lambert et al, 2011)

Bdellovibrio can glide in both lifestyles HD and HI, however visualisation of HI cells gliding is rarer. Lambert and co-workers showed that gliding motility in *Bdellovibrio* is independent of other bacterial appendages such as type IV pili and flagella. This was done by observing deletion mutants pilA (no PilA pilus fibre protein) and flic3 (no functional flagella). Both these mutant strains still exhibited surface motility (Lambert et al, 2011).

1.5.2.1. Overview of the potential gliding operons of *Bdellovibrio*

The mechanism of gliding motility in *Bdellovibrio* is yet to be determined however Luciano and co-workers have shown that the genome of *Bdellovibrio bacteriovorus* HD100 contains four operons with protein products that share homology with the Tol like complexes (suggested to be) involved in adventurous gliding motility in *Myxococcus xanthus* (Lambert et al, 2011; Luciano et al, 2011). These operons are *bd0416-0420, bd0828-0838, bd1471-1483,* and *bd2368-2377,* the operon and length was inferred from RNAseq data (Lambert unpublished work). Operons and additional gliding proteins of *Bdellovibrio* are shown in Figure 1.8, Luciano and co-workers suggested that the operon (B in Figure 1.8) *bd0828-838* was phylogenetically most similar to the genes involved in *Myxococcus Xanthus* gliding (Luciano et al, 2011). Though *bd1473-1483* (C in Figure 1.8) is the only operon that encodes for CglF/GltF protein which when applied exogenously in *Myxococcus* cglF deletion strain can restore gliding motility, suggesting this protein is localised at the cell surface and is important for functional gliding (Pathak & Wall, 2012). So *bd1473-1483* is the most complete operon, where structural and Tol proteins are co-encoded (Luciano et al, 2011).

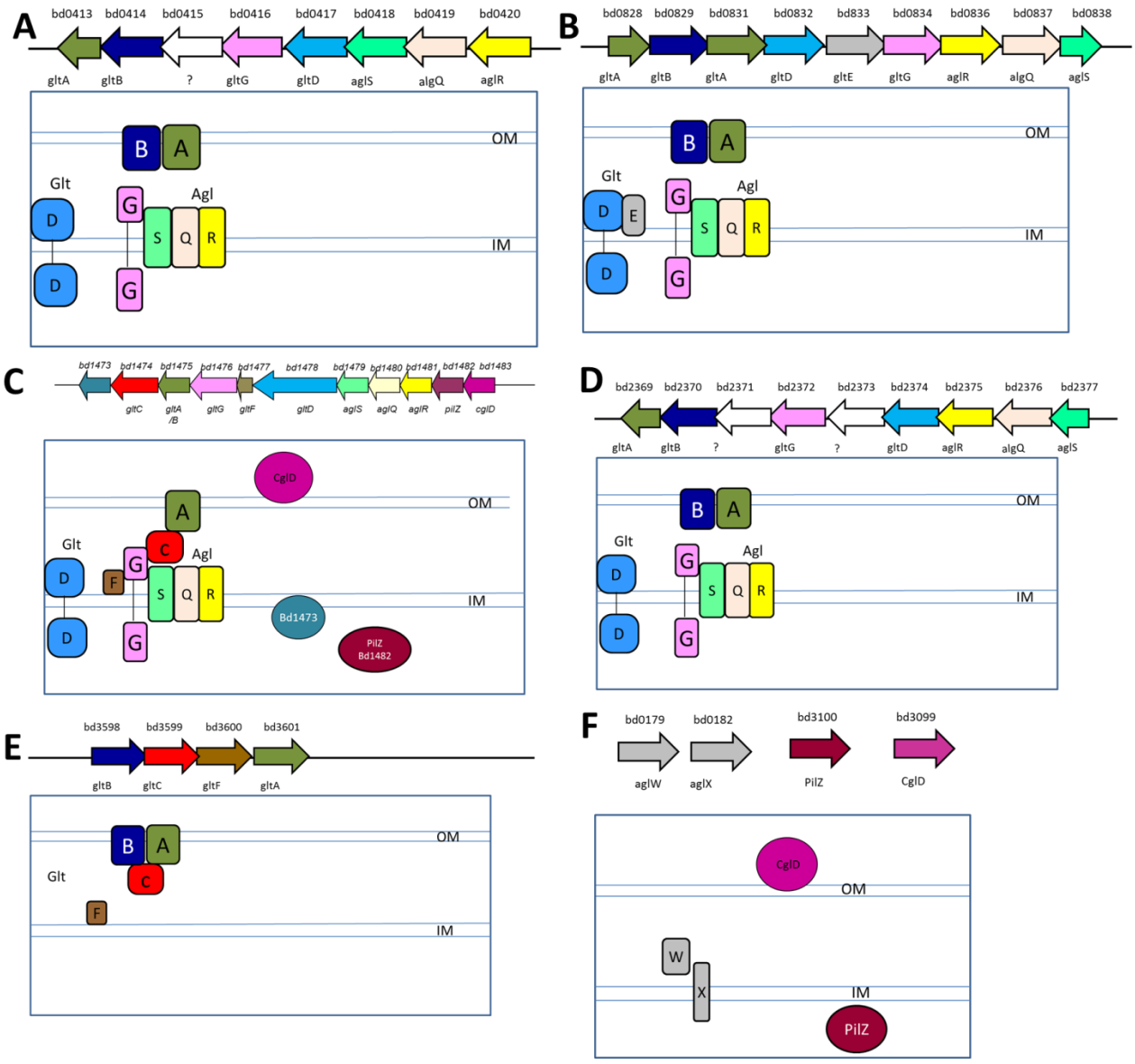

Figure 1.8 Genes and proteins implicated in *Bdellovibrio* gliding. The operons shown in A B C and D are operons that encode gliding motor complex genes. The genes are displayed above a presentation of the predicted protein locations in a similar style to Figure 1.6 and the colours of the proteins correspond to the colours of the gene. The predicted protein locations were made using PSORTb or by using locations of homologous *Myxococcus* proteins (Islam & Mignot, 2015; Jakobczak et al, 2015).

1.5.2.2. Initial examination of gliding operons in *Bdellovibrio*

In preliminary investigations Dr Lambert deleted the gene encoding Bd0416, this is a *tolb*-like gene predicted to be involved in in ion conductance. This deletion did not alter the motility phenotype, which suggested that functional redundancy between the homologous operons may mask phenotypes (Lambert et al, 2011).

In contrast Kadouri and co-workers examined two genes from the other speculative gliding operon *bd1481* and *bd1483*, these were disrupted using transposon mutagenesis. Both of these alterations hindered the ability of *Bdellovibrio* to reduce a preformed *E. coli* biofilm, this suggests that gliding motility or predation on a surface may have been impaired however direct visualisation of impaired gliding is was not investigated (Medina et al, 2008).

The presence of a predicted PilZ domain protein Bd1482 in the *bd1473-1483* operon is of interest as it may link c-di-GMP signalling and gliding motility regulation. The potential gliding proteins of *Bdellovibrio* are further discussed in chapter 6.

1.6. Summary

Although more has been discovered about both *Bdellovibrio* and c-di-GMP in the past decade there are still many unanswered questions. Such as:

How is c-di-GMP signalling specificity determined in *Bdellovibrio*?

What are the functions of the large number of PilZ domain proteins in *Bdellovibrio*?

How is DGC activity in *Bdellovibrio* regulated? Do protein interactions and/ or phosphorylation play a role?

What is the effect of large global changes in intracellular c-di-GMP levels on *Bdellovibrio* phenotypes?

My examination in this study of the c-di-GMP network in *Bdellovibrio* with such an apparently distinct local/specific c-di-GMP system aims to provide an insight into the broader questions in c-di-GMP research about how specificity of c-di-GMP signalling pathways is achieved.

1.7. How this study builds on previous work

In studies preceding this work Bd0367 was identified as an active DGC with an informatically predicted RR domain and a deletion phenotype showing no bdelloplast exit or gliding motility requiring routine culturing of Δ*bd0367* as a HI strain (Hobley et al, 2012). Additionally a PilZ domain protein Bd3100 with a deletion phenotype that produced a gliding defect had also been identified (Taylor, 2013).

The work presented in this thesis builds on these discoveries examining the possible ways that Bd0367 DGC activity may be regulated through protein interactions and phosphorylation. This study also pursues a potential link between DGC Bd0367 and PilZ domain protein Bd3100. During the course of this research a broader examination of how the global c-di-GMP signal could be integrated with or potentially over-ride local c-di-GMP signalling was investigated by examining the effects of a high and low c-di-GMP intracellular environment on *Bdellovibrio* surface motility.

1.7.1. Research objectives

- To identify a *Bdellovibrio* network of c-di-GMP related protein-protein interactions by bacterial two hybrid assays in *E.coli.*
- To find the cognate histidine kinase involved in regulating DGC Bd0367 and to phenotype the effect of histidine kinase gene deletion.
- To investigate the role of phosphorylation on Bd0367 DGC activity
- To initiate studies into the global effects of high and low cellular c-di-GMP levels in *B. bacteriovorus* focusing on gliding motility behaviour.
- To phenotype the gliding defects in the Bd3100 PilZ deletion strain and examine the links between the PilZ and DGC Bd0367.
- To begin to investigate the roles that other PilZ domain proteins may having in gliding motility.

1.7.2. Timeline of experimentation

1.7.2.1. Year 1

After completing my doctoral training program rotations in May 2013 I set out to find the cognate Histidine Kinase (HK) for Bd0367. Potential HKs had been selected informatically by our collaborator Dr Steven Porter of The University of Exeter and were cloned by myself to examine protein interactions with Bd0367 by bacterial two hybrid

assays (B2H). One HK Bd2584 was selected as a potential cognate HK candidate due to significant B2H interaction detailed.

1.7.2.2. Year 2

I constructed a deletion strain of Δ*bd2584* HK and assayed it for similar phenotypes to ⊿*bd0367* strain. This strain appeared similar to the wild type. Due to this I moved on to investigating other potential proteins interacting with Bd0367.

I examined the protein interaction network of Bd0367 by investigating interactions between other c-di-GMP proteins and Bd0367. This was carried out by extensive B2H assays and built on work carried out by Dr Milner and on work on an EAL protein carried out by Dr Basford.

I also assessed the B2H protein interactions of the potential cognate HK with the other c-di-GMP proteins.

In parallel I analysed the PilZ domain protein Bd3100 by fully phenotyping the ⊿*bd3100* deletion strain made by Aidan Taylor and Dr Milner. This was done by setting up gliding motility microscopy videos and assessing the motility phenotype. I also analysed the complemented and WT strains.

1.7.2.3. Year 3

To discover the activation state of Bd0367 as a DGC the phospho-receiving Aspartate 63 was mutated to an alanine. I observed the motility and exit phenotype of this strain compared to the ⊿*bd0367* strain and Bd0367-mCherry HI strain. I also compared the level of extracted c-di-GMP for these strains to assess the role of phosphorylation of Bd0367 on cellular c-di-GMP levels.

The interaction of the HK Bd2584 and Bd0367 was probed further by mutating the phosphotransfer and receiving amino acids to assess if this effected the B2H interaction.

In parallel the phenotype of a strain containing the HK with a mutated phosphotransfer H_{389} was assessed to observe if promiscuous phosphorylation had been occurring in the deletion strain in the absence of the HK. However the strain appeared the same as WT.

Additionally during this year I took my 3 month BBSRC DTP 'professional internship for PhD students' (PIP) at the Parliamentary Office of Science and Technology.

1.7.2.4. Year 4

To establish the relationship between potential cognate HK Bd2584 and Bd0367 the phosphotransfer profile between the two was examined by myself at The University of Exeter with the help of Dr Porter and Dr Francis. No transfer was observed and led to the conclusion that other HKs should be tested and that if Bd2584 did transfer in vivo then further proteins may be required for phospho-transfer.

I attempted to confirm the B2H protein interactions identified in this study by a protein pull down methods. However further optimization of the method is required.

I carried out further analysis on c-di-GMP proteins involved in gliding motility and analysed the effect of different c-di-GMP levels and genetic backgrounds on the location of Bd3100mCherry and Bd0367mCherry in *Bdellovibrio* and how surface motility affected these.

I began to study the PDE Bd1971 in year 3 through B2H interaction studies which inferred a role in the Bd0367 signalling network. I went on to study the gliding phenotype of a ⊿*bd1971* strain, a Bd1971 active site mutant. I also analysed the levels of extracted c-di-GMP from these strains to hypothesise the role of global c-di-GMP signalling in gliding motility in *Bdellovibrio*.

Chapter 2. Materials and Methods

2.1. Bacterial strains and plasmids

Escherichia coli DH5α was used for cloning plasmid constructs, these constructs were transformed into the *E.coli* strain S17-1 to be conjugated into various *Bdellovibrio bacteriovorus* strains. The *E.coli* strain BTH101 was used for bacterial two hybrid assays, this strain is deficient in adenylate cyclase (*cyaA*-), and this *cyaA* mutant strain is used to assay for plasmid derived adenylate cyclase to activate the *lac* operon. For protein overexpression, the *E.coli* strain XL-1 BLUE was used for cloning plasmid constructs, these constructs were transformed into the *E.coli* strain M15 pREP for protein over expression.

Table 2.1 Strains used in this study: Abbreviations N/A – previously confirmed strains. Gen PCR- amplification of relevant section; Kan selection these strains were maintained using kanamycin.

Strain	Description	Confirmation	Reference
General *Escherichia coli* strains			
DH5α intermediate cloning host	F^- endA1 hsdR17 (r_k^- mk^-) supE44 thi-1 recA1 *gyrA* (Nal^r) relA1 Δ(laclZYA-argF) U169 deoR (80dlacΔ(*lacZ*)M15) used as a cloning strain	N/A	(Hanahan, 1983)
S17 – one conjugation donor strain	thi,pro,hsdR-,hsdM+,recA; integrated plasmid RP4-Tc::Mu-Kn::Tn7; used as donor for conjugating plasmids into B. bacteriovorus	N/A	(Simon et al, 1983)
S171::pMAL_ p2mCherry	S17-1 with Amp^r plasmid containing mCherry gene with a malE signal sequence for localised periplasmic fluorescence to use as	N/A	(Fenton et al, 2010)

	lit prey background.		
XL-1 BLUE	Cloning strain recA1 endA1 gyrA96 thi-1 hsdR17 supE44 relA1 lac [F´ proAB lacIq ZΔM15 Tn10 (Tetr)	N/A	Gift from Dr Porter at the University of Exeter
M15 pREP	contains pREP4 expression host used in combination with most pQE-vectors (Qiagen) kan	N/A	Gift from Dr Porter at the University of Exeter
BTH101	F-,Δ*cya99*, *galE15, galK16, rpsL1, hsd*R2, *mcrA1, mcrB1* Adenylate cyclase⁻ strain used for protein:protein interaction studies by bacterial two hybrid analysis.	N/A	(Karimova et al, 2001) (Battesti & Bouveret, 2012) .
General *Bdellovibrio bacteriovorus* strains			
HD100	Host dependent wild type Bdellovibrio strain	N/A	(Rendulic et al, 2004) (Stolp & Starr, 1963)
HID13	Host independent naturally derivative from WT HD100 containing a G to A substitution in the start codon bd108.	N/A	(Lambert et al, 2010b)
Chapter 3 strains			
HD100 pK18::*bd0367*-mCherry	HD100 with pK18::*bd0367*mCherry integrated into the *bd0367* locus	N/A	(Hobley et al, 2012)
HD100 pK18::*bd1971*-mCherry	HD100 with pK18::*bd1971*mCherry integrated into the	N/A	(Basford, 2015)

	bd1971 locus		
HD100 pK18::*bd3125*-mCherry	HD100 with pK18::*bd3125*mCherry integrated into the *bd3125* locus	N/A	(Hobley et al, 2012)
HI ⊿*bd0367* pk18::*bd3125*mCherry	HI Δ*bd0367* with pK18::*bd3125*mCherry integrated into the *bd3125* locus	Kn selection	This study
HI pK18::*bd3125*mCherry	Host independent derivative of HD100 pK18::*bd3125*mCherry integrated into the *bd3125* locus	N/A	(Hobley et al, 2012)
XL-1BLUE pQE60_*bd0367*	XL-1Blue with vector for bacterial expression of C-terminally 6xHis tagged insert; amp resistance. Containing the gene *bd0367*.	Plasmid seq and antibiotic resistance-Amp 100	This study
M15pREP4 pQE60_*bd0367*	M15pREP4 with pQE60 vector for bacterial expression of C-terminally 6xHis tagged insert; amp resistance. Containing the gene *bd0367*	Plasmid seq and antibiotic resistance-Amp 100	This study
Chapter 4 strains			
HD100 pK18::*bd2584*mCherry	HD100 with pK18::*bd2584*mCherry single cross over integrated into the *bd2584* locus	Kn Selection Gen PCR, seq	This study
HI pK18::*bd2584*mCherry	Host Independent derivative of HD100 with pK18::*bd2584*mCherry single cross over integrated into the *bd2584* locus	Kn selection, Gen PCR, seq	This study
HD100 ⊿*bd2584*	HD100 with *bd2584* markerless deletion	Gen PCR, seq	This study
HD100 ⊿*bd2584*	HD100 with *bd2584*	Gen PCR, seq	This study

pK18::*bd2584*(H389V)	markerless deletion with a single cross over of pK18:: *bd2584*(H389V)		
XL-1BLUE pQE60_*bd2584*	XL-1Blue with vector for bacterial expression of C-terminally 6xHis tagged insert; amp resistance. Containing the gene *bd2584*	Plasmid seq and antibiotic resistance- Amp 100	This study
XL-1BLUE pQE80L_*bd0367*	XL-1Blue with Bacterial lacIq vector for expressing N-terminally 6xHis-tagged proteins, amp resistant. Containing gene *bd0367*	Plasmid seq and antibiotic resistance- Amp 100	This study
XL-1BLUE:: pQE80L *bd0367*RR(34-417bp)	XL-1Blue with Bacterial lacIq vector for expressing N-terminally 6xHis-tagged proteins, amp resistant. Containing truncated gene *bd0367* (34-417 bp)	Plasmid seq and antibiotic resistance- Amp 100	This study
XL-1BLUE pQE60_*bd0367*	XL-1Blue with vector for bacterial expression of C-terminally 6xHis tagged insert; amp resistance. Containing the gene *bd0367*.	Plasmid seq and antibiotic resistance- Amp 100	This study
XL-1BLUE pQE60_*bd0367*RR *(34-417bp)*	XL-1Blue with vector for bacterial expression of C-terminally 6xHis tagged insert; amp resistance. Containing the truncated gene *bd0367*	Plasmid seq and antibiotic resistance- Amp 100	This study
M15pREP4 pQE60 *bd2584*	M15pREP4with Vector for bacterial expression of C-terminally 6xHis tagged insert; amp resistance. Containing the gene *bd2584*	Plasmid seq and antibiotic resistance- Amp 100	This study
M15pREP4 pQE80L *bd0367*	M15pREP4 with Bacterial lacIq vector for expressing N-	Plasmid seq and antibiotic resistance-	This study

	terminally 6xHis-tagged proteins, amp resistant. Containing gene *bd0367*	Amp 100	
M15pREP4 pQE80L_*bd0367 (34-417)*	M15pREP4 with Bacterial lacIq vector for expressing N-terminally 6xHis-tagged proteins, amp resistant. Containing truncated gene *bd0367*	Plasmid seq and antibiotic resistance-Amp 100	This study
M15pREP4 pQE60_*bd0367*	M15pREP4with Vector for bacterial expression of C-terminally 6xHis tagged insert; amp resistance. Containing the gene *bd0367*	Plasmid seq and antibiotic resistance-Amp 100	This study
M15pREP4pQE60_*bd0367* (34-417)	M15pREP4with Vector for bacterial expression of C-terminally 6xHis tagged insert; amp resistance. Containing the truncated gene *bd0367*	Plasmid seq and antibiotic resistance-Amp 100	This study
Chapter 5 strains			
HI Δ*bd0367*	HD100 with *bd*0367markerless deletion	N/A	(Hobley et al, 2012)
HI Δ*bd0367* pK18:: *bd0367*(D63A)	HI with markerless deletion Δ*bd0367* with a single cross over of pK18::*bd0367*(D63A)	Kn Selection Gen PCR, seq	This study
HD100 pK18::*bd0367*mCherry	HD100 with pK18::*bd0367*mCherry integrated into the *bd0367* locus	N/A	(Hobley et al, 2012)
HI pK18::*bd0367*mCherry	Host Independent derivative of HD100 with pK18::*bd0367*mCherry single cross over integrated into the bd0367 locus	N/A	(Hobley et al, 2012)
HD100 Δ*bd1971*	HD100 with Δ*bd1971*	Gen PCR, Seq	Constructed by Rob Till

	markerless deletion		for this study
HI Δ*bd1971*	HI generate from HD100 with Δ*bd1971* markerless deletion		This study
HD100 pK18::*bd1971*(D307,308A)	HD100 with Δ*bd1971* markerless deletion with a single cross over of pK18:: *bd1971*(D307,308A)	Gen PCR, Seq	Constructed by Rob Till for this study
HI pK18::bd1971(D307,308A)	Host Independent derivative of HD100 with Δ*bd1971* markerless deletion with a single cross over of pK18:: *bd1971*(D307,308A)		Constructed by Rob Till for this study
HD100 Δ*bd1971*pK18::*bd0367*mCherry	HD100 with Δ*bd1971* markerless deletion with pK18::*bd0367*mCherry integrated into the *bd0367* locus	Kn selection	This study
Chapter 6 strains			
HD100 Δ*bd3100*	HD100 with Δ*bd3100* markerless deletion	N/A	(Taylor, 2013)
HD100 Δ*bd3100* pK18::*bd3100*(+ 450bp upstream)	HD100 Δ*bd3100* deletion containing the complementation construct pK18::*bd3100*(+1kb upstream) which contains the *bd3100* gene, plus 450 bp upstream and 100 bp downstream flanking regions, integrated into the *bd3100* locus.	Gen PCR, Seq	This study
HD100 pK18::*bd3100*-mCherry	HD100 with pK18::*bd3100*mCherry integrated into the *bd3100* locus	N/A	(Taylor, 2013)

HI pK18::*bd3100*-mCherry	HI strain generated from HD100 with pK18::*bd3100*mCherry integrated into the *bd3100* locus	N/A	(Taylor, 2013)
HI ⊿*bd0367*pK18::*bd3100*mCherry	HI with Δ*bd0367* markerless deletion with pK18::*bd3100*mCherry integrated into the *bd3100* locus	Kn selection	This study
HD ⊿*bd1971*pK18::*bd3100*mCherry	HD100 with Δ*bd1971* markerless deletion with pK18::*bd3100*mCherry integrated into the *bd3100* locus	Kn selection	This study
HD100 pK18::*bd1473*mCherry	HD100 with pK18::*bd1473*mCherry integrated into the *bd1473* locus	N/A	(Milner, 2014)
HD100 Δ*bd3100* + pK18::*bd1473*mCherry	HD100 with Δ*bd3100* markerless deletion with pK18::*bd1473*mCherry integrated into the *bd1473* locus	Kn selection	This study
HD100 pK18::*bd1482*mCherry	HD100 with pK18*::bd1482*mCherry integrated into the *bd1482* locus	N/A	Amy PilZ?

Table 2.2 Plasmids used in this study: cloned plasmids were confirmed by four restriction digests by double digests (DD) one enzyme cut in out the cloned fragment and the other two digests cut within the vector and the cloned fragment. These were analysed on an agarose gel and band sizes calculated. Some plasmids were also sequenced.

Plasmid	Description	Confirmation	Reference
<u>General Plasmids</u>			
pUC19	Amp^r high-copy number cloning vector in E. coli	N/A	(Yanischperron et al, 1985)

pK18*mob*sac*B*	Kn^r suicide vector in Bdellovibrio used to create clones for conjugation and recombination into *Bdellovibrio* genome (referred to as pK18 here).	N/A	(Schafer et al, 1994)
pZMR100	λ defective vector, Knr. Transformed in to S17-1 to create Knr prey to use with Knr Bdellovibrio predators.	N/A	(Rogers et al, 1986)
pMAL_p2_mCherry	Ampr vector containing mCherry gene with a malE signal sequence for localised periplasmic fluorescence	N/A	(Fenton et al, 2010)
pAKF56	Ampr vector for fusion of the mCherry gene-tag to the 3' end of a gene of interest during intermediate cloning stage	N/A	(Fenton et al, 2010)
pQE60	Vector for bacterial expression of C-terminally 6xHis tagged insert; amp resistance.	N/A	Gift from Dr Porter at the University of Exeter
pQE80L	Bacterial lacIq vector for expressing N-terminally 6xHis-tagged proteins, amp resistant	N/A	Gift from Dr Porter at the University of Exeter
<u>Deletion plasmids</u>			
puc19::⊿*bd2584*	The gene deletion construct was created using Bd2584F with delBd2584R primers to form the 5' region, and delBd2584F with Bd2584R primers to form the 3' region. These primer pairs were used to amplify DNA from the *bd2584* ORF. The resulting amplified products were used as template to link the 5' and 3' regions in a secondary PCR reaction, using the Bd2584F and Bd2584R primers. This PCR product was then cut with restriction enzymes EcoRI and HindIII and cloned into pUC19, which had been cut with the same restriction enzymes.	DD,	This study

pK18::⊿*bd2584*	The Δ*bd2584* deletion construct was cut from pUC19 using EcoRI/HindII before being ligated into pK18*mob*sacB which and been cut with the same enzymes. The construct was conjugated into B. bacteriovorus HD100.	DD, seq	This study
Complementation plasmids			
pK18::*bd3100*(+ 450 bp upstream)	The *bd3100* ORF (plus 450 bp 5', 100 bp 3') was amplified from HD100 genomic DNA using the primers bd3100_comp_F and bd3100_comp_R. The PCR productwas cut with HindIII and ligated into pK18*mob*sacB cut with HindIII.	DD, seq	This study plasmid constructed by David Milner
Amino acid alteration Plasmids			
pK18::*bd2584*(H389V +1kb upstream)	The *bd2584*(H389V) mutant in pUT18C was amplified from plasmid DNA using primers 2584 F gibson and 2584 R gibson. The 1 kb upstream region was amplified from HD100 genomic DNA using 2584 upstream F and 2584 upstream R primers. The PCR products were incubated with pK18 cut with EcoRI and HindIII in a isothermal Gibson reaction to join overlapping regions	DD, seq	This study
pK18::*bd0367*(D63A +1kb upstream)	The *bd0367*(D63A) mutant in pUT18C was amplified from plasmid DNA using primers 367 F gibson and 367 R gibson. The 1 kb upstream region was amplified from HD100 genomic DNA using 367 upstream F and 367 upstream R primers. The PCR products were incubated with pK18 cut with EcoRI and HindIII in a isothermal Gibson reaction to join overlapping regions	DD, seq	This study
pK18::*bd1971*(D307308A +1kb upstream)	The *bd1971*(D307308A) mutant in was amplified from HD100 genomic DNA using mutational primers 1971D307308AF and 1971D307308AR on conjunction	DD, seq	Constructed by Rob Till for this study

	with 1971 gib F or 1971 gib R. Then using 1971 gib F and 1971 gib R primer the two mutated PCR products were combined. The 1 kb upstream region was amplified from HD100 genomic DNA using 1971 upstream F and 1971 upstream R primers. The PCR products were incubated with pK18 cut with BamHI and HindIII in a isothermal Gibson reaction to join overlapping regions		
<u>mCherry plasmids</u>			
pKA56*bd2584*mCherry	The *bd2584* ORF (minus the stop codon) was amplified from WT HD100 genomic DNA using Bd2584HisF and 2584MCH_R. The resultant PCR product was digested with EcorI and KpnI and ligated to pAKF56 upstream of the mCherry ORF.	DD	This study
pK18 *bd2584*mCherry	The *bd2584*-mCherry ORF was cut out of pAKF56::*2584*mcherry using EcoRI and HindIII and ligated to pK18mobsacB	DD, seq	This study
pK18 *bd1971*mCherry	pK18mobsacB vector Kan Resistance, *bd1971* fused to mCherry.	N/A	(Basford, 2015)
pK18 *bd3125*mCherry	pK18mobsacB vector Kan Resistance, *bd3125* fused to mCherry.	N/A	(Hobley et al, 2012)
pK18 *bd3100*mCherry	pK18mobsacB vector Kan Resistance, *bd3100* fused to mCherry.	N/A	(Taylor, 2013)
pK18 *bd1473*mCherry	The *bd1473*-mCherry fragment was cut out of the pAKF56::*bd1473* plasmid using SacI and XbaI and blunted using a fill-in reaction. This was ligated into pK18mobsacB cut with SmaI.	N/A	(Milner, 2014)

pK18 *bd1482*mCherry	pK18mobsacB vector Kan Resistance, *bd1482* fused to mCherry.	N/A	Amy
Bacterial two hybrid plasmids			
General Bacterial two hybrid plasmids			
pKT25	Kn^r vector for fusion of gene to C-terminus of Cya-T25 in bacterial 2 hybrid analysis	N/A	(Karimova et al, 2001)
pUT18C	Amp^r vector for fusion of gene to C-terminus of Cya-T18 in bacterial two-hybrid analysis	N/A	(Karimova et al, 2001)
pKT25-zip	pKT25 containing the leucine zipper region from yeast GCN4 used as positive control for bacterial two-hybrid	N/A	(Karimova et al, 2001)
pUT18C-zip	pUT18c containing the leucine zipper region from yeast GCN4 used as positive control for bacterial two-hybrid	N/A	(Karimova et al, 2001)
Chapter 3			
pKT25::*bd0367*	The *bd0367* open reading frame (from adenine at base 34) was amplified from *B. bacteriovorus* HD100 genomic DNA and inserted into the pKT25 plasmid	N/A	(Milner, 2014)
pUT18C::*bd0367*	As above but ligated to pUT18C	N/A	(Milner, 2014)
pKT25::*bd0367* REC	The first 417 bp from start of *bd0367* open reading frame (from adenine at base 34) was amplified from *B. bacteriovorus* HD100 genomic DNA and inserted into the pKT25 plasmid	DD,	This study
pUT18C:: Bd0367 REC	As above but ligated to pUT18c	DD,	This study
pKT25::bd0367 DGC	Base pairs 418 to the end of the bd0367 open reading frame was amplified for *B. bacteriovorus* HD100 genomic DNA using primers 0367_DGC_B2H_F and 0367_DGC_B2H_R. The DNA	DD,	This study

	fragment and pKT25 plasmid were cut using KpnI and XbaI and ligated		
pUT18C::*bd0367* DGC	As above but ligated to pUT18c	DD,	This study
pKT25::*bd0367*(D63A)	The *bd0367* pKT25 plasmid was used as template DNA and pimers: Bd0367D63AF and BD0367D63AR were used to carry out site directed mutation PCR. This PCR product was then digested by DpnI to leave only newly amplified plasmid. These plasmids were sequenced to confirm amino acid mutation	DD, seq	This study
pUT18C::*bd0367*(D63A)	The *bd0367* pUT18C plasmid was used as template DNA and primers: Bd0367D63AF and BD0367D63AR were used to carry out site directed mutation PCR. This PCR product was then digested by DpnI to leave only newly amplified plasmid. These plasmids were seqeucned to confirm amino acid mutation	DD, seq	This study
pKT25::*bd1971*	The *bd1971* open reading frame was amplified for *B. bacteriovorus* HD100 genomic DNA using primers bd1971_BTH_F and bd1971_BTH_R. The DNA fragment and pKT25 plasmid were cut using KpnI and XbaI and ligated.	N/A	(Basford, 2015)
pUT18C:: *bd1971*	As above but ligated to pUT18C	N/A	(Basford, 2015)
pKT25::*bd1971* cNMP	The first 435 bp of the *bd1971* open reading frame was amplified for *B. bacteriovorus* HD100 genomic DNA using primers bd1971_BTH_F and Front_1971_R. The DNA fragment and pKT25 plasmid were cut using KpnI and XbaI and ligated.	N/A	(Basford, 2015)
pUT18C:: *bd1971* cNMP	As above but ligated to pUT18c	N/A	(Basford, 2015)
pKT25::*bd1971* EAL	Base pairs 433 to the end of the *bd1971* open reading frame was amplified for *B. bacteriovorus* HD100 genomic DNA using primers 1971_end_F and bd1971_BTH_R.	N/A	(Basford, 2015)

	The DNA fragment and pKT25 plasmid were cut using KpnI and XbaI and ligated		
pUT18C:: *bd1971* EAL	As above but ligated to pUT18c	N/A	(Basford, 2015)
pKT25::*bd3125*	The *bd3125* open reading frame was amplified for *B. bacteriovorus* HD100 genomic DNA using primers bd3125_BTH_F and bd3125_BTH_R. The DNA fragment and pKT25 plasmid were cut using KpnI and XbaI and ligated.	N/A	(Basford, 2015)
pUT18C:: *bd3125*	As above but ligated to pUT18c	N/A	(Basford, 2015)
pKT25::*bd1434*	The *bd1434* open reading frame (from thiamine base 118) was amplified for *B. bacteriovorus* HD100 genomic DNA using primers bd1434_BTH_F and bd1434_BTH_R. The DNA fragment and pKT25 plasmid were cut using KpnI and XbaI and ligated.	N/A	(Basford, 2015)
pUT18c::*bd1434*	As above but ligated to pUT18c	N/A	(Basford, 2015)
Chapter 4			
pKT25:: *bd2843*	The *bd2843* ORF was amplified from *B. bacteriovorus* HD100 genomic DNA using primers bd2843_BTH_F and Bd2843_BTH_R and the PCR product was cut with XbaI and KpnI and ligated into pKT25	DD	This study
pUT18C:: *bd2843*	As above but ligated to pUT18c	DD	This study
pKT25:: *bd2576*	The *bd2576* ORF was amplified from *B. bacteriovorus* HD100 genomic DNA using primers bd2576_BTH_F and Bd2576_BTH_R and the PCR product was cut with XbaI and KpnI and ligated into pKT25	DD	This study
pUT18C::*bd2576*	As above but ligated to pUT18c	DD	This study
pKT25::*bd2849*	The *bd2849* ORF was amplified from *B. bacteriovorus* HD100 genomic	DD	This study

	DNA using primers bd2849_BTH_F and Bd2849_BTH_R and the PCR product was cut with XbaI and KpnI and ligated into pKT25		
pUT18C::*bd2849*	As above but ligated to pUT18c	DD	This study
pKT25::*b*d3779	The *bd3779* ORF was amplified from *B. bacteriovorus* HD100 genomic DNA using primers bd3779_BTH_F and Bd3779_BTH_R and the PCR product was cut with XbaI and KpnI and ligated into pKT25	DD	This study
pUT18C:: Bd3779	As above but ligated to pUT18c	DD	This study
pKT25::*bd2335*	The *bd2335* ORF was amplified from *B. bacteriovorus* HD100 genomic DNA using primers bd2335_BTH_F and Bd2335_BTH_R and the PCR product was cut with XbaI and KpnI and ligated into pKT25	DD	This study
pUT18C::*bd2335*	As above but ligated to pUT18c	DD	This study
pKT25::*bd2584*	The *bd2584* ORF was amplified from *B. bacteriovorus* HD100 genomic DNA using primers bd2584_BTH_F and Bd2584_BTH_R and the PCR product was cut with XbaI and KpnI and ligated into pKT25	DD, seq	This study
pUT18C::*bd2584*	As above but ligated to pUT18c	DD, seq	This study
pKT25::*bd2584(*H389V)	The *bd2584* pKT25 plasmid was used as template DNA and plasmids Bd2584H389VF and Bd2584H389VR were used to carry out site directed mutation PCR. This PCR product was then digested by DpnI to leave only newly amplified plasmid. These plasmids were sequenced to confirm amino acid mutation	DD, seq	This study
pUT18C::*bd2584*(H389V)	The *bd2584* pUT18c plasmid was used as template DNA and plasmids Bd2584H389VF and Bd2584H389VR were used to carry out site directed mutation PCR. This PCR product was then digested by DpnI to leave only newly amplified plasmid. These plasmids were	DD, seq	This study

	sequenced to confirm amino acid mutation		
Chapter 6			
pKT25::*bd3100*	The *bd3100* ORF (starting at adenine at base 37) was amplified from *B. bacteriovorus* HD100 genomic DNA using primers bd3100BTHF and Bd3100BTHR and the PCR product was cut with XbaI and KpnI and ligated into pKT25	N/A	(Milner, 2014)
pUT18C::*bd3100*	As above but ligated to pUT18c	N/A	(Milner, 2014)
pKT25::*bd1482*	The *bd1482* ORF (starting at adenine at base 94) was amplified from *B. bacteriovorus* HD100 genomic DNA using primers Bd1482BTHF and Bd1482BTHR and the PCR product was cut with XbaI and KpnI and ligated into pKT25	N/A	(Milner, 2014)
pUT18C::*bd1482*	As above but ligated to pUT18C	N/A	(Milner, 2014)
Protein Purification plasmids			
pQE80L::*bd0367* tib full	The *bd0367* ORF (from adenine at base 34) was amplified from B. bacteriovorus HD100 genomic DNA by primer Bd0367_pQE80L_F and Bd0367_pQE80L_R, the PCR was cut with BamHI and HindIII and ligated into pQE80L cut with BamHI and HindIII	DD, seq	This study
pQE80L::*bd0367* RR	The *bd0367* response regulator ORF (from adenine at base 34 to 417) was amplified from *B. bacteriovorus* HD100 genomic DNA by primer Bd0367_pQE80L_F and Bd0367_reconly_PQE80L_R, the PCR was cut with BamHI and HindIII and ligated into pQE80L cut with BamHI and HindIII	DD, seq	This study
pQE60::*bd2584*	The *bd2584* open reading frame minus the stop codon was amplified from *B. bacteriovorus* HD100 genomic DNA by primer Bd2584_pQE60_F	DD, seq	This study

	and Bd2584_pQE60_R and the PCR was cut with NcoI and ligated into pQE60 cut with NcoI		
pQE60::*bd0367* tib full	The *bd0367* open reading frame (from adenine at base 34 and minus stop codon) was amplified from *B. bacteriovorus* HD100 genomic DNA by primer 367tib startPQE60F and 367fullPQE60R, the PCR was cut with BsmBI and BglII and ligated into pQE60 cut with NcoI and BglII	DD, seq	This study
pQE60::*bd0367* RR	The *bd0367* response regulator open reading frame (from adenine at base 34) to bp 417 was amplified from *B. bacteriovorus* HD100 genomic DNA by primer 367tib startPQE60F and 367reconlypqe60R and the PCR was cut with BsmBI and BglII and ligated into pQE60 cut with NcoI and BglII	DD, seq	This study

Table 2.3 Primers used in this study

Primer	Description	Sequence (5'-3')
Primers for Bacterial Two Hybrid cloning		
Candidate histidine kinases bacterial two hybrid primers		
Bd2843_BTH_F	Has six random 5' bases for cutting efficiency, then has a XbaI site, followed by an additional C to keep ORF in frame and the first 20 bases of predicted *bd2843* ORF.	CCAGACTCTAGACTTGTTCGGAGGTTTCATGTC
Bd2843_BTH_R	Has six random 3' bases for cutting efficiency, then has a KpnI site followed by a reverse complemented sequence of the 3' end of *bd2843*	AATGTGGGTACCCTAATGCAGTGACCGATCAC
Bd2576_BTH_F	Has six random 5' bases for cutting efficiency, then has a XbaI site, followed by an additional C to keep ORF in frame and the first 20 bases of predicted *bd2576* ORF.	CCAGACTCTAGACATGTTCTTAAAGAAAATCTA

Bd2576_BTH_R	Has six random 3' bases for cutting efficiency, then has a KpnI site followed by a reverse complemented sequence of the 3' end of *bd2576*	AATGTGGGTACCTTA AATGTTTTTAATTTCA A
Bd2849_BTH_F	Has six random 5' bases for cutting efficiency, then has a XbaI site, followed by an additional C to keep ORF in frame and the first 20 bases of predicted *bd2849* ORF.	CCAGACTCTAGACAT GTTCCAACGACTTTTA AA
Bd2849_BTH_R	Has six random 3' bases for cutting efficiency, then has a KpnI site followed by a reverse complemented sequence of the 3' end of *bd2849*	AATGTGGGTACCCTA GCGATGCTGGTGTCG TTC
Bd3779_BTH_F	Has six random 5' bases for cutting efficiency, then has a XbaI site, followed by an additional C to keep ORF in frame and the first 20 bases of predicted *bd3779* ORF.	CCAGACTCTAGACAT GAACCAATCAAGGGG CGG
Bd3779_BTH_R	Has six random 3' bases for cutting efficiency, then has a KpnI site followed by a reverse complemented sequence of the 3' end of *bd3779*	AATGTGGGTACCTTA AGCCTCTTCCAACGG CAG
Bd2584_BTH_F	Has six random 5' bases for cutting efficiency, then has a XbaI site, followed by an additional C to keep ORF in frame and the first 20 bases of predicted *bd2584* ORF.	CCAGACTCTAGACAT GGAATCTCGTTACGA AGC
Bd2584_BTH_R	Has six random 3' bases for cutting efficiency, then has a KpnI site followed by a reverse complemented sequence of the 3' end of *bd2584*	AATGTGGGTACCTTA TTTTGATCCCAGAGG TAG
Bd2335_BTH_F	Has six random 5' bases for cutting efficiency, then has a XbaI site, followed by an additional C to keep ORF in frame and the first 20 bases of predicted *bd2335* ORF.	CCAGACTCTAGACAT GAACCAAAAGCAACT GCC

Bd2335_BTH_R	Has six random 3' bases for cutting efficiency, then has a KpnI site followed by a reverse complemented sequence of the 3' end of *bd2335*	AATGTGGGTACCTCA AATACTGGGTGAGGG TG
Split domain and amino acid bacterial two hybrid primers		
0367_Tib_RR_F	Has six random 5' bases for cutting efficiency, then has a XbaI site, followed by an additional C to keep ORF in frame and the first 20 bases of predicted *bd0367* ORF (from adenine at base 34)	CCAGACTCTAGACAT GAGTTTTGAAGTAAG CCC
0367_RR_B2H_R	Has six random 3' bases for cutting efficiency, then has a KpnI site followed by a reverse complemented sequence of the 3' end of response regulator domain of *bd0367* (397-417bp)	AATGTGGGTACCGAA AAGCAGCTGCTCGTG CA
0367_DGC_B2H_F	Has six random 5' bases for cutting efficiency, then has a XbaI site, followed by an additional C to keep ORF in frame and the first 20 bases of the diguanlyate cyclase domain of *bd0367* (418-437bp)	CCAGACTCTAGACGC CAATGAAAAACTCAA AGA
0367_DGC_B2H_R	Has six random 3' bases for cutting efficiency, then has a KpnI site followed by a reverse complemented sequence of the 3' end of *bd0367*	AATGTGGGTACCTTA GCCGGCCGCTTTACG AC
BD0367D63AF	Has 13 bases immediately upstream of the *bd0367* 'D' codon (amino acid 63) to be changed, followed by the altered codon of GCC in place of GAC (A in place of D), with 15 bases immediately downstream.	CATTGTCATTTTAGCC TGGATGGCGCCTTcc
Bd0367D63AR	Reverse complement of Bd0367D63AF	GGAAGGCGCCATCCA GGCTAAAATGACAAT G
Bd2584H389VF	Has 13 bases immediately upstream of the *bd2584* 'H' codon (amino acid 389) to be changed, followed by the altered codon of GTG in place of CAC (V in place of H), with 13 bases immediately	GGCCAACATGAGTGT GGAAATTCGCACGC

	downstream.	
Bd2584Ht389VR	Reverse complement of Bd2584H389VF	GCGTGCGAATTTCCA CACTCATGTTGGCC
Primers for fluorescent tagging		
Bd2584hisF	Has six random 5' bases for cutting efficiency, then a EcoRI site followed by the first 20 bases of the *bd2584* ORF	TCACTGGAATTCATG GAATCTCGTTACGAA GC
2584MCH_R	Has six random 5' bases for cutting efficiency, then a KpnI site followed by the reverse complemented sequence at the 3' of *bd2584* with the TAA stop codon deleted.	TCACTGGGGTACCCT TTTGATCCCAGAGGT A
Gene deletion construct primers		
delBd2584F	Has, 13 bp upstream of the start of the bd2584ORF, 7 bp of *bd2584* then an XbaI site, followed by a 20 bp sequence, 12 bases from the 3' end of the *bd2584* ORF and 7bp from the downstream region.	TTAAGATTTCTCAATG GAATTCTAGAGGATC AAAATAAGAGTCTT
delBd2584R	Reverse complement of delBd2584F used with Bd2584F	AAGACTCTTATTTTGA TCCTCTAGATTCCATT GAGAAATCTTAA
Bd2584F	Has six random 5' bases for cutting efficiency followed by sequence 987 bp upstream of *bd2584* ORF. Use natural EcoRI site 94 bases into bd2584ORF.	TTTGTCGTGCTGATTC TGGG
Bd2584R	Has six random 5' bases for cutting efficiency then a HindIII site followed by reverse complemented sequence 942 bp downstream of *bd2584* ORF.	AGTCATAAGCTTGTTC CATCATCTCTTCATCC
RT-PCR Primers		
Bd2584RTF	Primers to amplify a 109 bp fragment of HD100 *bd2584* ORF.	ACGAGGCTCTGTGTG TTGTG

Bd2584RTR	Primers to amplify a 109 bp fragment of HD100 *bd2584* ORF	GTCAGATCCATGCTCCAGGT
His tagged protein constructs		
Bd2584_pQE60_F	Has four random 5' bases for cutting efficiency, then a NcoI site which uses the first 4 bp of the *bd2584* ORF, followed by 16 bp from start of *bd2584*	TACTCCATGGAATCTCGTTACGAAGC
Bd2584_pQE60_R	Has four random 3' bases for cutting efficiency, then a NcoI site followed by the reverse complemented sequence at the 3' of *bd2584* with the TAA stop codon deleted and an additional base to keep in frame.	CAGCCCATGGGTTTTGATCCCAGAGGTAGCG
Bd0367_tib_Pqe80L_F	Has four random 5' bases for cutting efficiency, then has a BamHI site, followed by the first 20 bases of predicted *bd0367* ORF (from adenine at base 34)	TCAGGGATCCATGAGTTTTGAAGTAAGCCC
Bd0367_pQE80L_R	Has four random 3' bases for cutting efficiency, then a HindIII site followed by the reverse complemented sequence at the 3' of *bd0367*	CAGCAAGCTTGCCGGCCGCTTTACGACGCT
Bd0367_rec_PQE80L_R	Has four random 3' bases for cutting efficiency, then a HindIII site followed by the reverse complemented sequence at the 3' of end of *bd0367* response regulator domain (397-417bp)	CAGCAAGCTTGAAAAGCAGCTGCTCGTGCA
367tib startPQE60F	Has six random 5' bases for cutting efficiency, then has a BsmBI site, followed by 2 additional bases (cc) to keep in frame then the first 19 bases of predicted *bd0367* ORF (from adenine at base 34)	GATACTCGTCTCCCATGAGTTTTGAAGTAAGCC
367fullPQE60R	Has four random 3' bases for cutting efficiency, then a BglII site followed by the reverse	CAGCAGATCTGCCGGCCGCTTTACGACGC

	complemented sequence at the 3' of end of *bd0367* with TAA stop codon deleted	
367reconlypqe60R	Has four random 3' bases for cutting efficiency, then a BglII site followed by the reverse complemented sequence at the 3' of end of *bd0367* response regulator domain (397-417bp)	CAGCAGATCTGAAAA GCAGCTGCTCGTGCA
<u>Gibson amino acid changing and adding 1kb upstream primers</u>		
Upstream 2584 F	Used on *B. bacteriovorus* HD100 genomic to amplify 1000 bp upstream of *bd2584* which has an overhang compatible with pk18 cut with EcoRI, Primers designed by http://nebuilder.neb.com/	CGACGGCCAGTGCCA TTTGACAGATATATTT GTCGTG
Upstream 2584 R	Used on *B. bacteriovorus* HD100 genomic to amplify 1000 bp upstream of *bd2584* which has an overlap compatible with pk18 cut with HindIII. Primers designed by http://nebuilder.neb.com/	AGATTCCATTGAGAA ATCTTAACAGGGTAA AAATC
2584 F gibson	Used on pUT18C_*bd2584*(H389V) template and has an overlap compatible with pk18 cut with EcoRI. Primers designed by http://nebuilder.neb.com/	GATTTCTCAATGGAA TCTCGTTACGAAG
2584 R gibson	Used on pUT18c::bd2584H389V template and has an overlap compatible with pk18 cut with HindIII. Primers designed by http://nebuilder.neb.com/	CTATGACCATGATTAC GTTATTTTGATCCCAG AGGTAG
Upstream 367 F	Used on *B. bacteriovorus* HD100 genomic to amplify 1000 bp upstream of *bd0367* which has an overhang compatible with pk18 cut with EcoRI, Primers designed by http://nebuilder.neb.com	TAAAACGACGGCCAG TGCCACGGATTTACC ATCGACCAC
Upstream 367 R	Used on HD100 genomic to amplify 1000 bp upstream of Bd0367 which has an overlap compatible with pk18 cut with HindIII. Primers designed by	CAAAACTCATCTTACA TACCAGTGTAACTTCT GC

	http://nebuilder.neb.com/	
367 F gibson	Used on Bd0367D63ApUT18c template and has an overhang compatible with pk18 cut with EcoRI. Primers designed by http://nebuilder.neb.com/	GGTATGTAAGATGAG TTTTGAAGTAAGCCCT AAACAAC
367 R gibson	Used on Bd0367D63ApUT18c template and has an overhang compatible with pk18 cut with HindIII. Primers designed by http://nebuilder.neb.com/	CAGCTATGACCATGA TTACGTTAGCCGGCC GCTTTACG
1971D307308AF	Has 12 bases immediately upstream of the *bd1971* 'DD' codon (amino acids 307 and 308) to be changed, followed by the altered codon of GCTGCT in place of GATGAT (A in place of D), with 10 bases immediately downstream.	GCAATTTCCATTGCTG CTTTCGGGACCG
1971D307308AR	Reverse complement of 1971D307308AF	CGGTCCCGAAAGCAG CAATGGAAATTGC
1971 upstream gib F	Used on HD100 genomic to amplify 1000 bp upstream of *bd1971* which has an overlap compatible with pk18 cut with HindIII, Primers designed by http://nebuilder.neb.com/	CGACGGCCAGTGCCA TTTTGAATACAATCTT TCAAGCTTC
1971 upstream gib R	Used on HD100 genomic to amplify 1000 bp upstream of *bd1971* which has an overlap compatible with pk18 cut with BamHI. Primers designed by http://nebuilder.neb.com/	TGCATTCATATGAGTT TTATTCTAGGGTCTTT G
1971 gib F	Used on HD100 genomic and has an overlap compatible with pk18 cut with HindIII. Primers designed by http://nebuilder.neb.com/ Primer was used in conjunction with 1971R67R or 1971D307308AR or 1971 gib R	TAAAACTCATATGAAT GCAGCAGCTCAG
1971 gib R	Used on HD100 genomic and has an overlap compatible with pk18 cut with BamHI. Primers designed	AGCTCGGTACCCGGG TTAGATCAGCTTTAA

	by http://nebuilder.neb.com/ Primer was used in conjunction with 1971R67F or 1971D307308AF or 1971 gib F	GAAGCG

2.2. Bacterial growth conditions

2.2.1. Growth media

A variety of growth media were used for culturing *E.coli,* this was dependent on the strain and purpose of growth. This study uses *E.coli* as prey to culture *Bdellovibrio* on, as a protein interaction system and to overexpress proteins. A variety of growth media were also used for culturing *Bdellovibrio* strains depending on the HD or HI growth phase (Section 2.3).

All media were made with 18 MΩ deionised water and autoclaved before use.

2.2.1.1. YT broth (per litre) for growth of *E. coli* cloning and conjugation strains

5 g NaCl ,5 g Difco Bacto Yeast Extract, 8 g Difco Bacto Tryptone. Adjusted to pH 7.5 with 2 M NaOH (Solidified with Sigma-Aldrich Select agar A5054 at 10 g L^{-1}).

2.2.1.2. 2YT (per litre) for growth of *E.coli* strains used for protein overexpression

Suspended 31 g in 1 L of demineralized water. (invirtrogen)

5 g NaCl, 16 g select Peptone, 10g Difco Bacto Yeast Extract

2.2.1.3. Mu broth (per litre) for growth of *E. coli* strain BTH101 for bacterial two-hybrid assays

10 g Difco Bacto Tryptone, 5 g Difco Bacto Yeast Extract, 10 g NaCl, 2 ml 1 M NaOH (to pH ~7.0).

2.2.1.4. Nutrient agar used for culturing BTH101 *E.coli* for bacterial two hybrid assays

Made up as per manufacturer's instructions: 28 g of nutrient agar per l.

2.2.1.5. SOC broth (per litre) for rescue of transformed *E. coli* strains

20 g Difco Bacto Tryptone, 5 g Difco Bacto Yeast Extract, 0.58 g NaCl, 0.186 g KCl,

2.03 g $MgCl_2$, 2.46 g $MgSO_4$, 3.6 g Glucose

2.2.1.6. SPY agar (per litre) for streaking of *B. bacteriovorus* HI strains from frozen stock and generating *Bdellovibrio* HI isolates

10 g Difco Bacto Peptone, 3 g Difco Bacto Yeast Extract, 10 g Sigma-Aldrich Select agar A5054. Adjusted to pH 6.8 with 2 M NaOH

2.2.1.7. PY broth (per litre) for growth of *B. bacteriovorus* HI strains

10 g Sigma-Aldrich Fluka Broadbean Peptone, 3 g Difco Yeast Extract. Adjusted to pH 6.8 with 2 M NaOH.

2.2.1.8. YPSC agar (per litre) for growth of HD *B. bacteriovorus* strains on overlay plates

1 g Difco Bacto Yeast Extract, 1 g Difco Bacto Peptone, 0.5 g Anhydrous Sodium Acetate, 0.25 g $MgSO_4.7H_2O$. Adjusted to pH 7.6 with 2 M NaOH Added sterile $CaCl_2$ from a 25 g L^{-1} stock to give 0.25 g L^{-1} after autoclaving. YPSC-Top agar was solidified with Sigma-Aldrich Select agar A5054 at 6 g L^{-1} whereas YPSC-Bottom agar was solidified with 10 g L^{-1}.

2.2.1.9. Calcium-HEPES buffer (per litre) for growth of HD *B. bacteriovorus* strains in liquid culture (on *E. coli* prey)

5.94g HEPES- N-(2-hydroxyethyl) piperazine-N'-(2-ethanesulphonic acid), 0.294 g $CaCl_2.2H_2O$. Adjusted to pH 7.6 with 2 M NaOH

2.2.1.10. Antibiotics and other supplements

Antibiotic/ Supplement	Stock concentration (mg ml^{-1})	Final concentration (μg ml^{-1})
Kanamycin Sulphate (Kn)	50 in AnalaR water	50/25
Ampicillin Sodium (Amp)	50 in AnalaR water	50/100
Isopropyl β-D-1-thiogalactopranoside (IPTG)	200 in AnalaR water	200
5-bromo-4-chloro-3-indolyl-β-D-galactopyranoside (X-gal)	20 in Dimethylformamide (DMF)	200/40

Table 2.4 Antibiotics and supplements used in this study. Abbreviations are shown in brackets. Solvents used to dissolve the supplements are shown in the stock concentrations column. The final concentration used varied depending on the *Bdellovibrio* or *E.coli* strain used.

2.3. Growth conditions

2.3.1. Growth of *B. bacteriovorus* host-dependent (HD) strains

2.3.1.1. Growth of Host-dependent *Bdellovibrio* strains on plates

Host-dependent (HD) *Bdellovibrio* strains were grown on lawns of *E.coli* in YPSC overlay plates. The overlay plates consisted of a bottom layer of YPSC-Bottom agar (supplemented with the appropriate antibiotics, when necessary), which was allowed to set before adding the top layer. The top layer consisted of 5 ml YPSC-Top agar, mixed with 150 μl of stationary phase *E. coli* S17-1 prey cells (or *E. coli* S17-1 (pZMR100) for kanamycin resistant strains).

For re-growing *Bdellovibrio* HD frozen stocks, 100 μl of the frozen stock was spotted onto the top of the *E.coli* containing YPSC overlay agar plate.

For enumerations of *Bdellovibrio* strains, 100 μl of a serial dilution was added to the moulten YPSC-Top agar/*E. coli* mix, prior to pouring on top of the YPSC bottom agar, allowing single plaques to form and be counted. The overlay plates were incubated at 29°C for 3-10 days (until individual plaques appeared).

2.3.1.2. Growth of Host-dependent *Bdellovibrio* strains in liquid

For growth of *Bdellovibrio* in liquid culture, individual plaques were picked into a predatory culture. The predatory culture was set up in bijou tubes and consisted of the picked plaque, 2 ml CaHEPES and 150 μl pre-grown *E. coli* S17-1 (or *E. coli* S17-1 pZMR100 for kanamycin-resistant strains and kanamycin at 50 μg ml^{-1}). Predatory cultures were incubated at 29°C, with 200 rpm shaking for 1-2 days (until prey were completely lysed, as viewed by microscopy). Predatory cultures of HD *Bdellovibrio* strains were then maintained by sub-culturing (at 24 hours intervals) into 10 ml predatory cultures (10 ml CaHEPES, 600 μl 16 hr pre-grown stationary phase *E. coli* S17-1, 200 μl previous *Bdellovibrio* culture in 50 ml falcon tubes) or 50 ml predatory cultures (50 ml CaHEPES, 3 ml 16 hr pre-grown stationary phase *E. coli* S17-1, 1 ml previous *Bdellovibrio* predatory culture in 250 ml conical flasks) incubated at 29°C with 200 rpm shaking.

2.3.2. Growth of *B. bacteriovorus* host-independent (HI) strains

50 μl of a *Bdellovibrio* HI frozen stock was spread onto SPY agar (supplemented with the appropriate antibiotics, when necessary) and incubated at 29°C for 3-12 days. As HI

strains exhibit density-dependent growth, colonies were picked into 500 µl PY broth and incubated at 29°C with 200 rpm shaking for 24-48 hr, until the broth became visibly turbid and was checked by microscopy. The volume of the culture was then doubled by addition of PY broth, until the volume reached 2 ml. At this point, the culture could be reliably diluted into larger volumes of PY broth.

2.3.3. *E. coli* growth

For *E. coli* strains to be used as *Bdellovibrio* prey, or for conjugating as donors with *Bdellovibrio*, these *E. coli* strains were streaked from frozen stocks to single colonies on YT agar (supplemented with the appropriate antibiotics, when necessary) and incubated at 37°C for 16 hours. Single colonies were picked into 50 ml of YT broth and incubated at 37°C for 16 hours with 200 rpm shaking. These stationary phase cultures typically yielded 1 x 10^9 cfu ml^{-1}.

For the *E. coli* strain BTH101 used to generate competent cells for bacterial two hybrid assays, the strain was streaked from frozen stocks to single colonies on NA agar and then grown in Mu broth at 29°C for 16 hours at 200 rpm. Details of growth conditions for the bacterial two hybrid assay are detailed in section 2.8.1, and details of growth conditions for competent cells are detailed in section 2.4.1.

2.4. Bacterial genetic manipulation

2.4.1. Production of chemically competent *E. coli* cells

To make chemically competent *E. coli*, *E. coli* DH5α, S17-1 or XL-BLUE cells were grown in 10 ml YT under standard growth conditions (37°C) (section 2.3.3). To make chemically competent *E.coli* M15pREP for protein overexpression the same protocol was followed however media was also supplemented with 25 µg ml^{-1} kan. The culture was back diluted 1:100 in 600 ml YT and grown to OD_{600} 0.4-0.6 at 37°C with 200 rpm shaking. The culture was then centrifuged in a Sigma 4K15 benchtop centrifuge at 5525 *x g* at 4°C for 5 minutes and the cell pellet re-suspended gently in 20 ml 4°C TFB1 (section 8.1.2.1) per 50 ml culture. The suspension was incubated on ice for 5 minutes and centrifuged for 5 minutes. Each cell pellet was then re-suspended in 2 ml 4°C TFB2 (section 8.1.2.2) and incubated on ice for at least one hour. The suspension was then divided into 200 µl aliquots in micro-centrifuge tubes and snap-frozen in liquid nitrogen. These were then stored at -80°C until required. Transformation efficiency of the

competent *E. coli* cells was assessed by transformation with a high copy-number plasmid (typically pUC19) and counting the number of colonies formed on the YT agar supplemented with the appropriate antibiotic (> 1000 transformants from 50 ng plasmid DNA).

Competent *E.coli* BTH101 were made as previously described with the replacement of YT by Mu broth and all incubation steps carried out at 29°C.

2.4.2. Transforming plasmids into competent *E. coli* strains

To transform plasmid DNA into aliquots of *E. coli* DH5α and S17-1 competent cells were thawed on ice and the DNA (typically from a ligation (section 2.5.4) or plasmid miniprep (section 2.4.3) was added and mixed by gentle pipetting. The cells were incubated on ice for 30 minutes and heat-shocked at 42°C for 1 minute, before recovery on ice for 5 minutes. 1 ml SOC medium was then added and the cells were incubated at 37°C, with 200 rpm shaking, for 1 hour to recover and allow the cells to express the plasmid-encoded antibiotic resistance gene. The cells were then centrifuged at 17000 *x g* for 1 minute, re-suspended in 100 µl YT and then plated onto YT agar supplemented with the appropriate antibiotic selection. Plates were incubated at 37°C for 16 hours. Control transformations were also performed: positive control = 1 µl intact plasmid; negative control = 1 µl water (no DNA). The same method above was used for transformation of M15pREP15 and XLBLUE except YT was supplemented with 2 % glucose and Kan 25µg ml^{-1} was used with M15pREP15 cells.

For transformation into *E. coli* BTH101, refer to section 2.8.1.

2.4.3. Plasmid isolation from *E. coli* strains

Two methods of plasmid extraction were used. The first method of extraction was a fast alkaline (fast mini prep) extraction method developed by (Cormack & Somssich, 1997). used to obtain low concentrations of plasmid DNA for screening large numbers of potential candidates. The second method used a GenEluteTM Plasmid miniprep kit (Sigma) to achieve higher concentration of purified plasmid.

The fast mini prep was performed by taking 300 µl of 16 hr overnight 37 °C *E.coli* culture and adding to 300 µl of alkaline SDS (1 % SDS, 0.2M NaOH) and mixing. This was neutralised with 300 µl of 3M potassium acetate pH 5.5 and mixed. These were then centrifuged for 10 minutes at 13000 rpm (17000 g) in an Accuspin Micro 17R bench

centrifuge (Fisher Scientific) chilled to 4 ºC. 700µl of supernatant was transferred to a 1.5 ml microcentrifuge tube containing 500 µl of 100% 4 ºC isopropanol, this was mixed and tubes were centrifuged as before. The supernatant was then removed by pouring, and 50 µl of 70% 4 ºC ethanol added to the pellet as a final wash. This was centrifuged for 2 minutes to harvest and solidify the pellet and then completely dried. The pellet was then resuspended in 25 µl of TE (10 mM Tris-HCl pH8, 1 mM EDTA) containing 10 µg ml^{-1} RNaseA. These samples were then digested once with a restriction enzyme which cuts in both the insert and plasmid backbone to determine possible clones containing the correct plasmid.

Potential clones were then grown up in to 10 ml of overnight 37 °C culture. Plasmid was extracted from 5 ml of this culture using GenEluteTM Plasmid miniprep kit used to extract high levels of pure plasmid. The extracted plasmid was then digested using four diagnostic tests to determine if any of the clones carried the desired gene inserts. If the diagnostic digests confirmed that correct plasmid, frozen stocks were made from the remaining culture. In most cases sequencing of gene regions cloned in the plasmid also occurred.

2.4.4. Isolation of genomic DNA from *B. bacteriovorus* strains

To isolate genomic (chromosomal) DNA from *B. bacteriovorus* strains, a Sigma-Aldrich GenEluteTM Bacterial Genomic DNA kit was used. Briefly, 10 ml of a *B. bacteriovorus* HD culture (typically 2.5 x 10^8 pfu ml^{-1}) was centrifuged in a Sigma 4K15 benchtop centrifuge at 5525 x g at 4°C for 20 minutes, or 2 ml of a *B. bacteriovorus* HI culture (typically 1 x 10^9 cfu ml^{-1}) was centrifuged at 17000 x g at 4°C for 2 minutes, before following the manufacturer's instructions.

2.4.5. Generating host-independent (HI) isolates of *B. bacteriovorus* strains

To generate *B. bacteriovorus* HI isolates, 10 ml of a *Bdellovibrio* predatory culture was filtered through a 0.45 µm filter and centrifuged in a Sigma 4K15 benchtop centrifuge at 5525 *x g* at 29°C for 20 minutes. The pellet was re-suspended in 100 µl residual supernatant, spread onto SPY agar (with antibiotic selection, if required) and incubated at 29°C until colonies appeared (typically 7-12 days).

2.4.6. Conjugating plasmids into host-dependent (HD) *B. bacteriovorus* strains

To transfer plasmids into *B. bacteriovorus*, conjugation is currently the most efficient method. In this excess *E.coli* donors are used so that although some are preyed upon the remainder can conjugate through the lateral sides of the *Bdellovibrio* cells. Conjugations involved pK18*mobsacB*, for single crossover recombination of fluorescent tags or deletion constructs integrated into the *Bdellovibrio* genome.

The recipient HD *B. bacteriovorus* strain was grown under standard conditions (section 2.3.1.1) in a 50 ml predatory culture. 10 ml of this culture was centrifuged in a Sigma 4K15 benchtop centrifuge at 5525 *x g* at 29°C for 20 minutes and re-suspended in 100 µl residual supernatant. This was pipetted onto a small piece of autoclaved Nytran SuPerCharge 0.45 µm Nylon Transfer Membrane (Whatman) immobilised on a SPY agar plate and allowed to dry.

The *E. coli* donor strain with the required plasmid was grown under standard conditions (section 2.3.3) in 50 ml YT with the appropriate antibiotic (typically Kn25). 10 ml of the *E. coli* donor strain was centrifuged at 5525 x g at 29°C for 10 minutes and re-suspended in 100 µl YT. This was pipetted onto the membrane, on top of the immobilised *B. bacteriovorus* cells and incubated at 29°C for 16 hours.

After incubation at 29°C, the membrane was removed using sterile forceps, and the cells were re-suspended in 1 ml PY. Overlay plates were then created by mixing dilutions of the resuspended cells (10 µl, 100 µl, 200 µl and 690 µl) with YPSC-Top agar containing 150 µl *E. coli* S17-1 pZMR100 prey cells, which was then poured onto set YPSC-bottom agar plates supplemented with 50 µg ml^{-1} kanamycin, to select for exconjugant *B. bacteriovorus* strains.

2.4.7. Conjugating plasmids into host-independent (HI) *B. bacteriovorus* strains

For conjugation of plasmids into HI strains, it is important to remove all residual *E.coli* donor cells prior to plating exconjugants onto rich SPY plates otherwise *E.coli* outgrow the HI cells. The recipient HI *B. bacteriovorus* strain was grown under standard conditions

(section 2.3.1.2) in a 10 ml culture. 500 µl of this culture was centrifuged at 17000 *x g* at 29°C for 2 minutes and re-suspended in 100 µl PY. This was pipetted onto a small piece of autoclaved Nytran SuPerCharge (SPC) 0.45 µm Nylon Transfer Membrane (Whatman) immobilised on a SPY agar plate and allowed to dry.

The *E. coli* donor strain with the required plasmid was grown under standard conditions in 50 ml YT with the appropriate antibiotic (typically kn25). 5 ml of the *E. coli* donor strain was centrifuged at 5525 *x g* at 29°C for 10 minutes and re-suspended in 100 µl PY. This was pipetted onto the membrane, on top of the immobilised *B. bacteriovorus* cells and incubated at 29°C for 16 hours.

After incubation at 29°C, the membrane was removed using sterile forceps, and the cells were re-suspended in 5 ml PY. This was allowed to recover at 29°C with 200 rpm shaking for 30 minutes. The culture was then filtered through a 0.45 µm filter to remove *E. coli* donor cells and centrifuged at 17000 *x g* at 29°C for 2 minutes and re-suspended in 200 µl PY. This was then spread onto SPY plates supplemented with 50 µg ml^{-1} kanamycin to select for exconjugant *B. bacteriovorus* strains.

2.4.8. Generating *B. bacteriovorus* deletion strains

To construct *B. bacteriovorus* deletion strains, approximately 1 kb genomic regions upstream and downstream of the gene to be deleted were amplified and joined together via touchdown PCR (section 2.5.2) using Phusion polymerase (NEB); plasmids constructions are described in detail in Table 2.2. The deletion constructs were initially cloned into the vector pUC19 (storage vector), before being cut out (using the required restriction enzymes, stated in Table 2.2) and ligated into the suicide plasmid, pK18*mobsacB*. The resulting vector was transformed into the *E. coli* donor strain S17-1 and conjugated into *B. bacteriovorus* HD100 (section 2.3.1.1).. Firstly, kanamycin-resistant merodiploid *B. bacteriovorus* strains were selected for by growing on *E.coli* S17-1 pZMR100 lawns (on YPSC overlay plates supplemented with 50 µg ml^{-1} kanamycin).

The resultant HD merodiploid strains, containing a single crossover from the plasmid to the genome, were grown in the presence of 2.5% or 5% sucrose (as pK18*mobsacB* is a sucrose suicide vector and so sucrose selects for cell that have undergone a second recombination event) with either live or heat-killed (5 minutes at 105°C) *E. coli* S17-1

prey, see Figure 2.1. Using heat-killed prey prevents *E. coli* from using the sucrose as a carbon-source, but *Bdellovibrio* are still able to invade the *E. coli*. Prey cleared cultures were plated on S17-1 lawns on YPSC overlay plates and single plaques were picked into predatory cultures in 96 well plates. Kanamycin-sensitive *Bdellovibrio* strains were screened by Taq polymerase PCR (Section 2.5.1) to confirm the gene deletion and verified by sequencing from outside gene.

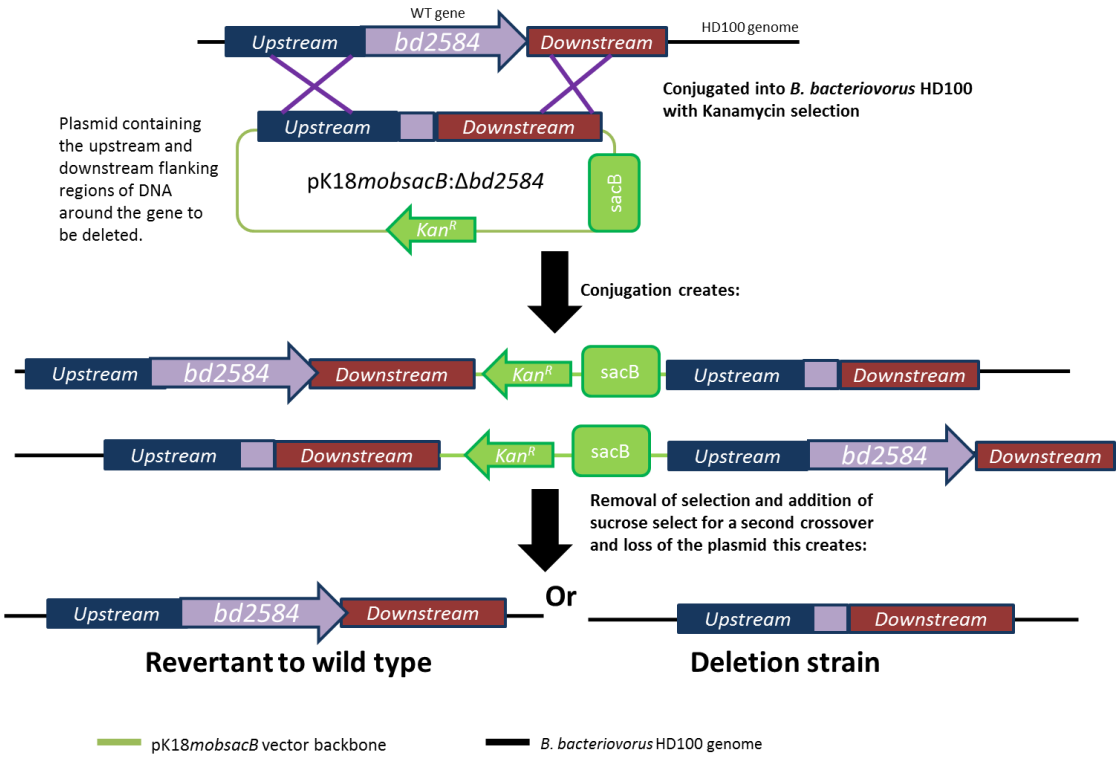

Figure 2.1 - The process of creating a markerless gene deletion of *bd2584* in *Bdellovibrio* HD100 genome. A plasmid is created containing upstream and downstream regions of DNA around the gene to be deleted. A single crossover event occurs to create a kanamycin resistant strain which contains both the wildtype region and the deletion strain sequence. A second crossover event occurs, this is selected for using sucrose, the second crossover causes the loss of the plasmid and kanamycin sensitivity. The strains are then screened using primers to separate wild type strains from deletions.

2.4.8.1. Site directed mutagenesis –amino acid change constructs

To carry out amino acid alterations for each case a pair of primers were designed to alter the target amino acid, taking into account preferred *Bdellovibrio* codon usage. The bacterial two hybrid plasmid containing the gene of interest was used as the template DNA and the alteration primers were used to amplify the plasmid by overlap extension PCR (Table 2.3). The resulting DNA was treated with DpnI (Fermentas, fast digest) to degrade the original, methylated (due to being cell-derived), template DNA, leaving behind the bacterial two hybrid plasmid containing the mutated gene of interest, see

Figure 2.2. This was transformed into *E. coli* DH5α and multiple colonies were screened; potential constructs were then sequenced (section 2.5.8).

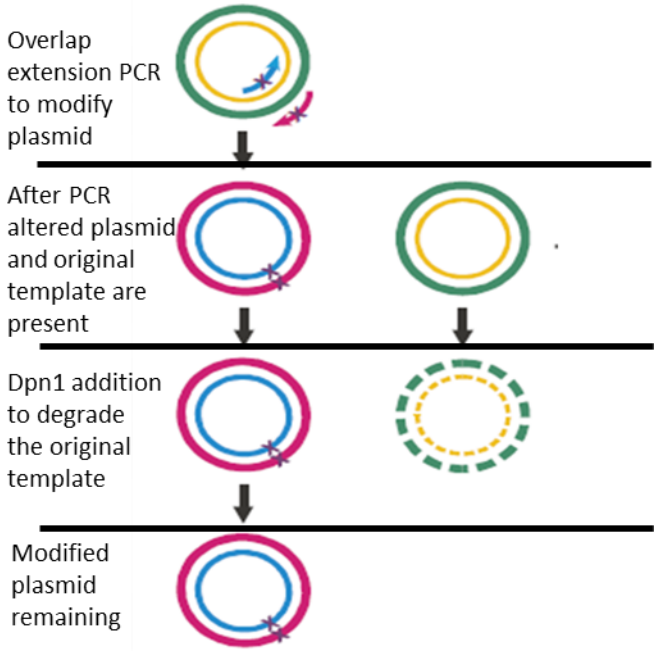

Figure 2.2 DpnI digest: when changing amino acids by overlap extension PCR, DpnI is useful for removing cell-derived, methylated plasmid template (green and yellow) from completed PCR reactions, leaving behind the un-methylated, modified plasmid produced in the reaction (containing gene of interest with a site-directed mutation) (pink and blue).

In some cases this amino acid change introduced an additional restriction site that could be used to help the screening process. However all altered genes in bacterial two hybrid vectors were confirmed via sequencing. These site directed alterations were used directly in bacterial two hybrid assays.

Additionally, the altered genes in these plasmids were used as PCR templates to allow amplification of the altered gene. This study used Gibson assembly cloning to combine the 1 kb region upstream of the gene of interest, with the mutated gene and the plasmid pK18*mobsacB,* see Figure 2.3 (Gibson et al, 2009). These constructs (amino acid alteration plasmids) were confirmed by sequencing.

The Gibson method allows for successful assembly of multiple DNA fragments, regardless of fragment length or end compatibility. Primers for Gibson assembly have regions which anneal to the DNA to be amplified and overhangs which overlap the neighbouring piece of DNA to be joined. Gibson Primers in this study were designed using the NEBuilder tool http://nebuilder.neb.com. The pK18 vector was cut with

EcoRI+HindIII and amplified DNA was compatible due to primer design. Gibson Assembly joins multiple overlapping DNA fragments in a single-tube isothermal reaction. Resulting in: 1 kb upstream, plus the gene with the amino acid alteration, together in pK18.

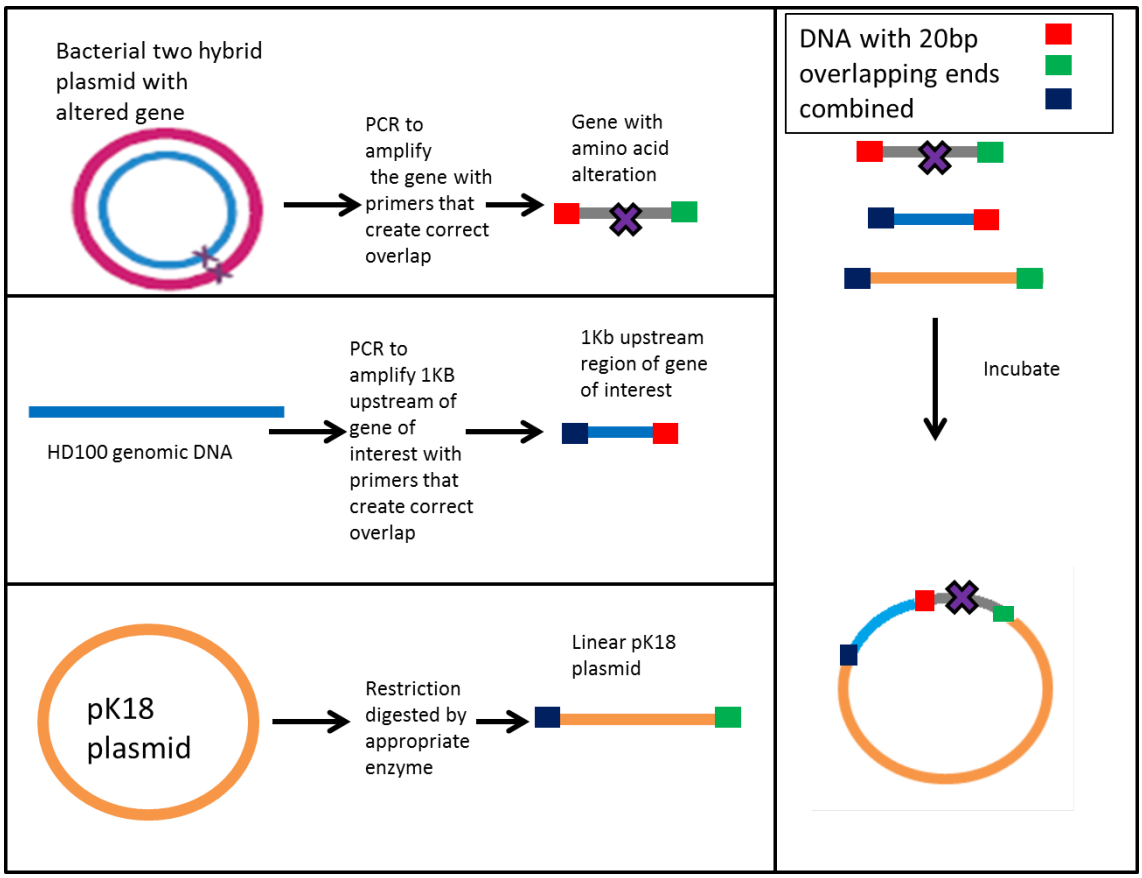

Figure 2.3 – The process of creating site directed amino acid alterations in pK18 plasmid. The miniprep of the bacterial two hybrid plasmid with altered gene was used as the template DNA to amplify the gene of interest. Another PCR reaction to get 1 kb upstream used genomic DNA as the template, and pK18 was digested to be linear. The primers used generate fragments with a 20 bp overlapping region. These fragments were all combined in a single-tube isothermal reaction to form the new pK18 plasmid.

This was then transformed into the *E. coli* donor strain S17-1 and conjugated into the *Bdellovibrio* deletion strain of interest. Merodiploid HD *B. bacteriovorus* strains were selected by growth on *E.coli* S17-1 pZMR100 lawns on YPSC overlay plates supplemented with 50 μg ml^{-1} kanamycin. Merodiploid HI *B. bacteriovorus* strains were selected by growth on SPY plates supplemented with 50 μg ml^{-1} kanamycin. These strains have a single cross over and require Kan. This method was used to create *B. bacteriovorus* strains with the

following gene mutations: *bd2584*(H389V) and *bd0367*(D63A), (Table 2.1) using Gibson amino acid changing primers in Table 2.3.

2.4.9. Generating fluorescently tagged gene constructs

Genes were tagged at the 3' with the mCherry gene by cloning the *Bdellovibrio* gene of interest (minus the upstream promoter region and STOP codon) into pAKF56 (a plasmid containing mCherry gene). This full length ORF-mCherry construct was sub-cloned into the pK18*mobsacB* plasmid and transformed into *E. coli* S17-1; the resulting strain was used as *E.coli* S17-1 donor for conjugation of the construct into *B. bacteriovorus* HD100. The fluorescently tagged gene recombined in a single crossover event at the gene of interest locus, with mCherry tagged exconjugants being positively selected for using kanamycin resistance (as pK18*mobsacB* still present). This resulted in merodiploid strains expressing fluorescently-labelled copies of the protein of interest, Figure 2.4. The gene was expressed in cis from its native promoter as the construct did not include this promoter region. This prevented expression of the wild type gene still present in the genome. Strains were further screened by primers to 300 bp upstream of the gene region included in the plasmid. This was used in conjunction with a primer which bound within the plasmid to amplify the region by PCR and then sequence though. This ensured that the crossover had occurred within the expected DNA sequence and that no additional mutations in the coding sequence had occurred during the cross-over event.

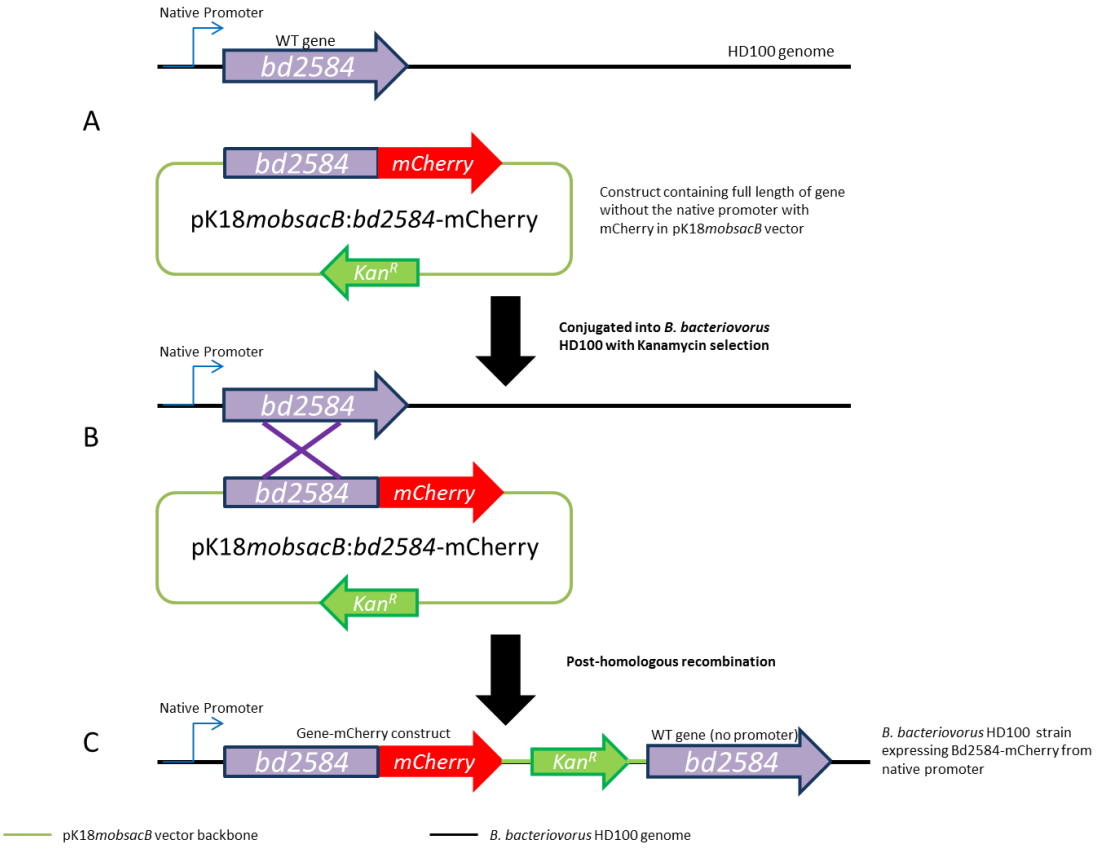

Figure 2.4 Illustration showing the process to obtain a single cross over *bd2584*-mCherry tag into the *Bdellovibrio* HD100 genome. The fluorescently tagged gene recombines in a single crossover event at the gene of interest locus (B) with mCherry tagged exconjugants being positively selected for using kanamycin resistance (as pK18mobsacB still present). This resulted in merodiploid strains expressing fluorescently-labelled copies of the protein of interest (C).

2.4.10. Isolating RNA from *B. bacteriovorus* strains

RNA was isolated from predatory cultures to assess transcription of particular genes across the predatory lifecycle. In all instances, a final concentration of 1% (v/v) phenol and 19% (v/v) ethanol was used to kill the cells, stop transcription and preserve nucleic acid prior to RNA extraction at particular points in the predatory cycle.

Phenol ethanol treated cell pellets were defrosted on ice and RNA was extracted using the Promega SV Total RNA Isolation System, following the manufacturer's instructions - this kit contains a single DNase treatment. RNA was eluted in 50 µl RNase-free water and then subjected to a second DNase (Ambion DNA-free) treatment to remove residual DNA. The RNA samples were then tested for absence of DNA using Taq PCR (section 2.5.1), typically using primers for amplifying a fragment of the *Bdellovibrio fliC1* gene; the Taq PCR would only produce a PCR product if DNA remained. RNA quality and yield

was then assessed using an Agilent 2100 bioanalyzer to ensure that the 16S and 23S rRNA was present.

2.4.10.1. RNA isolation from a predatory time-course

A 1 litre *B. bacteriovorus* HD100 culture, grown under standard conditions, was grown 24 hours prior to starting the protocol. Complete prey-lysis in the *B. bacteriovorus* culture was determined by light microscopy and the culture was centrifuged at 17,000 *x g* in a Sorvall RC-5B Plus centrifuge for 30 minutes. The pellets were re-suspended in a total of 100 ml CaHEPES buffer and incubated at 29°C with 200 rpm shaking for 3 hours to stabilise expression. Simultaneously, a 50 ml culture of *E. coli* S17-1, grown under standard conditions, was centrifuged at 5,000 *x g* in a Sigma 4K15 benchtop centrifuge at 29°C for 10 minutes. The pellet was re-suspended in 50 ml CaHEPES, then back-diluted to an OD_{600} of 1.0 and incubated at 29°C with 200 rpm shaking for 3 hours to stabilise expression.

The synchronous predatory culture was started by addition of 40 ml OD_{600} 1.0 *E. coli* grown as in section 2.3.3 and 50 ml *Bdellovibrio* culture grown as in section 2.3.1.1 to 30 ml CaHEPES. *E. coli*-only control (40 ml OD_{600} 1.0 *E. coli* and 80 ml CaHEPES) and *Bdellovibrio*-only control; (50 ml *Bdellovibrio* and 70 ml CaHEPES) were also set up. Both the *E. coli* and *Bdellovibrio* controls were enumerated from these controls to calculate the ratio of *Bdellovibrio* to *E. coli* (the multiplicity of infection); this was always greater than three. At each time-point, the synchronicity of the culture was assessed by microscopy and 4 ml of the culture was removed and added to 1 ml 5% (v/v) phenol/ethanol. The remainder of the method for RNA isolation from HD strains (Section 2.4.10) was then performed.

2.4.11. Frozen stocks of *E. coli* and *B. bacteriovorus* strains

For long-term storage of *E. coli* and *B. bacteriovorus* (both HD and HI) strains, 150 µl of 80% glycerol (v/v) was added to 700 µl of a freshly grown bacterial culture in a 2 ml screw-cap tube and mixed by inversion. The samples were then snap-frozen in liquid nitrogen and stored at -80°C.

2.5. DNA manipulation

2.5.1. Polymerase Chain Reaction

PCRs were carried out to amplify sections of DNA for cloning, using DreamTaq DNA polymerase (Fermentas) and Phusion® High-fidelity DNA polymerase (NEB), using the mixtures and programs shown below (Tables 2.5 and 2.6). Phusion® High-fidelity DNA polymerase was used when amplifying products for use in cloning or sequencing. DreamTaq DNA polymerase was used in PCR screening reactions at it lacks 3' to 5' exonuclease proofreading activity and is, therefore, low fidelity. Primers were designed, where possible, to be 20 bp long, with a 50 % GC ratio and a GC clamp at the 3' end, with the extra addition of any restriction enzyme sites in cloning.

All PCR amplifications and RT-PCR tests were carried out using Thermo Hybaid MBS satellite thermo cyclers, which take 0.5 ml or 0.2 ml tubes and controlled using Thermo Hybaid Multiblock system.

PCR component	Phusion	DreamTaq
Buffer (including $MgCl_2$)	5 µl (5x)	2.5 µl (10x)
10 mM dNTPs	0.2 µl	1 µl
Primers (100 pmol/µl)	0.5 µl	0.3 µl
Template genomic DNA	0.5 µl	0.5 µl (or 2 µl Bdellovibrio culture)
DNA Polymerase	0.25 µl	0.2 µl
AnalaR water	17.25 µl	20.2 µl (or 18.7 µl if used with direct culture)
TOTAL	25 µl	25 µl

Table 2.5: The typical reaction mixes used for Phusion or Taq DNA polymerase PCR amplification. The Phusion reaction mix could be scaled up for production of more DNA or split to run across a gradient to determine the optimum temperature for maximum DNA amplification with minimal non-specific amplification

Stage	Temperature	Duration	# Cycles	Description
1	98°C	5 minutes (Phusion)	1	Initial Denaturation
	95°C	10 minutes (DreamTaq)		
2	98°C	10 seconds (Phusion)	30 or 35 for direct amplification from colony (Phusion and Taq)	Denaturation
	95°C	1 minute (DreamTaq)		
	50-70°C	30 seconds (Phusion)		Annealing
		1 minute (DreamTaq)		
	72°C	30 seconds per kb (Phusion)		Extension
		1 minute per kb (DreamTaq)		
3	72°C	10 minutes (all)	1	Final Extension

4	4°C	Hold	1	Hold

Table 2.6 PCR program for Phusion or Taq DNA polymerases. The table indicates temperatures and timings used for each step of the PCR. Stage 2 cycled through denaturation, annealing and elongation stages 30 times for Phusion reactions and Taq amplifications on genomic DNA. This was increased to 35 cycles when screening of deletion mutants.

2.5.2. Touchdown PCR to form deletion constructs

Gene deletions are created in *Bdellovibrio* by joining the upstream and downstream flanking DNA using a touchdown PCR. This means that the two segments do not need to be sequentially cloned in a plasmid vector. In this reaction, complementary sequences of primer DNAs on the forward and reverse sequence anneal to connect the two sections of flanking DNA, removing the targeted gene. Primers from the outside ends of the DNA fragments aid in amplifying the DNA product. The reaction mix and PCR programme are detailed below in Table 2.7 and Table 2.8 .

PCR component	Amount µl
Buffer (5x stock including 7.5 mM $MgCl_2$)	60 µl
10 mM dNTPs	6 µl
Primers (100 pmol/µl)	3 µl
Template genomic DNA (~200ng/µl)	30 µl
Phusion DNA Polymerase (error rate is 4.4 X 10^{-7})	3 µl
AnalaR water	165 µl
TOTAL	300 µl

Table 2.7 The typical reaction mix used for touchdown PCR. This mix was split between 6 reaction tubes.

Stage	Cycles		Temperature °C	Duration
1	1	Hot Start	98	5 min
2	4	Denaturing	98	30 sec
		Annealing	65	1 sec
		Elongating	72	1 min
3	16	Denaturing	94	30 sec
		Annealing	65	1 sec
		Elongating	72	1 min
4	5	Denaturing	94	30 sec
		Annealing	50	30 sec
		Elongating	72	1 min

5	1	Final elongation	72	5 min

Table 2.8 Program used for DNA amplification during a touchdown PCR.

2.5.3. Restriction Digests

DNA digests were used as a diagnostic test and to create fragments required for sub cloning. Fermentas Fast DigestsTM enzymes were used where possible; otherwise NEB restriction enzymes were used. The Fermentas enzyme system has the advantage that one buffer is compatible with all Fermentas enzymes and includes a green dye so digest products could be run directly on an agarose gel. The NEB restriction enzyme system uses one of four buffers depending on which enzyme or combination is used. 10 µl reactions were used for diagnostic digests and 50-70 µl reactions for the creation of cloning fragments. These were set up as per manufacturer's instructions. Digests were incubated at the optimum temperature for the enzyme used and cut for 2 hours.

To reduce the number of self-ligations which occur, when empty plasmid vectors were digested, a phosphatase enzyme was added to the mixture. The dephosphorylation of cloning vector DNA was done to prevent recircularization during ligation. Empty plasmid vectors were digested in the presence of 1 µl Fermentas FastAP Thermosensitive Alkaline Phosphatase (TAP).

2.5.4. Ligation

Ligations were performed in 20 µl volumes using T4 DNA Ligase (Fermentas) as per manufacturer instructions and with a 1:3 ratio of vector to insert. A self-ligation was used as a control for each ligation performed. The reaction was left for a minimum of 1 hour at room temperature (<20 ºC) or for 16 hours at 16 °C. Ligation mixtures were then transformed straight into competent cells. For the initial stages, *E. coli* DH5α was used. *E. coli* S17-1 was used when creating a donor strain for conjugation of plasmids into *Bdellovibrio*.

2.5.5. Purification of DNA from restriction digests or PCR products

DNA was purified for use downstream using PCR clean-up or gel extraction. Sections of DNA that have been digested at each end to make compatible "sticky ends" were purified using GenEluteTM PCR Clean-up Kit (Sigma). Other DNA fragments,

produced by PCR or by digesting a fragment from a plasmid were separated by gel electrophoresis (section 2.5.6). Bands with the required fragment size were isolated by illuminating with a UVP (UV) transilluminator at 280 nm and cut out using a scalpel. This transilluminator has lowered intensity so as not to damage the DNA fragments. The DNA was then removed from the residual gel using GenEluteTM Gel Extraction Kit. Both PCR clean-up (Sigma) and gel extraction processes were performed as per the manufacturer's instructions. The products were typically eluted in 50 µl Elution buffer (or 30 µl should a higher product concentration be required). The purified DNA was then stored frozen at -20 °C.

2.5.6. Agarose gel Electrophoresis

After a PCR or plasmid extraction, concentrations of the nucleic acid were determined by running out 1 µl with 9 µl loading buffer on a 0.8 % agarose gel in TBE buffer (section 8.1.1.1) with a lane at each end containing 10 µl 1 Kb DNA ladder (NEB), bands of which show size and concentration. DNA electrophoresis gels were run in 1 % TBE buffer containing 0.1 µg ml^{-1} ethidium bromide. Gels are run at 100 V for 1 hour and imaged using UV light in a BioRadTM gel documentation system.

2.5.7. Extraction of *Bdellovibrio* Genomic DNA

DNA was collected from a 10 ml culture of a HD *Bdellovibrio* incubated overnight in which prey cells had been cleared. These cultures were pelleted by centrifugation at 5,525 *x g* for 20 minutes. For a host independent culture 2 ml of the *Bdellovibrio* strain (with OD_{600} 1-1.5) was pelleted for 3 minutes at 17,000 *x g*. Genomic DNA was extracted from the pellets using a GenEluteTM Bacterial Genomic DNA Kit (Sigma), as directed in the instructions. DNA was eluted into 200 µl and stored at 4 °C.

2.5.8. Sequencing DNA

Sanger Sequencing by Source Bioscience was used to confirm that plasmids contained the expected DNA sequence before conjugation into *Bdellovibrio* to form deletion strains or amino acid mutations. *Bdellovibrio* strains were sequenced to ensure that cross-over events occurred without additional mutations to those intended.

For plasmid sequencing, primers were used which bind to the plasmid, outside the cloning regions, these provided sequence into the inserted region. For sequencing DNA

from *Bdellovibrio* deletion strains (section 2.4.8), screening primers were designed 150 bp upstream and downstream from the end of the flanking sequences used for cloning. These were used to amplify the region by PCR and then the whole section between the two primers was sequenced. This ensured that no additional mutations were created when forming the deletion strain.

For strains with a single cross-over insertion, such as mCherry tagged strains and complementation strains (section 2.4.9), primers were obtained 300 bp upstream of the region included in the plasmid. This was paired with a primer which bound within the plasmid to amplify the region by PCR and then sequence though. This ensured that the crossover had occurred within the expected DNA sequence and that no additional mutations had occurred during the cross-over event.

Plasmids were diluted to 100 ng/µl and PCR products to 1 ng/µl per 100 bp of sample product in AnalaR Normapur water. Primers were diluted to a concentration of 3.2 pmol/µl in sterile AnalaR Normapur water. Samples and primers were sent for Sanger sequencing by Source BioScience in Nottingham.

2.6. Reverse-transcriptase polymerase chain reaction (RT-PCR)

RT-PCRs were performed using the Qiagen OneStep RT-PCR kit with the following 25 µl reaction mixture, and the cycling programme detailed in Table 2.9. The mixture used was as follows: Buffer (including 2.5 mM $MgCl_2$) 5 µl (5x),Q solution 5 µl (5x), 10 mM dNTPs 1 µl, Primers (100 pmol μl^{-1}) 0.15 µl, Template (DNA/RNA) 0.5 µl (50-500 ng), Polymerase 1 µl, sterile AnalaR water 12.2 µl.

Stage	Temperature °C	Duration (min)	Cycles
Reverse transcription	50	30	1
Initial denaturation	94	1	1
Denaturation	94	1	30
Annealing	50	1	
Extension	72	1	
Final extension	72	10	1
Hold	4	∞	1

Table 2.9 : RT-PCR programme. Table indicates temperatures and duration of each stage of the RT-PCR programme

2.6.1. RT-PCR on an RNA timecourse across the predatory cycle.

RNA was isolated from timepoints throughout the *Bdellovibrio* predatory cycle as described in Section 2.4.10. Primers specific to a particular gene of interest (amplifying a fragment of approximately 100 bp) were used to semi-quantitatively compare transcript levels at each timepoint. Typically 28-30 amplification cycles were used to avoid saturation of the PCR product and allow comparison in transcript levels to be compared across the predatory cycle. Each RT-PCR is representative of at least two repeats from independently-isolated RNA samples. For each RT-PCR controls are carried out, *B. bacteriovorus* HD100 genomic DNA (the positive control), *E. coli* S17-1 RNA (the negative control against residual prey *E. coli* RNA in the *Bdellovibrio* RNA samples) and no-template reactions were also performed.

2.7. Microscopy

2.7.1. Fluorescence/brightfield microscopy

Brightfield-phase-contrast and fluorescent microscopy was performed using a Nikon Eclipse E600 microscope equipped with a 100 x objective lens (Nikon). All images were taken at this magnification. A Prior Lumen 200PRO metal halide lamp was used for illumination for epifluorescence, in combination with the appropriate filter block for each fluorophore. Images were captured using a Hamamatsu ORCA-ER camera and SimplePCI software (version 5.3.1 Hamamatsu). All fluorescent images were taken through the green fluorescence channel at maximum (255) gain in Simple PCI. An hcRED filter block (excitation: 550–600nm; emission: 610–665nm) was used for visualisation of mCherry tags. Image clarity was improved by a whole image single 'sharpen' pass and two 'smooth' image enhancement passes in Simple PCI (as described previously (Fenton et al, 2010).

For immobilising cells, agarose pads were made by pipetting approximately 2 ml 1% agarose/CaHEPES onto microscope slides (VWR) and allowed to set for 5 minutes. For gliding timelapse and other extended experiments, two reservoirs were introduced into the ends of the slides and filled with sterile distilled water to keep the pad hydrated for the experiments duration. In all instances, the sample was spotted onto the centre of the pad and covered with a 22 x 22mm (0.13-0.17 mm thick) coverslip.

2.7.2. Surface-expressed fluorescence of mCherry tagged proteins

An assay was developed by Dr Milner (Milner, 2014) to observe changes in fluorescence intensity or localisation after a period of surface incubation. A 10 ml *B. bacteriovorus* HD culture, was grown (as section 2.3.1.2) 24 hours prior to starting the protocol. 1 ml of the *B. bacteriovorus* culture (containing $2.5x10^8$ pfu ml^{-1}) was centrifuged at 17000 *x g* at 29°C for 2 minutes and re-suspended in 100 µl supernatant. 10 µl of the re-suspended sample was pipetted onto the centre of a 1% agarose/CaHEPES pad (with reservoirs, as described 2.7.1) and initial fluorescent images were taken. The brightfield and fluorescence exposures were noted and kept consistent, the slide was incubated at room temperature, with the reservoir filled every 30 minutes. After 400 minutes (a value chosen to allow prolonged incubation on a surface, and for gliding motility to commence), fluorescent images were taken at the same brightfield and fluorescence exposures as at t = 0 minutes, to ensure images were comparable. Images were then analysed using MicrobeJ .

MicrobeJ allowed for the quantitation of the fluorescent signal at T0 and T400. The collected images were analysed using the MicrobeJ plugin for the ImageJ (FIJI distribution) software which automates detection of bacteria within an image (Ducret et al, 2016). The HD *Bdellovibrio* cells were identified by defining them as Cell Type 2 as: area 0-1 μm^2, length 0.5-1.5 µm, width 0.2-0.8 µm and all other parameters as default. Manual inspection of the analysed images confirmed that the vast majority of cells were correctly assigned. However it is of note MicrobeJ was only used to analyse HD *Bdellovibrio* cells in this study and not the more irregular shaped HI cells. The background-corrected mean fluorescent intensity (INTENSITY.ch2.mean_c) was measured for each cell and then the mean of these measurements was determined for each timepoint and for each independent experiment. This analysis allowed comparison of relative fluorescence

intensities for mCherry tagged proteins at 0 mins vs 400 mins (measured in arbitrary relative fluorescence units) to determine fold changed and significance via a t-test.

2.7.3. Timelapse microscopy for bdelloplast exit assay

Timelapse video microscopy was used to observe the growth and exit of various *Bdellovibrio* strains within the prey bdelloplast. This utilised a Prior H101A ProScan III controlled motorised stage, which allowed automated image capture, of various set locations on a microscope slide. The prey cells for these experiments were S17-1 containing the plasmid pMALmcherry (Table 2.2), this has an inducible mCherry gene with a signal sequence to give periplasmic as well as cytoplasmic fluorescence. S17-1::pMALmcherry was grown overnight supplemented with Amp50 and 1µl IPTG per ml media. 5 ml HI *Bdellovibrio* strains were also grown overnight. 1 ml of S17-1::pMALmcherry was centrifuged and resuspended in 500 µl CaHEPES. This was combined with 400 µl HI *Bdellovibrio* and 300 µl CaHEPES were placed in a bijou and incubated at 29°C 200 rpm for 3 hours to allow invasion of the prey cells.

After incubation the sample was checked by microscopy, then centrifuged and resuspended in 100 µl CaHEPES, from this 10 µl was placed on a 1% CaHEPES/Agarose slide with reservoirs, as described above, to keep the pad hydrated. The bdelloplasts were observed for 9 hours with timelapse conditions of 0.1 seconds exposure and pass delay of 150 seconds.

2.7.4. Timelapse microscopy (gliding assay)

Timelapse video microscopy was used to observe gliding motility of *B. bacteriovorus* cells on a surface as described in (Lambert et al, 2011). This utilised a Prior H101A ProScan III controlled motorised stage, which allowed automated image capture, of various set locations on a microscope slide. 1ml from a 10 ml *B. bacteriovorus* culture was centrifuged at 17000 *x g* at 29°C for 2 minutes and re-suspended in 100 µl supernatant, (and in some cases 2 µl of washed 0.3 µm latex polystyrene beads (sigma) 8 µl of sample was then immobilised on a 1% agarose/CaHEPES slide with reservoirs (as section 2.7.1). Fields of view with approximately 100 cells were selected if possible, with the fields of view in close proximity to prevent large movements of the stage; 6 FOVs were typically selected.

Timelapse settings included a Z-refresh at every frame, for auto-focusing, and a 150 second pass delay for all gliding assays.

2.7.5. ImageJ- analysing location of cellular fluorescence

Images had the 'sharpen' and 'smooth' function applied to the whole image a maximum of 5 times to improve the clarity of the image. For easy detection of the distinct locations of cellular fluorescence the colour balance of the image was adjusted to reduce the red brightness. The general brightness and contrast of the image was also adjusted to allow easy foci detection. The plugin Cell Counter was used to track the different types of location of cellular fluorescence, e.g monopolar, dominant monopolar, bipolar, throughout. This data was processed in Excel to determine the percentage of distinct fluorescence types between strains and at particular time-points.

2.7.6. SimplePCI image analysis –measuring fluorescence associated with cells with specific motile behaviours

To analyse the fluorescent intensity in gliding cells vs stationary cells SimplePCI image analysis was used. This allowed selection and analysis of fluorescence level in only the cells of interest (e.g gliding). To analyse this a ROI Circle was drawn (the same size ROI was used for all analyses) around each cell of interest and 'TOTAL_GREEN' was measured for each ROI in the Measure Image option menu. Five blank ROIs (where no cells were present) were also measured. These data were then used to create a mean background fluorescence value of the green channel, and the following formula was used to calculate a fluorescence value for each cell or a population of cells:

Average Cell Total Green- Average Background Total Green= Net Cell Total Green.

2.7.7. SimplePCI image analysis – measuring gliding motility in timelapse videos

2.7.7.1. Measuring gliding reversal frequency

To measure gliding reversal frequencies in SimplePCI, the 'Register' of the video was first adjusted manually using a non-moving object as a guide to ensure that each frame was superimposed correctly over the previous.

Reversal frequency: Cells were selected by generating random regions of interest (ROIs) of a standard width and height of 250 x 300 to included approximately 10 cells in selected

region. Following the cells through each frame allowed the time at which each cell started gliding to be observed. After an individual cell had been gliding for one hour (allowing an establishment period), the number of direction changes (reversals) was counted manually and recorded.

2.7.7.2. Measuring the percentage of cells that glide

Cells were selected by generating random regions of interest (ROIs) of a standard width and height of 250 x 300 to included approximately 10 cells in selected region. Following the cells through each frame allowed a record to be made of which cells glide across the course of a 6-8 hour video and which remain stationary. This was repeated across multiple fields of view and multiple biological repeats then the percentage of gliding vs stationary cells was calculated.

2.7.8. Synchronous predatory cultures

2.7.8.1. Small-scale synchronous predatory cultures

For examining Bd2584-mCherry fluorescence localisation during predatory growth of *B. bacteriovorus*, small-scale synchronous predatory cultures were used. 10 ml of a *Bdellovibrio* predatory culture, grown under standard conditions, was centrifuged in a Sigma 4K15 benchtop centrifuge at 5525 *x g* at 29°C for 20 minutes and re-suspended in 2 ml CaHEPES supplemented with kanamycin (50 μg ml^{-1} final concentration). Simultaneously, 5 ml *E. coli* S17-1 pZMR100, grown under standard conditions for 16 hours, was centrifuged and re-suspended in 1 ml CaHEPES supplemented with kanamycin. These cultures were allowed to recover for 90 minutes at 29°C with 200 rpm shaking. 100 μl of the *E. coli* culture was then added to 2 ml of the *Bdellovibrio* sample and incubated at 29°C with 200 rpm shaking. Samples were removed at intervals, where 10 μl was spotted onto a 1% agarose/CaHEPES pad for analysis by fluorescent microscopy.

2.8. Protein interaction studies

2.8.1. Bacterial two hybrid

For bacterial two hybrid analysis (B2H) the method was conducted as in (Karimova et al., 1998). The bacterial strain used to examine protein interactions in our study was the *E.coli* BTH101 strain which is a *cyaA*$^{-}$ strain devoid of cAMP production. Each gene of interest was cloned in-frame downstream the T18 and T25 gene fragment, which are catalytic domains of adenylate cyclase (from *Bordetella pertussis*). This was done by ligating the gene

of interest into vectors pUT18C and pKT25; these vectors tagged the N terminus of the protein of interest.

If the proteins of interest interact the T18 and T25 fragments are brought into close proximity (in the BTH101 cell) these two fragments are able to re-join which enables the production of cAMP (Karimova et al, 1998). The cAMP produced binds with endogenous catabolite activator protein (CAP), promoting expression of the reporter gene *lacZ*. The protein product of *lacZ* is the enzyme β-galactosidase which can cleave X-gal (5-bromo-4-chloro-3-indolyl-β-Dgalactopyranoside), this property allows colorimetric screening for positive interactions as cleavage of X-gal by β-galactosidase yields an insoluble blue precipitate which colours *E.coli* colonies which contain it, this can be observed on spot plates. When the test proteins did not interact, the two fragments were not re-joined so not able to produce cAMP and white colonies were observed on plates see Figure 2.5.

In all cases, interactions were tested with each test gene expressed from both plasmids (e.g. pUT18cA with pKT25-B and pUT18c-B with pKT25-A). Positive controls were run using pUT18c-zip and pKT25-zip. These contain the leucine zipper region from yeast GCN4 and interact strongly (Karimova et al, 2001). Empty plasmids were also transformed as a negative control.

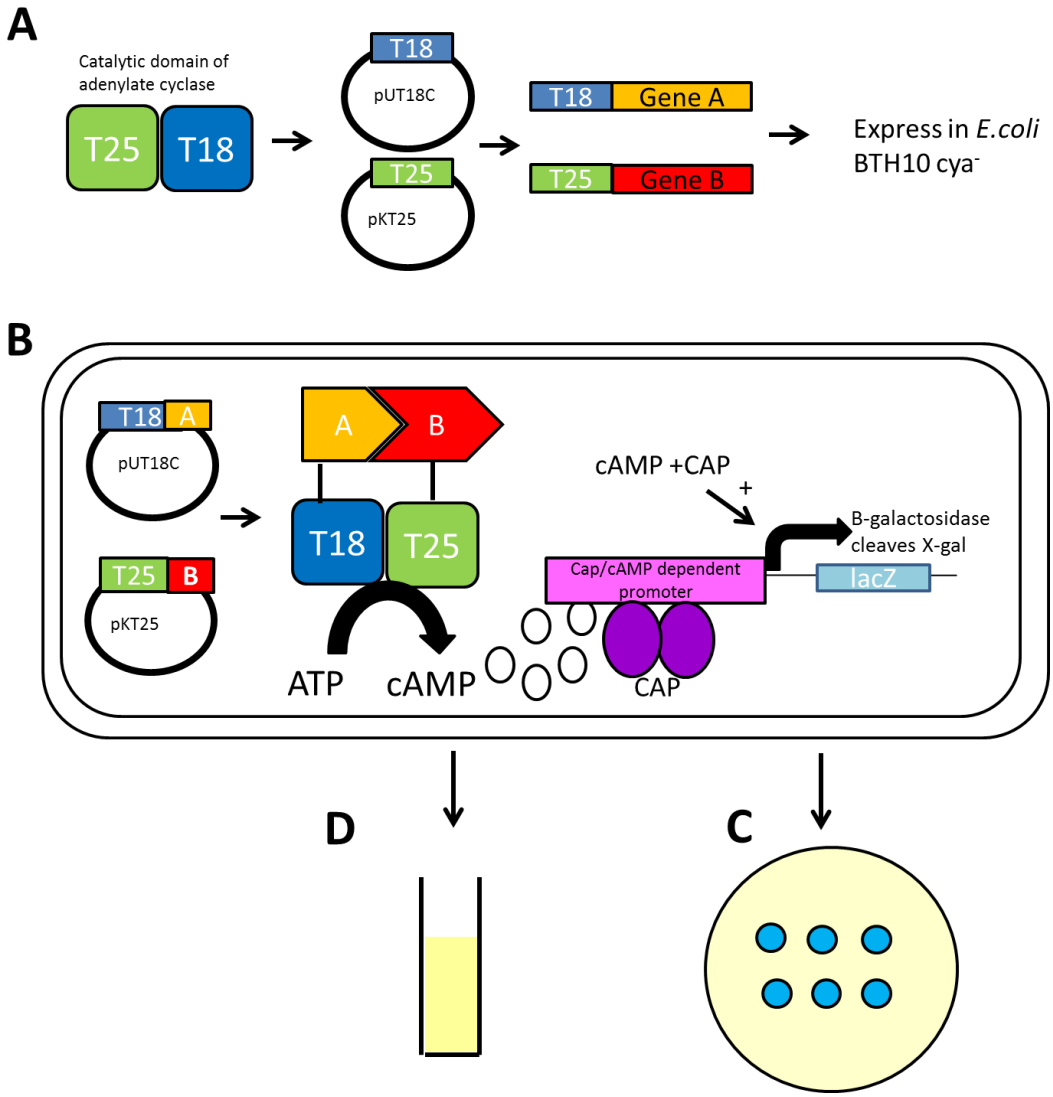

Figure 2.5 Illustration of Bacterial Two Hybrid assay. (A) The catalytic domain of adenylate cyclase is split into T25 and T18 these fragments are expressed in the plasmids pUT18C and pKT25, genes of interest can be cloned into these plasmids to investigate protein interactions. **(B)** If the two fragments of adenylate cyclase are fused to proteins which interact, the two fragments are brought into close proximity and the two fragments can reform the catalytic site of adenylate cyclase. This allows the production of cAMP from ATP. When cAMP is present in the cell, the messenger interacts with the Catabolite Activator Protein (CAP) and promotes the binding of *E.coli* RNA Polymerase to the promoter of the *lacZ* reporter gene. The *lacZ* gene encodes β-galactosidase which cleaves the X-gal present in the Nutrient Agar plates on which the colonies are grown on. **(C)** This cleavage reaction turns the bacterial colonies blue therefore this provides a colorimetric assay to assess protein interactions, where positive interactions result in blue colonies and negative interactions result in white colonies. (D) Liquid β-galactosidase assay uses ONPG (ortho-nitrophenyl β-D-galactopyranoside) which is an artificial substrate of β-galactosidase; the colourless ONPG is cleaved by β-galactosidase to produce yellow ortho-nitrophenol (ONP) which is measured by spectrophotometry.

The process of the bacterial two hybrid assay was carried out as follows: BTH101 competent cells were thawed on ice and 1 μl each plasmid was added and mixed by gentle pipetting. The cells were incubated on ice for 30 minutes and heat shocked at 42°C for 1 minute, before being allowed to recover on ice for 5 minutes. 1 ml SOC medium was then added and the cells were incubated at 29°C with 200 rpm shaking for 1 hour to recover. The cells were then centrifuged at 17000 x g for 1 minute, washed with 1 ml Mu broth (to remove glucose-rich SOC medium), re-suspended in 100 μl Mu and plated onto Nutrient Agar (Oxoid) supplemented with 50 μg ml^{-1} Ampicillin, 25 μg ml^{-1} Kanamycin and 40 μg ml^{-1} X-gal and incubated at 29°C for 48 hours. Three transformants (experimental repeats, to allow for variation) for each interaction were grown in 5 ml Mu broth supplemented with ampicillin and kanamycin (final concentrations 50 ug ml^{-1} and 25 ug ml^{-1} respectively) for 16 hours at 29°C with 200 rpm shaking. 5 μl of each culture was spotted onto Nutrient Agar supplemented as above and incubated for 48 hours at 29°C. Plates were then scanned on an Epson Perfection 1200U scanner to observe the colour of the culture spots on the plates. All experiments were carried out in triplicate and had multiple biological replicates.

2.8.2. Measurements of β-galactosidase activity

To quantify the β-galactosidase activity of bacterial two-hybrid strains, and hence the interaction strength of the test proteins in *E.coli* cytoplasmic conditions, a method based on that of (Miller, 1972) was used. This used ONPG (ortho-nitrophenyl β-D-galactopyranoside): which is an artificial substrate of β-galactosidase; colourless ONPG is cleaved by β-galactosidase to produce yellow ortho-nitrophenol (ONP) (Miller, 1992).

The 5ml cultures, grown for bacterial two-hybrid spot tests, were used for all β-galactosidase assays. A 1 ml aliquot of cells was pelleted by centrifugation in a Sigma 4K15 benchtop centrifuge at 3275 *x g* at 4°C for 10 minutes. The pellet was re-suspended in 2 ml 4°C Z-buffer (section 8.1.3.1). 0.5 ml of the resuspension was added to a fresh tube containing 0.5 ml 4°C Z-buffer and kept on ice (a tube containing 1 ml Z-buffer served as a blank). The cells were then permeabilised by addition of 100 μl 0.1% SDS and 100 μl chloroform. The samples were then incubated at 29°C with 200 rpm shaking for 10 minutes. The OD_{600} of the remaining 1.5 ml cells in Z-buffer was recorded during this incubation.

After incubation of the samples, 200 µl of ONPG solution (section 8.1.3.3) was added. The reaction mixture was incubated at 29°C with 200 rpm shaking until the samples turned yellow. At this point the reaction was quenched by addition of 500 µl 1 M Na_2CO_3, and the time from addition of ONPG to quenching was recorded. For any reactions that did not turn yellow, these were quenched after 20 minutes. 1.5 ml of each of the quenched reactions was centrifuged at 17000 *x g* for 1 minute and 1 ml of this was removed. The OD_{420} and OD_{550} values of each reaction were recorded. Miller units were then calculated using the following equation (where T = reaction time in minutes and V = culture volume in millilitres)

$$Miller\ units = \ 1000\ x \frac{OD_{420} - 1.75\ x\ OD_{550}}{T\ x\ V\ x\ OD_{600}}$$

2.9. Protein purification

Protein expression constructs were made using the expression plasmids PQE80L and pQE60. pQE80L allows the gene of interest to be tagged at the 5' in order to generate a protein product with an N-terminal 6xHis-tag, whereas pQE60 tags the gene at the 3', forming a C-terminally 6xHis-tagged protein product. These constructs were transformed into *E.coli* M15pRep4 and the resulting colonies were picked into 50 ml of 2YT supplemented (with 100 µg ml^{-1} Ampicillin, 25 µg ml^{-1} Kanamycin, 2% glucose). After 16 hrs incubation at 37°C, 25 ml of the culture was added into 500 ml of 2YT and grown to an OD_{600} between 0.4-0.8. At this point 1 mM IPTG was added to induce expression and the cultures were incubated for 20 hrs at 18°C in a 200 rpm shaking incubator. The cells were centrifuged at 8000 *x g* for 20 min at 4°C and re-suspend in 30 ml lysis buffer (section 8.1.5.2) and kept on ice. The resuspension was then sonicated and centrifuged at 17500 *x g* 4°C for 20 minutes. The supernatant was filtered using a 0.45 µm filter and added to columns containing Qiagen Ni-NTA agarose that had been pre-equilibrated with wash buffer (section 8.1.5.3). Once the supernatant had run through the column 50 ml of lysis solution was added to wash the column. Then the elution buffer (section 8.1.5.4) was added and after the column colour change 1.5 ml of elute was collected. The samples were boiled with Laemmli buffer (section 2.9.2.6) and run on a 12.5% SDS-

PAGE gel (section 2.9.2.3) to check purity levels; a Lowry assay was also carried out to assess the concentration of the protein samples.

2.9.1. Lowry total protein concentration

Lowry assays, with Markwell's method to include solubilizing membrane proteins by addition of SDS were used to determine protein concentrations (Lowry et al, 1951)(Markwell et al, 1978).

A standard curve was produced using BSA (bovine serum albumin, Sigma B4287). A 1 mg ml^{-1} solution of BSA in water was made fresh. This was diluted using the following quantities before being made up to 500 µl with water in cuvettes: 0, 20, 40, 60, 80 and 100 µl. The test samples were also made up to 500 µl. Solution C was made by adding 49.5 ml solution A to 0.5 ml solution B (section 8.1.4) in a Falcon tube and mixed by inversion. Each cuvette had 1.5 ml of solution C added and was mixed by pipetting and incubated in the dark for 20 minutes at room temperature. Folins' mix was set up using 1 ml of Folin-Ciocalteu reagent with 1 ml of deionised water and 150 µl of this mix was added to the cuvettes and mixed by pipetting. The cuvettes were incubated again for 45 minutes in the dark. The OD_{750} of the samples was then measured, using the 0 BSA test as the blank. The readings were compared to the standard curve produced to give the absolute amount of protein in the cuvette.

2.9.2. SDS-PAGE gel

Protein fractions from the His tag affinity purification step were incubated in Laemmli buffer for 10 minutes at 100°C then separated on a SDS-PAGE gel. The gel was used to assess purity and quantity of desired His tagged protein or to examine novel bands of interest from protein pull down experiments. The purified His tagged proteins and the novel protein bands of interest were excised from the gel, and sent for identification by LC-MS/MS analysis at the University of Leicester

2.9.2.1. Coomassie Blue stain

0.1% (w/v) Coomassie brilliant blue (BioRad), 30% (v/v) Methanol, 10% (v/v) Glacial acetic acid. Made up to required volume with deionised water.

2.9.2.2. SDS-PAGE destain solution

30% (v/v) Methanol, 10% (v/v) Glacial acetic acid. Made up to required volume with deionised water.

2.9.2.3. Resolving gel (12.5%)

3.3 ml sterile H_2O, 4 ml 40% acrylamide (29:1 acrylamide:bisacrylamide) (Fisher-Scientific UK), 2.5 ml 1.5 M Tris-HCl (pH 8.8), 200 µl 20% SDS (Melford), 200 µl 10% (w/v) Ammonium persulphate (APS) (Sigma), 7 µl Tetramethylethylenediamine (TEMED) (Sigma).

2.9.2.4. Stacking gel

3.5 ml sterile H_2O, 0.68 ml 40% Acrylamide (Fisher-Scientific UK), 0.5 ml

1 M Tris-HCl (pH 6.8), 150 µl 10% (w/v) SDS (Melford), 50 µl 10% (w/v)

APS, 5 µl TEMED (Sigma).

2.9.2.5. Running Buffer

200 mM Glycine (Sigma), 0.1% (w/v) SDS (Sigma), 25 mM Tris base (Fisher).

2.9.2.6. Laemmli Buffer

62.5 mM Tris HCl (Invitrogen) 10% (v/v) glycerol (Sigma) 2% (w/v) SDS (Sigma-Aldrich) 0.01 mg ml^{-1} Bromophenol blue (Invitrogen) 0.02% (v/v) β-Mercaptoethanol (Sigma-Aldrich)

2.9.2.7. Silver staining

Silver staining is a highly sensitive method for detecting proteins in polyacrylamide slab gels. The Bio-Rad Silver Stain was used in this study, it was derived from the method of Merril and co-workers (Merril et al, 1979), is 10-50 fold more sensitive than Coomassie brilliant blue R-250 for proteins (detection is ~0.1 ng/mm^2). The gel was placed in 400ml fixative (40% methanol/10% acetic acid (v/v)) for 30 min, then 400 ml fixative (10% ethanol/5% acetic acid (v/v)) for 15 min, this step was repeated. Gel was then incubated in 200 ml of Oxidizer for 5 min followed by 2 washes of 400 ml of water with 5 min duration. The gel was then combined with 200 ml of silver reagent for 20 min, the gel was then washed with water and developed, 400 ml of 5% acetic acid (v/v) was used to stop the developing.

2.10. His-Tag Protein Pulldown

This assay used Bd2584-His or Bd0367-His which had been purified as described above. These protein samples were dialysed twice (section 8.1.5.5) to remove imidazole previously used in the elution buffer. This dialysed protein was diluted and bound to the 200 µl of pre equilibrated Qiagen Ni-NTA agarose beads (washed and centrifuged twice) to act as the bait protein. Other Qiagen Ni-NTA agarose columns contained wash buffer (section 8.1.5.4) only to act as controls.

3 litres of attack phase *B. bacteriovorus* HD100 were grown (section 2.3.1.2), centrifuged for 20 minutes at 10,000 rpm (4°C) and resuspended in 4 ml lysis buffer (section 8.1.5.2). These cultures were sonicated on ice 6 minutes total, with 30 seconds pulses at a time. The sample were then centrifuged at 13,000 rpm in SS34 rotor for 30 minutes to remove membrane fractions, the supernatant was removed and passed through a 0.45 µm filter . 1 ml of cell lysate was incubated with the Ni-NTA agarose beads with or without the bait protein for 4 hours at 4°C on a rotor. These beads were then pelleted by centrifugation at 2,500 *x g* and washed twice with wash buffer. The beads were mixed with Laemmli buffer, boiled for 10 minutes and run on 12.5% SDS-PAGE gel to look for potential interacting proteins through protein bands present in Bait-His mixed with HD100 lysate samples and not in the controls. Potential bands were cut out and sent for LC-MS/MS analysis at the University of Leicester.

2.11. mCherry Protein Co-purification

To find proteins that interact with PilZ protein Bd3100 a novel in vivo co-purification assay was attempted. The strain used was the host dependent *B. bacteriovorus* Bd3100-mCherry strain, this strain has mCherry fused to the C terminus of the protein, so this could be used as the bait protein. The native levels of Bd3100-mCherry tagged bait protein in the host dependent *B. bacteriovorus* Bd3100-mCherry strain was hoped to bind to the RFP-TRAP chromo-Tek beads by the mCherry portion of the protein. This would allow interacting proteins bound to Bd3100 to be pulled out and analysed by LC-MS/MS.

800ml of the host dependent Bd3100mCherry strain was pelleted in attack phase by 20 minutes of centrifugation at 8,000 x g at 4°C and resuspended in 4 ml lysis buffer (section 8.1.5.7). These cultures were sonicated on ice 6 minutes on and off for 30 seconds at a time. The samples were then centrifuged in 1.5 ml tubes at 17,000g 45 minutes. The

supernatant was then concentrated to 2 ml using centricon concentration tubes (10 kDa cut off). RFP-TRAP chromo-Tek beads were prepared by resuspension in wash buffer (section 8.1.5.8) and centrifugation at 2,500 *x g* 2 mins (this was repeated twice). 1 ml of cell lysate was combined with 30 µl of the prepped RFP-TRAP beads (chromo-Tek) and was incubated for 2 hours at 4°C. These beads were then pelleted by centrifugation at 2,500 *x g* and washed twice with wash buffer. The beads were mixed with Laemelli buffer and boiled for 10 minutes and run on 12% SDS-PAGE gel and stained in Instant blue (Expedeon) (or silver stained where necessary) to look for potential interacting protein bands present in Bd3100mCherry strain lysate sample that are not present on the control HD100 lysate. Any bands of interest were cut out for analysis by LC-MS/MS at Leicester University to allow identification.

2.12. Phosphotransfer assay in Dr Porter's lab at The University of Exeter

Histidine kinase auto-phosphorylation and phosphotransfer experiments to response regulator protein Bd0367 were carried out in Dr Steve Porter's lab at The University of Exeter with assistance from Dr Francis and used the technique from (Porter et al., 2007). Briefly a tube containing the standard phosphotransfer buffer had the relevant proteins at the correct concentrations added to it. This tube then has radioactive ATP added at time 0 and 10 µl of the sample is collected at the set time points and put into the quenching tube. The quenching tube was stored on ice until gel loading. The SDS-PAGE gel is run and this gel was then cut and placed in the phosphoimager, these images were then analysed using MultiGauge ver 2.0 software.

2.12.1. Detail of Phosphotransfer assays carried out in this study

The variety of test proteins were added to: a mixture of 5x phosphotransfer buffer (section 8.1.6.2) water and 5.5 µl $MgCl_2$/KCl made to a final volume of 100 µl. The final concentrations of the test proteins added were 40 µM, 20 µM, or 5 µM. Samples were incubated at room temperature or 29°C for 10 mins. A 2 mM [γ-32P] ATP solution with a specific activity 14.8 GBq $mmol^{-1}$ was added to samples (Porter et al, 2007). 11.5 µl of this was added to each tube to start the reaction. Alterations were made depending on the desired reaction, in some cases c-di-GMP at 75 µM or 100 µM was added immediately before ATP addition in other samples c-di-GMP was added at 14.5 min post ATP addition to observe its effect. In other samples a test protein was added to the reaction

mix after the histidine kinase had been exposed to ATP for 30 minutes to see if differences in phosphotransfer transfer occurred. At the selected time-point 10 µl of the reaction mix was added to 20 µl of quenching solution (section 8.1.6.1) vortexed then placed on ice. Three sets of time points were used to investigate the speed of autophosphorylation and potentially phosphotransfer transfer speed.

The time courses used were:

- 15 sec, 30 sec, 45 sec, 60 sec after ATP addition,
- 1, 15, 20, 30 min after ATP addition
- 1, 15, 30, and 60 minutes after ATP addition.

These samples were run on a 12.5% SDS-PAGE gel cooled by antifreeze. The resulting gel was cut and placed in between two sheets of acetate with ladder to left and the ATP standards (200, 160,120, 80, 40, 20, 16, 8,4, 2, 0 µM) at the base. This was then placed on a phosphoimaging sheet in a cassette for 1 hr. This sheet was then visualized on a phosphoimager and analysed using MultiGauge version 2.0 software.

2.13. Bioinformatics

A variety of online tools were used in the bioinformatics analysis of gene products studied in this work. These included:

• Nucleotide and protein sequences were retrieved from xBase http://www.xbase.ac.uk/and http://rrc22a.vet.cam.ac.uk/xbase/ These sequences were compared using NCBI BLAST (National Center for Biotechnology Information Basic Local Alignment Tool - http://blast.ncbi.nlm.nih.gov/) on its default settings.

• The presence of predicted secretion signals was tested using SignalP4.1. (http://www.cbs.dtu.dk/services/SignalP/) and location information for non-secreted proteins was predicted using PSORTb (Petersen et al, 2011; Yu et al, 2010).

• Transmembrane regions were predicted using TOPCONs topology analysis, which combines 5 topology prediction programs (Tsirigos et al, 2015).

Signal transduction proteins in the *B. bacteriovorus* HD100 genome were predicted using Mist2.2 http://mistdb.com/ which identifies protein domains implicated in signal transduction.(Ulrich & Zhulin, 2010).

Similarity and identity of full length predicted protein products were analysed using the Clustal omega http://www.ebi.ac.uk/Tools/msa/clustalo/

2.14. *Bdellovibrio* analysis methods

2.15. Quantification of c-di-GMP

Levels of cyclic-di-GMP were determined for BTH101 *E.coli* and *Bdellovibrio* in Host Dependent and Host Independent growth conditions. In all cases the Bobrov method was used for the extraction, however the growth of the strains before extraction varied, as outlined below (Bobrov et al, 2011).

2.15.1. Preparation before c-di-GMP extraction from liquid cultures of *Bdellovibrio* attack phase strains

The HD strains extracted in this study were: *B. bacteriovorus* HD100, Δ*bd1971*, *bd1971*(D307308A) (Table 2.1).

For extraction of c-di-GMP large amounts of *Bdellovibrio* in order to collect the required amounts c-di-GMP for detection. Recent modifications in *Bdellovibrio* growth protocol allows a concentrated 50 ml culture to result in a quantity of *Bdellovibrio* comparable to that of a previous 500 ml culture. Four cultures were set up per strain (equivalent to an 'old fashioned' 2L culture) and per repeat. These cultures consisted of 10 ml S17-1 *E.coli*, 10 ml *Bdellovibrio* strain, 30 ml CaHEPES. This was split between two 50 ml falcons and incubated at 29°C 200 rpm for 24 hours. These cultures were then filtered through a 0.45 µl filter into a 50 ml falcon and the culture was checked by microscopy to check any residual *E.coli* had successfully been removed. There cultures were centrifuged at 15,000 *x g* for 20 minutes at 4°C. The cell pellet was resupendend in the residual supernatant and transferred to a pre-weighed 1.5 ml microcentrifuge tube. These tubes were centrifuged at 4°C for 3 minutes at 17,000 *x g* and all the supernatant carefully removed. The tubes with cell pellet were re-weighed so that the wet weight of the cells could be calculated. The pellets were then snap frozen in liquid nitrogen and stored at -80 ºC.

2.15.2. Preparation before c-di-GMP extraction from liquid cultures of Host-Independent *Bdellovibrio* strains

The HI strains extracted in this study were: *B. bacteriovorus* Δ*bd0367*, *bd0367*-mCherry, *bd0367*(D63A), HID13, Δ*bd1971*, *bd1971*(D307308A) (Table 2.1).

HI cultures were all grown the same way, doubling the culture volume each day. These HI cultures were back-diluted in to 10 ml PY (with or without Kan at 50 μg ml^{-1}) to a starting OD_{600} of 0.2 and grown to an OD_{600} of 0.6. These were then pelleted by centrifugation at 15,000 *x g* for 20 minutes at 4ºC before being resuspended in 1 ml PY and transferred to a weighed 1.5 ml microcentrifuge tube. This was cetrifuged for 3 minutes in micro centrifuge at 17,000 *x g* at 4 ºC. The supernatant was all carefully removed and the tube reweighed so the wet pellet weight could be calculated. The tube was snap frozen in liquid nitrogen and stored at -80 ºC until the c-di-GMP could be extracted.

2.15.3. Extraction technique for c-di-GMP

The method of extraction of c-di-GMP was the same for the three different types of culture investigated. This method was the same as previously used for *Bdellovibrio* c-di-GMP determination (Hobley et al, 2012), an adaption from the method used by Bobrov for the analysis of c-di-GMP in *Yersinia pestis* (Bobrov et al, 2011). To extract c-di-GMP the pellets were vortexed in 100 μl of extraction buffer (40% methanol, 40% acetonitrile in 0.1 N formic acid) per 48 ng wet weight of cells and incubated at -20 ºC for 30 minutes. The cell debris was pelleted by spinning at 17,000 *x g* for 3 minutes at 4 ºC. The supernatant was then removed and neutralised with 4 μl 15% NH_4HCO_3 per 48 ng wet weight and stored at -20°C. The extraction process was repeated with the same volumes of extraction buffer on the remaining pellet and neutralised. The two supernatants removed were combined per sample and stored at -20 ºC until they were shipped to The RTSF Mass Spectrometry and Metabolomics Core at East Lansing, MI for analysis using liquid chromatography tandem mass spectrometry (LC-MS/MS).

Chapter 3. The Bd0367 signalling pathway in *Bdellovibrio bacteriovorus*

3.1. Introduction

3.1.1. Regulation of diguanylate cyclase activity and function by response regulator domains

As previously mentioned diguanylate cyclases (DGC) contain GGDEF domains and synthesize c-di-GMP. GGDEF domains can also be part of proteins with regulatory and sensory domains, such as response regulator (RR) domains. The integration of a RR and an enzymatic domain allows control at a post-translational level. This post-translational control can result in conformational rearrangement and activation in response to changing environmental or internal signals. Phosphorylation of RR domains is a common mechanism used to activate GGDEF domains enzymatic activity (De et al, 2009; Ryjenkov et al, 2005; Wassmann et al, 2007). These control mechanisms relayed through the RR domain regulate GGDEF activity and allow tight control c-di-GMP production, this regulation is used to correctly time c-di-GMP signalling cascades in order to have the correct output and to prevent overproduction of c-di-GMP that could cause an undesired molecular output.

3.1.1.1. RR domains can effect DGC oligomerization, activity and protein interactions

PleD is a well-studied *Caulobacter crescentus* DGC with two N terminal RR domains. The RR domains are phosphorylated by two cognate kinases PleC and DivJ, this activates PleD DGC activity and also results in sequestration of PleD to the differentiating pole (Aldridge et al, 2003; Paul et al, 2004). PleD DGC activity is also only active when PleD is in a dimeric state and the dimer formation is mediated by phosphorylation (Paul et al, 2007). This leads to only phosphorylated dimeric PleD proteins being sequestered to the pole, it is hypothesised that dimeric phosphorylated PleD is recognised at the pole by specific polar interaction partners. It is also suggested that dimerization of PleD may increase diversity of protein interaction by enabling the simultaneous binding of two interacting proteins and that interacting partners of PleD may discriminate between

binding monomeric or dimeric forms (Marianayagam et al, 2004; Paul et al, 2007). This example shows how important the RR phosphorylation state can be for protein interactions and enzyme function.

3.1.2. *Bdellovibrio* diguanylate cyclase Bd0367

As previously mentioned in chapter 1 *Bdellovibrio bacteriovorus* HD100 has four DGC proteins. Each of these proteins were deleted and three resulted in distinct phenotypes indicating a specific c-di-GMP signalling system in *Bdellovibrio* with a lack of cross talk between parallel c-di-GMP outputs (Hobley et al, 2012).

The focus of my study is the DGC Bd0367. Bd0367 has been suggested to be a key component in the signalling cascade that is important in gliding motility and prey cell exit.

During the course of my study new research by Hallberg et al 2016 has shown that Bd0367 can be considered a promiscuous substrate-binding or Hypr GGDEF (see section 1.4.5). This new class of GGDEF can also produce cyclic AMP-GMP (cAG), the study showed that Bd0367 can produce cAG in vitro (Hallberg et al, 2016). From Hobely et al it is known that Bd0367 produces c-di-GMP as expected in vivo. More research is ongoing into this new class of GGDEF proteins which will hopefully lead to a better understanding of the role Hypr GGDEF proteins are performing in bacteria.

Bd0367 has a RR domain as well as a GGDEF domain; this suggests that the enzymatic activity is controlled by phosphorylation from a currently unknown histidine kinase (HK). The investigation to find the cognate HK is covered in Chapter 4 and the investigation into the effect of phosphorylated on Bd0367 DGC activity and hence c-di-GMP levels and phenotype is discussed in Chapter 5.

3.1.3. The *Bdellovibrio* EAL domain protein Bd1971

3.1.3.1. Bd1971 structure

The *Bdellovibrio bacteriovorus* HD100 genome encodes one EAL domain phosphodiesterase (PDE) protein Bd1971. Bd1971 consists of an EAL domain but also has a cNMP (cyclic nucleotide) binding domain (predicted by SMART) Figure 3.1, which we postulate can activate its EAL activity. The Bd1971 cNMP binding domain is predicted to bind adenosine 3',5'-cyclic monophosphate (cAMP) (Basford, 2015). This suggests that the interaction of cAMP with Bd1971 allows the integration of two signalling pathways..

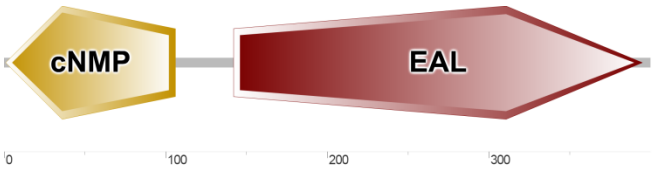

Figure 3.1 : Predicted domains of *B. bacteriovorus* HD100 EAL Bd1971 protein Predicted using SMART sequence analysis tool. The cNMP domain is predicted to bind cAMP and EAL domain degrades c-di-GMP.

3.1.3.2. Gene deletion of *bd1971*

Work on Bd1971 was started in the Sockett lab by Rashidah Ahmad and Rowena Fung for their Masters projects (Ahmad, 2007; Fung, 2008). From their work a kanamycin cassette Bd1971 deletion strain was obtained, this strain could grow via HI or HD growth and formed 'rafts' of aggregated cells in liquid culture. The cause of the aggregation is thought to be due to the elevated levels of c-di-GMP that were shown by Dr Basford to be present in the HI mutant Δ*bd1971*Kan (Basford, 2015). These high levels of c-di-GMP could be causing the biofilm like phenotype in the EAL mutant. Recently a silent Δ*bd1971* strain has been made by Rob Till and preliminary analysis of the phenotype is detailed in chapter 5.

3.1.3.3. Bd1971 protein interaction studies

Further work by Dr Basford suggested Bd1971 interacts with degenerate GGDEF Bd3125 by B2H assays. This interaction had a slightly increased strength when Bd3125 was tested with the cNMP N terminus of Bd1971. She proposed that the Bd3125 interaction with the cNMP domain may block cAMP binding (Basford, 2015).

Bd1971 expression was evaluated via RT-PCR and is constitutive throughout the predatory cycle. Dr Basford also did preliminary analysis of the varied location of Bd1971-mCherry fluorescence throughout the HD predatory cycle and in HI cells and which showed it mostly located throughout the cell.

The current data available about Bd1971 begins to give an indication of its structural nature, its molecular function, the potential protein interaction network and location of its action in the *Bdellovibro* cell. However work is ongoing in the Sockett lab and in this study to full characterise the role of Bd1971 in life cycle of *Bdellovibrio*.

3.1.4. The degenerate diguanylate cyclase of *Bdellovibrio* Bd3125

Bd3125 has a degenerate GGDEF motif (DVNEF) this protein is unable to make c-di-GMP but can bind it through the conserved RxxD I site, suggesting this protein acts as a c-di-GMP receptor (Hobley et al, 2012). The deletion of *bd3125* results in a slower entry speed into prey cells and the mCherry location of Bd3125 is found to be at the predatory pole of the attack-phase *Bdellovibrio* cell (Hobley et al, 2012). Work by Dr Milner showed that Bd3125 interacts with a complex of predatory proteins at the predatory pole of *Bdellovibrio*, Bd3125 interacted with RomR and TPR protein Bd2492 see Figure 3.2 (Milner et al, 2014). The c-di-GMP receptor function of Bd3125 allows a c-di-GMP signalling input into the process of predation. Additionally as previously mentioned Dr Basford discovered Bd3125 interacted with the c-di-GMP component protein Bd1971 PDE, so may be part of an extended protein network regulating c-di-GMP levels at the predatory pole in order to control the predation process.

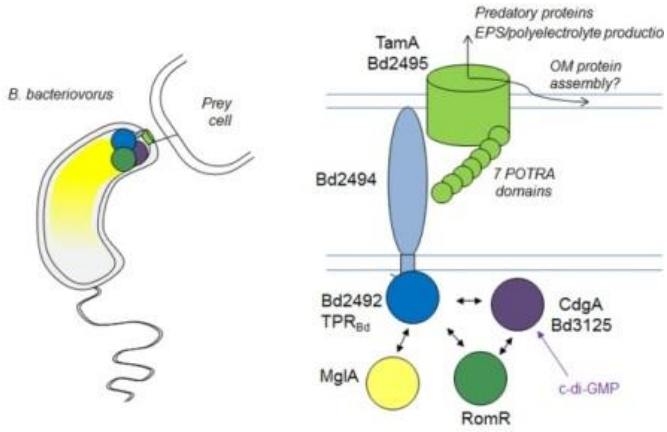

Figure 3.2 Interactions of Bd3125 at the predatory pole of *Bdellovibrio* Figure taken from (Milner et al, 2014). Bd3125 interacts with RomR and Bd2492 and is only located at the predatory pole. These proteins make up a predatory hub involved in predation.

3.1.5. Achieving specificity of c-di-GMP signalling by direct protein interactions

Bacterial cells cope with numerous c-di-GMP signalling systems happening in parallel to each other, how this signalling is kept to a specific cascade has become a growing field of investigation. From these investigations evidence for local c-di-GMP signalling by specific DGCs and PDEs that operate on separate targets with little or no cross talk have been found (Dahlstrom et al, 2015; Hobley et al, 2012; Lindenberg et al, 2013).

One way that this local model can operate is by direct protein-protein interactions or functional sequestration, where these physical interactions can aid in mediating parallel

the signalling outcomes without cross talk (Dahlstrom et al, 2015; Hengge, 2009; Lindenberg et al, 2013).

In this study the above model by which c-di-GMP signalling specificity is achieved by physical interaction or sequestration is of particular interest. As in *Bdellovibiro* single gene deletions of three DGC proteins results in three clear phenotypes this suggests a c-di-GMP control cascade with local and specific signalling (Hobley et al, 2012).

An example of functional sequestration where a protein complex has differing roles depending on the local c-di-GMP levels, was studied by (Lindenberg et al, 2013). This system was studied in *E.coli* and consists of 2 c-di-GMP modules, Module 1 contains YegE (DGC) and YhjH (PDE) and Module 2 contains YdaM (DGC) and YciR (PDE) see Figure 3.3. Module 1 controls the c-di-GMP that is sensed and degraded by the PDE YciR. YciR acts a bifunctional trigger enzyme and has a role additional to PDE function, this is to directly inhibit YdaM (DGC) and MlrA. When YciR is active as a PDE due to high cellular c-di-GMP levels the inhibition on YdaM (DGC) and MlrA is relieved. When YdaM (DGC) is not bound to YciR (PDE) its DGC activity is activated, contributing to the c-di-GMP pool produced by Module 1 and it can also activate MlrA by direct interaction. MlrA in turn regulates transcription of *csgD* which is essential for production of amyloid curli fibre in the biofilm matrix (Lindenberg et al, 2013).

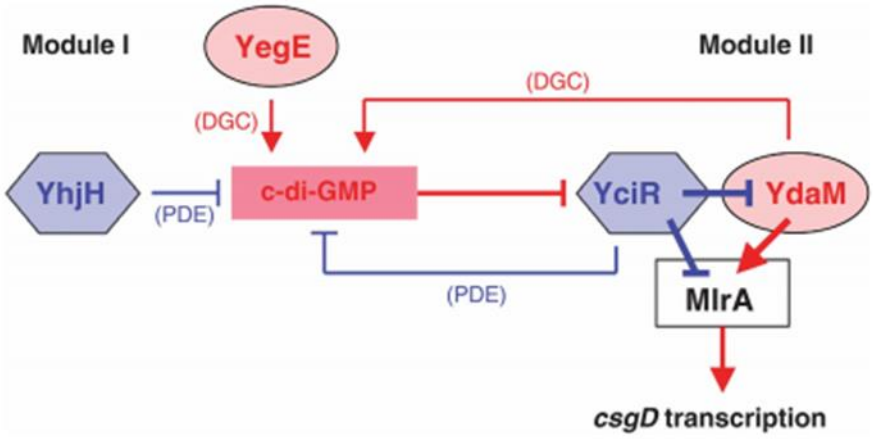

Figure 3.3 Model of csgD c-di-GMP signalling. Figure taken from Lindenberg et al 2013. Module I control the c-di-GMP level that is then degraded by the PDE YciR, which together with the DGC YdaM constitutes module 2. YciR is also trigger enzyme whose secondary activity is the direct inhibition of YdaM and MlrA. The inhibition is relieved when YciR is active as a PDE. DGCs are indicated by ovals and PDEs by hexagons. DGCs and high c-di-GMP-driven processes are shown in red, and PDEs and processes occurring at low c-di-GMP levels are shown in blue.

Lindenberg et al investigated the location of these direct protein interactions further by splitting the proteins of interest in to specific domains and testing the interactions by B2H assays seen in Figure 3.4. This allowed interactions to be assigned to specific domains (Lindenberg et al, 2013).

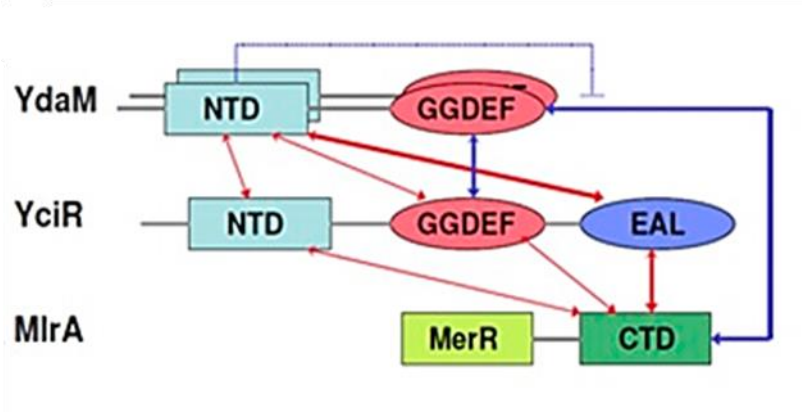

Figure 3.4 Modular *csgD* c-di-GMP interactions network mediated by direct protein interactions. Figure taken from Lindenberg et al 2013. The thickness of the line represents the strength of the interaction and the blue lines show conditional interactions that are only observed in the split domain constructs. For example the c-di-GMP producing domain of YdaM can make a direct contact with the putative ligand-binding domain of MlrA (CTD).

This implies that DGC proteins are not just a simple c-di-GMP releasing system that acts globally but a more nuanced system acting locally relying on additional macromolecular interactions.

However the purpose of multiprotein complexes containing c-di-GMP related proteins is not always linked to modulating the cellular c-di-GMP levels. An example of a multiprotein complex that forms independently of its enzymatic activity is shown by Ryan and co-workers in *Xanthomonas campestris* (Ryan et al, 2012). The physical interaction between RpfG and two GGDEF domain proteins were shown to control motility (Ryan & Dow, 2010). The process of this interaction is as follows, the diffusible signal factor (DSF) binding may cause auto phosphorylation of histidine kinase RpfC. This phosphorylation results in phosphotransfer to RpfG (RR and HD-GYP domain protein). Once RpfG is phosphorylated it interacts with two GGDEF domain proteins, this interaction was confirmed by yeast two hybrid, FRET and Far Western blotting and the location of the interaction site was also examined (Ryan et al, 2012). When this multi-protein complex is established it can recruit the PilZ protein XC_2249 which then interacts with PilT and PilU pilus motor proteins (see Figure 3.5)(Ryan et al, 2012). The

importance of the enzymatic function of the c-di-GMP components on the interactions was examined by mutating the active site or c-di-GMP binding site on the proteins of interest. Addition of these enzymatic mutations to gene deletion strains restored motility, indicating that the output of this multi-protein complex is independent of the proteins enzymatic, c-di-GMP function. This indicates that that these proteins may have dual functions, one which modulates pilus function and motility via the protein interactions formed in the complex that does not require proteins to be enzymatically active, and an unknown function which does require the regulatory modulation of varying c-di-GMP levels yet to be discovered.

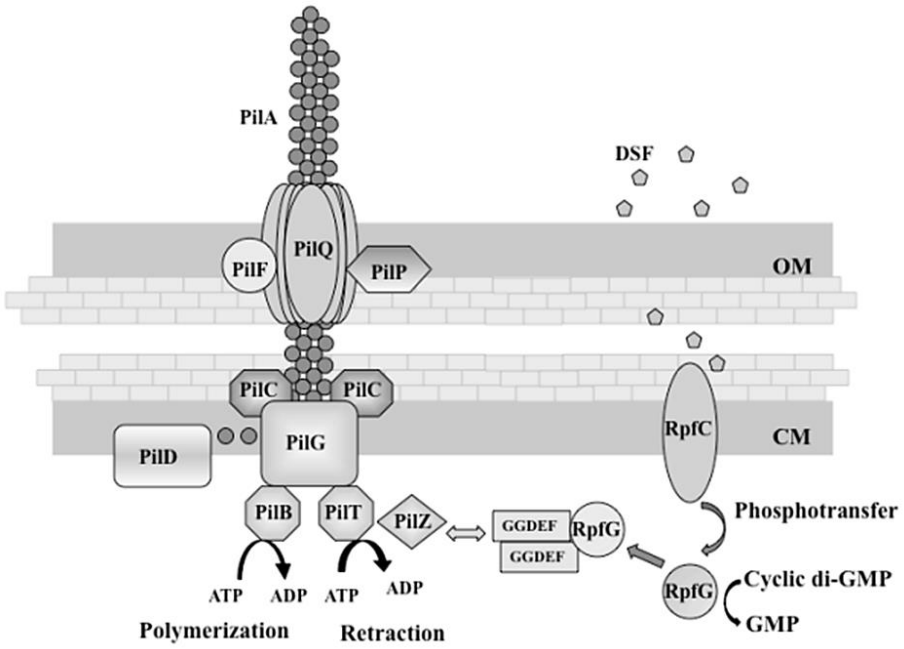

Figure 3.5 Protein interactions between c-di-GMP related components in *Xanthomonas campestris*. Figure reproduced from (Ryan et al, 2012) showing the protein interactions which lead to modulated pilus function and hence motility.

Both examples show how direct protein-protein interactions can be used to produce specific molecular outputs. In this study I aimed to identify part of the signalling network that regulates the enzymatic function of Bd0367 or a protein network that mediates a role independent of the enzymatic function of Bd0367. The examination of this interaction network from Bd0367 may show the cascade of events that lead to outputs such as successful bdelloplast exit and implementation of gliding motility.

3.1.6. Background to the work presented in this chapter

3.1.6.1. Previous protein interactions with c-di-GMP components in the Sockett Lab

At the same time that I was investigating B2H interactions with Bd0367, a PhD student Dr Basford was doing similar investigations using Bd1971 and Bd3125, when interactions were found between these two (Bd1971, Bd3125) and Bd0367 by spot plate analysis but not by her preliminary β-galactosidase analysis I took over the investigation and found interactions detailed in sections 3.4.3.and 3.4.4.

3.2. Specific Research Aims

- To assess the self-interaction of Bd0367 by testing dimer formation by B2H and β-galactosidase assays.
- To investigate if Bd0367 is phosphorylated or un-phosphorylated in the B2H expression system by examining the dimerization strengths between a WT Bd0367 construct and a predicted non-phosphorylatable mutant Bd0367D63A via β-galactosidase assays.
- To assess the interaction between EAL protein Bd1971 and RR/DGC subdomains of DGC protein Bd0367 via B2H and further quantify the previously discovered full length interaction by β-galactosidase assays.
- To assess the interaction between subdomains of EAL protein Bd1971 with the full length and subdomains of DGC protein Bd0367 via B2H and quantify by β-galactosidase assays.
- To assess the dimerization interaction of Bd1971 by B2H assay and to quantify by β-galactosidase assays.
- To analyse the location and intensity of Bd1971-mCherry protein when incubated on a surface by examining the fluorescence.
- To assess the interaction between degenerate GGDEF protein Bd3125 and protein subdomains of DGC protein Bd0367 via B2H and further quantify the previously discovered full length interaction by β-galactosidase assays.
- To assess the self-interaction of Bd3125 by B2H assay and to quantify by β-galactosidase assays.
- To investigate the location of Bd3125-mCherry protein in an in-frame deletion strain of Δ*bd0367* by examining fluorescence profile.

- To analyse the location and intensity of Bd3125-mCherry protein when incubated on a surface by examining the fluorescence.
- To try and develop a method to pull out native interacting protein partners of Bd0367, using Bd0367-His protein purified in *E.coli*, attached to beads and incubated with sonicated HD100 attack phase culture.
- To assess the interaction found by the Bd0367-His pull down by B2H analysis and quantify the interaction by β-galactosidase assays.

3.3. Hypotheses

- Bd0367 will weakly dimerize as the cognate kinases predicted to phosphorylate the protein and promote dimerization is not likely to be present in *E.coli BTH101* strain.
- Bd0367 and Bd1971 will interact and will have a preferential interaction site located on one domain of Bd0367. This will suggest if Bd1971 plays a regulatory role in the activity of Bd0367.
- Bd0367 will interact specifically with one domain of Bd1971 aiding the investigation of the specific interaction site. Bd197-mCherry intensity or location will alter to suggest a role for Bd1971 in gliding motility.
- Bd1971 will interact as a dimer by B2H as structural studies by Dr Lovering at University of Birmingham suggest.
- Bd0367 and Bd3125 will interact. This could suggest that c-di-GMP produced by Bd0367 is directly transferred to Bd3125 (degenerate GGDEF acting as an effector protein) to mediate a specific signal.
- Bd3125 will interact as a dimer by B2H assays due to the degenerate GGDEF structure.
- Bd0367 may be involved in aiding localisation of its interacting partners, in the HI *bd0367* deletion strain mCherry-tagged interacting proteins Bd3125 may be visualised in altered locations to WT HI strain.
- Bd3125-mCherry fluorescence location and intensity will likely not alter on surface incubation due to the previously determined role for Bd3125 in predation.

- The interaction pull down assay will identify unknown partner proteins and may confirm interactions that have already been investigated by B2H analysis. Unknown partner proteins may be involved in gliding motility or bdelloplast exit.

3.4. Results

3.4.1. Investigating the dimerization interaction of Bd0367 construct in wildtype and non-phosphorylated forms by B2H assay

Many proteins interact with themselves in order to self-associate and form higher order aggregates such as dimers, trimers etc. This self-association can enable proteins to have different functionality in monomer vs dimer confirmation. DGCs are active upon dimerisation (Chan et al, 2004; Schirmer & Jenal, 2009). RR domains also have a role in dimerization and commonly phosphorylation can stimulate the dimerization and trigger conformational change that can alter for example enzymatic activity (Paul et al, 2007).

B2H analysis (see section 2.8.1) in an adenylate cyclase negative BTH101 *E.coli* was used to test this interaction (Karimova et al, 1998). The genes were cloned into plasmids pUT18c and pKT25 which tagged the N terminus of the proteins with the T18 or T25 sections of adenylate cyclase. The tagged constructs of Bd0367 were cloned by Dr Milner and Rob Till. The *bd0367* construct was cloned from base 34 as the HD100 genome start site was compared with *B. bacteriovorus Tiberius* genome and with RNA sequencing data (section 8.3.1.1) for Bd0367, predicting this as the correct start site and that HD100 annotation is incorrect. If the test proteins interact the T25 and T18 fragments are brought together and reform adenylate cyclase, cAMP causes the expression of the LacZ reporter gene, this results in blue colonies on plates containing X-gal see Figure 3.6.

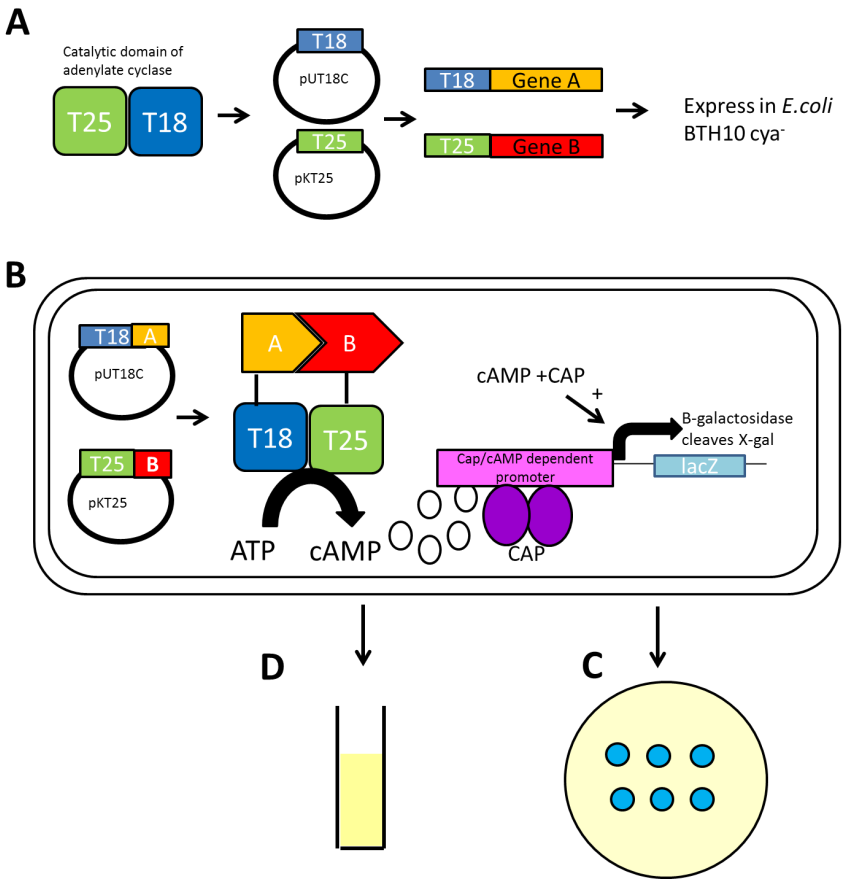

Figure 3.6 Illustration of B2H assay. (A) The catalytic domain of adenylate cyclase is split into T25 and T18 these fragments are expressed in the plasmids pUT18C and pKT25, genes of interest can be cloned into these plasmids to investigate protein interactions. (B) If the two fragments of adenylate cyclase are fused to proteins which interact, the two fragments are brought into close proximity and the two fragments can reform the catalytic site of adenylate cyclase. This allows the production of cAMP from ATP. When cAMP is present in the cell, the messenger interacts with the Catabolite Activator Protein (CAP) and promotes the binding of RNA Polymerase to the promoter of the lacZ reporter gene. The lacZ gene encodes β-galactosidase which cleaves the X-gal present in the Nutrient Agar plates on which the colonies are grown on. (C) This cleavage reaction turns the bacterial colonies blue therefore this provides a colorimetric assay to assess protein interactions, where positive interactions result in blue colonies and negative interactions result in white colonies. (D) Liquid β-galactosidase assay uses ONPG (ortho-nitrophenyl β-D-galactopyranoside) which is an artificial substrate of β-galactosidase; the colourless ONPG is cleaved by β-galactosidase to produce yellow ortho-nitrophenol (ONP) which is measured by spectrophotometry.

3.4.1.1. The Bd0367 full length WT construct interacts significantly with itself

The result of a typical B2H assay between the self-interaction of Bd0367 is shown in Figure 3.7. The self-interaction consistently produced blue spots indicative of a positive interaction.

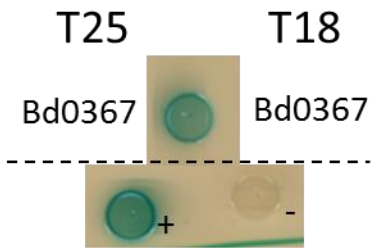

Figure 3.7 Spot plate of Bd0367 self-interaction. A Blue spot suggests an interaction between Bd0367 and Bd0367. Results displayed are a typical representation of the results of three biological repeats with nine technical repeats. Positive (+) = pUT18c-zip with pKT25-zip. Negative (-)= pUT18c with pKT25.

The B2H spot plate analysis allows for a qualitative assessment of the interaction between Bd0367 and itself. Further testing of this interaction was carried out by β-galactosidase assays, these assays were used to quantify the strength of the interaction between the two proteins Figure 3.8. The WT DGC protein Bd0367 interacted significantly with itself however the interaction strength observed was not as high as other self-interacting proteins seen later in this chapter. Suggesting that Bd0367 may be un-phosphorylated in the B2H system.

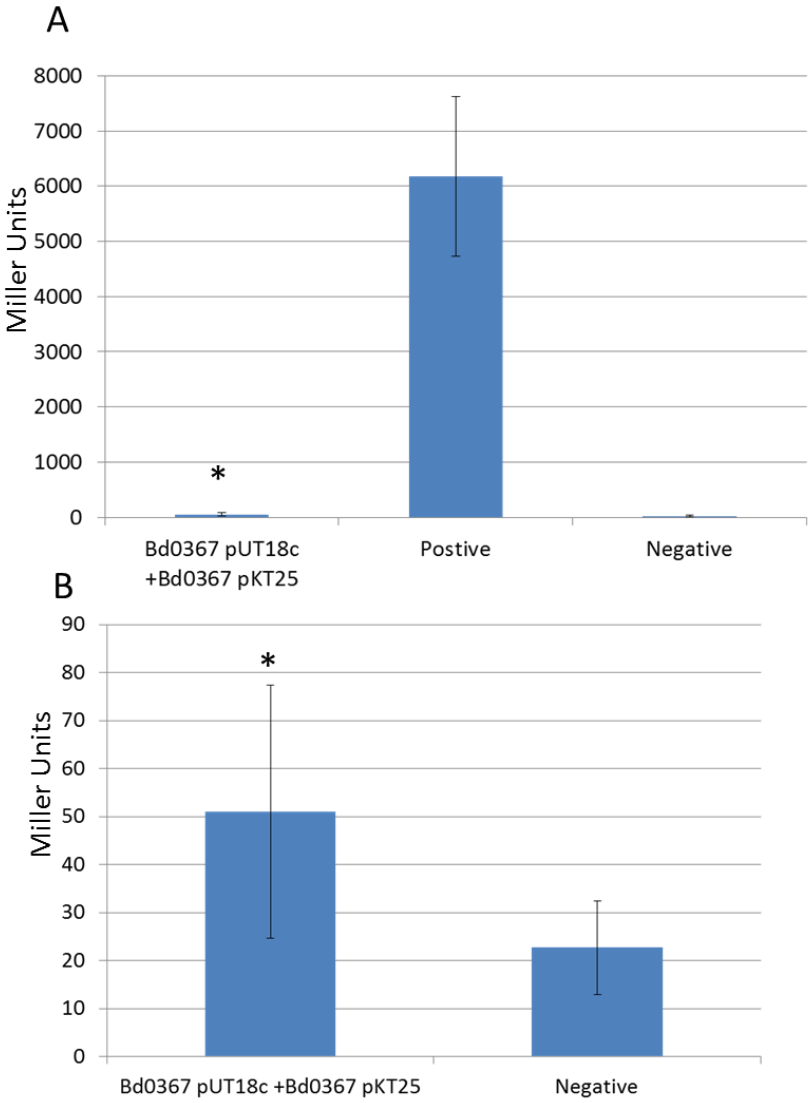

Figure 3.8 β-Galactosidase activity assay for Bd0367-Bd0367 self-interactions. Error bars show standard deviation. The results show the mean value from 3 biological repeats and comprise a total of 6 technical repeats. Bd0367 interacts significant with itself when compared to the negative control. Asterisks show significance of Student t-test compared to the negative (pUT18c, pKT25) *≤0.05

3.4.1.2. Investigation of the Bd0367 dimerization strength when using a predicted non-phosphorylatable mutant.

To determine the reason for the lower than expected dimerization interaction strength a non-phosphorylatable mutant of Bd0367 was made. As Bd0367 has a RR domain, it also has a conserved aspartate Aspartate residue at position 63 which is phosphorylated by a specific kinase (Hobley et al, 2012).

The phosphorylation site was identified by putting the RR domain through protein annotation resource CDD (conserved domains output) (see Figure 3.9) and by protein alignments (Marchler-Bauer et al, 2015). The phosphorylation state of Bd0367 may have effects on its conformation. These conformational changes may promote dimerization, enzymatic activity and possibly alter interactions with partner proteins. To test this the Aspartate 63 was mutated to an Alanine in the full length Bd0367 B2H construct (Bd0367D63A) as it was anticipated that this would remove phospho-receiver functionality without affecting structure. This mutation means that the self-interaction of the non-phosphorylated version of Bd0367 can be examined and compared with the strength of WT Bd0367 self-interaction.

Figure 3.9 Bd0367 Phosphorylation site identified by CDD search as amino acid 63. (Marchler-Bauer et al, 2015)

3.4.1.3. The predicted non-phosphorylatable Bd0367 self-interaction is not significantly different from that of the WT Bd0367 self-interaction.

The result of a typical B2H assay between the self-interaction of the WT Bd0367and predicted non-phosphorylatable Bd0367D63A is shown in Figure 3.10. Both self-interactions consistently produce blue spots indicative of a positive interaction.

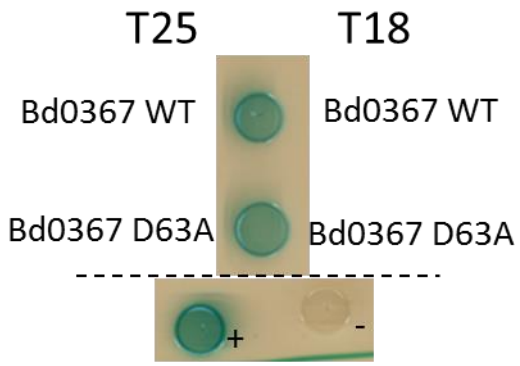

Figure 3.10 Spot plate of WT Bd0367and Bd0367D63A self-interactions. Blue spots suggests an interaction between Bd0367D63A and Bd0367D63A. Results displayed are a typical representation of the results of three biological repeats with nine technical repeats. Positive (+) = pUT18c-zip with pKT25-zip. Negative (-)= pUT18c with pKT25.

Further testing of this interaction was carried out by β-galactosidase assays Figure 3.11. From these liquid assays there is no significant difference between the Bd0367WT self-interaction and the Bd0367D63A self-interaction. This suggests that Bd0367WT is in a non-phosphorylated state in the B2H expression system BTH101.

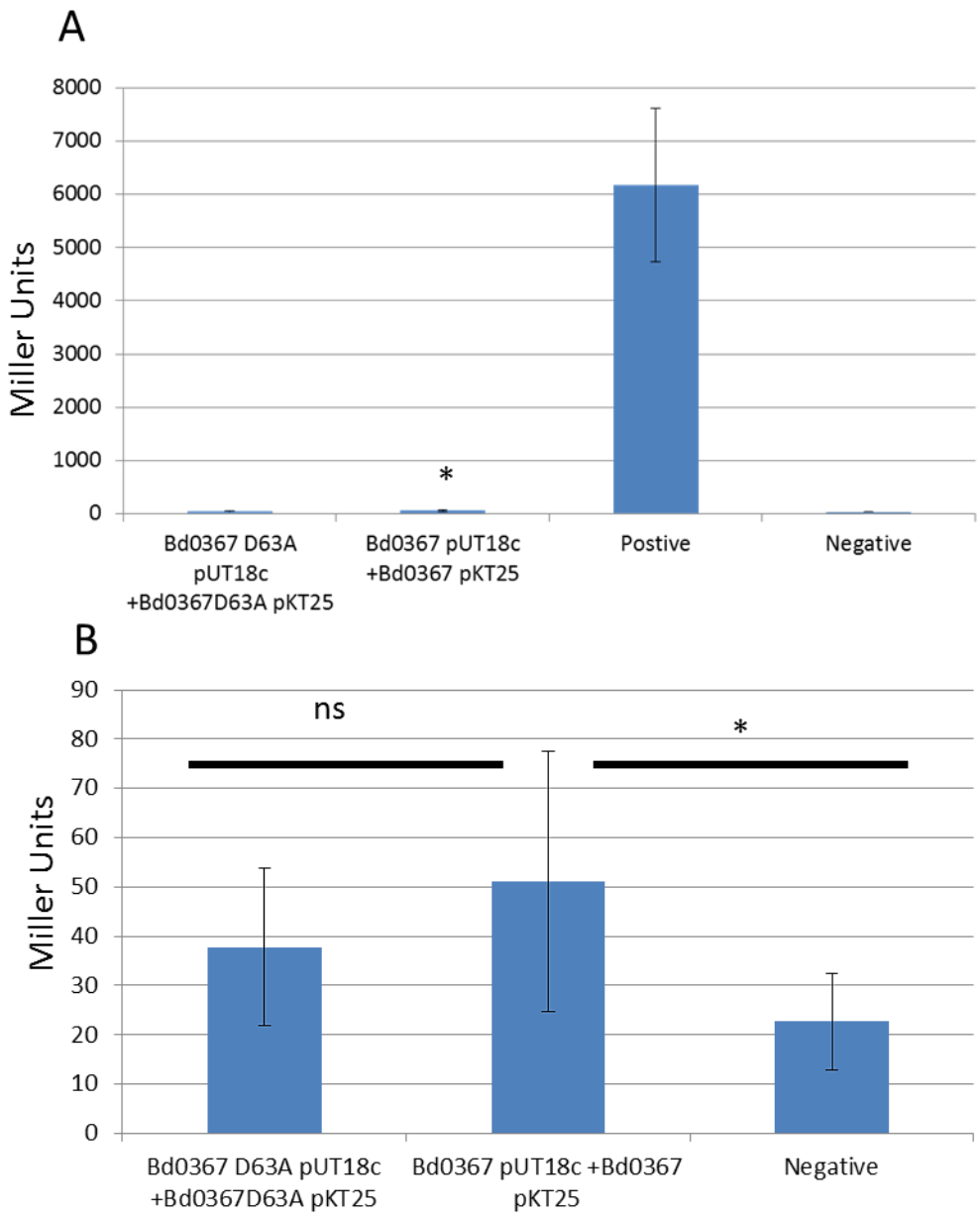

Figure 3.11 β-galactosidase activity assay to compare Bd0367D63A self-interactions with Bd0367WT self-interaction strengths. Error bars show standard deviation. The results show the mean value from 3 biological repeats and comprise 6 technical repeats. (A) shows the Miller units for the Bd0367 self-interactions with both the positive and negative controls. (B) This graph allows better observation of the similarity of the Bd0367WT and Bd0367D63A self-interactions compared to that of the negative control. Bd0367WT interacts significant with itself when compared to the negative control. However the Bd0367WT interaction strength is not significantly

different from the Bd0367D63A self-interaction strength. Asterisks show significance of Student t-test compared to the negative (pUT18c, pKT25) *≤0.05

This result led to the assumption that the interactions demonstrated later in the chapter are occurring with the non-phosphorylated, probably enzymatically inactive version of Bd0367.

3.4.2. Confirming interactions between DGC protein Bd0367 and other c-di-GMP components

Due to the increasing evidence that many DGC and PDE proteins are regulating more than just c-di-GMP turnover through protein interactions and multiprotein complexes (Lindenberg et al, 2013; Ryan et al, 2012) members of the Sockett lab began to investigate protein interactions between the multiple c-di-GMP components of *Bdellovibrio* via B2H assays. These interaction studies led to promising results and my study continues this B2H work and advances it through the use of split domains as previously presented in (Lindenberg et al, 2013).

PhD student Dr Basford, discovered that Bd3125 (degenerate GGDEF) and Bd1971 (EAL) interacted via B2H assay. Bd1971 was also found to interact with Bd0367 however this interaction was not upheld in her preliminary β-galactosidase assays showing no interaction between the EAL domain protein and Bd0367 (Basford, 2015). After this she tested Bd3125 with Bd0367, she found positive interactions between Bd3125 and Bd0367 through B2H spot plate analysis. Her preliminary data obtained from β-galactosidase assays showed Bd3125 and Bd0367 had highly variable interaction strength so was not found to be significant.

The putative interaction discovered between Bd1971-Bd0367 and Bd3125 –Bd0367 are further investigated in this study, qualitatively and quantitatively by B2H and β-galactosidase assays.

3.4.3. Investigating the nature of the protein interaction between Bd1971 (PDE) and Bd0367 (DGC)

As DGC protein Bd0367 can produce c-di-GMP it seemed possible that forming an interaction with a PDE which degrades c-di-GMP may allow fine tuning regulation to control c-di-GMP levels. This may be achieved by the EAL protein binding causing the DGC protein to become inactive as demonstrated by (Lindenberg et al, 2013). Or the

interaction may create a protein complex that recruits a specific PilZ domain protein for a particular molecular output as demonstrated by Ryan and co-workers (Ryan et al, 2012).

Bd1971 was cloned into plasmids pUT18c and pKT25 which tagged the N terminus of the proteins with the T18 or T25 sections of adenylate cyclase. The tagged constructs of Bd1971 were cloned by Dr Basford (Basford, 2015).

3.4.3.1. Full length Bd0367 interacts with Bd1971 via B2H spot plates

The result of a typical B2H for Bd1971 with full length Bd0367 (Bd0367full) is shown in Figure 3.12. Bd1971 when tested with Bd0367 consistently produced uniform blue spots in both orientations tested indicative of a positive interaction.

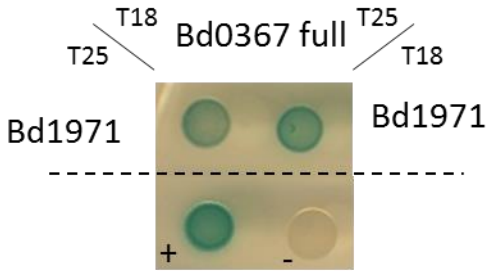

Figure 3.12 Spot plate interactions GGDEF protein Bd0367 with EAL protein Bd1971. Blue spots suggests an interaction between Bd0367 and Bd1971 in both orientations. Results displayed are a typical representation of the results of five biological repeats with 15 technical repeats. Positive (+) = pUT18c-zip with pKT25-zip. Negative (-)= pUT18c with pKT25.

Further testing of this interaction was carried out by β-galactosidase assays, Figure 3.13 these assays were used to quantify the strength of the interaction between the two proteins. From these results Bd0367 and Bd1971 do not appear to interact significantly more than the negative control. This was an unexpected result, however the consistent results obtained from the spot plate analysis led this study to analyse this possible interaction further, by splitting the two domains of Bd0367.

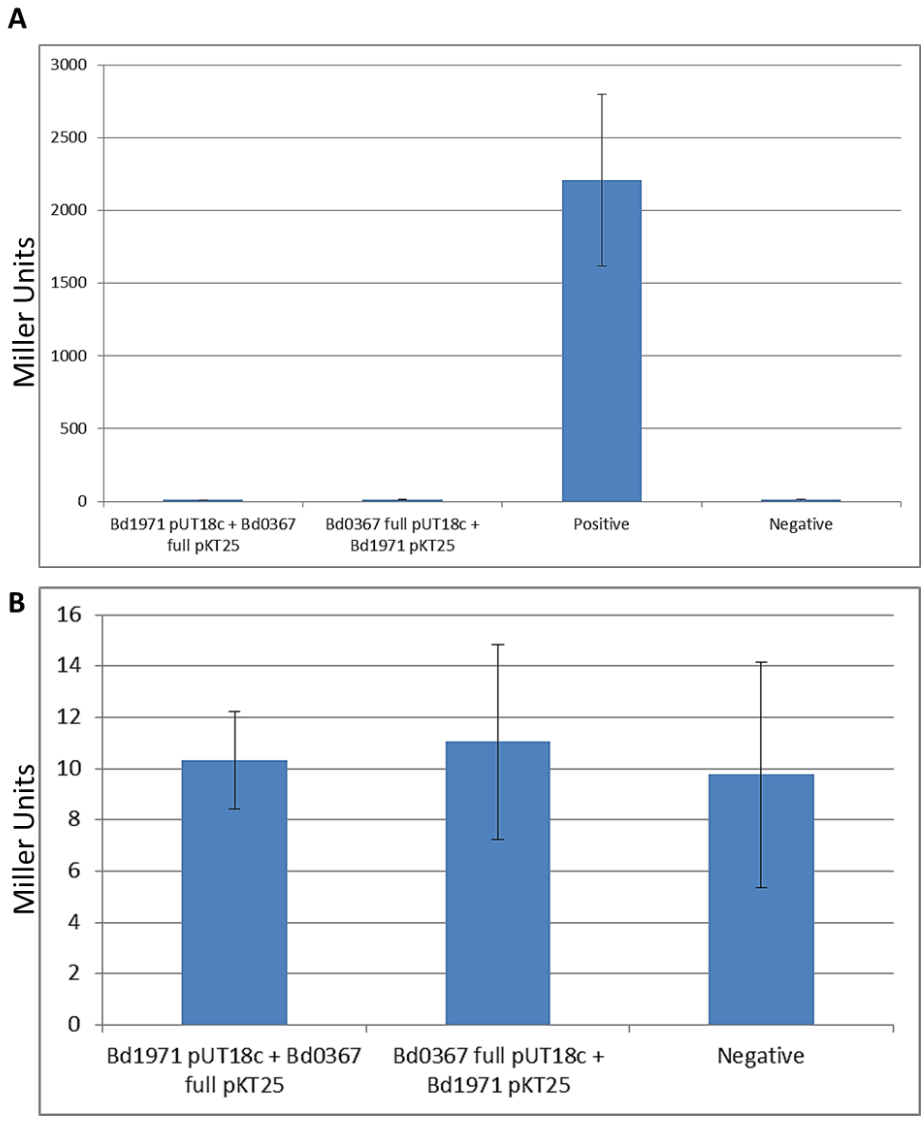

Figure 3.13 Full length Bd0367 and Bd1971 do not significantly interact by β-galactosidase activity assay. Error bars show standard deviation. . The results show the mean value from five biological repeats and comprise 10 technical repeats. (A) shows the Miller units for the Bd0367-Bd1971 interaction with both the positive and negative controls. (B) This graph allows better observation of the similarity of the Bd0367-Bd1971 interaction to that of the negative control.

3.4.3.2. Investigation of Bd0367 split domain protein interactions

Bd0367 has two distinct domains, an N terminal RR domain and a C terminal DGC domain joined by a linker region. In this study B2H constructs were made that split this protein in two, Figure 3.14 . The cloned 'response regulator domain' (RR) was taken from amino acids 1 to139. This construct contains the response regulator domain, the linker region and the first 3 amino acids of the DGC domain. The cloned 'digunalyate cyclase domain' (DGC) comprises of amino acid 140 to the end of the protein (332), this domain is deficient in its first 3 amino acids of the DGC domain and contains the

unknown C terminal region. These constructs were used to further investigate the location of the Bd0367-Bd1971 interaction.

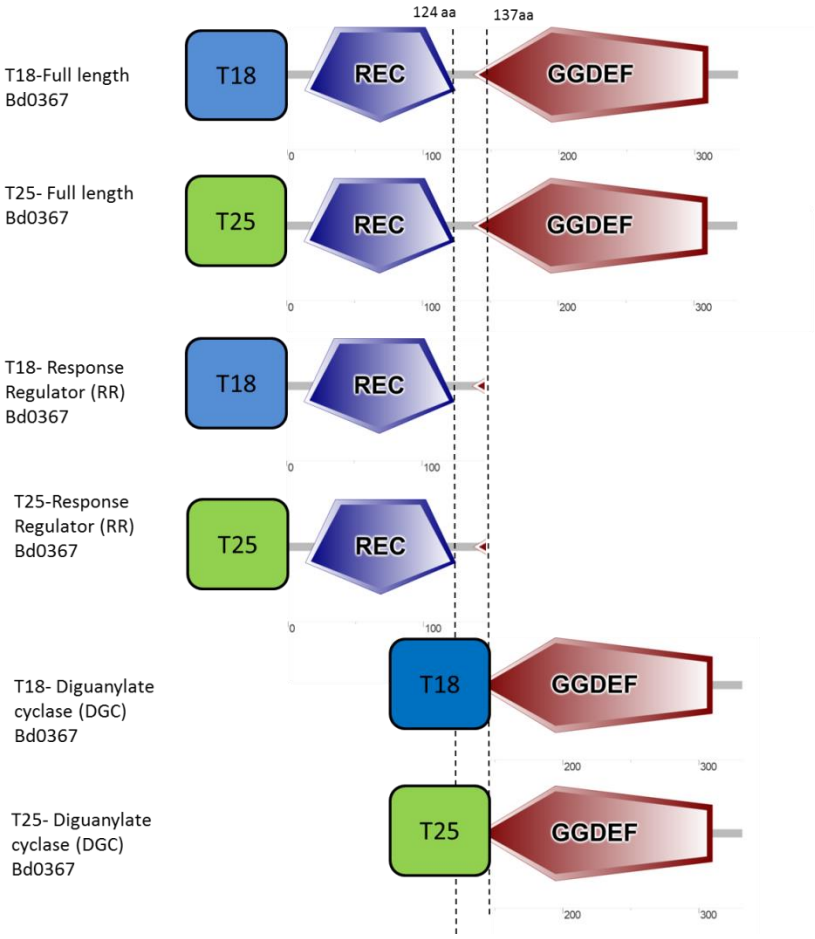

Figure 3.14 Illustration of the various Bd0367 constructs used in B2H analysis. The diagram shows the domains of Bd0367 as predicted by SMART, the dotted line demonstrated the amino acids at which the designated domain ends or started. The split domains of Bd0367 are split into the response regulator domain and the diguanylate cyclase domain.

3.4.3.3. Bd1971 does not interact with the DGC domain of Bd0367

The result of a typical B2H assay for Bd0367DGC and Bd1971 is shown in Figure 3.15. Bd0367DGC and Bd1971 consistently produced white spots in both orientations indicating no interaction between the two test proteins.

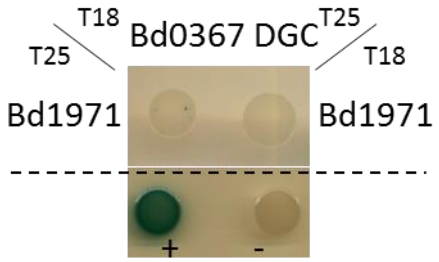

Figure 3.15 Spot plate interactions of split GGDEF protein Bd0367 DGC with EAL protein Bd1971. White spots suggest no interaction between the DGC fragment of Bd0367 and Bd1971 in either orientation. Results displayed are a typical representation of the results of three biological repeats with nine technical repeats. Positive (+) = pUT18c-zip with pKT25-zip. Negative (-)= pUT18c with pKT25.

Despite this negative result the interaction was further quantified for completeness via β-galactosidase activity assay. This confirmed that the interaction between Bd0367 DGC and Bd1971 was not significantly higher than the negative control, Figure 3.16.

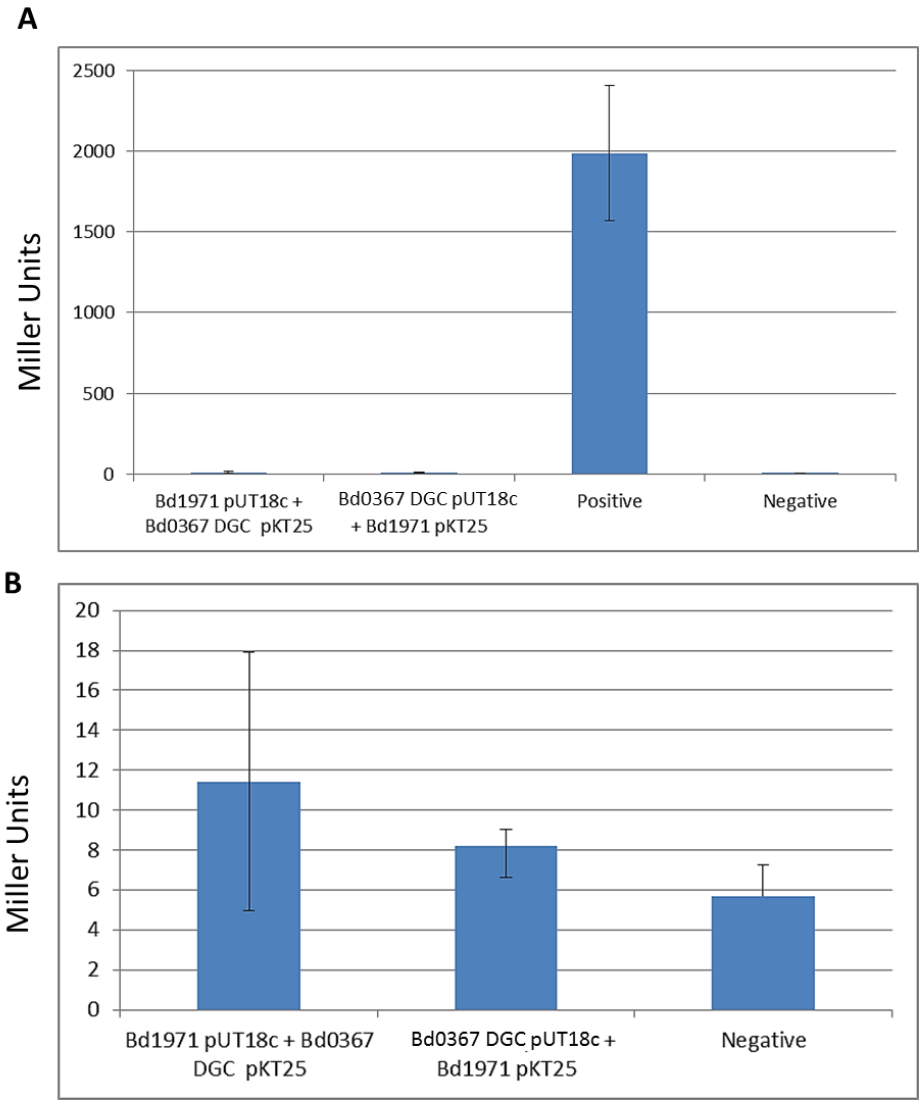

Figure 3.16 Split domain proteins Bd0367 DGC and Bd1971 do not significantly interaction by β-galactosidase activity assay for. Error bars show standard deviation. The results show the mean value from three biological repeats and comprise of six technical repeats. (A) Shows the Miller units for the Bd0367DGC and Bd1971 interactions with both positive and negative controls. (B) This graph allows easier observation of Bd0367DGC and Bd1971 interaction strengths, these are similar to the negative control.

3.4.3.4. Bd1971 interacts with the RR domain of Bd0367

The result of a typical B2H assay for Bd0367 RR and Bd1971 is shown in Figure 3,17. Bd0367 RR and Bd1971 consistently produced uniform blue spots in both orientations tested.

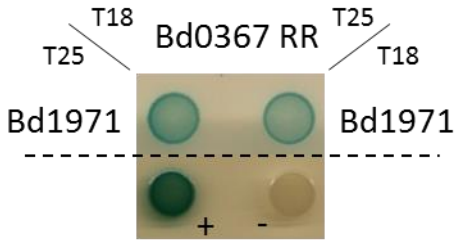

Figure 3.17 Positive spot plate interactions of split GGDEF protein Bd0367 RR with EAL protein Bd1971. Blue spots suggest an interaction between the RR fragment of Bd0367 and Bd1971 in both orientations. Results displayed are a typical representation of the results of four biological repeats with 12 technical repeats. Positive (+) = pUT18c-zip with pKT25-zip. Negative (-)= pUT18c with pKT25.

This positive interaction between Bd0367RR and Bd1971 was then quantified by β-galactosidase assays, see Figure 3.18. From these results Bd0367 RR and Bd1971 interact significantly more than the negative control in both orientations. Investigating the split domains of Bd0367 has allowed a dissection of the Bd1971- Bd0367 interaction, and allowed us to obtain a positive quantifiable interaction in liquid when the DGC domain of Bd0367 is not present.

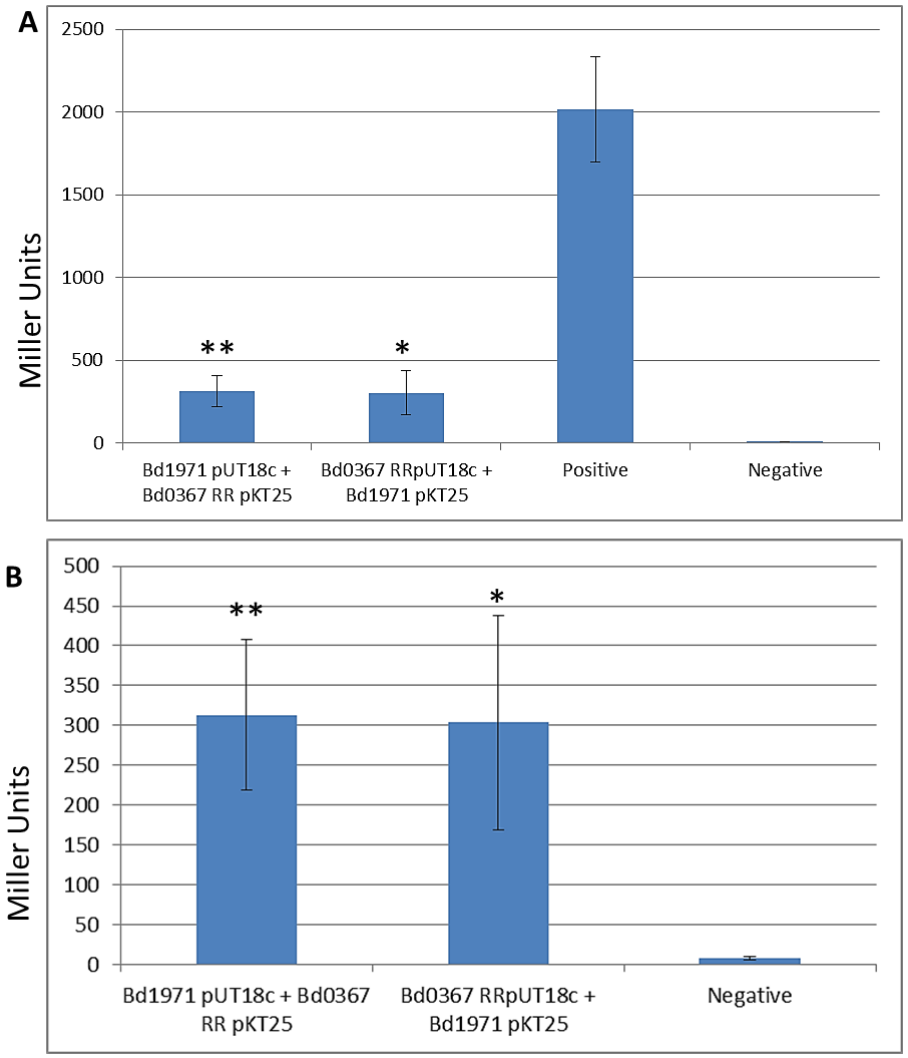

Figure 3.18 Split domain proteins Bd0367 RR domain and Bd1971 interacted significantly by β-galactosidase activity assay. Error bars show standard deviation. The results show the mean value from four biological repeats and comprise eight technical repeats. (A) shows the miller units for the Bd0367 RR and Bd1971 interaction with both the positive and negative controls. (B) This graph allows for better observation of the significant difference between Bd0367RR-Bd1971 (both orientations) from the negative control. Asterisks show significance of Student t-test compared to the negative (pUT18c,pKT25) *≤0.05 **≤0.01.

Due to the success of the Bd0367 RR domain interaction with Bd1971 it was decided to investigate the interaction location further. Rob Till had made Bd1971 split domain B2H constructs for a previous study. These were used to continue the investigation of the Bd0367-Bd1971 interaction.

3.4.3.5. Investigation of Bd1971 split domains interactions with Bd0367

Bd1971 has two distinct domains, an N terminal cNMP domain and a C terminal EAL domain joined by a linker region. B2H constructs were made that split this protein in two see Figure 3.19 . The cloned N terminal cNMP domain was taken from amino acids 1 to145. The cloned EAL domain comprises of amino acid 145 to the end of the protein (400).

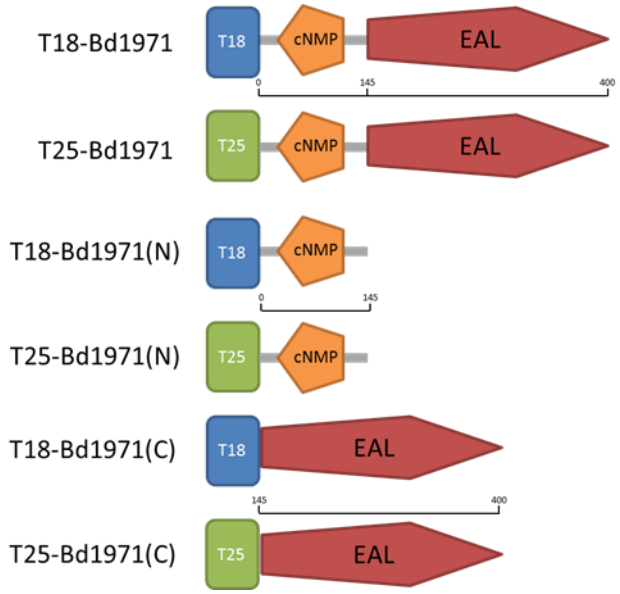

Figure 3.19 Illustration of the various Bd1971 constructs used in B2H analysis. This diagram was produced by Dr Basford to show how the domains of Bd1971were separated in split constructs (Basford, 2015).

3.4.3.6. The N and C terminal constructs of Bd1971 interact variably with full length Bd0367

The result of a typical B2H for full length Bd0367 and the two domains of Bd1971 is shown in Figure 3.20. Both the Bd1971 N terminal cNMP domain and C terminal EAL domain consistently produced blue spots when tested with Bd0367 in one orientation. This orientation was when Bd1971 was tagged with the T25 fragment. This suggests that splitting/truncating Bd1971 has had a slightly negative effect on the interaction between Bd1971-Bd0367.

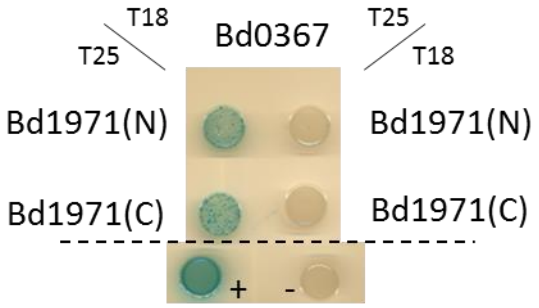

Figure 3.20 Spot plate interactions of split EAL protein Bd1971 with full length GGDEF Bd0367. White spots suggest no interaction between the N or C terminus of Bd1971 and Bd0367 when Bd1971 is T18 tagged. However both split domains of Bd1971 interact with Bd0367 when T25 tagged Results displayed are a typical representation of the results of three biological repeats with nine technical repeats. Positive (+) = pUT18c-zip with pKT25-zip. Negative (-)= pUT18c with pKT25.

Further testing of this interaction was carried out by β-galactosidase assays. From these liquid assays there is no significant difference in interactions between N or C terminal Bd1971 constructs and Bd0367 see Figure 3.21. This result is similar to the β-galactosidase assay result observed for full length Bd1971 and full length Bd0367, with a positive spot plate interaction but no interaction in the liquid assay.

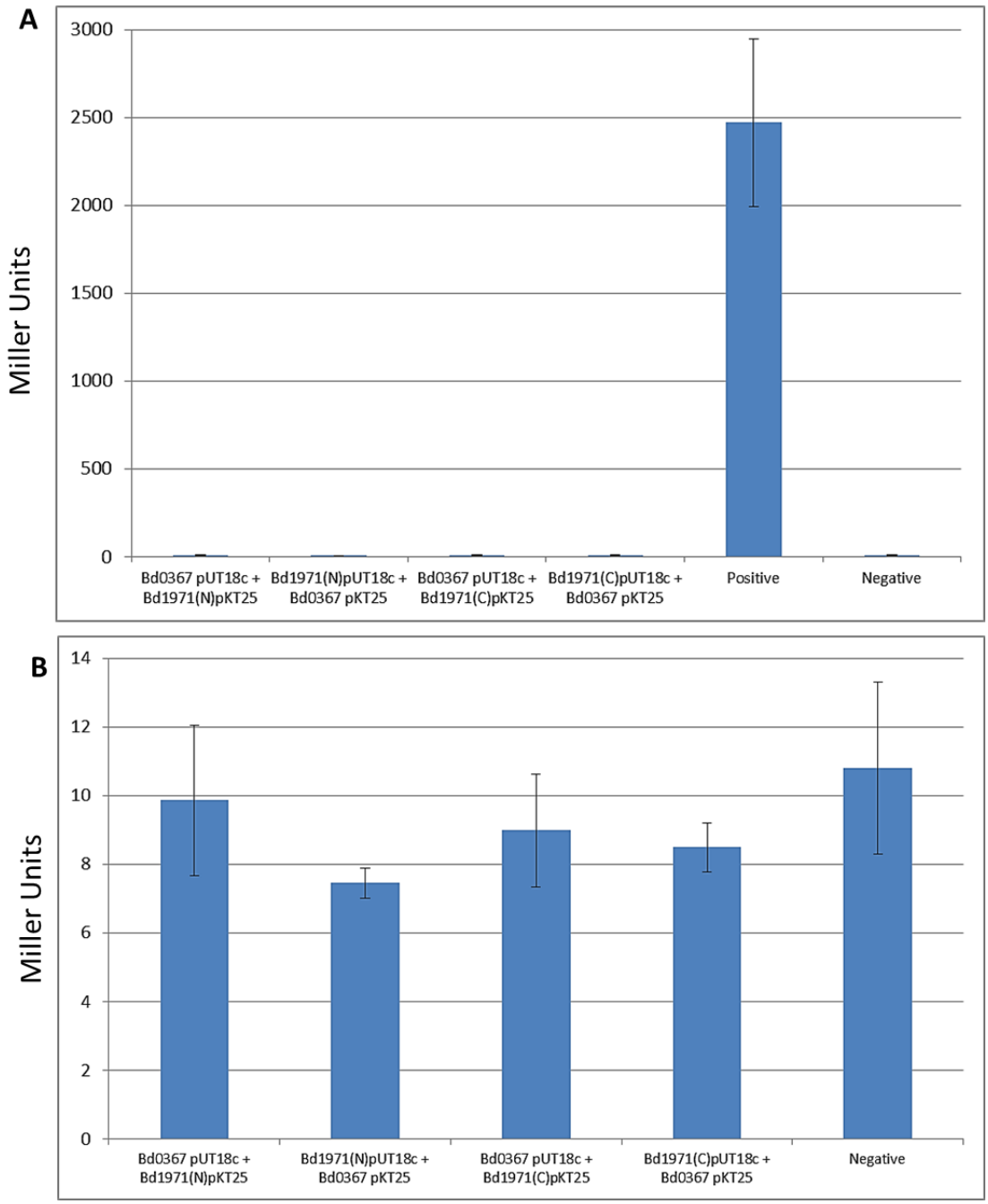

Figure 3.21 Bd0367 and split Bd1971 domains do not interact significantly by β-galactosidase activity assay. Error bars show standard deviation. The results show the mean value from two biological repeats and comprise four technical repeats. (A) shows the Miller Units for the Bd0367 and Bd1971 split domain interactions with both positive and negative controls. (B) this graph allows observation of the similar interaction strengths for the test interactions when compared to the negative control, indicating no interaction.

3.4.3.7. The C terminal construct of Bd1971 interacts more consistently than the N terminal construct with RR domain of Bd0367

The split domains of Bd1971 were tested against the RR domain of Bd0367. This was done as full length Bd1971 interacts more strongly with the RR domain Bd0367 than the full length Bd0367, so it was hypothesised that the interaction location may be easier to determine using the RR construct.

The result of a typical B2H for Bd0367 RR domain and the two domains of Bd1971 is shown in Figure 3.22.. The Bd1971 N terminal cNMP domain (T25) produced uniform blue spots when tested with Bd0367 RR in one orientation. Whereas the C terminal EAL domain produced uniform blue spots when tested with Bd0367 RR in both orientation. This may suggest a slightly stronger preference for Bd0367 RR to bind the C terminal EAL domain.

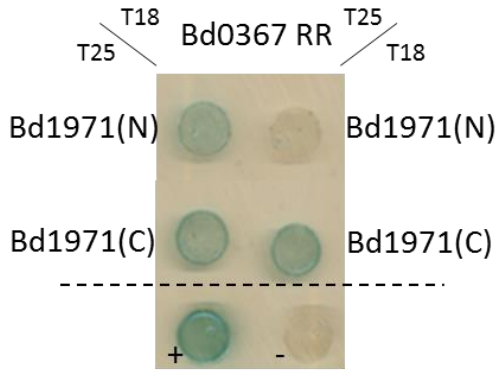

Figure 3.22 Spot plate interactions of Bd0367 RR domain with the split domains of Bd1971. Blue spots suggest an interaction between the C terminal (EAL) Bd1971 and the Bd0367 RR domain in both orientations tested. The Bd1971 N terminal construct has a positive interaction with Bd0367 RR when T25 tagged and a negative interaction when T18 tagged. Results displayed are a typical representation of the results from four biological repeats and 12 technical repeats. Positive (+) = pUT18c. Negative (-)=pKT25

Further testing of this interaction was carried out by β-galactosidase assays see Figure 3.23. From these liquid assays there is no significant difference in interactions between B1971N terminal cNMP domain and Bd0367 RR domain compared to the negative control. However the C terminal EAL domain Bd1971 with the T18 tag interacts with Bd0367RR significantly more than the negative control. The interaction strength observed was variable and weaker than the previously seen full length Bd1971-Bd0367RR interaction but may provide an indication of the location of the specific interaction pad.

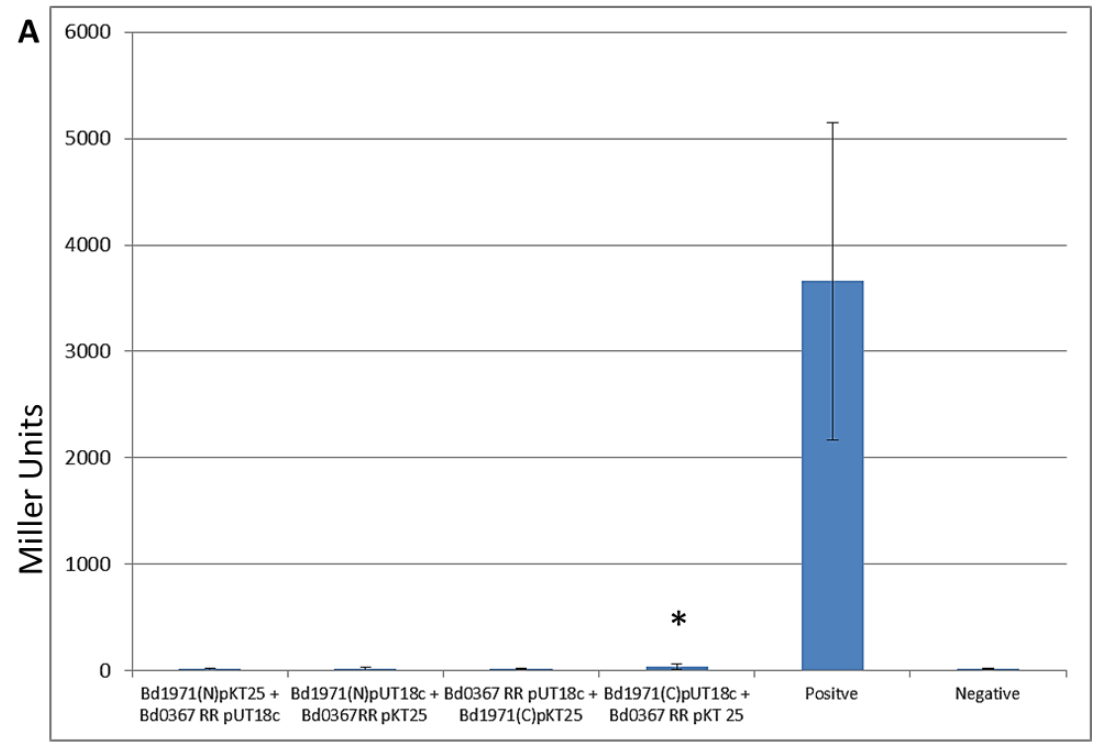

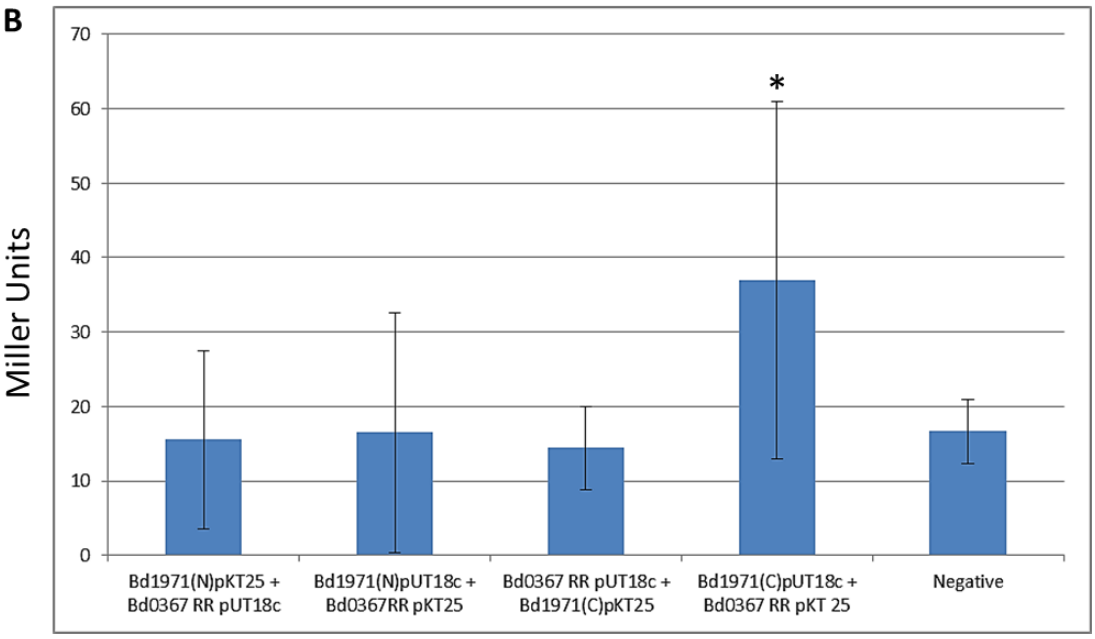

Figure 3.23 β-galactosidase activity assay for split domains of Bd1971 and Bd0367 RR domain. Error bars show standard deviation. The results show the mean value from three biological repeats and comprise six technical repeats. (A) Shows the Miller Units for the split Bd1971 and Bd0367 RR interactions with both the positive and negative control. (B) This graph allows better observation of the variable but significantly different interaction Bd1971CpUT18c-Bd0367RRpKT25. Asterisks show significance of Student t- test compared to the negative (pUT18c, pKT25) *≤0.05.

In summary Bd1971 only interacts strongly by β-galactosidase assay when tested with the Bd0367 RR domain and Bd1971 split domain analysis showed a possible preference of interaction with the C terminal (EAL domain) of Bd1971.

3.4.3.8. Investigating Bd1971 dimer interaction strength via B2H assay

The EAL domain protein Bd1971 is under investigation with our collaborator at Birmingham University, Dr Andy Lovering. His unpublished data of the Bd1971 crystal structure indicates that Bd1971 dimerises. This led us to test this result via B2H analysis. The result of a typical B2H for Bd1971 self-interaction is shown in Figure 3.24. Bd1971 resulted in blue spots when paired with itself indicating a positive self-interaction.

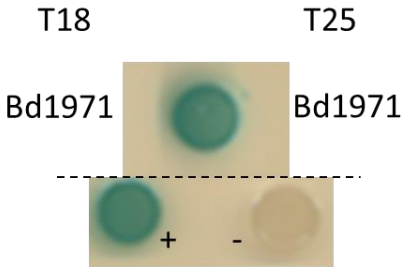

Figure 3.24 Spot plate self-interactions of Bd1971. A blue spot suggests an interaction between Bd1971-Bd1971. Results displayed are a typical representation of the results from three biological and nine technical repeats. Positive (+) = pUT18c-zip with pKT25-zip. Negative (-) = pUT18c with pKT25.

Further testing of these interactions was carried out by β-galactosidase activity assays, to quantify the strength of the interaction between the self-interacting Bd1971. From these results Bd1971-Bd1971 interacted incredibly strongly, suggesting a tight interaction and an interaction significantly higher than the negative control. See Figure 3.25.

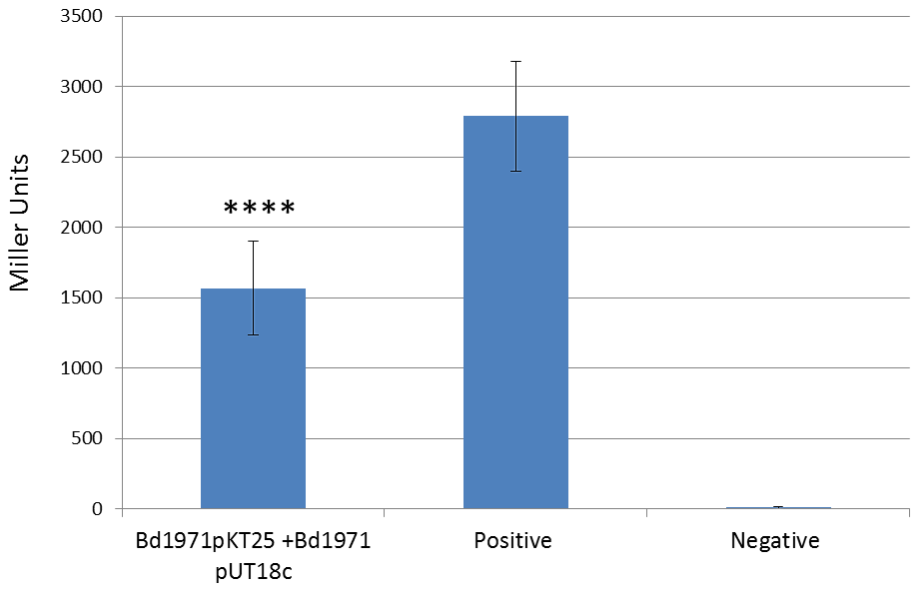

Figure 3.25 Bd1971 interacts significantly with itself by β-galactosidase activity assay. Error bars show standard deviation. The results show the mean value from 3 biological repeats and comprise 6 technical repeats. Bd1971 interacts significant with itself. Asterisks show significance of Student t-test compared to the negative (pUT18c, pKT25) ****≤0.0001.

3.4.3.9. *B. bacteriovorus* Bd1971-mCherry cells do not show increased fluorescence on incubated on a surface.

Due to the developing evidence for a signalling network link between Bd0367, which is involved in gliding motility, and Bd1971 it was decided to examine if Bd1971 was involved in gliding motility.

Bd1971-mCherry had previously been constructed by fusion of *bd1971*, lacking its stop codon, in frame with a C terminal mCherry tag. This was then integrated into the *B. bacteriovorus* chromosome by single crossover at the *bd1971* gene, resulting in a strain where Bd1971 was fused to the mCherry gene. Previous investigations of mCherry tagged proteins hypothesised to be involved in gliding motility resulted in a visible alteration in mCherry intensity, resulting in brighter cells after surface incubation (Milner, 2014).

The expression of protein Bd1971 in *B. bacteriovorus* Bd1971-mCherry attack phase cells did not increases when incubated on a surface. This was studied by observing the intensity of the mCherry fluorescence at the first point of surface contact and at time 400 minutes; as at time 400 minutes most cells will be exhibiting gliding motility (methods

2.7.2). A typical Bd1971-mCherry image at T0 and T400 is shown in Figure 3.26 and there is no observable change in fluorescence level.

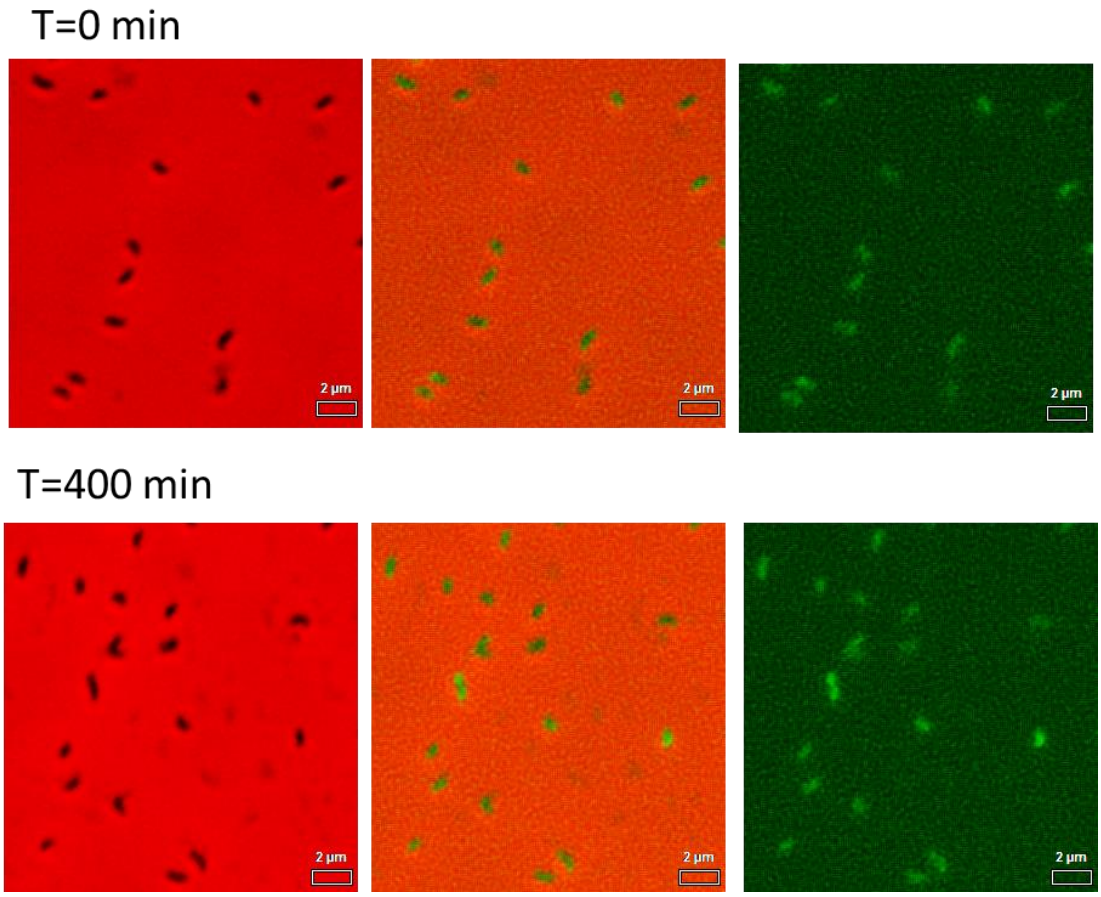

Figure 3.26 *B. bacteriovorus* Bd1971-mCherry attack phase cells show no change in fluorescence when incubated on a surface. The cells were placed on a 1% agarose slide and images were collected at time 0 and time 400 min. during this time the slide was kept consistently hydrated and at room temperature of 25°C. The panel of images shows time 0 at the top and time 400 minutes bellow. The panels left to right show the brightfield channel, the merged channel and the fluorescence channel. There is not observable difference between the two time points and Bd1971-mCherry fluorescent intensity.

Despite no noticeable difference in fluorescence intensity by visual analysis the images were further examined by a programme called MicrobeJ, section 2.7.2, which can measure bacterial fluorescent intensity. This analysis showed that there was no significant difference between the fluorescent intensity of the two time points. This suggests that the expression of Bd1971 does not increase on surface incubation, Figure 3.27.

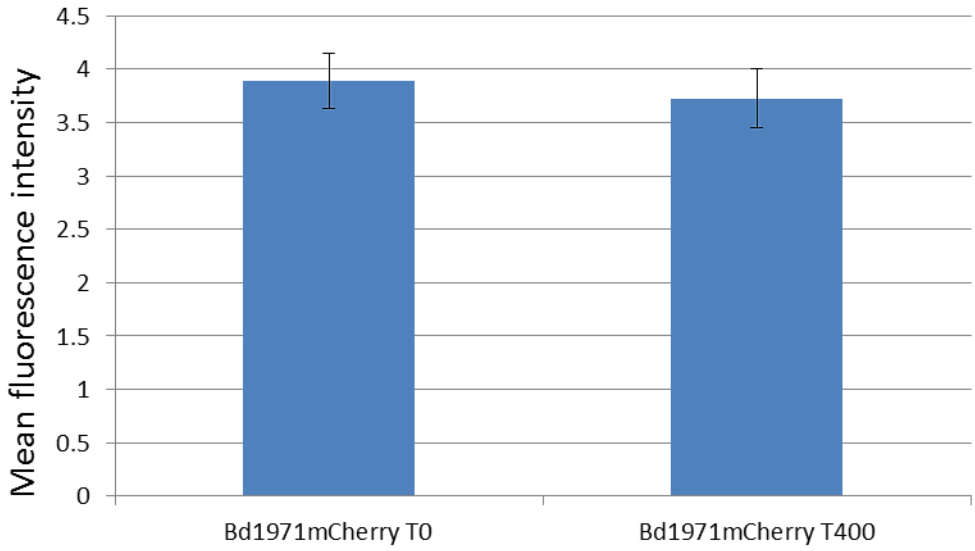

Figure 3.27 *B. bacteriovorus* Bd1971-mCherry attack phase cells show no change in fluorescence intensity when incubated on a surface. Analysis using MicrobeJ on a population of 450 cells per time point gathered from three biological repeats each with three technical repeats showed that there was no significant change in mean fluorescence intensity between time points. Error bars represent 95% confidence interval.

3.4.3.10. Bd1971-mCherry fluorescent location does not alter significantly when incubated on a surface

In other mCherry tagged proteins analysed in this study (chapter 6) surface incubation has a notable effect on the cellular location of fluorescence. For this reason Bd1971-mCherry fluorescence was further analysed despite no increase in mean fluorescence intensity on surface incubation. The difference in Bd1971-mCherry location between time 0 and time 400 minutes is small, was a 5% increase in bipolar foci upon surface incubation. Attack phase cells were analysed using the analyse counter function of ImageJ section 2.7.5. Images were processed in ImageJ to allow easier observation of the points of fluorescence. A typical image for each time point is show in in Figure 3.28 showing predominantly diffuse fluorescence throughout the cell at both time points.

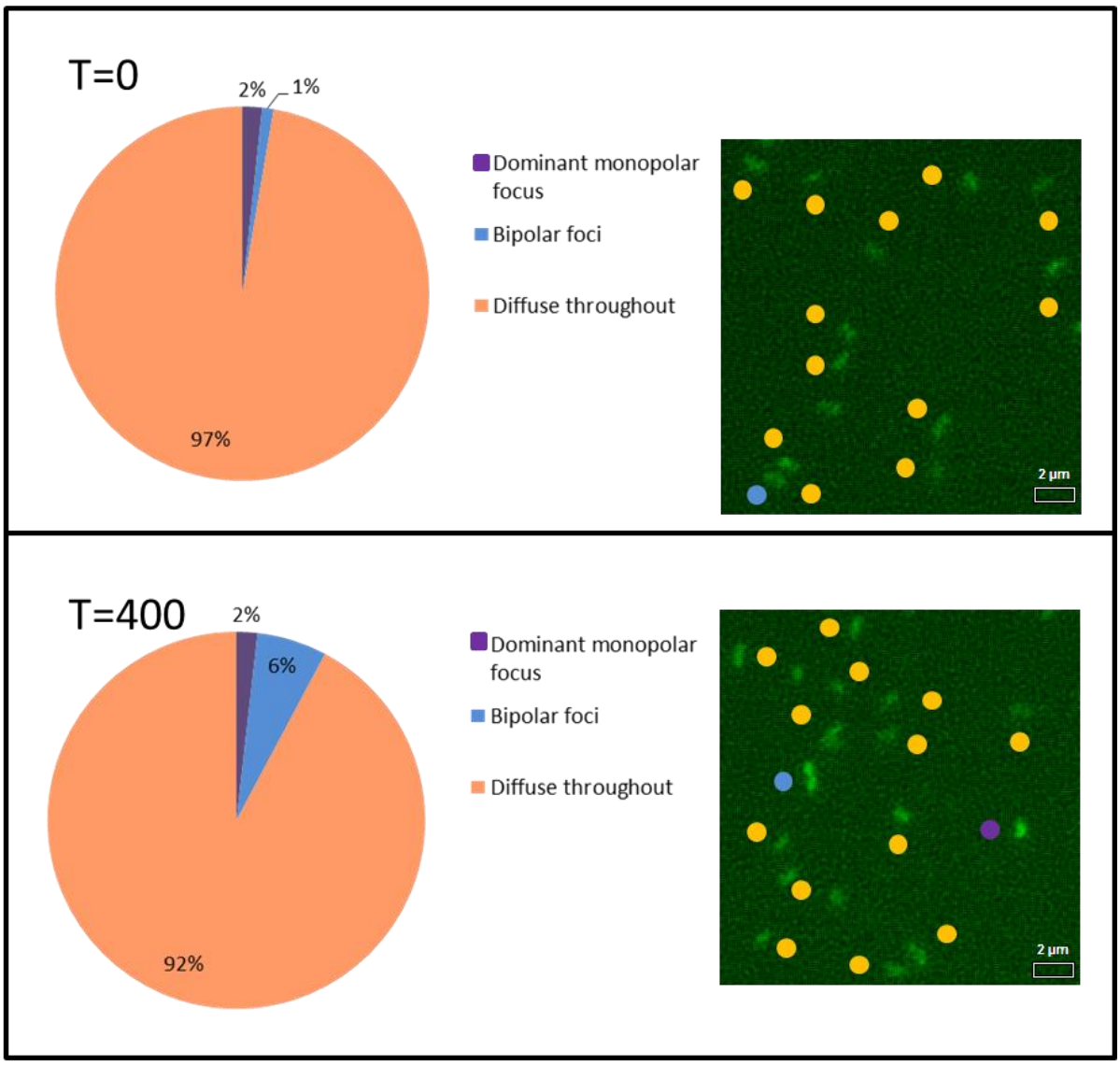

Figure 3.28 Bipolar fluorescence foci increase in frequency on surface incubation of *B bacteriovorus* Bd1971-mCherry attack phase cells. The pie charts show the % distribution of different fluorescent locations at T0 and T400. To demonstrate this visually the location of fluorescence in the cell (dominant monopolar, bipolar, diffuse) is highlighted by a dot of colour next to the cell which indicates which section of the pie chart this cell is representative of. At time 0 *B bacteriovorus* Bd1971-mCherry attack phase cells show a predominately diffuse fluorescence distribution, with rare occurrences of monopolar and bipolar foci. At T400 most of the cell population is still observed with diffuse fluorescence however the occurrence of bipolar foci increased from 1% to 6%. A total of 411 cells with analysed at T0 and 334 at T400 these cells were counted across three biological repeats each with three technical repeats.

3.4.4. Investigating the nature of the protein interaction between Bd3125 (degenerate GGDEF) and Bd0367 (DGC)

The degenerate GGDEF domain protein Bd3125 was found to interact with Bd1971 by Dr Basford's previous work. Also preliminary analysis showed that Bd3125 may interact with Bd0367 (Basford, 2015). In this case it is possible that Bd3125 is acting as a receptor protein for c-di-GMP and is transducing a specific signal from Bd0367. The strength of the interaction between Bd0367 and Bd3125 was re-examined by β-galactosidase assays and investigated further through the use of the Bd0367 split domain constructs in this study.

3.4.4.1. Full length Bd0367 interacts with Bd3125 by B2H analysis

The result of a typical B2H assay for Bd3125 and Bd0367 is shown in Figure 3.29. Bd3125 and Bd0367 consistently produced a uniform blue spot in both orientations tested indicative of a positive interaction.

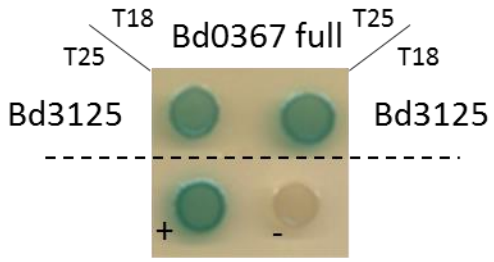

Figure 3.29 Positive spot plate interactions of full length GGDEF protein Bd0367 with degenerate GGDEF Bd3125. Blue spots suggest an interaction between Bd0367 and Bd3125 in both orientations. Results displayed are a typical representation of the results of three biological repeats with nine technical repeats. Positive (+) = pUT18c-zip with pKT25-zip. Negative (-)= pUT18c with pKT25.

Dr Basfords' previous investigation of this interaction resulted in β-galactosidase values that were highly variable, so did not result in a significant interaction. However in this study the further investigation of Bd3125 and Bd0367 by β-galactosidase assay showed they interacted significantly more than the negative control in one orientation (Bd3125-T25 and Bd0367-T18) and the variability of this interaction was much reduced from the previous investigation, see Figure 3.30. Additionally the strength of the interaction between Bd3125 and Bd0367 can be considered a strong rather than transient interaction.

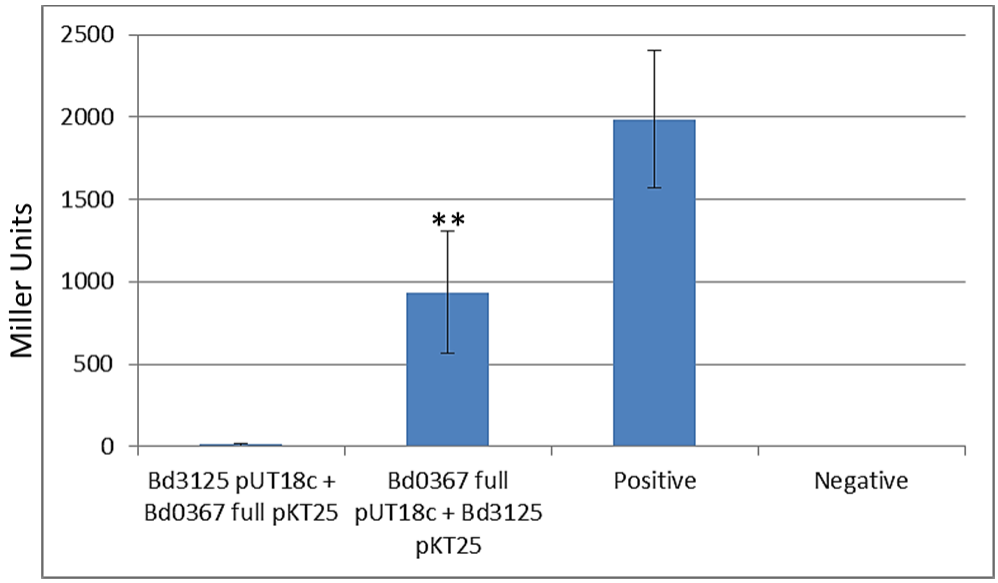

Figure 3.30 Bd3125 and Bd0367 interact significantly by β-galactosidase activity assay Error bars show standard deviation. The results show the mean value from three biological repeats and comprise six technical repeats. The graph shows the Miller Units for the Bd3125 and Bd0367 interactions with both positive and negative controls. Asterisks show significance of Student t-test compared to the negative control (pUT18c, pkT25) **≤0.01

Due to the significant interaction shown by β-galactosidase between Bd3125 and Bd0367, investigations continued to determine if Bd3125 bound preferentially to either of the domains of Bd0367.

3.4.4.2. Bd3125 does not interact with the DGC domain of Bd0367 by B2H analysis

The result of a typical B2H for Bd3125 and Bd0367 DGC is shown in Figure 3.31. Bd3125 and Bd0367 DGC consistently produced white spots comparable to the negative control, suggesting that Bd3125 and Bd0367 DGC do not interact.

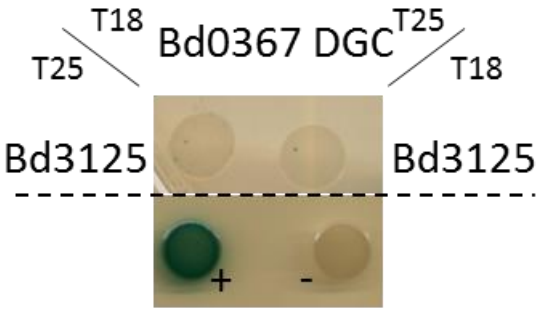

Figure 3.31 Negative spot plate interactions of split GGDEF protein Bd0367 DGC with degenerate GGDEF Bd3125. White spots suggest no interaction between the DGC fragment of Bd0367 and Bd3125 in either orientation. Results displayed are a typical representation of the results of three biological repeats with nine technical repeats. Positive (+) = pUT18c-zip with pKT25-zip. Negative (-)= pUT18c with pKT25.

Despite the negative interaction indicated by spot plate analysis β-galactosidase assays were carried out to allow quantification of the interaction strength, even if weak. These results confirm what the spot plates suggested, that Bd0367 DGC and Bd3125 do not interact significantly more than the control, Figure 3.32.

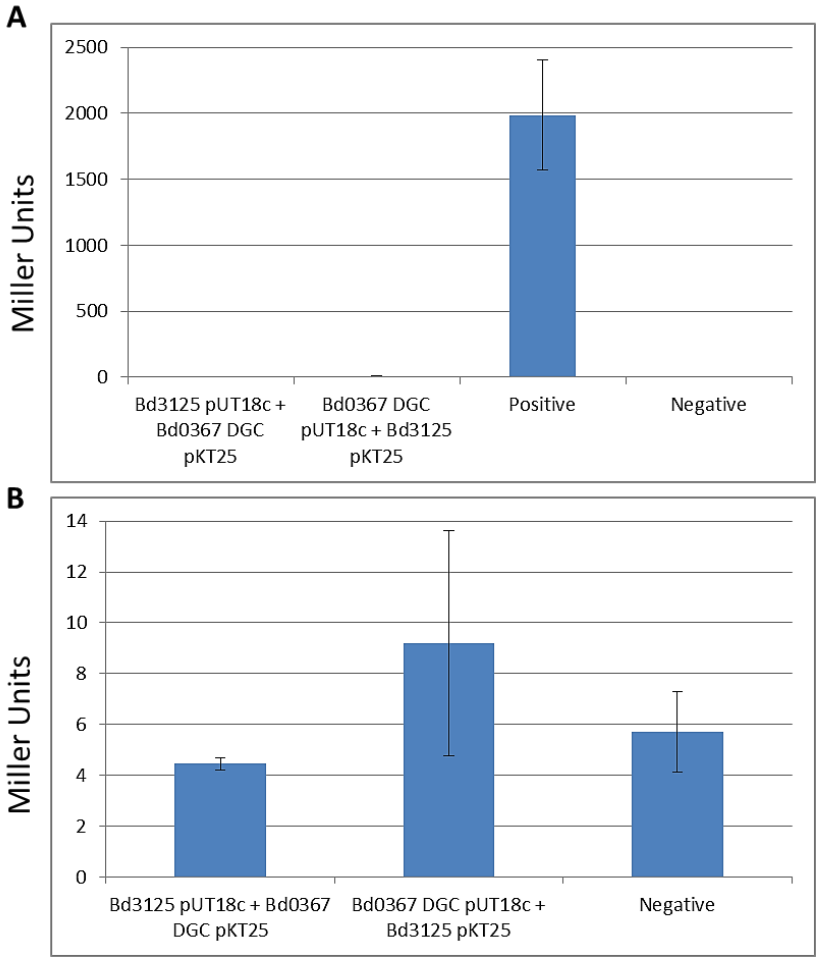

Figure 3.32 β-galactosidase activity assay for Bd3125 and Bd0367 DGC interactions. Error bars show standard deviation. The results show the mean value from three biological repeats and comprise six technical repeats. (A) The graph shows the Miller Units for the Bd3125 and Bd0367 DGC interactions with both positive and negative controls. (B) This graph allows better observation of the similarity in interaction strengths between the test proteins and that of the negative control, the test proteins to not interact significantly more than the negative.

3.4.4.3. Splitting the domains of Bd0367 showed that the Bd0367 RR domain interacts with Bd3125

The result of a typical B2H for Bd3125 and Bd0367 RR is shown in Figure 3.33. Bd3125 and Bd0367 RR consistently produced uniform blue spots in both orientations tested indicative of a positive interaction,

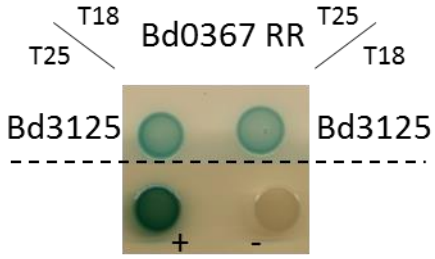

Figure 3.33 Positive spot plate interactions of split GGDEF protein Bd0367 RR with degenerate GGDEF Bd3125. Blue spots suggest an interaction between the RR fragment of Bd0367 and Bd3125 in both orientations. Results displayed are a typical representation of the results of three biological repeats with nine technical repeats. Positive (+) = pUT18c-zip with pKT25-zip. Negative (-)= pUT18c with pKT25.

Further testing of this interaction was carried out by β-galactosidase assays, these assays were used to quantify the strength of the interaction between the two proteins. From these results Bd0367 RR and Bd3125 interact significantly more than the negative control in both orientations. See Figure 3.34.

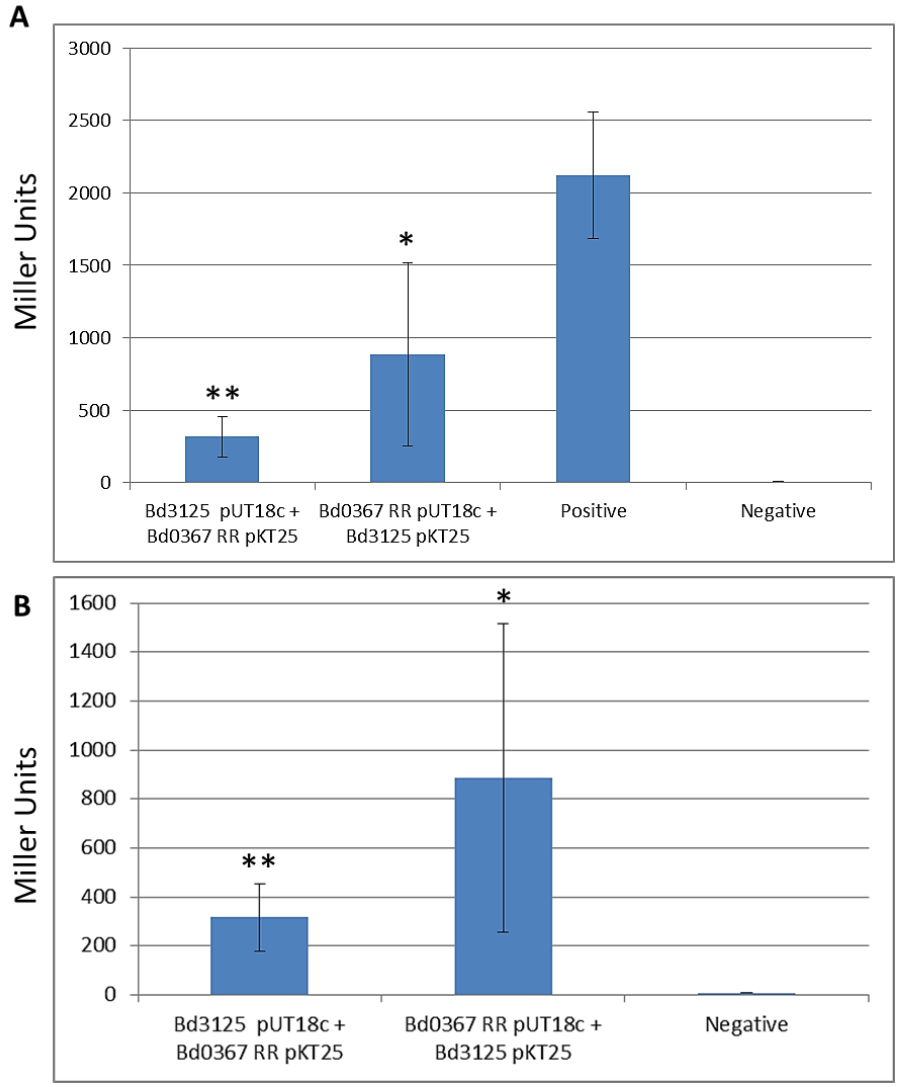

Figure 3.34 β-galactosidase activity assay for Bd3125 and Bd0367 RR interactions. Error bars show standard deviation. The results show the mean value from three biological repeats and comprise six technical repeats. (A) The graph shows the Miller Units for the Bd3125 and Bd0367 RR interactions with both positive and negative controls. (B) This graph allows better observation of the difference in interaction strengths between the test proteins and that of the negative control. Asterisks show significance of Student t-test compared to the negative (pUT18c, pKT25) *≤0.05 **≤0.01.

It is interesting to note that Bd3125 can interact with Bd0367 RR in both orientations but only interact with full Bd0367 in one orientation.

A summary of the positive interactions between Bd0367 and Bd3125 are shown in Figure 3.35. This shows that there is no significant difference between the Bd3125-T25 interaction with Bd0367 full length or Bd0367 RR, however the Bd3125-T25 interaction with Bd0367 RR is slightly more variable that the interaction with the full length Bd0367. It also shows that there is a significant difference between the interaction strength Bd3125-T18 with the full length Bd0367 or the Bd367 RR construct. This suggests that the truncation of Bd0367 has removed previous steric hindrance present in the full length construct allowing the Bd3125 T18 fragment to interact.

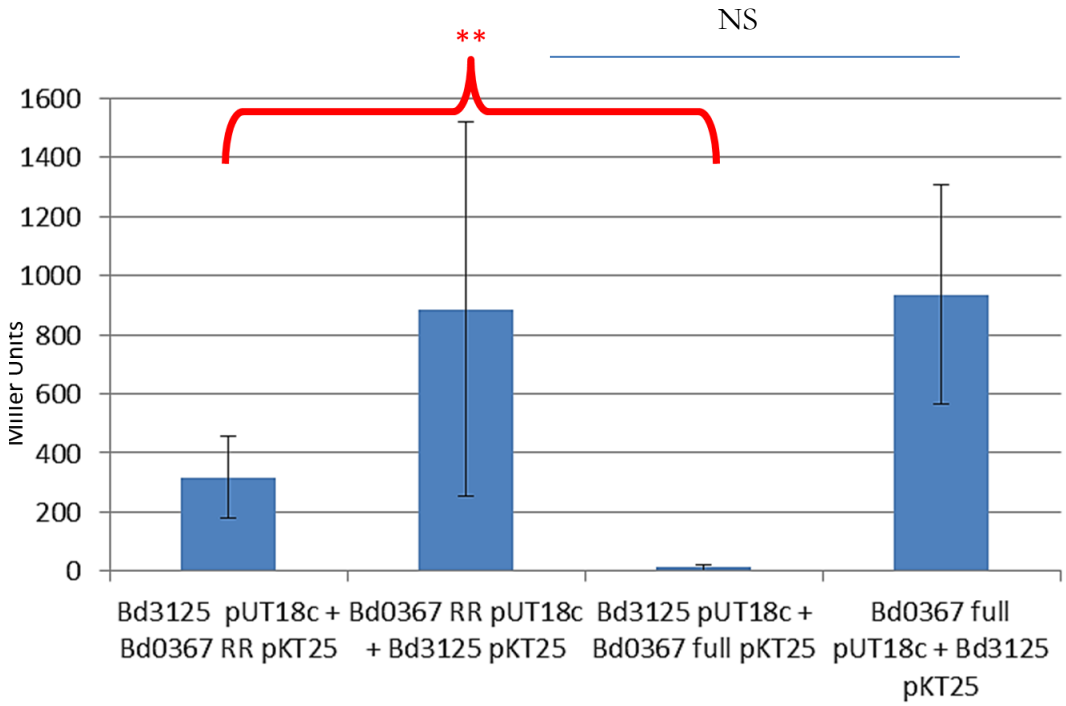

Figure 3.35 Summary of positive β-galactosidase activity assays for Bd3125 and a variety of Bd0367 constructs. Error bars show standard deviation. The results show the mean value from three biological repeats and 6 technical repeats. The graph shows there is no significant difference in the Bd3125-T18 interaction with Bd0367 or Bd0367RR. However there is a significant increase in interaction strength when Bd3125-T25 interacts with the RR domain only compared to the full length Bd0367. The red asterisks show significance by Student t-test **≤0.01.

3.4.4.4. Investigating Bd3125 dimer interaction strength via B2H assay

As Bd3125 is a degenerate GGDEF it was likely that the protein retained the common ability of many DGC of being able to interact with itself and form higher order structure, most commonly through dimerization this theory was tested by B2H analysis The result

of a typical B2Hfor Bd3125 self-interaction is shown in Figure 3.36. Bd3125 resulted in blue spots when paired with itself indicating a positive self-interaction.

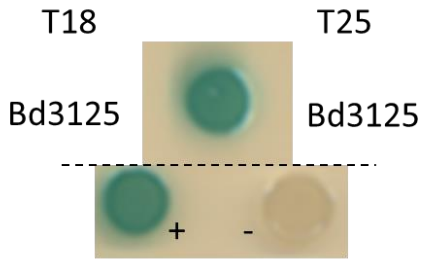

Figure 3.36 Positive spot plate self-interactions of Bd3125. Blue spots suggest an interaction between Bd3125-Bd3125. Results displayed are a typical representation of the results from three biological and nine technical repeats. Positive (+) = pUT18c-zip with pKT25-zip. Negative (-) = pUT18c with pKT25.

Further testing of these interactions was carried out by β-galactosidase activity assays, to quantify the strength of the interaction between the self-interacting proteins. From these results Bd3125-Bd3125 interacted strongly, suggesting a tight interaction and an interaction significantly higher than the negative control. See Figure 3.37.

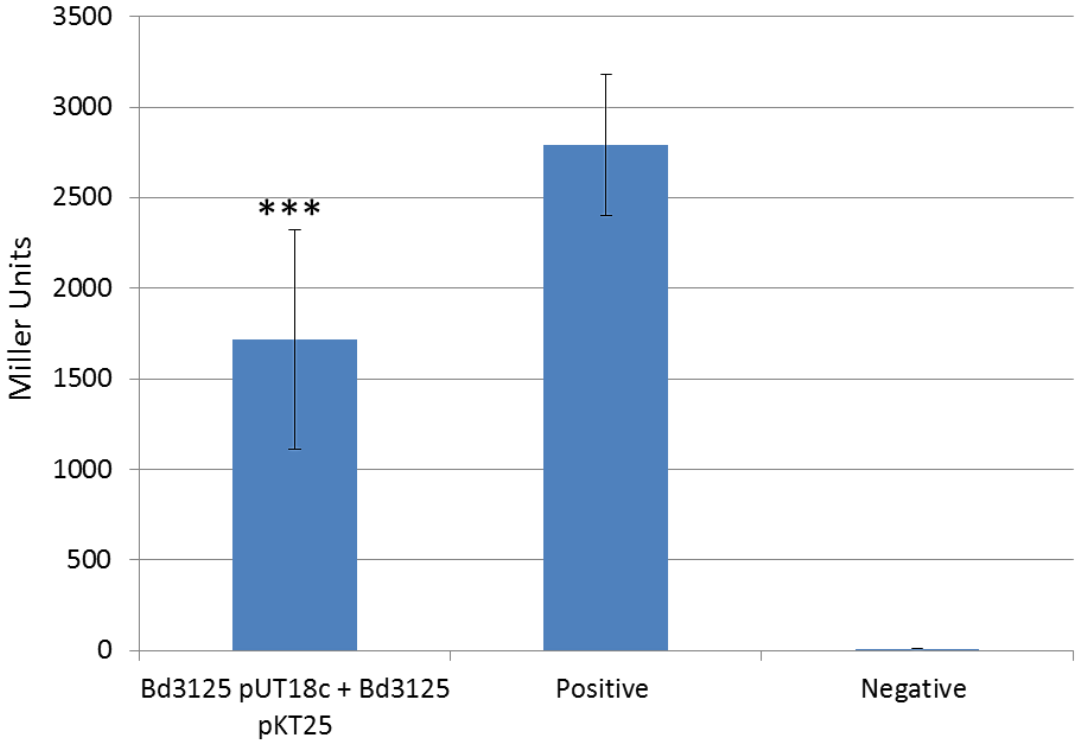

Figure 3.37 β-galactosidase activity assay for Bd3125-Bd3125 self-interaction. Error bars show standard deviation. The results show the mean value from 3 biological repeats and comprise 6 technical repeats. Bd3125 interacts significantly with itself. Asterisks show significance of Student t-test compared to the negative (pUT18c, pKT25) ***≤0.001

3.4.5. Investigating if Bd0367 gene deletion affects localisation of Bd3125

Bd0367 has been found in this study to interact via its RR domain with Bd3125 by B2H analysis. This led to the hypothesis that Bd3125-mCherry fluorescence location may be altered in the absence of Bd0367, not because of the loss of an interacting protein that potentially sequesters Bd3125 to the pole but due to the large reduction in c-di-GMP levels in the absence Bd0367. This global reduction in c-di-GMP may show that c-di-GMP binding Bd3125 is important in regulating its distinct polar localisation. To study this hypothesis the location of Bd3125-mCherry was studied in a Bd0367 absent strain, Δ*bd0367*. This was achieved by conjugating the Bd3125-mCherry into the Δ*bd0367* HI strain.

3.4.5.1. Location of Bd3125-mCherry in HI Δ*bd0367* strain shows no significant change in mCherry localisation

Interestingly the location of Bd3125-mCherry fluorescence in HI Δ*bd0367* cells was similar to the location of Bd3125-mCherry fluorescence in WT HI cells, suggesting the absence of c-di-GMP produced by Bd0367 or the absence of Bd0367 itself does not play a role in Bd3125 location. The localisation of Bd3125-mCherry in the *bd0367* deletion strain remained dominantly mono-polar (92%) with a small proportion of bipolar cells (8%) Figure 3.38. There was small change in bipolar cells observed in the Bd3125mCherry in WT HI cells (4% more) compared to in the Δ*bd0367*strain however this is a small difference.

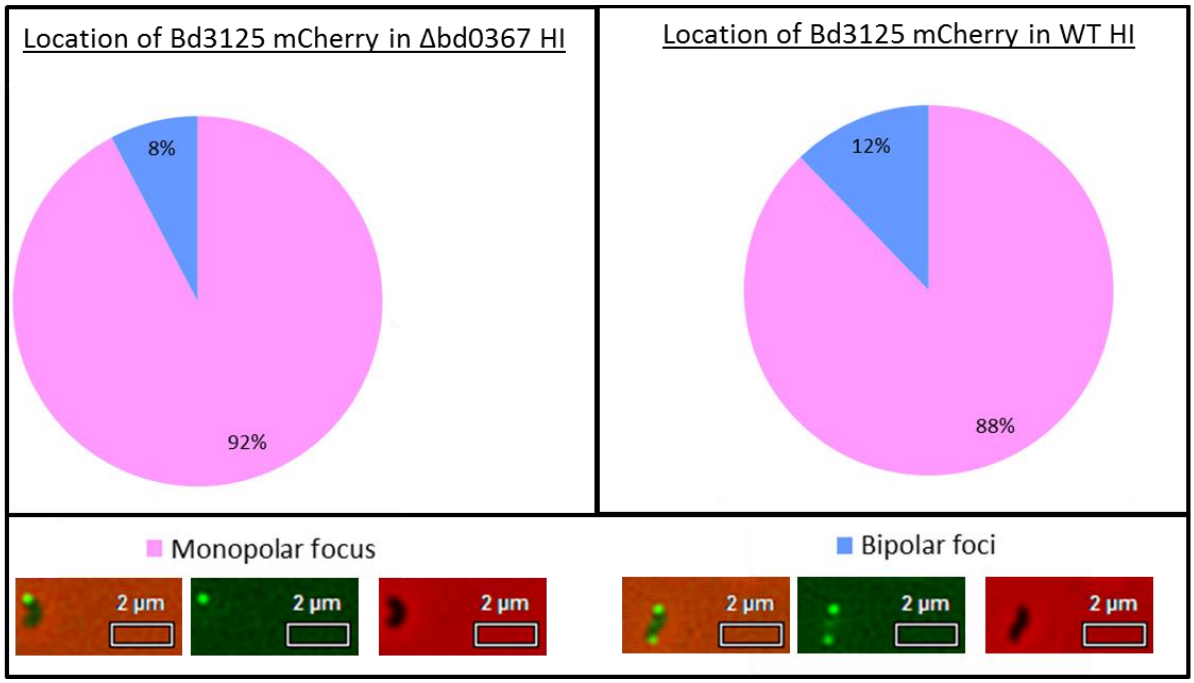

Figure 3.38 Bd3125-mCherry fluorescence is still predominantly mono-polar in location in the absence of *bd0367*. The pie chart shows the distribution of Bd3125mCherry fluorescence between the two strains and has a representative image of a monopolar and bipolar cell. A total of 298 Bd3125mCherry Δ*bd0367* and 229 Bd3125 mCherry WT HI cells were counted across three biological repeats.

3.4.5.2. The intensity and distribution of Bd3125-mCherry fluorescence in attack phase cells does not alter on surface incubation

Despite the *bd3125* gene deletion being related to predation this study has shown interaction evidence between Bd3125 and Bd0367. This suggests the involvement of Bd3125 in the signalling network of Bd0367 which led this study to test the possibility that Bd3125 was also involved in the gliding motility pathway that Bd0367 regulates.

Expression of protein Bd3125 in *B. bacteriovorus* Bd3125-mCherry in attack phase cells did not increase when incubated on a surface. This was studied by observing the intensity of mCherry fluorescence at the first point of surface contact and at time 400 minutes, as at time 400 mins most cells should be gliding. A typical Bd3125 T0 and T400 image is shown in Figure 3.39.

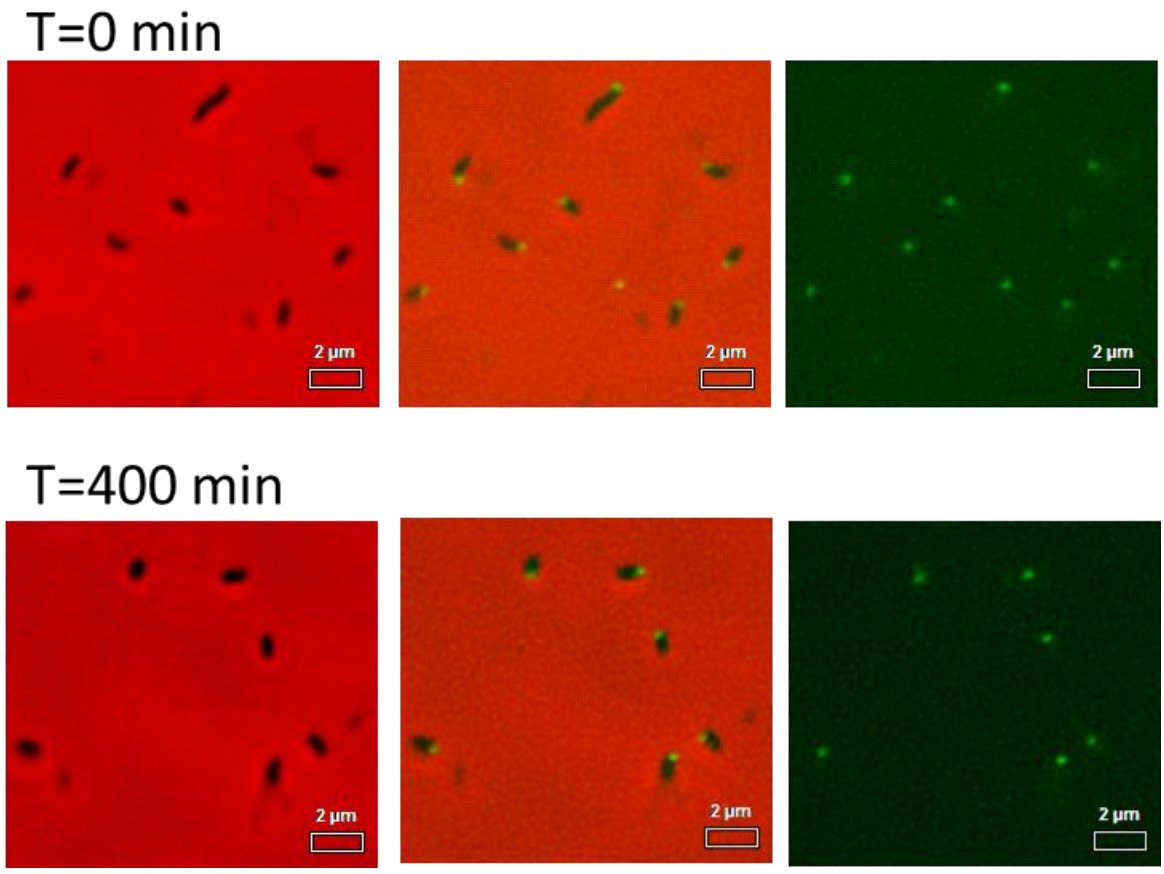

Figure 3.39 *B. bacteriovorus* Bd3125-mCherry cells show no difference in fluorescence intensity when incubated on a surface. The cells were placed on a 1% agarose slide and images were collected at time 0 and time 400 minutes. During this time the slide was kept consistently hydrated and at room temperature of 25°C. The panel of images shows the time 0 at the top and the time 400 below. The panels left to right show the brightfield channel, the merged channel and the fluorescence channel. At both time points distinct monopolar fluorescence is observed.

The program MicrobeJ (section 2.7.2) was used to quantify the fluorescence intensity observed at time 0 and time 400 min. This quantification was used to detect any differences between the intensity which are not apparent by visual observation. This analysis confirmed that there was no significant difference in fluorescent intensity of Bd3125-mCherry on surface incubation Figure 3.40.

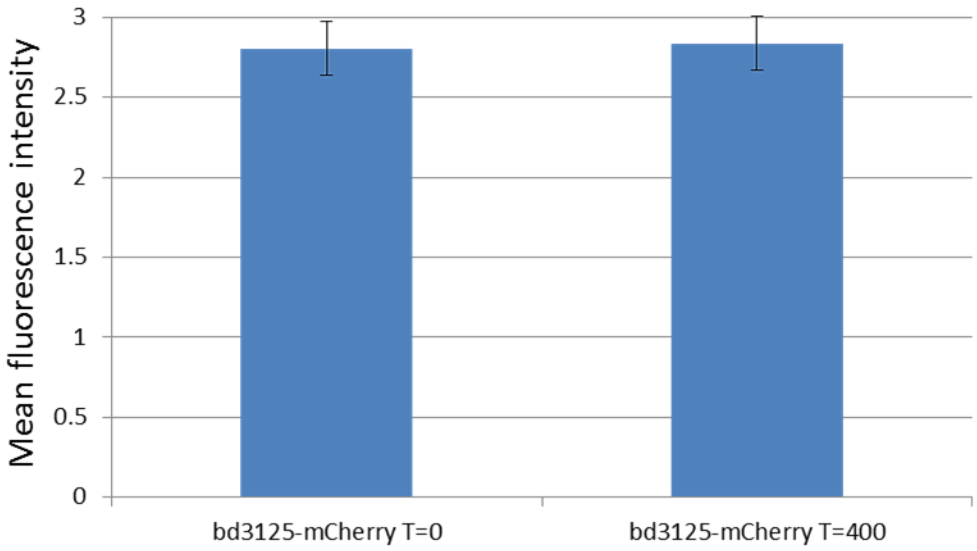

Figure 3.40 MicrobeJ shows fluorescence intensity of *B. bacteriovorus* Bd3125-mCherry attack phase cells is unaltered on surface incubation. Analysis using MicrobeJ on a population of 450 cells gathered across three biological repeats and three technical repeats showed no significant difference in mean fluorescence intensity between timepoints. Error bars represent 95% confidence interval.

In other mCherry tagged proteins analysed in this study surface incubation has a notable effect on the location of the tagged protein fluorescence. For this reason Bd3125-mCherry fluorescence in attack phase cells was further analysed despite no increase in mean fluorescence intensity on surface incubation. The difference between time 0 and time 400 minutes was negligible, with 1% less bipolar cells at T400. These cells were counted using the analyse counter function of ImageJ, section 2.7.5. A typical image for each time point is shown in in Figure 3.41 showing a predominantly monopolar localisation in the cell at both time points.

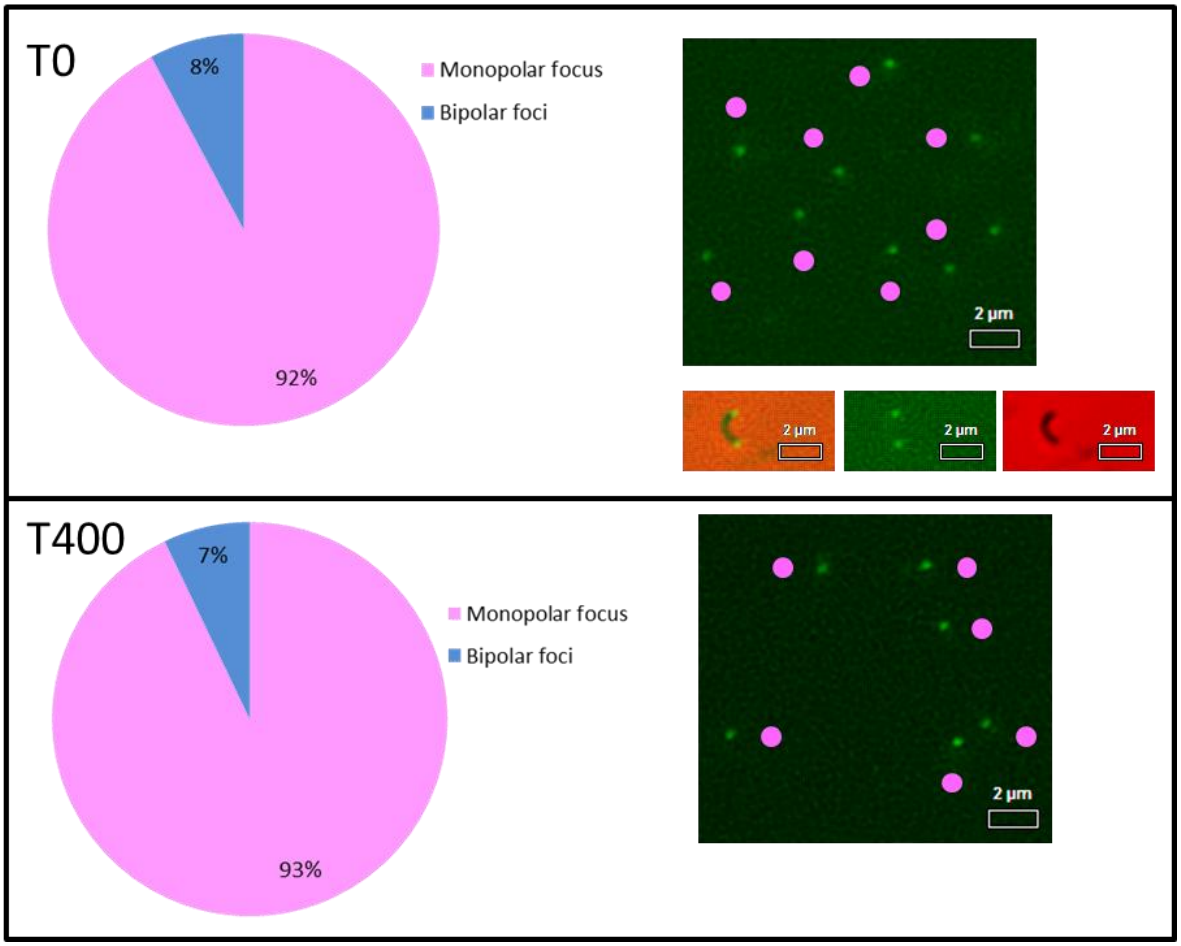

Figure 3.41 Surface incubation causes no change in location of Bd3125-mCherry fluorescence in attack phase cells. At time 0 and time 400 the cells show a primarily monopolar localisation. To demonstrate this visually the location of fluorescence in the cell (monopolar or bipolar) is highlighted by a dot of colour next to the cell which indicates which section of the pie chart this cell is representative of. Cells were placed on 1% agarose slide at room temperature 25°C and kept hydrated. These slides were imaged at T0 and T400minutes. A total of 384 cells were analysed at T0 and 367 at T400, these cells were counted across three biological repeats each with three technical repeats.

This data showed that Bd3125 fluorescence intensity and localisation did not alter on surface incubation. This suggests that Bd3125 may not be involved in the gliding motility network that Bd0367 controls, however Bd3125 may still have role in an alternative signalling pathway in conjunction with Bd0367.

3.4.6. Testing for partner proteins of Bd0367 through an interaction pull down assay

To find proteins that interact with Bd0367 in vivo and confirm interactions found by B2H assays an interaction pull down assay was developed (see section 2.10). This assay used Bd0367-His (C terminally tagged) which had been purified via over production in *E.coli*, this protein was bound to the Ni-agarose beads to act as the bait protein. Large cultures of attack phase HD100 were used, the cultures were centrifuged and lysed. Once these cultures were broken open and membrane factions removed they were incubated with the Ni-agarose beads with or without the bait protein. These beads were later washed, boiled and run on SDS gel to look for potential interacting proteins through protein bands present in Bd0367-His + HD100 lysate and not in the control lanes. These bands were cut out and sent for analysis by LC-MS/MS at Leicester University.

3.4.6.1. Purification of Bd0367-His after overproduction in *E. coli* was successful

Bd0367-His was cloned into pQE-60(C terminal) this was then over produced in M15pRep4 *E.coli* and purified on Ni-Agarose column (see methods 2.9). The purified Bd0367-His obtained from two elution fractions is shown in Figure 3.42.

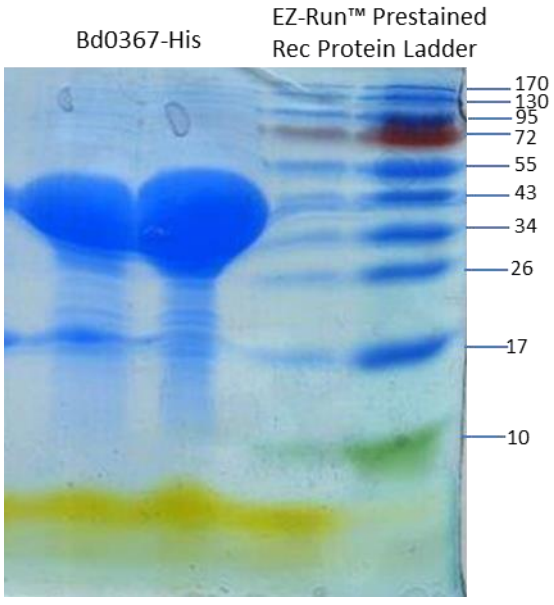

Figure 3.42 Bd0367-His purified from *E.coli*. SDS-PAGE on 12.5% gel with EZ-Run Prestained Rec Protein Ladder (right lane). The two right hand lanes show (loaded 25 µl) two fractions of eluted Bd0367-His from *E.coli* purification, using pQE-60 with C terminally tagged Bd0367. The expected weight for Bd0367-His is ~40kDa.

The eluted Bd0367-His protein was dialysed twice to remove high imidazole concentration so that the protein could be bound to the Ni-Agarose beads. See methods 2.10 for detail.

3.4.6.2. Interaction Pull-down assay

The bait protein Bd0367-His was successfully bound to the beads and incubated with HD100 cell extract or wash solution as a control, HD100 cell extract was also applied to bead with no Bd0367 bound as a control. The resulting gel is shown in Figure 3.43. The doublet of presumed Bd0367-His was split into Band 3 and 4, these were sent for LC-MS/MS analysis to confirm the bands identity as Bd0367-His. There were no unique bands present in the test lane (Bd0367beads+HD100) when compared to the two control lanes. However there was a small difference in band intensity between Band 1 in Bd0367beads + HD100 and Band 2 in HD100 alone on beads, band 1 appeared darker in the test lane compared to the corresponding band in the control lane band 2. Bands 1 and 2 were extracted and sent for LC-MS/MS analysis to investigate any differences between the proteins obtained from these bands.

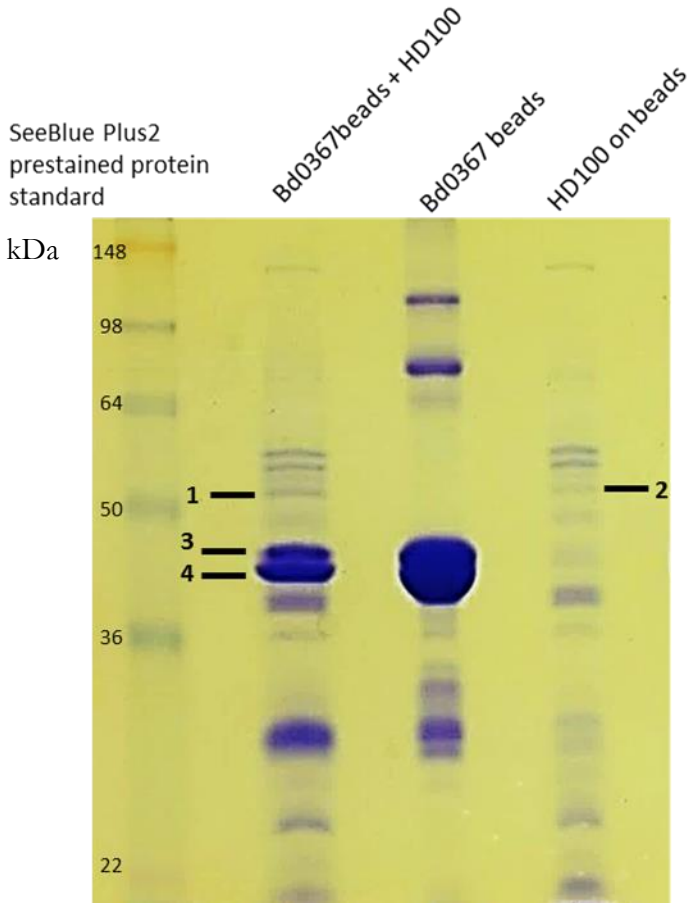

Figure 3.43 One potential interaction pair from Bd0367-his pulldown were sent for analysis by LC-MS/MS. Description of conditions for each lane**.** Bd0367beads+HD100: Bd0367-His was purified from *E. coli*, dialysed and diluted, then 200 µl was applied to beads, this was incubated with HD100 lysate. Bd0367 beads: 200 ul of dialysed Bd0367-His was applied to beads and incubated with buffer. HD100 lysate on beads: The Ni beads were washed and HD100 lysate was incubated with washed beads. All these conditions were then washed, boiled and run on 12.5% SDS-PAGE gel. The expected weight of Bd0367-His is 40kDa and seeblueplus2 prestained standard ladder is used. A doublet of Bd0367-his has developed, possibly due to dialysis and storage, making part of the doublet potentially a breakdown product.

3.4.6.3. Results of LC-MS/MS analysis

The Bands 3 and 4 that were the doublet of the presumed purified Bd0367-His from the test lane were analysed by LC-MS/MS and confirmed that both bands contained Bd0367. The Table 3.1shows that they had the same number of unique peptides and percentage coverage (percentage coverage section8.3.1.2).

Table 3.1 Identity of Bd0367 confirmed by LC-MS/MS

	Bdellovibrio Protein	Putative function	Size Kda	Hits (exclusive unique peptides)	Percentage coverage
Band 3	Bd0367-His	GGDEF	40kDa	20	65
Band 4	Bd0367-His	GGDEF	40kDa	20	65

Table 3.2 GGDEF protein additional to Bd0367 was found in much lower amounts

	Bdellovibrio Protein	Putative function	Size Kda	Hits (exclusive unique peptides)	Percentage coverage
Band 4	Bd1434	GGDEF	47.3	10	29

Interestingly another GGDEF protein additional to Bd0367 was found in much lower amounts in band 4 from the test band Bd0367-His+HD100. This was identified as Bd1434, details of the peptides and percentage coverage are detailed in Table 3.2 and section 8.3.1.3.

The observation of Bd1434 in the test lane in a band containing Bd0367 was interesting however the control band of this region was not sent for analysis so it cannot be said that this is a specific interaction, but it does warrant additional investigation.

The potential interaction Band 1 from the test lane and Band 2 from the control lane were sent for LC-MS/MS analysis to find differences between the identified proteins in the two samples. Unfortunately a contamination occurred during the LC-MS/MS process at Leicester University; this allowed another concentrated protein that I sent for analysis (discussed in Chapter 4) to carry over from the previous run into the next two runs, which were Band 1 and 2. Table 3.3 shows the peptide and percentage coverage details for the Bd2584 contamination of Bands 1 and 2.

	Bdellovibrio Protein	Putative function	Size Kda	Hits (exclusive unique peptides)	Percentage coverage
Band 1					
	Bd2584	Histidine kinase	69.8	28	64
Band 2					
	Bd2584	Histidine kinase	69.8	23	54

Table 3.3 LC-MS/MS analysis of contamination from previous reaction

Once the contaminating protein is excluded both Band 1 and Band 2 have the same top 5 protein hits, listed in table 3.4, the number of unique peptides and percentage coverage is also very similar.

				Band 1 (Test lane)		Band 2 (Control lane)	
	Bdellovibrio Protein	Putative function	Size Kda	Hits (exclusive unique peptides)	Percentage coverage	Hits (exclusive unique peptides)	Percentage coverage
1	Bd0134	Aspartokinase	50	19	55	17	49
2	Bd2608	Major anaerobically induced transmembrane protein	50.8	18	50	20	55
3	Bd0761	phoH like ATPase	50	18	59	19	59
4	Bd0407	Putative hydrolase	51	16	45	15	41
5	Bd3395	flE: Flagella hook protein	45.9	14	42	14	43

Table 3.4 Top hits in band 1 and 2 identified by LC-MS/MS were the same.

The top five different proteins present in Band 1 and absent in Band 2 are shown in Table 3.5. However these differences do not provide any confirmation of previous interacting partners of Bd0367 or identify any new interacting proteins for Bd0367. The proteins identified are proteins that are commonly pulled down due to high abundance and that have been observed previously in other non-related *Bdellovibrio* pull down experiments.

	Bdellovibrio Protein	Putative function	Size Kda	Hits (exclusive unique peptides)	Percentage coverage
Band 1 (Test lane)					
1	Bd1066	rpsA: 30s ribosomal protein S1	65.9	12	23
2	Bd0367-His	GGDEF	40	9	34
3	Bd2983	rpoC: DNA-directed RNA polymerase subunit beta	151.8	9	10
4	Bd3780	rpsB: 30s ribosomal protein S2	34.5	9	30
5	Bd2259	Cah: Carbonic anhydrase	27.9	7	34

Table 3.5 Top 5 hits present in the test band 1 and not int the control identified by LC-MS/MS

In conclusion the Bd0367-His pull down assay that was developed using HD100 attack phase cells did not discover or confirm any interaction partners for Bd0367. The presence of Bd1434 in the test lane in Band 4 could be an interaction however the control band was not examined so this cannot be confirmed. The potential interaction of Bd1434 with Bd0367 is investigated further below by B2H.

3.4.6.4. B2H analysis of potential interaction partner Bd1434

The pull down assay tentatively identified one interaction partner candidate, the DGC protein Bd1434. To investigate this potential interaction further B2H and β-galactosidase

assays were carried out between the potential interaction partner Bd1434 and Bd0367 and additionally between Bd0367 and other GGDEF protein Bd0742 to act as a control DGC protein.

A result of a typical B2H assay is shown in Figure 3.44 between Bd0367 and Bd1434 and Bd0367 with Bd0742. Both interactions consistently produce white spots indicative of a negative interaction.

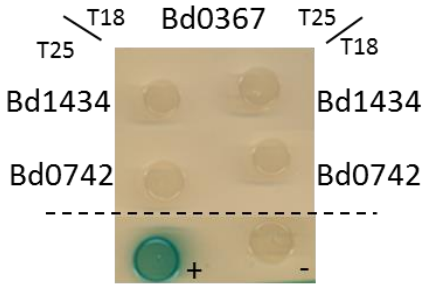

Figure 3.44 GGDEF Bd1434 and Bd0742 do not interact with Bd0367. White spots suggest no interaction between these proteins in either orientation when N terminally tagged. Results displayed are a typical representation of the results from three biological repeats and nine technical repeats. Positive (+) = pUT18c. Negative (-)=pKT25

Further testing of this interaction was carried out by β-galactosidase assays for completeness. From these liquid assays there is no significant difference in interactions between Bd0367 and Bd1434, Bd0742 and the negative control, Figure 3.45.

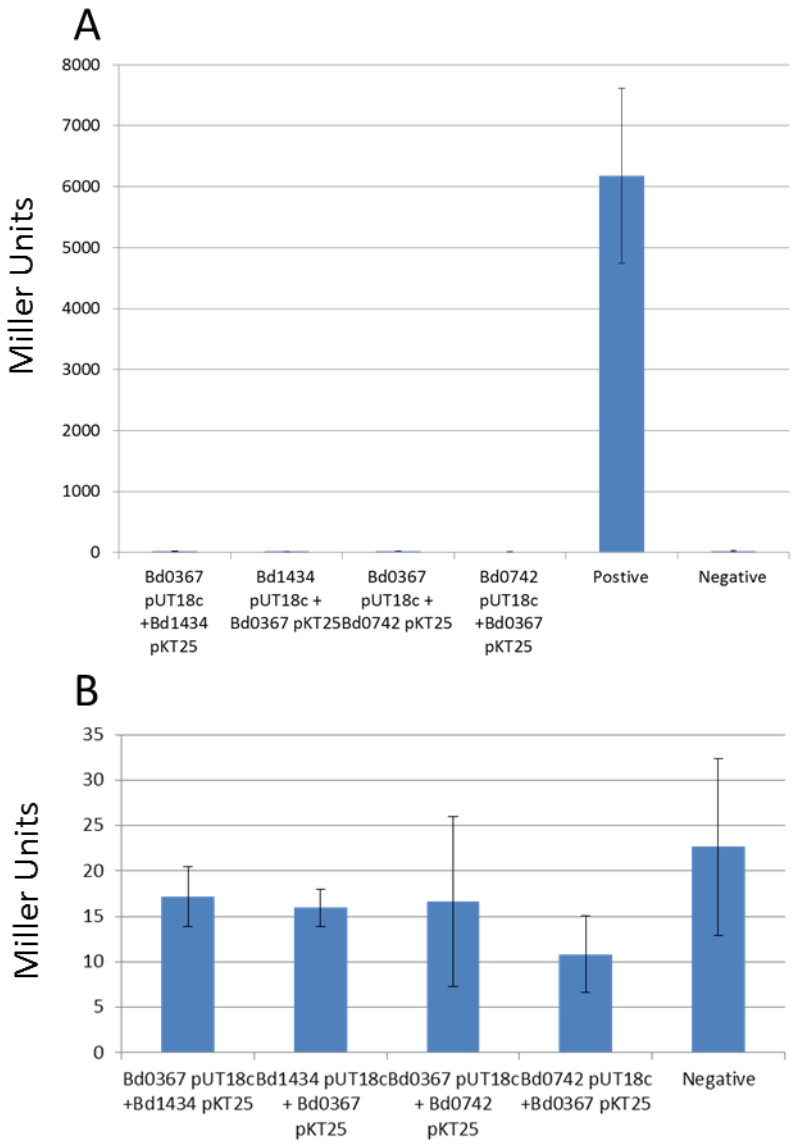

Figure 3.45Bd0367 does not significantly interact with other GGDEF proteins Bd1434 and Bd0742 by β-galactosidase assay. Error bars show standard deviation. The results show the mean value from three biological repeats and comprise six technical repeats. (A) Shows the Miller Units for Bd0367 with Bd1434, Bd0742 both the positive and negative control. (B) This graph allows better observation of the low interaction strengths with the absence of the positive control.

From these results it appears that N terminally tagged Bd1434 does not interact with N terminally tagged Bd0367 in a BTH101 background.

3.5. Discussion

3.5.1. The advantages and limitations to using B2H as a protein identification method

B2H can be a powerful method to identify protein interactions. Previously B2H studies were used to successfully identify the interactions between the *Bdellovibrio* proteins that make up the predatory hub showing B2H to be a useful technique in isolating interactions that are occurring in vivo in *Bdellovibrio*.

The limitations of our investigations using B2H is that T18 and T25 tags have always been added to the N terminus of the test protein. To fully examine and exclude the possibility of an interaction addition of the tags to the C terminus of the test protein should be carried out. This altered tagging location could alter misfolding or any steric hindrance that N terminal tagging may have caused that resulted in no interaction being observed previously.

An additional limitation of the B2H plasmid set used in this study is that the T18 tag is in a higher copy number plasmid than the T25 tag plasmid. This results in a different quantity of the test proteins dependent on the tagging and can cause changes in the observed level of interaction seen. There are now plasmids available designed to give the same copy number of each interacting protein which may be helpful where stoichiometry is a critical feature in an interaction (Jervis & Green, 2007).

General issues with this technique is that some proteins have an intrinsic tendency to interact with any protein making them 'sticky proteins' which result in false positive interactions in B2H.

Overall this technique is a relatively simple, fast and reliable method to identify protein interactions. The ease of manipulating the proteins that are tagged has allowed for further characterisation of domains or residues that are importance for an interaction to occur. B2H has proved a useful technique through-out this study and others studies (Battesti & Bouveret, 2012; Karimova et al, 2005).

3.5.2. Self-interaction and phosphorylation state of Bd0367 in BTH101

The most commonly described self-interaction for DGC proteins is to form an active homodimer (Chan et al, 2004). On occasion there are more complex self-interactions

such as WspR where higher order structures form and this can regulate activity of the DGC (Huangyutitham et al, 2013).

From the B2H analysis in this study we can confirm that Bd0367 does interact with itself, we presume this is a dimeric interaction; however further testing by other methods would be required to confirm this. These methods would involve cross-linking assays (using chemical cross linker disuccinimidyl suberate (DSS)) with Bd0367 incubated with or without BeF_3 present to mimic phosphorylation. This would enable detection of Bd0367 in monomeric and dimeric forms, possibly higher order oligomers too. These states could also be probed for DGC activity level to see if the Bd0367 mechanism of activation agrees with the commonly supported 'activation by dimerization mechanism' (Paul et al, 2007).

The strength of the self-interaction of Bd0367 was not as high as observed in the rest of this study. I hypothesised that the reason for the weaker self-interaction is due to the phosphorylation state of the Bd0367 RR domain, as the cognate kinase to phosphorylate the RR domain of Bd0367 is not present in the BTH101 strain. In the DGC PleD in *Caulobacter*, it has been shown that dimerization is coupled to the phosphorylation state and that dimer formation can be a mechanism to control enzyme activity (Paul et al, 2007).

For this reason the self-interaction of a non-phosphorylated Bd0367 construct Bd0367D63A was analysed and found to not be significantly different from the Bd0367WT. From this evidence it seems likely that Bd0367 is not phosphorylated in the BTH101 strain and that the lack of phosphorylation may explain the low self-interaction strength.

3.5.3. Interactions between DGC protein Bd0367 and other c-di-GMP components

The B2H and β-galactosidase assays carried out in this study have confirmed expected interactions and established which domains of these proteins are interacting. These experiments showed that Bd1971 interacted with Bd0367RR and that Bd3125 interacted with Bd0367RR, Figure 3.46. Additionally previous work showed that Bd3125 can

interact with Bd1971 (Basford, 2015). This suggests potential for a regulation of c-di-GMP metabolism and molecular outputs by physical interactions in *Bdellovibrio*.

Currently the amino acid residues that make up the interaction sites are unknown as is the function and effects of these physical interactions in vivo. The possibilities raised by the discovery of these interactions are discussed further here.

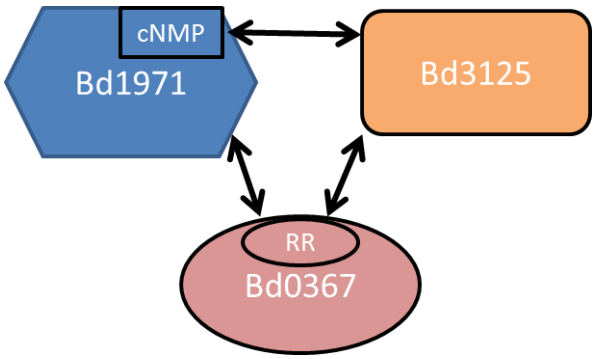

Figure 3.46 Interactions with Bd0367 identified by B2H

3.5.3.1. Bd1971 and Bd3125 can both self-interact

The interacting partners Bd1971 and Bd3125 were both investigated for self-interaction properties by B2H and β-galactosidase analysis. These showed that Bd1971 interacts with itself, this interaction is assumed to be a dimer due to unpublished X-ray crystallography work by Dr Lovering showing a structural dimer for Bd1971. Bd3125 also interact with itself this interaction is presumed to be dimeric due to its degenerate DGC structure.

3.5.3.2. Cellular locations of Bd0367 Bd1971 and Bd3125

The cellular location of these proteins in *Bdellovibrio* is important to establish if these interactions isolated in vitro are possible in vivo. Bd3125mCherry has a distinct location with ~90% of cells demonstrating a mono-polar localisation and ~10% with a bipolar localisation (see section 3.4.5.2). Bd1971mCherry is localised predominantly throughout the cytoplasm, ~97% of the time (see section 3.4.5.10). Bd0367mCherry is also located predominantly throughout the cytoplasm ~80% of the time (see section 5.4.1.2). These locations suggest that Bd1971 and Bd0367 are commonly located in the same region so can potentially interact in vivo. The location of Bd3125 at the pole suggests that in vivo the interactions occurring at the predatory pole between Bd1971-Bd0367-Bd3125 may have a different effect to the Bd1971-Bd0367 interaction occurring in the rest of the cell.

3.5.3.3. Bd0367 is not necessary to aid Bd3125 localisation

Bd3125 localisation is not controlled by its interaction with Bd0367, as in the absence of Bd0367 Bd3125-mCherry is still monopolar. Additionally the Δ*bd0367* cells have a lower c-di-GMP level than WT; the lack of alteration of Bd3125mCherry location in a low c-di-GMP background suggests that the RxxD c-di-GMP binding site of Bd3125 is not used to mediate its polar location. The localisation of Bd3125 is probably controlled by a membrane protein involved in the predatory hub such as Bd2492.

3.5.3.4. Investigating potential role of Bd0367 interacting partners in gliding motility

Due to the interactions discovered by B2H it was tempting to suggest that Bd1971 or Bd3125 may function in the same pathways as Bd0367. The possible role in gliding motility was examined using HD Bd1971mCherry or Bd3125mCherry strains and incubating them on a surface to see if an alteration in fluorescence intensity occurred, which may indicate increased production of these proteins. In both cases no change in mCherry intensity was observed on surface incubation. This suggested that Bd3125 is not involved in gliding motility which fits as the Δ*bd3125* strain has a pre-established role in predation. The lack of increased fluorescent intensity of Bd1971mCherry on surface incubation does not rule out its involvement in gliding motility as this gives no indication of the possible alterations in PDE enzyme activity on surface incubation. The role of Bd1971 in gliding motility is further investigated in chapter 5.

3.5.3.5. Bd1971 EAL interacts with Bd0367 RR domain by B2H

There is reliable and repeatable spot plate evidence that Bd1971 and Bd0367 interact by B2H, however this interaction has been shown to be confined to the Bd0367 RR domain when studied by β-galactosidase assays. It could be that the full length interactions are transient or that testing with the RR domain only has relieved some steric hindrance (introduced by the B2H tags.)

The function of interaction between Bd1971 and the regulatory RR domain of Bd0367 in vivo can currently only be speculated on until further evidence is collected. However the models showing the possible mechanisms of this interaction are discussed below.

Model 1: Bd1971 binding to Bd0367 regulates DGC enzyme activity

(A) Bd1971 binding inhibits Bd0367 DGC activity

Bd1971 could inhibit Bd0367 DGC activity by holding Bd0367 in an inactive state, perhaps by preventing dimerization. Or Bd1971 binding to the RR domain of Bd0367 could potentially prevent the cognate HK phosphotransfer reaction to the RR domain from occurring resulting in no activation of enzyme activity, see Figure 3.47.

To test if this interaction causes a direct inactivation could be examined in the future by investigating the DGC activity of Bd0367 in vitro compared to when incubated with Bd1971WT and compared to incubation with Bd1971 active site mutant. If Bd0367 DGC activity decreases on incubation with Bd1971 active site mutant this suggests Bd1971 binding Bd0367 inhibits its enzymatic abilities.

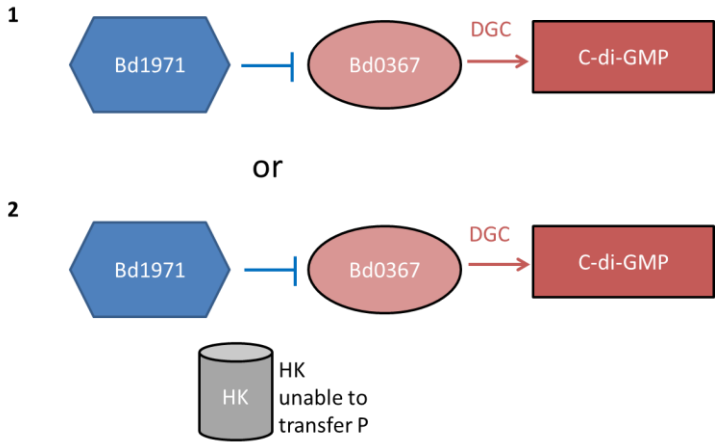

Figure 3.47 Bd1971 binding inhibits Bd0367 DGC activity. This could be done by binding causing an inactive DGC conformation (1) or by preventing phosphorylation interaction from HK (2). DGC actions and high c-di-GMP driven processes are shown in red and PDE actions and processes occurring at low level c-di-GMP levels are shown in blue.

(B) Bd1971 binding stimulates Bd0367 DGC activity

The cellular conditions under which the Bd1971-Bd0367RR interaction occurs is currently unknown. However it is possible that the Bd1971 interaction is regulated by the global level of cellular c-di-GMP. If this is the case Bd1971 may interact with Bd0367 when the c-di-GMP concentration is low as a signal to stimulate production of more c-di-GMP. This stimulation could occur by Bd1971 acting as an accessory protein or bridging protein to stabilize the cognate HK interaction to stimulate increased phosphotransfer and hence increases DGC activity see Figure 3.48.

To test this identification of the relevant HK would be necessary and then phosphotransfer experiments and enzyme activity experiments could be conducted with the HK-Bd0367 compared to HK, Bd1971, Bd0367.

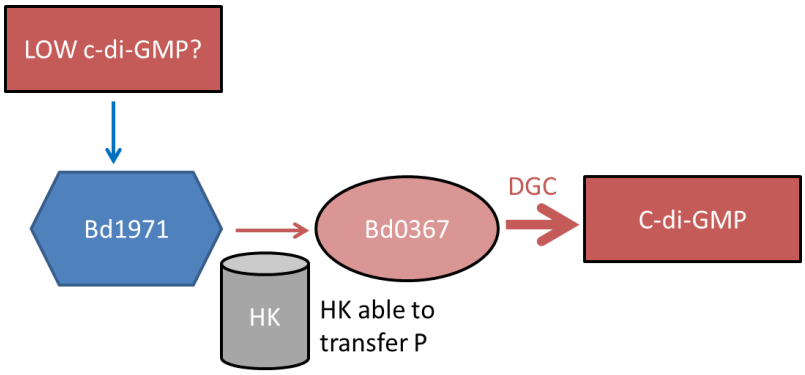

Figure 3.48 Bd1971 binding stimulates Bd0367 DGC activity. This could be done by Bd1971 aiding phosphotransfer from HK to RR of Bd0367 as accessory protein.

Model 2: Specific c-di-GMP signalling systems are controlled in *Bdellovibrio* by Bd1971 acting as a 'trigger enzyme'

There is no genetic or biochemical data to suggest Bd1971 is a trigger enzyme similar to YciR as shown in (Lindenberg et al, 2013). However it is a tempting to acknowledge the theory as *Bdellovibrio* has very specific phenotypes associated with DGC deletions and how these 'local pools' of c-di-GMP are regulated is still currently unknown.

Bd1971 could potentially inhibit Bd0367 DGC activity and inhibit a specific DGC-PilZ interaction, this coordination would mean the molecular output caused by the DGC-PilZ interaction would only occur at specific c-di-GMP levels which could regulate Bd1971 binding, see Figure 3.49.

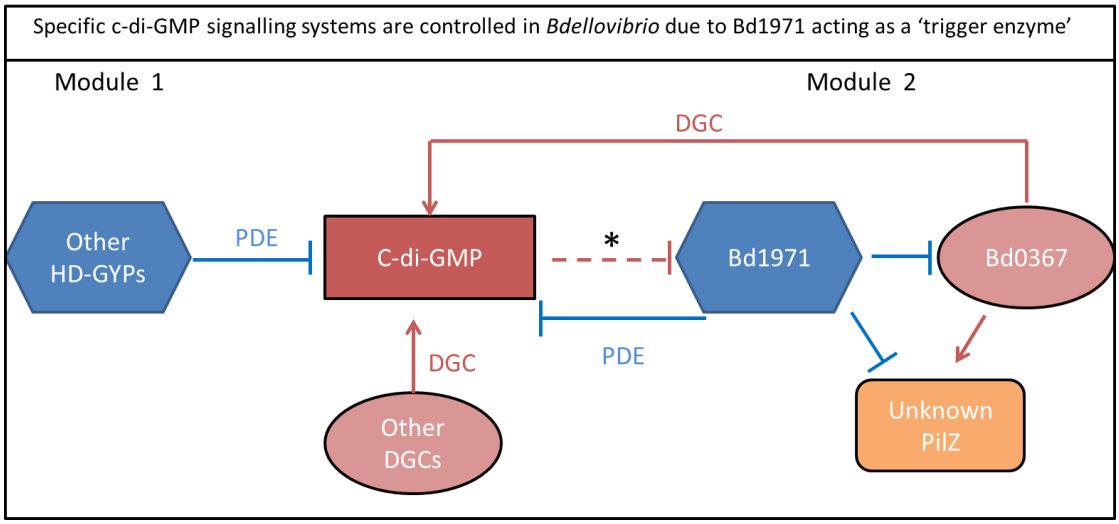

Figure 3.49 Bd1971 acts as a trigger enzyme DGC Bd0367 and PDE Bd1971 comprise a separate module, where Bd1971 interacts with Bd0367 and this interaction inhibits the Bd0367 DGC activity and the PDE activity of Bd1971. I propose that when the cellular c-di-GMP level is elevated (depicted by line with *) the PDE Bd1971 will no longer interact with Bd0367, and instead use its PDE activity to degrade pool of c-di-GMP. This allows Bd0367 DGC activity to resume and interactions with PilZ proteins to transduce molecular outputs. DGC actions and high c-di-GMP driven processes are shown in red and PDE actions and processes occurring at low level c-di-GMP are shown in blue.

Model 3: Together Bd1971 and Bd0367 form a multiprotein complex that recruits other proteins to result in a molecular output – such as gliding or bdelloplast exit

(A) Bd1971, Bd0367 and effector protein interaction is regulated by the c-di-GMP metabolising and binding abilities of the proteins in the complex as in (Lindenberg et al, 2013). With Bd1971 potentially aiding or preventing effector protein interaction with Bd0367 dependent on cellular c-di-GMP levels, Figure 3.50.

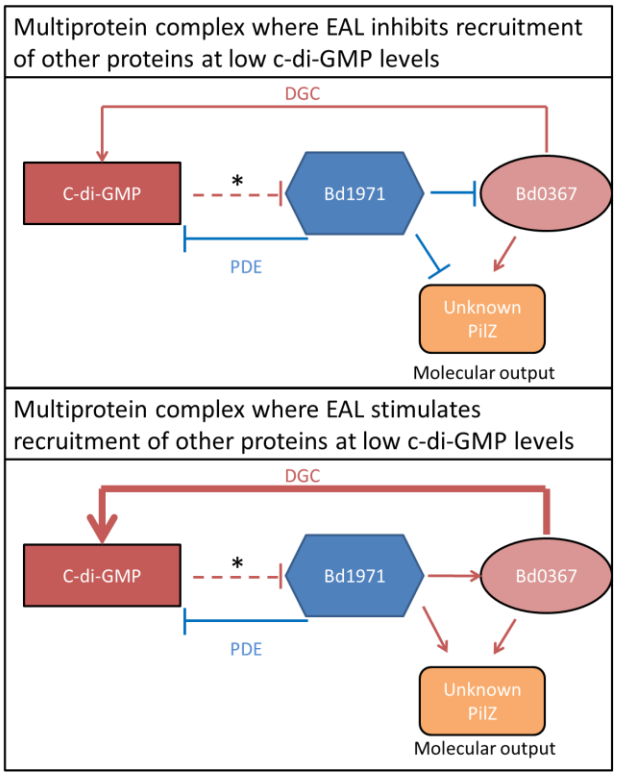

Figure 3.50 Multi-protein complex reliant on enzymatic properties of interacting proteins to regulate formation and dissociation of complex. When the cellular c-di-GMP level is elevated (depicted by line with *) the PDE Bd1971 will no longer interact with Bd0367 and act as PDE. The loss of the PDE interaction with Bd0367 may allow a PilZ interaction to occur, or it may result in the loss of a PilZ interaction which was mediated by the PDE-DGC complex. DGC actions and high c-di-GMP driven processes are shown in red and PDE actions and processes occurring at low level c-di-GMP levels are shown in blue.

(B) Bd1971, Bd0367 and effector protein interaction is independent of the proteins primary c-di-GMP roles as shown in (Ryan et al, 2012). This could suggest these proteins have dual functions, in c-di-GMP regulated outputs and separately through the regulation achieved through physical interactions that are not effected by c-di-GMP, Figure 3.51.

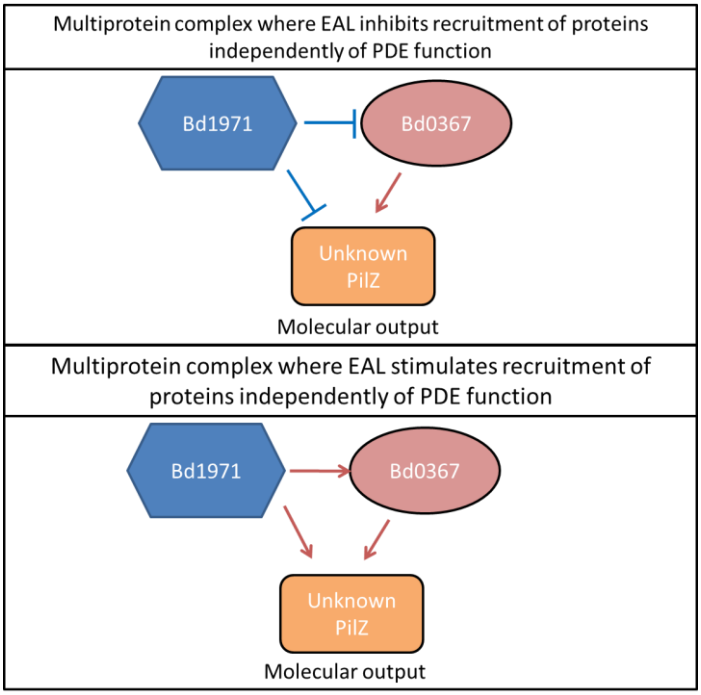

Figure 3.51 Multi-protein complex independent of interacting proteins enzymatic properties. The multiprotein complex where PDE stimulates or inhibits protein recruitment is unaffected by the enzymatic role of these proteins. Eluding to protein dual functionality.

3.5.3.6. Bd3125 (degenerate GGDEF) interacts with Bd0367 RR domain by B2H interaction

From this study there is evidence that Bd3125 and full length Bd0367 interact by B2H and by β-galactosidase assays. From the spilt domain analysis it was found that the location of the Bd3125 interaction was located at the RR domain of Bd0367. The location of the interaction at the RR domain suggested that Bd3125 binding was having a regulatory role on the enzymatic function of Bd0367. This was a surprise as Bd3125 can bind c-di-GMP as it had been speculated that Bd3125 may bind at the DGC domain to act as a specific effector protein that bound c-di-GMP produced by Bd0367.

Bd3125 has previously been shown to interact with Bd1971 and 'predatory pole proteins' RomR and TPR protein Bd2492. The number of interactions implies that Bd3125 may have dual roles, one of which requires the c-di-GMP effector ability and another function that is independent of this.

Dr Basford speculated that Bd3125 binding the cNMP domain of the Bd1971 EAL may prevent cAMP binding, which in itself may alter the EAL activity of Bd1971.

The interaction between Bd0367full or RR and Bd3125 was strong but variable, this may be due to the c-di-GMP bound state of Bd3125, as levels of c-di-GMP within BTH101 *E.coli* will be variable even under standardised conditions . This could be investigated in the future by making a B2H construct with the RxxD motif mutated in Bd3125. Recent investigations by (Baker et al, 2016) into PilZ FlgZ have shown that the RxxxR site is crucial for the FlgZ-MotC B2H interaction.

Due to distinct location of Bd3125 at the predatory pole of *Bdellovibrio* I propose a separate model for interactions occurring at the predatory pole

Model 4: The predatory pole of *Bdellovibrio* is a separately regulated c-di-GMP module.

Bd3125 interacts with Bd1971 and Bd0367 at the predatory pole. In this model the function of this interaction is to ensure both PDE and DGC activities of the pair are inactive. I propose that Bd3125 simultaneously binds to the cNMP and RR domains to either enhance the already DGC inhibitive interaction between Bd1971-Bd0367 by stabilizing it, or to repress the potentially DGC stimulating interaction by binding the proteins in an inactive form. This creates a specific c-di-GMP level at the predatory pole which is controlled by the DGC implicated in predatory function, Bd0742 see Figure 3.52. This tight regulation of c-di-GMP levels at the predatory pole may aid in coordinating the predatory process as Bd1971 is prevented from degrading this 'specific' c-di-GMP and Bd0367 is prevented potentially swamping the area with 'non-specific' c-di-GMP by the Bd3125 inhibitory interaction. In the Δ*bd3125* deletion strain prey entry was slower. I suggest this slow entry is due to the loss of tight control of the predatory c-di-GMP module, without Bd3125 present both Bd0367 and Bd1971 can act as c-di-GMP metabolising proteins at the cell pole which disrupts the specific c-di-GMP level normally determined by Bd0742 which affects the process of initiating predation., Figure 3.53.

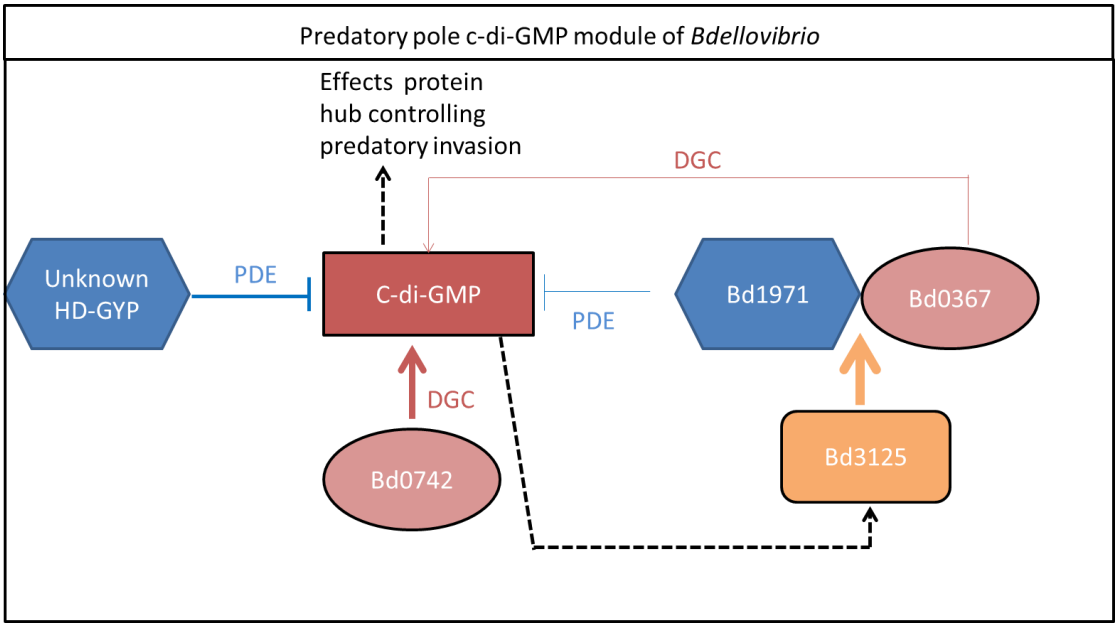

Figure 3.52 Predatory pole c-di-GMP module: Bd3125 interacts with Bd0367 and Bd1971 its binding holds both enzymes in an inactive form. This limits the ability of Bd1971 or Bd0367 to alter the cellular c-di-GMP level at the predatory pole. The c-di-GMP level at the predatory pole is specifically controlled so that the c-di-GMP specifically produced by Bd0742 mediates an efficient predatory response, possibly in a c-di-GMP concentration dependent manner. The Bd3125-Bd1971-Bd0367 interaction may be influenced by the c-di-GMP bound state of Bd3125.

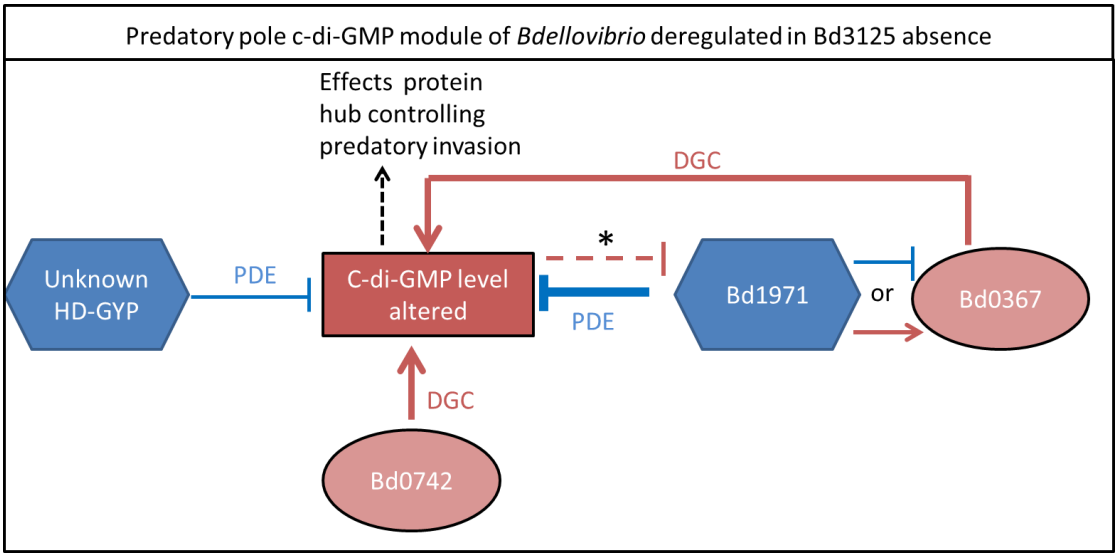

Figure 3.53 Deregulation of predatory pole c-di-GMP module in *Δbd3125* strain. Bd0367 and Bd1971 are no longer permanently in an inactive state and can respond to the c-di-GMP pool. This altering of the c-di-GMP level at the predatory pole may result in slower co-ordination of prey entry.

3.5.4. Interacting partners of Bd0367 identified by B2H were not confirmed by the pull down assay

The identity of purified Bd0367-His bait protein was confirmed by LC/MS (section 8.3.1.2).

The lack of identification of any previously found or unique protein interactions is thought to be because of reasons relating to the conditions of this assay, this suggests further optimization of this process is necessary.

The cells used were attack phase *Bdellovibrio*. Using HD cells brings multiple problems, firstly a large volume of these cells are required to obtain significant protein quantify and secondly retaining this protein after cell harvesting and cell lysis is difficult due to the high number of proteases present in attack phase *Bdellovibrio* due to its predatory nature. Protease inhibitor cocktail was added, however this assay needs to consider either other protease inhibitors, larger amounts of HD100 cells, or consider using HI cells which may have less active proteases.

Additionally the lack of some interaction partners may have been due to the liquid conditions that the HD100 attack phase cells were grown in. Assaying for proteins expressed on surface incubation was attempted but this process did not result in usable protein bands. It is expected that the conditions used such as prolonged incubation on a surface after centrifugation caused cell stress resulting in increased protease activity.

The pull down assay attempted in this study excluded the membrane region as the interactions that we were trying to confirm are cytoplasmic proteins, however it is possible that for example Bd3125, that interacts with membrane bound Bd2492 was retained in the membrane fraction so was not present to interact with Bd0367-His. To include the membrane fraction consideration of different detergents should be investigated.

Overall it could be better to find another technique to confirm the B2H interactions as optimising pull down assays in *Bdellovibrio* has proved difficult in this study and in previous studies by the lab.

3.6. Further Experiments

To progress this work further and help determine a mode of action the following experiments are recommenced

1. Make more B2H constructs. To examine the effect of a Bd0367 phosphomimic mutation on the previously studied interactions. To assess interactions on alanine substitution mutagenesis to locate the exact interaction site for each of the interacting proteins. Then observe Bd3125 interactions when RxxD site is mutated to see if the c-di-GMP bound state of Bd3125 influences these interactions.
2. Confirm the B2H interactions by another experimental method. The His-tag pull downs could be repeated using HI cells and in larger volumes. However other techniques such as far western blotting or affinity chromatography using Glutathione S-transferase (GST) tagged proteins, or co-precipitation methods should be considered.
3. Investigate the effect these protein interactions have on Bd0367 enzymatic activity. For example the DGC activity of purified Bd0367 could be investigated in vitro using radiolabelled GTP and c-di-GMP, by examining the level of c-di-GMP produced by thin layer chromatography. This level could then be compared to the result when incubated with Bd1971, and with Bd1971 with a mutated active site. By examining this it would indicate if Bd1971 interaction inhibits Bd0367 c-di-GMP production.
4. Mutate interaction proteins act their interaction site and conjugate these into *Bdellovibrio* to observe the phenotypic effects caused by the loss of the interaction.
5. Mutate the active sites of the interaction proteins and conjugate these into *Bdellovibrio* gene deletion strain to see if the phenotypic effects caused by the loss of the proteins can be restored by protein presence without restoring enzyme activity.

6. Examine the locations of the protein interactions in vivo. Using an in vivo FRET system would be optimal however the system is not currently possible in *Bdellovibrio* as the plasmids for this are not yet developed. An alternative would be to cross a fluorescently tagged gene on interest onto the chromosome and conjugate a different protein of interest with a different fluorescent tag into the same strain and observe any co-localisation.

3.7. Chapter conclusions

My investigations suggest that Bd0367 physically interacts with Bd1971 and Bd3125. The role of these interactions at the predatory pole of the cell compared to the rest of the cell may be different due to the influence of polar Bd3125. My work suggested that these interactions occur on the RR domain of Bd0367 suggesting these protein interactions may have a regulatory role on the c-di-GMP production ability of Bd0367. From this I have suggested 4 models for the role of these interactions in vivo, however further experimentation is needed to elucidate the true purpose of these interactions.

Chapter 4. Testing for the cognate HK for Bd0367

4.1. Introduction

4.1.1. Two component systems

Two component systems (TCS) are the most widely used of all signal transduction enzymes in nature, present in bacteria, archaea and eukarya (Grebe & Stock, 1999; Koretke et al, 2000). They are used to sense the cells environment, in bacteria this is sensing conditions such as, nutrients, osmotic conditions, temperature, antimicrobials and many more conditions via a sensor Histidine Kinase (HK). The HK relays the message through phosphotransfer to an Asp residue on the Response Regulator (RR) domain protein.

The responses generated by two component signalling are mediated by RR proteins. Many RR proteins (~60%) have DNA binding domains and act as transcriptional regulators. The remaining RR proteins are comprised of either: a stand-alone RR domain (~14%) or a mixture of enzymatic (GGDEF, EAL, HD-GYP), RNA-binding, protein- or ligand-binding (PAS, GAF, TPR, and HPt) domains, or domains of unknown function (Galperin, 2006).

Many HKs also function as phosphatases, which catalyse the removal of the phosphoryl group from the Asp residue of the RR. This process is controlled by the sensory input to the HK, in the form of ligand-binding or other environmental signal, this regulates the balance between HK kinase and phosphatase activities (Bhate et al, 2015). This allows stringent control over bacterial responses to external and internal stimuli.

4.1.2. Overview of HKs

4.1.2.1. Genetics

TCS are found in nearly all bacterial species (except *Mycoplasma*) (Koretke et al, 2000) however the number of TCS between bacterial species varies greatly with the average in bacteria being 52 TCS (Cock & Whitworth, 2007; Ulrich & Zhulin, 2010). In many bacterial species the relationship between these signalling proteins are reflected in their gene organisation with many cognate HK and RR pairs found on a single operon. However there are also cognate HK and RR that are not on the same operon these are known as orphans, it can be harder to find the cognate pair when this is the case.

4.1.2.2. Conserved structural regions and domains of HK proteins

HKs have conserved domains required for kinase activity, however within these conserved domains there are differences which allows HKs to be classified into 11 subfamilies (Wolanin et al, 2002). HK activity depends on the core domains, these are the catalytic domain (CA) which binds ATP, at the DHP which is the dimerization and histidine phosphotransfer domain, Figure 4.1.

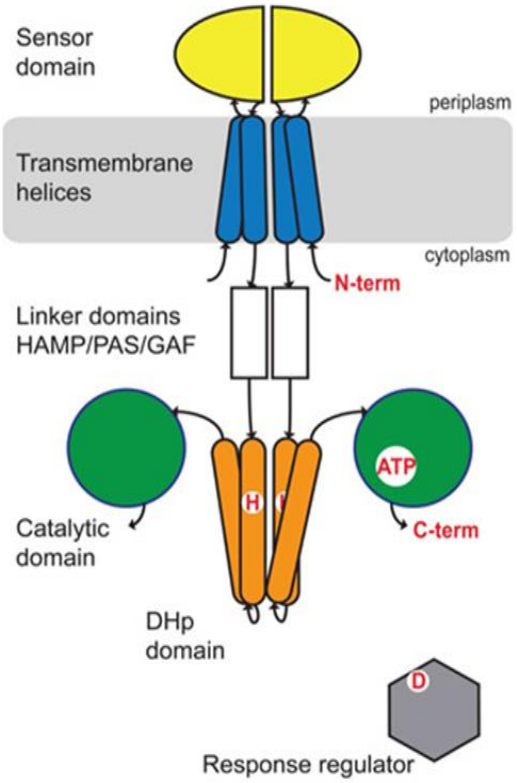

Figure 4.1 The basic HK structural architecture of a transmembrane HK dimer. Figure reproduced from (Bhate et al, 2015) the basic structure is similar for a cytoplasmic HK but without the transmembrane region and external sensor. The diagram shows the DHp domain with the autophoshorylatable histidine and the catalytic domain binding to ATP.

The dimerization domain allows HK homodimer formation and the H box is found within this domain, the H box contains the site of autophosphorylation. Within the catalytic domain there are four conserved motifs, N,D,F and G boxes that are involved in ATP binding, catalysis and phosphotransfer see Figure 4.2. These motifs are used to determine HK subfamilies (Bilwes et al, 2001; Marina et al, 2001). The structure of the catalytic core domain forms an ATP binding pocket from the conserved residues of the N, G and F boxes, this is a flexible region of the protein suggesting conformational

changes may accompany ATP binding (Kim & Forst, 2001) these alterations may modulate protein-protein interactions.

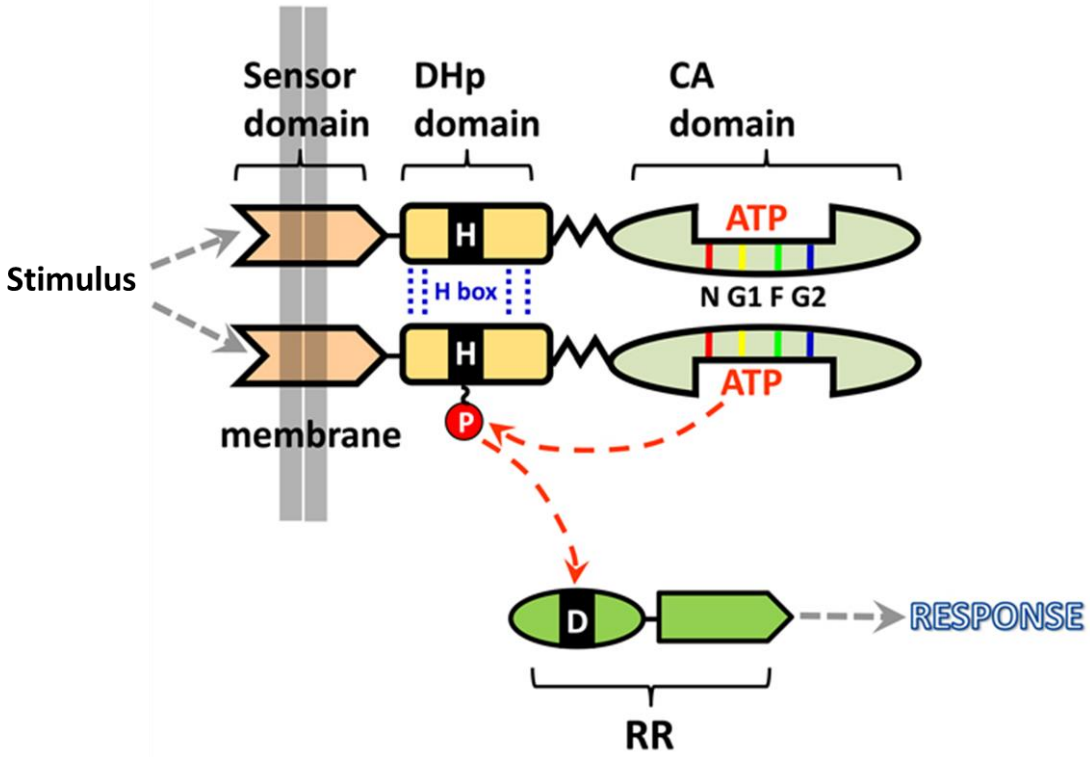

Figure 4.2 The three key structural domains: of a transmembrane sensor, a sensor domain, a DHp domain, and a CA domain. Figure reproduced from (Stewart, 2010).. Within DHp is the H box that spans the phospho-accepting histidine. In addition, there are other homology boxes located within the CA domain near the ATP binding pocket: N, G1 (also called the D box), and G2 (also called the G box) are conserved in all HKs, while the F box is present in some, but not all, HKs. (shows autophosphorylation via an intradimer *cis* mechanism; some HKs utilize a trans mechanism, which is a interdimer mechanism where the H on one HK receives the phosphoryl group from the ATP molecule bound to the CA domain of the HK protein (Ashenberg et al, 2013; Casino et al, 2014; Gao & Stock, 2009; Goldberg et al, 2010)

Another key domain of a HK is the linker domain; this joins the sensor domain to the kinase catalytic core domain. The linker domain may be crucial for proper signal transduction. The linker region is thought to promote intracellular associations or relay conformational changes from the sensor domain to the kinase core (Aravind & Ponting, 1999).

4.1.2.3. Signal perception by HKs

HK proteins are commonly linked to a variety of different sensing domains, such as a key transmembrane helix or extracellular loop or HAMP, PAS, and GAF domains. These

domains can bind and respond to a diverse range of ligands and respond to a broad range of stimuli resulting in a responsive signalling system.

PAS domains are the most frequent sensor domain found with HK proteins (Krell et al, 2010). PAS domains are versatile domains that can bind to many different ligands to monitor cellular changes such as redox potential, oxygen, light and small ligands depending on the co-factor (Zhulin & Taylor, 1999).

Another mechanism of HK signal perception in through accessory proteins, these additional proteins can act as signal-sensing antennae. The signal binds to the accessory protein and this protein transmits the stimulus to the HK. When this occurs it can be known as a three component system, this system was once thought rare but there is increasing evidence that the use of accessory proteins is more common than originally thought (Buelow & Raivio, 2010). Accessory proteins belong to many different protein families; this can connect TCS to other regulatory networks in the cell and result in a response to an expanded range of stimuli. The accessory protein binding works in a variety of ways, it can influence HK activity by interacting with and altering the activity of the enzymatic domain, this can increase phosphatase or phosphotransferase activity of the HK (Buelow & Raivio, 2010).

4.1.2.4. HK phosphotransfer mechanisms

The simplest mechanism of autophosphorylation, phosphotransfer and dephosphorlyation are outlined below.

HKs undergo an ATP dependent autophosphorlyation at a histidine residue in the kinase core, depicted as: HK-His + ATP↔HK-His~P + ADP. This autophosphorylation event can occur in *trans* or in *cis*, in *trans* this is a bimolecular reaction between HK homodimers where one monomer catalyses the phosphorylation of the other (Hoch & Silhavy, 1995). In *cis* this is an intradimer reaction where the ATP from the CA domain catalyses the phosphorylation of the histidine on the same monomer (Casino et al, 2009). In both cases this phosphorylation creates a high energy phosphoryl group that is transferred to an aspartate residue on the RR, this is referred to as the phosphotransfer step and is shown as: HK-His~P+ RR~Asp ↔HK~His+ RR-Asp~P.

The autophosphorylation activity of a HK can be regulated by transmembrane domains binding ligands or indirect detection of signals through interaction with other protein components.

The phosphotransfer step is catalysed by the RR domain, this was shown as phosphodonors were seen to result in RR-Asp~P, this showed that phosphotransfer could occur independent of any assistance from the HK (Lukat et al, 1992). The phosphoryl transfer causes RR conformation to change over a large surface of the domain via repositioning of secondary structures. This is because the phosphorylation of the RR-Asp results in acyl phosphate, the energy within the acyl phosphate bond may then be used to drive these conformational changes in proteins (Jencks, 1980). The changed molecular surface alters inter and intra molecular interactions which can result in a precise molecular output (Stock et al, 2000). Phosphorylation of the RR domain can also: promote dimerization, further oligomerization, protein interactions, relief of inhibition and trigger enzymatic activity of other domains (Blat & Eisenbach, 1994; Fiedler & Weiss, 1995; Sanders et al, 1989; Simms et al, 1985; Weiss et al, 1992).

Finally the phosphoryl group is transferred from the RR-Asp to water in a hydrolysis reaction Figure 4.3. RR-Asp~P +H_2O ↔RR-Asp + Pi. The half-lives of the RR-Asp~P varies, depending on the auto-phosphatase activity of the RR, this autophosphatase activity ensures that the RR proteins are not permanently activated by phosphorylation (Goudreau et al, 1998; Hess et al, 1988; Zapf et al, 1998). A water molecule executes a nucleophilic attack on the phosphorus, resulting in a PO_3 transition state coordinated by the conserved Thr/Ser, conserved Lys, and metal ion (Bourret, 2010).

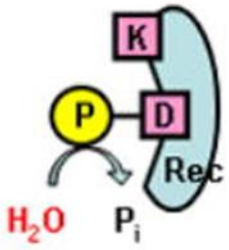

Figure 4.3 RR autophosphatase activity. Reproduced from (Huynh & Stewart, 2011) The RR exhibits autophosphatase activity, where the phosphoryl group is hydrolysed by a water molecule. The Lys residue participates directly in dephosporylation reactions

This system is expanded upon by some HKs which have multiple phosphotransfer steps known as phosphorelays. This increased complexity may reflect the need to integrate both positive and negative signals into the output of the pathway. The extended phosphotransfer cascade can incorporate the histidine of HPt domains, involve hybrid HKs and RRs, with the transfer to a secondary kinase (Hoch, 2000).

4.1.2.5. HK phosphatase activity

Many HKs are bifunctional meaning input signals can either stimulate kinase or phosphatase activity (Laub & Goulian, 2007). However not all HKs have phosphatase activity (Stock et al, 2000). Phosphatase activity is not just reverse phosphotransfer, but does result in de-phosphorylation of the cognate RR. This de-phosphorylation can reset the system but can also limit cross talk between non-cognate partners (Perego & Hoch, 1996). There are currently multiple hypothesises about the mechanism of de-phosphorylation, one of which suggests the importance of the T/N amino acid after the H in the H box: H E/DxxN/T is in involved in phosphatase activity see Figure 4.4. When the T/N amino acid was substituted in CpxA and VanS it resulted in loss of phosphatase activity (Baptista et al, 1997), (Raivio & Silhavy, 1997) (Dutta et al, 2000; Huynh & Stewart, 2011).

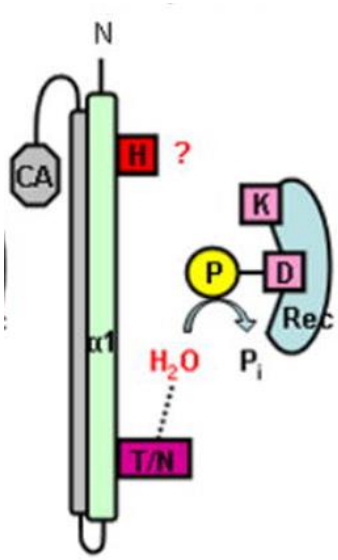

Figure 4.4 Example of HK phosphatase activity. It is hypothesized to employ a conserved Asn or Thr residue. However the role for the phospho-accepting His residue in phosphatase activity is uncertain. Figure reproduced from (Huynh & Stewart, 2011)

4.1.3. Specificity residues between cognate two component system partners

A key means of ensuring specificity of the interactions between a HK and its cognitive RR is determined at the level of molecular recognition by protein-protein interactions (Newman & Keating, 2003). This molecular recognition allows an 'exquisite specificity of HK- RR interactions' (Skerker et al, 2008). This specificity means that HKs have a distinct preference for their cognitive RR, therefore excluding interactions with non-

cognate RRs. Identifying the crucial residues for molecular recognition was carried out using computational and co-variation analysis (which does not require structural data) this resulted in two clusters of importance. Then the group of amino acids located below the active site histidine (Capra et al, 2010) was seen to be sufficient to determine the substrate specificity of the HK, which tends to correlate with the presumed location of the molecular interface generated during phospho-transfer see Figure 4.5 (Skerker et al, 2008).

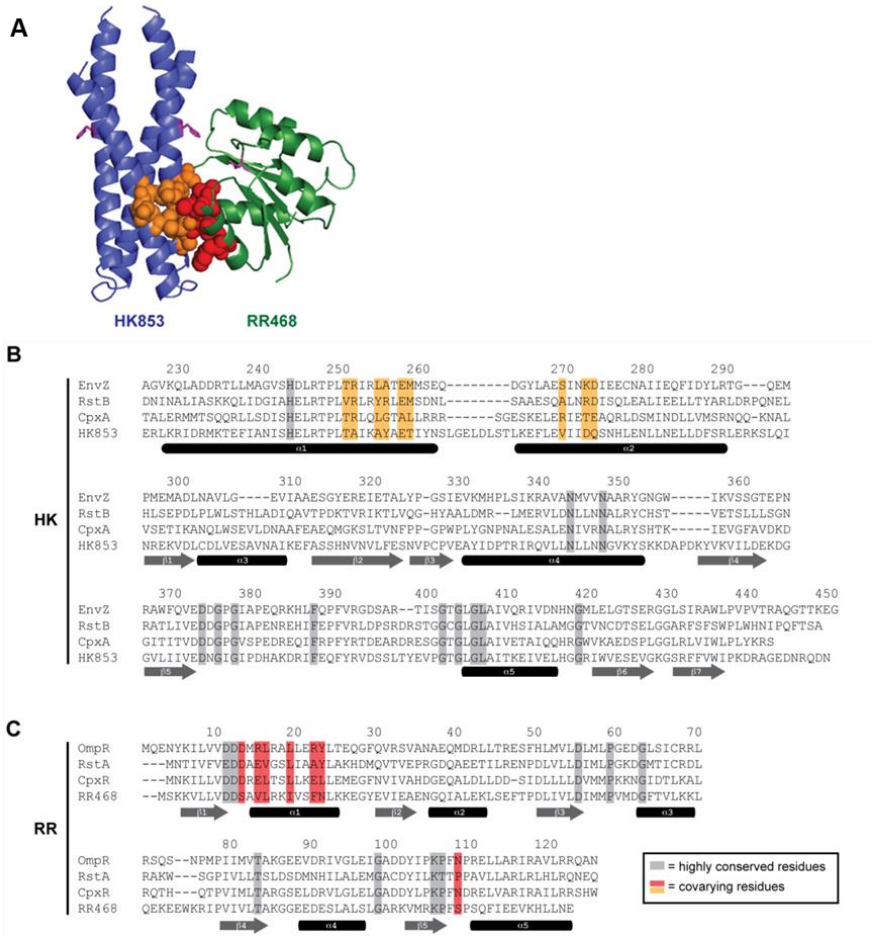

Figure 4.5 Specificity residues between TCS partners. (A) shows the interacting regions : the blue is a HK with its cognate RR in green. The orange and red residues proved to be the sufficient in determining RR specificity to a particular kinase. These residues are located under the active site histidine. (B) and (C) that highlight the co varying residues through protein alignment. Figure reproduced from (Capra et al., 2010)

Skerker and co-workers showed that each kinase has a "kinetic preference" for its cognate substrate, which was mediated by amino acid differences in the specificity residues between the kinase and the RR affecting the reaction rate (Skerker et al, 2005). If the RR interacts for a longer time with its correct kinase, this both prevents access to the

kinase by the incorrect substrate and drains the kinase of all available phosphate, resulting in phosphorylation of only the correct RR. This hypothesis, was supported by changes to the kinase at the specificity residues, which resulted in a shift in kinetic preference that altered HK-RR specificity (Skerker et al, 2008). In summary HKs exhibit a kinetic preference in vitro for their in vivo cognate RR relative to other non-cognate RRs (Skerker et al, 2005). These favourable kinetics for the cognate pairs limits the crosstalk between non-cognate pairs (Groban et al, 2009).

4.1.4. Number of HKs two component systems in *Bdellovibrio*

Mist2.2 identifies 29 HKs, 14 hybrid HKs, 40 RR and 2 hybrid RRs in *B. bacteriovorus* HD100, these are examined further in section 4.4.1. To date there has been no research into characterising TCS in *Bdellovibrio.*

4.2. Specific Research Aims

- To identify the binding potential of candidate HKs to Bd0367 by B2H analysis and β-galactosidase analysis.
- To assess the interaction between the putative cognate HK and Bd0367 on phosphorylation site mutation by B2H and β-galactosidase analysis.
- To assess the dimerization interaction of the cognate HK with a WT and phosphorylation mutation.
- To investigate the possible network of interactions between the putative cognate HK and other c-di-GMP components known to interact with Bd0367 by B2H analysis and β-galactosidase analysis.
- To make an in-frame deletion of the putative cognate HK and analyse the resulting phenotype.
- To supply the HK deletion strain in *cis* with a version of the gene that is predicted to be unable to auto phosphorylate and analyse the resulting phenotype.
- To analyse the location and intensity of the HK-mCherry protein throughout predation and when incubated on a surface.
- To investigate the phospho-transfer profile between the putative cognate kinase and Bd0367 by radioactive phosphotransfer assays under varying conditions.

- To develop a method to pull out native interacting protein partners of the HK, using His-tagged *Bdellovibrio* protein purified in *E. coli*.
- To re-test the original potential candidate HKs for dimerization interactions to confirm that validity of B2H tagging.

4.3. Hypotheses

- One of the candidate HKs will interact significantly with Bd0367 by B2H assay, suggesting it to be the cognate HK for Bd0367.
- Mutation of the phosphorylation sites on the RR and the HK will result in a slightly weaker interaction, as the region where transfer phosphotransfer occurs has been altered but key cognate specificity residues still remain.
- Due to the interaction between Bd0367 and the cognate kinase, the kinase could be in close proximity with the c-di-GMP components Bd1971 and Bd3125 that also interact with Bd0367. I hypothesise that these other c-di-GMP component proteins will interact with the HK and this interaction could be considered accessory proteins providing a mechanism of sensing of the c-di-GMP level of the cell and that this could in turn modulate the phospho-transfer to Bd0367 and hence its activity.
- The deletion of the cognate kinase will result in a phenotype similar to the Bd0367 deletion as I hypothesise that phosphotransfer activates Bd0367 activity and in this mutant no phosphotransfer should occur.
- The mutation in the HK resulting in the predicted loss of auto-phosphorylation should ensure that Bd0367 is not promiscuously phosphorylated by alternative HK. This should result in Bd0367 in its un-phosphorylated (predicated inactive) state leading to a phenotype similar to the Bd0367 deletion strain.
- Analysis of the location of the HK mCherry throughout the time course will show increased fluorescence at the end of the predatory cycle as progeny *Bdellovibrio* prepare to exit the bdelloplast and an increase when incubated on a surface suggesting a link to gliding motility.
- The candidate cognate kinase will phosphotransfer to Bd0367. This will indicate that the kinase investigated is the correct candidate.
- The HK His tagged pull down assay will confirm interactions established by B2Hanalysis and identify other potential interacting partners.

- The original candidate HKs will form dimers as expected as N terminal tags will not impair the DHp region located at the C terminus.

4.4. Results

4.4.1. Profile of two component systems in *Bdellovibrio bacteriovorus* HD100

Mist2.2 was used to analyse the potential TCS in *Bdellovibrio*. These have been grouped into Table 4.1 of suspected cognate partners due to predicted location in the same operon by and orphans Table 4.2 (Taboada et al, 2012). Microarray analysis of the expression of *Bdellovibrio bacteriovorus* HD100 genes was undertaken by (Lambert et al, 2010a) and compared the expression of genes during the attack phase of the predatory cycle and to the expression of the same gene in a HI strain. These data were used to look at the gene expression of various HKs and RRs identified by Mist2.2 (Ulrich & Zhulin, 2010). These data give an indication of which HK are more important for HD or HI growth phases.

HK	Response regulator	Expression patterns by microarray data (Lambert et al 2010)
Bd0620	Bd0621	Up in HI growth
Bd1018	Bd1017	Up in HI growth
Bd1335	Bd1347	Down in HI growth
Bd1506	Bd1505	Up in HI growth
Bd1512	Bd1513	Up in HI growth
Bd1758	Bd1759	Down in HI growth
Bd2141	Bd2139	Down in HI growth
Bd2576	Bd2575	Up in HI growth
Bd2838	Bd2837	Up in HI growth
Bd3036	Bd3035	Up in HI growth
Bd3357	Bd3360	Up on 30 min prey incubation

Bd3367	Bd3366	Up in HI growth
Bd3428	Bd3431	Down in HI growth
Bd3450	Bd3451	Up in HI growth
Bd3648	Bd3649	Constitutive
Bd3750	Bd3751	Down in HI growth
Hybrid HK	Response regulator	Expression patterns by microarray data
Bd0300	Bd0299	Down in HI growth
Bd1828	Bd1825	Up in HI growth
Bd3430	Bd3431	Up in HI growth
Bd3528	Bd3527	Down in HI growth

Table 4.1 Potential cognate HK and RR proteins in *Bdellovibrio*

Orphan HKs and orphan hybrid HKs are harder to group with their potential cognate response regulator. The expression of these genes is outlined in Table 4.2.

Orphan HKs and orphan hybrid HKs			
Up in HI growth	Down in HI growth	Up on 30 min prey incubation	Constitutively expressed
Bd1571, Bd1657, Bd3126, Bd3613	Bd0216, Bd1855, Bd1899, Bd2184, Bd2833, Bd3779 Bd2335 Bd2843 Bd2849, Bd0584, Bd0596, Bd1381, Bd1382, Bd1535	Bd1258	Bd2584, Bd0499

Table 4.2 Orphan HK and hybrid HK proteins in *Bdellovibrio*

4.4.2. Selecting possible cognate HKs informatically

Dr Steve Porter used the specificity residue data from various studies (Burger & van Nimwegen, 2008; Capra et al, 2010) to predict kinase: regulator partners, and employed them in generating the candidate HKs that may specifically interact with the RR domain in Bd0367. This analysis was necessary as Bd0367 does not have a co-transcribed kinase. He found that Mext1821 from *Methylobacterium extorquens* had similar specificity residues to Bd0367, sharing 4/7 residues (see Figure 4.6). These residues are Bd0367: DDSIEPV and Mext1821:DDIIRGV. The cognate kinase for Mext 1821 is Mext1822 and its

specificity residues of are TVGEDL. This suggested Bd2576 with residues TIGEEL (4/6) or Bd2849 with residues NVGMDL (4/6) as possible cognate kinases in *Bdellovibrio*.

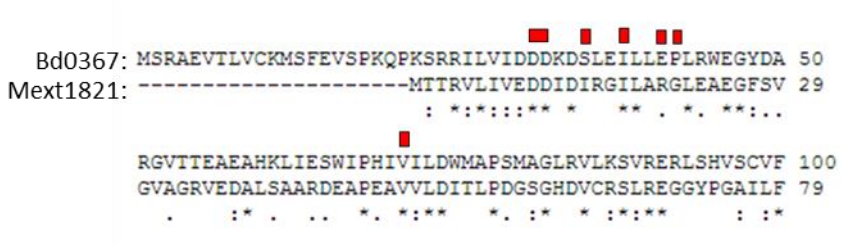

Figure 4.6 Location of specificity residues for Mext1821 compared to Bd0367. The RR domain of Bd0367 compared to the RR region of Mext 1821. The residues indicated by red rectangles are the proposed specificity residues.

However another method was also employed looking at similar RR specificity residues to those for Bd0367 with in the *B. bacteriovorus* HD100 genome; this found hybrid HK Bd2843 with residues DDSVTVA at its RR domain. As Bd2843 is a hybrid HK its kinase specificity residues could be noted, these are NSGWEI. Other HK in *Bdellovibrio* then had their specificity residues compared to those of Bd2843. This resulted in suggestions of Bd3779: NSGFDI (4/6), Bd2584:NSGMEL (4/6) and Bd2335: NSGMEL (4/6). This made six candidate kinases to test for interaction with Bd0367 by B2H analysis. See table 4.3 for further analysis of these six candidate kinases and figure 4.7 for diagrams of SMART domains.

Gene Number	SMART Domains	Predicted cellular compartment (PSORTb)(Yu et al, 2010)	Signal peptide prediction (predisi) (Hiller et al, 2004)	Specificity residues	Expression in predatory life cycle array data (Lambert et al, 2010a)
Bd2335	8 transmembrane regions, MASE1, HisKA, HK CA:1, REC	Cytoplasmic membrane	Signal sequence predicted: cleavage site amino acid 57 (predicted for secretion)	N_{341}SVLGMLEL$_{349}$	decrease in HI growth
Bd2576	2TM domains, HAMP, HisKA, HK CA:2	Cytoplasmic membrane	Signal sequence predicted: cleavage site amino acid 31	T_{278}IMRGEMEL$_{286}$	Up in HI growth
Bd2584	PAS 3, PAS4, HisKA, HKCA:1 (HATPase_c)	Cytoplasm/ cytoplasmic membrane	None predicted	N_{396}SIMGMSEL$_{404}$	constitutive,
Bd2843	GAF, HisKA, HATPase_c, REC	Cytoplasm/ cytoplasmic membrane	None predicted	N_{198}SIMGWAEI$_{206}$	decrease in HI growth
Bd2849	7transmembrane domains, Chase,	Cytoplasmic membrane	Signal sequence predicted: cleavage	N_{512}VIVGMSDL$_{520}$	decrease in HI growth

	HisKA, HATPase_c, REC		site amino acid 37		
Bd3779	5transmembrane domains, HisKA, HK CA:1	Cytoplasmic membrane	Signal sequence predicted: cleavage site amino acid 60	N_{240}SIIGFSDI$_{248}$	decrease in HI growth

Table 4.3 Candidate cognate HKs for Bd0367. This table shows the predicted domains, cellular location, specificity residues and array data for the HKs being investigated. The bold residues indicate the key specificity residues from within the surrounding sequence.

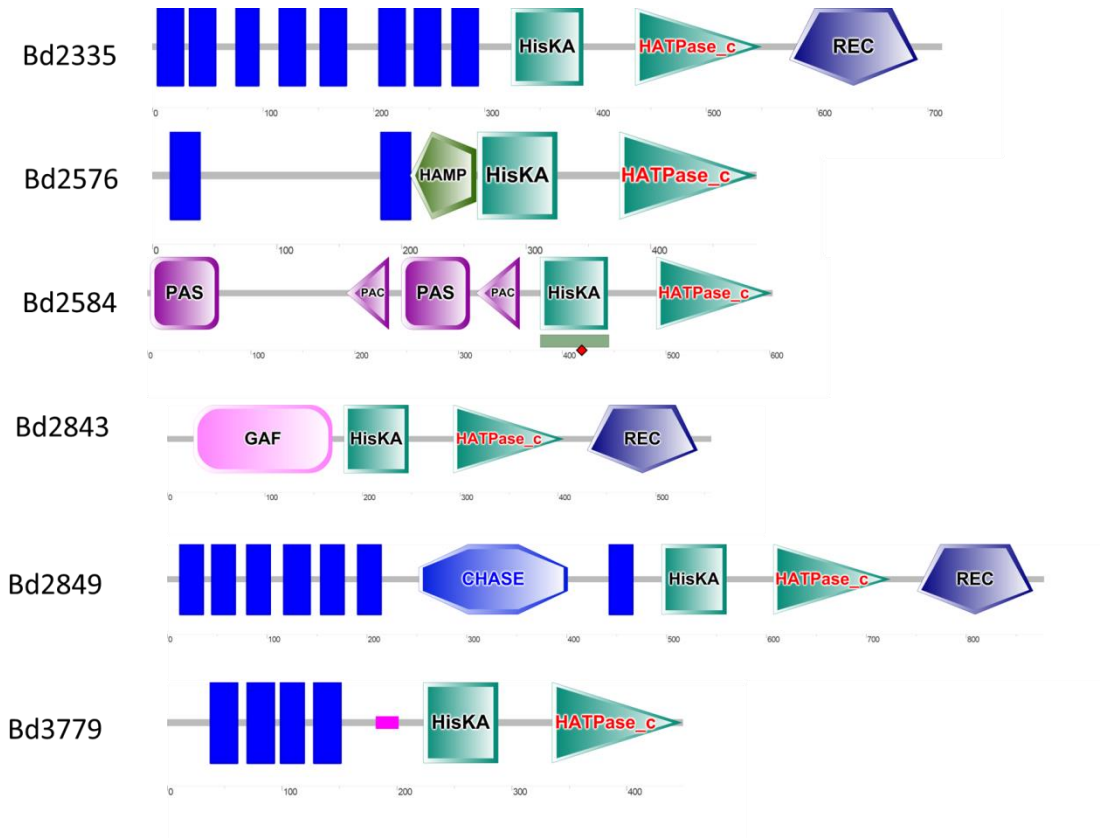

Figure 4.7 The SMART domains of the 6 candidate HK. The blue rectangles represent the transmembrane regions. HisKA is a dimerization and phosphoacceptor domain. HATPase_c domains are found in ATP binding proteins such as HKs. REC domains contain phosphoacceptor sites that are phosphorylated by HKs. HAMP domains are 50-amino acid alpha-helical linker regions that can transmit conformational changes. PAS domains are found in many proteins and acts as a signal sensor. GAF domains are small-molecule-binding regulatory domains found in many proteins and have a similar fold to the PAS domain. CHASE domains are extracellular or periplasmic in location and are predicted to be ligand binding domains.

4.4.3. Investigating interactions between six HKs and DGC and RR protein Bd0367

To determine which of the six bioinformatically identified kinases were most likely to be the cognate kinases for Bd0367 the method of B2H in BTH101 *E.coli* was used. This technique has been used previously in other literature to investigate interaction strengths between cognate and non-cognate pairs in regards to a cross regulation system in which they determined results from differential binding affinities between different sensor–regulator pairs (Huynh et al, 2015).

This suggested that the cognate HK would be the protein that interacted most strongly by β-galactosidase assay with Bd0367.

All six of these genes were cloned into the B2H plasmids pUT18c and pKT25 which tagged the N terminus of the proteins with the T18 or T25 sections of adenylate cyclase. In retrospect in addition to this these proteins should have been C terminally tagged or truncated due to the transmembrane nature of 4 of the 6 test proteins, figure 4.8 shows the location of 6 HK and the position of the B2H tags.

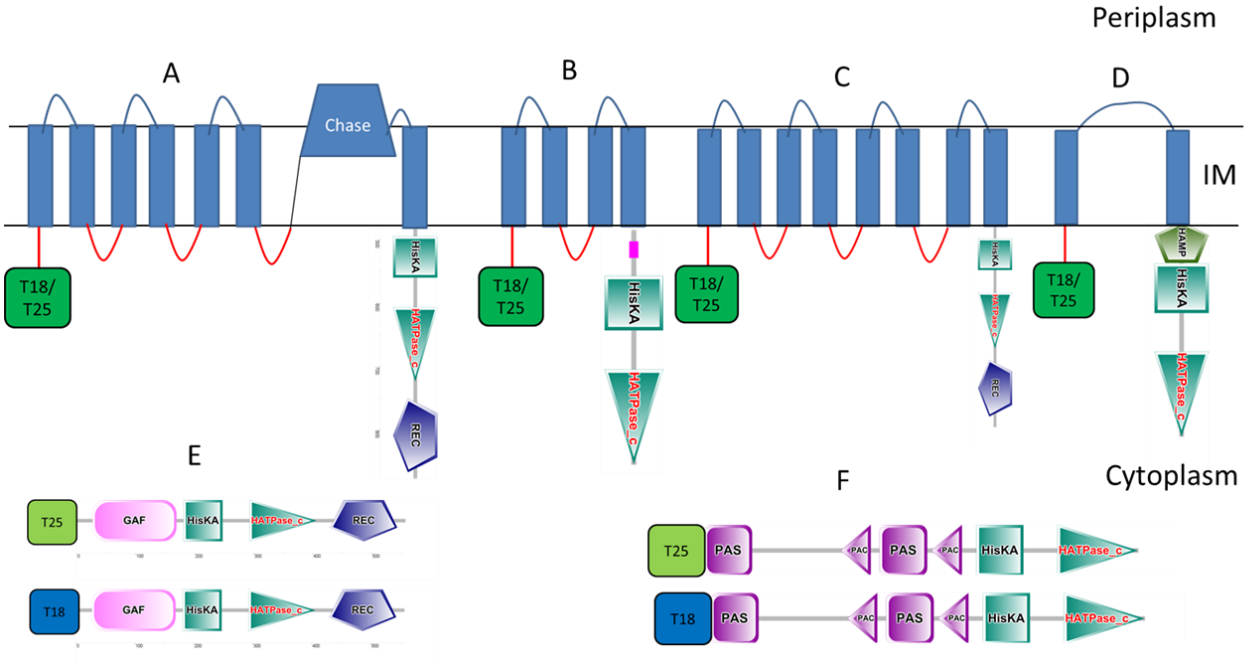

Figure 4.8 Predicted cellular location of HKs with B2H tags. Membrane orientation of transmembrane regions of the candidate kinases predicted by Topcons (Tsirigos et al, 2015), with N terminal B2H tags (T18/T25). (A) Bd2849 membrane associated (B)Bd3779 membrane associated (C) Bd2335 membrane associated (D)Bd2576 membrane associated (E) Bd2843 cytoplasmic (F) Bd2584.cytoplasmic.

4.4.3.1. B2H and β-galactosidase assays suggest that Bd0367 interacts with HK Bd2584

If a candidate HK and Bd0367 interact the T18 and T25 fragments are brought together and reform adenylate cyclase, cAMP cause the expression of the *lacZ* reporter gene, this results in blue colonies on plates containing X-gal, see methods 28.1.

The results of a typical B2H assay for Bd0367 and the candidate kinases are shown in Figure 4.9. A strong interaction between Bd2584 and Bd0367 was observed in both orientations tested resulting in two blue spots. A slight interaction was also detected between Bd2843 and Bd0367 resulting in light blue spots.

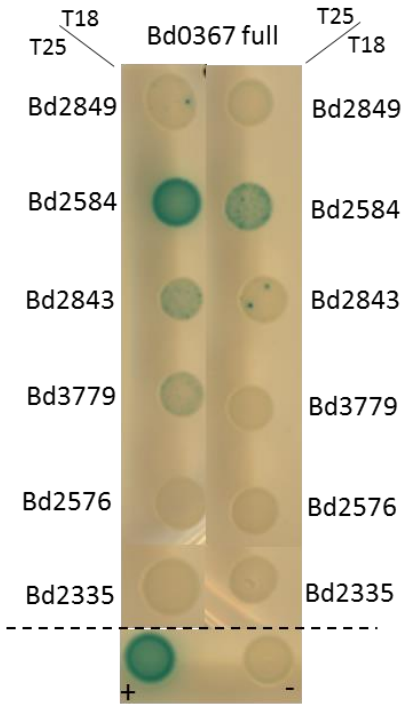

Figure 4.9 Spot plate interactions of Bd0367 GGDEF protein with 6 HK proteins. Blue spots suggest an interaction between Bd0367 and Bd2584, this interaction is seen in both tag orientations. There are also faint blue spots between Bd2843, Bd3779 and Bd0367. Results displayed are a typical representation of the results from three biological repeats and nine technical repeats. Positive (+) = pUT18c-zip with pKT25-zip. Negative (-) = pUT18c with pKT25.

Further testing of these interactions was carried out by β-galactosidase assays, these assays were used to quantify the strength of the interaction between the pairs of proteins. From these results Bd0367-T18 and Bd2584-T25 were seen to interact significantly more than the negative control but only in this orientation suggesting that the other orientation experiences steric hindrance (Figure 4.10. The interaction strength seen is not as strong as those in the previous chapter 3 however it is presumed that the interaction between HK and RR is transient in nature. None of the other test pairs result in an interaction greater than the negative control Figure 4.11.

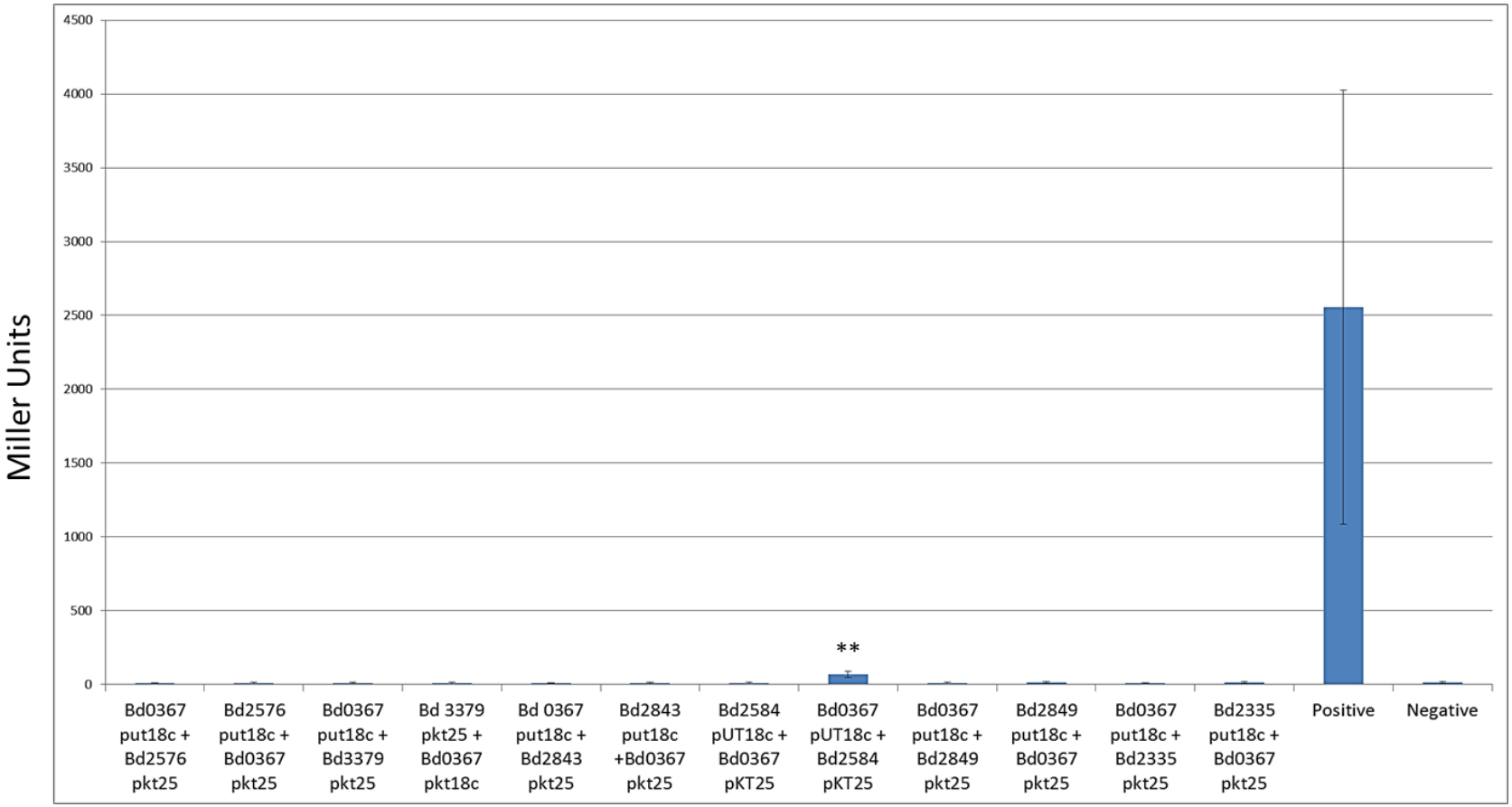

Figure 4.10 β-galactosidase activity assay for interactions between Bd0367 and six test HK proteins. Error bars show standard deviation. The results show the mean value from three biological repeats and comprise six technical repeats. The figure shows the interaction strengths of each kinase in each either vector with both the positive and negative controls. Only one interaction, Bd0367-18 and Bd2584-25, was found to be significantly different from the negative control by Student t-test. Asterisks show significance of student t-test compared to the negative (pUT18c,pKT25) **≤0.01

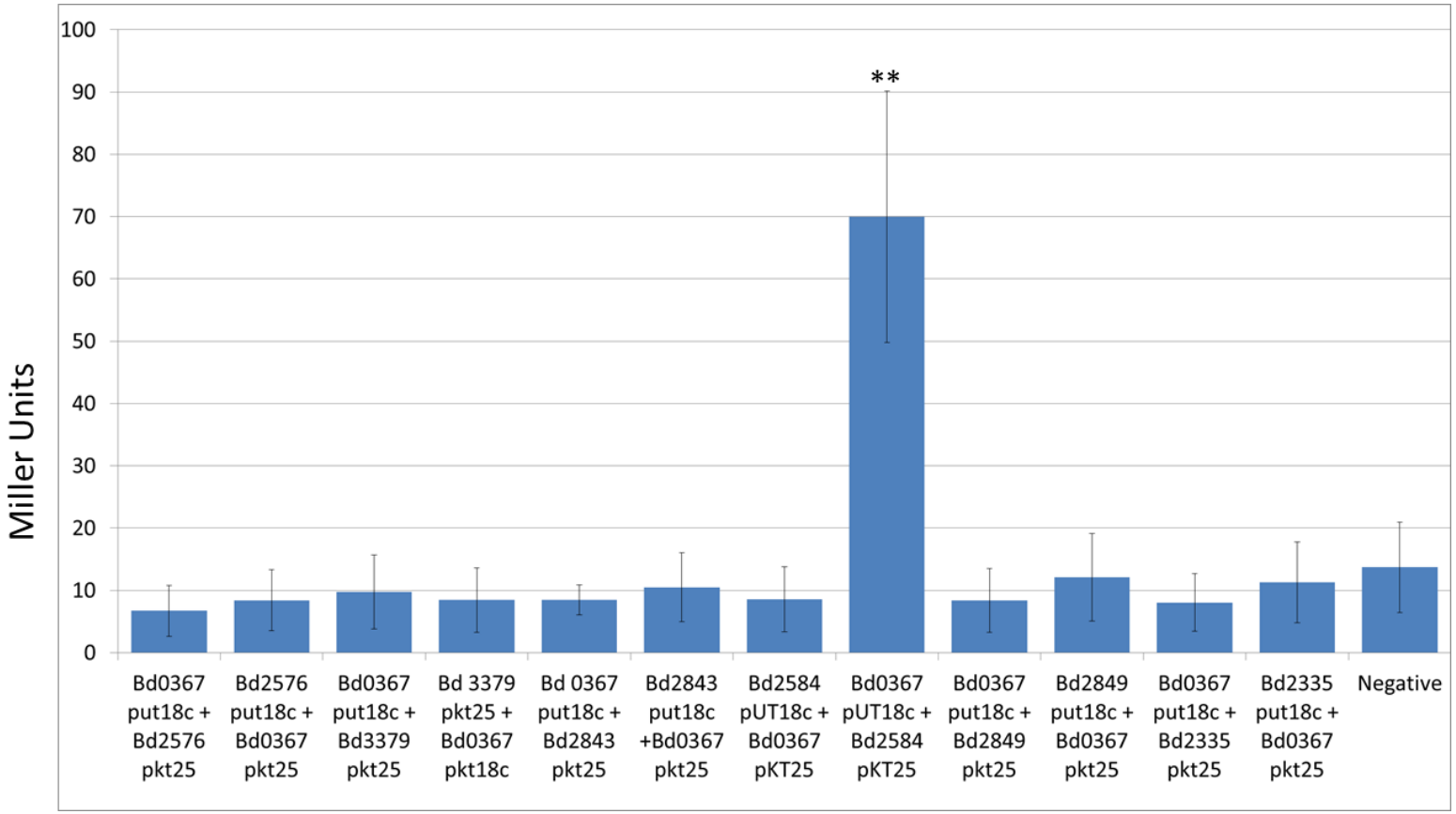

Figure 4.11 β-galactosidase activity assay (enlarged scale) for interactions between Bd0367 and six test HK proteins without the positive control. Error bars show standard deviation. The results show the mean value from three biological repeats and comprise six technical repeats. The figure shows the interaction strengths of each kinase in each either vector with the negative control, to allow better observation of the difference in interaction strength when compared to the negative. Only one interaction, Bd0367-18 and Bd2584-25, was found to be significantly different from the negative control by Student t-test. Asterisks show significance of Student t-test compared to the negative (pUT18c,pKT25) **≤0.01

4.4.4. Bioinformatics of HK Bd2584

From the results of the B2H and β-galactosidase assays Bd2584 appeared to be the most convincing candidate for the role of cognate HK to Bd0367.

Further bioinformatic analysis of Bd2584 showed it is conserved in *B. bacteriovorus Tiberius* (Bdt_2508) found by BLAST to share 88% protein identity. This suggests that role for Bd2584 may be conserved between the *Bdellovibrio* species. However there are no strong protein homologues in other bacteria.

4.4.4.1. Domain structure of Bd2584

As shown in Table 4.3 and Figure 4.7 Bd2584 has multiple conserved domains. There are two PAS domains, where the ligand of these PAS domains is not established. However the observation of a haem pocket bioinformatically suggests a potential role in oxygen binding as seen in FixL PAS domain (LukatRodgers & Rodgers, 1997). Haem is a common cofactor, the coordination state of the haem can regulate kinase activity (LukatRodgers & Rodgers, 1997; Miyatake et al, 1999). The other conserved domains comprise the HK region of the proteins HisKA involved in dimerization and HATPase_c involved in ATP binding and catalysis.

Bd2584 is a cytoplasmic HK so does not have a transmembrane sensor region. This suggests that Bd2584 could be responding to an intracellular signal, or that it may receive a signal from a transmembrane protein.

4.4.4.2. HK Bd2584 is part of the HK 1 subfamily

As stated in the introduction HK can be split into subfamilies of 11 varieties (Wolanin et al, 2002). The majority of HK are classed in the type 1 subfamily, the sub group is determined by the motifs for the H, N, D and G boxes. Table 4.4 shows the homology box motifs for subfamily 1, Bd2584 has very similar motifs to subfamily 1, suggesting it is part of this family of kinases.

Motifs	Type 1 HK homology motifs	Bd2584 motifs
H box	Fhxxh(S/T/A)H(D/E)h(R/K)TPLxxh	$_{383}$FLANMSHEIRTPMNSI$_{398}$
N box	(D/N)xxxhxxhhxNLhxNAh.(F/H/Y)(S/T)	$_{492}$DATRFQQVLINLIGNGLKFT$_{511}$
D and F box	hxhxhxDxGxGhxxxxxxxhFxxF	$_{527}$LWVGVKDTGIGMAPEQMQGLFTRF$_{550}$
G box	GGxGLGLxhhxxhhxxxxGxhxhxxxxxxGxxFxhxh	$_{562}$GGTGLGLSISKQLVEKMGGTIGVTSEIGQGSVF$_{594}$

Table 4.4 Shows the similarity between the subtype 1 HK homology motifs (as described in (Wolanin et al, 2002)) and those found in HK Bd2584. Where the amino acids in Bd2584 are the same as in the type 1 motif they are underlined, when they deviate from the type one they are in bold. The D and G box of Bd2584 match the motif for a subtype 1 HK perfectly. In the Bd2584 motif there is one deviation on the H box and two changes in the N box when compared to the subtype 1 motifs. Conserved hydrophobic residues are I, L, V, M are designated by ' h' and x represents any amino acid.

Additionally another study suggested that H box of 'HEhRTPh' is enough to suggest subfamily 1 with this consideration Bd2584 has a subfamily 1 H box motif: HEIRTPM, (Kim & Forst, 2001).

4.4.4.3. Auto-phosphorylation site of Bd2584

Through CDD and H box analysis the H at position 389 in Bd2584 was defined as the site of *trans* or *cis*-autophosphorylation, Figure 4.12 (Marchler-Bauer et al, 2015).

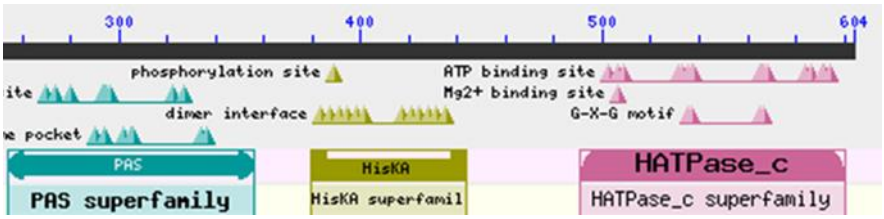

Figure 4.12 Putative phosphorylation site for HK Bd2584 as predicted by the CDD (Marchler-Bauer et al, 2015).

4.4.4.4. Is Bd2584 a bifunctional kinase?

Many HKs are bifunctional meaning input signals can either stimulate kinase or phosphatase activity (Laub & Goulian, 2007). Previous studies have shown the T or N in the H box are important for phosphatase activity (Dutta et al, 2000; Raivio & Silhavy, 1997; Willett & Kirby, 2012) and Bd2584 possesses a T at this position, suggesting it may also possess phosphatase activity. However more than bioinformatic analysis would be required to confirm this.

4.4.5. Investigating the interaction between the HK Bd2584 and split domains of Bd0367 (RR and DGC)

As in Chapter 3 Bd0367 was split into two domains, the RR region and the DGC domain (Figure 4.13). This allowed the site of Bd2584 interaction with Bd0367 to be investigated, and confirm that Bd2584 was binding at a biologically relevant region of Bd0367. Other studies such as (Chen et al, 2015) have investigated the interaction between truncated protein RR domains and HK proteins via B2H method to confirm regions of interaction.

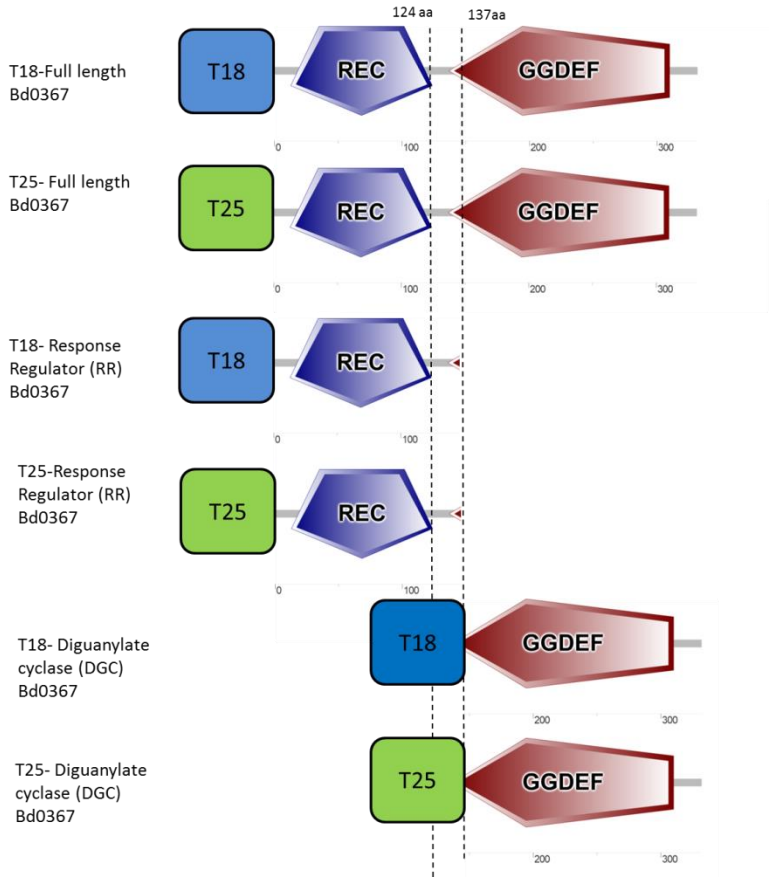

Figure 4.13 B2H constructs of Bd0367 split domains used to study site of HK Bd2584 interaction.

4.4.5.1. HK Bd2584 interacts specifically with the RR domain of Bd0367 as expected

The split domain constructs of Bd0367 used in the previous chapter were used again here to determine if the location of the HK Bd2584 interaction resides in the RR domain or the DGC domain. As expected the interaction region is found in the RR domain of Bd0367, Figure 4.14, and no interaction was observed with the DGC domain, Figure 4.15. This result suggests that the interaction is not due to an intrinsic 'stickiness' of Bd2584 as the interaction is occurring at the biologically relevant domain. However the Bd2584-Bd0367RR interaction no longer occurs in both orientations as seen in the full length Bd0367 spot plates suggesting the truncating of Bd0367 has had a negative effect on the interaction when Bd2584 is tagged with T18.

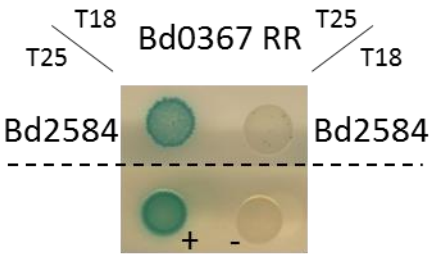

Figure 4.14 Spot plate interactions with RR domain of Bd0367 with HK Bd2584. Blue spots suggest an interaction between Bd0367 RR domain and Bd2584, this interaction is seen in one tag orientation. Results displayed are a typical representation of the results from three biological repeats and nine technical repeats. Positive (+) = pUT18c-zip with pKT25-zip. Negative (-) = pUT18c with pKT25.

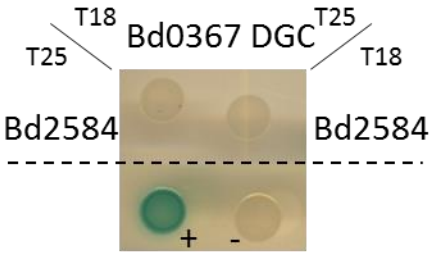

Figure 4.15 Spot plate interactions with digunaylate cyclase domain of Bd0367 with HK Bd2584. White spots suggest no interaction between Bd0367 RRdomain and Bd2584.. Results displayed are a typical representation of the results from three biological repeats and nine technical repeats. Positive (+) = pUT18c-zip with pKT25-zip. Negative (-) = pUT18c with pKT25.

β-galactosidase interactions were carried out to quantify the interaction strengths. The average strength of Bd2584-T25 + Bd0367RR-T18 interaction is higher than seen in the full length β-galactosidase assay and is significantly different from the negative control (figure 4.16 A and B). However the variability of this interaction had increased.

B-galactosidase assays were also carried out the Bd2584 and Bd0367DGC interaction for completeness. This resulted in neither interaction being significantly different to the negative control Figure 4.17.

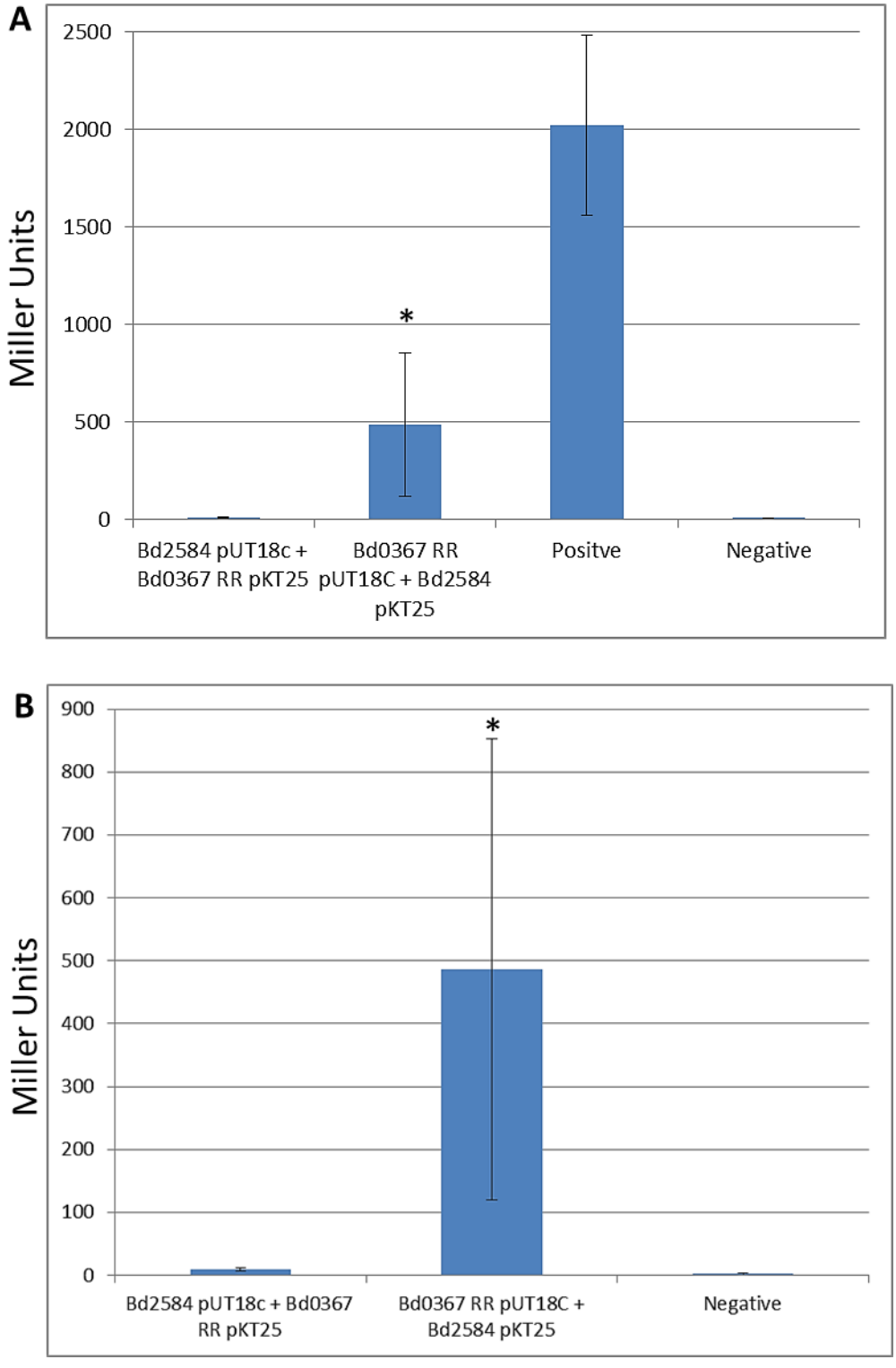

Figure 4.16 β-galactosidase activity assay for Bd0367 RR domain and HK protein Bd2584. Error bars show standard deviation. The results show the mean value from three biological repeats and comprise six technical repeats. (A) The graph shows the Miller units for the Bd2584 and Bd0367 RR interactions with both positive and negative controls. (B) This graph allows better observation of the difference in interaction strengths between the test proteins and that of the negative control. Only one orientation, Bd2584-18 and Bd0367-25, was found to be significantly different from the

negative control by Student t-test. Asterisks show significance of Student t-test compared to the negative (pUT18c,pKT25) *≤0.05

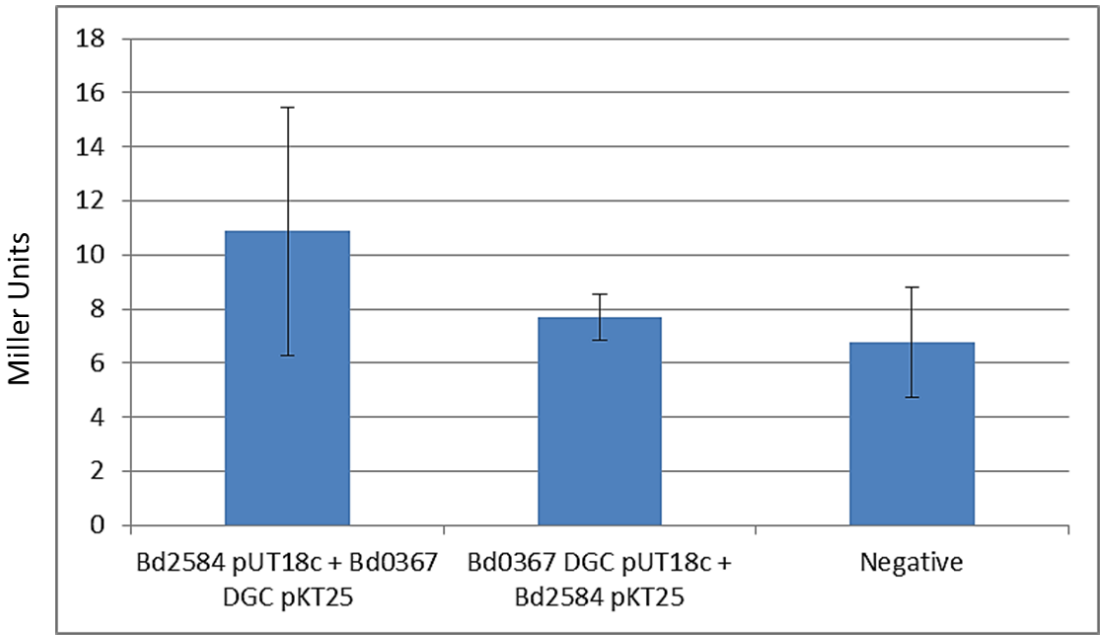

Figure 4.17 β-galactosidase activity assay for interactions between diguanylate cyclase domain of Bd0367 and HK Bd2584 without the positive control . Error bars show standard deviation. The results show the mean value fromthree biological repeats and comprise six technical repeats. The figure shows the interaction strengths of each test interaction with only the negative control, to allow better observation of the difference in interaction strength when compared to the negative. No interactions were found to be significantly different from the negative control by Student t-test.

A summary of the positive interactions between Bd2584 and a variety of Bd0367 constructs is shown in Figure 4.18. The increase in interaction strength between Bd2584 and Bd0367 RR was compared to the interactions strength between Bd2584 and full length Bd0367 and found to be significantly higher.

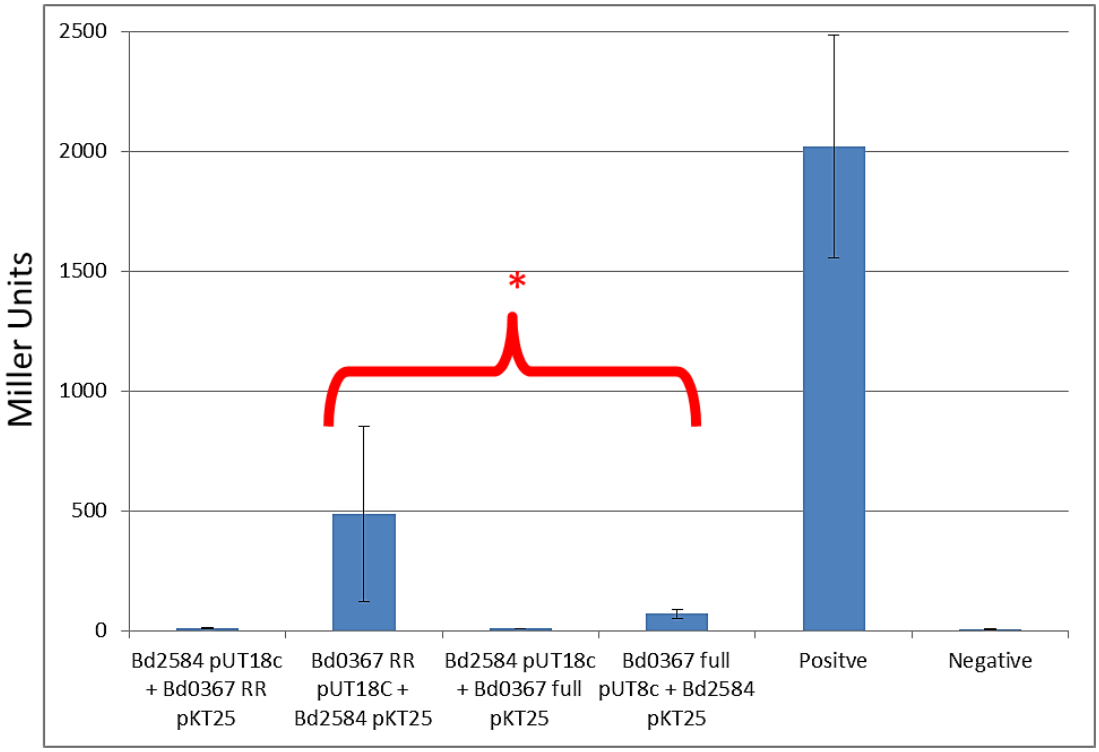

Figure 4.18 Summary of positive β-galactosidase activity assays for Bd2584 and a variety of Bd0367 constructs. Error bars show standard deviation. The results show the mean value from three biological repeats and 6 technical repeats. The graph shows there was no significant difference in the Bd2584-T18 interaction with Bd0367full or Bd0367RR. However there was a significant increase in interaction strength by Student t.test when Bd2584-T25 interacts with the RR domain only compared to the full length Bd0367. This is shown by the red asterisk *≤0.05.

4.4.6. Investigating interactions between HK Bd2584 and Bd0367 when residues important to phosphorylation are mutated

The interaction between HK and RR is thought to be determined by their specificity residues (Capra et al, 2010). However other mutations that affect the conformation of the two proteins may also impact the strength of a protein interaction. By identifying the histidine that is autophosphorylated by the conserved domain database, alignments, the H box, the autophosphorylation site Histidine at position 389 in the kinase Bd2584 was mutated to a Valine residue, Figure 4.19.

In this mutant autophosphorylstion should no longer occur so phospho-transfer to Bd0367 should no longer be able to take place. This strategy has been employed by numerous groups when investigating the relationship between EnvZ and OmpR, with a valine substitution being adequate to prevent auto-phosphorylation in EnvZ (Forst et al, 1989; Zhu et al, 2000). As the H resides in the dimerization region of Bd2584 it is

possible that dimerization of Bd2584 is effected and this could affect the strength of the Bd2584-Bd0367 interaction. Additionally the mutated H residue is only 6 amino acids from the specificity residues identified by Dr Porter, it is possible that the mutation of Histidine to Valine results in an altered environment for the specificity residues and impairs the Bd2584-Bd0367 interaction.

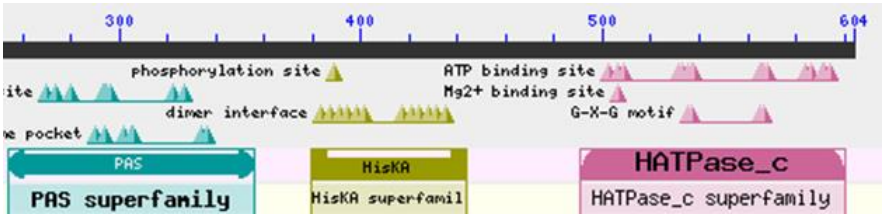

Figure 4.19 Putative phosphorylation site for HK Bd2584 as predicted by the CDD (Marchler-Bauer et al, 2015).

This was used in conjunction with Bd0367D63A mutant outlined in chapter 3 this resulted in a Bd0367 that could not receive phosphate, this was used to examine if the Bd2584-Bd0367 interaction was effected by residues involved in phosphotransfer being mutated.

4.4.6.1. Strength of interaction between Bd2584 and Bd0367 is reduced by mutating the autophosphorylation site on Bd2584 H389V, and mutating the phospho receiving D63A

The result of a typical B2H is show in Figure 4.20. This shows that Bd2584H389V-T25 and Bd0367D63A-T18 interact in one orientation. However the blue colour observed is lighter and more speckled in appearance than previous interaction seen between these two proteins. Additionally in the full length interactions described in section 4.4.3.1 the interaction was observed in both orientations suggesting a slight impairment in the interaction between Bd2584H389V and Bd0367D63A in comparison to wild type spot tests.

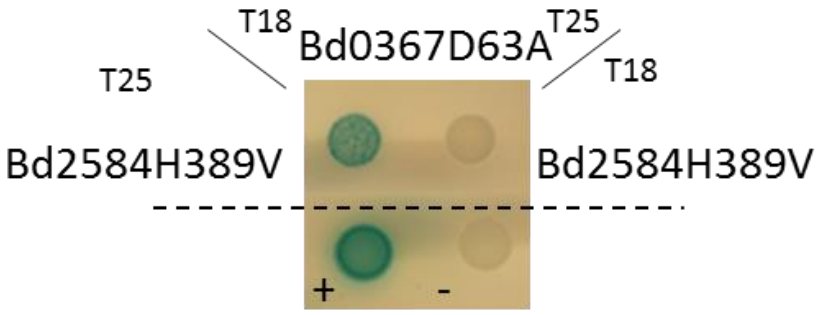

Figure 4.20 Spot plate interactions with Bd0367 D63A with HK Bd2584 H389V . The results look similar to the Bd0367-Bd2584 non mutated interaction, with a blue spot indicative of a positive interaction in one orientation only. The blue spot is slightly speckled however which is different to the consistent blue spot observed previously. Results displayed are a typical representation of the results from three biological repeats and nine technical repeats. Positive (+) = pUT18c-zip with pKT25-zip. Negative (-) = pUT18c with pKT25.

B-galactosidase assays were used to quantify the strength of interaction between these two altered proteins in comparison to the wild type strength. From these results Bd2584H389V and Bd0367D63A do not interact significantly more than the negative control (see Figure 4.21). Also when compared to the interaction strength observed for wild type Bd2584 and Bd0367 the mutated interaction is seen to be significantly lower.

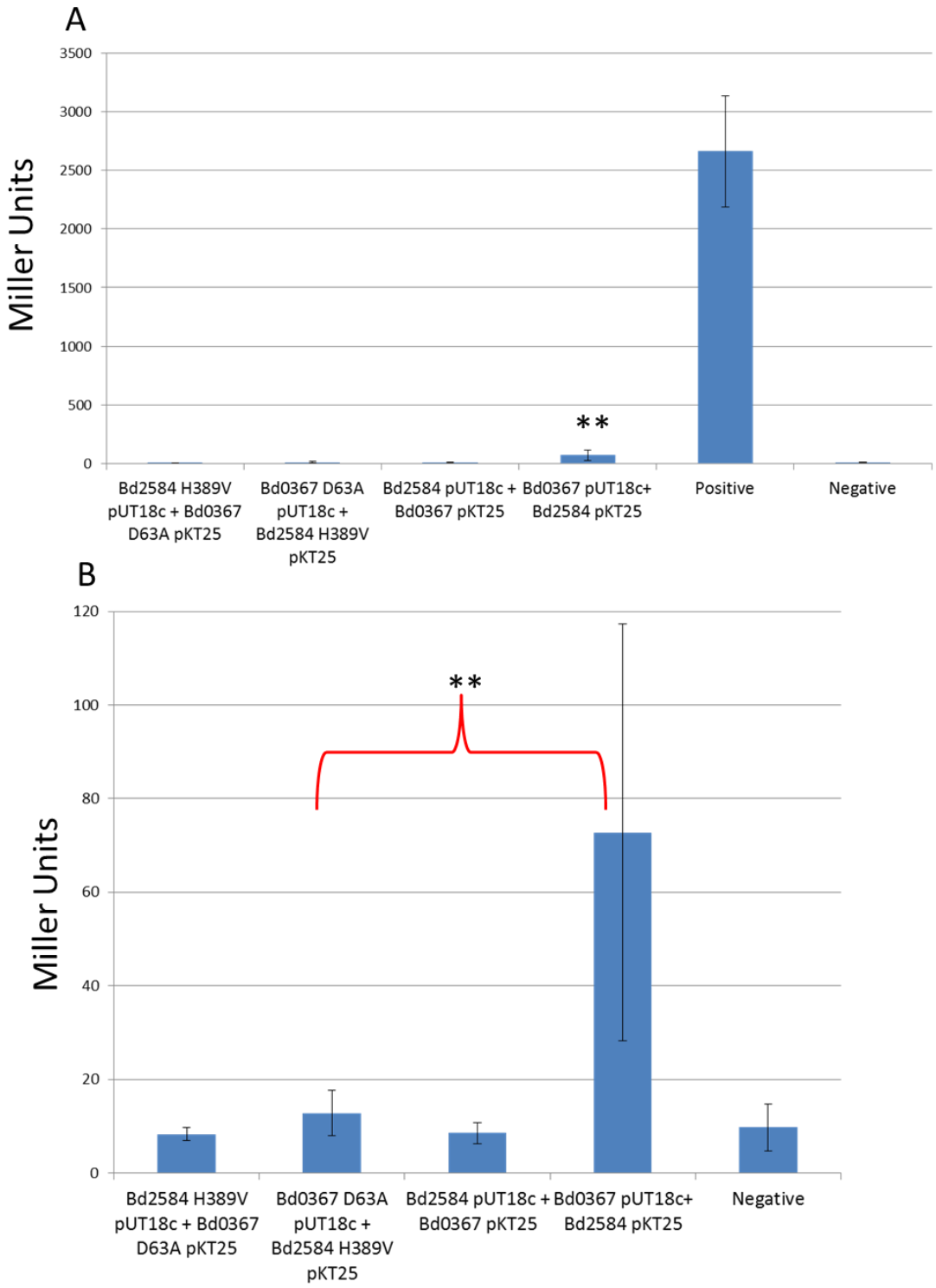

Figure 4.21 Summary of β-galactosidase activity assays for the wild type and phosphoaccepting mutated amino acid version of Bd0367 and a Bd2584. Error bars show standard deviation. The results show the mean value from three biological repeats and 6 technical repeats. (A) The graph shows the Miller units for the wild type and phosphoaccepting mutated amino acid version of Bd0367 and a Bd2584 interactions with both positive and negative controls. (B) This graph allows better observation of the difference in interaction strengths between the test proteins and that of the negative control. The graph shows there is a significant decrease in interaction strength by Student

t-test when comparing Bd2584-T25-Bd0367T18 with Bd2584H389V-Bd0367D63A. This is shown by the red asterisks **≤0.01.

4.4.7. Investigating dimer interaction between HK Bd2584

HKs are well established to act as dimers so the strength of the Bd2584-Bd2584 interaction was tested by B2H and β-galactosidase assays. Due to the reduced interaction strength between Bd2584H389V and Bd0367D63A the ability of Bd2584H389V to dimerise was also investigated to compare to wild type.

4.4.7.1. Bd2584 dimerises and interacts with itself

As expected Bd2584 interacts with itself when tested by B2H, the interaction produces consistently uniform blue spots, Figure 4.22.

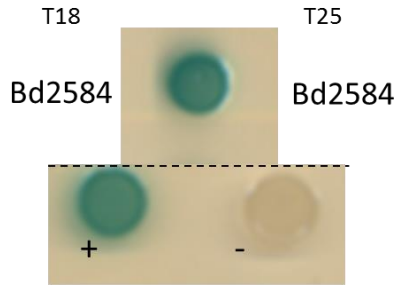

Figure 4.22 Spot plate interactions investigating self-interactions between HK Bd2584. The blue spot indicates a positive interaction between Bd2584 and itself, suggesting dimer formation. Results displayed are a typical representation of the results from three biological repeats and nine technical repeats. Positive (+) = pUT18c-zip with pKT25-zip. Negative (-) = pUT18c with pKT25.

The interaction strength was then quantified using β-galactosidase assay, this resulted in a very high average interaction strength that was significantly different from the negative control (see Figure 4.23). This strong interaction is thought to be due to the importance of HK dimerization interaction.

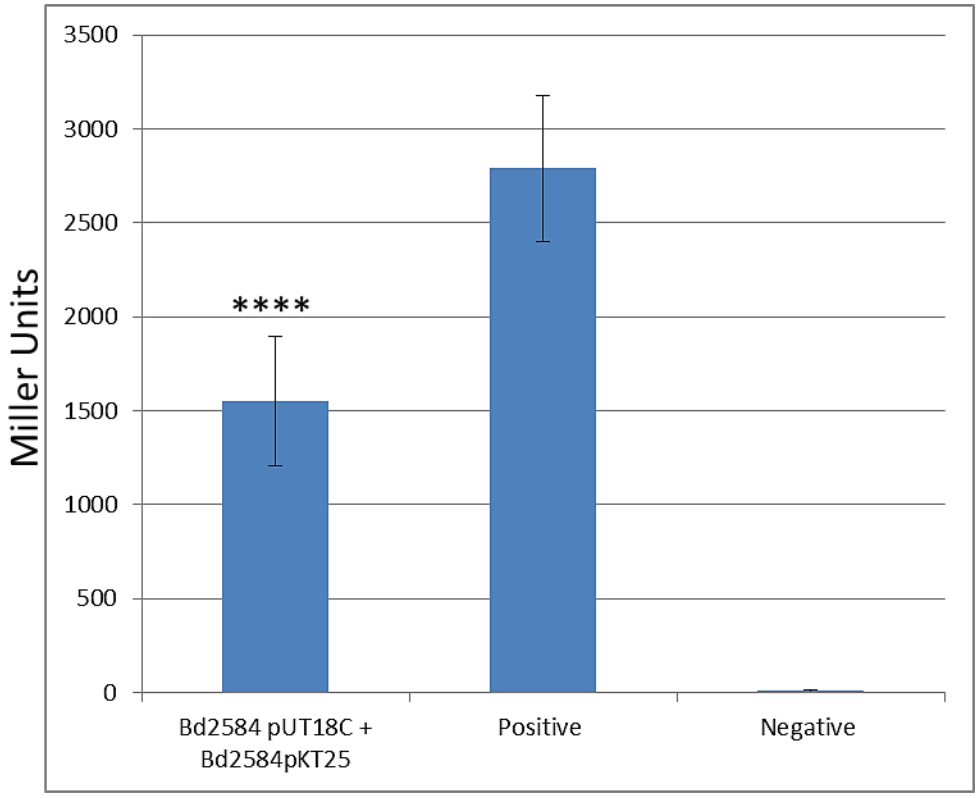

Figure 4.23 β-galactosidase activity assay for Bd2584 self-interactions. Error bars show standard deviation. The results show the mean value from three biological repeats and comprise 6 technical repeats. HK Bd2584 interacts significant with itself. Asterisks show significance of Student t-test compared to the negative (pUT18c, pKT25) ****≤0.0001.

4.4.7.2. Bd2584 dimerization ability is negatively affected by H389V mutation

There was a reduction in interaction strength between Bd2584-Bd0367 when the autophosphorlyation H389 was altered to V in Bd2584. This reduction could be due to the H residing in the dimerization region of Bd2584 so the ability of Bd2584H389V to dimerize was investigated below.

The result of a typical B2H spot plate is shown in Figure 4.24. This shows that Bd2584 and Bd2584H389V form blue spots and consistently interact with themselves.

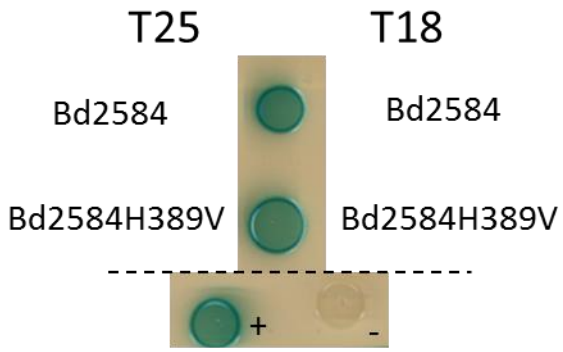

Figure 4.24 Spot plate interaction of Bd2584 and Bd2584H389V dimers. The blue spot indicates a positive interaction between Bd2584H389V and itself, suggesting dimer formation. Results displayed are a typical representation of the results from three biological repeats and nine technical repeats. Positive (+) = pUT18c-zip with pKT25-zip. Negative (-) = pUT18c with pKT25.

B-galactosidase assays were used to quantify the strength of the interaction between Bd2584H389V and itself see Figure 4.25. This resulted in an interaction that was significantly different from the negative control.

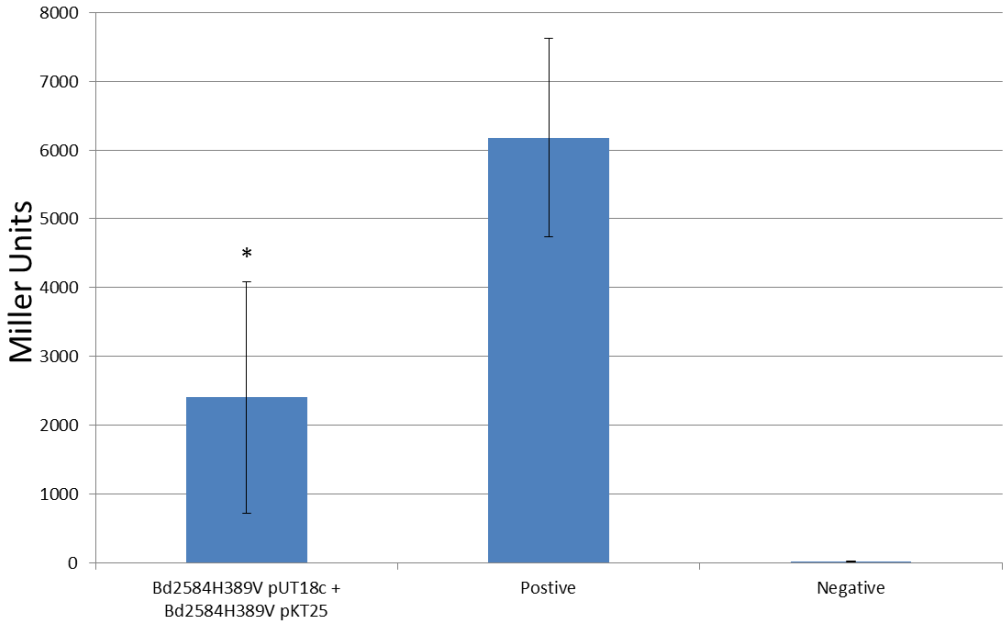

Figure 4.25 β-galactosidase activity assay for Bd2584H389V self-interactions. Error bars show standard deviation. The results show the mean value from three biological repeats and comprise 6 technical repeats. HK Bd2584H389V interacts significant with itself. Asterisks show significance of Student t-test compared to the negative (pUT18c, pKT25) *≤0.05

The Bd2584WT self-interaction was repeated at the same time as the Bd2584H389V interaction to have a direct comparison of interaction strengths this is shown in Figure 4.26.

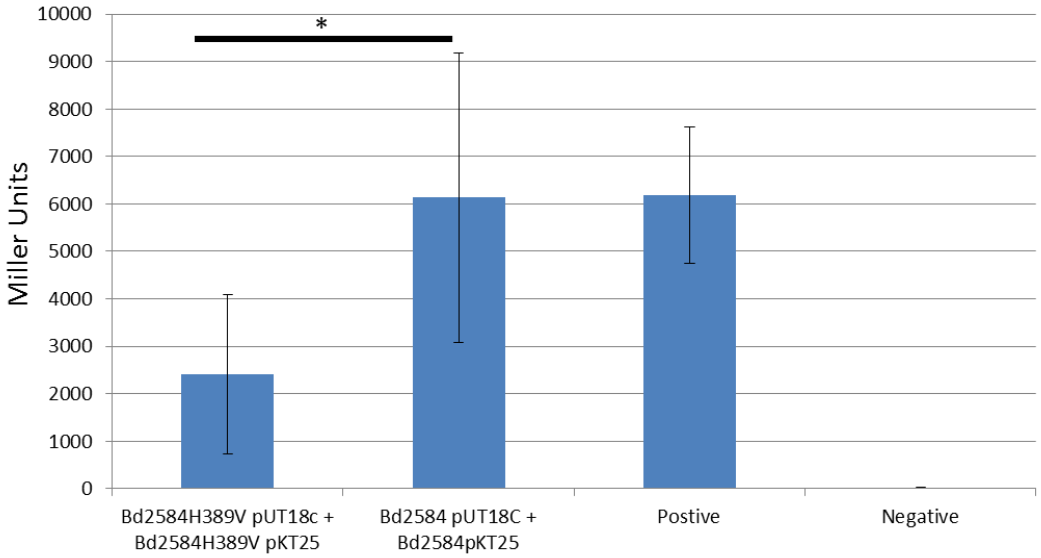

Figure 4.26 β-galactosidase activity assay for Bd2584H389V self-interaction compared to Bd2584WT self-interaction. Error bars show standard deviation. The results show the mean value from three biological repeats and comprise six technical repeats. HK Bd2584H389V interaction strength is significantly lower than Bd2584WT. Asterisks show significance of mutant Bd2584 dimer student t-test compared to the wt (pUT18c, pKT25) *≤0.05

This result suggested that Bd2584 cannot dimerize as strongly when H389 is mutated to V. This reduction in dimerization strength may provide a reason for the reduction in the Bd2584H389V-Bd0367 interaction strength.

4.4.8. Investigating interactions between HK Bd2584 and other cyclic di-GMP related proteins

In chapter 3 I showed that Bd0367 had multiple interaction partners which are also involved in the c-di-GMP network, these were Bd1971 EAL domain protein and Bd3125 degenerate GGDEF protein. As the RR domain of Bd0367 appeared already to be a hub of interactions, the identification of HK Bd2584 interacting with Bd0367 RR led to the hypothesis that Bd2584 could potentially be in close proximity to the c-di-GMP components Bd1971 and Bd3125. Bd2584 also has two PAS domains that could be binding a specific ligand or could be used to interact with proteins. If these other c-di-

GMP component proteins interacted with Bd2584 it would suggest that Bd2584 could be receiving a sense of the c-di-GMP level of the cell through these accessory protein interactions and that this could in turn modulate the phospho-transfer to Bd0367 and hence its activity.

4.4.8.1. Investigating the nature of the protein interaction between Bd1971 (EAL) and Bd2584 HK

Firstly the possible interaction between Bd2584 and Bd1971 was investigated. A variety of tagged B2H constructs of Bd1971 were tested, these consisted of: the full length protein, the N terminal and the C terminal domains, Figure 4.27. All the Bd1971 constructs had previously been made as stated in chapter 3 by Dr Basford and Rob Till.

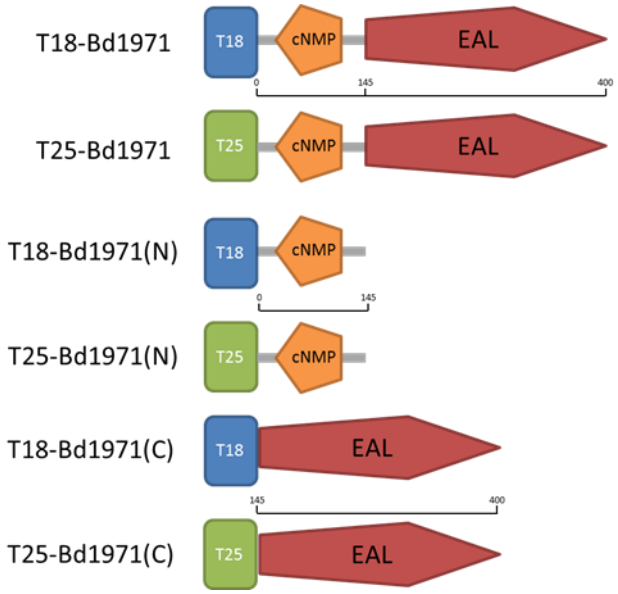

Figure 4.27 Illustration of the various Bd1971 constructs used in B2H analysis. This diagram was produced by Dr Basford to show how the domains of Bd1971 were separated in split constructs.

4.4.8.2. HK Bd2584 interacts with EAL domain protein Bd1971

The result of a typical B2H assay for full length Bd1971 with Bd2584 is shown in Figure 4.28. Bd1971 when tested with Bd2584 consistently produced uniform blue spots in both orientations tested.

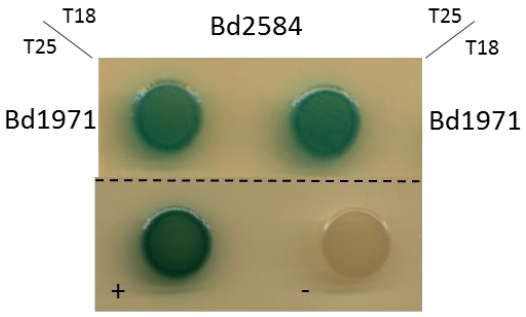

Figure 4.28 Spot plate interactions with HK Bd2584 and EAL domain protein Bd1971. Blue spots suggest an interaction between Bd2584 and Bd1971 this interaction is seen in both orientations. Results displayed are a typical representation of the results from three biological repeats and nine technical repeats. Positive (+) = pUT18c-zip with pKT25-zip. Negative (-) = pUT18c with pKT25.

Further testing of this interaction was carried out by β-galactosidase assays, Figure 4.29, these assays were used to quantify the strength of the interaction between the two proteins. From these results Bd2584 and full length Bd1971 interact significantly more than the negative control. This was a relatively strong interaction strength suggesting a more fixed than transient interaction.

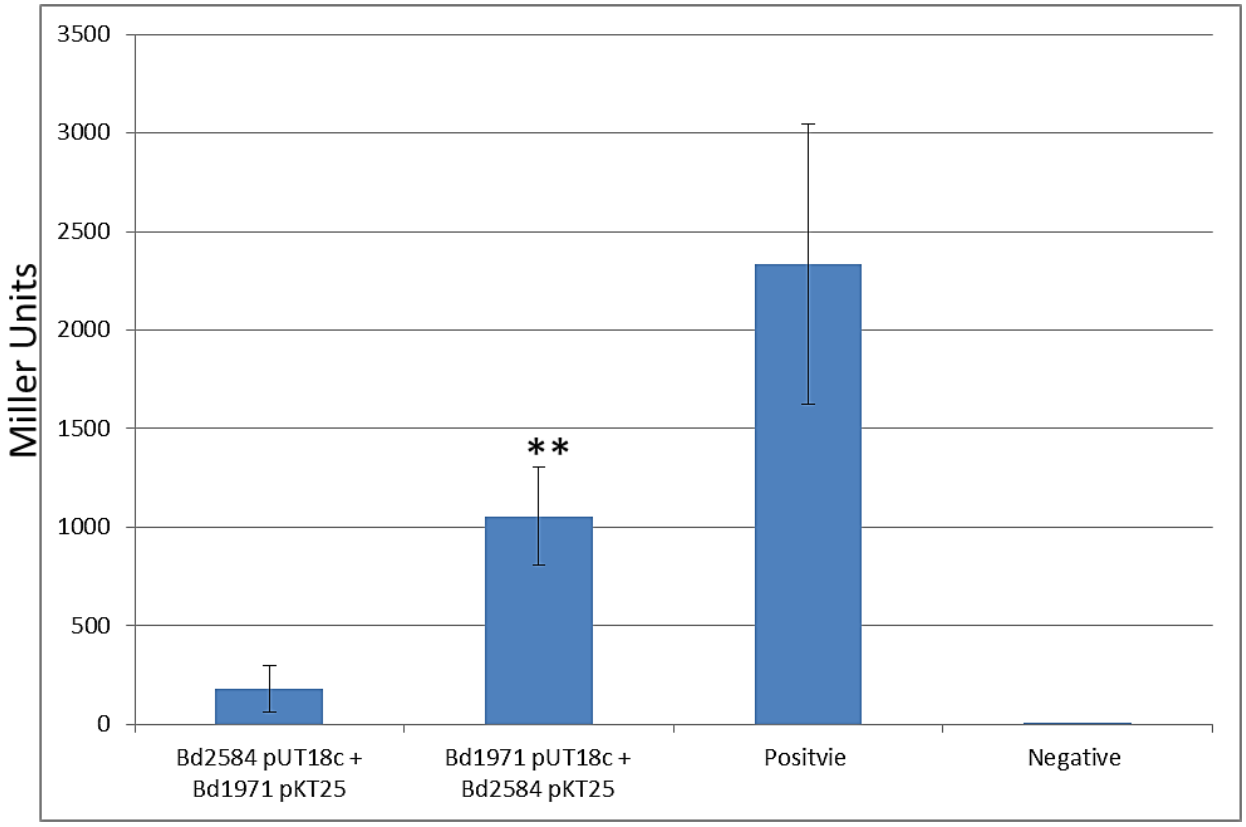

Figure 4.29 β-galactosidase activity assay for HK Bd2584 and EAL domain protein Bd1971. Error bars show standard deviation. The results show the mean value from three biological repeats and comprise six technical repeats. Bd2584 interacts significant with Bd1971 in one orientation Bd1971-T18 + Bd2584-T25. Asterisks show significance of Student t-test compared to the negative (pUT18c, pKT25) **≤0.01

4.4.8.3. HK Bd2584 interacts with N (cNMP) terminal domain of Bd1971

The result of a typical B2H assay for C terminus EAL Bd1971 with Bd2584 is shown in Figure 4.30. Bd1971 when tested with Bd2584 consistently produced uniform blue spots in one orientation tested Bd2584-T18 and Bd1971(C)-T25.

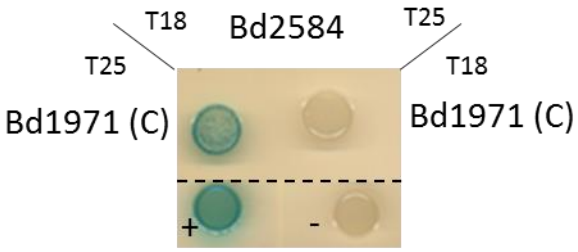

Figure 4.30 Spot plate interactions with HK Bd2584 and C terminal (EAL domain) of Bd1971. Blue spots suggest an interaction between Bd2584 and Bd1971 (C) this

interaction is seen in one orientation. Results displayed are a typical representation of the results from three biological repeats and nine technical repeats. Positive (+) = pUT18c-zip with pKT25-zip. Negative (-) = pUT18c with pKT25.

The result of a typical B2H assay for N terminus cNMP Bd1971 with Bd2584 is shown in Figure 4.31. Bd1971 when tested with Bd2584 consistently produced uniform blue spots in both orientations tested. This suggested Bd2584 may interact more strongly with the N terminal region of Bd1971.

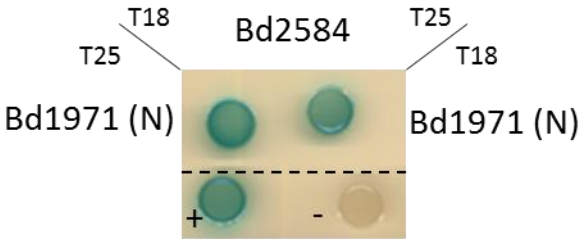

Figure 4.31 Spot plate interactions with HK Bd2584 and N terminal (cNMP domain) of Bd1971. Blue spots suggest an interaction between Bd2584 and Bd1971 (N) this interaction is seen in both orientations. Results displayed are a typical representation of the results from three biological repeats and nine technical repeats. Positive (+) = pUT18c-zip with pKT25-zip. Negative (-) = pUT18c with pKT25.

Further testing of these interactions were carried out by β-galactosidase assays, Figure 4.32, these assays were used to quantify the strength of the interaction between the two proteins. From these results Bd2584 and N terminal Bd1971 interact significantly more than the negative control. This is relatively strong interaction strength particularly in one orientation.

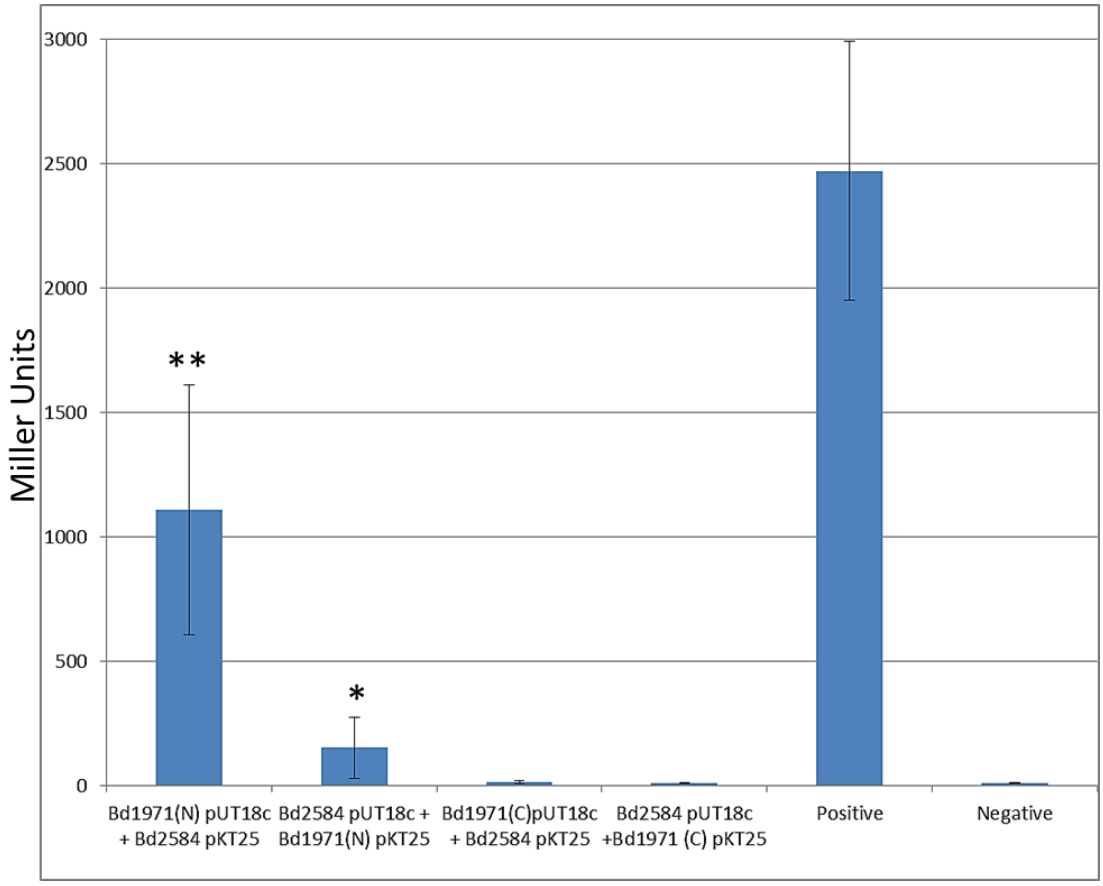

Figure 4.32 β-galactosidase activity assay for split domains of Bd1971 and Bd2584. Error bars show standard deviation. The results show the mean value from three biological repeats and comprise six technical repeats. Both orientations of the Bd1971(N) constructs interact significant with Bd2584. Neither of the Bd1971(C) constructs interact with Bd2584. Asterisks show significance of Student t-test compared to the negative (pUT18c, pKT25) *≤0.05 **≤0.01

4.4.8.4. Summary of variety of Bd1971 constructs interactions with Bd2584

These interaction studies have shown that Bd2584 interacts with Bd1971 and the interaction is located at the N terminal of Bd1971 (cNMP domain). However when the full length Bd1971 interaction with Bd2584 is compared to the Bd1971(N) construct interaction with Bd2584 there is not a statistical difference in interaction strength (T.test). This shows that truncating Bd1971 does not remove steric hindrance and does not cause structural alterations that effect the ability of Bd2584 to interact.

4.4.8.5. Investigating the nature of the protein interaction between Bd3125 degenerate GGDEF and Bd2584 HK

The interaction between Bd3125 a degenerate GGDEF and Bd2584 HK was investigated. Both these proteins interact at the RR domain of Bd0367 so it is possible

that they maybe in close proximity to each other within the *Bdellovibrio* cell at particular times. This possibility led this study to investigate the possibility of a direct interaction between Bd3125 and Bd2584.

4.4.8.6. HK Bd2584 interacts with degenerate GGDEF Bd3125

The result of a typical B2H assay for Bd3125 with Bd2584 is shown in Figure 4.33. Bd3125 when tested with Bd2584 consistently produced uniform blue spots in both orientations tested suggesting an interaction.

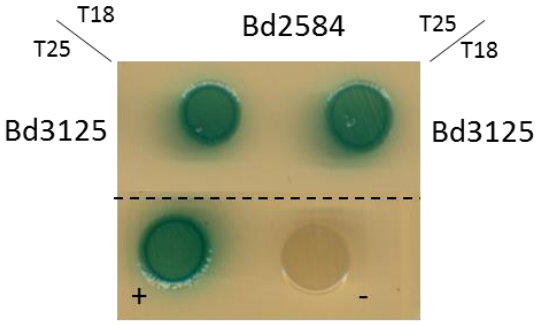

Figure 4.33 Spot plate interactions with HK Bd2584 and degenerate GGDEF domain protein Bd3125. Blue spots suggest an interaction between Bd2584 and Bd3125 this interaction is seen in both orientations. Results displayed are a typical representation of the results from three biological repeats and nine technical repeats. Positive (+) = pUT18c-zip with pKT25-zip. Negative (-) = pUT18c with pKT25.

Further testing of these interactions were carried out by β-galactosidase assays, Figure 4.34, these assays were used to quantify the strength of the interaction between the two proteins. From these results Bd2584 and Bd3125 interact significantly more than the negative control. This is relatively strong interaction strength in both orientations.

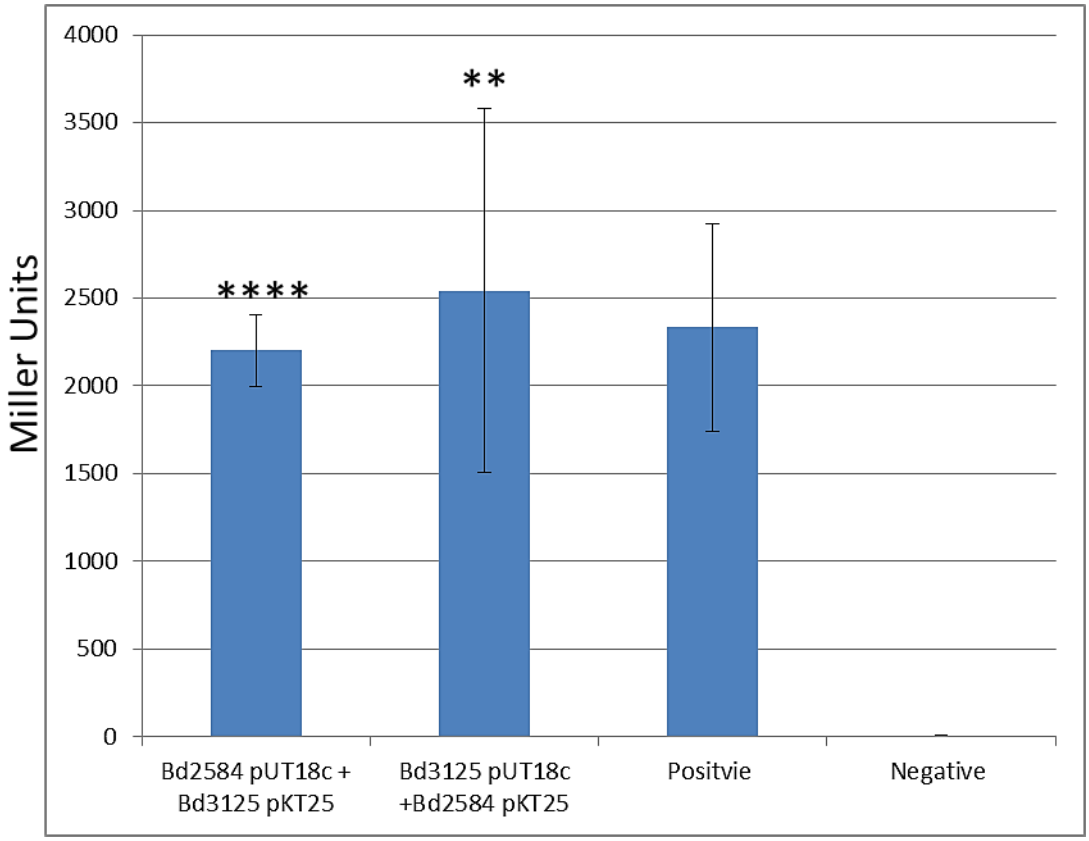

Figure 4.34 β-galactosidase activity assay for HK Bd2584 and degenerate GGDEF Bd3125.. Error bars show standard deviation. The results show the mean value from three biological repeats and comprise six technical repeats. Bd2584 and Bd3125 interact significant with in both orientations. Asterisks show significance of Student t-test compared to the negative (pUT18c, pKT25) **≤0.01 ****≤0.0001.

4.4.8.7. HK Bd2584 does not interact with a unrelated protein Bd0316

Bd0316 is a predicted ATP dependent RNA helicase that was under investigation in another study (conducted by PhD student Dr Somers) and has no known link to c-di-GMP signalling. This construct was used to ensure Bd2584 was not an intrinsically 'sticky' protein that would give a positive interaction when tested against most proteins. The negative interaction between Bd2584 and Bd0316 shows that Bd2584 does not indiscriminately interact with proteins, suggesting the interaction observed previously are specific and potentially biologically relevant interactions, Figure 4.35.

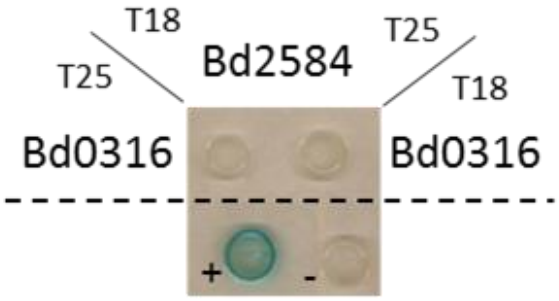

Figure 4.35 Spot plate interactions between HK Bd2584 and a unrelated protein Bd0316. White spots suggest no interaction between Bd2584 and Bd0316. Results displayed are a typical representation of the results from three biological repeats and nine technical repeats. Positive (+) = pUT18c-zip with pKT25-zip. Negative (-) = pUT18c with pKT25.

4.4.8.8. Bd1971 and Bd3125 interactons tested by B2H with other cytoplasmic HK Bd2843

To determine if Bd1971 and Bd3125 would interact indiscriminately with any HK B2H analysis was carried out using the cytoplasmic candidate HK Bd2843. A typical B2H assay shows that Bd1971 does not interact with Bd2843, Figure 4.36.

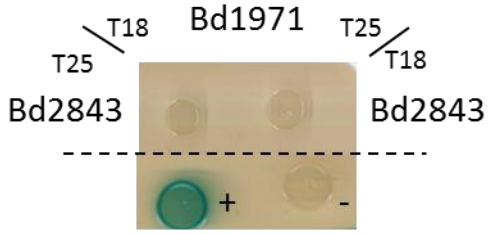

Figure 4.36 Spot plate interactions between HK Bd2843 and Bd1971. White spots suggest no interaction between Bd2843 and Bd1971. Results displayed are a typical representation of the results from three biological repeats and nine technical repeats. Positive (+) = pUT18c-zip with pKT25-zip. Negative (-) = pUT18c with pKT25.

B-galactosidase assays were also carried out on the Bd2843 and Bd1971 interaction for completeness. This resulted in neither interaction being significantly different to the negative control figure 4.37.

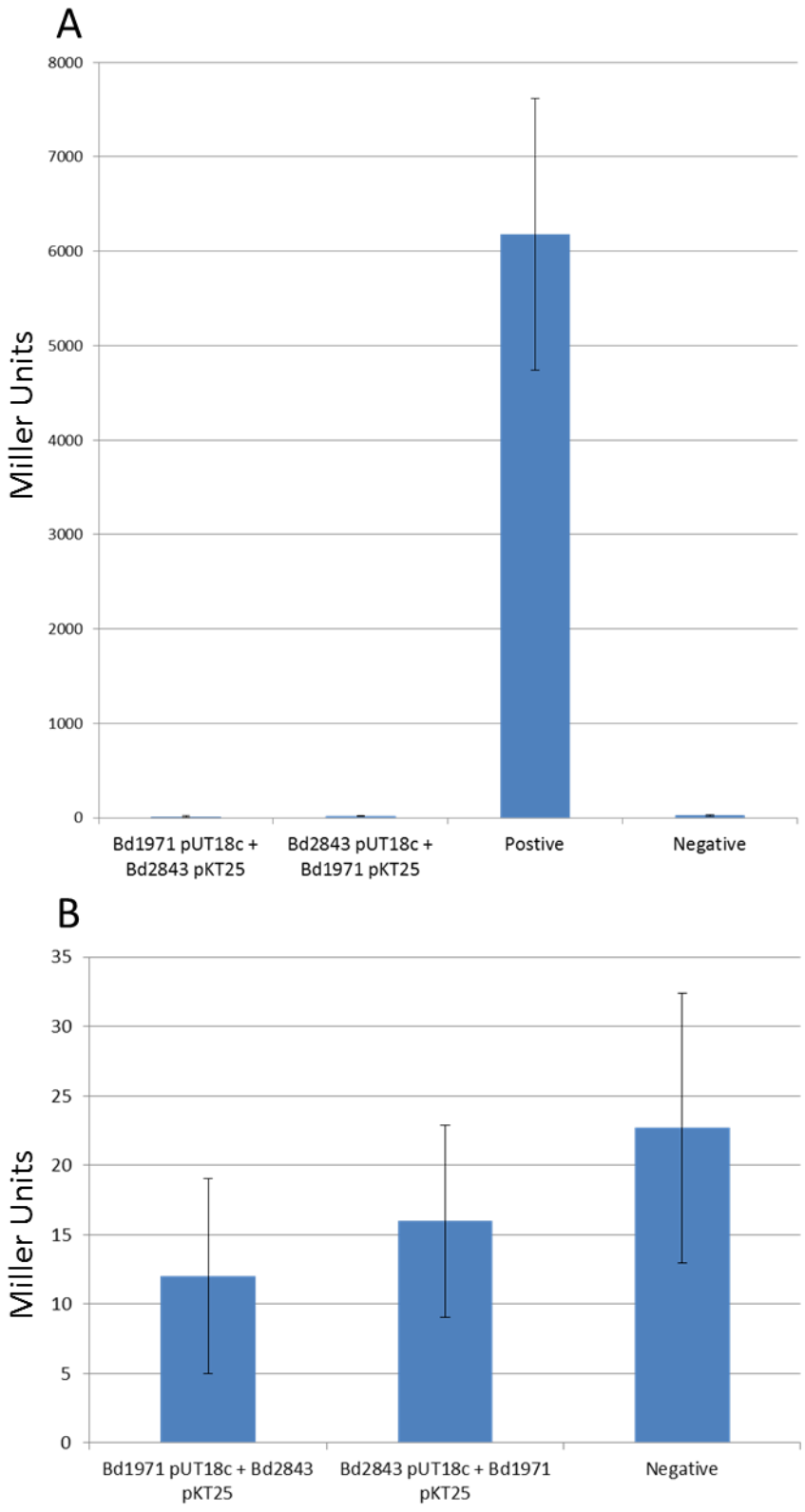

Figure 4.37 β-galactosidase activity assay for interactions between HK Bd2843 and Bd1971. Error bars show standard deviation. The results show the mean value from three biological repeats and comprise six technical repeats. (A) The graph shows the Miller units for the Bd2843 interactions with Bd1971, with both positive and negative controls displayed. (B) This graph allows better observation of the interaction strengths

between the test proteins and that of the negative control, showing them to be of similar values. There is no significant difference by Student t.test between the test interactions and the negative control.

This confirmed that the interaction between Bd2584 and Bd1971 is biologically relevant.

However B2H assay shows that Bd3125 consistently interacts with Bd2843, see Figure 4.38. These blue spots suggest that Bd3125 may have an intrinsic ability to interact with cytoplasmic HKs.

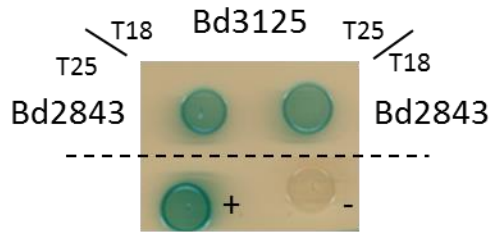

Figure 4.38 Spot plate interactions between HK Bd2843 and Bd3125. Blue spots suggest an interaction between Bd2843 and Bd3125. Results displayed are a typical representation of the results from three biological repeats and nine technical repeats. Positive (+) = pUT18c-zip with pKT25-zip. Negative (-) = pUT18c with pKT25.

B-galactosidase assays were carried out to investigate this interaction further. This resulted in one orientation being significantly different from the negative control figure 4.39.

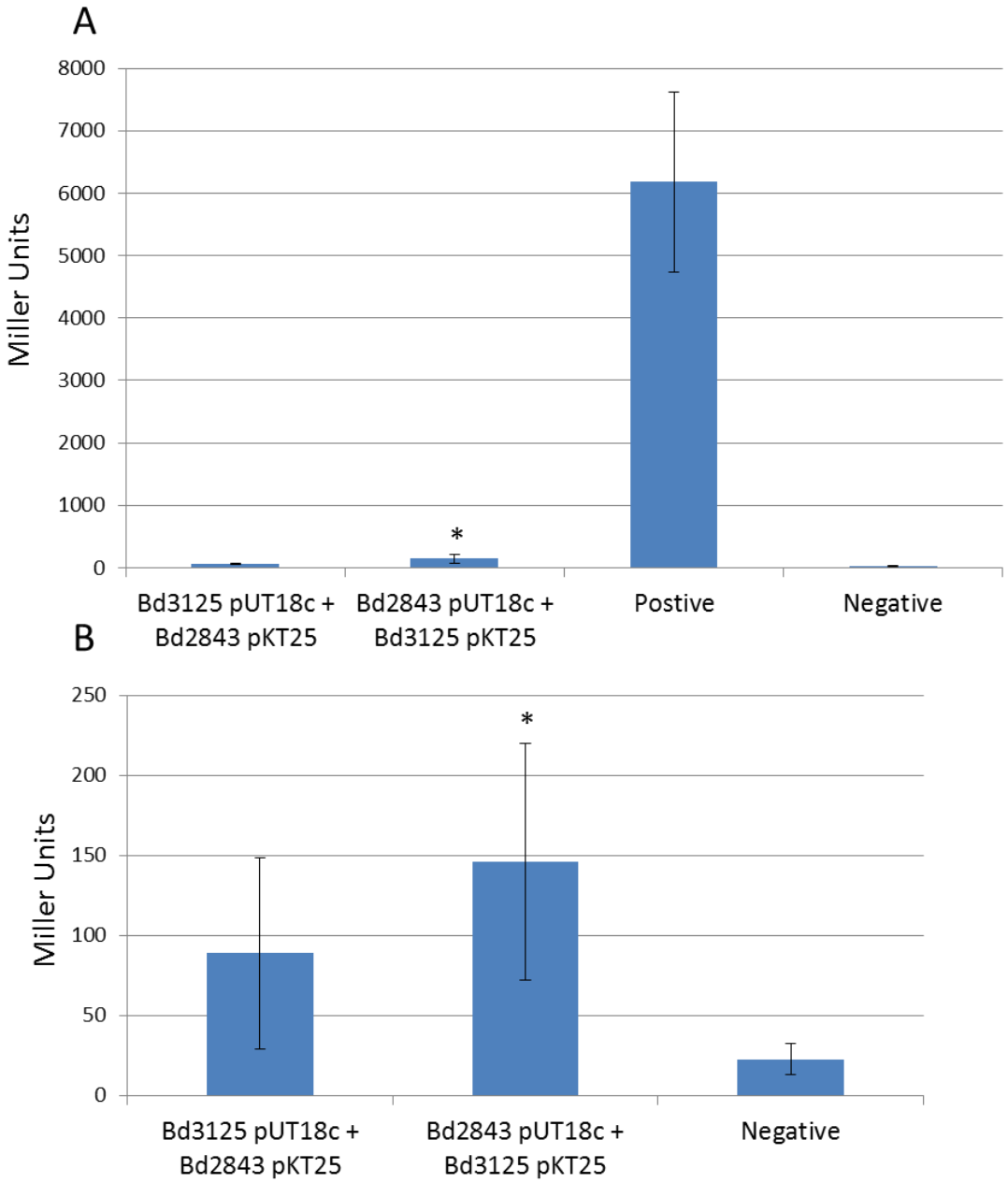

Figure 4.39 β-galactosidase activity assay for interactions between HK Bd2843 and Bd3125. Error bars show standard deviation. The results show the mean value from three biological repeats and comprise six technical repeats. (A) The graph shows the Miller units for the Bd2843 interactions with Bd3125, with both positive and negative controls displayed. (B) This graph allows better observation of the interaction strengths between Bd2843-Bd3125 and that of the negative control, showing one orientation to be significantly different from the negative control. Asterisks show significance of Student t-test compared to the negative (pUT18c, pKT25) *≤0.05.

These results suggest that the interaction between Bd2584 and Bd3125 is not biologically relevant and is due to Bd3125 having an affinity for another cytoplasmic HK.

4.4.9. Gene transcription of *bd2584* exhibits constitutive expression

To assess whether Bd2584 was present at bdelloplast exit (4hr) (a crucial point for Bd0367 function) reverse transcriptase PCR (RT-PCR) was used. Synchronous predatory cultures of *B. bacteriovorous* HD100 were set up with *E. coli* as the prey (details in section 2.6.1) and RNA was isolated at specific timepoints associated with the life cycle stages. Using primers specific to *bd2584* the transcription profile of the gene across the predatory cycle was identified and can be seen in Figure 4.40.

The transcription profile of *bd2584* is constitutive which is what would be expected for a sensor HK as it will only be active as a kinase when the specific signal is present.

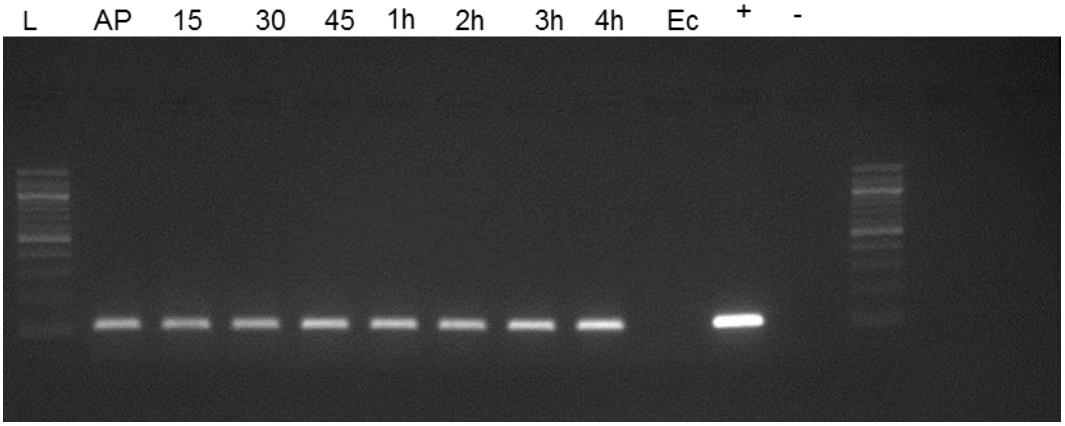

Figure 4.40 RT-PCR showing the transcriptional profile of *bd2584* in *B. bacterivorous* HD100 Synchronous predatory cultures of *B. bacteriovorous* HD100 were set up with *E.coli* as the prey and RNA was isolated at specific time points annotated on the diagram (minutes and then hours since addition of *Bdellovibrio* to prey). Primers were used to amplify a fragment of the gene (30 cycles). AP= attack phase, free swimming *B. bacteriovorous* HD100; 15-45minutes attachement and rounding of prey cell into a bdelloplast; 1hr-4hr= intracellular filamentous growth of *B. bacteriovorous*, septation and lysis of the bdelloplast for exit. Ec= S17-1 *E.coli* RNA, += *B. bacteriovorous* HD100 genomic RNA, - = no template control, L= NEB 100bp DNA ladder.

4.4.10. HK Bd2584 was successfully C terminally mCherry tagged

To assess cellular localisation of Bd2584 and to examine the expression pattern of Bd2584 fluorescence protein during predation and under different conditions a strain with a C-terminally fluorescently tagged Bd2584 was generated. Bd2584-mCherry was constructed by fusion of *bd2584*, lacking its stop codon, in frame with an mCherry tag.

This fused gene was then integrated into the *B. bacteriovorus* chromosome by single crossover at the *bd2584* gene, resulting in a strain where Bd2584 is fused to the mCherry (section 2.4.9).

4.4.10.1. *B. bacteriovorus* Bd2584mCherry fluorescence was too low for visualisation during a predatory time course.

The level of Bd2584mCherry during predation on *E.coli* was too low for clear visualisation. The very low level fluorescence appeared to be diffuse throughout the cell and there did not appear to be any points in the predatory cycle where expression of Bd2584mCherry significantly increased Figure 4.41. The constitutively low level Bd2584mCherry observed suggests that HK Bd2584 is present in low quantities suggesting that the presence of the specific signal is important rather than the quantity of Bd2584 protein in the cell.

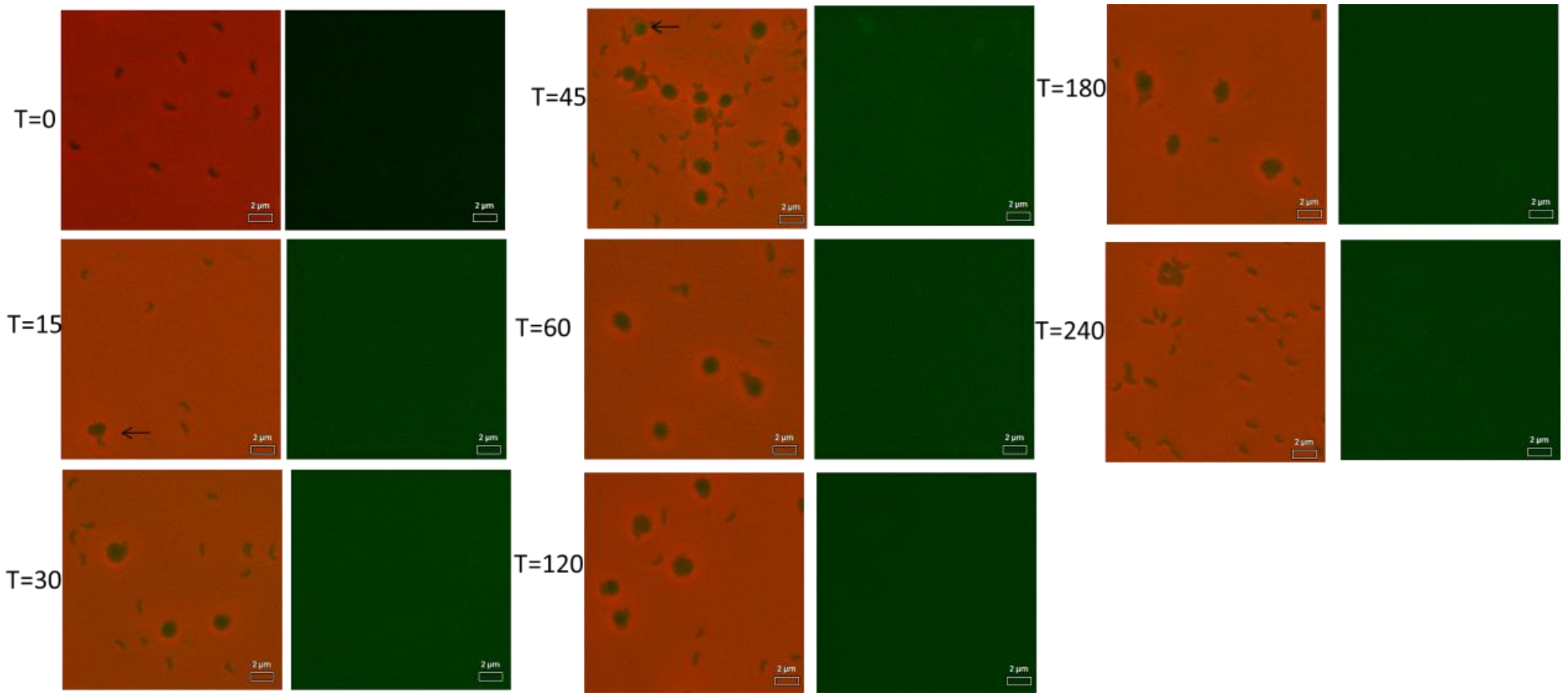

Figure 4.41 Timepoint images of Bd2584mCherry location throughout the predatory life cycle shows very low level expression. A synchronous infection was set up in liquid broth and 10 µl immobilized on 1 % agarose/Ca-HEPES and imaged at each timepoint shown in minutes. Panels show the merged image and the fluorescence in green (mCherry false coloured). Images were taken with 1.5 seconds fluorescence exposure and maximum gain, then sharpened and smoothed using tools in Simple PCI. Scale bar shows 2 µm.

4.4.10.2. *B. bacteriovorus* Bd2584mCherry fluorescence is low when examined in HI strain

Due to the low expression of Bd2584mCherry in the HD strain the HI strain was isolated and examined to investigate if expression levels were altered in the HI life style. Visualisation of the Bd2584-mCherry HI strain showed low level fluorescence as seen previously in the HD strain, Figure 4.42.

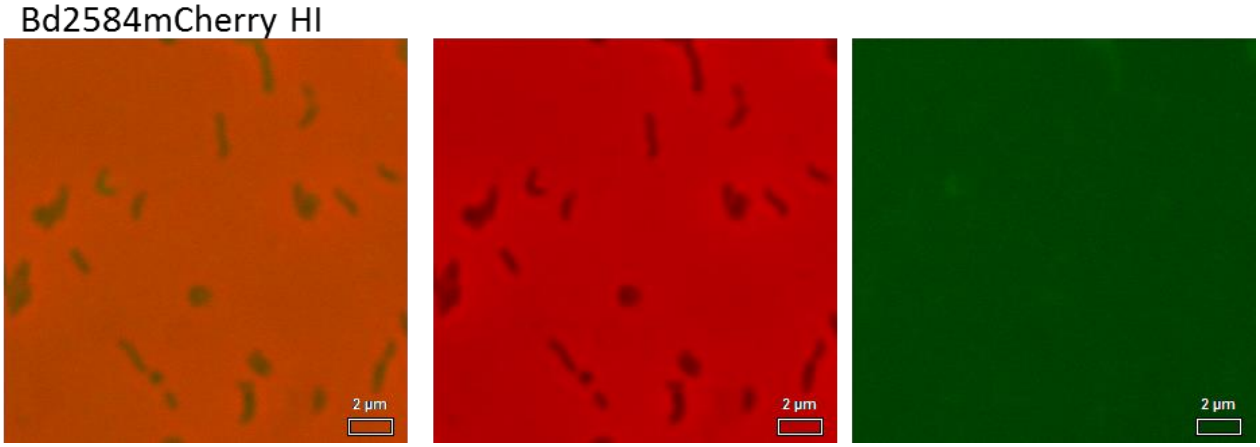

Figure 4.42 Bd2584mCherry strain grown HI shows low level fluorescence. 10 µl of Bd2584mCherry cells were immobilized on 1 % agarose/Ca-HEPES. Panels show merged image, phase image in red and fluorescence in green. Images were taken with 1.5 seconds fluorescence exposure and maximum gain, then sharpened and smoothed using tools in Simple PCI. Scale bar shows 2 µm

4.4.10.3. *B. bacteriovorus* Bd2584mCherry cells do not show increased fluorescence when incubated on a surface

Expression of protein Bd2584 in *B. bacteriovorus* Bd2584mCherry attack phase cells upon surface incubation was investigated by measuring changes in fluorescence. This was studied by observing the intensity of mCherry fluorescence at the first point of surface contact and at time 400 minutes, at time 400 minutes most cells should be utilising gliding motility (see Figure 4.48). This was investigated as Bd2584 is hypothesised to regulate Bd0367 which has been implicated to be of importance in gliding motility. However no visible increase in fluorescence was observed on surface incubation.

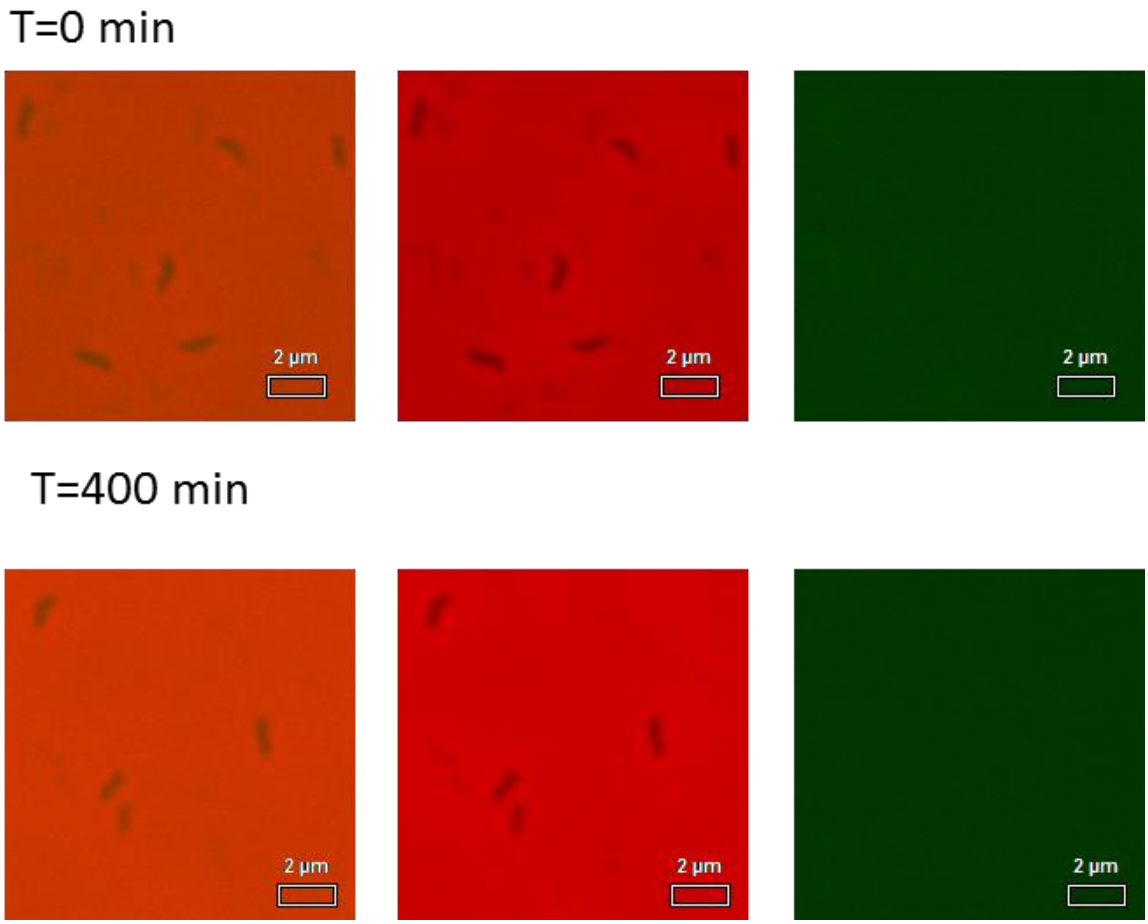

Figure 4.43 *B. bacteriovorus* Bd2584mCherry attack phase cells did not show increased fluorescence when incubated on a surface. The cells were placed on a 1% agarose Ca-HEPES slide and images were collected at time 0 and time 400 minutes. During this time the slide was kept consistently hydrated and at room temperature of 25°C. The panel of images shows time 0 at the top and time 400 minutes below. The panels left to right show the merged channel, bright field channel and fluorescent channel. There is no visual difference between Bd2584mCherry at T0 and T400.

MicrobeJ was used to measure the fluorescent intensity of a at each timepoint (section 2.7.2) (T0 and T400minutes). MicrobeJ which can detect small variations allowed analytical quantification of the mean fluorescent intensity (Ducret et al, 2016). This showed that Bd2584-mCherry mean fluorescent intensity was much lower than some previously analysed proteins in this thesis and that there is not significant change in mean fluorescent intensity on surface incubation (see Figure 4.44).

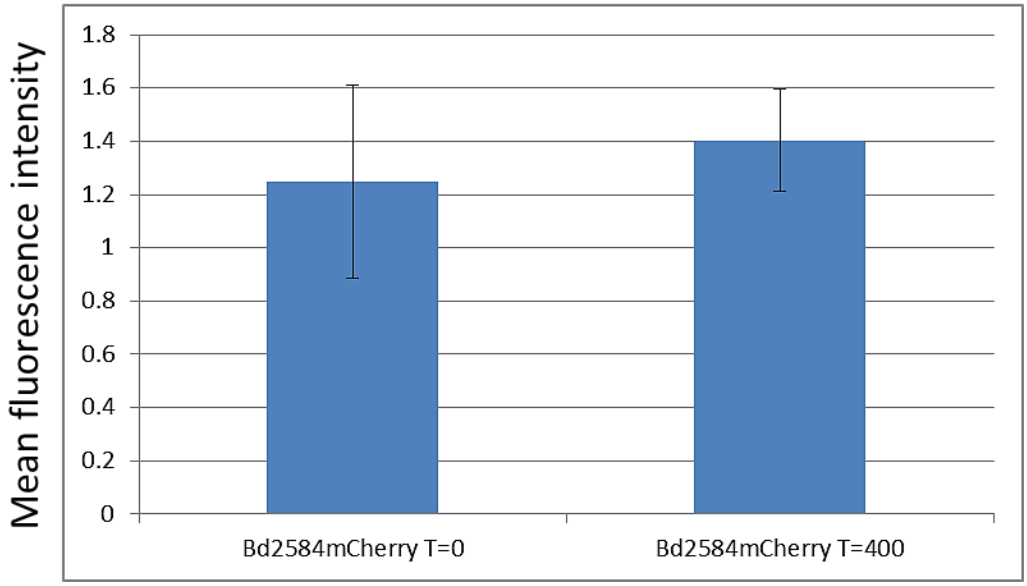

Figure 4.44 *B. bacteriovorus* Bd2584mCherry attack phase cells did not show a change in mean fluorescent intensity when incubated on a surface. Analysis using MicrobeJ on a population of 450 cells across 3 biological repeats each with 3 technical repeats showed no significant change in mean fluorescent intensity between timepoints. Error bars represent 95% confidence interval. Significance was tested by Students t test.

As the fluorescence measured by MicrobeJ (Ducret et al, 2016) for Bd2584mCherry was lower than seen in previously examined mCherry strains, the fluorescence was compared to the fluorescence of WT HD100 with no mCherry. MicrobeJ picked up no fluorescence for HD100 cells at T=0 and low level fluorescence at T=400. The HD100 T=400 mean fluorescence intensity values were compared to the Bd2584mCherry T=400 mean fluorescence intensity values, this found the Bd2584 levels of fluorescence to be significantly higher than the WT HD100 control see Figure 4.45. This suggests that the low level Bd2584mCherry fluorescence found by MicrobeJ analysis is specific to the expression of Bd2584mCherry and not due to residual cellular fluorescence. This data suggests that Bd2584 is present in low levels in the cell.

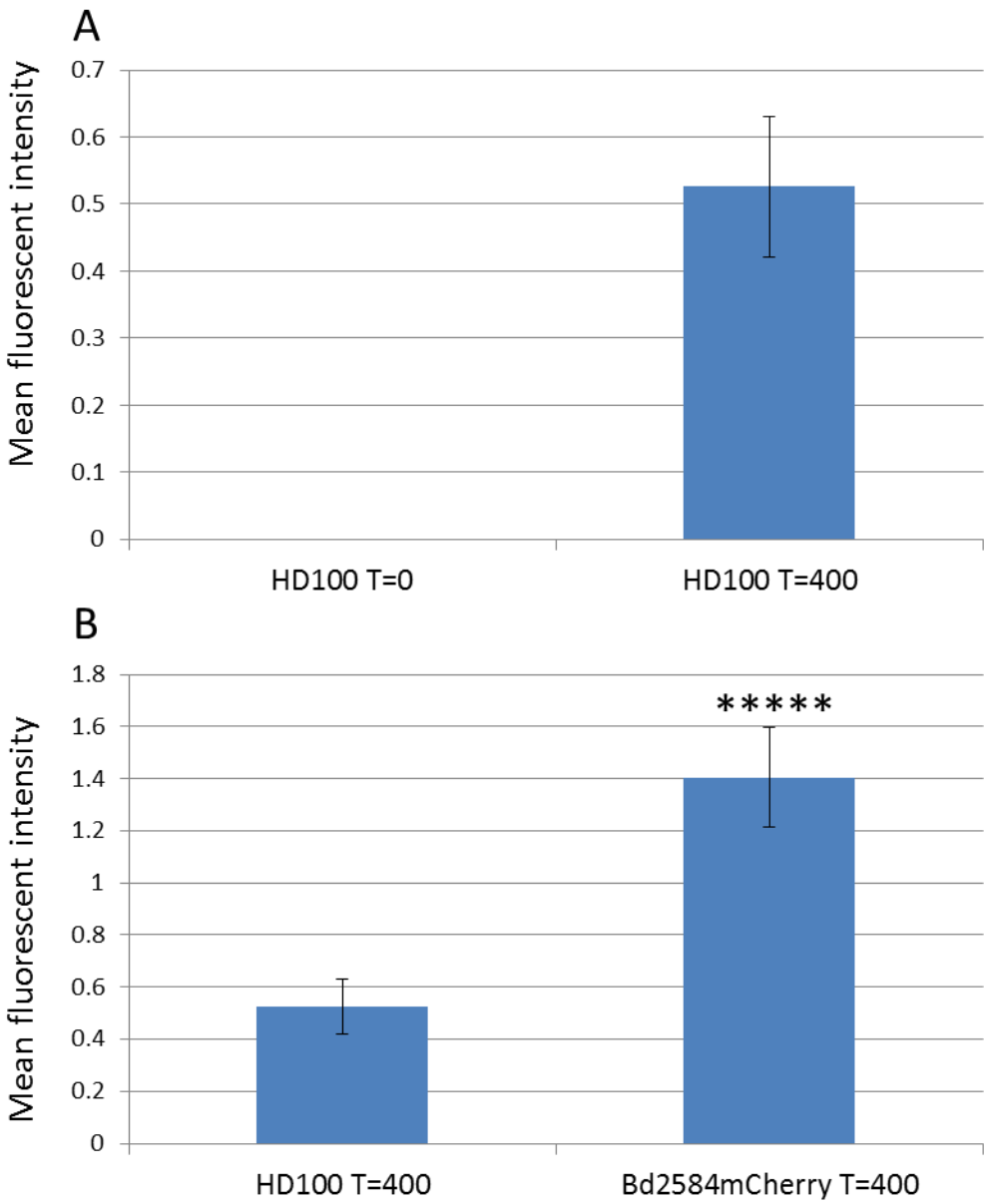

Figure 4.45 *B. bacteriovorus* Bd2584mCherry attack phase cells have greater fluorescent intensity than HD100. A) Analysis using MicrobeJ showed that there is a small residual fluorescent in HD100 cells at T=400. B) Analysis using MicrobeJ on a population of 450 cells showed a significant change in mean fluorescent intensity between HD100 T=400 and Bd2584mCherry T=400 suggesting that there is more fluorescence in the mCherry strain than in a non mCherry strain. This suggest Bd2584mCherry is being expressed at low levels. Error bars represent 95% confidence interval. Significance was tested by Students t test *****≤0.00001.

4.4.11. A deletion strain of *bd2584* was successfully obtained

An in frame deletion strain of HK *bd2584* was obtained as described in section 2.4.8 of methods. The strain was isolated in a HD *B. bacteriovorus* strain, (and independently as a HI *B. bacteriovorus* strain). The Δ*bd2584* strain was confirmed by DNA sequencing of the region at which the crossover event occurred.

4.4.12. Deletion of HK Bd2584 did not result in a phenotype similar to the Δ*bd0367* strain.

The *B. bacteriovorus* Δ*bd2584* strain was expected to result in a phenotype similar to that of the Δ*bd0367* strain, due to the supposed link between these proteins from the above B2H analysis. The Δ*bd0367* strain could only be isolated as a HI strain, though when offered prey it could invade it could not exit the prey cell when incubated on a surface, additionally no gliding motility was observed. For this reason the Δ*bd2584* strain was examined for gliding motility and bdelloplast exit phenotypes.

4.4.12.1. Predatory growth

The first difference in the Δ*bd2584* strain compared to the Δ*bd0367* strain was its isolation in a HD strain. This suggests that the absence of Bd2584 does not inhibit the predatory nature of the *Bdellovibrio* strain as was the case for Δ*bd0367* strain. The Δ*bd2584* strain was found to be able to clear a culture of prey *E. coli* within a 24 hr time period which is the same for HD100 WT. Due to this no further investigation into defects in predation occurred.

4.4.12.2. Testing for the gliding phenotype of *B. bacteriovorus* Δ*bd2584* strain

The Δ*bd0367* HI strain was unable to using gliding motility when incubated on a surface; this was shown by time-lapse microscopy (Hobley et al, 2012). Due to this the gliding ability of Δ*bd2584* was investigated, it was hypothesised that without *bd2584* activation of Bd0367 may not occur, meaning that c-di-GMP levels may not be adjusted to enable wildtype gliding motility to commence.

4.4.12.3. *B. bacteriovorus* Δ*bd2584* cells and HD100 cell commenced gliding motility at similar times after surface incubation

Time-lapse microscopy was used to investigate the time taken from cell application to the 1% agarose slide surface to first visualisation of cell movement using gliding motility.

Figure 4.46 shows that the deletion of *bd2584* does not have a significant effect on the time taken to commence gliding.

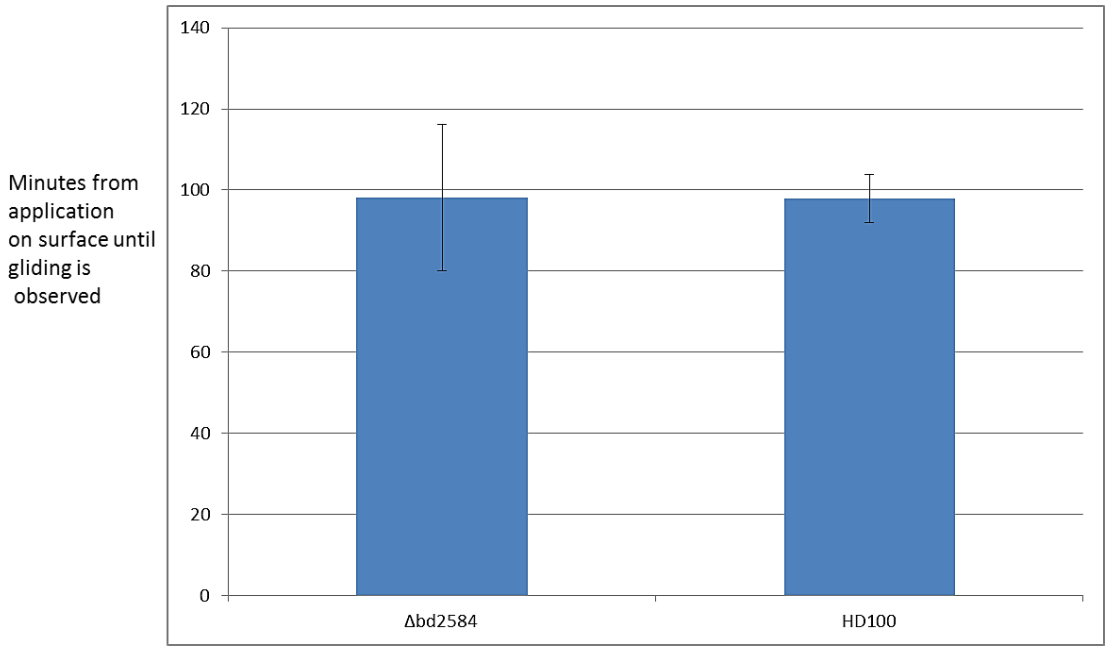

Figure 4.46 *B. bacteriovorus* Δ*bd2584* attack phase cells did not differ in the time taken to commence gliding when compared to wild type HD100 cell. The cells were applied to a 1% agarose pad with 25mM HEPES 2mM $CaCl_2$ and cell movements were recorded by time-lapse microscopy. The graphs show the mean value obtained from 2 biological repeats for Δ*bd2584* and 3 biological repeats for HD100. The mean start times from a total of 45Δ*bd2584* cells and 116 HD100 cells were gathered. Error bars represent 95% confidence interval. Frame rate: 1 frame per 150 sec.

4.4.12.4. *B. bacteriovorus* Δ*bd2584* cells do not exhibit an altered gliding reversal frequency when compared to wildtype cells.

A previous study by Dr Milner into *B. bacteriovorus* gliding motility on agarose showed that the gene can effect gliding motility reversals. This was established by observing the lack of net forward motion and then measuring the reversal frequency of gliding cells (Milner 2014) and has been successful for documenting gliding defects later in this study (chapter 6). This technique was used to see if the gliding motility exhibited by the Δ*bd2584* strain was impaired by increased reversals, this would result in less progressive gliding movement which may link this gene *bd2584* to the non-gliding phenotype of Δ*bd0367*. Figure 4.47 shows that the Δ*bd2584* strain does not vary significantly in mean gliding reversal frequency in comparison to the wild type suggesting that Bd2584 is not involved in gliding motility, which matches the mCherry surface data from section 4.4.10.3. Figure 4.48 shows the typical images of a Δ*bd2584* cell gliding, with 3 reversal event occurring in an hour.

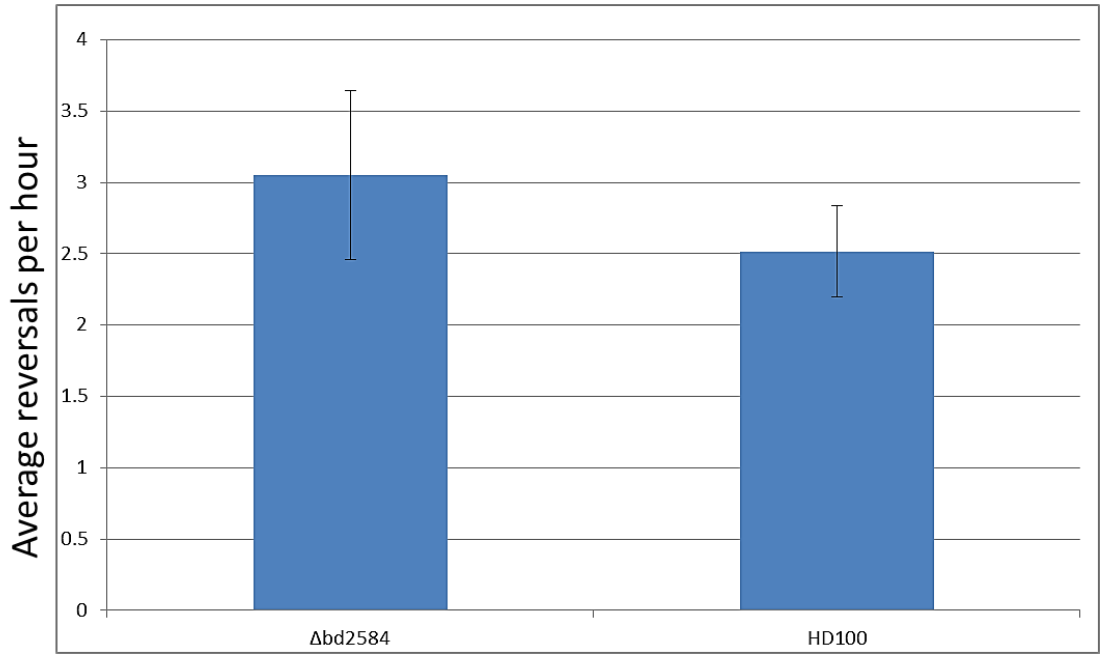

Figure 4.47 *B. bacteriovorus* Δ*bd2584* attack phase cells did not differ in reversal frequency when compared to wild type HD100 cells. The cells were applied to a 1% agarose pad with CaHepes and cell movements were recorded by time-lapse microscopy. The number of reversals per hour was analysed in the second hour after gliding commenced. The graphs show the mean value obtained from 2 biological repeats for Δ*bd2584* and 3 biological repeats for HD100. The average reversals per hour from a total of 40Δ*bd2584* cells and 97 HD100 cells were gathered. Error bars represent 95% confidence interval. 1 frame per 150sec.

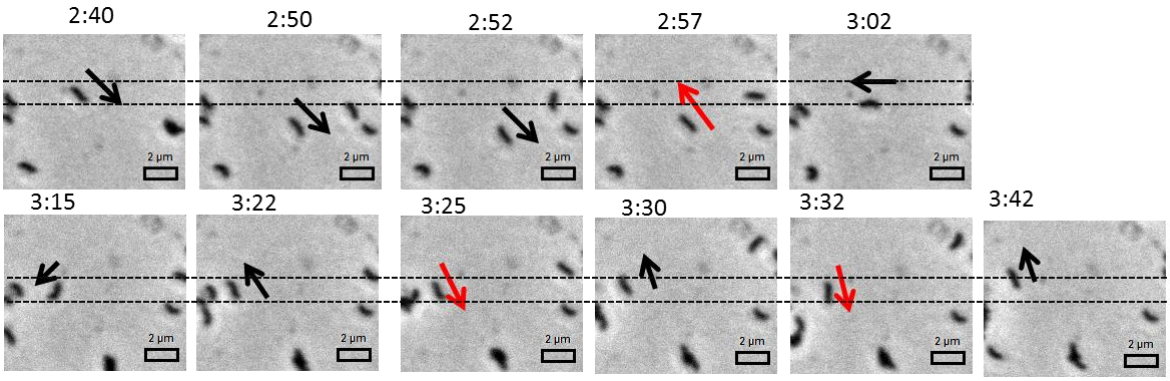

Figure 4.48 *B. bacteriovorus* Δ*bd2584* attack phase cells exhibited a normal gliding reversal frequency. The panel shows stills from video footage of gliding motility. A movie of this process can be located on the USB stick attached, titled 'Bd2584 gene deletion gliding' with a movie titled 'HD100 gliding' as a comparison, further details of these movies are found in section 8.2.1. The selected stills show a variety of events that occur to 1 cell captured in the dotted line to allow observation of progressive movement within 1 hour. The time is hr:min since the addition of the cell to the agarose pad (frames of the video were captured every 150 seconds). The black arrow shows the

direction of travel of the Δ*bd2584* cell and the red arrow shows when the cell reverses back on itself.

4.4.12.5. Exit phenotype of *B. bacteriovorus* Δ*bd2584* strain

The Δ*bd0367* strain was unable to exit the bdelloplast after it lysed the prey cell, this greatly impaired the predatory ability of the Δ*bd0367* strain. As Bd2584 is hypothesised to phosphorylate Bd0367 and activate Bd0367 c-di-GMP production, it is still possible that in the absence of Bd2584 the exit ability of theΔ*bd2584* progeny was impaired compared to the wildtype due to inactive Bd0367.

4.4.12.6. *B. bacteriovorus* Δ*bd2584* strain exits prey bdelloplast without impairment

Time-lapse microscopy was used to observe the growth of the Δ*bd2584* strain within a fluorescent pmal *E .coli* strain (as described in Methods 2.7.3). This allows for the observation of the point at which the bdelloplast is broken open and the time taken for the progeny *Bdellovibrio* to glide out. Figure 4.49 shows that the Δ*bd2584* strain can exit the bdelloplast unlike the Δ*bd0367* strain that have never been observed leaving the bdelloplast and takes approximately 1 hour to do so.

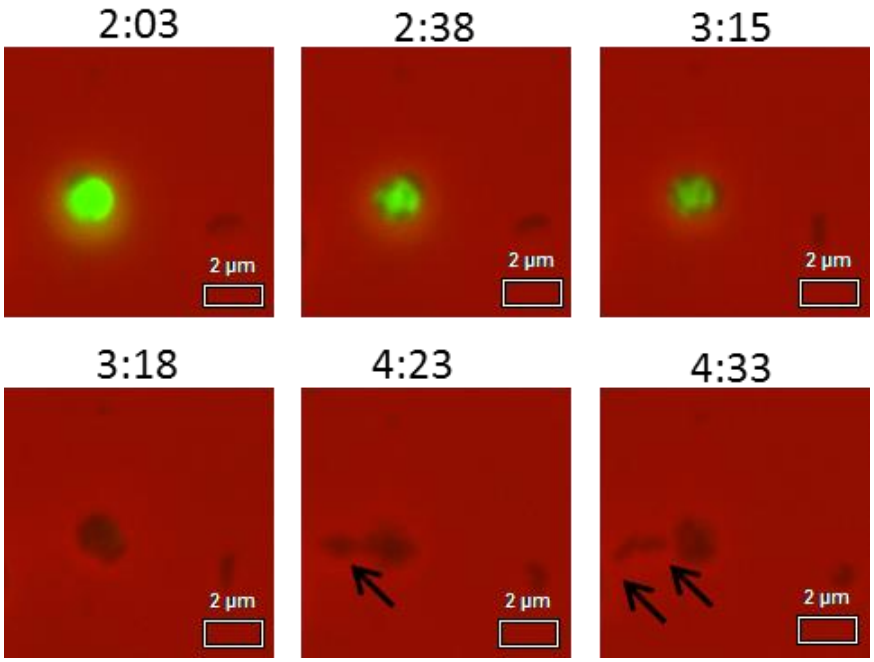

Figure 4.49 *B. bacteriovorus* Δ*bd2584* cells glide out of the exhausted bdelloplast. The panels show stills from video footage of progeny cells growing within the bdelloplast and exiting. A movie of this process can be located on the USB stick attached, titled 'Bd2584 gene deletion bdelloplast exit', with a movie titled 'HD100 bdelloplast exit' as a comparison, further details of these movies are found in section 8.2.1. The time is hr:min since the addition of prey to the *Bdellovibrio* culture, after

incubation to allow infection the cells are applied to the 1%agarose pad and frames of the video were captured every 150 seconds. 55 minutes after prey cell lysis progeny *Bdellovibrio* are observed gliding (black arrow), movement was observed prior to this but only within the 'ex' bdelloplast circle. At 4:33 it is clearer that 2 progeny cells are gliding away.

4.4.13. Complementation of HK Bd2584 deletion with Bd2584 H389V alteration was successfully achieved

An in frame deletion strain of HK *bd2584* had previously been obtained, as was Bd2584 H389V in B2Hvectors. The Gibson cloning technique outlined in section 2.4.8.1 of methods was used to join *bd2584H389V* to the 1 kb upstream, and express this in vector pK18. This construct was conjugated into the Δ*bd2584* deletion strain resulting in the only copy of Bd2584 in this strain having the H389V mutation predicated to prevent phosphotransfer. The strain was isolated as a HD *B. bacteriovorus* strain, and was confirmed by DNA sequencing of the region at which the crossover event occurred.

It was hypothesised that the *bd2584H389V* strain may show a phenotype more similar to the Δ*bd0367* strain. The reasoning for this was that in the Δ*bd2584* strain it is possible that the absence of Bd2584 may have allowed a promiscuous kinase to phosphorylate Bd0367 and that this caused Bd0367 to be active despite lack of Bd2584, masking any potential phenotype. Whereas in the *bd2584H389V* strain Bd2584 will theoretically be present to bind and interact with Bd0367 which would block any other kinase promiscuously phosphorylating Bd0367. However the H389V mutation means that Bd2584 will no longer phosphorylate Bd0367, therefore this strain could result in a phenotype similar to the Δ*bd0367* deletion strain.

4.4.14. Strain *bd2584H389V* did not result in a phenotype similar to the Δ*bd0367* strain.

4.4.14.1. Predatory growth

The *bd2584H389V* strain was isolated as a HD strain, this suggests that the absence of Bd2584 phosphorylation does not inhibit the predatory nature of the *Bdellovibrio* strain unlike the Δ*bd0367* strain. The *bd2584H389V* strain was found to be able to clear a

culture of prey *E.coli* within a 24hr time period which is the same for HD100. Due to this no further investigation into defects in predation occurred.

4.4.14.2. Gliding phenotype

As mentioned above the Δ*bd0367* strain was unable to use gliding motility. Due to this the gliding ability of the *bd2584H389V* strain was investigated.

4.4.14.3. *B. bacteriovorus bd2584H389V* cells and HD100 cell commence gliding motility at similar times

Time-lapse microscopy was used to investigate the time taken from cell application to the 1% agarose CaHEPES slide surface to first visualisation of cell movement using gliding motility. Figure 4.50 shows that the *bd2584H389V* does not have a significant effect on the time taken to commence gliding compared to HD100 WT or Δ*bd2584*. A movie of this process can be located on the USB stick attached, titled 'Bd2584H389V gliding' with a movie titled 'HD100 gliding' as a comparison, further details of these movies are found in section 8.2.1.

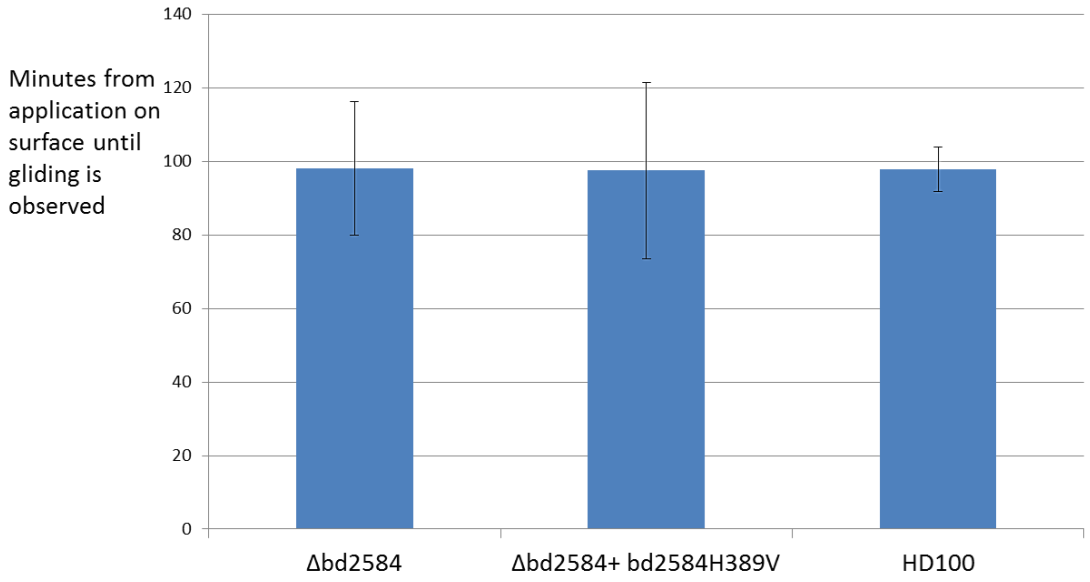

Figure 4.50 *B. bacteriovorus bd2584H389V* attack phase cells did not differ in the time taken to commence gliding when compared to wild type HD100 cell. The cells were applied to a 1% agarose pad with CaHepes and cell movements were recorded by time-lapse microscopy. The graphs show the mean value obtained from 2 biological repeats for Δ*bd2584* and *bd2584H389V* and 3 biological repeats for HD100. The average start times from a total of 24 *bd2584H389V*, 45Δ*bd2584* cells and 116 HD100 cells were gathered. Error bars represent 95% confidence interval. Frame rate 1 per 150 sec.

4.4.14.4. *B. bacteriovorus bd2584H389V* cells do not exhibit an altered gliding reversal frequency when compared to wildtype cells

As mentioned previously measuring the reversal frequency of gliding cells can allow detection of impaired gliding behaviour. This technique was used to see if the gliding motility exhibited by the *bd2584H389V* strain was impaired, this would result in less progressive gliding movement. Figure shows that the *bd2584H389V* strain does not vary significantly in average gliding reversal frequency in comparison to the wild type suggesting that the *bd2584* is not involved in gliding motility, Figure 4.51.

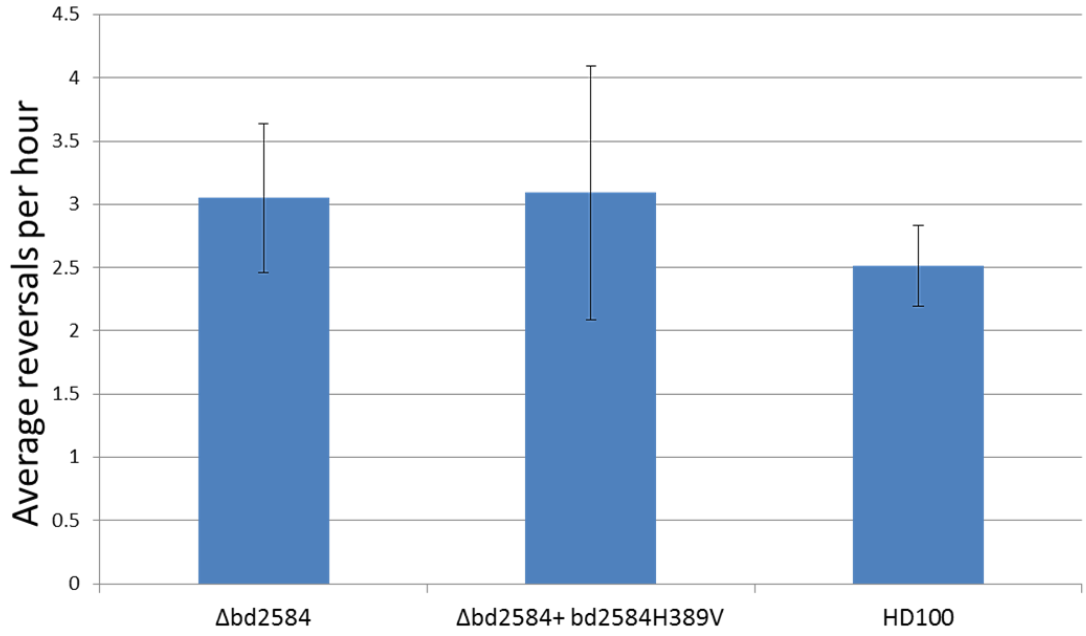

Figure 4.51 *B.bacterivorus bd2584H389V* attack phase cells did not differ in reversal frequency when compared to wild type HD100 cells. The cells were applied to a 1% agarose pad with CaHepes and cell movements were recorded by time-lapse microscopy. The number of reversals per hour was analysed in the second hour after gliding commenced. The graphs show the mean value obtained from 2 biological repeats for *bd2584H389V*, Δ*bd2584* and 3 biological repeats for HD100. The average reversals per hour from a total of 11 *bd2584H389V*, 40Δ*bd2584* cells and 97 HD100 cells were gathered. Error bars represent 95% confidence interval. Frame rate 1 per 150 sec.

4.4.14.5. Exit phenotype of *B. bacteriovorus bd2584H389V* strain

As mentioned before the Δ*bd0367* strain was unable to exit the bdelloplast after it lysed the prey cell. It is possible that in the absence of Bd2584 phospho-transfer to Bd0367 but with the presence of Bd2584H389V still binding the HK could block promiscuous phosphorylation to Bd0367 resulting in a altered the exit phenotype of the Bd2584H389V progeny compared to the wildtype.

4.4.14.6. *B. bacteriovorus bd2584H389V* strain exits prey bdelloplast without impairment

Time-lapse microscopy was used to observe the growth of the *bd2584H389V* strain within a fluorescent pmal *E.coli* strain (as described in methods 2.7.3). This allows for the observation of the point at which the bdelloplast is broken open and the time taken for the progeny *Bdellovibrio* to glide out. Figure 4.52 shows that the *bd2584H389V* strain can exit the bdelloplast unlike the Δ*bd0367* strain and takes approximately 1 hour to do so.

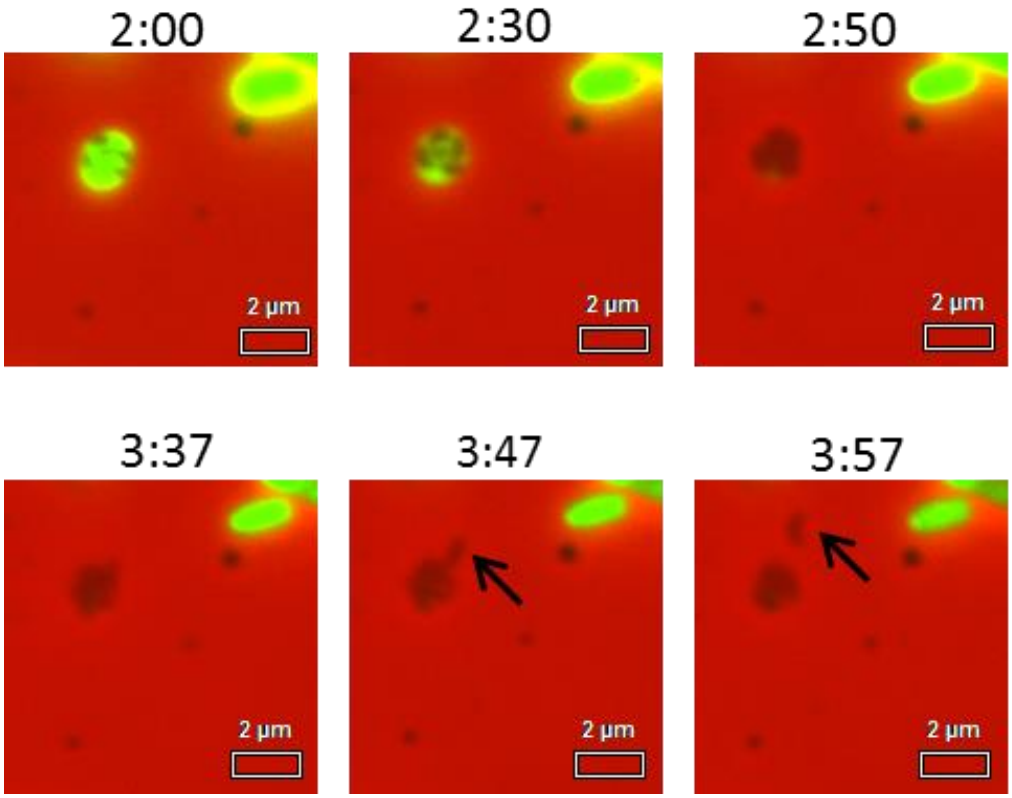

Figure 4.52 *B. bacteriovorus bd2584H389V* cells glide out of the exhausted bdelloplast. The panels show stills from video footage of progeny cells growing within the bdelloplast and exiting. A movie of this process can be located on the USB stick attached, titled 'Bd2584 gene deletion bdelloplast exit', with a movie titled 'HD100 bdelloplast exit' as a comparison, further details of these movies are found in section 8.2.1.The time is hr:min since the addition of prey to the *Bdellovibrio* culture, after incubation to allow infection the cells are applied to the 1%agarose pad and frames of the video were captured every 150 seconds. 55 minutes after prey cell lysis progeny *Bdellovibrio* are observed gliding (black arrow), movement was observed prior to this but only within the 'ex'bdelloplast circle. At 3:47 it is clear that a progeny cell is gliding away.

4.4.15. Investigating phospho-transfer between HK Bd2584 and RR and DGC domain protein Bd0367

In vitro phosphorylation assays using purified proteins have been widely used to study signal transduction mechanisms between HKs and RRs in order to establish which proteins are the cognate pair (Hess et al, 1991; Scharf, 2010). This involves incubating the kinase with radiolabelled ATP, when the kinase auto-phosphorylates the P incorporated is radiolabelled, this P is then transferred to the RR aspartate if phospho-transfer occurs between the proteins, this transfer is observed by running the sample on a SDS-PAGE gel and then placing the gel in a phosphorimaging screen (see methods 2.12). Bands corresponding to phosphorylated protein will then be visible and can be quantified using pixel intensity. *In vitro* phosphorylation assays were carried out between Bd2584 and Bd0367 at The University of Exeter with the assistance of Dr Porter and Dr Francis. These experiments aimed to further investigate if HK Bd2584 could phosphorylate Bd0367. As this would increase the experimental evidence for Bd2584 being the cognate HK to RR Bd0367.

4.4.15.1. Successfully purified proteins Bd2584, Bd0367 and truncated Bd0367 from *M15pRep4 E.coli* using pQE80L(N) and pQE60 (C) vectors

Protein expression constructs were made using the expression plasmids pQE80L and pQE60. The RR Bd0367 was cloned in a full and truncated version into pQE80L which used an N terminal His tag and pQE60 which used a C terminal his tag. The HK Bd2584 was cloned into pQE60 which used a C terminal his tag. These constructs were transformed into *M15pRep4 E. coli* for overproduction and purification (detailed in methods 2.9). A high yield of protein was obtained determined by Lowry assays (see methods 2.9.1).

The eluted over produced proteins shown in Figure 4.53 on SDS-PAGE shows that the proteins of interest are in high abundance and have some co-eluted proteins.

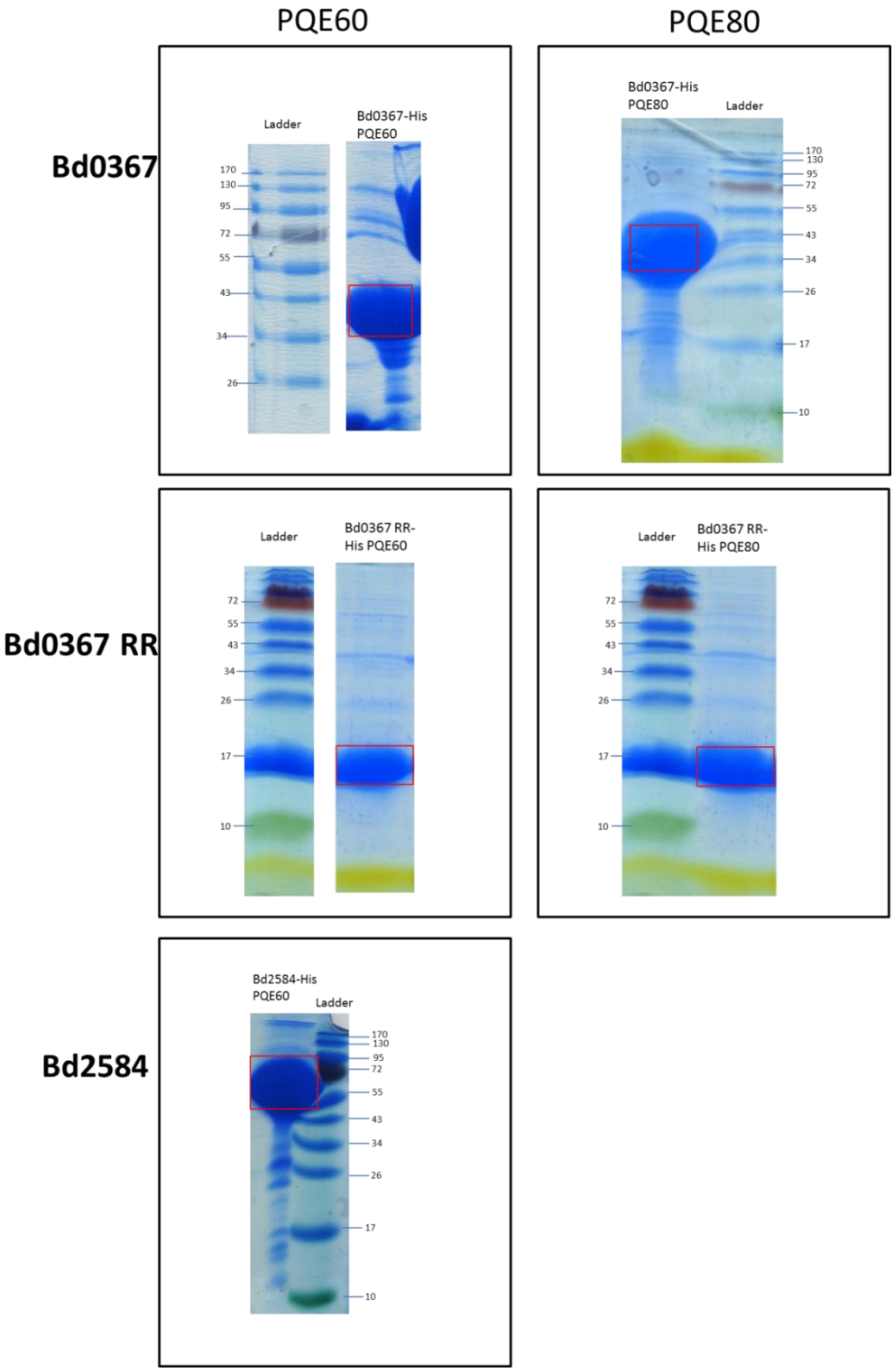

Figure 4.53 Proteins Bd2584, Bd0367 and Bd0367RR were successfully purified from *E. coli*. The pQE60 constructs are His-tagged at the C-terminus the protein of interest is indicated by a box around the purified band. The pQE80L constructs are His tagged at the N-terminus the protein of interest is indicated by a box around the purified band. All purified protein constructs were obtained were of a high yield. Ladder used was ez rec prestained.

4.4.15.2. No phospho-transfer was observed between Bd2584 and Bd0367 under the conditions tested

Many conditions were tested to try and stimulate phospho-transfer between Bd2584 and Bd0367. First an experiment using a long time course 1-60 minutes was used with a high concentration of both Bd2584 and Bd0367 present in the mixture. The conditions for this are shown in Table 4.5, a band of Bd2584-P is visible due to auto-phosphorylation by 1 minute but there is no transfer to Bd0367 even after 60 minutes

Due to the link of Bd2584 and Bd0367 to c-di-GMP signalling this experiment was repeated with the addition of 75μM c-di-GMP (Table 4.6), as I hypothesised that c-di-GMP may stimulate phospho-transfer rather than phosphatase activity as seen in (Lori et al, 2015). However there was no difference in the phospho-transfer profile of Bd2584.

Next we investigated the rapid phosphorylation rate of Bd2584 by carrying out a short time course 15 seconds-60 seconds (see Table 4.7), this established that Bd2584 is auto-phosphorylated at approximately 15 seconds. This experiment also investigated the possibility of a rapid phospho-transfer to Bd0367 followed by rapid phosphatase activity which could result in Bd0367-P being missed in a longer time course however this was not seen to be the case.

As before this shorter time course (15-60 sec) was repeated with the addition of in this case 100 μM c-di-GMP, as used in (Petters et al, 2012) (see Table 4.8) to see if this could stimulate a phospho-transfer event between Bd2584 and Bd0367, however there was no difference in the phospho-transfer profile.

In all cases full length Bd0367 N or C terminally tagged and Bd0367 truncated N or C terminally tagged were tested in combination with Bd2584 C terminally tagged and no transfer occurred.

Other experiments were carried out to try and optimise the assay but the results are not shown. This includes pre-incubating the HK with radiolabelled ATP and adding Bd0367 to the mixture later in case prolonged incubation with the phospho-transfer buffer was causing Bd0367 to degrade. However no transfer occurred. Additionally the temperature was altered from room temperature of 25°C to 29°C to see if a biologically relevant temperature (Najnin et al, 2016) stimulated phosho-transfer however this did not result in any difference to the previously described phosphorylation profile. Furthermore addition

of c-di-GMP at a later point in the time course was tried to see if this might impact the phosphorylation profile but it did not (Lori et al, 2015).

A positive control showing phosphotransfer between a known cognate HK and RR was not carried out and in retrospect would have been useful. However a positive control for autophosphoylation was carried out, this reaction showed that the radioactive ATP used was functional and that $MgCl_2$ and KCl were present in the phosphotransfer buffer. This control took the form of the autophosphorylation reaction of HK CheA2 (*Rhodobacter sphaeroides*), which Dr Porter regularly uses as a control in his studies (data not shown). This control was validated by the multiple successful Bd2584 autophosphorlyation reactions (Table 4.5-4.8). This suggests that the lack of phosphate transfer to RR Bd0367 was not due to lack of ATP, $MgCl_2$ or KCl.

This data suggests that Bd2584 is not the cognate kinase of Bd0367, however stimulating transfer between proteins can be difficult and it could be that the conditions were still not optimal, or that currently unknown additional factors were required for phosphotransfer in vitro (Shikuma et al, 2009).

Proteins added	Concentration of proteins	C di GMP	Time points(min)	Temp °C	Result	
Bd2584	20 μM	No	1,15,30,60	25	Bd2584 auto Phosphorylates at T=1 min	
Bd2584 Bd0367pQE80 (N)	20 μM	No	1,15,30,60	25	Bd2584 auto Phosphorylates at T=1 min No transfer to Bd0367	
Bd2584, Bd0367pQE60 (C)	20 μM	No	1,15,30,60	25	Bd2584 auto Phosphorylates at T=1 min No transfer to Bd0367	

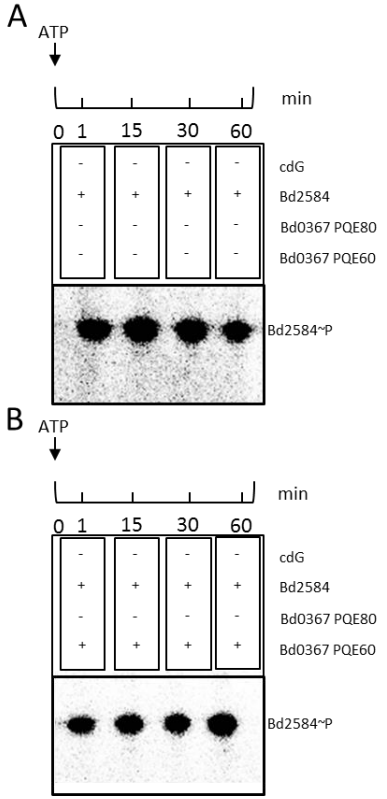

Table 4.5 Auto-phosphorylation of Bd2584 was observed under the standard phosphotransfer conditions but no phoshotransfer to Bd0367 was detected. Each test protein was added at a 20 μM concentration and observed over a long time course 1 min-60 min. Figure A shows Bd2584 incubated alone with radiolabelled ATP with samples taken at 1,15,30 and 60 minutes, the results were obtained from a phoshoimager and B shows a typical representation of the result when Bd2584 and any of the Bd0367 constructs were incubated together, Bd2584 auto-phosphorylates but there is no transfer of the radiolabelled phosphate to Bd0367.

Proteins added	Concentration of proteins added	C-di-GMP	Timepoints (min)	Temp °C	Result	
Bd2584	20 μM	75 μm	1,15,30,60	25	Bd2584 auto Phosphorylates at T=1 min	
Bd2584, Bd0367pQE80 (N)	20 μM	75 μm	1,15,30,60	25	Bd2584 auto Phosphorylates at T=1 min No transfer to Bd0367	
Bd2584, Bd0367pQE60 (C)	20 μM	75 μm	1,15,30,60	25	Bd2584 auto Phosphorylates at T=1 min No transfer to Bd0367	

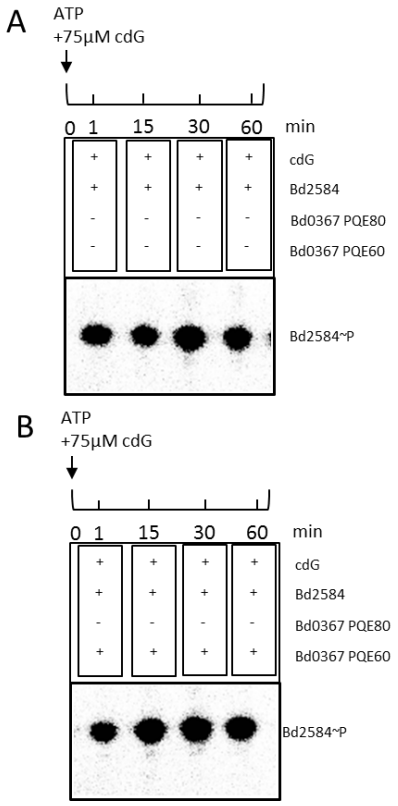

Table 4.6 Auto-phosphorylation of Bd2584 was observed in the presence of c-di-GMP but this did not stimulate phoshotransfer to Bd0367. Each test protein was added at a 20 μM concentration and observed over a long time course 1min-60min this time with an addition of 75 μM c-di-GMP. Figure A shows Bd2584 incubated alone with c-di-GMP and radiolabelled ATP with samples taken at 1,15,30 and 60 minutes, the results were obtained from a phoshoimager and B shows a typical representation of the result when Bd2584 and any of the Bd0367 constructs were incubated together in presence of 75μM c-di-GMP, Bd2584 auto-phosphorylates but there is no transfer of the radiolabelled phosphate to Bd0367.

Proteins added	Concentration of proteins added	C-di-GMP	Time points (sec)	Temp °C	Results	
Bd2584	5 μM	No	15, 30, 45, 60	25	Bd2584 starts to auto phosphorylate at T=15 sec	
Bd2584, Bd0367pQE80 (N)	5 μM, 40 μm	No	15, 30, 45, 60	25	Bd2584 starts to auto phosphorylate at T=15 sec No transfer to Bd0367	
Bd2584, Bd0367pQE60 (C)	5 μM, 40 μm	No	15, 30, 45, 60	25	Bd2584 starts to auto phosphorylate at T=15 sec No transfer to Bd0367	

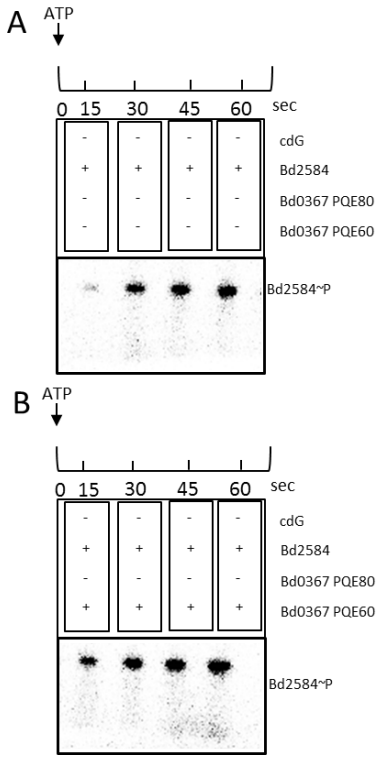

Table 4.7 A short time-course showed that Bd2584 auto-phosphorylation is rapid but no phosphotranfer to Bd0367 was detected. Test proteins concentration were varied to increase the RR(40 μM) and decrease the kinase (5 μM) and observed over a short time course 15 sec-60 sec Figure A shows Bd2584 incubated alone with radiolabelled ATP with samples taken at 15,30,45 and 60 seconds, this shows auto-phosphorylation at 15 seconds. The results were obtained from a phoshoimager and B shows a typical representation of the result when Bd2584 and any of the Bd0367 constructs were incubated together, Bd2584 auto-phosphorylates but there is no transfer of the radiolabelled phosphate to Bd0367.

Proteins added	Concentration of proteins added	C di GMP	Time-points (sec)	Temp °C	Result	
Bd2584	5 μM	100 μm	15, 30, 45, 60	25	Bd2584 starts to auto phosphorylate at T=15 sec	
Bd2584, Bd0367pQE80 (N)	5 μM, 40 μm	100 μm	15, 30, 45, 60	25	Bd2584 starts to auto phosphorylate at T=15 sec No transfer to Bd0367	
Bd2584, Bd0367pQE60 (C)	5 μM, 40 μm	100 μm	15, 30, 45, 60	25	Bd2584 starts to auto phosphorylate at T=15 sec No transfer to Bd0367	

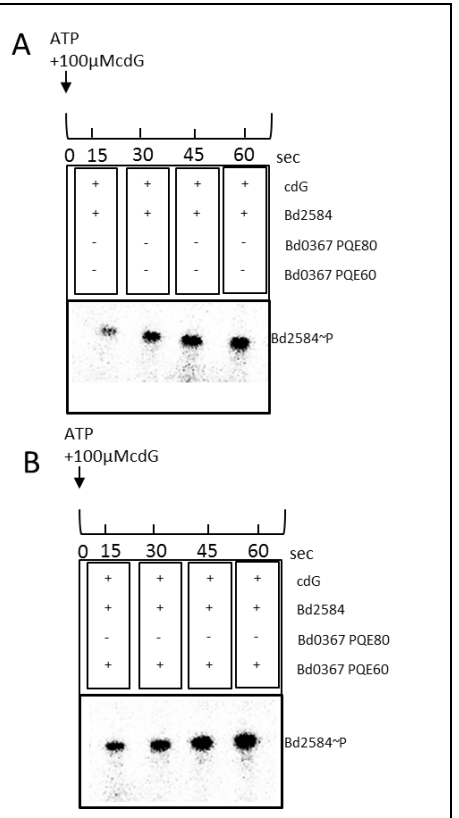

Table 4.8 A short time-course showed that Bd2584 auto-phosphorylation is rapid and is un-affected by c-di-GMP but no phosphotranfer to Bd0367 was detected. Test proteins concentration were varied to increase the RR(40 μM) and decrease the kinase (5 μM) and observed over a short time course 15 sec-60 sec Figure A shows Bd2584 incubated alone with c-di-GMP and radiolabelled ATP with samples taken at 15,30,45 and 60 seconds, this shows auto-phosphorylation at 15 seconds. The results were obtained from a phoshoimager and B shows a typical representation of the result when Bd2584 and any of the Bd0367 constructs were incubated together with c-di-GMP, Bd2584 auto-phosphorylates but there is no transfer of the radiolabelled phosphate to Bd0367.

Overall this data shows Bd2584 can autophosphorylate, but does not transfer phosphate to Bd0367 under the conditions tested. This and other data collected in this study began to suggest Bd2584 is not the cognate kinase for Bd0367.

4.4.16. Testing for partner proteins of Bd2584 through a interaction pull down assay using His-tagged Bd2584

To find proteins that interact with Bd2584 *in vivo* and confirm interactions found by B2H an interaction pull down assay was developed. This assay used Bd2584-His (C terminal) which had been purified via expression in *E. coli* (for previous phosphotransfer experiment), this protein was bound to the Ni-agarose beads to act as the bait protein. Large cultures of attack phase HD100 were used. Once these cultures were sonicated and membrane factions removed they were incubated with the Ni-agarose beads with or without the bait protein, Bd2584-His. These beads were later washed, boiled and run on SDS gel to look for potential interacting proteins through protein bands present in Bd2584-His + HD100 lysate and not in the controls see Figure 4.54. These experiments were carried out in parallel with Dr Lowry, who was conducting a similar investigation into separate *Bdellovibrio* protein interactions, this resulted in sharing of buffers and SDS-PAGE gels. These bands were cut out and sent for analysis by LC-MS/MS at Leicester University.

4.4.16.1. Interaction Pull-down assay

The bait protein Bd2584-His was successfully bound to the beads so was available to pull out potential interacting partners. The box number 1 shows predicted Bd2584-His, this band was sent for LC-MS/MS analysis to confirm the bands identity as Bd2584-His (Section 8.3.2.1). Box 2 shows a protein band that only appears in the Bd2584beads+HD100 lane suggesting an interacting partner may have been pulled out. Box 3 is a control for box 2 to check that any protein identified in box 2 is not present in the control lane. These 3 bands were cut out and sent for LC-MS/MS analysis to investigate any differences between the proteins obtained from these bands.

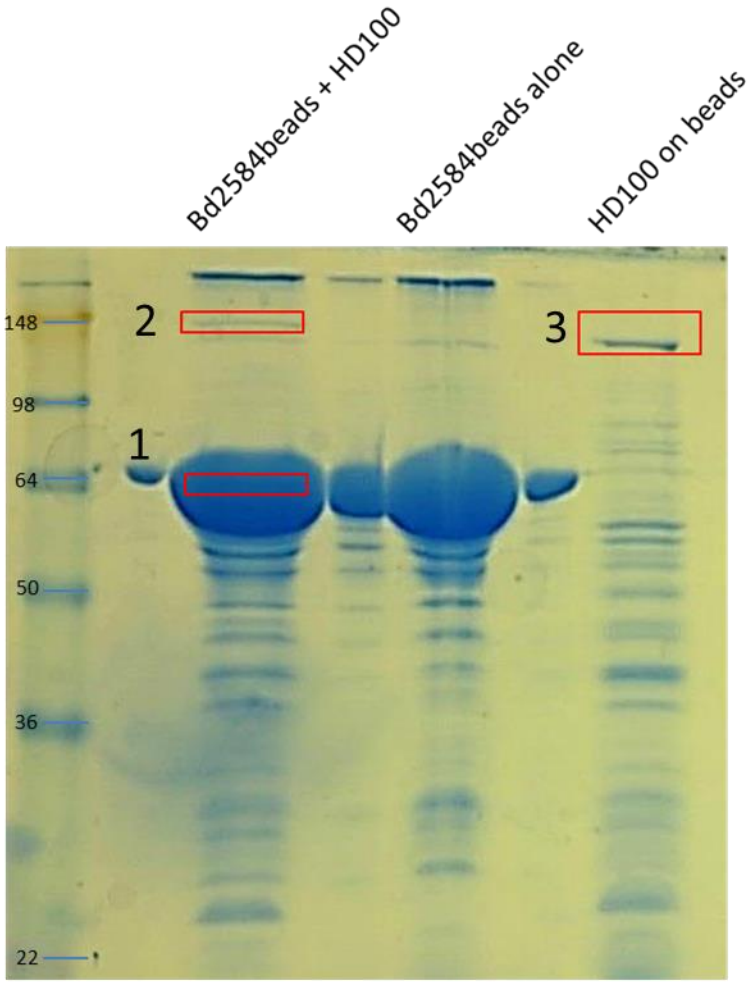

Figure 4.54 One potential interaction pair from Bd2584-His pulldown were sent for analysis by LC-MS/MS. Description of conditions for each lane**.** Bd2584beads+HD100: Bd2584-His was purified from *E. coli*, dialysed and diluted, then 580 µl was applied to beads, this was incubated with HD100 lysate. Bd2584 beads: 580 ul of dialysed Bd2584-His was applied to beads and incubated with buffer. HD100 on beads: The Ni beads were washed and HD100 lysate was incubated with washed beads. All these conditions were then washed, boiled and run on 12.5% SDS-PAGE gel. The expected weight of Bd2584-His is ~69 kDa and seeblueplus2 prestained standard ladder was used. The Bd2584-His appears not to have been sufficiently diluted.

4.4.16.2. Results of LC-MS/MS analysis

Purified Bd2584-His from the test lane were analysed by LC-MS/MS and confirmed that band 1 contained Bd2584-His. The Table 4.9 shows the number of unique peptides and percentage coverage.

	Bdellovibrio protein	Putative function	Size Kda	Hits (exclusive unique peptides)	Percentage coverage
Band 1					
	Bd2584	HK	69.8	45	79

Table 4.9 Identity of Bd2584 confirmed

The potential interaction Bands 2 and 3 were sent for LC-MS/MS analysis to find differences between the identified proteins in the two samples. However Band 2 and Band 3 have the same top 3 *Bdellovibrio* protein hits, listed in Table 4.10, the number of unique peptides and percentage coverage is also very similar. The top 2 proteins identified are proteins that are commonly pulled down in other *Bdellovibrio* pull down assays. The low level of Bd2584 present in band 3 could be there due to overspill from the neighbouring lane or column contamination.

				Band 2		Band 3	
	Bdellovibrio protein	Putative function	Size Kda	Hits (exclusive unique peptides)	Percentage coverage	Hits (exclusive unique peptides)	Percentage coverage
1	Bd2984	rpoB: DNA-directed RNA polymerase subunit beta	157	67	58	72	58
2	Bd2983	rpoC: DNA-directed RNA polymerase subunit beta	151.8	55	54	59	59
3	Bd2584	HK	69.8	31	58	17	17

Table 4.10 Top 3 *Bdellovibrio* protein hits for Bd2584 pulldown: There were no unique *Bdellovibrio* proteins identified in band 2.

So in conclusion none of the interactions found by B2H studies were confirmed by this method and no new interactions between Bd2584 and other *Bdellovibrio* proteins were found.

4.4.17. Re-evaluating the original test for putative cognate kinases

Re-evaluation of the original B2H HKs was carried out due to the lack of further evidence that Bd2584 is the cognate kinase for Bd0367. It was hypothesised that the N terminal tagging of the transmembrane HKs may have impaired their localisation to the membrane and the tag may have caused disorder at the N terminal region. It is possible that this disordered N terminal prevented the true cognate HK from interacting with Bd0367. To assess the possible disorder caused by N terminal tagging the dimerization of these HK was tested by B2H assay and quantified by β-galactosidase assay.

4.4.17.1. Other candidate HK dimers investigated by bacterial two hybrid

The results of a typical B2H assay for all the candidate kinases interactions with themselves is shown in Figure 4.55. All HK apart from Bd2576 resulted in blue spots signifying a dimer interaction. This suggested that N terminal tagging only disrupted the ability of Bd2576 to dimerize.

Figure 4.55 Spot plate interaction of candidate HK dimers. Blue spots suggest a dimerization interaction between most of the candidate HKs. Bd2576 did not dimerize and resulted in white spots. Results displayed are a typical representation of the results from three biological repeats and nine technical repeats. Positive (+) = pUT18c-zip with pKT25-zip. Negative(-)= pUT18c with pKT25.

Further testing of these interactions was carried out by β-galactosidase assays see Figure 4.56. These assays were used to quantify the strength of the HK dimer interactions identified by spot plate analysis. Bd2584 has the highest dimerization strengths, however the other 4 HK with positive spot plate interactions also have interactions significantly stronger than the negative control. This suggests N terminal tagging only stops Bd2576 from dimerizing.

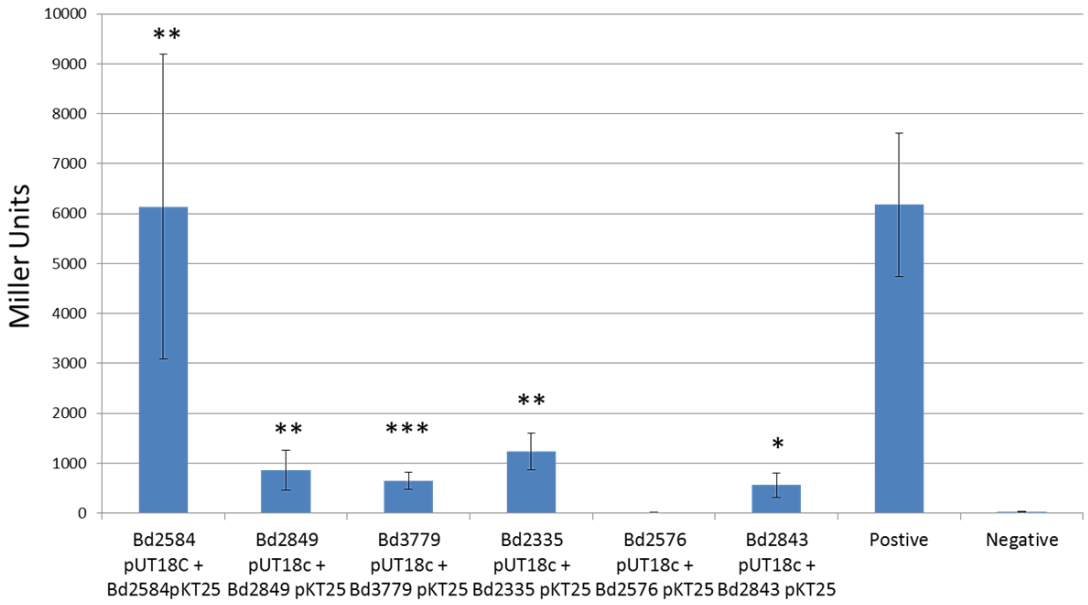

Figure 4.56 β-galactosidase activity assay for dimer interactions for the six test HKs proteins. Error bars show standard deviation. The results show the mean from three biological repeats and six technical repeats. The figure shows the interaction strengths of each kinases interacting with itself. Five of the six HK tested were found to have interaction strengths significantly different from the negative control. Asterisks show the significance of Student t-test compared to the negative (pUT18c,pKT25) *≤0.05 **≤0.01 ***≤0.001.

These dimerization interactions suggest that N terminal tagging did not significantly disrupt the structure of five candidate HK as self-interaction still occurs. This suggests that the lack of interaction between these four other HK and Bd0367 is due to there being no interaction or only a very transient interaction and not the fault of the N terminal tag.

4.5. Discussion

These data suggest that Bd2584 is probably not the cognate HK regulating DGC Bd0367 activation, due to lack of phenotypic evidence in *bd2584* deletion strains and absence of observed phosphotransfer between Bd2584 and Bd0367. However interaction studies have placed HK Bd2584 in a network of proteins that are all of a c-di-GMP nature. What the function of Bd2584 is in this context is not yet established and these physical interactions are still to be verified by an alternative method to B2H.

4.5.1. Selection of candidate kinases

The selection of the candidate kinases was done by Dr Porter by generating partner predictions through the most recent observations of (Burger & van Nimwegen, 2008;

Skerker et al, 2008; Weigt et al, 2009; White et al, 2007). However Burger and co-workers observed that predictions for orphan HK and RR pairs were much less reliable than of paired proteins this indicates that it is possible that none of the 6 candidate kinases are the true cognate kinase for Bd0367.

There are 17 orphan HK and hybrid HK in *Bdellovibrio* that have not been investigated by B2H analysis, and 21 orphan HK and hybrid HK that have not been analysed by phosphotransfer assay. It is possible that to find the true cognate HK for Bd0367 all 21 of these HK and hybrid HK proteins may have to be analysed by phosphotransfer assay in the future.

4.5.2. HK Bd2584 interacts with the RR and DGC protein Bd0367 by B2H assays

From the B2H and β-galactosidase data Bd2584 was the strongest proposed candidate HK. Due to Bd2584 being the proposed cognate HK to RR Bd0367 further investigation into Bd2584 was carried out.

4.5.2.1. Validity of the B2H method to screen candidate HKs

The method of B2H to narrow the selection of the six candidate kinases was done due to various published studies that examine HK-RR interactions by B2H screens or the similar technique, yeast two hybrid (Huynh et al, 2015; Ohta & Newton, 2003; Ryan et al, 2012).

An example of a successful B2H HK and RR interaction study is shown by Huynh et al. In this study B2H analysis revealed significant interactions for cognate pairs NarX–NarL, and NarQ–NarP. They also found a much weaker interaction for the non-cognate pair (NarX-NarP), this demonstrated that cognate HK-RR interactions can be detected by B2H (Huynh et al, 2015). However these techniques are not perfect as yeast two hybrid was used to screen for interactions the between the cognate HK and PleD–but no kinases were identified, this suggested that not all HK- RR interactions have stable enough interactions to screen for via methods such as yeast or B2H assays (Ohta & Newton, 2003). Other studies have shown the HK-RR interactions to be transient and loose associations due to the affinity of these interactions being ~1 μm (Stites, 1997). This interaction strength is far lower than the average K_D observed for normal protein

interactions (average 17 nM) for this reason detection of all HK-RR interactions by B2H may not always be possible.

4.5.2.2. Validity of the B2H method to screen membrane proteins

B2H if done correctly can be used to probe interactions with membrane proteins, however (Battesti & Bouveret, 2012) noted that for membrane proteins, an unspecific weak interaction signal is more often observed than for soluble proteins, resulting in more false positives. In the case of the 4 membrane associated HKs in this study no consistent 'false positives' were found, however this may be due to the N terminal tagging of these proteins. The N terminal tag may have impaired the targeting and insertion of these proteins into the membrane. However even if these proteins had a disordered N terminus due to transmembrane regions being forced to remain in the cytoplasm I predict that the C terminal HK regions are located sufficiently far from the disorder at the N terminus hence would not be too affected structurally and still able to interact with RR interaction partners.

This reasoning was tested by checking the dimerization interaction of the candidate kinases, only one HK would not dimerize, suggesting in this case that the structure of HK Bd2576 had been negatively affected by N terminal tagging. However Bd2576 is unlikely to be the cognate kinase to Bd0367 as it is found in an operon with a different RR.

An interaction study by (Ohta & Newton, 2003) suggested that the region of autophosphorylation phosphotransfer and dimerization (located at the C terminus of the 4 candidate membrane HKs) is sufficient for recognition specificity between cognate HK and RR. Considering this if one of the other candidate HKs was the cognate HK for Bd0367 this study suggests the interaction could have occurred despite the potential disorder at the N terminus. So these HKs had the potential to result in a positive interaction within the constraints previously mentioned about the limitations of B2H in detecting transient interactions.

4.5.2.3. Bd2584 interacts with Bd0367 full length and Bd0367 RR domain

The B2H interaction studies carried out between the six candidate HK and Bd0367 showed reliable spot plate and β-galactosidase evidence that HK Bd2584 interacted with Bd0367. This interaction was further investigated by B2H and quantified by β-galactosidase assays to confirm that Bd2584 interacted specifically with the RR domain of

Bd0367. This result suggested that the interaction between Bd2584 and Bd0367 was occurring at the biologically relevant protein domains and was stronger than the full length interaction. At this point the data suggested that Bd2584 was the cognate HK for RR and DGC protein Bd0367.

4.5.2.4. Mutating the phosphotransfer and phosphoaccepting amino acids on Bd2584 and Bd0367 had a stronger effect than expected

When the Bd2584H389V and Bd0367D63A B2H constructs were made it was thought that the interaction between the two would become weaker due to 2 key functional residues (involved in phospho-transfer and phospho-receiving) being mutated. However I assumed that an interaction would still occur due to the specificity residues being un-altered. The result of this interaction by B2H analysis suggested a very weak interaction may occur between Bd2584H389V and Bd0367D63A in one orientation due to the blue colonies on the spot plate, however there was no significant interaction when tested by β-galactosidase assay and it is significantly lower than the WT interaction. The removal of this interaction by mutating the phospho-transfer H may be caused by the reduced ability of the HK Bd2584 to dimerise due to the H lying with in the dimerization region or by conformational changes that have altered the 3D location and environment for the specificity residues. It was observed that though dimerization of Bd2584H389V did occur it was significantly weaker than WT dimerization strength. This removal of interaction upon mutation of key functional residues for phosphotransfer again confirmed that the HK-RR interaction was occurring in a biologically relevant location.

4.5.3. HK Bd2584 interacts with another component of the *Bdellovibrio* c-di-GMP network

In chapter 3 it was shown that RR domain of Bd0367 interacted with the degenerate GGDEF Bd3125 and EAL domain protein Bd1971. In this chapter it has been shown that HK Bd2584 interacts with the cNMP domain of the EAL protein Bd1971, in addition to interacting with RR of Bd0367 see Figure 4.57.

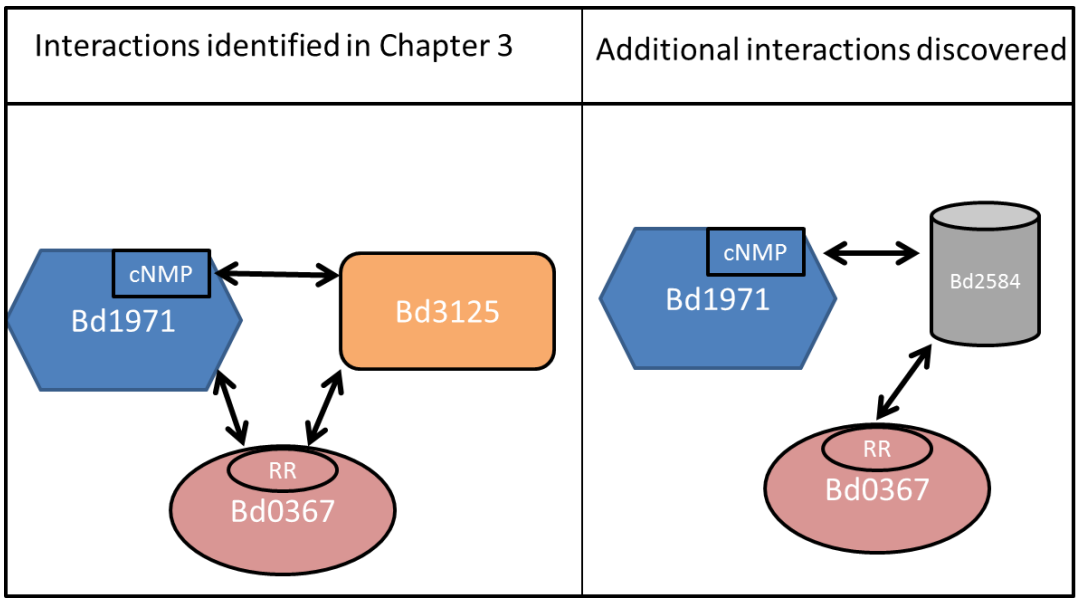

Figure 4.57 Adding to the protein interaction network of Bd0367

4.5.3.1. HK Bd2584 interacts with EAL domain protein Bd1971 by B2H assays

Bd2584 interacted with Bd1971 by B2H analysis; this interaction was isolated and found to be occurring between Bd2584 and the cNMP domain of Bd1971. The cNMP domain is the proposed binding site of cAMP. Both Bd1971 and Bd2584 are predominately located diffusely throughout the cell; this gives the pair an opportunity to interact in vivo.

The function of the Bd1971-Bd2584 interaction has not been established however there are a number of hypothesise outlined below starting with two models in which Bd2584 is not the cognate HK and 2 in which Bd2584 is potentially the cognate HK for Bd0367.

Model 1: Bd2584 sequesters Bd1971 from Bd0367

Bd2584 may interact with Bd1971 when it is in complex with Bd0367 and relieve any hypothesised repressive effect that the Bd1971-Bd0367 interaction could have on the ability of Bd0367 to produce c-di-GMP (as theorized in model 1 in chapter 3) see figure 4.58. The problem with this model is mCherry studies of Bd2584 expression have shown it is only present in low levels, so is unlikely to be present in high enough quantities to sequester large quantities of Bd1971 from Bd0367.

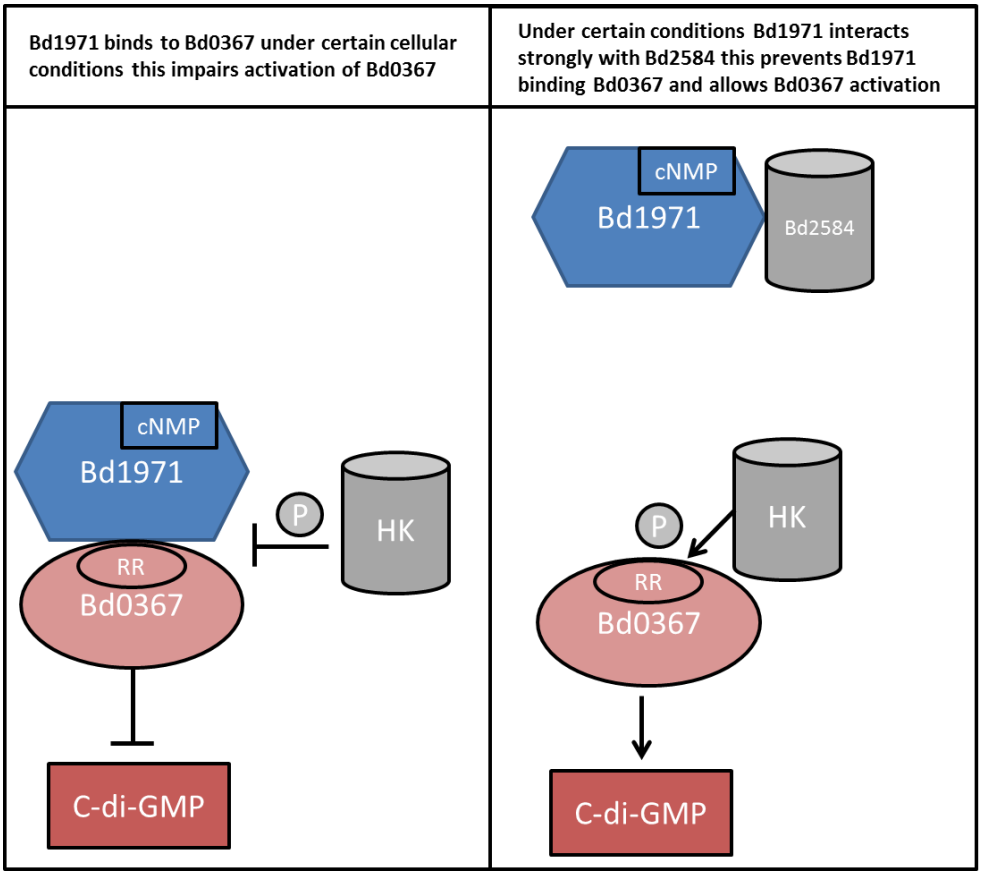

Figure 4.58 Hypothesis 1: Bd2584 sequesters Bd1971 allowing Bd0367 DGC activation. When Bd1971 interacts with Bd0367 this blocks the interaction between Bd0367 RR and the cognate HK. This results in Bd0367 not being phosphorylated, so not producing c-di-GMP. However in certain conditions Bd2584 can bind to Bd1971 and this interaction causes Bd1971 to leave the RR domain of Bd0367, this enables the cognate HK to phosphorylated Bd0367 and c-di-GMP to be produced.

Model 2: Bd2584 binding to Bd1971 regulates PDE enzyme activity

Under certain conditions Bd2584 binds to the cNMP domain of Bd1971, this may prevent cAMP binding and potentially prevent the PDE activity of Bd1971. This hypothesis would work to shift the level of c-di-GMP in the cells from low to high see figure 4.59. However the same issue of low abundance of Bd2584 in the cell makes this hypothesis unlikely.

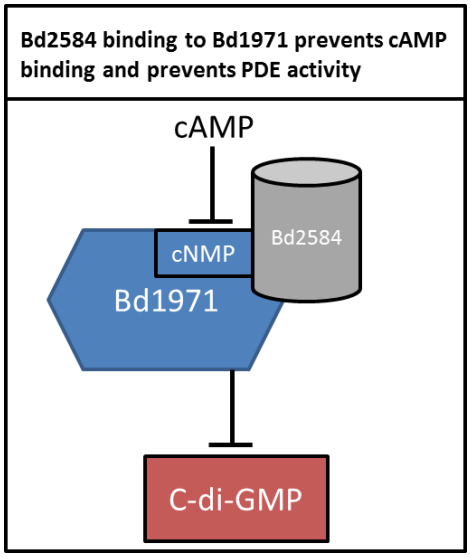

Figure 4.59 Bd2584 prevents cAMP binding to Bd1971, this prevents PDE activity. This function would cause the cellular c-di-GMP level to rise.

Model 3: Bd1971 acts as an accessory protein to regulate the catalytic abilities of Bd2584

As mentioned in the introduction to this chapter accessory proteins can act to enhance autophosphorylation, or phosphatase activity of HKs (Buelow & Raivio, 2010). The physical interaction between an accessory protein CpxP and HK CpxA has recently been demonstrated by B2H and this interaction is mediated by specific conditions(Tschauner et al, 2014). Bd1971 could have a role additional to its PDE activity and act as an accessory protein regulating Bd2584 HK catalytic abilities and this physical interaction could be dependent on the cellular c-di-GMP levels. Bd1971 binding could stimulate phospho-transfer or phosphatase activity of Bd2584 to the RR domain of Bd0367 see figure 4.60. I propose that phospho-transfer may be stimulated as this would suggest Bd1971 binding Bd2584 is required for transfer to occur and would explain why no phosphotransfer was observed in the in vitro phosphotransfer assay as Bd1971 was the missing factor that provides the c-di-GMP level signal rather than c-di-GMP itself as seen previously (Lori et al, 2015). In this model it is possible that Bd2584 is the cognate HK for Bd0367. Additionally it is possible Bd1971 acts as an accessory protein to Bd2584 to control phosphorylation of an unknown RR domain.

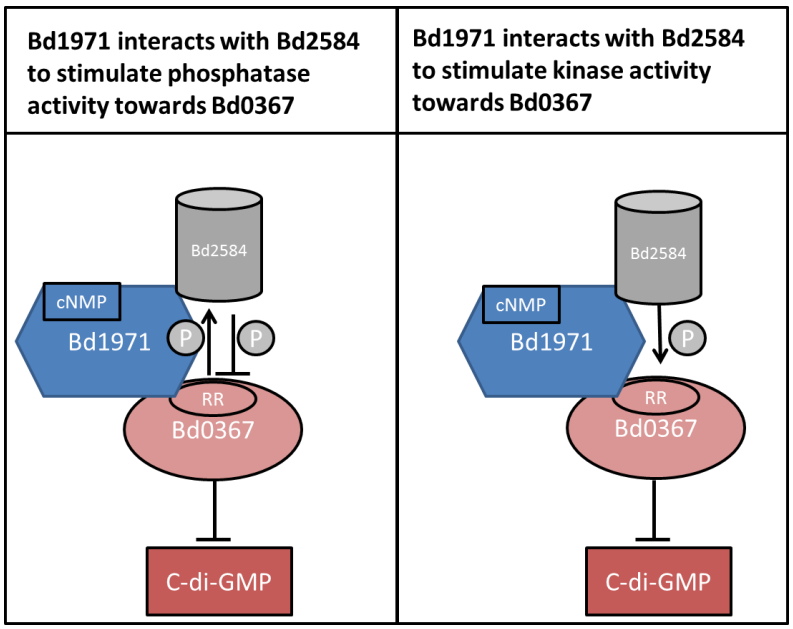

Figure 4.60 Bd1971 acts as an accessory protein to Bd2584 and regulates phosphotransfer to Bd0367.

Model 4: Bd1971 provides a signal of the cellular c-di-GMP level and Bd2584 is involved in a phospho-relay interaction

In this model Bd1971 interacts with Bd2584 to act as a signal of the cellular level of c-di-GMP for Bd2584, which regulates Bd2584 catalytic activity. Bd2584 is involved in Bd0367 signalling cascade, however it is part of a phosphorelay, so does not phosphotransfer directly to Bd0367. In phosphorelays, phosphate is transferred initially from the His of the sensor HK (Bd2584) to a RR domain that is uncoupled from an output domain. In many cases, this domain is fused to the HK in what is known as a hybrid HK (currently unknown candidate). After phosphorylation of the RR domain on the hybrid HK, phosphate is passed to an HPt domain. Finally, the phosphorylated HPt domain serves as a phosphate donor for the terminal RR proposed as Bd0367 (Galperin et al, 2001; Gao & Stock, 2009).

The example of a phosphorelay would explain the weak interaction between Bd0367 and Bd2584 by B2H but the lack of phosphotransfer *in vitro*. This would also explain the lack of phenotype on *bd2584* deletion as in this model the unknown hybrid HK could be receiving phosphate from another donor (due to potential incorporation of multiple signals) and transferring this to Bd0367 in Bd2584 absence. Additionally the Bd1971 interaction with RR Bd0367 and Bd2584 may keep all signalling proteins for the cascade in close proximity to each other to allow signalling to occur. To determine if there is a

hybrid HK involved in phosphotransfer to Bd0367, a wide range of *in vitro* phosphotransfer assays would have to be carried out.

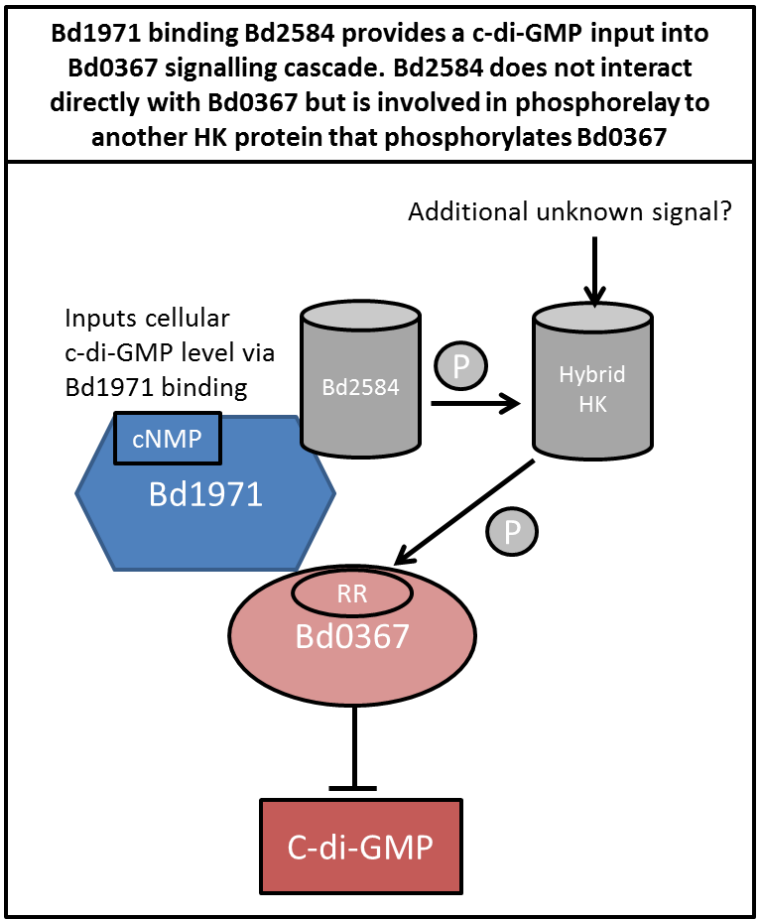

Figure 4.61 Bd2584 acts as part of a phosphorelay to regulate Bd0367 phosphorylation and activation. Bd2584 phosphotransfer is stimulated by cellular c-di-GMP level. This phosphate is transferred to currently unknown HK protein which then phosphorylated Bd0367. This method allows Bd2584 to indirectly regulate Bd0367 DGC activity and allows multiple steps for further regulatory control to be applied, as well as additional input sensing systems.

In conclusion I think that models 3 and 4 are the most convincing theories to pursue.

4.5.3.2. HK Bd2584 does not interact specifically with the degenerate GGDEF protein Bd3125

Bd2584 interacted strongly with Bd3125 by B2H analysis; however on further analysis Bd3125 was shown to interact with another HK Bd2843 casting doubt over the biological relevance of the Bd2584-Bd3125 interaction. This result suggested that the degenerate GGDEF Bd3125 may have tendency to interact with cytoplasmic HKs.

4.5.4. Fluorescent imaging of Bd2584 did not aid in elucidating its cellular function

The low level fluorescence observed in Bd2584mCherry strains was not a surprise as the proposed role of Bd2584 as a constitutively expressed HK that is activated by a signal binding the PAS domains, this means that the level of the 'signal' is controlling the level of Bd2584 autophosphorylation and phospho-transfer, so low levels of this protein are sufficient for it to regulate phosphorylation state of its cognate RR.

4.5.5. HK Bd2584 is not important for predation, gliding motility or bdelloplast exit

The investigation of two Bd2584 strains, the deletion of *bd2584* and the Bd2584H389V mutant was hoped to elicit a phenotype similar to that of the Δ*bd0367* strain. As has been observed previously with other HK deletions, for example; HK RavA deletion resulted in attenuation of *Xanthomonas campestris* virulence due to the lack of phosphotransfer from RavA to cognate partner RavR affecting RavR c-di-GMP turnover activity (Tao et al, 2014).

However this was not the case in our study with no impairment of the Δ*bd2584* strain or Bd2584H389V strain found when compared to wild type. This led to the possibility that Bd2584 was not the cognate kinase and that Bd0367 was still phosphorylated by its true cognate kinase, so was still active.

In the deletion strain it was possible that in the absence of the proposed cognate HK (Bd2584) Bd0367 was being phosphorylated by a promiscuous kinases, hence was still being activated. Promiscuous phosphorylation *in vivo* upon cognate pair disruption has been documented previously by (Kellogg & Kristich, 2016). However this possibility was investigated further by the *bd2584H389V* strain which was proposed to bind but not phosphorylate Bd0367, this aimed to prevent promiscuous phosphorylation and result in a phenotype similar to Δ*bd0367* strain.

However studies by (Willett & Kirby, 2012) previously have found that while alterations in the H box can have independent enzymatic effects alterations in this region could also alter other properties. In our case unfortunately the alteration removes the interaction between Bd2584H389V when tested with Bd0367D63A when tested by B2H study. If this is the case in the *Bdellovibrio* Bd2584H389V strain this would mean that this strain is

very similar to the Δ*bd2584* strain as Bd0367 would still be open to promiscuous phosphorylation from other kinases engaging in cross talk.

4.5.6. HK Bd2584 does not phosphotransfer to Bd0367

Phosphotransfer assays were carried out as these experiments are the best way to investigate cognate partners in two component systems in vitro. These experiments hoped to establish that Bd2584 was the cognate HK to the RR Bd0367 despite no phenotypic evidence to this effect. Previous use of this technique in multiple studies has successfully isolated cognate pairs (Hess et al, 1991; Scharf, 2010).

Bd2584 was seen to autophosphorylate at approximately 15 seconds, this is a fast autophosphorylation. However no transfer of this phosphate to Bd0367 over long (1 hour) or short time(1 min) courses was seen. The conditions used were standard conditions used in Dr Porter's lab and documented in (Porter et al, 2007). Many HKs will transfer under these standard conditions but some others require conditions to be optimised, a common optimisation is altering the temperature to be physiologically relevant (Najnin et al, 2016). Using a biologically relevant temperature was also carried out in this study however no transfer occurred.

Another possibility was that Bd2584 was rapidly transferring phosphate to Bd0367 and just as rapidly de-phosphorylating Bd0367, due to phosphatase activity, so the transfer of phosphate to Bd0367 was not observed. There is also the possibility that Bd0367 itself possesses a rapid intrinsic autodephosphorylation activity. Rates of autodephosphorylation vary greatly between RRs however faster autodephosphorylation rates correspond with faster biological processes such as motility (Pazy et al, 2009).

However this can probably be ruled out for the case of Bd2584-Bd0367 as no change in Bd2584-P32 levels were seen and no transfer to Bd0367 was observed even over the short time course.

The lack of transfer under standard conditions was not ideal however further investigation into phospho-profiling of the predicted pair was continued by examining the effect on c-di-GMP addition to the reaction mix. This was inspired by the work of (Lori et al, 2015) in their 2015 paper they demonstrated that c-di-GMP binds the HK CckA inhibits its kinase activity and stimulates its phosphatase activity. As Bd2584 also has a proposed kinase role within a c-di-GMP signalling network I hypothesised that

perhaps in this case c-di-GMP was required to stimulate phospho-transfer to Bd0367. No transfer was observed under these conditions and no alteration in Bd2584 autophosphorylation was observed, this suggested that the addition of c-di-GMP did not stimulate the phospho transfer to Bd0367.

Many studies into *in vitro* 'cross talk' in phospho profiling assays have been carried out, these studies show that after prolonged incubation some HKs can phosphotransfer to a non-cognate RR (Groban et al, 2009; Skerker et al, 2005; Willett et al, 2013; Yamamoto et al, 2005). One of these cases was with HK CrdS, this HK was seen to phosphotransfer to 3 additional targets but only at the later timepoint, of an hour incubation. (Willett et al, 2013)

Bd2584 did not even appear to demonstrate 'cross talk' at the longer incubations, as no transfer was observed even at an hour incubation, this may suggest that purified Bd0367 was not stable or was negatively affected by the experimental conditions.

There are few papers documenting the difficulties of finding the optimal transfer conditions for predicted cognate kinases and RRs. However in one study no phosphotransfer was observed between LuxU~P to LuxO, the predicted cognate pair, and it is hypothesised that this may require additional factors for phosphotransfer in vitro (Shikuma et al, 2009).

So it is possible that Bd2584 could transfer to Bd0367 but additional unknown factors are needed for this to be seen *in vitro*. However in the majority of cases HKs can transfer to their cognate RRs without extensive optimisation, this fact in conjunction with the lack of a phenotype in the Bd2584 deletion strain leads me to suggest that Bd2584 may not be the cognate kinase of Bd0367.

4.5.7. No additional interacting partners of Bd2584 were identified and none of the interactions shown by B2H were confirmed

The identity of purified Bd2584-His used in phosphotransfer assays was confirmed by LC/MS, however no protein interaction partners were found.

The lack of identification of any previously identified or unique protein interactions is thought to be because of reasons relating to the conditions of this assay discussed previously in chapter 3. This suggests that further optimization of this process is necessary.

A smaller amount of Bd2584-His should also be used as the amount used may have masked other interactions. Additionally variation in the imidazole concentration used to wash the beads could be attempted as perhaps the concentration added not only got rid of non-specific proteins but also removed some specific interactions. Another consideration is the washing the beads step without disrupting weak or transient interactions, which the RR interaction is expected to be.

Over all it could be better to find another technique to confirm the B2H interactions as optimising pull down assays in *Bdellovibrio* has proved difficult.

4.6. Chapter Conclusions

In conclusion, this study has not found sufficient evidence to conclude that Bd2584 is the cognate HK for Bd0367. However investigation of HK Bd2584 has shown that it may have a role in the c-di-GMP signalling network of *Bdellovibrio* due to it interactions with EAL protein Bd1971. The function of the Bd2584 protein interactions are currently unknown, however I have formed a number of hypothesises. The model that I think is the mostly likely is that Bd1971 acts as an accessory protein to Bd2584. This is independent of the enzymatic function of Bd1971 and acts as c-di-GMP sensing mechanism, this interaction stimulates either phospho-transfer or phosphatase activity of Bd2584 on Bd0367or an unknown RR or possibly to an additional kinase which transfers to Bd0367. This would potentially fit with model 1 from chapter 3 where Bd1971-Bd0367RR interaction is proposed to stimulate DGC activity.

4.7. Further Experiments

Further experiments will be required to find and confirm the cognate HK for Bd0367.

1. Make more B2H constructs. These constructs would C terminally tag the candidate HKs and also would contain truncated versions of the HKs without the membrane spanning regions to see if these alterations found an interaction with Bd0367.
2. Examine candidate HKs by phosphotransfer assay with Bd0367. This technique could also be extended to examine all *Bdellovibrio* orphan HK and hybrid HKs for potential phosphotransfer to Bd0367. However this would be best suited to labs who regularly work on HK-RR partners.

3. Investigate the possibly of adapting *in vivo* phosphorylation assays using Phos-tag for *Bdellovibrio* and carried this out on various HK deletion strains, to examine the level of Bd0367~P in different genetic backgrounds (Barbieri & Stock, 2008; Tao et al, 2014).
4. Confirm B2H interaction by another experimental method, (Bd2584-Bd0367, Bd1971-Bd2584) such as isothermal titration calorimetry could be used to quantify the interacting proteins binding affinity. Or far western blotting with Bd2584 as the probe protein could be carried out on *Bdellovibrio* cell lysate (Wu et al, 2007). Or Co-immunoprecipitation could be used as this could pull out a protein complex. However both far western blotting and co-immunoprecipitation present similar challenges to affinity pull down experiments attempted in this study.

4.8. Concluding remarks

In conclusion, the cognate HK of Bd0367 has not yet been found. However another HK that is involved in c-di-GMP signalling has been discovered, the role that HK Bd2584 plays in the c-di-GMP signalling cascade of Bd0367 is yet to be fully determined.

Chapter 5. Investigating the role of phosphorylation on Bd0367 diguanylate cyclase activity and assessing the role of increased global c-di-GMP level on gliding motility

5.1. Introduction

5.1.1. Role for DGC proteins regulated by RR domains in c-di-GMP signalling systems

Many DGC domains are joined to response regulator (RR) domains, these types of proteins make up ~2.3% of all RR investigated (Galperin, 2010). This suggests that RR domains are a common mechanism of regulating DGC activity through phosphorylation. RR domains exist in equilibrium between two conformational states, active and inactive, phosphorylation by the cognate HK normally shifts the equilibrium to the active state. The difference in conformation can cause different molecular surfaces to be displayed, which can facilitate different protein-protein interactions and regulate enzymatic activity of protein (Stock et al, 2000).

5.1.1.1. Examples of the role of RR domains in modulating DGC activity

There are two well-known examples of DGC enzymes with RR domains, these are PleD in *Caulobacter* and WspR in *Pseudomonas*. Both proteins show that RR domains can provide an extra layer of regulatory control and specificity.

The Wsp signalling system involves WspR, this DGC protein in *P. aeruginosa* contains a RR domain, which allows WspR to be activated via phosphorylation by the HK WspE (Hickman et al., 2005). WspE itself is activated by WspA, a membrane-bound protein that detects a surface associated signal. The presence of this RR domain allows WspR to respond specifically to a surface signal, the c-di-GMP produced by WspR stimulates synthesis of the EPS Pel, which is important for biofilm formation (Hickman et al, 2005).

The phosphorylation of WspR by WspE results in the formation of WspR-P tetramers these tetramers can oligomerise into clusters which enhance the activity of WspR DGC

(Huangyutitham et al., 2013). These clusters could allow for a c-di-GMP feedback mechanism on WspR activity, with the suggestion that high c-di-GMP levels potentially result in dissociation of the clusters, or that the clusters may be more resistance to c-di-GMP inhibition, however neither theory has yet been experimentally demonstrated (Huangyutitham et al, 2013).

The examples demonstrate the control and diverse regulation that can occur when a DGC domain is paired with a RR domain.

5.1.1.2. C-di-GMP production by DGC Bd0367 in *Bdellovibrio*

Bd0367 is a *Bdellovibrio* DGC protein with an RR domain. It has previously been established by Hobley and co-workers that Bd0367 is an active DGC. This was determined by several methods. The GDDEF domain of Bd0367 was fused to a maltose binding protein and expressed in a motile strain of *E. coli*. It was shown that elevated c-di-GMP levels inhibit *E. coli* motility in swim agar plates, and this occurred when the Bd0367 fusion was expressed which was consistent with its predicted DGC activity. This activity was further demonstrated by purifying the maltose binding protein fusion Bd0367 and investigating the activity *in vitro* by HPLC analysis. This confirmed that Bd0367 could process GTP to c-di-GMP. Finally c-di-GMP levels were determined from the *⊿bd0367* HI strain and compared to the wild type strain HID13. This confirmed that the deletion of Bd0367 resulted in a fall in c-di-GMP levels when compared to the wild type strain. This showed that Bd0367 is an active DGC and produces c-di-GMP to contribute to the cellular c-di-GMP level present in *Bdellovibrio*.

However the role of the RR domain of Bd0367 on DGC activity was not investigated. In this study the role of phosphorylating the RR domain of Bd0367 on DGC activity and phenotype is investigated by amino acid mutation.

5.1.2. C-di-GMP levels and phenotypes

Levels of c-di-GMP in bacteria are controlled by the activity of DGC and PDE proteins. The regulation of these enzymes is important in order to correctly control the c-di-GMP level and hence the downstream effects. The ways in which DGC and PDE proteins are controlled can be mediated by tightly regulating when these proteins are expressed. For example the gene encoding DGC DmxB in *Myxococcus* has been shown by qRT-PCR to be up regulated at the transcriptional level specifically in response to starvation (Skotnicka et al, 2016b). Additionally these proteins commonly also have signal input

domains such as PAS, GAF or RR domains, this allows ligand binding to control activity (Galperin et al, 2001). Another method of controlling the downstream effects of c-di-GMP levels is through the differing affinity for the receptor proteins to c-di-GMP, this allows regulation, with a downstream response only occurring at set threshold levels of c-di-GMP (Pultz et al, 2012).

Controlling the level of c-di-GMP in the cell is very important as the molecular responses to differing levels of c-di-GMP can result in very different phenotypes. Generally there is a correlation between high cellular c-di-GMP levels and increased sessility and biofilm formation (Romling et al, 2013). For example when the DGC activity of WspR in *P. aeruginosa* increases the protein produces more c-di-GMP and this can stimulate EPS production allowing biofilm formation (D'Argenio et al, 2002). These globally high c-di-GMP levels can cause TFs to relieve repression of genes for example c-di-GMP binding reduces FleQ affinity to *pel* promoter in *P. aeruginosa* allowing EPS biosynthesis transcription and increased biofilm formation (Baraquet et al, 2012). The opposite is true at low c-di-GMP levels this increases motility and virulence (Romling et al, 2013; Tischler & Camilli, 2005). For example a PilZ domain protein FlgZ interacts with a stator motor protein MotC in a c-di-GMP dependent manner, when FlgZ is c-di-GMP bound this interaction impairs swarming motility in *P. aeruginosa* (Baker et al, 2016).

5.1.3. Global and local c-di-GMP signalling mechanisms

A number of global and local c-di-GMP signalling mechanisms have been studied, in many bacteria it appears both these mechanisms are being used in parallel to carefully control cellular responses (Dahlstrom et al, 2015; Lindenberg et al, 2013).

5.1.3.1. Global

An example of when global c-di-GMP levels are used to have a specific effect is through the use of threshold values. When the global c-di-GMP level reaches a certain concentration PilZ domain proteins with varying affinities for c-di-GMP can become active. A good example of this are the two PilZ domain proteins YcgR and BcsA in *S. enterica*, BcsA has a 40 fold lower affinity than YcgR for c-di-GMP so is only active at higher global c-di-GMP levels (Pultz et al, 2012).

Another mechanism that can achieve global changes in the c-di-GMP level is controlling the transcription of DGCs or PDEs. For example *Y. pseudotuberculosis* regulates biofilm formation, pathogenesis and motility through the Rcs phosphorelay system. RcsB can

activate DGC *hmsD* transcription but when interacting with auxiliary protein RcsA it represses *hmsD* transcription, leading to global changes in c-di-GMP level (Guo et al, 2015).

5.1.3.2. Local

Overall global low or high c-di-GMP levels can have similar overall phenotypic effects however there is not always a correlation between the concentration of global c-di-GMP and the extent of the phenotypic effect observed. This lack of correlation suggests local mechanisms are also at work in this system, where particular DGC proteins and effector proteins are working to transduce a specific response without cross talk. This is reflected in gene deletion studies where some DGC deletions result in a clear cut phenotype and other DGC deletions do not, seeming that these DGC proteins may have been mediating local pools and other DGCs may have been contributing to the overall global cellular pool (Ha et al, 2014; Romling et al, 2013; Shikuma et al, 2012).

One way that this local model can operate is by direct protein-protein interactions, (as discussed in Chapter 3) where these physical interactions can aid in mediating parallel signalling outcomes without cross talk (Dahlstrom et al, 2015; Hengge, 2009; Lindenberg et al, 2013).

Work by Dahlstrom and colleagues has progressed the field in protein-protein interactions being an important method of controlling local signalling. They showed that effector LapD and DGC GcbC interact by B2H and that GcbC localises to the inner membrane to interact with LapD (Dahlstrom et al, 2015). However they admit that it is unknown at this point how global c-di-GMP signalling may be integrated within this local signalling model. In the cases of work by Lindenberg and colleagues the multiprotein interaction complex described controls a local module and specific effect (interaction-activates MlrA to stimulate *csgD* transcription important in biofilms) however this interaction complex is influenced by the global c-di-GMP level and this integration of local and global is mediated by YciR PDE acting like a trigger enzyme (Lindenberg et al, 2013).

5.1.4. Background to the work presented in this chapter

Work in previous chapters has examined the interaction partners of Bd0367 and tried assess the role of phosphorylation of Bd0367 by attempting to identify the cognate kinase for Bd0367. This chapter instead assesses the function of Bd0367 phosphorylation by site directed mutation of Bd0367. This chapter also begins to assess the function of differing cellular levels of c-di-GMP in *Bdellovibrio* on cell motility by PDE gene deletion studies. While this research was being carried out a study by (Hallberg et al, 2016) was published indicating that Bd0367 is a bifunctional enzyme that can produce cAG. Due to the timing of this discovery this thesis has not researched Bd0367 cAG production and function. However work into this is now being carried out by Dr Lowry, she has recently made a new complement of the Bd0367 deletion strain. Additionally she has carried out site directed mutagenesis on an amino acid considered important for cAG production to assess the phenotype when cAG is no longer produced. These strains are currently still being assessed for phenotypes and will hopefully provide more information about *Bdellovibrio* signalling.

5.2. Specific Research Aims

- To analyse levels of cellular fluorescence in the HD Bd0367mCherry strain when incubated on a surface vs liquid.
- To analyse the location of the HD Bd0367mCherry and see if this location is altered on surface incubation.
- To determine if Bd0367 is activated by phosphorylation by investigating the c-di-GMP levels in the Δ*bd0367*::Bd0367D63A HI strain.
- To investigate the effects of the presence of a non-phosphorylated Bd0367 on *Bdellovibrio* gliding motility.
- To investigate the effects of the presence of a non-phosphorylated Bd0367 on the ability of *Bdellovibrio* progeny to exit the bdelloplast.
- To determine if Bd0367mCherry HI strain has impaired c-di-GMP production due to the mCherry tag potentially impairing dimerization via analysing c-di-GMP levels.
- To analyse the effect of potentially altered c-di-GMP levels due to Bd0367mCherry on bdelloplast exit in the HI strain.

- To analyse the effect of potentially altered c-di-GMP caused by Bd0367mCherry on gliding motility in the HI strain.
- To investigate the effect of *bd1971* deletion and Bd1971D307308A inactivation mutation strain on c-di-GMP levels in HI and HD strains through c-di-GMP extraction.
- To investigate the effect of high global c-di-GMP levels on gliding motility through investigating gliding motility of Δ*bd1971* strain.
- To determine if gliding impairment in the Δ*bd1971* strain is due to high c-di-GMP levels or due to loss of Bd1971 as an interaction partner for Bd0367. Via using a Bd1971 D307308A mutant which was predicted to disrupt PDE function but would still be present to interact with Bd0367 and other interaction partners.
- To investigate if the location or intensity of Bd0367mCherry fluorescence alters in silent in-frame deletion strain of Δ*bd1971* where c-di-GMP levels are high.
- To assess if different Bd0367mCherry levels in Δ*bd1971* cells correspond to particular motility behaviours.

5.3. Hypotheses

- The expression of Bd0367mCherry will increase on surface exposure, continuing to suggest a role in gliding motility.
- The ⊿*bd0367*::Bd0367D63A HI strain will show the DGC activity to be inactive, in the un-phosphorylated state. Resulting in a similar c-di-GMP level to the *bd0367* deletion strain.
- This lower level of c-di-GMP in the ⊿*bd0367*::Bd0367D63A HI strain will have a similar phenotype to the deletion strain with no *Bdellovibrio* exiting from the bdelloplast and no gliding motility
- The phenotype of the Bd0367mCherry HI strain will be partially restored to wildtype levels due to the slightly higher levels of c-di-GMP.
- ⊿*bd1971* HD strain gliding motility will be altered, with high c-di-GMP levels possibly impairing motility.
- Bd1971D307308A HD strain will have altered gliding motility due to globally high cellular c-di-GMP levels impairing motility by an unknown mechanism.

- The mCherry tagged Bd0367 may be visualised in altered location or altered intensity in the Δ*bd1971* HD strain in response to the increased level of cellular c-di-GMP or due to loss of interacting partner Bd1971.

5.4. Results

5.4.1. Surface incubation effects expression of Bd0367mCherry

Originally to assess cellular localisation of Bd0367 a strain a C-terminally mCherry tagged Bd0367 HD strain was made (Hobley et al, 2012). Bd0367mCherry was constructed by fusion of *bd0367* lacking its stop codon in frame with a mCherry tag. This was integrated into the *B. bacteriovorus* chromosome by single crossover at the *bd0367* gene. Bd0367 has a proposed role in gliding motility due to the lack of gliding motility observed in the Δ*bd0367* HI strain (Hobley et al, 2012). Due to this the levels of Bd0367mCherry expression were investigated when incubated on a surface.

5.4.1.1. *B. bacteriovorus* Bd0367mCherry cells show increased fluorescence when incubated on a surface.

Expression of protein Bd0367 in *B. bacteriovorus* Bd0367mCherry attack phase cells was seen to increase when incubated on a surface, a representation of this is shown in Figure 5.1. This increase in expression was quantified by using image analysis software (MicrobeJ) (Ducret et al, 2016). Time 0 min was obtained by observing the cellular fluorescence at the first point of surface contact and by time 400 min most cells would be exhibiting gliding motility (see Methods 2.7.2).

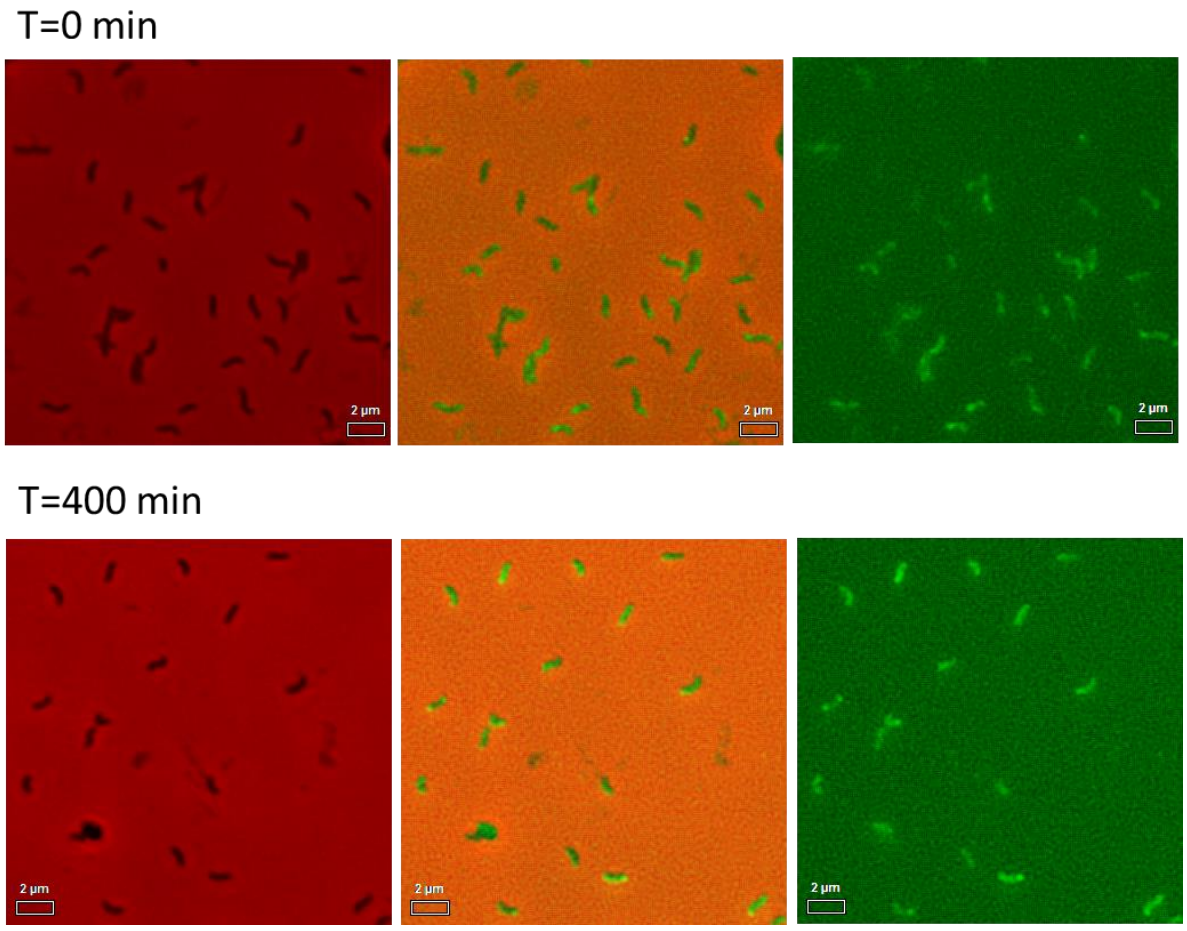

Figure 5.1 *B. bacteriovorus* Bd0367mCherry cells show increased fluorescence when incubated on a surface. The cells were placed on 1% CaHEPES agarose slide and images were collected at time 0 and time 400 min. during this time the slide was kept hydrated and at room temperature of 25°C. The panel of images shows time 0 at the top and time 400 minutes below. The panels left to right show brightfield channel, merged channel and fluorescence channel.

MicrobeJ was used to measure the fluorescence intensity of the individual cells. This data shown in Figure 5.2 found a 1.18 fold increase on surface incubation and that the intensity of the time 0 and time 400 min samples were significantly different from each other by student t.test.

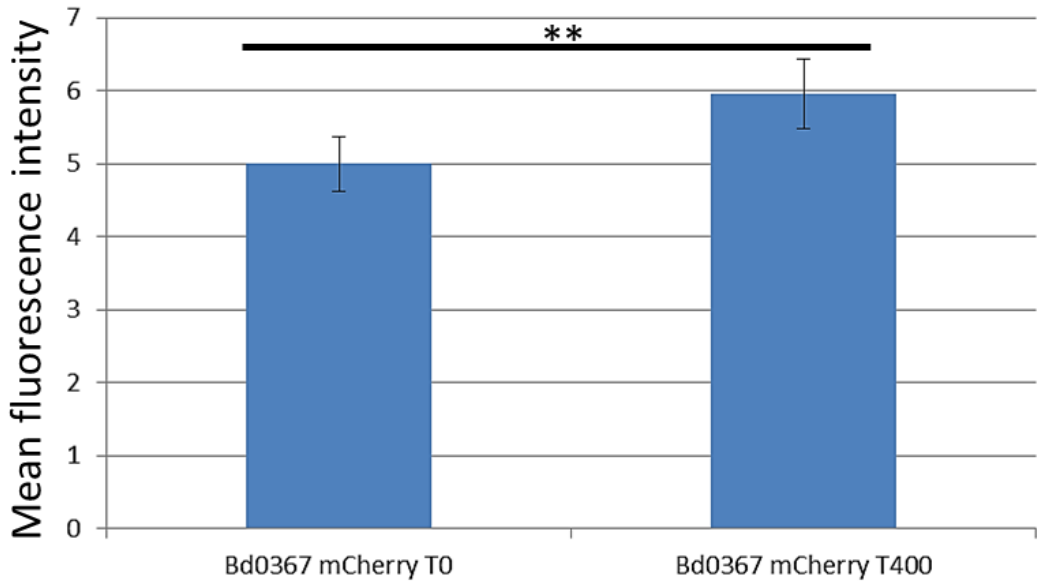

Figure 5.2 *B. bacteriovorus* Bd0367mCherry attack phase cells show an increase of 1.18 fold fluorescent intensity when incubated on a surface. Analysis using MicrobeJ on a total population of 393 cells at T0 and 389 cells at T400 sampled across 3 biological repeats each with 3 technical repeats, showed a significant increase in mean fluorescence intensity between time points. Error bars represent 95% confidence interval. Asterisks show the values of the Students t.test **≤0.01.

5.4.1.2. The distribution of Bd0367mCherry fluorescence in attack phase cells alters when incubated on a surface

Surface incubation increases Bd0367mCherry expression and also altered the localisation of Bd0367mCherry with in the cell. Bd0367mCherry localisation is split into 3 categories, throughout the cell, this is diffuse fluorescence throughout the cytoplasm with no obvious foci., bi-polar which has 2 foci, one at each pole and dominant mono-polar with a focus at one pole, with some diffuse fluorescence. The most common location at time 0 and time 400 min was throughout the cell, this location increased by 7% on surface incubation. Interestingly bi-polar localisation decreased on surface incubation dropping by 10% and becoming the least common localisation. Dominant mono-polar are the least common at time 0 and increases in frequency at time 400 by 3% suggesting this location is relatively constant in both situations (see Figure 5.3). This suggests that bipolar localisation of Bd0367 may be less advantageous on surface incubation. The most common location throughout the cell is consistent with Bd0367 interacting with multiple proteins all at various cellular locations.

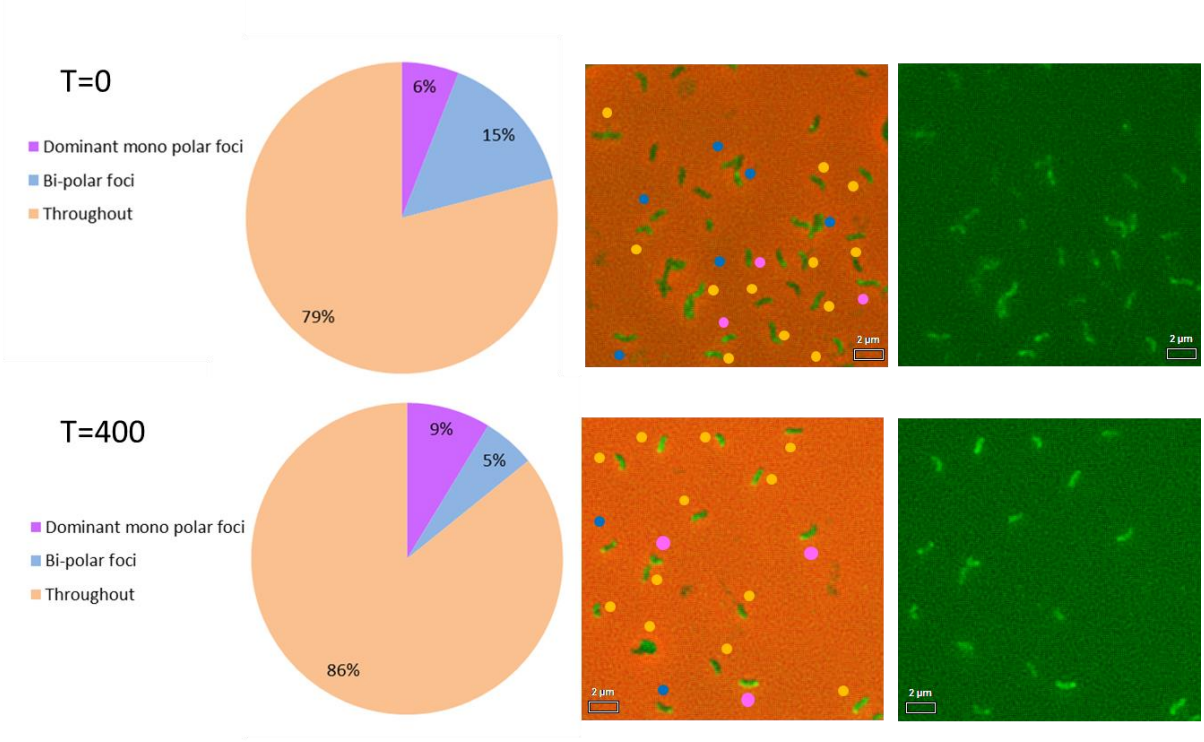

Figure 5.3 The frequency of bi-polar localisation of Bd0367mCherry decreases on surface incubation. At time 0 and 400 min *B. bacteriovorus* Bd0367mCherry cells showed primarily a diffuse fluorescence distributed throughout the cell, with a decrease in bipolar distribution at T 400. To demonstrate this visually the location of fluorescence in the cell (dominant monopolar, bipolar, diffuse) is highlighted by a dot of colour next to the cell which indicates which section of the pie chart this cell is representative of. Cells were placed on a 1% agarose CaHEPES slide at room temperature and kept hydrated. These slides were imaged at time 0 and time 400. A total of 1080 cells were analysed at t0 and 1206 at t400 min, these cells were counted across 3 biological repeats each with 3 technical repeats.

5.4.2. Cloning Bd0367D63A into the *Δbd367* HI strain

The D that is phosphorylated in Bd0367 RR domain was identified in Chapter 3 as D63. This amino acid was altered to an alanine via site-directed PCR in a B2H plasmid. The change of the D to an A results in a predicted non-phosphorylate-able version of Bd0367, as others have done by mutating the D to an N, cloning this into the gene deletion strain allows observation of the effect that phosphorylation has on Bd0367 enzymatic function (Skotnicka et al, 2016b). The Bd0367D63A construct was cloned out of the B2H construct (used in Chapter 3) and combined with 1 Kb of the Bd0367 upstream region and plasmid pK18 by Gibson cloning (see Methods 2.4.8.1). This construct was then integrated into the Δ*bd0367* HI *B. bacteriovorus* chromosome by single crossover at the upstream region of the *bd0367* gene, resulting in a strain where the only Bd0367 expressed has the mutated D63A. The genomic DNA of this construct was

extracted and the crossover and *bd0367* region were sequenced to confirm successful cross over and that the Bd0367 gene still had the relevant mutation.

5.4.3. Assessing the c-di-GMP production ability of *⊿bd0367*::Bd0367D63A HI strain in comparison to other HI strains

The levels of c-di-GMP can be quantified by extracting the c-di-GMP from a pellet of cells using the method described by (Bobrov et al, 2011) (see Methods 2.15). Since then this method has been used for the successful determination of the c-di-GMP levels present in *Bdellovibrio* HI strains. This method was used to analyse c-di-GMP levels in the *⊿bd0367* HI strain (Hobley et al, 2012) and was also used by Dr Basford to investigate the levels of c-di-GMP in the Kan Δ*bd1971* HI strain (Basford, 2015) and Mike White to investigate the levels of c-di-GMP in the HD-GYP deletions *bd2325* and *bd2421*(White, 2012). These previous results have given an indication that HI strains can have quite varied c-di-GMP levels between biological repeats, the reasons for this will be discussed further in Section 5.5.3.

The strains picked for investigation via c-di-GMP extractions were: *⊿bd0367* HI strain, *⊿bd0367*::Bd0367D63A HI strain, Bd0367mCherry HI strain and wild type HID13. Bd0367mCherry was chosen as the *⊿bd0367* HI strain was complemented by Bd0367mCherry previously (Hobley et al, 2012) and this resulted in only partial complementation, suggesting the mCherry may have some effect on the function of Bd0367, so the c-di-GMP level of this was also investigated.

For this experiment 1 biological repeat was examined this consisted of two independent isolates for each strain, which were grown and maintained in parallel in the same conditions (see Figure 5.4 showing all pellet weights obtained were similar). These strains were then grown overnight in broth to an OD_{600} of 0.6, pelleted by centrifugation and these pellets were resuspended in extraction buffer and processed as in the Bobrov method to extract the c-di-GMP from the pellet (see Methods 2.15). These samples were sent for analysis at RTSF Mass Spectrometry & Metabolomics Core at Michigan State University by Dr Lijun Chen and the nM/mg wet cell weight concentration of c-di-GMP was determined for each strain by HPLC.

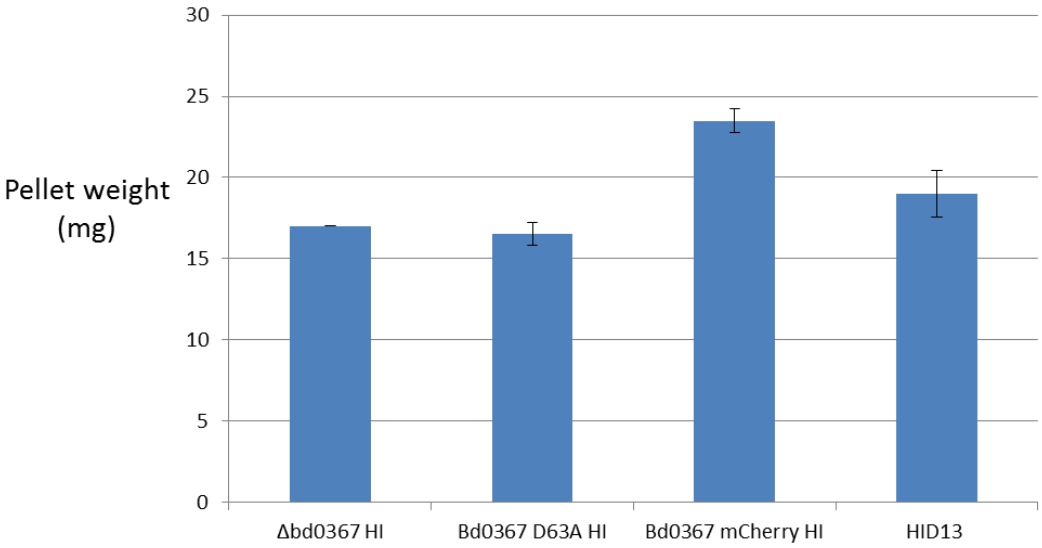

Figure 5.4 HI cell pellet weights for all HI strains investigated at this time were of similar value. Data was collected from one biological repeat with 2 technical repeats with the mean value shown. Error bars show standard deviation.

At the time of these experiments there was no true complementation strain to use as a control, however recently the complementation strain of Bd0367 has been successfully created by Dr Lowry. This c-di-GMP levels of this strain will be investigated in future studies.

5.4.3.1. Phosphorylation of Bd0367 is required for activation of the DGC activity of Bd0367

The results show that the normalised, relative concentration of c-di-GMP (nM) per mg of cell wet weight, in the ⊿*bd0367*::Bd0367D63A HI strain were lower than the in the wild type control HID13 suggesting that phosphorylation is required for activation of Bd0367 DGC activity. See Figure 5.5.

The ⊿*bd0367*::Bd0367D63A HI strain had a 93% reduction in cellular c-di-GMP compared to the wild type control HID13. Whereas the ⊿*bd0367* HI strain had a 91.5% reduction in c-di-GMP compared to HID13. The ⊿*bd0367*::Bd0367D63A HI was not significantly different from the ⊿*bd0367* HI strain.

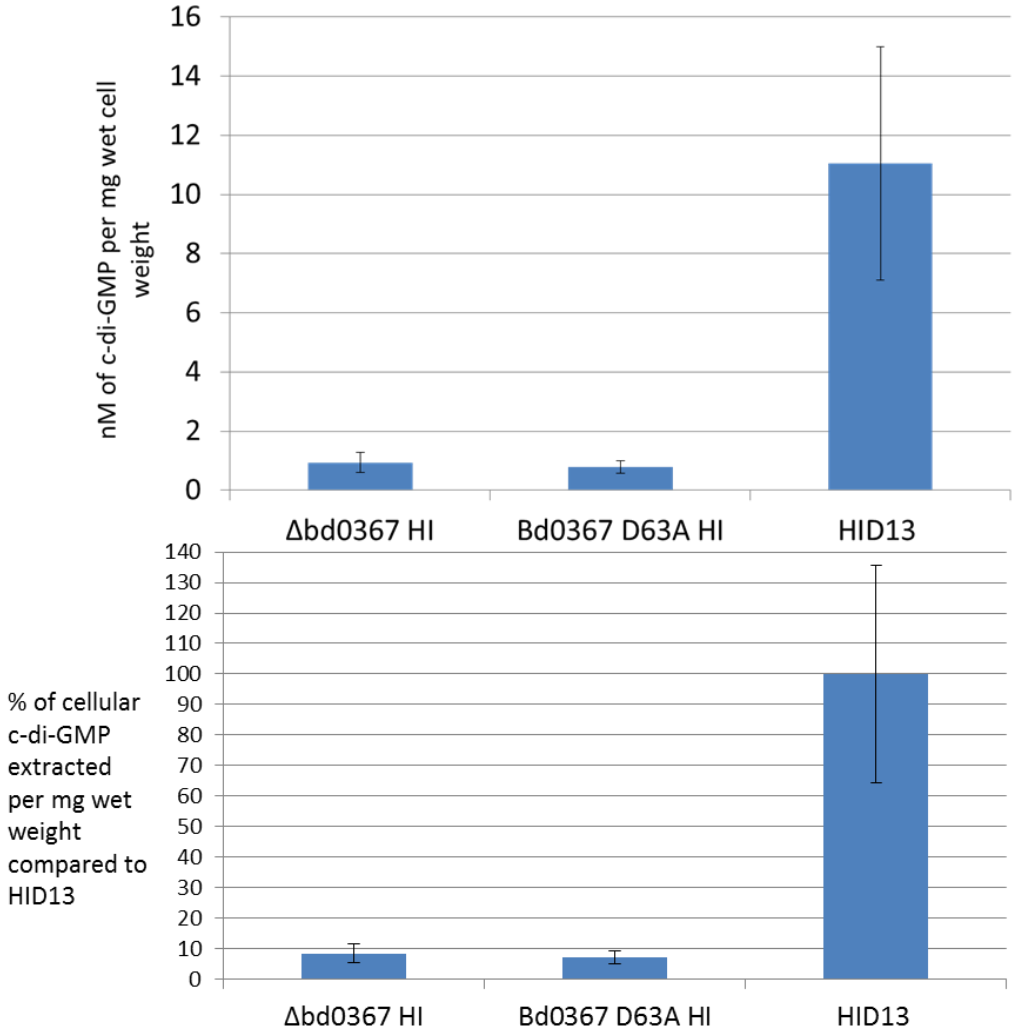

Figure 5.5 Bd0367D63A HI c-di-GMP levels are less than the wildtype control. HID13 contains more c-di-GMP per mg of wet cell weight than Bd0367D63A. Bd0367D63A does not contain significantly more nM of c-di-GMP than Δ*bd0367*. This was also represented as a % of c-di-GMP level in comparison to WT level. Data was collected from one biological repeat with 2 technical repeats with the mean value shown. Error bars show standard deviation, Student t test was used for significance but no significance shown as only two repeats.

5.4.3.2. Bd0367mCherry HI strain had an 88% reduction in c-di-GMP compared to the control

The Bd0367mCherry HI strain had an 88% reduction in the extracted amount of c-di-GMP (nM/mg wet weight) compared to the HID13 wild type making it different from wild type and similar to the levels seen in the deletion strain (see Figure 5.6). This suggests that the C terminal mCherry tag had a detrimental effect on the ability of Bd0367 to potentially dimerise and produce c-di-GMP.

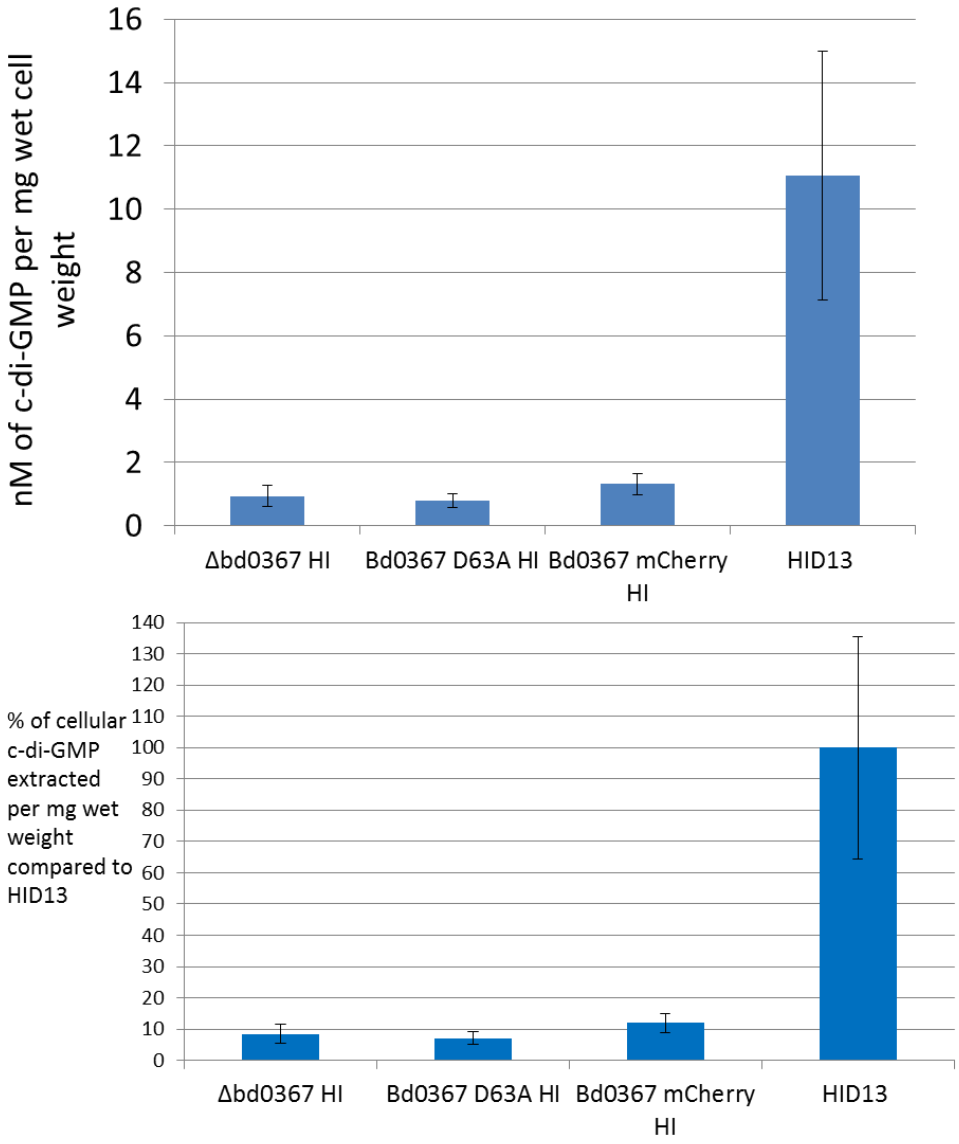

Figure 5.6 Bd0367mCherry HI strain c-di-GMP levels are less than the wildtype control. The HID13 cells contained more c-di-GMP per mg/wet weight than Bd0367mCherry HI cells. The Bd0367mCherry HI cells do not contain significantly more c-di-GMP than Δ*bd0367* or Bd0367D63A strains. Data was collected from one biological repeat with 2 technical repeats with the mean value shown. Error bars show standard deviation Student t test was used for significance but no significance shown as only two repeats.

5.4.4. Phenotyping Bd0367D63A strain

The Bd0367D63A construct in the Δ*bd0367* strain background was isolated as a HI. The introduction of the mutated Bd0367 did not restore the predatory ability of the strain and it was not possible to grow it efficiently on *E.coli* prey cells. The reasons for the lack of effective predatory growth are investigated bellow.

5.4.5. Bd0367 D63A bdelloplast exit vs HID13

A key phenotype in the Δ*bd0367* strain was the inability to exit the *E.coli* prey cell after the lysis of the bdelloplast (Hobley et al, 2012). As the Δ*bd0367* and Bd0367D63A strain can only propagate as HIs the predation ability of this strain could only be tested as a HI. WT HI *Bdellovibrio* can still enter prey but at a lower rate than HD cells, so it was possible to test prey exit in these strains but the number of bdelloplasts formed is low due to rare entry cases due to HI nature.

My study showed the Bd0367D63A strain has a c-di-GMP levels comparable to the Δ*bd0367* strain for this reason the phenotype of bdelloplast exit was examined. Across 5 biological repeats, 92 bdelloplasts created by the Bd0367D63A HI strain were examined for progeny cell exit and no exiting was observed. Bdelloplast lysis would still occur causing the fluorescence to dissipate from prey cell but the progeny remained motionless In comparison when the wild type HID13 was presented with prey 37.5% of the 32 bdelloplasts examined resulted in progeny cells exiting the bdelloplast, this occurred approximately 1 hr after the fluorescence of the prey dissipated. The rate of successful bdelloplast exit is lower for HID13 than HD100 due to its HI nature and recent re-introduction to prey. A typical representation of bdelloplast non-exit for the Bd0367D63A strain compared to the bdelloplast exit for the HID13 strain is shown in Figure 5.7 and 5.8.

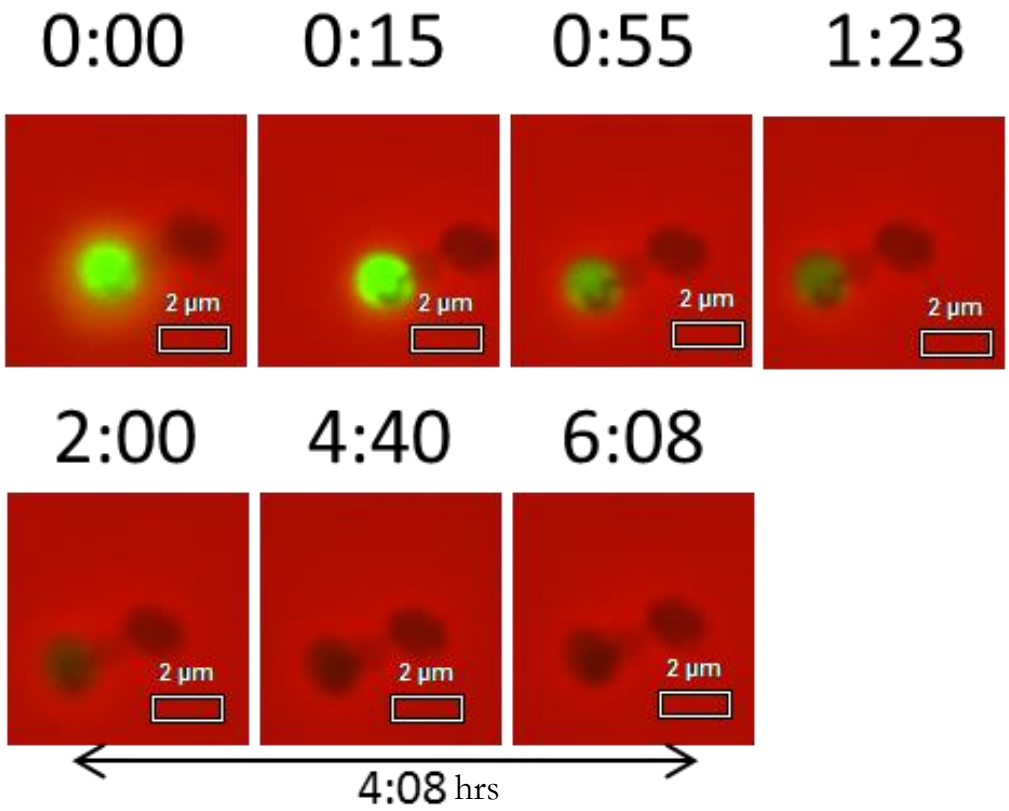

Figure 5.7 *Bdellovibrio* strain Bd0367D63A progeny do not exit the bdelloplast. This range of images is a typical representation of the process leading to prey cell lysis. Data was gathered from 92 bdelloplasts analysed over 5 biological repeats. The Bd367D63A strain grows and elongates within the cell and septates. Then the cell lyses, at this point the fluorescence from the prey dissipates (2:00) the progeny remain motionless within the empty bdelloplast for more than 4 hrs after lysis. Hr:min. 0:00 is the start of the timelapse video after 3 hrs of *Bdellovibrio* incubation with prey. Scale bar shows 2 µm. A movie of this process can be located on the USB stick attached, titled 'Bd0367D63A no bdelloplast exit' with a movie titled 'HID13 bdelloplast exit' as a comparison, further details of these movies are found in Section 8.2.2.

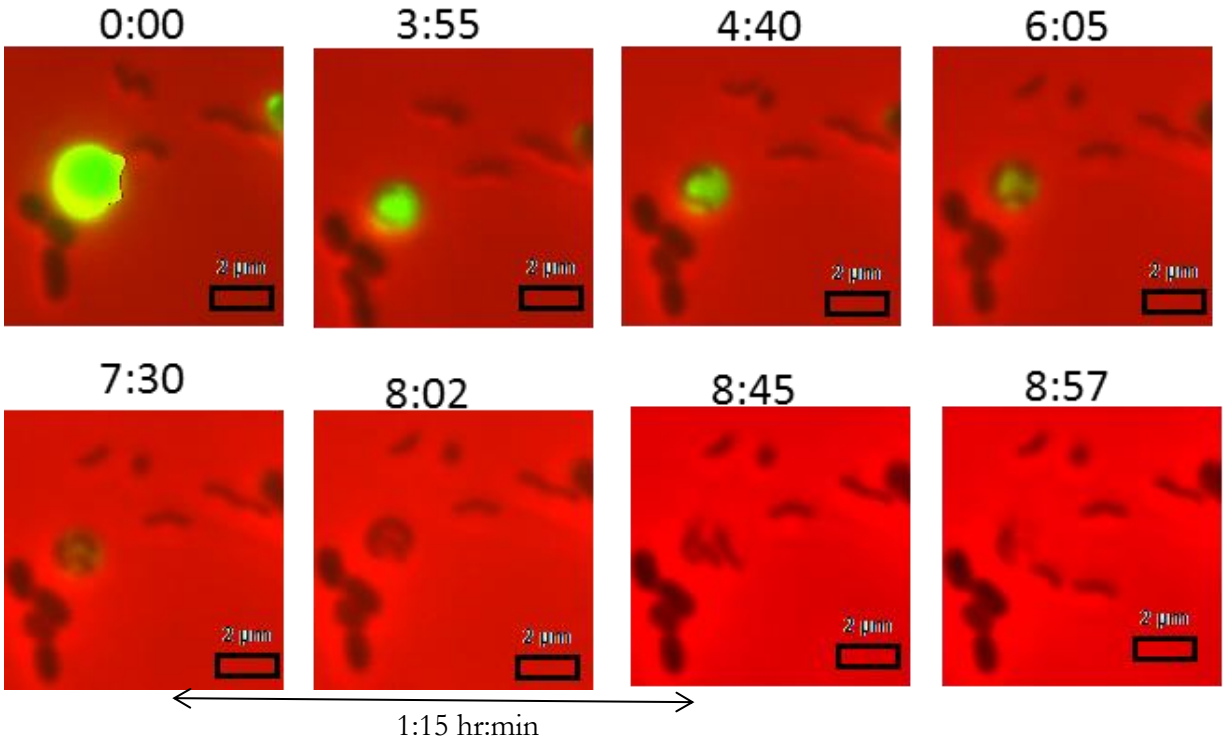

Figure 5.8 *Bdellovibrio* strain HID13 progeny exit the bdelloplast within 2hr from fluorescence dissipating. This range of images is a typical representation of the process leading to prey cell lysis and exit for 37.5% of HID13 cells across 4 biological repeats with a total of 32 bdelloplasts observed. The HID13 strain grows and elongates within the cell and septates. Then the cell lyses, at this point the fluorescence from the prey dissipates (7:30) the progeny begin moving via gliding motility and exit the bdelloplast within 1 hr and 15 minutes from cell lysis. .hr:min. 0:00 is the start of the timelapse video after 3hrs of *Bdellovibrio* incubation with prey. Scale bar shows 2 µm. A movie of this process can be located on the USB stick attached, titled 'HID13 bdelloplast exit' further details of these movies are found in Section 8.2.2.

5.4.6. Bd0367 D63A gliding motility outside prey vs HID13 gliding

As the Bd0367D63A mutant has similar c-di-GMP levels to Δ*bd0367* strain and the same inability to exit the bdelloplast, the next step was to examine the gliding ability of the Bd0367D63A strain which is separate from prey exit. Gliding motility is rarer in HI strains than in HD strains, as most (94%) HD cells will glide, however this study found that only just over 1% of wild type HID13 strains glide on surface incubation.

The analysis of gliding motility was carried out via timelapse microscopy and later video analysis.

5.4.6.1. Bd0367D63A cells can utilise gliding motility outside prey on agarose

From this analysis it was shown that 0.32% of Bd0367D63A strain HI cells can glide see Figure 5.9. This analysis studied 636 Bd0367D63A cells across 6 biological repeats an example of a Bd0367D63A cell gliding is shown in Figure 5.10. This is less frequent gliding motility than the 1.07% of HID13 cells observed gliding. This percentage resulted from analysis of 1126 HID13 cells across 4 biological repeats. However 0.32% is more frequent than the 0% observed in the Δ*bd0367* HI strain originally documented by (Hobley et al, 2012) and reconfirmed in this study by analysing 292 Δ*bd0367* cells across 2 biological repeats (data not shown). This shows that gliding motility can occur in the absence of specific c-di-GMP production from Bd0367 which suggests Bd0367 may be having an effect on gliding through another mechanism, perhaps by protein interactions. However this reduction in c-di-GMP does make gliding motility an even rarer phenotype for HI cells suggesting c-di-GMP level may be important. This also begins to suggest it is not the abolition of gliding motility causing the Bd0367D63A strain to be unable to exit the bdelloplast but another signalling or sensing mechanism, possibly monitoring bdelloplast bursting. However further observation is required to gather the sample size needed to definitively prove this.

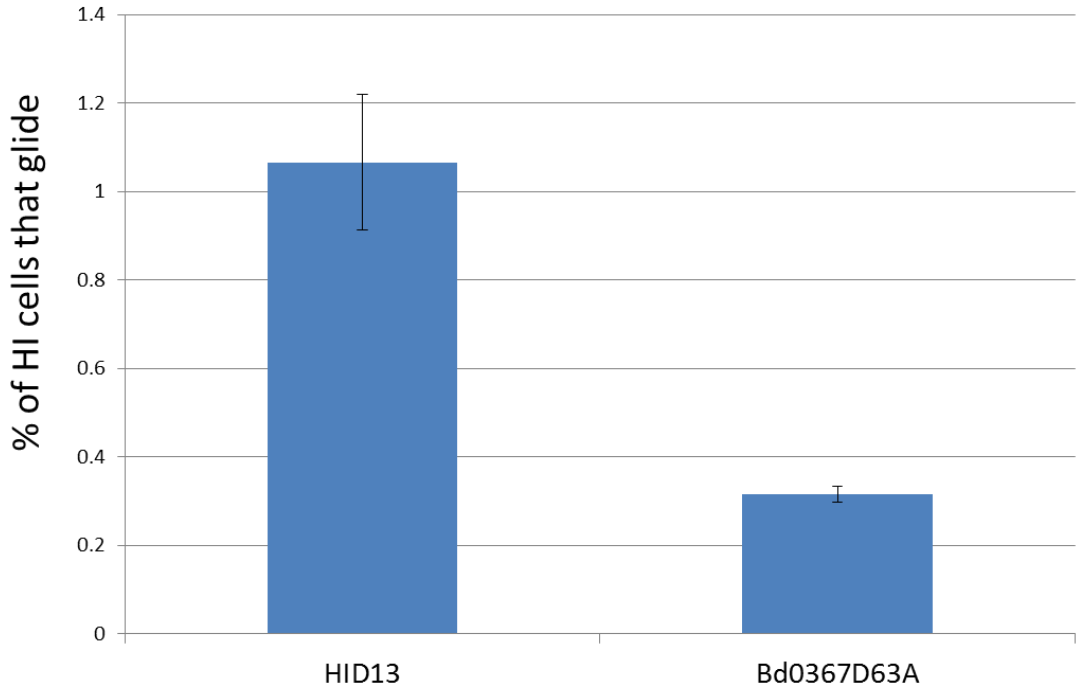

Figure 5.9 The percentage of Bd0367D63A HI cells that exhibit gliding motility. Just over 1% of HID13 cells are observed to glide. 1126 HID13 cells across 4 biological repeats were studied for signs of gliding motility. Only 0.32% of the Bd0367D63A cells

were observed to glide. 636 Bd0367D63A cells across 6 biological repeats were studied for signs of gliding motility.

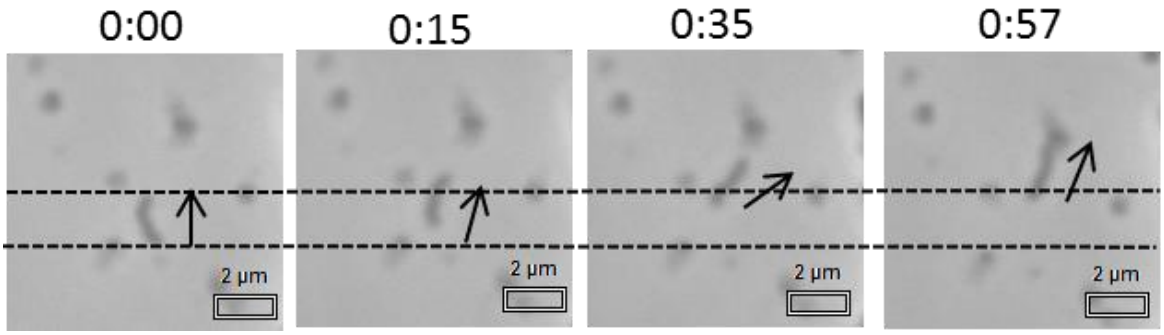

Figure 5.10 Free HI cells of strain Bd0367D63A very rarely glide. An example of this rare gliding is shown in the frames above. The gliding cell observed is between the dotted lines and the arrows represent the direction of its movement over the course of 1 hr. hr:min. scale bar 2 µm. A movie of this process can be located on the USB stick attached, titled 'Bd0367D63A gliding cell' with a movie titled 'HID13 gliding' as a comparison, further details of these movies are found in Section 8.2.2.

5.4.7. Phenotyping the Bd0367mCherry HI strain

Similar low cellular c-di-GMP levels were found in Bd0367mCherry HI cells when compared to the Δ*bd0367* and 367D63A strains. The Bd0367mCherry HI strain had an 88% reduction in c-di-GMP production when compared to wild type HID13 and ~3.5% more c-di-GMP than the Δ*bd0367* strain. In these other two strains bdelloplast exit and gliding motility were abolished or impaired, for this reason these phenotypes were examined in the Bd0367mCherry HI cells.

5.4.8. Bd0367mCherry HI strain bdelloplast exit vs HID13

Bd0367mCherry HI has lower than HID13 level of c-di-GMP but a higher level than Δ*bd0367* or Bd0367D63A, the effect of this slightly higher level of c-di-GMP was investigated by examining the Bd0367mCherry HI bdelloplast exit phenotype. In HID13 37.5% of the 32 bdelloplasts examined resulted in progeny successfully cells exiting whereas the Bd0367mCherry strain is different from the Δ*bd0367* and Bd0367D63A strain with 24.75% of the 101 bdelloplasts observed resulting in successful progeny exit see Figure 5.11 and 5.12.

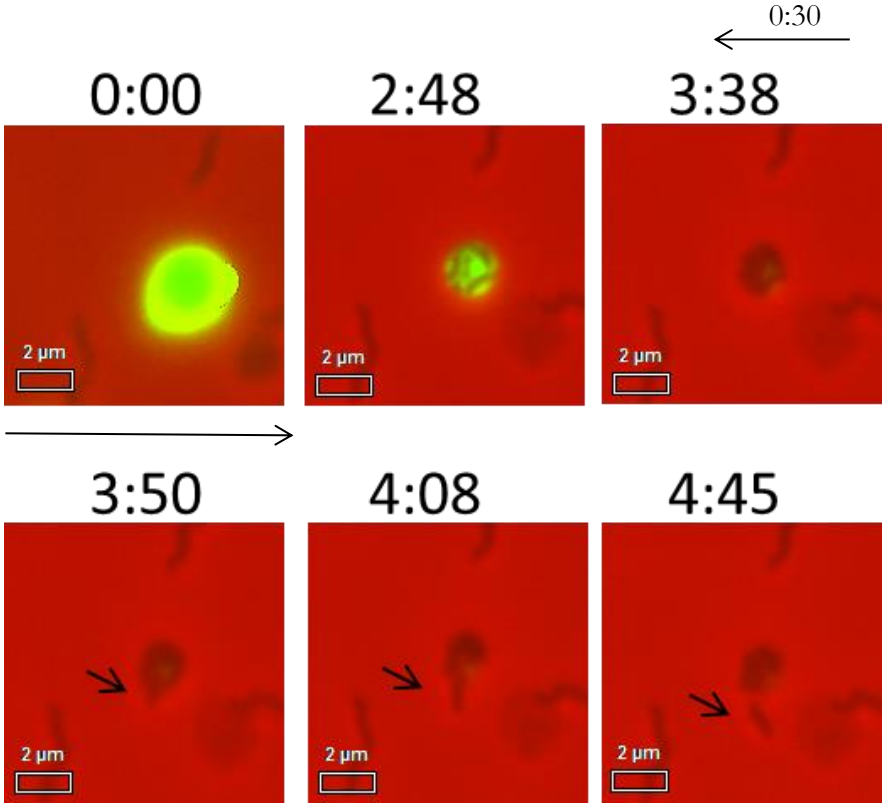

Figure 5.11 *Bdellovibrio* strain Bd0367mCherry (HI) progeny exit the bdelloplast with in 1hr. This range of images is a typical representation of the process leading to prey cell lysis and exit for 24.75% of Bd0367mCherry HI cells across 3 biological repeats observing a total of 101 bdelloplasts. The Bd0367mCherry strain grows and elongates within the cell and septates. Then the cell lyses, at this point the fluorescence from the prey dissipates (3:38) the progeny begin moving via gliding motility and exit the bdelloplast within 1 hr from cell lysis. Hr:min. Black arrow shows the first progeny cell to glide out of bdelloplast. A movie of this process can be located on the USB stick attached, titled 'Bd0367mCherry HI bdelloplast exit and cells gliding' with a movie titled 'HID13 bdelloplast exit' as a comparison, further details of these movies are found in Section 8.2.2.

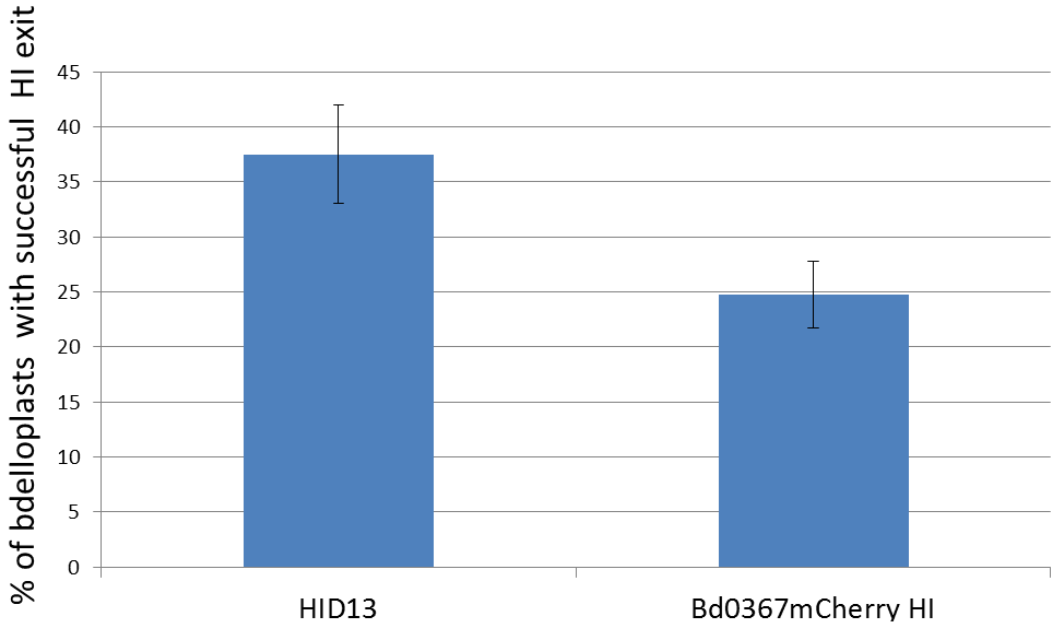

Figure 5.12 Bd0367mCherry HI progeny have only mildly impaired bdelloplast exit. The Bd0367mCherry HI strain shows that when Bd0367 is present with a mCherry tag bdelloplast exit can occur. However exit is not fully restored to WT levels. 37.5% bdelloplasts formed by HID13 result in successful exit of progeny cells. This was a total of 32 bdelloplasts observed across 4 biological repeats. 24.75% bdelloplasts formed by Bd0367mCherryHI result in successful exit of progeny cells. This was found from observing a total of 101 bdelloplasts observed across 3 biological repeats. Error bars represent 95% confidence interval.

5.4.9. Bd0367mCherry HI strain glides more frequently than HID13

Observation of the Bd0367mCherry strain gliding out of prey bdelloplasts suggests that Bd0367mCherry strain can glide. However the frequency of gliding motility in this strain when HI cells were incubated on a surface without prey still needed to be determined. Examination of Bd0367mCherry gliding frequency showed that 34.2% of the cells observed could glide see Figure 5.14 . This is significantly higher than the ~1% of HID13 cells that can glide. This provides more evidence that gliding motility in *Bdellovibrio* is effected by Bd0367. Reasons for this alteration in gliding frequency will be discussed in Section 5.5.7.

The analysis of gliding motility was carried out via timelapse microscopy and later video analysis, a Figure of a gliding Bd0367mCherry HI cell is shown in Figure 5.13.

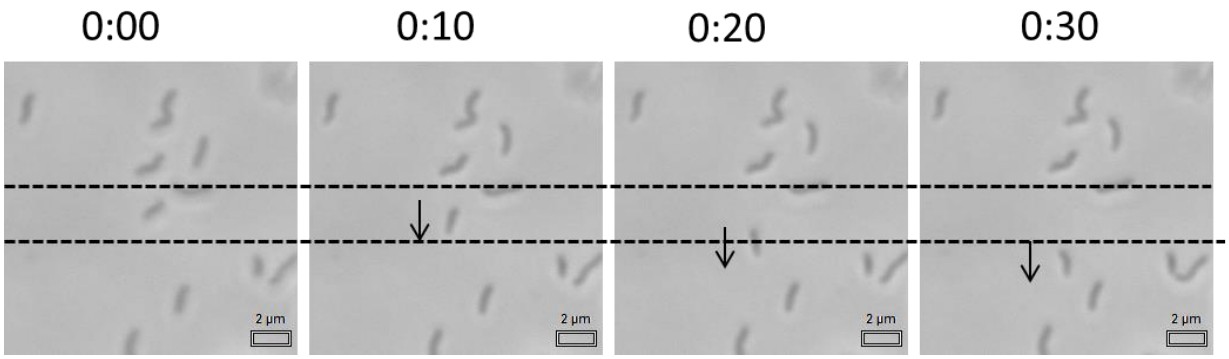

Figure 5.13 HI cells of strain Bd0367mCherry glide more frequently than HID13 WT. An example of this frequent gliding is shown in the frames above. The gliding cell observed is between the dotted lines and the arrows represent the direction of its movement over the course of 30 min. hr:min. scale bar 2 µm. A movie of this process can be located on the USB stick attached, titled 'Bd0367mCherry HI bdelloplast exit and cells gliding' with a movie titled 'HID13 gliding' as a comparison, further details of these movies are found in Section 8.2.2.

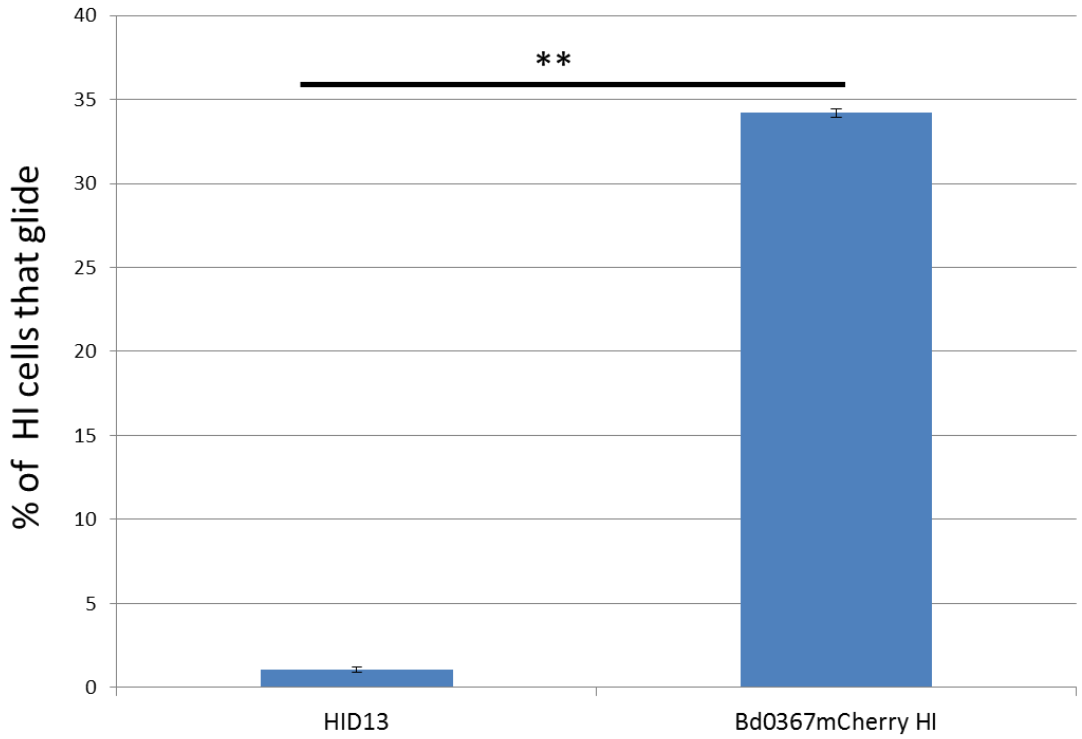

Figure 5.14 A higher percentage of Bd0367mCherry HI cells glide in comparison to HID13. Just over 1% of HID13 cells are observed to glide. 1126 HID13 cells across 4 biological repeats were studied for signs of gliding motility. Whereas 34.2% of the Bd0367mCherry HI cells observed were seen to glide. A total of 538 Bd0367mCherry HI cells were observed across 3 biological repeats. Error bars represent 95% confidence interval. Asterisks show values of the Student t-test **≤0.01.

5.4.10. Investigating the effect of a global increase in cellular c-di-GMP on gliding motility in *Bdellovibrio*

The results above continue to suggest that DGC protein Bd0367 is involved in gliding motility in *Bdellovibrio*. However the gliding phenotypes of the 3 HI strains Δ*bd0367*, Bd0367D63A and Bd0367mCherry are all different despite having similar c-di-GMP levels. This is interesting as c-di-GMP levels have regularly been linked with motility phenotypes in other bacteria (Romling et al, 2013). It appears Bd0367 may have a role in gliding motility which is independent of its enzymatic DGC role, so another method of studying the effect of c-di-GMP levels on *Bdellovibrio* gliding was investigated.

This method involved silently deleting and mutating PDE protein Bd1971 (cloned by Rob Till for this study). This gene was selected as previous work on the Kan Δ*bd1971* strain suggested that cellular c-di-GMP levels increase significantly upon its deletion (Basford, 2015). This large global increase in cellular c-di-GMP would allow investigation into the effect of varied c-di-GMP levels on *Bdellovibrio* gliding motility.

The selection of Bd1971 also provided the opportunity to attempt to characterise the role of the Bd0367-Bd1971 interaction described in Chapter 3. This was done by creating an enzymatically inactive Bd1971 protein through mutating D307 and D308 to alanine see figure 5.15. Bd1971 has been worked on structurally by our collaborator at the University of Birmingham, Dr Andy Lovering. He suggested this D307308A mutation in Bd1971 as he predicted it would inactivate the EAL function of Bd1971. This strain was cloned by Rob Till and quantified and phenotyped by me for this study. This mutation was made independently to the Δ*bd1971* strains and double crossed over strains were selected for, so this mutation is present without Kan selection. This mutant was originally created in the HD life style, and was then additionally generated as a HI strain.

Figure 5.15 CDD analysis of EAL domain of Bd1971 showing the 307 308 Ds which were mutated and the proximity to the EAL residues (at 370-372) (Marchler-Bauer et al, 2015).

Using these two strains allowed for the phenotypic comparison of high global c-di-GMP levels in the presence and absence of Bd1971 to identify if gliding motility was regulated by potential Bd0367-Bd1971 multiprotein complexes/trigger enzyme or by the global cellular c-di-GMP level.

The c-di-GMP level of Δ*bd1971* EAL silent deletion and mutation strains was quantified by Dr Chen at Michigan University and the gliding phenotype of these strains with elevated global c-di-GMP levels were observed and described in the following sections.

5.4.11. Assessing the c-di-GMP levels in the Bd1971 deletion and mutation strains in comparison to wildtype HI and HD strains

The silent Δ*bd1971* strain and Bd1971D307308A double cross over strain were obtained in the HD lifestyle by Rob Till. These strains were then also generated as HI strains by myself and Rob Till. The ability to grow in both lifestyles provided the opportunity to measure c-di-GMP levels in both the HI and HD lifestyles.

For the HI strain experiment 1 biological repeat was examined this consisted of two independent isolates for each strain, which were grown and maintained in parallel in the same conditions. These strains were then grown overnight in a 10 ml culture to an OD_{600} of 0.6, pelleted by centrifugation and these pellets were resuspended in extraction buffer and processed as in the Bobrov method to extract the c-di-GMP from the pellet (see 2.15 methods).

For the HD strain experiment 1 biological repeat was examined this consisted of two independent isolates for each strain, which were grown and maintained in parallel in the same conditions. These strains were then grown over night in multiple concentrated 50 ml predatory cultures, in order to have sufficient cell mass, these cultures were then filtered to remove residual *E. coli* and pelleted by centrifugation. These pellets were then resuspended in extraction buffer and processed as in the Bobrov method to extract the c-di-GMP from the pellet (Bobrov et al, 2011)(see Methods 2.15).

Both HI and HD control strains examined here resulted in similar pellet weights as shown in Figure 5.16 from using the liquid growth conditions described above and did

not differ significantly in the relative levels of c-di-GMP extracted for this biological repeat between HI and HD controls, Figure 5.17.

However there are differences between the two distinct lifestyles that potentially result in differing quantities of c-di-GMP being extracted with differing variation. Most notably are the varied morphologies of the HI strain compared to the synchronous HD culture this is discussed in more detail in section 5.5.3.

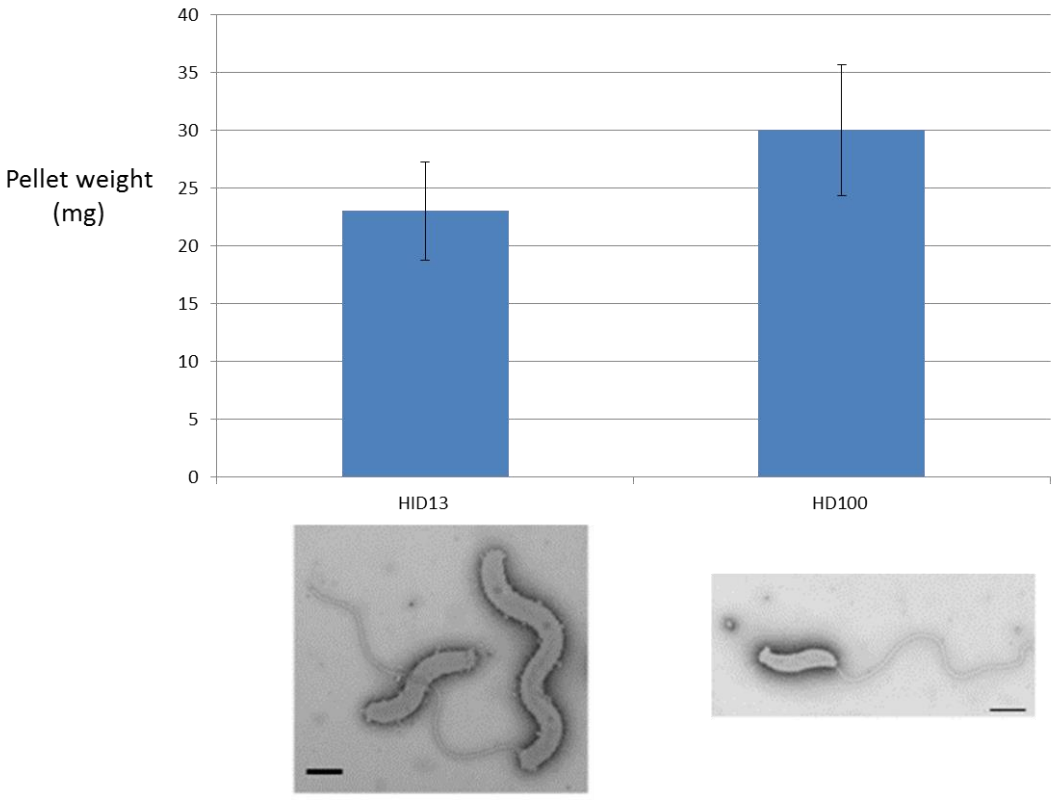

Figure 5.16 Mean pellet weights obtained for HID13 and HD100 c-di-GMP extractions were not significantly different. This also shows the difference in morphology between these two cell types. The HI cell is a Δ*bd3125* HI strain with typical HI morphology, the HD cell is HD100, these images are from (Hobley et al, 2012). The cells were stained with 1% PTA (pH 7.0), scale bars = 0.5 μm.

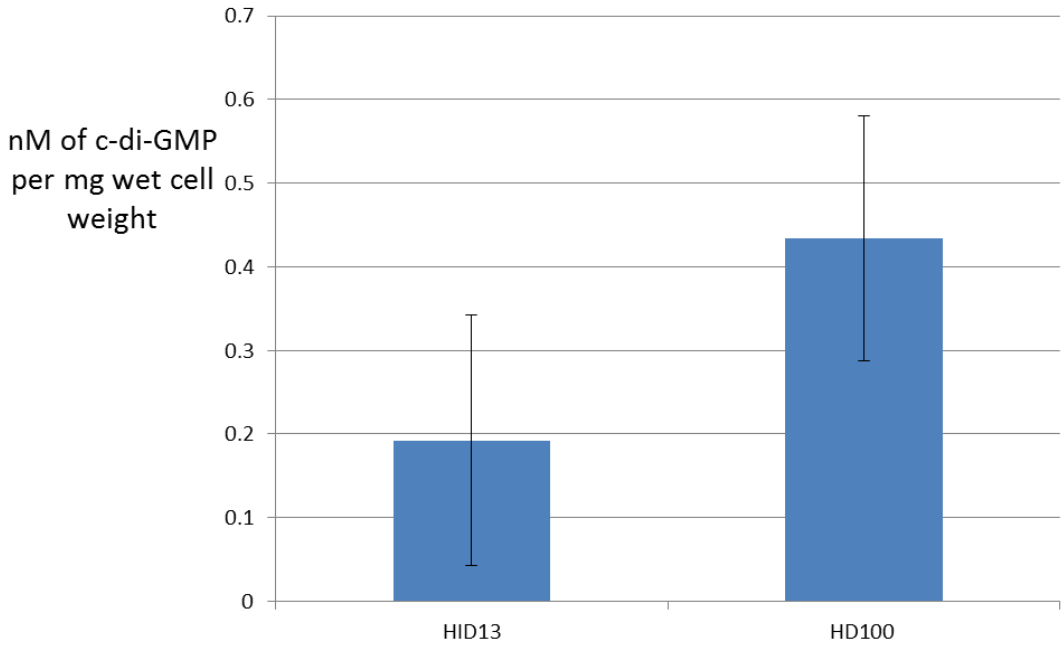

Figure 5.17 The relative c-di-GMP levels extracted from HID13 and HD100 cells in this biological repeat were not significantly different. The HID13 strain in this example has a slightly lower mean c-di-GMP level than the HD100 culture.

These samples were sent for analysis at RTSF Mass Spectrometry & Metabolomics Core at Michigan State University by Dr Lijun Chen and the nM concentration of c-di-GMP was determined for each strain by HPLC.

5.4.11.1. Cellular c-di-GMP levels are higher in *Δbd1971* and Bd1971D307308A HI strains than WT control

Results from the c-di-GMP extraction of the HI strains showed that Δ*bd1971* and Bd1971D307308A HI strains had approximately 200% more c-di-GMP extracted from the cell pellets than HID13. This suggests that in these strains the loss of Bd1971 as a PDE resulted in a higher than wild type level of cellular c-di-GMP.

The nM of c-di-GMP per mg wet cell weight for HID13 is lower than previously reported in this study (Section 5.4.3) so is not comparable to the levels assessed for Bd0367 strains. However the percentage change shows that under these biological conditions there was more c-di-GMP present in the mutant strains compared to HID13.

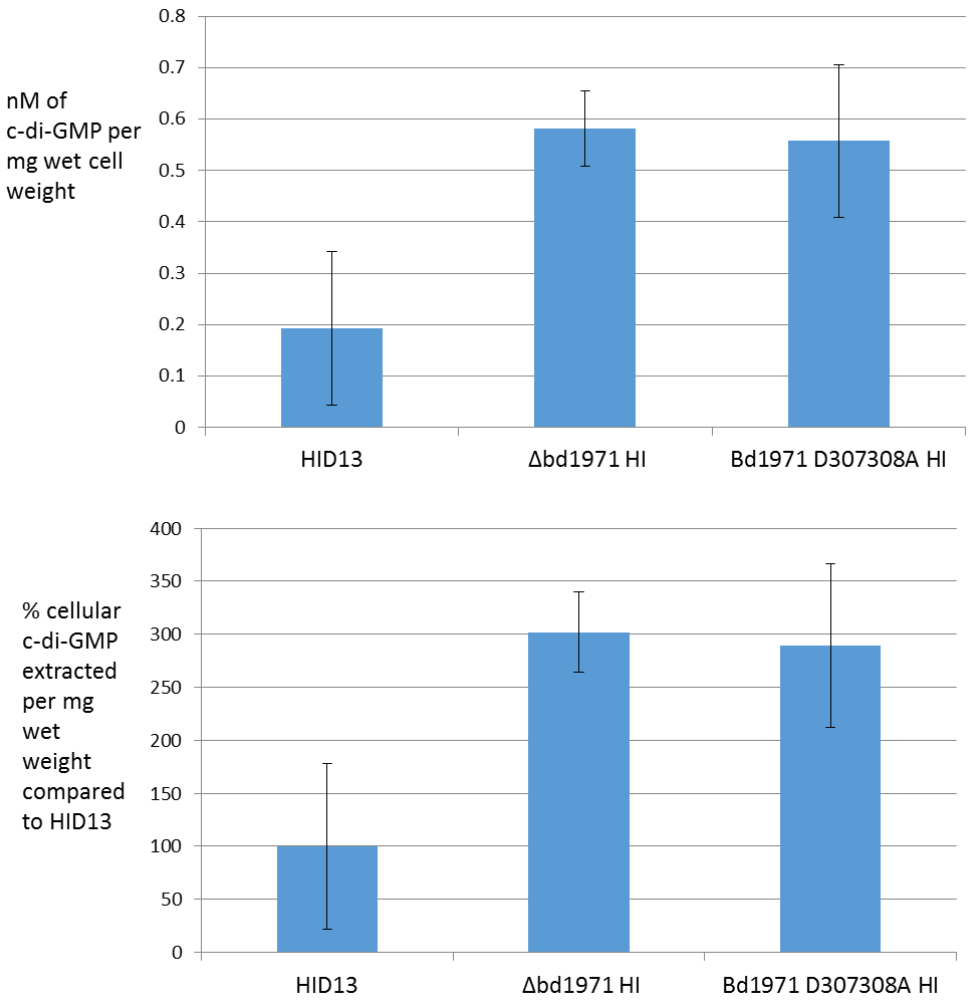

Figure 5.18 *Δbd1971* and Bd1971D307308A HI strains had higher mean c-di-GMP levels than the wildtype control. The HID13 cells contained ~200% less c-di-GMP per mg wet cell weight than both Δ*bd1971* and Bd1971D307308A HI cells when grown in liquid culture. Data was collected from one biological repeat with 2 technical repeats Error bars show standard deviation. Student t test was used for significance but is not included due to only two repeats.

5.4.11.2. Cellular c-di-GMP levels are higher in *Δbd1971* and Bd1971D307308A HD strains than the HD100 control

Results from the c-di-GMP extraction of the HD strains showed that Δ*bd1971* and Bd1971D307308A HD strains had more c-di-GMP extracted from these cell pellets than HD100 pellets. Δ*bd1971* had approximately 100% more c-di-GMP extracted than HD100 and interestingly Bd1971D307308A had over 400% more c-di-GMP extracted when compared to HD100. This is interesting and suggests that in the HD lifestyle the Bd1971 protein may be having a function independent to its enzymatic function that is stimulating c-di-GMP production. As in the Bd1971D307308A strain the protein is

present but inactive as a PDE and this has a greater effect on increasing the cellular c-di-GMP levels than removing Bd1971 as in the Δ*bd1971* strain.

This is the first study that has achieved a mean value with a small standard deviation for the c-di-GMP level of HD100, due to new pellet preparation (see methods 2.15). This work needs to be repeated to confirm that the nM of c-di-GMP per mg wet cell weight for HD100 is consistent across multiple biological repeats.

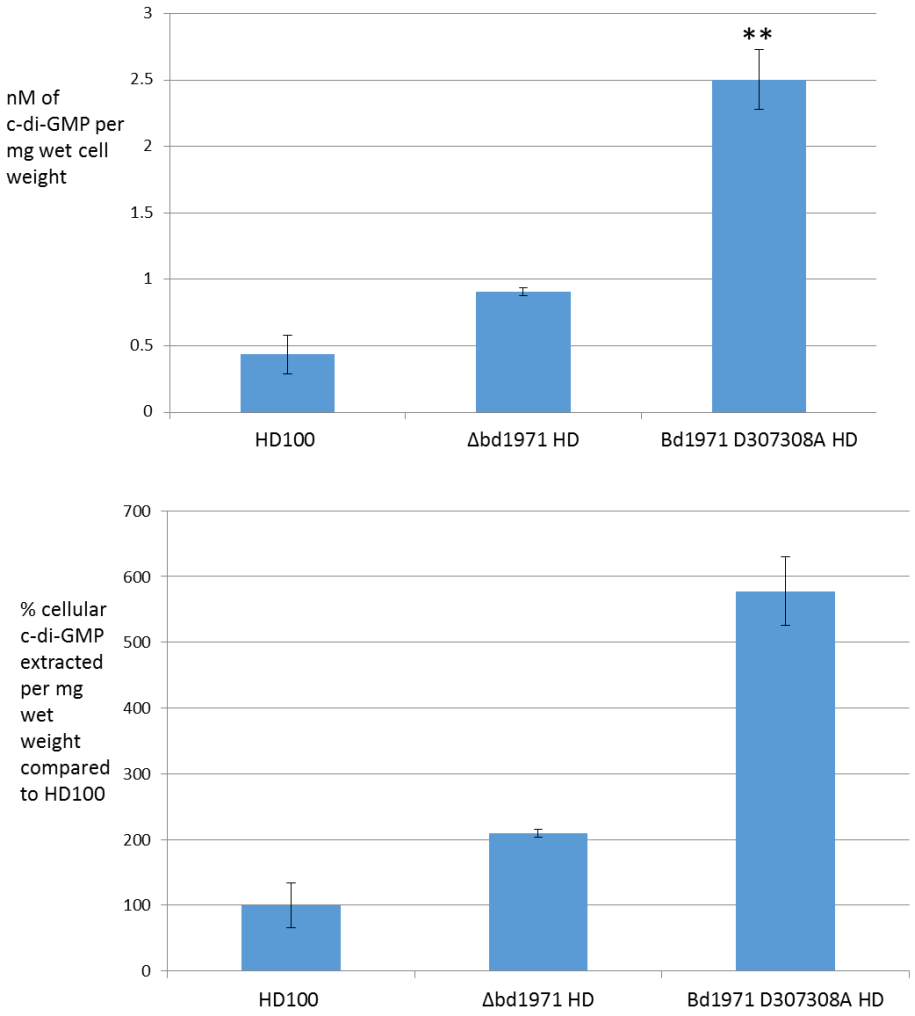

Figure 5.19*Δbd1971* and Bd1971D307308A HD strains had higher mean c-di-GMP levels than the HD100 control. The HD100 cells contained ~100% less c-di-GMP per mg wet cell weight for Δ*bd1971* and 400% less for Bd1971D307308A HD cells. Data was collected from one biological repeat with 2 technical repeats Error bars show standard deviation. Student t test was used for significance. **≤0.01

5.4.12. Investigating gliding motility in the *B. bacteriovorus Δbd1971* strain

A different gliding phenotype to WT was postulated in the Δ*bd1971* strain despite the Bd1971mCherry strain showing no significant difference in fluorescent intensity or location of fluorescence on surface incubation. It has been shown in this study that the silent deletion strain Δ*bd1971* has higher than WT levels of c-di-GMP in HD and HI strains due to the loss of the PDE activity of this protein. Levels of c-di-GMP have proven important in motility for many bacteria, with high c-di-GMP normally being associated with biofilm like behaviour and low c-di-GMP being associated with increased motility (Romling et al, 2013). The effect of high c-di-GMP levels on gliding motility in *B. bacteriovorus* are investigated here.

Additionally in *B. bacteriovorus* the lack of DGC protein Bd0367 results in HI cells that cannot glide. As Bd0367 and Bd1971 are predicted to be part of an interaction network (see Chapter 3) it is possible that Bd1971 interacts with Bd0367 to regulate gliding motility in *B. bacteriovorus*, and this regulation could occur through protein interactions and forming multiprotein complexes rather than by altering cellular c-di-GMP levels.

5.4.12.1. The percentage of *B. bacteriovorus Δbd1971* attack phase cells that glided was less than in WT HD100

The Δ*bd1971* strain was obtained as a HD strain and the following gliding motility experiments were carried out in the HD lifestyle.

When observing HD100 attack phase cells glide it was apparent that almost 100% of the cells will glide within a 6 hr video with most of these cells demonstrating gliding motility within the first 120 minutes. The reasons for the 6% of HD100 cells that do not glide could be due to a number of reasons such as these cells possibly being dead or represent some heterogeneity in the population. Initial observation of the attack phase *B. bacteriovorus* Δ*bd1971* strain via microscopy showed a noticeable difference in the percentage of cells able to glide under the standard conditions tested. When the time-lapse microscopy videos were analysed it showed that only 34% of Δ*bd1971* cells could glide. See Figure 5.20. This result suggests that Bd1971 or regulated c-di-GMP levels are necessary for a part of the gliding motility process. Currently there is no complementation strain to ensure that gliding levels are restored to WT levels on reintroduction of Bd1971.

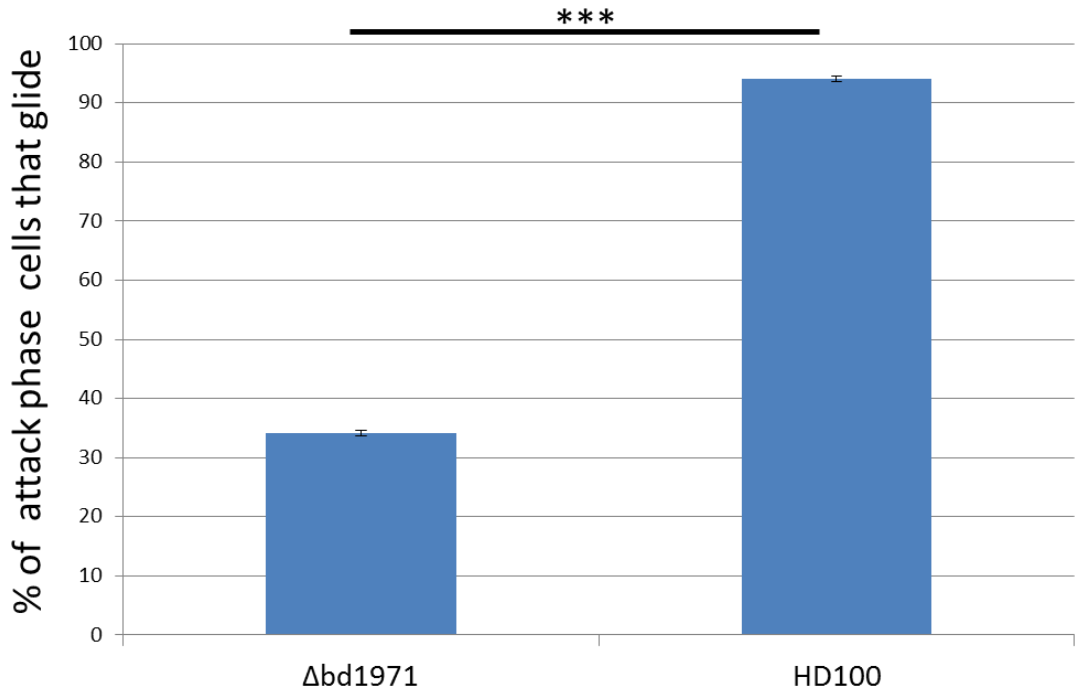

Figure 5.20 Only 34% of *B. bacteriovorus Δbd1971* attack phase cell can glide under standard conditions. The data are obtained from three biological repeats with the total number of cell observed for gliding or no gliding being 232 HD100 cells and 126 Δ*bd1971* cells. Error bars represent 95% confidence interval. Asterisks show values of the Student t-test ***≤0.001. A movie of this process can be located on the USB stick attached, titled 'Bd1971 gene deletion gliding' with a movie titled 'HD100 gliding' as a comparison, further details of these movies are found in Section 8.2.2.

5.4.12.2. The *B. bacteriovorus Δbd1971* cells that glide took longer to initiate gliding motility compared to wild type cells

The differences in gliding motility between HD100 and Δ*bd1971* cells were further investigated by studying the time taken from placement on a surface to gliding initiation. This measurement is taken as the time taken from application of cells on a surface to the cells first movement using gliding motility observed via time-lapse microscopy. Of the 34% of Δ*bd1971* cells that can glide, the start times showed that the mean gliding start time was significantly longer, over an hour later than WT HD100 cells, Figure 5.21. There is currently no complemented Δ*bd1971* strain to test if this strain would have restored WT gliding start times.

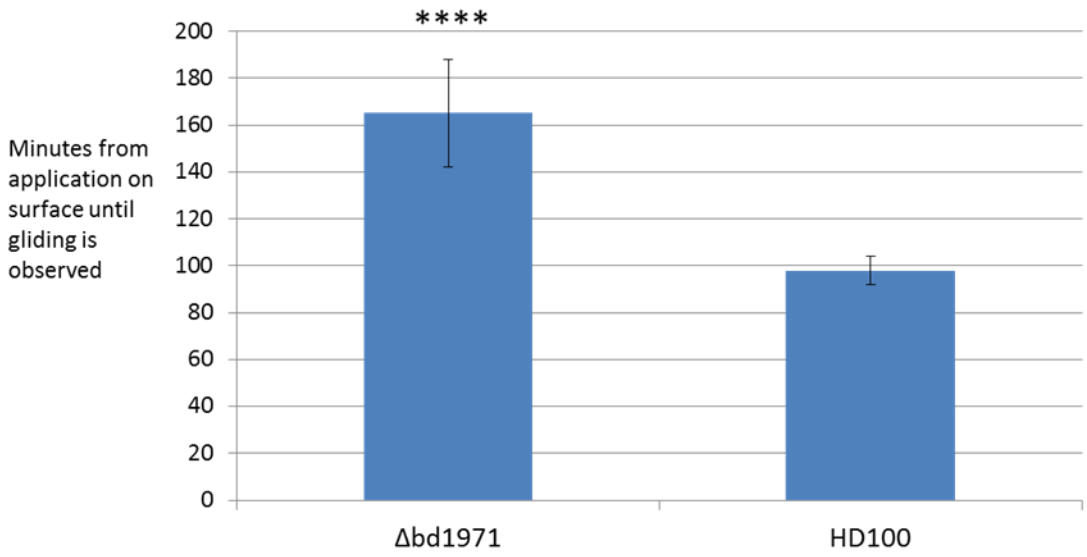

Figure 5.21 *B. bacteriovorus Δbd1971* attack phase cells took significantly longer to initiate gliding motility compared to wild type cell. The data was obtained from three biological repeats with the means from a total of 43 Δ*bd1971* cells and 116 HD100 wild type cells. Error bars represent 95% confidence interval. Asterisks show values of the Student t-test ****≤0.0001.

5.4.13. Investigating gliding motility in the *B. bacteriovorus* Bd1971 D307308A HD strain

Due to the aberrant gliding phenotype observed in the HD Δ*bd1971* strain the gliding phenotype of attack phase HD Bd1971D307308A strain was also investigated.

5.4.13.1. The percentage of *B. bacteriovorus* Bd1971D307308A attack phase cells that glided was less than in WT HD100

Initial observation of the *B. bacteriovorus* Bd1971D307308A strain via phase contrast timelapse microscopy showed a noticeable difference in the percentage of cells able to glide under the standard conditions tested (Section 2.7.4) when compared to WT HD100. When the time-lapse microscopy videos were analysed it showed that only 47% of Bd1971D307308 cells could glide within 6 hrs, Figure 5.22. This is much lower than seen for WT HD100 (94%) and slightly higher than observed for Δ*bd1971* (34%). This suggests that even when Bd1971 is present to interact with Bd0367 the high global c-di-GMP level caused by non-functioning of the EAL domain impairs the cells ability to glide.

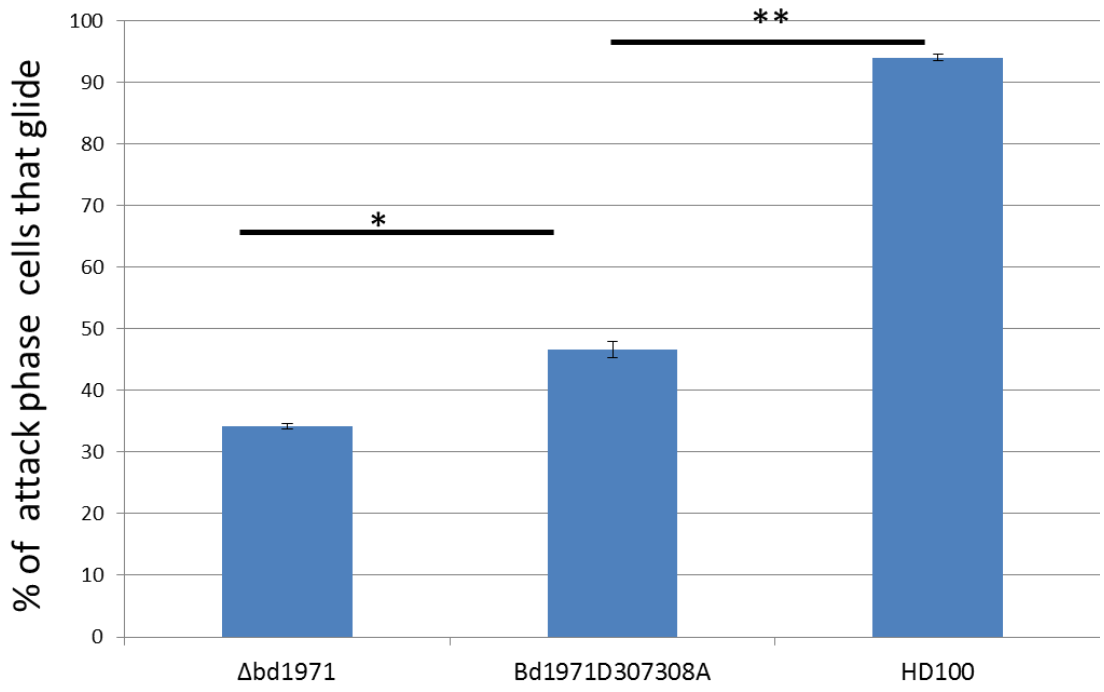

Figure 5.22 Only 47% of Bd1971D307308A attack phase cells can glide under standard conditions compared to 34% of *B. bacteriovorus* Δ*bd1971* attack phase cells and 94% of HD100 cells. The data are obtained from three biological repeats with the total number of cell observed gliding or not gliding being 346 Bd1971D307308A, 232 HD100 cells and 126 Δ*bd1971* cells. Error bars represent 95% confidence interval. Asterisks show values of the Student t-test *≤0.05 between Δ*bd1971* and Bd1971D307308A. A movie of this process can be located on the USB stick attached, titled 'Bd1971 D307308A HD gliding' with a movie titled 'HD100 gliding' as a comparison, further details of these movies are found in Section 8.2.2

5.4.13.2. The *B. bacteriovorus* Bd1971 D307308A cells that did glide took longer to initiate gliding motility compared to wild type cells

The differences in gliding motility between HD100 and Bd1971D307308 cells were further investigated by studying the time taken from placement on a 1% agarose CaHEPES surface to gliding initiation. This measurement is taken as the time taken from application of attack phase cells on a surface to the cells first movement using gliding motility observed via time-lapse microscopy. A sample of the Bd1971D307308A cells that could glide were analysed, the start times measured showed that the mean gliding start time was significantly longer, over an hour later than WT HD100 cells, Figure 5.23. The Bd1971D307308A strain gliding start time was not significantly different from the Δ*bd1971* strain. This suggests that gliding start time is influenced by the high global c-di-GMP level and not by the protein interaction between Bd1971 and Bd0367.

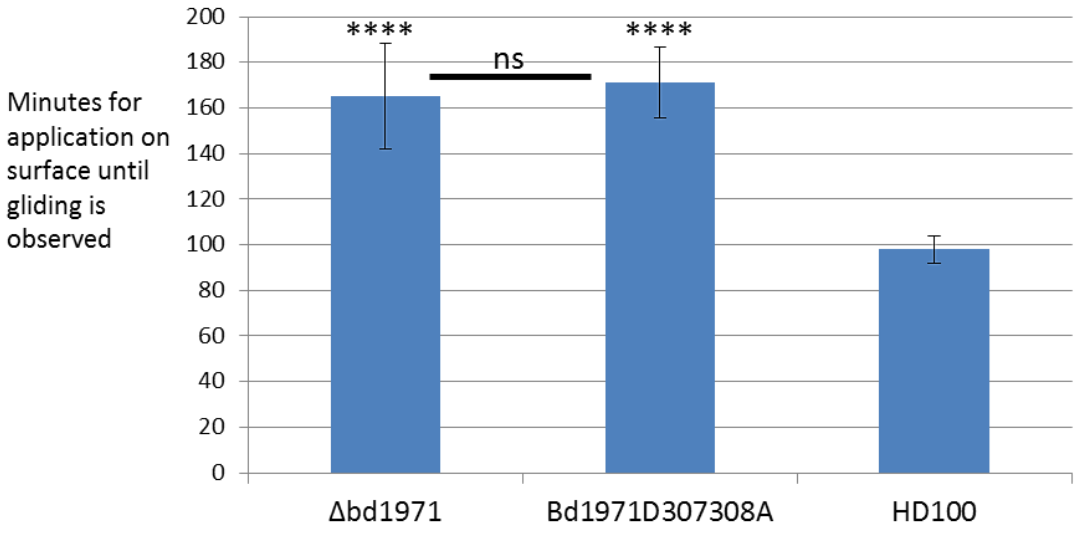

Figure 5.23 *B. bacteriovorus* Bd1971D307308A attack phase cells took significantly longer to initiate gliding motility compared to WT HD100. However the gliding start times of Bd1971D307308A and Δ*bd1971* attack phase cells was not significantly different.. The data was obtained from three biological repeats with the means from a total of 57 Bd1971D307308A, 43 Δ*bd1971* cells and 116 HD100 wild type cells. Error bars represent 95% confidence interval. Asterisks show values of the Student t-test ****≤0.0001.

In summary the Bd1971D307308A strain displays an aberrant gliding phenotype which is not significantly different from the phenotype displayed by Δ*bd1971*. This suggests that high cellular c-di-GMP levels are causing the abnormal gliding phenotype. The possible mechanisms for high c-di-GMP levels mediating reduced gliding motility phenotype will be discussed in Section 5.5.7.

5.4.14. Investigating expression of Bd0367mCherry in the *B. bacteriovorus Δbd1971* strain

Various results collected in this study such as: the B2H interaction between Bd1971 and Bd0367 (Chapter 3), the importance of the Bd0367 protein in gliding motility and the altered gliding phenotype of the Δ*bd1971* led to the investigation of the distribution of Bd0367mCherry in the background of Δ*bd1971* strain which has a elevated cellular c-di-GMP level due to EAL gene deletion. The Bd0367mCherry was conjugated into the Δ*bd1971* strain as a single cross over and the distribution of Bd0367mCherry was compared to the distribution of Bd0367mCherry fluorescence in WT HD100 attack phase cells previously analysed in Section 5.4.1.2.

5.4.14.1. Bd0367mCherry expression level is altered when expressed in the *Δbd1971* HD strain

The distribution of Bd0367mCherry in WT attack phase cells after 0 minutes on a surface was 79% diffuse throughout the cell, 15% bi-polar and 6% mono-polar. Interestingly in the Δ*bd1971*::bd0367mCherry strain there was a pronounced decrease in the percentage of cells that had Bd0367mCherry located throughout the cytoplasm. This decrease was due to the appearance of previously absent 'dark cells', where very low levels of Bd0367mCherry was present, these types of cells were not observed in the HD100::bd0367mCherry strain. This population of 'dark' cells is made up of approximately half of the Δ*bd1971*::bd0367mCherry cell population that was previously described as diffuse throughout fluorescence which is approximately 40% of the total cell population, Figure 5.24. The reasons for this reduction in Bd0367mCherry expression in a proportion of Δ*bd1971* cells will be discussed in Section 5.5.8.3. However it did appear possible that the 37% of dark cells may correspond to the 34% of Δ*bd1971* cells that can glide seen in Section 5.4.12.1. so this was tested for.

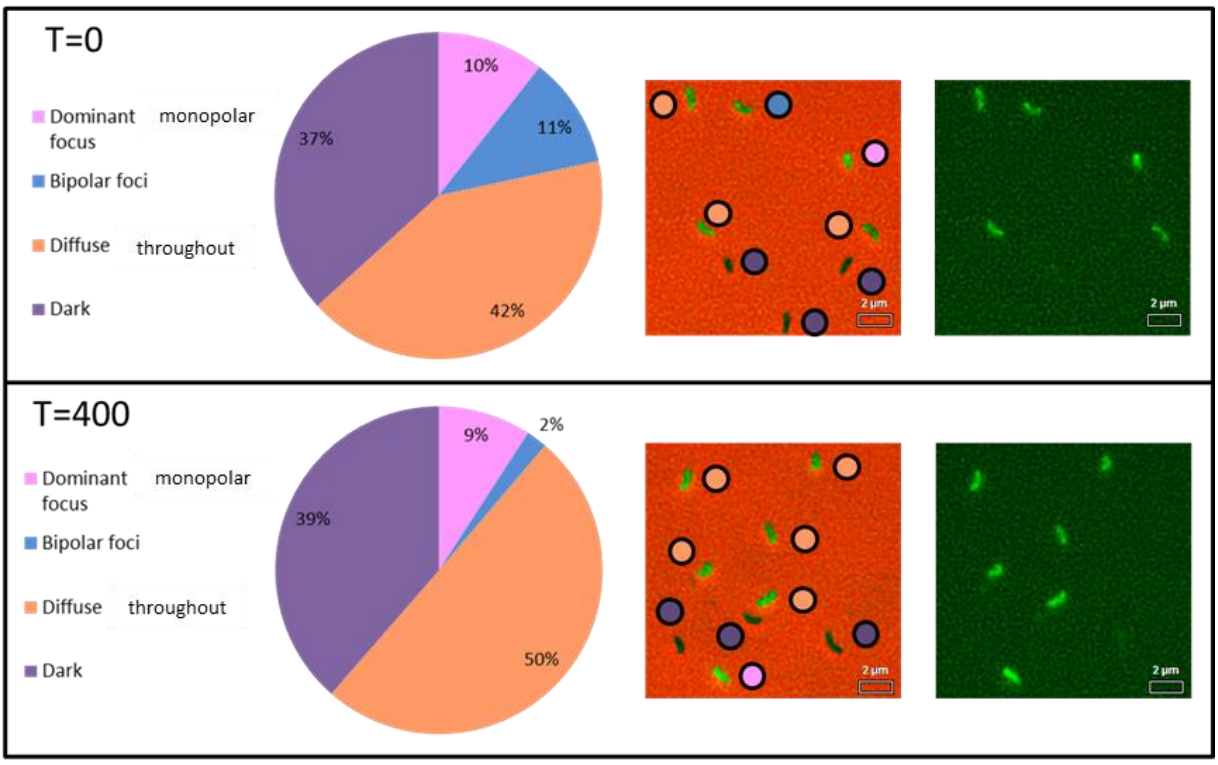

Figure 5.24 Bd0367mCherry expression in *Δbd1971* attack phase cells changes compared to HD100. The pie charts show the % distribution of different fluorescent locations at T0 and T400. To demonstrate this visually the location of fluorescence in the cell (dominant monopolar, bipolar, diffuse or dark) is highlighted by a dot of colour next to the cell which indicates which section of the pie chart this cell is representative of. The cells were placed on 1% CaHEPES agarose slide and images were collected at time 0 and time 400 min. during this time the slide was kept hydrated and at room temperature of 25. The panel of images shows time 0 at the top and time 400 minutes below. The panels on the right show example categories from merged channel and fluorescence channel. A combined total of 982 cells were analysed at T0 and 1082 cells at T400, from images obtained from three biological repeats each with three technical repeats.

5.4.14.2. The majority of *Δbd1971*::Bd0367mCherry attack phase cells that glide are expressing a significantly lower level of Bd0367mCherry

In this study a small number of gliding Δ*bd1971*::Bd0367mCherry attack phase cells were observed gliding via timelapse microscopy and fluorescent microscopy. This involved brightfield time-lapse microscopy to investigate gliding paired with fluorescence microscopy to look at the location of fluorescence during gliding motility. Fluorescent microscopy could not be used continually for this gliding analysis due to bleaching of mCherry. Cells were incubated on the surface (for 400 min) so that gliding had time to initiate then a region of cells was picked and imaged by fluorescence microscopy to have an initial record of the fluorescent location. Immediately bright field time-lapse

microscopy was used to capture timelapse movies of the gliding of the cells. The video was run for 30 minutes in only bright field illumination and another fluorescent image was captured of the region at the end an example of video shown in Figure 5.25.

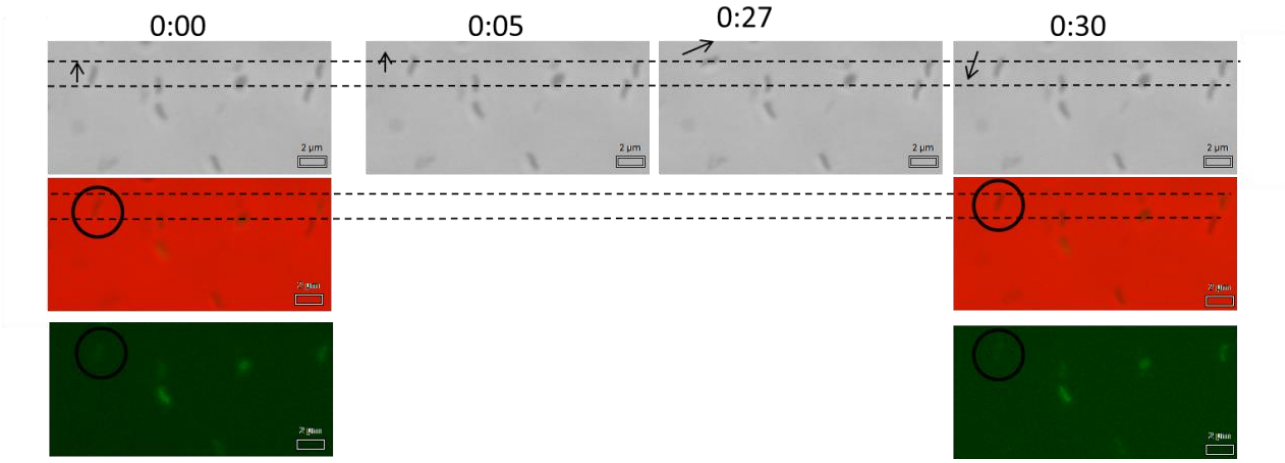

Figure 5.25 An example of a single *Δbd1971*::bd0367mCherry cells that glides with low level fluorescence. The actively gliding cell is circled, showing merged and fluorescent channels. Movement of the cell on 1% agarose CaHEPES is monitored by its position between the dotted line. The image shows that the cell has low fluorescence and glides over the 30 min period shown with no change in fluorescence intensity. Hr:min. 2 μm scale

This showed the location and quantity of Bd0367mCherry in actively gliding cells. Across 3 biological repeats a total of 16 cells were observed gliding, the average fluorescent intensity of actively gliding cells was quantified as 2062.7 by SimplePCI net total green measurements (see Methods 2.7.6). The cells that were not seen to demonstrate gliding had brighter average net fluorescence of 8151.3. This suggests that actively gliding cells have mean of 3.95 fold less Bd0367mCherry present than stationary cells see Figure 5.2.6.

This suggests that when Bd0367 is at low levels in the high cellular c-di-GMP Δ*bd1971* strain gliding is possible.

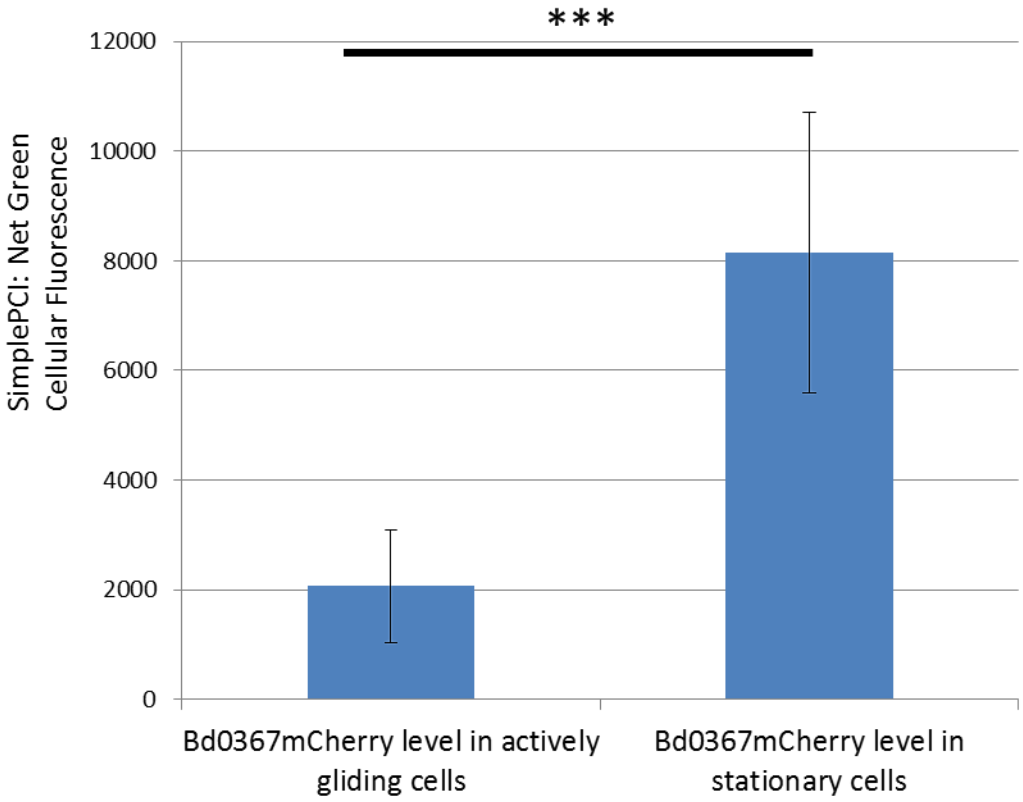

Figure 5.26 Bd0367mCherry cellular fluorescence in the stationary *Δbd1971*:Bd0367mCherry cells was higher than that observed in the actively gliding cells. The Average Net Total 'Green' was calculated for the Δ*bd1971*:Bd0367mCherry gliding and non-gliding cells**.** This resulted in a noticeable difference in strength of cellular fluorescence. Bd0367mCherry in stationary cells was 3.95 higher than that observed in actively gliding cells. The mean cellular fluorescence of 16 gliding cells and 16 non gliding cells across 3 biological repeats was analysed. The error bars show 95% confidence and the difference between the samples was found to be significant by Student test. *** ≤0.001.

It appeared from these results that Bd0367mCherry was present in the gliding cells but at a much lower level. To confirm that Bd0367mCherry was present in the gliding cells the cellular fluorescence measured for Bd0367mCherry in Δ*bd1971* gliding cells was compared to cellular fluorescence measured for HD100 without a mCherry construct see Figure 5.27. This showed that the cellular fluorescence measured for Bd0367mCherry in Δ*bd1971* gliding cells was significantly higher than that measured in HD100. Suggesting Bd0367mCherry is present at low levels in these 'dark' gliding cells.

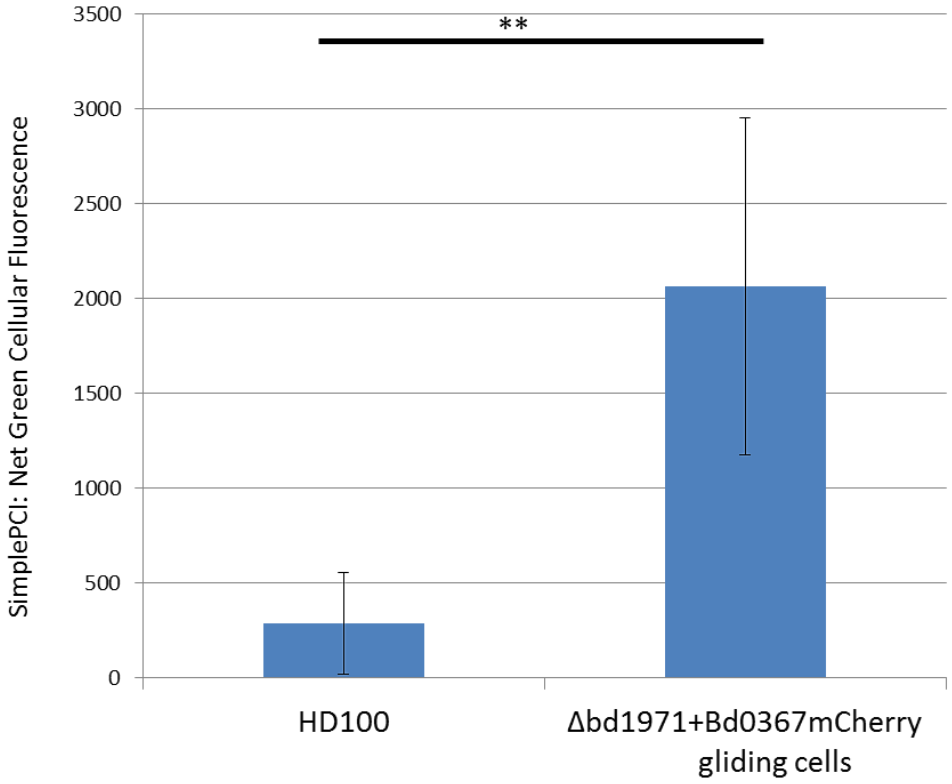

Figure 5.27 Bd0367mCherry cellular fluorescence in actively gliding *Δbd1971*:Bd0367 cells was higher than in HD100 control. The Average Net Total Green was calculated for HD100 cells with no mCherry tag compared to the level in Δ*bd1971*:Bd0367mCherry gliding cells. This resulted in a significant different mean Net Total Green cellular fluorescence suggesting Bd0367mCherry is expressed in gliding cells at low level. A total of 16 HD100 cells were analysed across 3 biological repeats and 16 Δ*bd1971*:Bd0367mCherry gliding cells over 3 biological repeats The error bars show 95% confidence and the difference between the samples was found to be significant by Student t test.. **≤0.01

This raises the question of how are Bd0367mCherry levels being controlled, is this control post-translational or transcriptional and is this regulation dependent on the global level of c-di-GMP.

5.5. Discussion

These data suggest that global c-di-GMP levels effect gliding motility in *Bdellovibrio bacteriovorus*, with high cellular c-di-GMP resulting in reduced frequency of gliding. However the process of bdelloplast exit still occurs in this high cellular c-di-GMP background suggesting this process of exit may be regulated by a specific c-di-GMP pool produced by Bd0367 or that this process is cAG regulated. The function of Bd0367 as a

HypGGDEF and role of cAG production in *Bdellovibrio* are still unknown. Taken together these data suggest that there may be an optimal cellular c-di-GMP level required for WT gliding motility to occur and that gliding is dependent on expression of Bd0367 even when lacking enzymatic functionality. Which suggests protein interactions with Bd0367 may have a key role in the regulation and control of gliding motility. These ideas are discussed further below.

5.5.1. Bd0367mCherry HD expression is increased on surface incubation

Fluorescent tagging of Bd0367 with mCherry in HD100 demonstrated that general fluorescent intensity increased after 400 minutes of surface incubation, this incubation time correlates with when the majority of cells are gliding. A 1.18 fold increase in fluorescent intensity indicated that Bd0367 was upregulated on surface incubation, which suggested a role in gliding motility. This result further validated the previous study that first showed Bd0367 was involved in gliding motility as deletion of *bd0367* resulted in an abolition of gliding motility (Hobley et al, 2012).

5.5.2. The location of Bd0367mCherry in HD100 cells is altered on surface incubation

In addition to the increase in fluorescent intensity there was an alteration in the location of Bd0367mCherry fluorescence within the cell. This change in location is smaller than the results to be covered in Chapter 6, however may still be of biological relevance. Most notable is the decrease in bipolar localisation by 10% on surface incubation, suggesting this location is not advantageous to surface related activities such as gliding. The most common localisation of Bd0367mCherry in attack phase cells is diffuse throughout the cell, this correlates with the interaction studies of Chapter 3 which show Bd0367 has multiple protein interaction partners in multiple cellular locations. Therefore a location throughout the cell enables Bd0367 to interact with particular partners in a range of cellular areas.

The dominant mono polar focus is the rarest localisation of Bd0367mCherry at time 0 6% and stays relatively steady on surface incubation increasing to 9%, it is unknown if this polar location occurs at the prey interaction pole or the flagellar pole, but interactions with Bd3125 from Chapter 3 suggest it may be the prey interaction pole. This is still a

rare localisation of Bd0367mCherry and suggests that cells with a mono-polar localisation of Bd0367mCherry may be involved in a very particular or rare cellular function.

In other DGC proteins with RR domains the phosphorylation state has proved important in regulating sequestration the DGC to specific subcellular localisations as observed by PleD locating to the pole in *Caulobacter* on phosphorylation and dimerization (Paul et al, 2007). It is possible that the distinct polar locations of Bd0367mCherry correspond to the phosphorylation state of this protein. This is worth investigation by mutating the phospho-receiving amino acid D63A in the Bd0367mCherry construct and observing any effect on localisation pattern. However I think this theory is unlikely in the case of Bd0367 as it would suggest that only 21% of the cell population observed at time 0 have phosphorylated and presumed active Bd0367 and only 14% of the cell population at time 400.

5.5.3. Challenges of determining intracellular c-di-GMP content of *Bdellovibrio*

5.5.3.1. Quantifying c-di-GMP levels in HI strains

Previous studies in the Sockett lab have obtained a range of values for HI c-di-GMP levels, despite the samples being prepared in consistent ways (ie. grown to the same OD_{600} and using the Bobrov method of c-di-GMP extraction). The variation between these separate biological experiments is thought to be due to the wide-ranging and mixed growth rates of HI cells. HI cells can have a diverse range of cellular morphologies, as mentioned in Chapter 1 and the distribution of these morphologies can vary between different cultures of the same HI strain. The unknown factors that lead to these diverse morphologies, with presumably differing physiologies and different growth mechanisms. As these factors are currently unknown they cannot be easily controlled for, this area will hopefully become more understood in the future.

However, it is interesting that values for HID13 in the Bd0367 investigation (Section 5.4.3) are comparable to those documented by Dr Basford, and the HID13 values in the Bd1971 investigation (Section 5.4.11) are comparable to those documented by Masters student Mike White (which lie half way between Mike White's values and those in c-di-GMP paper (Hobley et al., 2010)(Basford, 2015; White, 2012).

A more detailed analysis into the variation observed in the HI control strains is recommended to see if alterations to the protocol can result in more consistent and standardised c-di-GMP levels between biological repeats of HI control strains. However, achieving this level of consistency is not just a difficult in *Bdellovibrio* research; a recent study in *Myxococcus* demonstrated that their absolute c-di-GMP levels varied up to 2-fold between experiments (Skotnicka et al, 2016a)

It is possible that the c-di-GMP level of HI *Bdellovibrio* may vary on transition into stationary phase (as demonstrated in *E. coli*)(Spangler et al, 2010). It is also possible that as HI cells do not always grow at the same rate, cells in a single culture may be in mixture of growth stages. In *E. coli*, the level of c-di-GMP was shown to increase on entry into stationary phase from ~1.2 pmol/mg protein to ~2.1 pmol/mg protein and then decrease during stationary phase (Spangler et al, 2010). There could be similar variations according to growth phase to be discovered in HI cells.

Additional measures that could be used to improve the current HI c-di-GMP extraction protocol would be to calculate the relative c-di-GMP value by comparing concentration of protein between samples (pmol/mg protein). This is currently being attempted and only future biological repeats will determine if this measurement reduces variation

5.5.3.2. Quantifying c-di-GMP levels in HD strains

The growth method used to obtain HD pellets is novel to this study, previous work on HD strains have resulted in variable values between cultures of the same strain prepared in the same biological experiment. This was thought to be due to the length of time taken to process the large culture volume (6 litres per strain) (Basford, 2015). The HD method presented in this thesis used a concentrated *Bdellovibrio* culture (Methods 2.15.1) whose use was pioneered by Dr Chris Moore (Sockett lab). This resulted in a high yield of *Bdellovibrio* that could be quickly processed up to the point of extraction.

It appears that this new method has reduced the variability of c-di-GMP levels extracted between different cultures of the same strain grown on the same day, which is an improvement on previous HD extraction techniques. It is hoped that the values obtained for HD100 in this study will be reproducible in future to allow comparison between different biological repeats for HD strains.

It is possible that now HD strains can be processed quickly, the c-di-GMP levels may not vary much due to the fact that HD cells are grown in synchronised cultures unlike HI cells and have a standard rod-shaped cell morphology when in attack phase.

5.5.4. Bd0367 c-di-GMP production is activated by phosphorylation

As with many other DGC proteins with RR domains the enzymatic function of Bd0367 was seen to be absent when phosphorylation of the RR domain was prevented by the construction of a Bd0367D63A strain with mutation of the conserved D receiver amino acid. The c-di-GMP level produced by the Δ*bd0367* and Bd0367D63A HI mutant strain were not significantly different. This suggested that phosphorylation by a cognate HK would activate Bd0367 DGC activity *in vivo*.

Additionally the reduction of c-di-GMP level on the removal or inactivation of Bd0367 greatly reduces the cellular percentage of c-di-GMP (between 91.5±3.07 to 93±1.93% less c-di-GMP) under the conditions tested; this may suggest that Bd0367 may be the most active major DGC contributing the most to the cellular pool of c-di-GMP under the conditions tested compared to the other DGC proteins in *Bdellovibrio* Bd0742, Bd1434 and Bd3766.

5.5.5. C-di-GMP production by Bd0367 is hindered by the C terminal mCherry tag

The c-di-GMP level recorded for the Bd0367mCherry HI strain was 88% less than WT and 3.5% more than the gene deletion strain. The reduction in c-di-GMP level is postulated to be due to steric hindrance introduced by the mCherry tag (see Figure 5.28). It is possible that the tag impaired Bd0367 dimerization resulting in a less active DGC activity from Bd0367 and hence less cellular c-di-GMP than WT.

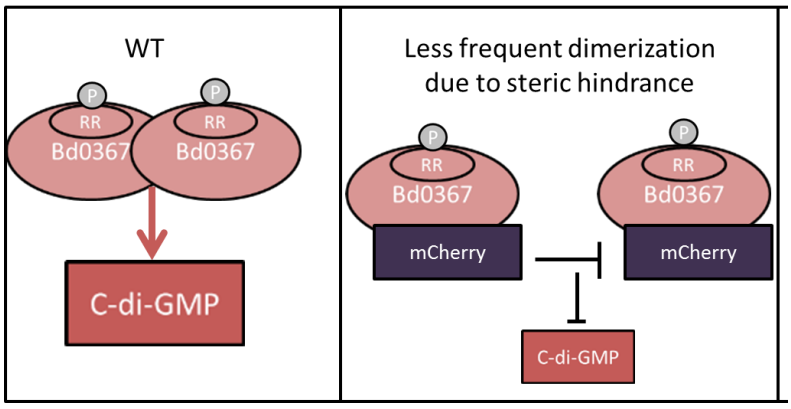

Figure 5.28 mCherry tag may impair Bd0367 dimerization. The C terminal mCherry tag introduces steric hindrance that can prevent dimerization of Bd0367 when activated by phosphorylation, this results in less efficient production of c-di-GMP.

5.5.6. A specific Bd0367 associated product is required for bdelloplast exit

Previous work on the Δ*bd0367* HI strain showed that *Bdellovibrio* could not leave the bdelloplast in the absence of Bd0367. In this study I have shown that *Bdellovibrio* progeny could not leave the bdelloplast when Bd0367 is present but unable to be post-translationally activated as a DGC by phosphorylation. Additionally when the Bd0367mCherry HI strain was investigated progeny cells could exit the bdelloplast however exit rates were not restored to WT levels suggesting the impairment of c-di-GMP production caused by the mCherry tag was hindering a process required for progeny bdelloplast exit (see Figure 5.29). The Bd0367mCherry HI strain also demonstrated that the difficulties exiting the bdelloplast were not due to gliding motility problems, as this strain had no hindrance in gliding motility outside prey. Additionally bdelloplast exit does not appear to be a process effected by changes in global levels of c-di-GMP as in a globally high cellular c-di-GMP level strain *(*Δ*bd1971*HD) bdelloplast exit occurs normally (clearing a whole predatory culture in 24 hrs). This suggests that the production of c-di-GMP by Bd0367 specifically is part of the stimulus to cause progeny *Bdellovibrio* to exit the bdelloplast. Or that bdelloplast exit is responding to cAG levels produced by Bd0367 due to an as yet unknown potential variation in ATP:GTP ratio in progeny cells in the bdelloplast.

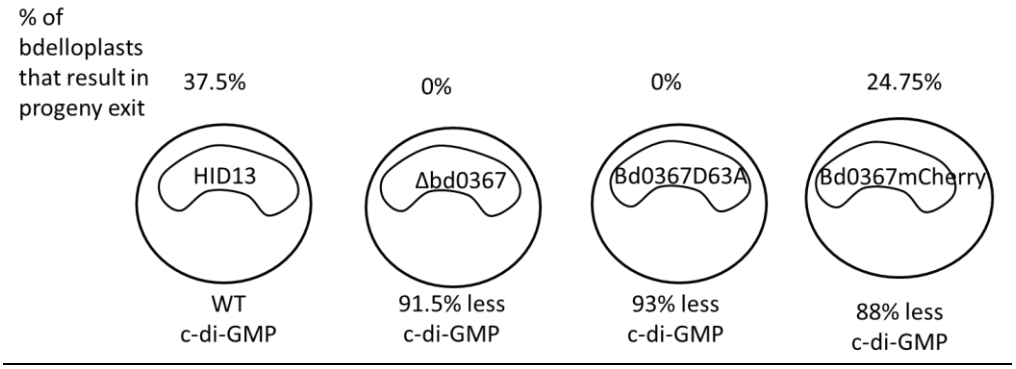

Figure 5.29 Percentage of bdelloplasts that result in successful progeny exit. In the WT HI HID13 37.5% of bdelloplasts will result in progeny cells exiting on a surface. Progeny exit is never observed in Δ*bd0367* or Bd0367D63A strain, suggesting that lack of Bd0367 or lack of phosphorylated Bd0367 (so inactive Bd0367) results in no prey cell exit. The exit frequency is partially restored in the Bd0367mCherry strain, this mutant is hypothesized to hinder dimerization of Bd0367 so result in low c-di-GMP levels, however this mutant is theorized to be more active than the Bd0367D63A strain and can be phosphorylated. In this strain the low level production of specific c-di-GMP or cAG may mediate the cell exit process.

5.5.7. Production of Bd0367 protein (active or inactive) is required for gliding motility to occur

Interestingly in this study we have shown that gliding motility is possible when Bd0367 is present but unable to be post-translationally activated by phosphorylation leading to an enzymatically inactive Bd0367. This strain Bd0367D63A HI results in lower c-di-GMP background that WT with 0.32% of cells gliding. Whereas in the Δ*bd0367* HI strain gliding motility was completely abolished. This suggests that gliding motility is not reliant on Bd0367 c-di-GMP levels in order to occur, however in HI growth for gliding motility to occur requires the protein Bd0367 to be produced/available. This result suggests that the protein interactions that Bd0367 forms (discussed more in Chapter 6) form potentially independently from Bd0367 DGC function to form part of the signalling system to control gliding motility. The frequency of HI strains gliding with the c-di-GMP percentage is shown in Figure 5.30.

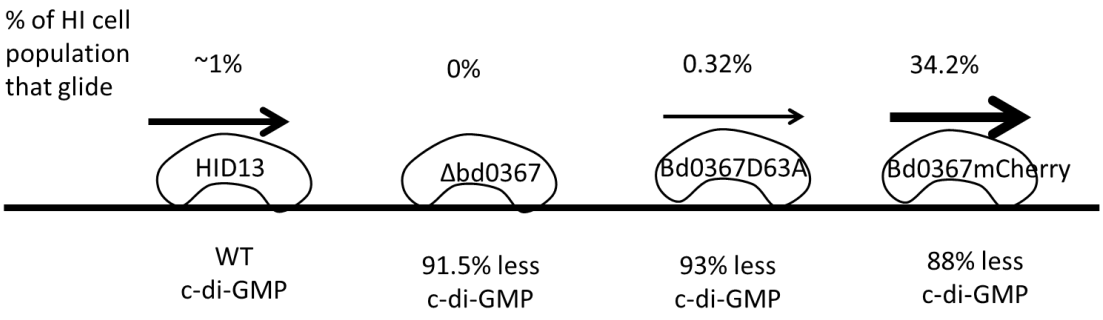

Figure 5.30 Percentage of HI cells that exhibit gliding motility. Gliding is rare in HI cells. However the protein Bd0367 is required for cells to glide, as 0% glide in the deletion strain. However gliding can occur in two low c-di-GMP level strains, Bd0367D63A and Bd0367mCherry (suggesting Bd0367 specific c-di-GMP does not regulate gliding). The reduced gliding frequency in Bd0367D63A mutant strain suggests phosphorylation may be an important protein modification in mediating protein interactions which stimulate gliding motility. The increase in gliding frequency in the Bd0367mCherry HI strain suggests that low c-di-GMP levels coupled with a Bd0367 that can be phosphorylated and presumably interact with partner proteins results in more frequent gliding.

5.5.7.1. Is gliding motility mediated by Bd0367 DGC activity or protein interactions?

The cellular level of c-di-GMP has been shown to have large effects on cell motility phenotypes in other bacteria. However in *Bdellovibrio* the presence of an enzymatically inactive Bd0367 does not increase c-di-GMP levels but does partially restore gliding motility suggesting protein interactions may be more important in this system. The theories are discussed below.

Model 1: Threshold cellular c-di-GMP level to initiate gliding motility

It is well documented that levels of cellular c-di-GMP can have vast effects on bacterial motility generally with low c-di-GMP stimulating motility and high c-di-GMP repressing motility phenotypes, via c-di-GMP receptors acting as post-translational brakes on motors or by synthesising surface adhesive polymers (Romling et al, 2013). However there has been a recent discovery in *Myxococcus* showing that an increase in c-di-GMP and a decrease in c-di-GMP level can cause defects in type IV pilus motility, suggesting there may be an optimum level of c-di-GMP for motility (Skotnicka et al, 2016b). For this reason our study considers the possibility that low c-di-GMP levels observed in the Bd0367D63A HI strain contribute to the reduced gliding phenotype, as the c-di-GMP level is below the set threshold value.

My hypothesis suggests that a set (relatively low) level of cellular c-di-GMP may be required to stimulate gliding motility and it is possible that the 93% reduction in c-d-GMP level created by the Bd0367D63A HI strain is just under or hovering around this threshold level allowing reduced gliding at 0.32% of cells. This threshold level theory would explain how an 88% reduction in cellular c-di-GMP in the Bd0367mCherry HI strain despite only being only 5% higher c-di-GMP level results in a large increase in the percentage of cells that glide. This would suggest that at 88% the threshold level of c-di-GMP enables gliding motility and that like many other bacterial lower levels of c-di-GMP (without complete reduction) increases motility in *Bdellovibrio* explaining the increased frequency of gliding in this strain (34.2%) compared to WT (~1%).

This threshold value may work by levels of cellular c-di-GMP controlling the interaction strengths of Bd0367 protein partners as observed in *E.coli* with proteins PgaC and PgaD. These proteins fail to interact at low c-di-GMP concentrations which results in PgaD degradation and less EPS production (Steiner et al, 2013). This could suggest that at very low cellular level of c-di-GMP Bd0367 cannot interact with partner proteins well and this results in less gliding motility, however when c-di-GMP levels in the cell are slightly higher this provides the optimal conditions for Bd0367- protein interactions, and results in increase gliding motility, Figure 5.31. This suggests that c-di-GMP may have a nuanced effect on strength of protein interactions in *Bdellovibrio*, however this requires further investigation.

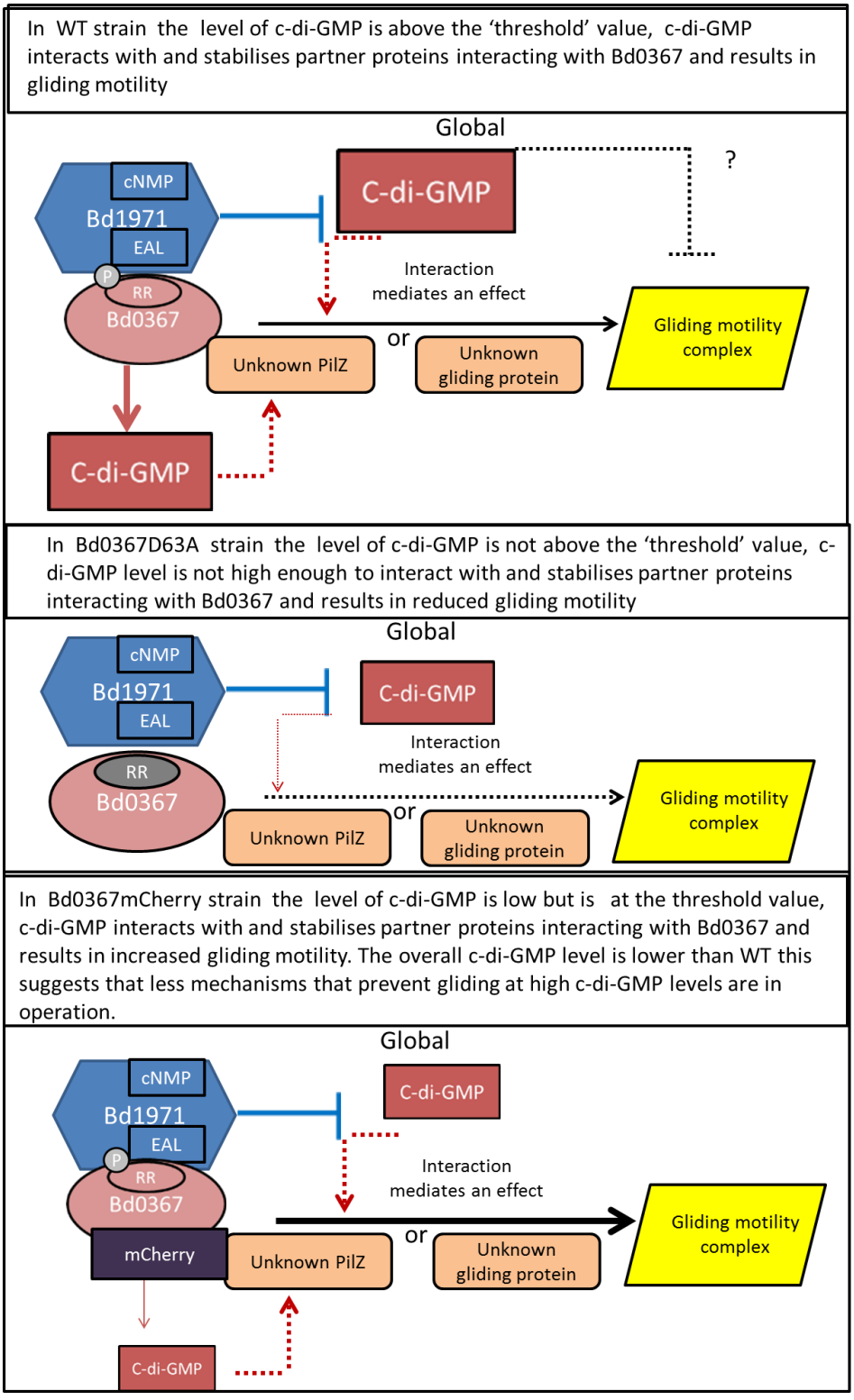

Figure 5.31 Threshold c-di-GMP level is needed for gliding motility, this stabilises Bd0367 partner protein interactions. If the c-di-GMP level is below the threshold value (Bd0367D63A) may lead to reduced gliding motility as protein interactions cannot be stabilised. Additionally a higher c-di-GMP level could led to repression of gliding motility through another mechanism that interferes with the gliding motility complex (WT dotted black line). There may be an optimal level of c-di-GMP for gliding motility, for example box 3 shows the Bd0367mCherry strain, which with ~5% higher c-di-GMP

levels than Bd0367D63A can glide more frequently than WT. PDE proteins and processes are show in blue, DGC and c-di-GMP producing/dependent processes are shown in red. The thickness of lines and size of c-di-GMP box represents the strength and quantity.

Model 2: Gliding motility is controlled by the phosphorylation state of Bd0367 due to changes in protein interactions

The reduction in gliding motility of the Bd0367D63A HI strain may be independent of the cellular c-di-GMP level as it could be that the D63A mutation prevents certain conformational changes that occur due to phosphorylation, for example protein dimerization, Figure 5.32. Bd0367 dimerization or other structural changes induced by phosphorylation may be important for the protein interactions occurring with Bd0367 which are hypothesised to mediate effects on gliding motility. A recent study showed that mutations destabilising the dimerization of DGC GcbC resulted in a loss of interaction between itself and its effector LapD (degenerate EAL) by B2H, it would be possible to investigate the dimerization region of Bd0367 and observe the effect of mutating this region by B2H in the future (Dahlstrom et al, 2015).

The Bd0367D63A HI strain may still be able to interact with partner proteins but these interactions may be weaker due to the lack of phosphorylation, resulting in the ~ 70% reduction in gliding frequency observed.

This could be investigated by examining the gliding phenotype of an active site mutant (in the GGDEF motif) of Bd0367. This strain could still be phosphorylated and dimerize, so may then be able to form more stable interactions with partner proteins but the c-di-GMP level of this strain should still be very low. This would allow a study to more fully dissect the role of c-di-GMP level vs protein interactions in Bd0367 signalling.

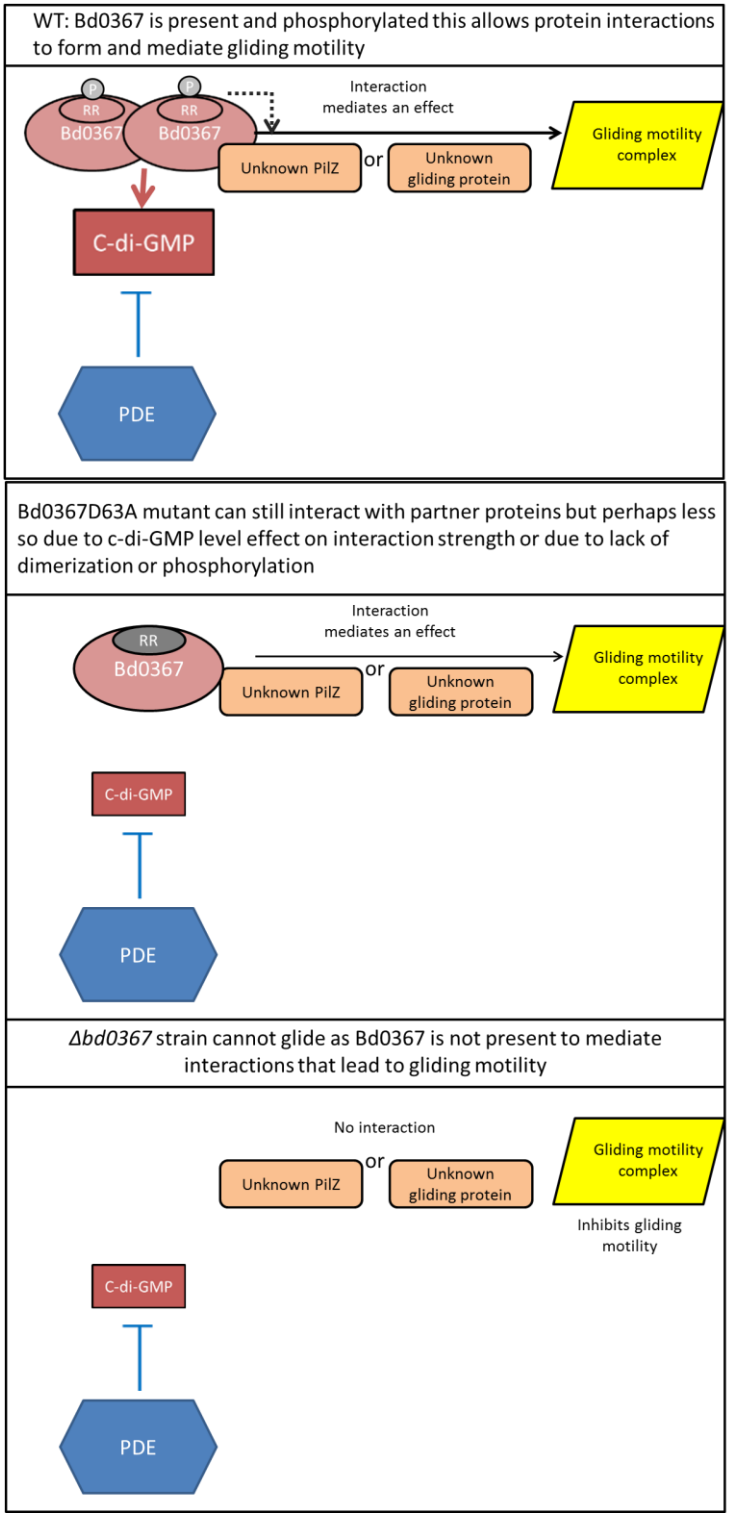

Figure 5.32 The phosphorylation state of Bd0367 is important for mediating proteins interactions and hence important for gliding motility. When Bd0367 is un-phosphorylated it is not in an optimal conformation to interact with its partner proteins, there may still be some weak interaction though allowing a low frequency of gliding to occur. Whereas in the *bd0367* deletion strain there is no Bd0367 so no chance of a weak interaction with partner protein so no gliding motility. PDE proteins and processes are

shown in blue, DGC and c-di-GMP producing/dependent processes are shown in red. The thickness of lines and size of c-di-GMP box represents the strength and quantity.

5.5.7.2. Role of mCherry tag in increasing gliding frequency

This study found that the Bd0367mCherry HI strain produced slightly more c-di-GMP (~4%) than the deletion and Bd0367D63A inactive strain and glides more frequently than the WT HID13 strain. This result could suggest that in this small difference the Bd0367mCherry HI strain c-di-GMP levels result in the optimal level of c-di-GMP for gliding motility to occur as discussed previously, or it could suggest that the mCherry tag is stabilizing a Bd0367 protein conformation conducive to protein interactions rather than blocking protein interactions with Bd0367, this increased stability of protein interactions may lead to increased frequency of gliding motility, see figure 5.33. Additionally the fact the Bd0367mCherry strain can be phosphorylated may also play a role in stabilising these interactions, however the frequency of dimer formation is unknown.

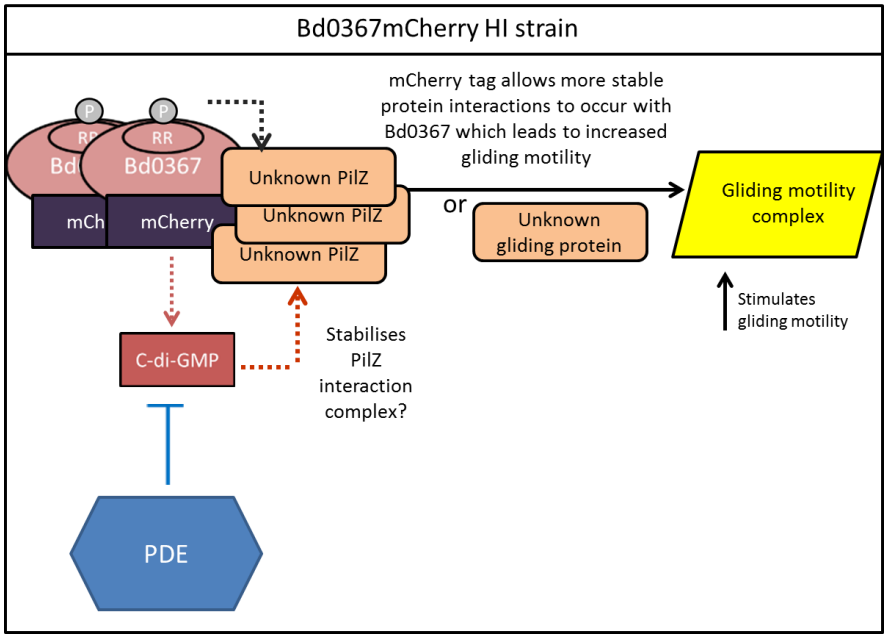

Figure 5.33 How does Bd0367mCherry increase gliding motility in the HI strain. It is proposed that Bd0367mCherry strain may have a c-di-GMP level which is optimal to stabilizing protein interactions, or that the mCherry tag or phosphorylation state keeps Bd0367 in a conformation that is favourable to protein interactions. These interactions with Bd0367 are hypothesised to influence gliding motility. PDE proteins and processes are shown in blue, DGC and c-di-GMP producing/dependent processes are shown in red. The thickness of lines and size of c-di-GMP box represents the strength and quantity.

5.5.8. How global cellular c-di-GMP levels regulate gliding motility in *Bdellovibrio*

Previously in Hobley 2012 it was suggested that the low c-di-GMP levels in the Δ*bd0367* strain in conjunction with loss of Bd0367 may have caused the defects in gliding motility. However further work in this study suggests that the presence of Bd0367 protein is more important for gliding motility than its DGC function as gliding can occur when DGC function is inactivated by a mutation in the phospho-accepting D63. Additionally the Bd0367mCherry HI strain has very low c-di-GMP levels similar to the inactivated strain but an enhanced gliding frequency suggesting that low c-di-GMP levels do not inhibit gliding motility and that Bd0367 protein interactions are the major factor missing from the deletion strain leading to abolished gliding motility.

However the mechanism of these protein interactions in meditating gliding motility is currently unknown and it remains possible that the strength of these interactions may be influenced by c-di-GMP levels. This suggested that varied levels of cellular c-di-GMP could still play a large role in orchestrating gliding motility in *Bdellovibrio*. For this reason the effect of a high cellular c-di-GMP level on *Bdellovibrio* gliding was examined by testing a silent Bd1971 PDE deletion strain and a silent PDE inactivated Bd1971 strain Bd1971D307308A to analyse the effect of high c-di-GMP on gliding phenotypes.

5.5.8.1. C-di-GMP levels increase in both *Δbd1971* and Bd1971D307308A strains

C-di-GMP extractions from both Δ*bd1971* and Bd1971D307308A strains in both HI and HD life styles has shown that these strains have higher c-di-GMP levels than the WT. This suggests that Bd1971 is an active PDE and that a D307308A mutation is sufficient to attenuate the PDE activity of this protein.

The increase in c-di-GMP in HI cells is similar between the two strains at ~200% higher than WT for this biological set. However in the HD attack phase cells the Bd1971D307308A strain has a noticeably higher extracted c-di-GMP than the deletion strain at ~300% higher.

This is an interesting effect and I propose that in the Bd1971D307308A strain Bd1971 interacts with Bd0367 (as demonstrated in Chapter 3) and that this interaction stimulates Bd0367 c-di-GMP production in attack phase cells (see Figure 5.34). However further

work is required to confirm this hypothesis such as finding and mutating the interaction binding site and analysing the effect of this strain on global c-di-GMP levels.

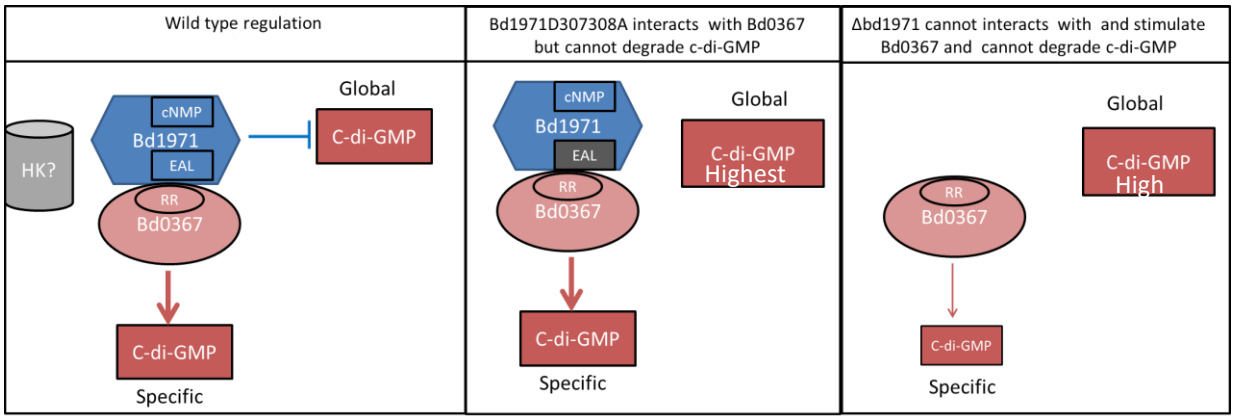

Figure 5.34 In the wild type HD100 cells Bd1971 may stimulate Bd0367 DGC activity. This activation of DGC Bd0367 may be implemented through Bd1971 binding alone or by acting as an accessory protein to the cognate HK to Bd0367. In the Δ*bd1971* strain there is no Bd1971 to stimulate DGC activity of Bd0367, this results is an increased level of global c-di-GMP compared to WT but a lower amount of Bd0367 specific c-di-GMP. In the Bd1971D307308A strain DGC activity of Bd0367 is still stimulated generating more specific c-di-GMP and the global pool of c-di-GMP increases due to lack of PDE activity from Bd1971, resulting in a higher level of c-di-GMP in this strain compared to the Δ*bd1971* HD strain. PDE proteins and processes are shown in blue, DGC and c-di-GMP producing/dependent processes are shown in red. The thickness of lines and size of c-di-GMP box represents the strength and quantity.

5.5.8.2. PDE Bd1971 is involved in gliding motility in *Bdellovibrio* outside prey

Once a silent deletion of *bd1971* was made the gliding ability of the strain was tested. These data showed that when Bd1971 was absent HD cell gliding was observed less frequently (34%) and took longer to initiate (~160 min). Additionally this gliding phenotype also occurred in the Bd1971D307308A (enzymatically inactive mutant) suggesting that the impaired gliding motility (47% cells gliding) is mostly due to the high c-di-GMP levels in this case and not due to the lack of Bd1971.

This correlates with the general principle that high c-di-GMP levels stimulate biofilm and stationary behaviours, however the role of c-di-GMP in mediating the variety of mechanisms employed to inhibit motility, remain poorly understood even in flagellar motility (McCarter & Gomelsky, 2015; Romling et al, 2013). As gliding motility is in the earlier stages of investigation than flagella motility even less in known about the possible c-di-GMP mechanism that may influence this type of motility. Interestingly a study

recently showed that gliding motility appeared to be unaffected by varied c-di-GMP levels in *Myxococcus* (Skotnicka et al, 2016a).

The regulatory mechanism by which the PDE protein Bd1971 controls cellular c-di-GMP levels and how these levels effect gliding motility is unknown, however four models are proposed below as possibilities.

Model 1: *Bdellovibrio* has four potential gliding operons for gliding motor synthesis it is possible that under different c-di-GMP levels different gliding motors are in operation

In this model I propose that the cellular c-di-GMP level effects the transcriptional expression of the four different gliding motors and complexes in *Bdellovibrio*. I suggest that the gliding motor/complex that is prevalent under high c-di-GMP levels is a 'bad' gliding motor which is less efficient and therefore results in less frequent gliding. This model comes from reading the work on c-di-GMP controlling flagellar swarming motility through the mechanism of the MotAB stator displacing the MotCD from the motor, when c-di-GMP levels are high and negatively affecting motility (Kuchma et al, 2015). This theory could be tested via RT-PCR of the gliding operons in high and low c-di-GMP strains incubated on surfaces.

Model 2: High levels of c-di-GMP influence gliding motor performance by unknown c-di-GMP receptor protein binding at high c-di-GMP and inhibiting gliding motility complex

In this model an unknown c-di-GMP receptor protein binds c-di-GMP when it is at a high cellular level, this binding then initiates a downstream signal transduction cascade that is predicted to result in the unknown receptor protein regulating post-translationally an aspect of the gliding motility complex in a c-di-GMP dependent manner, Figure 5.35. This mechanism is inspired by the c-di-GMP binding protein YcgR, which regulates flagellum-based motility in a c-di-GMP-dependent manner (Ryjenkov et al, 2006). YcgR has been found to interact with the flagellar switch-complex proteins FliG and FliM strongly in the presence of c-di-GMP, this results in disruption through conformational changes which inhibit motility (Paul et al, 2010). It is tempting to speculate that PilZ

domain protein Bd1482 may act in this manner due to its location in one of the *Bdellovibrio* gliding operons. This could be assessed by B2H studies with Bd1482 and the gliding motility complex proteins, with a particular focus of the gliding proteins isolated by Rotem and co-workers in c-di-GMP capture compound study (Rotem et al, 2016).

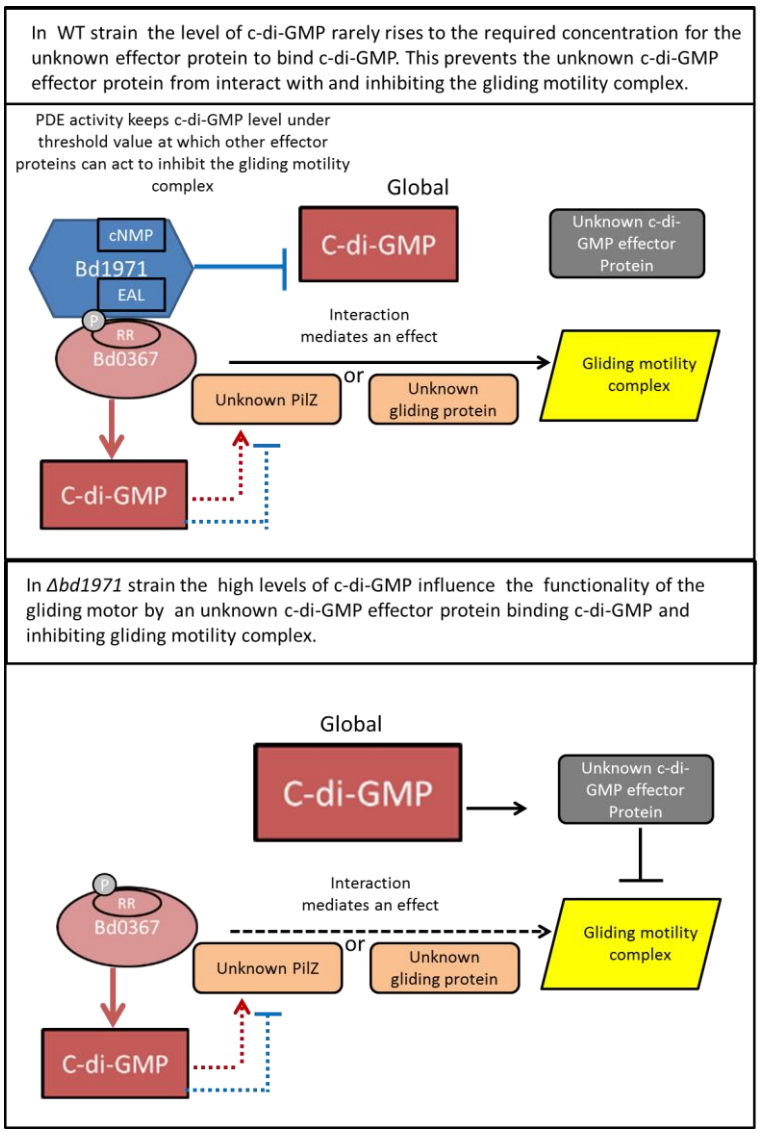

Figure 5.35 When c-di-GMP levels are high a c-di-GMP effector protein binds to the gliding motility complex and inhibits gliding. It is possible that the cellular c-di-GMP level also impacts on the strength of Bd0367 interactions. PDE proteins and processes are shown in blue, DGC and c-di-GMP producing/dependent processes are shown in red. The thickness of lines and size of c-di-GMP box represents the strength and quantity.

Model 3: High cellular c-di-GMP disrupts protein interactions between Bd0367 and protein partners

Another potential model is that a multiprotein complex involving Bd0367 may be needed to stimulate gliding motility. In this case the interaction strength between proteins and Bd0367 may be influenced by the cellular c-di-GMP levels, with high c-di-GMP levels causing weaker protein interactions and the multiprotein complex to dissociate, so less gliding occurs, Figure 5.36. This may be due to the interaction partners being PilZ domain proteins that bind c-di-GMP at high levels, so when c-di-GMP levels are high enough these proteins bind c-di-GMP and potentially change in conformation and no longer interact with Bd0367, this lost interaction may result in targeted degradation of the partner proteins as in the case of PgaD at low levels of c-di-GMP in *E.coli* (Steiner et al, 2013). Or another c-di-GMP effector protein may bind to c-di-GMP at these levels and this may enable these other unknown proteins to interact with and sequester the Bd0367 partner proteins.

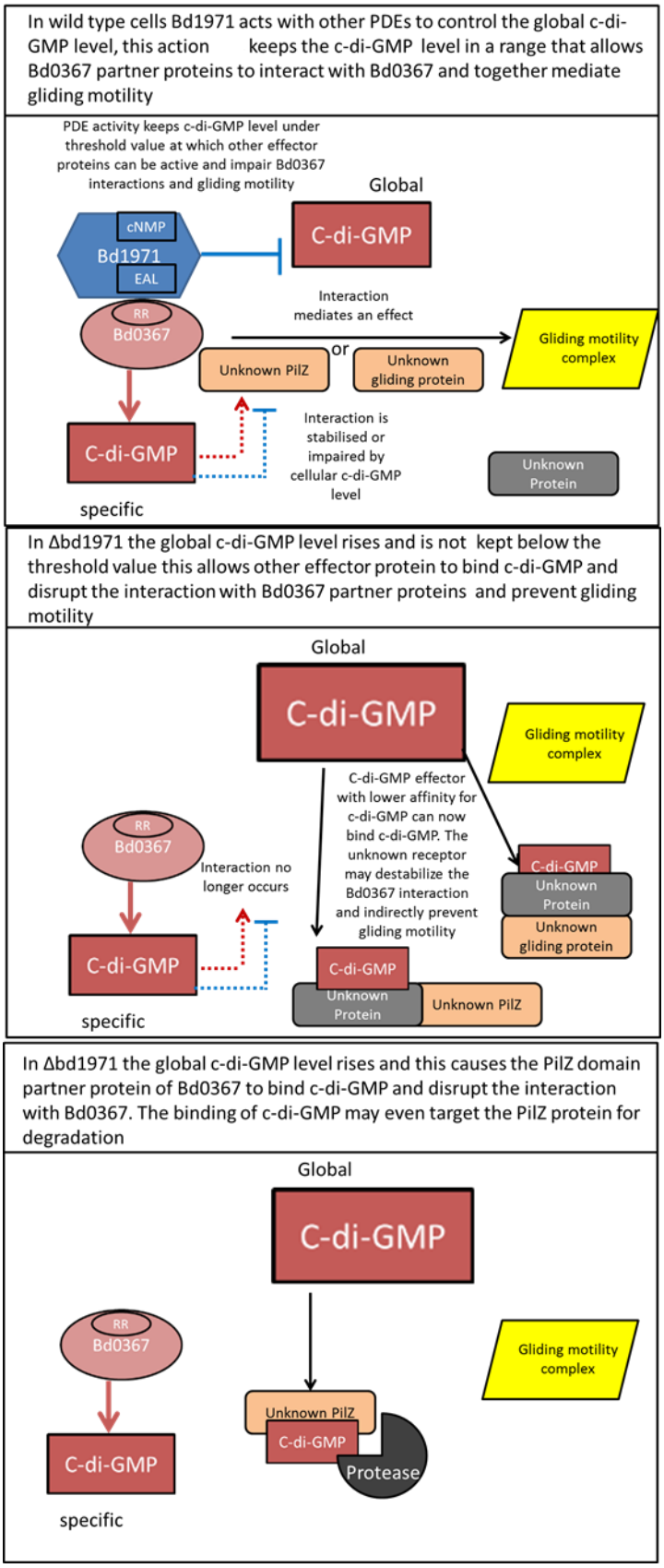

Figure 5.36 High cellular c-di-GMP disrupts protein interactions between Bd0367 and protein partners. Either by other proteins sequestering the partners, or the Bd0367 partner proteins bind to c-di-GMP altering the protein conformation so that the

interaction can no longer occur. PDE proteins and processes are shown in blue, DGC and c-di-GMP producing/dependent processes are shown in red. The thickness of lines and size of c-di-GMP box represents the strength and quantity.

Model 4: There is an increase in EPS in the *Δbd1971* and Bd1971D307308A strains impairing gliding motility by 'trapping' *Bdellovibrio* cells

A common outcome of increased cellular c-di-GMP levels is increased production of EPS, EPS is commonly used in bacteria to adhere to surfaces, stimulate biofilm formation and inhibit motility. The increased production of EPS in high c-di-GMP conditions can be mediated by transcriptional regulators (e.g FleQ *P. aeruginosa*) or by a c-di-GMP binding a PilZ protein (such as BcsA in *Salmonella*) which then synthesizes cellulose (Hickman & Harwood, 2008) (Zorraquino et al, 2013).

I propose in the high c-di-GMP level strains Δ*bd1971* and Bd1971D307308A there is an increase in EPS possibly due to unknown transcriptional regulator, (as there is no BcsA PilZ cellulose synthase homologue in *Bdellovibrio).* This additional EPS sticks down *Bdellovibrio* cells and prevents gliding despite presence of gliding machinery see Figure 5.37. EPS has been seen to prevent motility in other bacteria in high cellular c-di-GMP conditions, for example in *L. monocytogenes*, where mutation of a EPS biosynthesis genes restored motility (Chen et al, 2014).

Previous investigation of EPS in the Δ*bd1971* Kan strain by Dr Basford by Calcofluor White stain showed fluorescence from EPS in HI plate cultures but the variation in these results meant that no conclusion could be drawn about level of EPS in the Δ*bd1971* Kan strain versus the control (Basford, 2015). The Calcofluor White stains for β-1,3 and β-1,4 polysaccharides, such as cellulose and chitin, it is possible that Δ*bd1971* Kan and Δ*bd1971* strains increase another component of the EPS, such as protein, glycoprotein, glycolipids, or DNA (Flemming et al, 2007; Harrington & Hageage, 2003). Further investigation into EPS levels should be considered to fully understand this gliding phenotype.

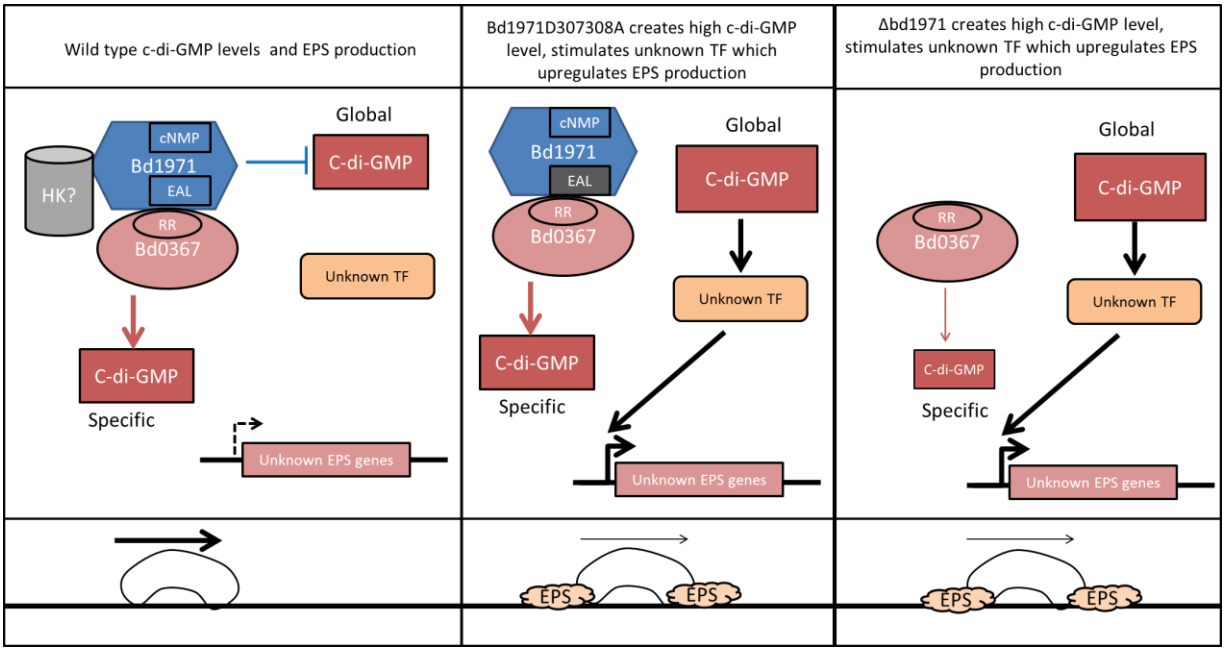

Figure 5.37 Comparison of EPS in WT attack phase cells compared to Bd1971 mutant strains. In WT the level of c-di-GMP does not cause TF to bind to the EPS genes often resulting in low level of EPS. In the Bd1971 mutant strains global c-di-GMP levels are elevated so the TF is frequently interacting and promoting EPS transcription, resulting in more EPS and less gliding motility due to cells being stuck. PDE proteins and processes are shown in blue, DGC and c-di-GMP producing/dependent processes are shown in red. The thickness of lines and size of c-di-GMP box represents the strength and quantity.

5.5.8.3. Level of Bd0367mCherry is effected by high cellular c-di-GMP levels

To assess the role of Bd0367 in the Δ*bd1971* strain the Bd0367mCherry construct was conjugated into the Δ*bd1971* strain. This allowed observation that 37% of these cells had very low fluorescence from Bd0367mCherry. This is different to the WT distribution of Bd0367mCherry fluorescence in attack phase cells where there are no 'dark' cells. The percentage of 'dark' cells where Bd0367mCherry is present at a low level was very similar to the percentage of Δ*bd1971* cells that could glide (34%). This led to the hypothesis that the *Bdellovibrio* attack phase cell population had heterogeneous levels of c-di-GMP and that the cells that could glide had lower c-di-GMP levels due to less DGC activity represented by less Bd0367mCherry fluorescence (see Figure 5.38). It is interesting that despite having post-translational control mechanisms such as phosphorylation and an I site to control DGC activity there appears to be another additional layer of control for Bd0367.

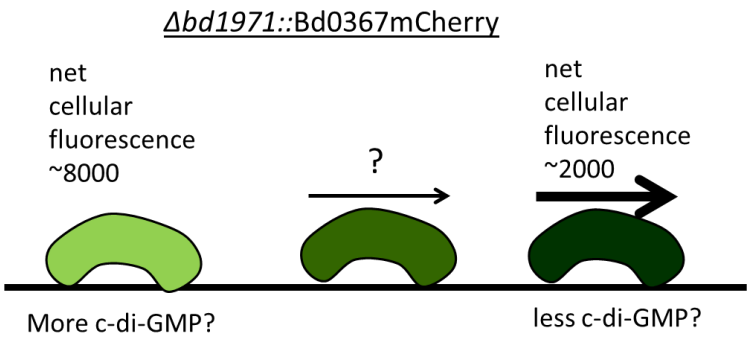

Figure 5.38 Stationary cells had high levels of Bd0367mCherry fluorescence whereas motile cells had low level cellular fluorescence.

Studying the Δ*bd1971*::Bd0367mCherry cells that could glide identified 16 cells, analysis of these cells confirmed that there was a significantly lower level of Bd0367mCherry in cells that could glide compared to stationary cells. This suggests a heterogeneous nature of the *Bdellovibrio* population and also suggests that the c-di-GMP level in the gliding cells may be lower than their non-gliding neighbours. This would be interesting to assess via c-di-GMP biosensors like the RNA-based fluorescent biosensors created by fusing the Spinach aptamer to variants of a natural GEMM-I riboswitch by (Kellenberger et al, 2013). This allowed live cell imaging experiments and fluorescence in response to c-di-GMP, these sensors are still being developed to allow accurate quantification of changes in the intracellular levels of cyclic di-nucleotides to be measured, but will be useful in the future.

This observation led to the two hypotheses, that the gliding cells may have lower c-di-GMP levels due to transcriptional regulation of Bd0367 at high c-di-GMP levels or due to post-translational regulation, in which Bd0367 is targeted by a specific protease for degradation at high c-di-GMP levels. The predicted promoter region of Bd0367 is shown in Section 8.3.3.1.

Model 1: Bd0367mCherry expression is controlled at the transcriptional level in response to changing levels of cellular c-di-GMP

This model suggests that increased cellular c-di-GMP levels in the Δ*bd1971* HD strain results in changes in *bd0367* transcription, these changes could be mediated by alterations in transcriptional regulators affinity to promotors. The first suggested mechanism is that high cellular c-di-GMP levels causes the destabilization of an unknown transcription factor (TF) from the promoter region of *bd0367*. This results in less transcription of

bd0367 in a similar manner to FleQ interaction being disrupted by c-di-GMP resulting in downregulation of flagella gene expression (Hickman & Harwood, 2008; Matsuyama et al, 2016). The alternative mechanism is that an unknown transcriptional regulator is stabilized by c-di-GMP binding at high cellular c-di-GMP levels, this transcriptional regulator with c-di-GMP bound can bind the promotor region of *bd0367* and at as a repressor to reduce the transcription of *bd0367*, see Figure 5.39.

However little work has been carried out into the roles of TFs in *Bdellovibrio*, it is tempting to speculate that Bd0156 a TF recently identified to bind c-di-GMP may be involved in this downregulation of *bd0367* this could be investigated by TF footprinting (Rotem et al, 2016)

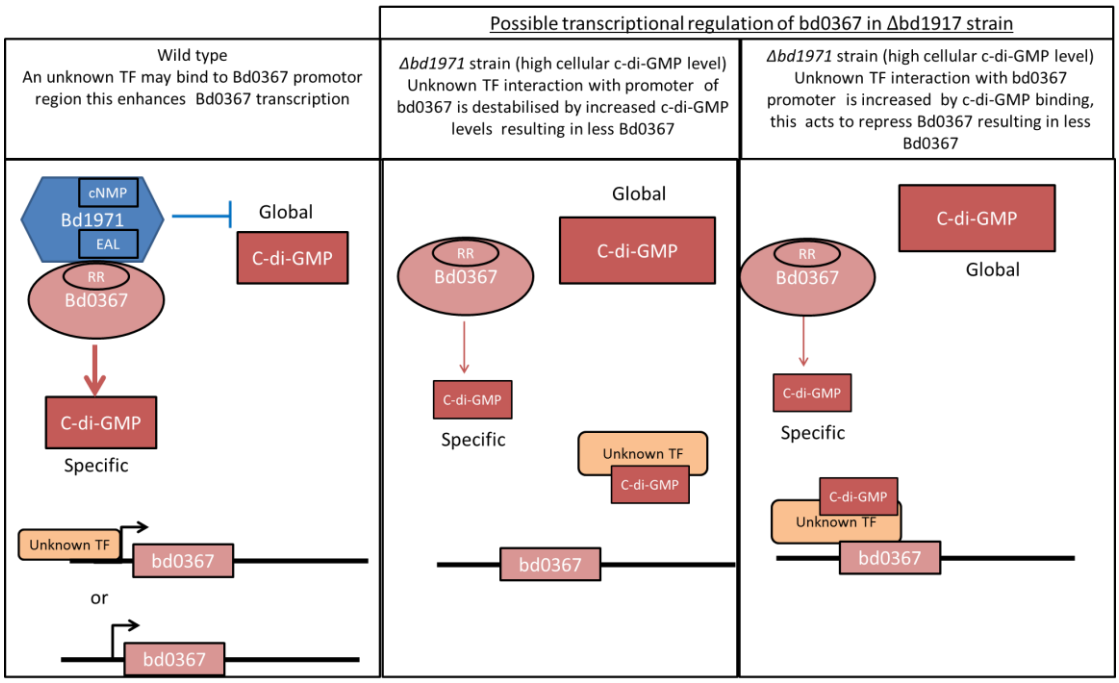

Figure 5.39 Model of transcriptional regulation of *bd0367*. In a high cellular c-di-GMP background of the Δ*bd1971* the fluorescent signal from Bd0367mCherry is reduced. This model proposes that the reduction in Bd0367 is controlled at the transcriptional level by an unknown transcription factor. The binding of the TF to the promotor region of *bd0367* is affected by the global cellular c-di-GMP level. The TF is predicted to bind c-di-GMP and that this binding will either remove an activating TF or stabilize a repressor, resulting in less *bd0367*. PDE proteins and processes are shown in blue, DGC and c-di-GMP producing/dependent processes are shown in red. The thickness of lines and size of c-di-GMP box represents the strength and quantity.

Model 2: Bd0367mCherry level is controlled at the post-translational level in response to changing levels of cellular c-di-GMP

This model suggests that increased cellular c-di-GMP levels in the Δ*bd1971* HD strain results in changes in the post-translational regulation of Bd0367. The increased cellular c-di-GMP levels could mediate Bd0367 degradation by the action of an unknown specific protease. This could occur by this protease being expressed or no longer repressed under high c-di-GMP conditions. Or the specific degradation of Bd0367 could be mediated by an unknown adaptor protein binding Bd0367 under high c-di-GMP conditions enabling recognition by the unknown protease, Figure 5.40. For example CpdR acts as an adaptor protein, binding PDE PdaA in specific conditions, which then enables PdeA degradation by ClpXP protease in *Caulobacter* (Abel et al, 2011).

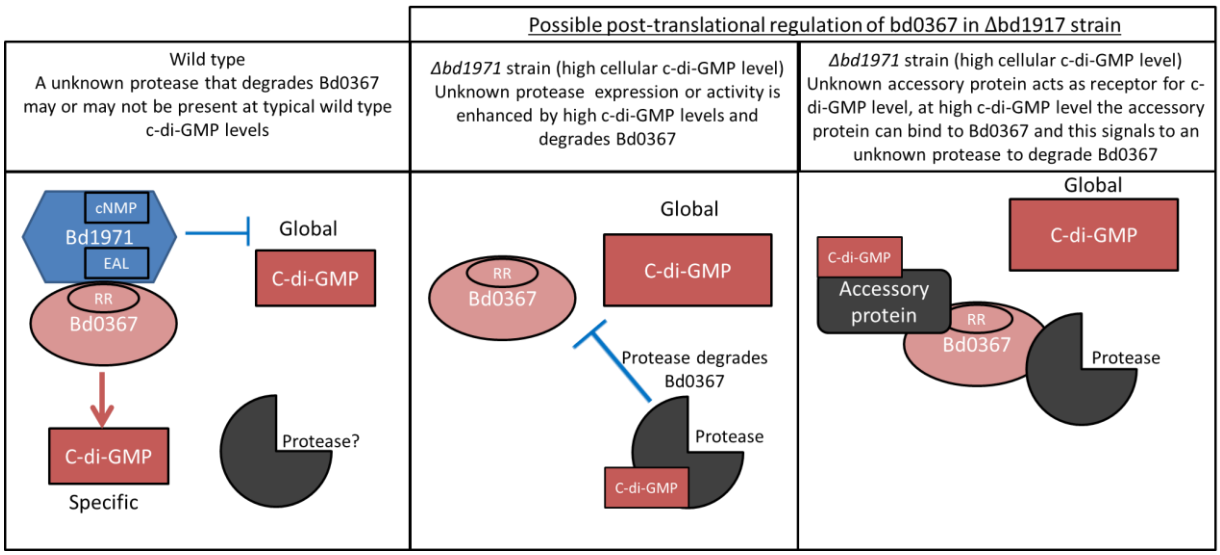

Figure 5.40 Model of post-translational regulation of *bd0367* by an unknown protease. High c-di-GMP levels act to stimulate protease action on Bd0367 this can occur alone of with the aid of an accessory protein. PDE proteins and processes are shown in blue, DGC and c-di-GMP producing/dependent processes are shown in red. The thickness of lines and size of c-di-GMP box represents the strength and quantity.

5.6. Further Experiments

To fully determine the mechanistic role of c-di-GMP signalling and elucidate the role of protein interactions on mediating gliding motility in *Bdellovibrio* the following experiments are recommended:

1. Make a site directed mutant of the phospho-receiving D63 in the Bd0367mcherry construct. Compare the location of Bd0367 when it is unable to be activated by phosphorylation. If the frequency of Bd0367D63A mCherry in polar locations alter this could suggest phosphorylation is important in mediating subcellular localisation of Bd0367.
2. To fully examine the role Bd0367 plays in c-di-GMP levels and protein interactions a number of new strains are required. Firstly the Bd0367 complement strain, which is currently under investigation by Dr Lowry to confirm restoration to WT c-di-GMP levels. Secondly a Bd0367 phospho-mimic and I site mutant strain to assess if this can cause overproduction of Bd0367 specific c-di-GMP and what phenotypic effects this may generate. Thirdly a Bd0367 GGDEF active site mutant should be created and analysed to determine if low frequency of gliding in the Bd0367D63A strain was caused by low c-di-GMP or by protein interactions being weakened due to lack of phosphorylation and dimer formation. As in the Bd0367GGDEF mutant c-di-GMP levels will be low but phosphorylation should still occur.
3. To begin to examine the role of cAG signalling by Bd0367 in *Bdellovibrio* requires a number of new strains. A mutation in an S amino acid has been identified by (Hallberg et al, 2016) to be critical for cAG production. A strain with this mutation in S214 amino acid has been constructed and is under investigation by Dr Lowry to determine the role of cAG in *Bdellovibrio*.
4. To fully examine the role of Bd1971 in c-di-GMP signalling requires further strain construction. Most importantly generation of the Bd1971 complementation strain and analysis of gliding phenotypes and c-di-GMP levels. Secondly it would be interesting to examine the mCherry fluorescence of the other DGC proteins of *Bdellovibrio* in this high c-di-GMP background to determine if other DGC proteins are being downregulated at high cellular c-di-GMP levels in addition to Bd0367mCherry. Thirdly a B2H alanine mutagenesis screen to observe the amino acids critical for the Bd1971- Bd0367 interaction, so this mutation lacking the specific interaction residues could be observed to see if this results in c-di-GMP levels similar to the gene deletion in the HD strain.
5. To try and identify the EPS utilised by *Bdellovibrio* and use different staining methods to determine if the high cellular c-di-GMP strains produce more EPS.

Also to find the genes necessary for EPS biosynthesis and mutate these genes to see if motility is restored in a high c-di-GMP background.

6. To establish if Bd0367 level is controlled by transcriptional regulation or protein degradation by investigating *bd0367* level by RT-PCR in the WT and Δ*bd1971*::bd0367mCherry strain.
7. To understand the heterogeneous levels of cellular c-di-GMP with in a *Bdellovibrio* population. To investigate this in real time via microscopy could be very useful in determining in the gliding cells had lower c-di-GMP than the stationary cells as well as quantifying variation in the cell population. However to do this requires the development of a c-di-GMP biosensor adapted for use in *Bdellovibrio*.

5.7. Chapter Conclusions

Overall my investigations have shown that Bd0367 DGC activity is activated by phosphorylation and that gliding motility can occur at low cellular levels of c-di-GMP, when Bd0367 protein is present. I have suggested that protein interactions and cellular c-di-GMP level may act together to control the percentage of *Bdellovibrio* cells that can glide. My work has demonstrated that high levels of cellular c-di-GMP impair *Bdellovibrio* gliding motility and has suggested ways to investigate the mechanisms behind that gliding impairment mechanism further.

Chapter 6. Investigation of PilZ domain genes in gliding motility

6.1. Introduction

As previously discussed in Chapter 1 gliding motility allows *Bdellovibrio* to encounter potential prey bacteria on solid surfaces (Lambert et al, 2011). HD attack phase *Bdellovibrio* cells can glide bi-directionally at speeds between 16 μm hr^{-1} and 35 μm hr^{-1}. *Bdellovibrio bacteriovorus* HD100 contains four operons with protein products AglR, AglQ and AglS, these proteins share homology with the MotA/B and TolQ/R proteins. In *Myxoccocus* it has been shown that AglR, AglQ and AglS are motor proteins and form a proton channel in the IM, and proteins AglQ and AlgR directly localise to clusters of gliding motility complexes indicating roles in adventurous gliding motility (Nan et al, 2011; Sun et al, 2011). The presence of AglR, AglQ and AglS in these four operons suggests these operons may be involved in *Bdellovibrio* gliding motility; these operons are *bd0416-0420, bd0828-0838, bd1471-1483*, and *bd2368-2377* shown in Figure 6.1 (Lambert et al, 2011; Luciano et al, 2011). The operon *bd1471-1483* is considered to be the most complete gliding operon present in *Bdellovibrio*. These gliding operons in *Bdellovibrio* also encode a selection of gliding transductor complex proteins (glt). In *Myxococcus* GltA-K proteins have been suggested to form a complex which spans from the cytoplasm to the OM and more specifically GltB and A have been shown to be OM β-barrel proteins that interact with periplasmic GltC forming an integral subcomplex for gliding motility in *Myxococcus* (Jakobczak et al, 2015; Luciano et al, 2011). To date little is known of the functions of the genes and proteins encoded in the *Bdellovibrio* gliding operons and most functionality is predicted from functions determined for similar proteins in *Myxococcus* as there has been extensive work into the particular protein functions in gliding motility within *Myxococcus* in recent years.

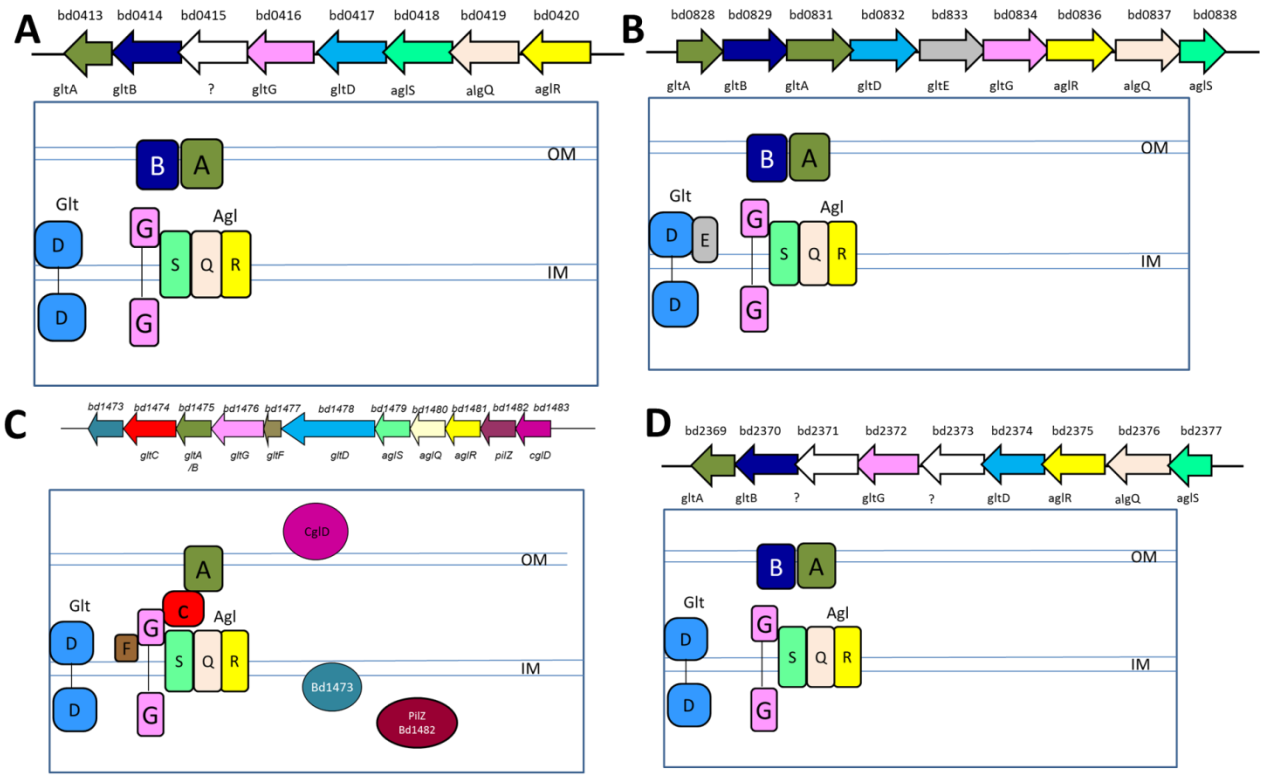

Figure 6.1 Four potential gliding operons in *Bdellovibrio*. The genes are colour coded to the proteins and are shown in their predicted cellular locations. The predictions were made using PSORTb or by using locations of homologous *Myxococcus* proteins from (Islam & Mignot, 2015; Jakobczak et al, 2015)(Yu et al, 2010).

6.1.1.1. Investigation of predicted gliding operons in *Bdellovibrio* by gene deletion and mCherry tagging studies

Work by Dr Milner on the potential gliding operon *bd1471-1483* (Figure 6.2) showed genes in this operon to be important in gliding motility, particularly Bd1481 (AglR homologue). *B. bacteriovorus* Bd1481-mCherry tagged strain was incubated on a 1% agarose CaHEPES surface to study fluorescence when gliding motility would be occurring. The cells fluorescence increased on surface incubation. Additionally Dr Milner's deletion of Bd1481 abolished gliding motility totally; however the deletion strain failed to complement when *bd1481* was reintroduced possibly due to polar effects. Another gene product of this operon was also C-terminally mCherry tagged, Bd1473 a novel protein with signal peptide and no homology to other known gliding proteins. The *B. bacteriovorus* Bd1473mCherry strain resulted in an altered gliding phenotype of hyper reversals. Additionally when incubated on a surface the cells fluorescence increased and resulted in a location change to dominant monopolar foci. RT-PCR also showed that *bd1473* transcription was up regulated when compared to RNA obtained from *B. bacteriovorus* before and after surface incubation (Milner, 2014).

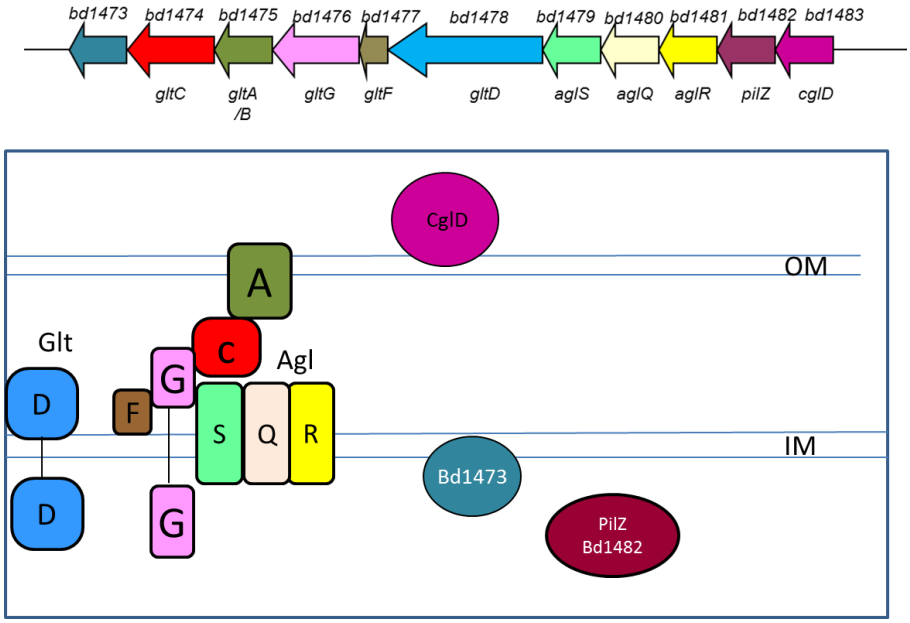

Figure 6.2 Most work to date has been carried out on the *bd1471-1483* gliding operon in *Bdellovibrio* . The genes are colour coded to the proteins and are shown in their predicted cellular locations. The predictions were made using PSORTb by using locations of homologous *Myxococcus* proteins shown in (Islam & Mignot, 2015; Jakobczak et al, 2015)(Yu et al, 2010) to assign predicted cellular location.

Dr Milner also worked on another gene *bd0836* from the other suggested gliding operon *bd0828-0838*. However RT-PCR data showed no increase in *bd0836* transcription on surface incubation suggesting there may be redundancy between the multiple operons (Milner, 2014). These current data show a surface response for genes encoded in the operon *bd1473-1483,* which suggests this may be a key operon for gliding motility in *Bdellovibiro.*

The proposed protein roles and homology for the proteins of the *Bdellovibiro* gliding operon *bd1473-1483* were analysed by Dr Milner and Figure 6.3 shows these proteins compared with *Myxococcus*.

Gene	Protein length (amino acids)	*Proposed M. xanthus* homologue	Conserved domains	Signal peptide? (SignalP)	Cellular compartment (PSORTb)
bd1473	217	Not significant	Coiled coil domain	Sec (1-24)	Unknown
bd1474	713	MXAN_2541 (GltC)*	TPR domain Coiled coil domain	Sec (1-24)	Unknown
bd1475	254	MXAN_2540 (GltA)*	OM channel	Sec (1-18)	Unknown
bd1476	488	MXAN_4867 (GltG)*	TolA/TonB C-terminal domain	Not predicted	Unknown
bd1477	82	MXAN_4868 (GltF)*	Transmembrane domain	Sec (1-21)	Unknown
bd1478	1237	MXAN_4870 (GltD)*	TPR domain	Sec (1-20)	Unknown
bd1479	167	MXAN_6860 (AglS)*	ExbD/TolR transport protein	Not predicted	Unknown
bd1480	185	MXAN_6861 (AglQ)*	ExbD/TolR transport protein	Not predicted	Cytoplasmic
bd1481	236	MXAN_6862 (AglR)*	Transmembrane domain MotA/ExbB proton channel	Not predicted	Cytoplasmic membrane
bd1482	206	N/A (PilZ)	PilZ domain	Not predicted	Cytoplasmic
bd1483	353	MXAN_0962 (CglD)	von Willebrand factor type A domain	Sec (1-19)	Extracellular

Figure 6.3 The *bd1473-1483* gliding operon protein homology in comparison to *Myxococcus*. Analysis conducted by Dr Milner to determine the conserved domains, cellular locations and proposed homologues. The * indicated the minimum protein requirements for gliding motility as predicted by Luciano (Milner, 2014)

6.1.2. Regulation of direction of travel when moving via gliding motility

The study of how gliding direction is determined in bacteria has been best examined in *Myxococcus*; where distinct proteins are used to define the leading and lagging poles and signals are sensed that mediate pole switching of gliding machinery from the leading to lagging pole. As mentioned in Chapter 1 these cells typically reverse direction every 8-10 minutes (Spormann & Kaiser, 1995).

6.1.2.1. Pole defining proteins in *Myxococcus* polarity module

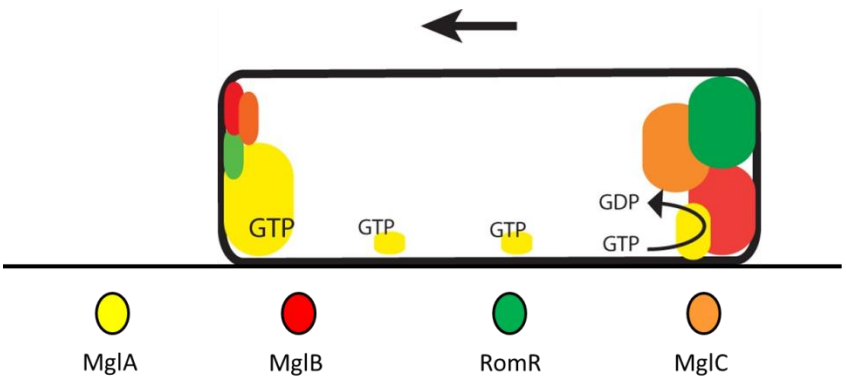

Figure 6.4 Regulation of motility polarity in *Myxococcus*. Figure shows the location of the pole defining proteins in *Myxococcus* in an actively gliding cell moving in the direction indicated by the arrow. The amount of the protein is represented by the size of the coloured patch and the role of MglA-GTP vs MglA-GDP is also shown. MglA is predominantly found at the leading pole, but is also associated with the gliding motility complexes along the cell, MglB is found predominantly at the lagging cell pole with RomR and newly discovered MglC Adapted from (McLoon et al, 2016)

As Figure 6.4 shows MglA, MglB, MglC and RomR are proteins used to determine cell polarity, creating a leading and lagging pole for gliding motility in *Myxococcus*. The roles of these proteins are outlined in Table 6.1.

Protein	Role	Deletion or mutation phenotype	Reference
MglA	It is a Ras-like GTPase and modulating its activity depending of the GTP or GDP bound state. When MglA is GTP it interacts with RomR When activated and GTP bound MglA is found at the leading pole and stimulates the formation of gliding motility complexes and moves with these complexes towards the lagging pole	Deletion results in no gliding motility	(Leonardy et al, 2010; Zhang et al, 2010)
MglB	MglB is located at the lagging pole and stimulates disassembly of motility complexes so prevents reversals. MglB is also an MglA GTPase Activating Protein (GAP) which causes MglA –GTP hydrolysis at the lagging pole leading to dissociation of MglA from the motility complex. This action prevents MglA accumulation at the lagging cell pole	Required for proper regulation of gliding frequency, on deletion hyper-reversal occurs.	(Leonardy et al, 2010; Zhang et al, 2010)
MglC	MglC is located at the lagging pole and correct polar localization of MglC depends on RomR and MglB.	Deletion results in hypo-reversal frequency.	(McLoon et al, 2016)
RomR	RomR is located predominantly at the lagging pole, with small cluster at leading pole. RomR acts as a link between Frz system and MglA/MglB. Phosphorylation of RomR causes polar release of MglA and MglB and reorganisation to opposite poles.	A phosphomimic resulted in hyper-reversals. Whereas when RomR cannot be phosphorylated there are hypo-reversals Deletion results in loss of A gliding motility	(Keilberg et al, 2012; Leonardy et al, 2007; Zhang et al, 2012)

Table 6.1 Pole defining proteins in *Myxococcus*

6.1.2.2. Gliding directional regulation in *Myxococcus*

The polarity axis formed in the actively gliding cell by MglA, MglB, MglC and RomR is stable unless it is contacted by upstream Frz signals, these signals can interface with the MglA/MglB/MglC/RomR module to invert cell polarity and cause a cellular reversal (Guzzo et al, 2015). The Frz chemosensory system regulates gliding directionality in *Myxococcus* by sensing chemotactic signals and transducing these signals (Figure 6.5). An unknown signal is sensed by inner membrane spanning FrzCD methyl-accepting chemotaxis proteins (MCP), FrzCD can be methylated, catalysed by FrzF. The signal is then relayed through phospho-relay involving phospho transfer from HK FrzE to FrzZ a RR domain protein (Inclan et al, 2008). Deletion of *frzCD*, *frzA*, *frzE* or *frzZ* genes cause *Myxococcus* to show hypo-cell reversal frequencies (Kaimer & Zusman, 2016). Whereas a point mutation (D709A) in the RR domain of FrzE (HK) affects the phosphorelay and results in hyper reversals as cells reverse more with increasing phosphorylation of FrzZ (Li et al, 2005) . This shows that the pole switching that leads to directionality changes in gliding motility is controlled by the Frz system, which therefore regulates cellular gliding reversals. However though FrzZ localises to the leading pole on phosphorylation it is not yet know what other proteins it may interact with to modulate this change (Kaimer & Zusman, 2013). The Frz system may interact via FrzE with RomR (which has a RR domain) to signal change but this has yet to be shown experimentally (Kaimer & Zusman, 2016).

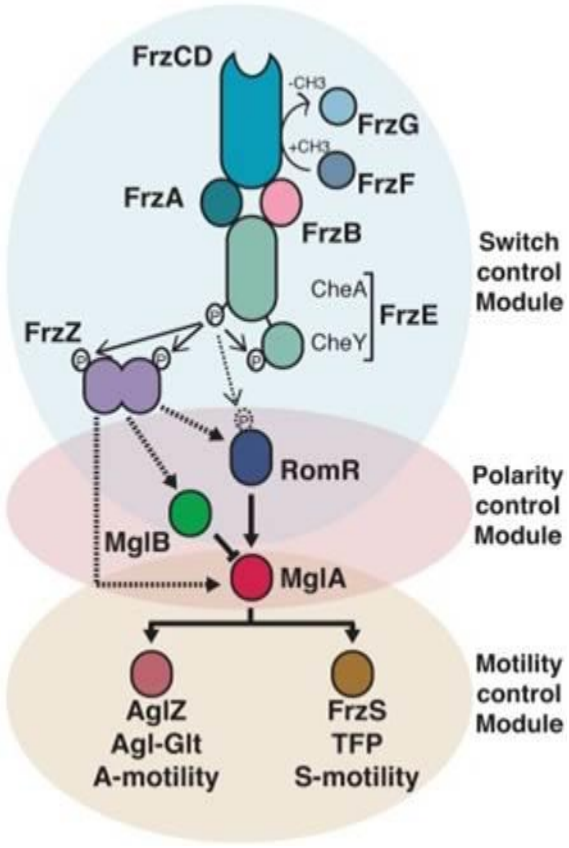

Figure 6.5 The Myxococcus Frz chemotaxis gliding signalling system. Reproduced from (Guzzo et al, 2015). The Frz system is thought to promote a phosphorylation cascade that activates reversals. Activation of the FrzCD receptor by unknown signals activates the auto-phosphorylation of the FrzE kinase through FrzA. The exact function of FrzB is unknown. HK FrzE then transfers a phosphoryl group to as many as three RR proteins, (FrzE RR), the FrzZ protein, and potentially to RomR. The phosphorylated events are thought to modulate the polarity proteins and trigger their re-localization to opposite poles. Plain arrows indicate established interactions and dotted arrows indicate suspected interactions.

.

6.1.2.3. Gliding directional regulation in *Bdellovibrio*

MglA and RomR are repurposed for predation

It was initially assumed that as *mglA* and *rom*R are conserved in *Bdellovibrio*, their products could play a role in regulating gliding direction in *Bdellovibrio*. However the FrZ system and *mglB* are not conserved in *Bdellovibrio* which suggested that an alternative signalling mechanism would be required to control reversals during gliding in *Bdellovibrio* compared to the regulation seen in *Myxococcus* (Blackhart & Zusman, 1985). Dr Milners' work on gliding regulation in *Bdellovibrio* established that deletion of MglA abolished prey invasion and reduced type IV pili formation but had no effect on gliding motility (Milner et al,

2014). This suggested that the role of MglA has been repurposed during evolution in *Bdellovibrio* to facilitate prey invasion. Interaction studies with MglA, identified an interaction with membrane associated TPR protein Bd2492 found at the prey interaction pole, this protein was also shown to be necessary for predation. Deletion of RomR could not be obtained suggesting that in *Bdellovibrio* RomR is essential in both life styles. Additionally $RomR_{Bd}$ did not directly interact with $MglA_{Bd}$ as was seen in *Myxococcus*. Taken together the study showed that MglA, RomR and a complex of other proteins work together to facilitate type IV pilus associated prey invasion in *Bdellovibrio* and do not regulate the direction of gliding, Figure 6.6.

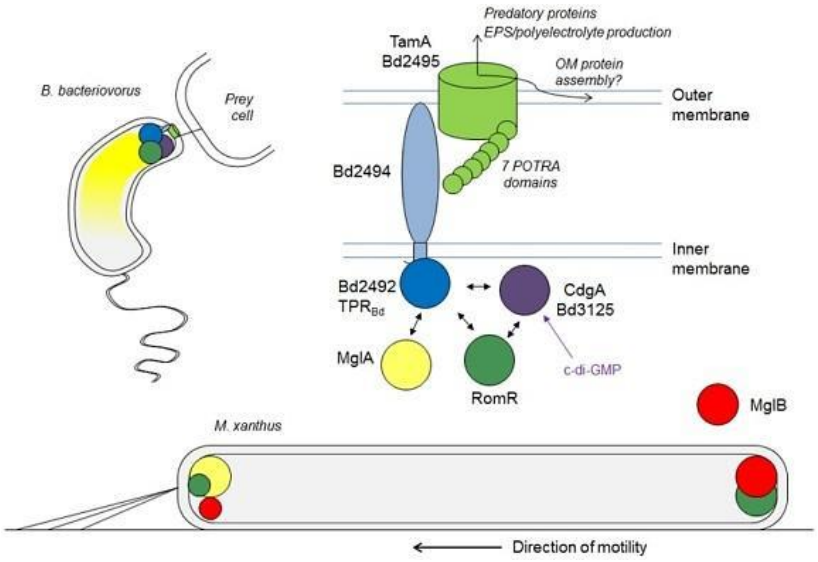

Figure 6.6 Predatory hub: shows the organisation and interaction structure of the MglA predatory complex in *Bdellovibrio* in comparison to the MglA gliding complex in M.xanthus. Figure reproduced from (Milner et al, 2014)

Unknown mechanism of gliding directional regulation in *Bdellovibrio*

It can be presumed that in *Bdellovibrio* the gliding motility system will still require proteins that localise asymmetrically to cell poles in order to determine which is the leading and lagging pole when cells are actively gliding and that during cell reversals these proteins are released from their poles and bind to the opposite pole, enabling inversion of cell polarity. Hence the leading pole is now the lagging pole. What these proteins are in *Bdellovibrio* is unknown

It is unknown how environmental signals are transduced in *Bdellovibrio* to result in an altered gliding direction but c-di-GMP is a candidate.

So the question remains as to which proteins are involved in coordinating and regulating direction of gliding in *Bdellovibrio*. It can be postulated that c-di-GMP levels and related proteins could be involved in this process, due to the abolition of gliding motility in the Bd0367 DGC deletion.(Hobley et al, 2012) and from work previously presented in this thesis show how differing levels of c-di-GMP can alter gliding motility. This line of inquiry was continued by the work carried out in this chapter.

6.1.3. PilZ domains and motility

PilZ domain proteins have been discovered to be important transducing c-di-GMP levels into outputs that regulate the degree of motility by targeting proteins that are involved in motility or biofilm processes. For example BcsA in *Salmonella* synthesizes cellulose on c-di-GMP binding promoting biofilm formation or YcgR regulates flagella based motility by interacting with flagellar switch complex proteins and inhibiting motility (Zorraquino et al, 2013) (Paul et al, 2010). Another PilZ domain protein FlgZ can been found to mediate swarming motility in *Pseudomonas aeruginosa* by c-di-GMP-bound FlgZ preventing motility by interacting with the MotCD stator (Baker et al, 2016). This was of interest to this study as DGC Bd0367 is involved in regulating gliding motility in *Bdellovibrio* suggesting a c-di-GMP input; but the mechanism by which this signal is transduced into an effect is unknown. It is possible that this signal is transduced by one of the many c-di-GMP proteins of *Bdellovibrio*.

6.1.3.1. PilZ domain proteins in *Bdellovibrio*

Bdellovibrio originally had 15 PilZ domain proteins identified bioinformatically (Amikam & Galperin, 2006; Hobley et al, 2012). Recent research by Rotem and colleagues has identified 4 more potential PilZ domain proteins and confirmed that c-di-GMP binds to 11 of these identified PilZ domain proteins (see Table 6.2) (Rotem et al, 2016).

For a number of years groups of undergraduate students have been investigating individual PilZ domain proteins of *Bdellovibrio* in the Sockett Lab. This work has involved fluorescent mCherry tagging of the PilZ domain proteins with analysis of the PilZ proteins expression throughout predatory time courses. More recently the students made B2H constructs of the PilZ domain proteins, some of these constructs were truncated versions of PilZ domain proteins and all were only N terminally tagged. These PilZ domain constructs were tested in *E. coli* cells for interactions against the *Bdellovibrio* DGC proteins Bd0367, Bd0742 and Bd1434.

This was investigated as physical interactions between PilZ domains or c-di-GMP receptor proteins and DGC protein has been postulated to be a mechanism that can be used to insulate signalling pathways and maintain signalling specificity (Dahlstrom et al, 2015; Lindenberg et al, 2013).

However to date only one PilZ domain protein Bd3100 has been found to directly interact with a DGC. Other specific PilZ- DGC interactions may yet be found as the non-interaction could be due to the tagged orientation of the proteins or to do with alterations in structure following truncation of some of the PilZ domain proteins to remove the transmembrane membrane region or the predicted signal sequence.

6.1.4. Background to the work presented in this chapter

As I started my PhD, Aidan Taylor (Undergraduate student) and Dr Milner identified a PilZ domain protein Bd3100 that interacts with Bd0367 via B2H analysis. Deletion of this PilZ domain protein from *B. bacteriovours* HD100 resulted in an alteration of gliding motility behaviour. The Bd3100 deletion strain exhibits a hyper reversal gliding phenotype. At this point I carried on the research that they began.

6.2. Specific Research Aims

- To assess the interaction between PilZ protein Bd3100 and protein subdomains of DGC Bd0367 via B2H assays and quantify this and the previously discovered interaction by β-galactosidase assays.

- To analyse levels of cellular fluorescence in the Bd3100-mCherry strain when incubated on a surface versus liquid.
- To fully quantify the gliding phenotype of the previously made in-frame deletion strain of *bd3100*.
- To complement the *bd3100* deletion mutant strain and analyse its phenotype.
- To investigate the location of Bd3100mCherry in a low and high c-di-GMP cellular background to assess if c-di-GMP binding effects localisation or expression of Bd3100.
- To analyse levels of cellular fluorescence of a protein in the gliding operon, Bd1473. The Bd1473-mCherry strain fluorescence was assessed when incubated on a surface versus liquid.

- To examine the effect that *bd3100* deletion had on localisation of other predicted gliding protein Bd1473.
- To investigate PilZ domain protein Bd1482, which has partial identity with Bd3100; changes in fluorescent PilZ domain protein Bd1482mCherry strain when incubated on a surface versus liquid.
- To analyse the gliding phenotype of the Bd1482mCherry strain.
- To investigate the possibility of PilZ protein Bd3100 interacts with other PilZ domain proteins implicated in gliding motility via B2H assays.
- To try to develop a protein co-purification assay using the Bd3100mCherry strain to identify native partner proteins of Bd3100.

6.3. Hypotheses

- DGC protein Bd0367 and PilZ protein Bd3100 will interact via the DGC domain as deletion of c-di-GMP producer Bd0367 abolishes gliding motility and PilZ c-di-GMP receptor protein Bd3100 is also involved in the regulation of gliding motility. This will suggest that the c-di-GMP produced by Bd0367 may have a specific role mediated by a contact dependent, direct transfer to Bd3100 as well as a role in controlling the global level of c-di-GMP in the cell.
- PilZ domain proteins that are also putative gliding proteins (Bd3100 and Bd1482) will likely be up-regulated when incubated on a surface. These proteins will be identified by observing increases in the fluorescently tagged proteins when placed on surfaces.
- As Aidan Taylor observed that the deletion of *bd3100* increased gliding reversals, I hypothesis that other aspects of gliding motility will also be effected by this gene deletion; and that complementation with Bd3100 should reduce reversal rate in towards wild type.
- Gliding protein Bd1473 will likely be up-regulated when incubated on a surface this will be identified by observing increases in the fluorescently tagged proteins when placed on surfaces.
- I predict that Bd3100 and Bd1473 may function in the same pathway due to the Bd1473mCherry strain also having a hyper-reversal gliding phenotype. In the absence of Bd3100 I predict the localisation pattern of Bd1473mCherry will alter.

- I predict that PilZ domain protein Bd1482 will have a role in gliding motility, and that this will cause an increase in fluorescence when Bd1482mCherry is incubated on a surface and potentially the mCherry tag will result in impairing Bd1482 function leading to gliding motility defects.
- The two PilZ proteins with one or more DUF4339 domains, Bd3100 and Bd1482 may have diverged sufficiently to control different aspects of gliding motility. However they may interact with each other to deliver a co-ordinated gliding response.
- Bd3100mCherry co-purification assay will identify other proteins hypothesised to be involved in gliding motility and potentially interact with novel proteins of unknown function.

6.4. Results

6.4.1. Bioinformatics analysis of Bd3100 PilZ domain protein

6.4.1.1. Data on PilZ domain proteins of *Bdellovibrio*

As mentioned in the introduction *Bdellovibrio* possesses a large array of PilZ domain containing proteins. The current data about these proteins is displayed in Tables 6.2 and 6.3. One table displays the data on the structural and c-di-GMP binding status of the PilZ domain protein and the other table shows the predicted expression profile using microarray data and the documented fluorescent location of mCherry tagged versions of these proteins.

The data for c-di-GMP binding status was gathered from work by Rotem and colleagues, they provided the first physiochemical proof as to which PilZ domain proteins were found to interact with the c-di-GMP capture compound, which allowed some PilZ domain proteins to be confirmed as c-di-GMP binders (Rotem et al, 2016). This group concluded that 11 out of the 19 PilZ domain proteins were c-di-GMP receptors and that one was a potential c-di-GMP binder.

The predicted expression patterns of these c-di-GMP receptor genes were collated from whole genome micro-array data and are displayed in Table 6.3. The micro-array data was obtained by extracting RNA from attack phase cells, HI cells and synchronously infecting cells at 30 minutes of predatory growth (Lambert et al, 2010a). The PilZ-mCherry tagged fluorescent cellular locations were compiled from data collected by multiple years of

undergraduate project. The location and timings of expression of the PilZ domain proteins can allow hypothesises of potential functions.

Table 6.2 PilZ domain protein structure, cellular location and c-di-GMP binding status. C-di-GMP binding data is taken from (Rotem et al, 2016). The red depicts the PilZ domain proteins investigated in this study.

Gene number	Domains	Predicted cellular compartment (PSORTb)	Did PilZ bind c-di-GMP capture compound? (Rotem et al, 2016)	RRXXXR and D/NXSXXG motif
Bd0064	PilZ domain	Unknown	No	$_{22}$RNYAR$_{26}$ $_{35}$NISITG$_{40}$
Bd0378	PilZ domain	Unknown	Yes	$_{236}$RLLFR$_{240}$ $_{199}$DISLSG$_{204}$
Bd0642	PilZ domain (hemolysin)	Cytoplasmic	Yes	$_{105}$RRVVYR$_{110}$ $_{140}$DLSSQE$_{144}$
Bd1007	PilZ domain Transmembrane domain	Unknown	Yes	$_{6}$RYHGR$_{10}$ $_{42}$NVSLFG$_{47}$
Bd1482	PilZ domain Low complexity region Duf4339	Cytoplasmic	Yes	$_{84}$RKCPR$_{89}$ $_{100}$SVSENG$_{105}$
Bd1996	PilZ domain Duf4339	Unknown	Yes	$_{127}$RRSHPR$_{132}$ $_{154}$SISEGG$_{159}$
Bd2059	PilZ domain 4 Transmembrane domains Signal sequence	Cytoplasmic membrane	Yes	$_{145}$RYDFR$_{149}$ $_{166}$DLSYTG$_{171}$

Bd2524	PilZ domain 4 Transmembrane domains	Cytoplasmic membrane	Yes	$_{151}$DLSYTG$_{156}$ Type 2
Bd2545	Subtilisin like serine protease domain PilZ domain 1 transmembrane 2 low complexity regions	Extracellular	No	$_{528}$RRKHDR$_{533}$ $_{555}$TISQGG$_{559}$
Bd2717	PilZ domain	Cytoplasmic	Yes	$_{111}$RRANAR$_{116}$ $_{145}$DVSAGG$_{150}$
Bd2880	PilZ domain	Cytoplasmic	Yes	$_{109}$RKNYR$_{113}$ $_{142}$DLSTEG$_{147}$
Bd3100	PilZ domain 2x Duf4339	Unknown	Yes- however was not significantly enriched in 3 out of 5 experiments.	$_{167}$RRRHVR$_{172}$ $_{194}$EISAGG$_{199}$
Bd3138	PilZ domain 4 transmembrane domains, signal peptide	Cytoplasmic membrane	Yes	- $_{156}$SISGGG$_{161}$ Type 2
Bd3232	PilZ domain	Unknown location	No	$_{60}$NISQTG$_{65}$ Type 2
Bd3527	PilZ domain	Cytoplasmic	No	$_{220}$RLWIR$_{225}$ -
Bd0760	PilZ domain	Cytoplasmic	Yes	$_{43}$RRDVKR$_{48}$ $_{73}$DISENG$_{78}$
Bd1466	No conserved domains	Unknown location	No	$_{30}$RGVVR$_{34}$ -
Bd1616	PilZ domain	Unknown location	No	$_{131}$RKQDR$_{135}$ $_{62}$NLSLRA$_{67}$

Bd2147	PilZ domain	Unknown location	No	$_{123}$RQDKR$_{127}$ $_{160}$NISLNG$_{165}$

Table 6.3 PilZ domain protein predicted expression profile from microarray data and fluorescent cellular location The red depicts the PilZ domain proteins investigated in this study.

Gene number	Predicted expression profile from microarray data (Lambert et al, 2010a)	Location of fluorescence data
Bd0064	Array data shows decrease in HI	Throughout cell in HD and HI
Bd0378	Array data shows decrease in HI	Monopolar in attack phase or throughout cell HD and HI
Bd0642	Array data shows no change in HD or HI	Unknown
Bd1007	Array data shows decrease in HI	Throughout cell in HD and absent in HI
Bd1482	Array data shows decrease in HI.	Throughout cell in HD and HI
Bd1996	Array data shows no change in expression in HD or HI	Unknown
Bd2059	Array data shows no change in expression HD or HI.	Periplasmic location HD and HI (higher in HI)
Bd2524	Array data shows decrease on prey entry and HI growth compared to attack phase.	Throughout cell HD and HI
Bd2545	Array data shows decrease on prey entry and HI growth compared to attack phase	Throughout cell HD no expression in HI
Bd2717	Array data shows increase in expression in HI.	No expression HD. Throughout cell HI
Bd2880	Array data shows decrease in HI	Mono-polar attack phase otherwise throughout cell
Bd3100	Array data shows decrease on prey entry and HI growth compared to attack phase	Mono-polar, bi-polar and throughout cell seen in HD and HI

Bd3138	Array data shows increase in HI	Throughout cell in HD and monopolar HI
Bd3232	Array data shows down in HI.	None visible in HD and monopolar in HI
Bd3527	Array data is down in HI.	None observed,
Bd0760	Array data shows down in HI and down on prey entry meaning attack phase specific	Unknown
Bd1466	Array data down in HI	Unknown
Bd1616	Array data down in HI	Unknown
Bd2147	Array data shows decrease on prey entry and HI growth compared to attack phase.	Unknown

6.4.1.2. Comparison of the three PilZ domains with DUF4339 domains

A PilZ domain protein of interest in this study Bd3100 has an additional two domains. These domains are both DUF4339 domains and two other PilZ domain proteins in *Bdellovibrio* also have a form of the DUF4339 domain, Bd1996 and Bd1482 Figure 6.7.

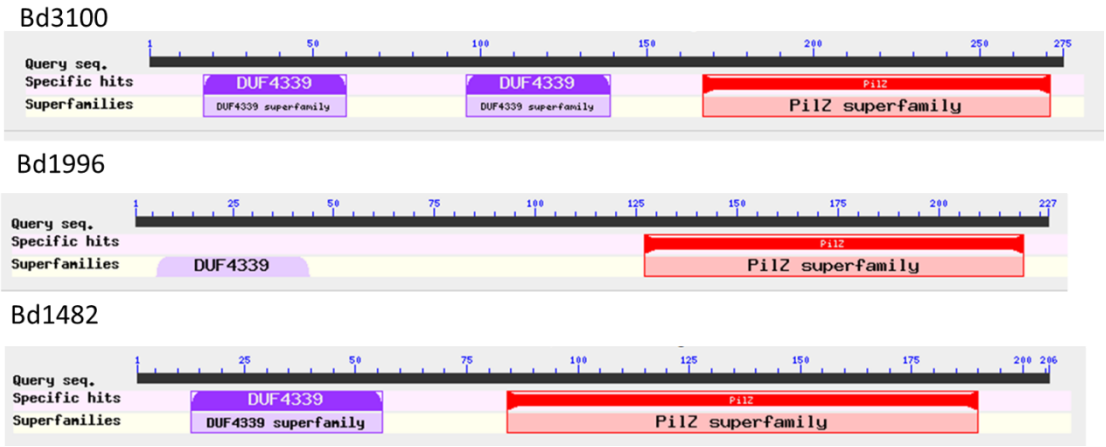

Figure 6.7 Three PilZ domain proteins in *Bdellovibrio* also have DUF4339 domains. Domains identified via CDD for Bd3100, Bd1996 and Bd1482 (Marchler-Bauer et al, 2015).

The DUF4339 domain is approximately 50 amino acids and of unknown function with a conserved G and W. It is found in bacteria, archaea and eukaryotes and has homology with the eukaryotic GYF proline binding domain, this is a fold that is involved in signalling through proline-rich sequences (Gu et al, 2005). Dr Milner previously

investigated DUF4339 domains and suggested that as the GYP domain recognised PPG-X-(R/K) a DUF4339 domain may bind a similar motif. From this he identified the potential binding motif in GltD homologues in *Bdellovibrio* Bd0832, Bd1478 and Bd2374. It was suggested these PilZ domain proteins (only Bd3100 and Bd1482 were tested) may interact with these proteins to regulate gliding motility, however these interactions were not established by the B2H analysis. This may have been due to Bd0832, Bd1478 and Bd2374 being truncated in the B2H constructs (Milner, 2014). So to date it is currently unknown which proteins this type of DUF4339- PilZ domain protein may interact with, however the potential interaction proteins are still hypothesised to be in the gliding proteins due to the location of Bd1482 in the gliding operon.

The relevance of *Bdellovibrio* having 3 proteins with similar domain architecture was of interest and it was speculated that these could be paralogs resulting from gene duplication, which could result in the proteins retaining the same function and being redundant or these proteins have evolved a divergence of function. The alignments by clustal omega (section 8.3.4.1) have shown that these domains are not identical and that the percentage identify between the three proteins is low. Bd3100 has 22.32% ID with Bd1996 and 27.75% with Bd1482. The percentage ID between Bd1482 and Bd1996 is 17.65%. When the proteins were split to compare only DUF4339 domains it was found that DUF4339 domains of Bd1996 and Bd1482 were only similar to the second DUF4339 domain of Bd3100 (section 8.3.4.1) however the percentage identify between these DUF4339 domains was still low. The second DUF4339 domain of Bd3100 has 26.19% ID with the DUF4339 domain of Bd1996 and DUF4339 domain of 35.56% ID with Bd1482. This suggests that the function of these three proteins cannot be inferred by homology and that these proteins have probably evolved to have different functions and binding partners in *Bdellovibrio*.

6.4.2. Investigating interactions between DGC proteins and PilZ domain proteins

These interactions studies were started as a result of published data from (Ryan et al, 2012) that showed how DGC proteins can have other regulatory roles in protein complexes, independent of their primary enzymatic role. In the cited study a protein complex that includes a GGDEF domain recruits a PilZ domain protein to control motility (Ryan et al, 2012). There is also other literature that demonstrates the role of c-

di-GMP receptor proteins in recruiting GGDEF proteins to particular cell poles (Dueriget al., 2009; Abelet al., 2011) and a recent study citing specific physical interactions between DGCs and effectors to result in co-ordinated responses to limit cross talk (Dahlstrom et al, 2015). There is increasing evidence that DGC domain proteins are regulating more than just c-di-GMP turnover, Dr Milner began to investigate interactions between the DGC protein Bd0367 and the PilZ domain proteins Bd3100 and Bd1482 via B2H assays. These proteins were chosen as Bd0367 has been shown to regulate gliding motility in *B. bacteriovorus* and PilZ proteins Bd3100 and Bd1482 had been postulated to be involved in gliding motility, due to operon location and DUF4339 domain similarity. His preliminary B2H assays showed that Bd3100 interacted with Bd0367 however the construct of Bd1482 did not (all were N terminally tagged). In this study the Bd0367-Bd3100 interaction was further investigated via additional B2H assays and quantitatively analysed via the first β-galactosidase assays. This interaction is further dissected by observing Bd3100 interactions with the split domains of Bd0367.

6.4.2.1. Bacterial two-hybrid and β-galactosidase assays suggests that DGC Bd0367 interacts with PilZ domain protein Bd3100

As Bd0367 and Bd3100 are both involved in gliding motility it was hypothesised that they would interact and by acting together coordinate gliding motility regulation. B2H analysis in an adenylate cyclase negative *E.coli* was used to test this interaction (Section 2.8.1) (Karimova et al, 1998). The genes were cloned into plasmids pUT18c and pKT25 which tagged the N terminus of the proteins with the T18 or T25 sections of adenylate cyclase. The tagged constructs of Bd0367 and Bd3100 were cloned by Dr Milner and Rob Till. The *bd0367* construct was cloned from base 34 as the HD100 genome start site was compared with *B. bacteriovorus Tiberius* genome and with RNA sequencing data, predicting this as the correct start site (section 8.3.1.1). If the test proteins interact the T25 and T18 fragments are brought together and reform adenylate cyclase, cAMP causes the expression of the *lacZ* reporter gene, this results in blue colonies on plates containing X-gal.

The result of a typical bacterial two-hybrid assay for Bd3100 and Bd0367 is shown in (Figure 6.8). Bd3100 and Bd0367 consistently produced uniform blue spots in both orientations tested as demonstrated in (Figure 6.8).

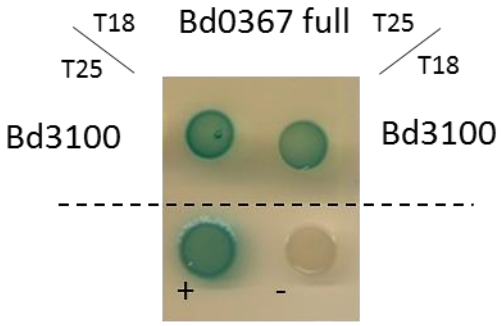

Figure 6.8: Spot plate interactions of full length GGDEF protein Bd0367 with full length PilZ protein Bd3100. Blue spots suggest an interaction between Bd0367 and Bd3100. This interaction is seen in both tag orientations. Results displayed are a typical representation of the results from three biological repeats and nine technical repeats Positive (+) = pUT18c-zip with pKT25-zip. Negative (-) = pUT18c with pKT25.

The bacterial two-hybrid spot plate analysis allows a qualitative assessment of the interaction between Bd0367 and Bd3100. Further testing of this interaction was carried out by β-galactosidase activity assays, these assays were used to quantify the strength of interaction between the two proteins. From these results Bd0367 and Bd3100 interact significantly more than the negative but only in one tagged orientation (Bd3100-T25 and Bd0367-T18) Figure 6.9. This suggests the other orientation experiences some steric hindrance or that protein stoichiometry is important. The interaction strength observed is significant even though it is lower than some other interactions previously described. This suggests that the interaction between Bd0367 and Bd3100 is of a transient nature.

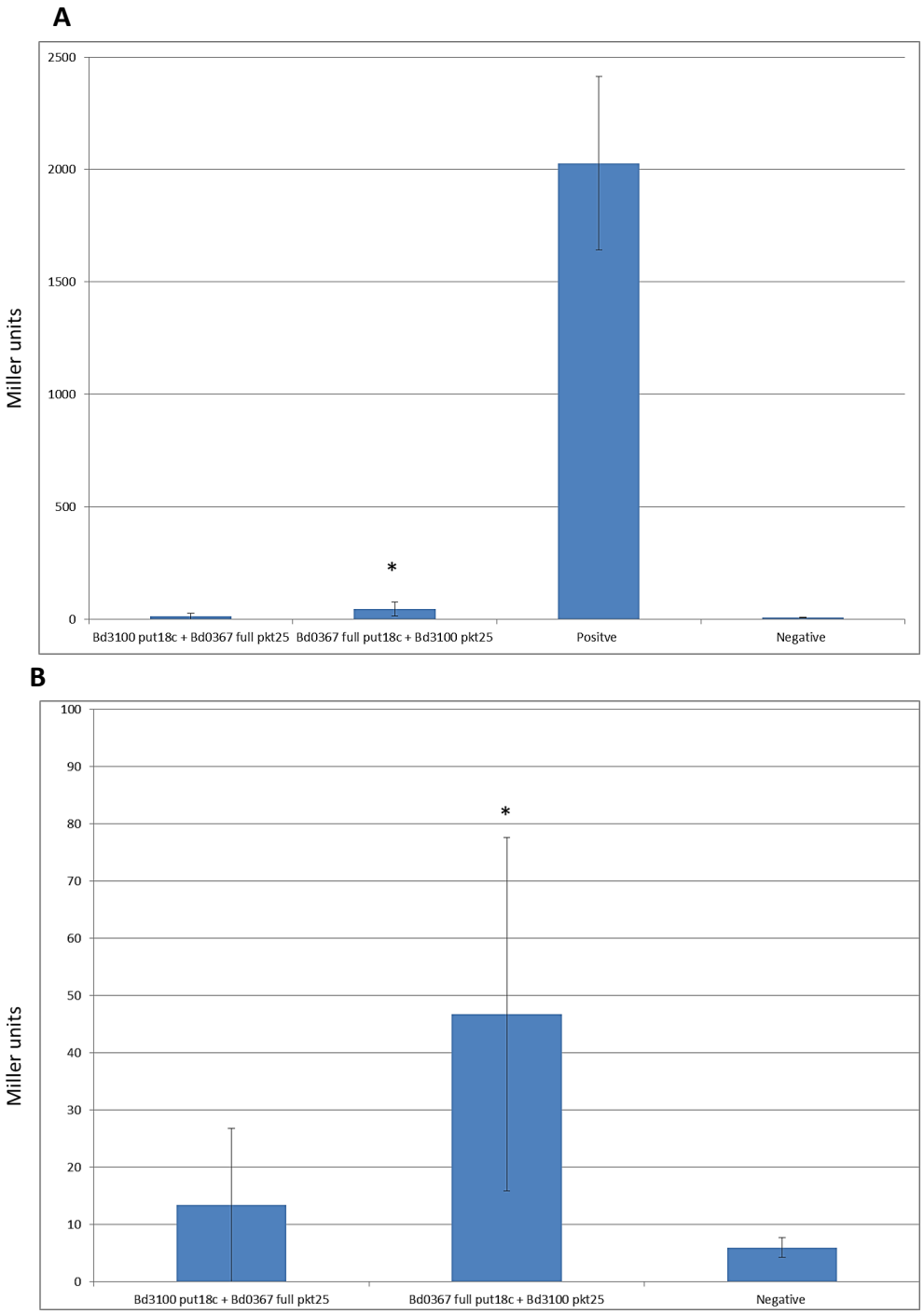

Figure 6.9 β-galactosidase activity assay for Bd3100 and Bd0367 interactions. Error bars show standard deviation. The results show the mean value from three biological repeats and comprise six technical repeats. Figure (A) shows the Miller units for the Bd3100 and Bd0367 interactions with both positive and negative controls. (B) This graph allows better observation of the significant difference between Bd0367 full pUT18c with Bd3100 pKT25 in comparison to the negative control only. Asterisks show significance of Student t-test compared to the negative (pUT18c, pKT25) *≤0.05.

6.4.2.2. PilZ domain protein Bd3100 interacts with the full length Bd0367 protein only with no interaction with Bd0367 split domains

Bd0367 has two distinct domains, an N terminal response regulator domain and a C terminal diguanylate cyclase domain joined by a linker region. B2H constructs were made that split this protein in two (Figure 6.10). The cloned 'response regulator domain' (RR) was taken from amino acids 1 to139. This construct contains the response regulator domain, the linker region and the first 3 amino acids of the DGC domain. The cloned 'digunalyate cyclase domain' (DGC) comprises of amino acid 140 to the end of the protein (332), this domain is deficient in its first 3 amino acids of the DGC domain and contains the unknown terminal region to further investigate the location of the Bd0367-Bd3100 interaction.

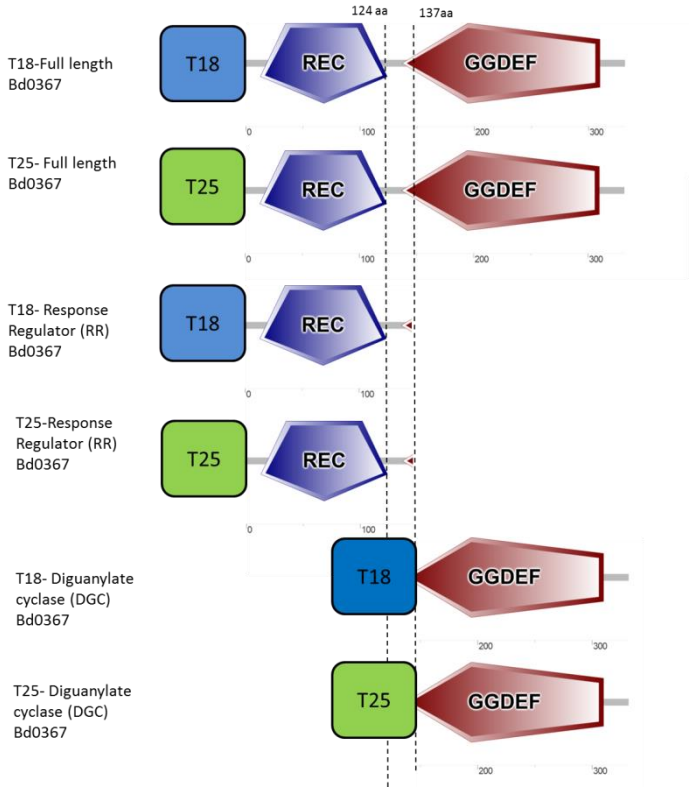

Figure 6.10 Illustration of the various Bd0367 constructs used in B2H analysis. The diagram shows the domains of Bd0367 as predicted by SMART, the dotted line demonstrates the amino acid at which the designated domain ends or started. The split domains of Bd0367 as split into the response regulator region and the diguanylate cyclase domain.

Bacterial two-hybrid assays showed that Bd3100 does not interact with the response regulator domain (RR) or diguanylate cyclase only domain (DGC) as spot plates resulted in white colonies, Figure 6.11. This suggests that Bd3100 requires the full length

construct of Bd0367 to interact this could be due to full protein conformation or the linker region being important.

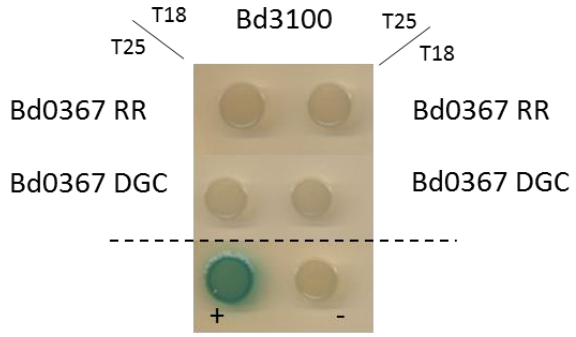

Figure 6.11 Spot plate interactions of split domains of Bd0367 with full length PilZ protein Bd3100. White spots suggest no interaction between Bd0367 RR or DGC with Bd3100. Results displayed are a typical representation of the results from three biological repeats and nine technical repeats. Positive (+) = pUT18c-zip with pKT25-zip. Negative (-) = pUT18c with pKT25.

β-galactosidase activity assays were also carried out on the split Bd0367 domains with Bd3100 to investigate if there was a quantifiable difference in interaction strengths between the two domains. However interactions with both the response regulator and diguanlyate cyclase domain were not significantly different from the negative or each other Figure 6.12. Leading to the conclusion that Bd3100 only interacts with the full length Bd0367, having no preference for a particular domain.

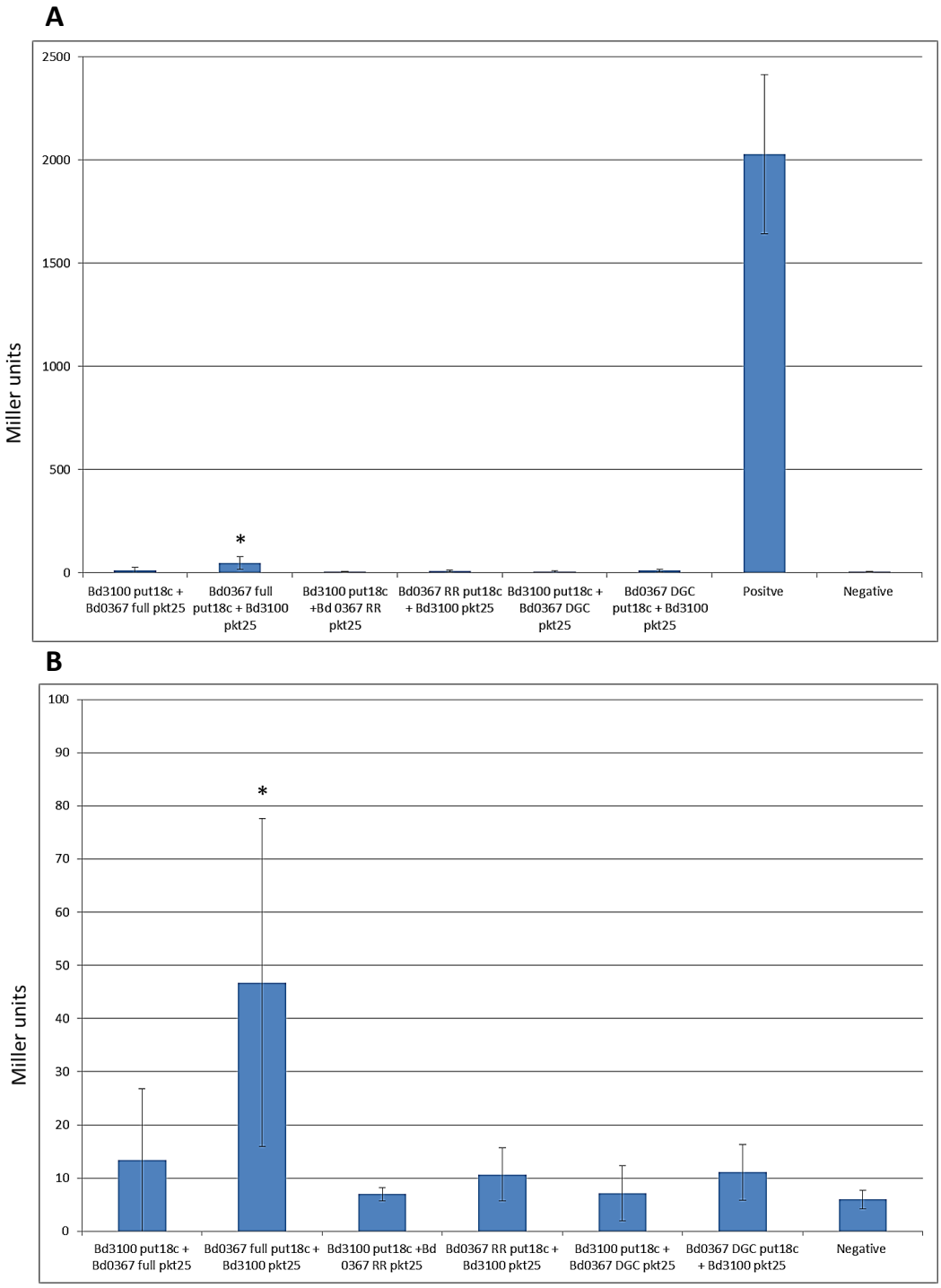

Figure 6.12 β-galactosidase activity assay for Bd3100 and a variety of Bd0367 interactions. Error bars show standard deviation. The results show the mean value from three biological repeats and comprise six technical repeats. Figure (A) shows the Miller units for the variety of Bd3100 and Bd0367 interactions with both positive and negative controls. (B) This graph allows better observation of the significant difference between Bd0367 varieties with Bd3100 in comparison to the negative control only. Only the full length Bd0367 puT18c + Bd3100 pKT25 interaction is significantly different from the negative Asterisks show significance of Student t-test compared to the negative (pUT18c, pKT25) *≤0.05.

6.4.3. Surface incubation affects expression of PilZ domain protein Bd3100mCherry

To assess cellular localisation of Bd3100, Aidan Taylor (an undergraduate student) generated a strain with C-terminally fluorescently tagged Bd3100. Bd3100mCherry was constructed by fusion of *bd3100*, lacking its stop codon, in frame with a mCherry tag. This was then integrated into the *B. bacteriovorus* chromosome by single crossover at the *bd3100* gene. Bd3100 has a proposed role in gliding motility, due to this prediction the expression of Bd3100mCherry when incubated on a surface was analysed. Aidan Taylor (with help from Dr Milner) first noticed this visible alteration in mCherry intensity, resulting in brighter cells after surface incubation. To quantify this he measured the intensity of fluorescence of some cells at time 0 and time 400 using SimplePCI (Milner et al, 2014; Taylor, 2013). In my study the work was furthered by taking significantly more images and by analysing them using a different ImageJ analysis program called MicrobeJ.

6.4.3.1. *B. bacteriovorus* Bd3100mCherry cells show increased fluorescence when incubated on a surface

Expression of protein Bd3100 in *B. bacteriovorus* Bd3100mCherry attack phase cells was seen to increase when incubated on a surface. This increase in expression was demonstrated by visibly increased fluorescence. This was studied by observing the intensity of the mCherry fluorescence at the first point of surface contact and at time 400 mins; as at time 400 mins most cells should be gliding (a typical Bd3100-mCherry image is shown in Figure 6.13).

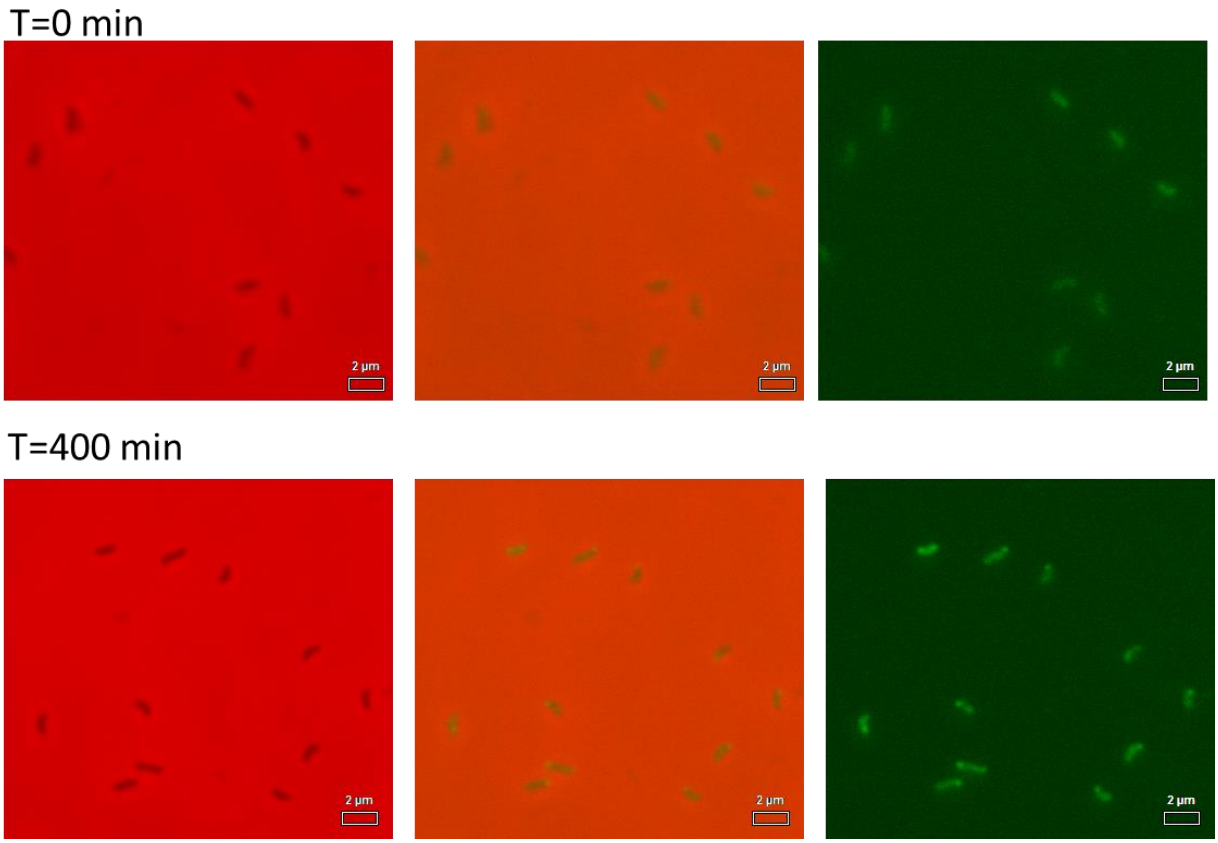

Figure 6.13 : *B. bacteriovorus* Bd3100-mCherry cells show increased fluorescence when incubated on a surface. The cells were placed on a 1% agarose CaHEPES slide and images were collected at time 0 and time 400 minutes. During this time the slide was kept consistently hydrated and at room temperature of 25°C. The panel of images shows time 0 at the top and time 400 minutes bellow. The panels left to right show the bright field channel, the merged channel and the fluorescent channel. At time 0 the image shows that the cells had faint cytoplasmic fluorescence. At time 400 min the fluorescence had increased and the localisation of fluorescence was less diffuse.

The program used in this study to analyse the large amount of additional images accrued is called MicrobeJ. Fluorescent intensity is just one of the many characteristics this program can analyse (section 2.7.2). A sample population of 450 cells at each time point (0 and 400 minutes) was gathered across 3 biological repeats and 3 technical repeats. The difference between the two time points was significantly different when analysed by Student t test. This analysis showed that Bd3100mCherry intensity increased 1.57 fold after surface incubation for 400 minutes on 1% agarose buffered with 25mM HEPES, 2 mM $CaCl_2$ which began to establish that Bd3100 plays a role in gliding motility in *B. bacteriovorus*.

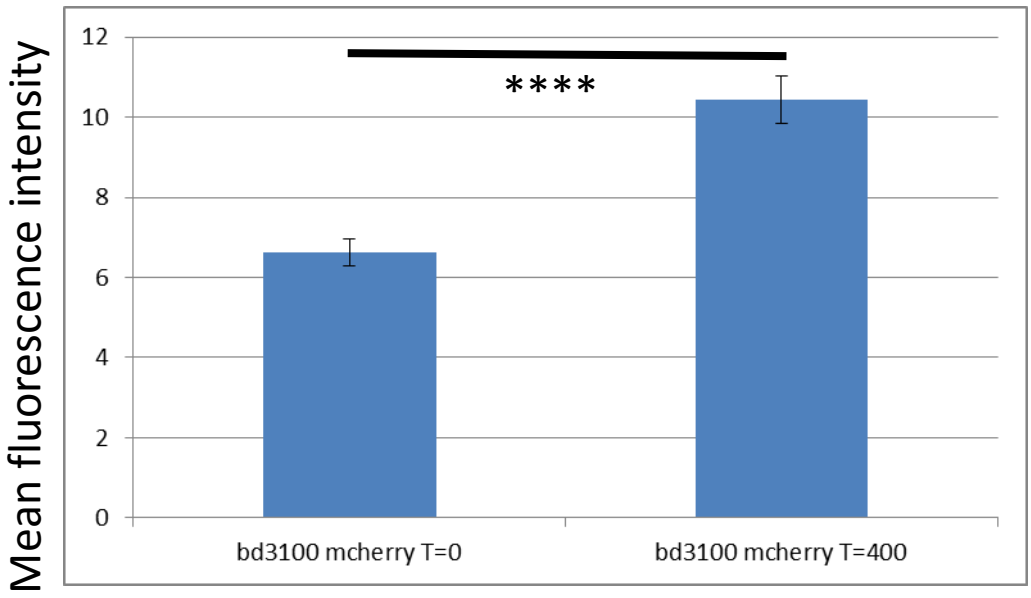

Figure 6.14 *B. bacteriovorus* Bd3100-mCherry attack phase cells show an increase of 1.57 fold fluorescence intensity when incubated on a surface. Analysis using MicrobeJ on a total population of 450 cells across 3 biological repeats and 3 technical repeats showed a significant increase in mean fluorescence intensity between the timepoints. Error bars represent 95% confidence interval. Asterisks show values of the Student t-test ****=<0.0001

6.4.3.2. The distribution of Bd3100mCherry fluorescence alters when incubated on a surface

During analysing the effect that surface incubation had on *B. bacteriovorus* Bd3100mCherry cells fluorescence, it was observed that the localisation of Bd3100mCherry formed more discreet foci. It was suggested that this change in localisation may be to do with formation of focal adhesion complex. Over 1000 cells at each time point across 3 biological repeats each with 3 technical repeats were analysed by hand via the 'analyse counter' function of ImageJ (Section 2.7.5). The results of this are shown in Figure 6.15 the most pronounced change was the decrease of diffuse fluorescence throughout the cell and the increase of the dominant mono polar foci.

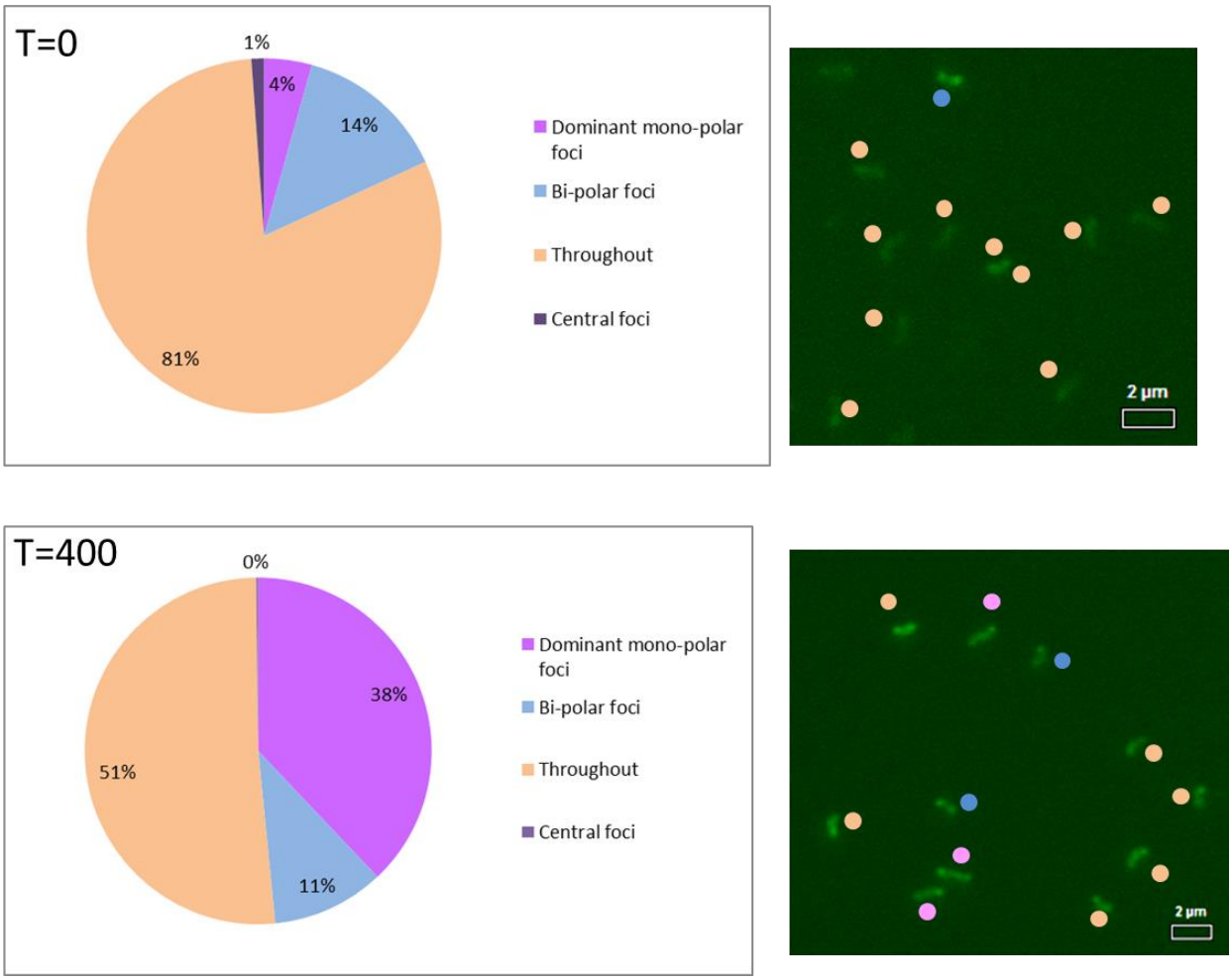

Figure 6.15 A dominant mono-polar fluorescence focus increased in frequency on surface incubation of *B. bacteriovorus* Bd3100mCherry cells. At time 0 min *B. bacteriovorus* Bd3100mCherry cells showed primarily a diffuse fluorescence distributed throughout the cell. To demonstrate this visually the location of fluorescence in the cell (dominant monopolar, bipolar, diffuse) is highlighted by a dot of colour next to the cell which indicates which section of the pie chart this cell is representative of. At time 400 the frequency of diffuse fluorescence dropped by 30%. The dominant mono-polar foci (this is a cell which is fluorescent throughout but with a distinct foci at one pole) had increased by 34% on surface incubation. Cells were placed on a 1% agarose CaHEPES slide at room temperature and kept hydrated. These slides were imaged at time 0 and time 400. A total of 1160 cell were analysed at t=0 and 1131 at t=400, these cells were counted across 3 biological repeats each with 3 technical repeats.

6.4.4. Investigating gliding motility in the *B. bacteriovorus Δbd3100* strain

The deletion of the PilZ domain protein *bd3100* was originally undertaken by undergraduate student Aidan Taylor with the help of PhD student Dr Milner. Initial observation of the *B. bacteriovorus* Δ*bd3100* strain via microscopy showed a noticeable difference in gliding motility. Aidan Taylor observed two videos of attack phase Δ*bd3100*

cells gliding by eye and noted without quantifying that 'the strain presented a hyper-reversal gliding phenotype'(Taylor, 2013). In this study further research was undertaken to fully characterise this strain and quantify the phenotype, which is outlined below. Additionally complementation of the Δ*bd3100* strain was achieved during this study by myself using a previously constructed plasmid made but not tested by PhD student Dr Milner.

6.4.4.1. *B. bacteriovorus Δbd3100* cells are slower at initiating gliding motility compared to wild type cells

When the deletion strain of *bd3100* was first made the attack phase cells gliding motility was observed via time-lapse microscopy. This was investigated as Bd3100 was hypothesised to be involved in gliding motility due to its interaction with Bd0367 and its similarity with Bd1482 which is encoded from a gliding operon. From the first video it was apparent that though gliding motility was still present it was not representative of movement typically seen in wild-type cells because cells did not make progress and reversed frequently. This required further investigation and so in this study multiple time-lapse microscopy videos were used to establish the differences observed. These were set up as per Methods (Section 2.7.4) using attack phase *Bdellovibrio* on 1% agarose buffered with 25 mM HEPES 2 mM $CaCl_2$. The first characteristic of gliding that was examined was the time taken from application of cells on a surface to the cells first movement using gliding motility. The time taken to initiate gliding can provide an insight into the regulation and induction of gliding proteins. Figure 6.16 shows that the deletion of *bd3100* does have a detrimental effect on the efficiency of initiating gliding motility.

The time taken to initiate gliding motility was investigated by applying cells to an 1% agarose pad and following the cells movement through time-lapse microscopy (as per methods section 2.7.4). Start times were taken as the time of the first image after one frame of movement was observed. The start times demonstrated by the Δ*bd3100* cells resulted in an average start time that was over an hour later than the HD100 wild type cells. This start time was partially restored towards a wild type level by complementation; the initiation of gliding time in the complementation strain sits half way between the wild type and the Δ*bd3100* strain start times. This partially complemented phenotype could be due to levels of Bd3100 encoded from the plasmid cross over being altered versus wild type or to do with operon organisation being disrupted.

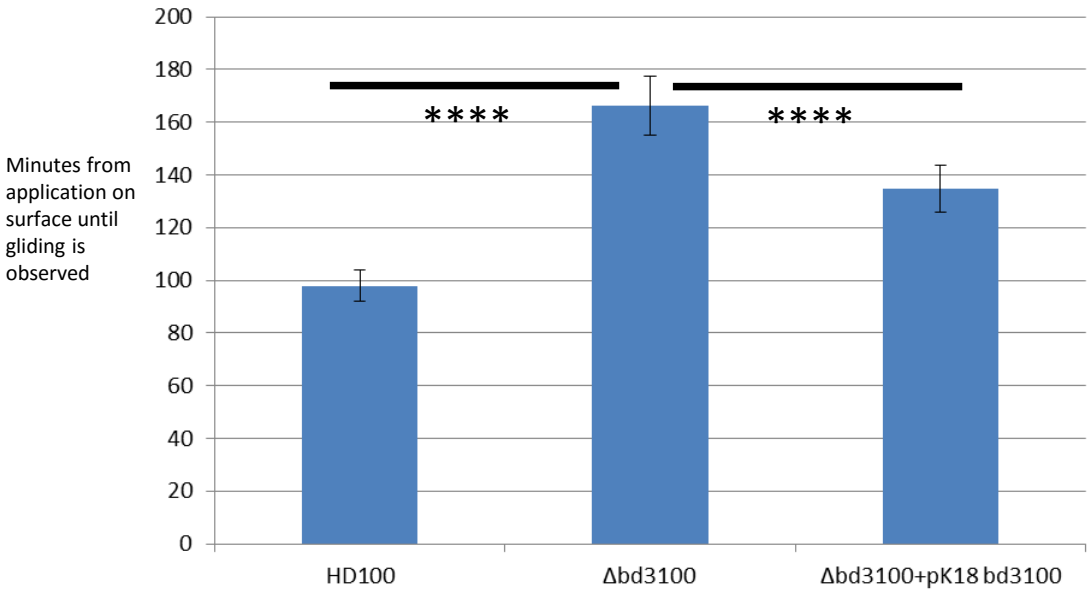

Figure 6.16 *B. bacteriovorus Δbd3100* attack phase cells took significantly longer to initiate gliding motility compared to wild type cells. The data are obtained from 3 biological repeats with means taken from a total of 116 HD100 wild type cells, 129 Δ*bd3100* cells and 123 Δ*bd3100* complemented with pK18 *bd3100*. Error bars represent 95% confidence interval. Asterisks show values of the Student t-test ****≤0.0001. Frame rate:1 frame per 150 sec.

6.4.4.2. *B. bacteriovorus Δbd3100* cells exhibit an increased gliding reversal frequency compared to wild type cells

A previous study by Dr Milner into *B. bacteriovorus* gliding motility observed that some mutant strains had a lack of net forward motion and this led to measuring the reversal frequency of gliding cells (Milner, 2014). A reversal is defined as a directional change. The technique was used in this study to further characterise the effect of the Δ*bd3100* strain on gliding motility, typical images of gliding are shown in Figure 6.17. By analysing the reversal frequency it was found that the Δ*bd3100* strain made significantly more reversals per hour than HD100 Figure 6.18, which supports initial observations made by Aidan Taylor. These results suggest that Bd3100 has a role to play in regulating sustained movement on a surface.

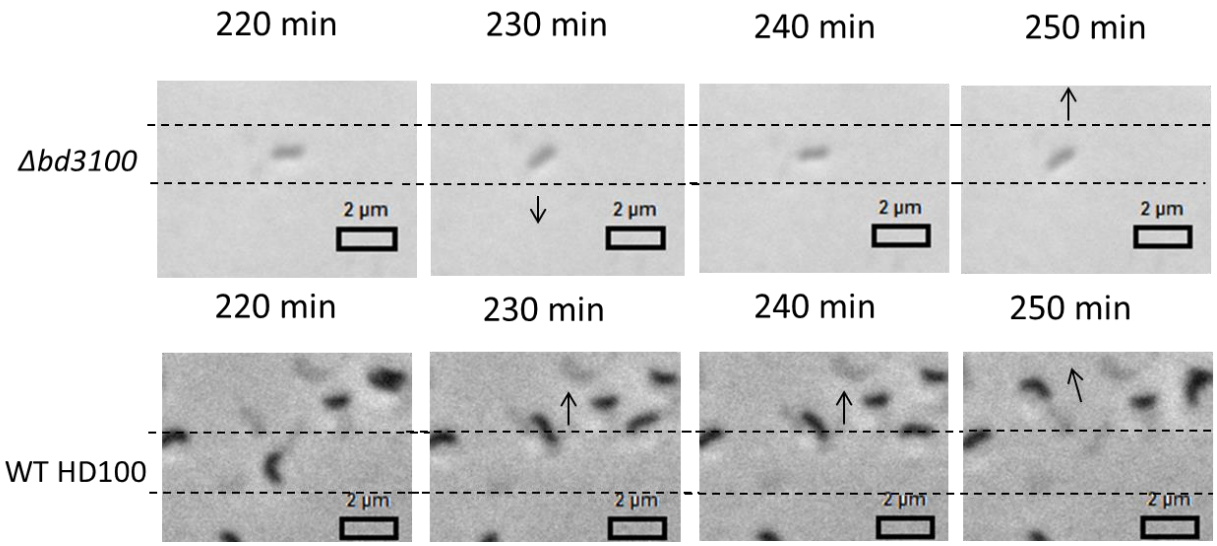

Figure 6.17 *B. bacteriovorus Δbd3100* HD cells exhibited a hyper-reversal gliding phenotype. The panel shows a selection of stills from video footage of gliding motility. A movie of this process can be located on the USB stick attached, titled 'Bd3100 gene deletion gliding' with a movie titled 'HD100 gliding' as a comparison, further details of these movies are found in Section 8.2.3. The selected stills are 10 minutes apart and show 30 minutes of gliding motility, 220 mins after addition of the cells to the agarose pad (frames of video were captured every 150 seconds). Δ*bd3100* cells show no progressive gliding motility, due to rapid back and forth movements; this can be seen by the cells inability to travel past the black dotted line. However wild-type cells show sustained runs of gliding motility resulting in progressive directional movement outside the black dotted lines.

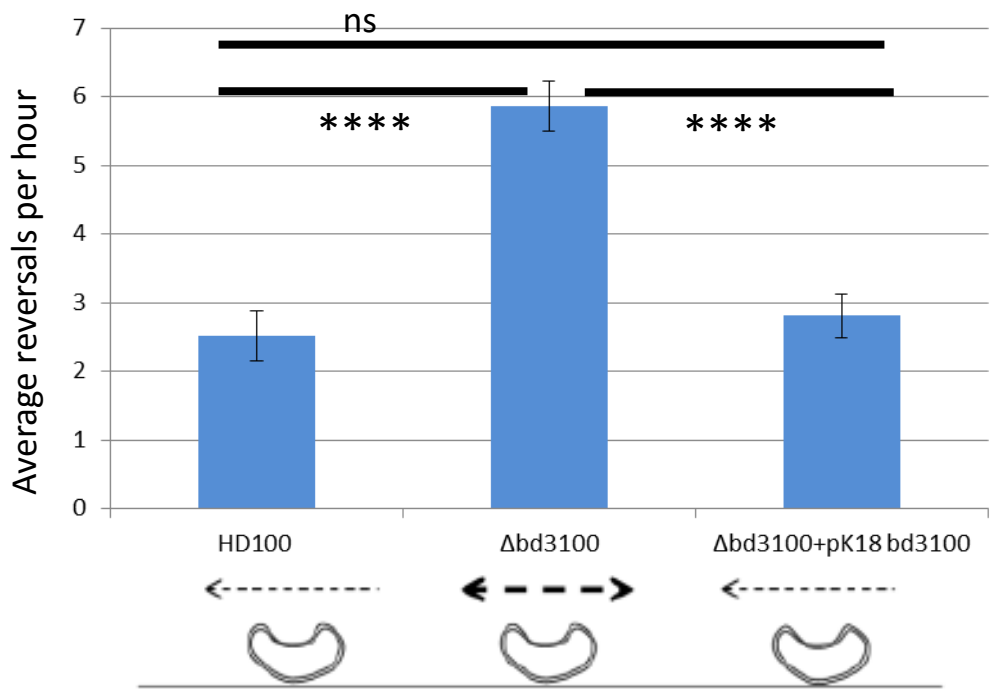

Figure 6.18 *B. bacteriovorus Δbd3100* attack phase cells made more directional reversals than wild-type when gliding. The cells were applied to a 1% agarose CaHEPES pad and time-lapse microscopy was used to record the cells movements (Section 2.7.4). The Δ*bd3100* cells made more gliding reversals than wild type cells. Reintroduction of *bd3100* through complementation restored the reversal frequency to wild type levels. A movie of this can be located on the USB stick attached, titled 'Bd3100 complemented gliding' further details of these movies are found in Section 8.2.3. These data were obtained from 3 biological repeats with means taken from a total of 97 HD100 wild type cells, 107 Δ*bd3100* cells and 108 Δ*bd3100* cells complemented with pK18 *bd3100* cells. The number of reversals per hour was analysed in the second hour after gliding commenced. Error bars represent 95% confidence interval. Asterisks show values of the Student t-test ****≤0.0001.

The deletion of *bd3100* resulted in less progressive gliding movement due to the increased frequency of reversals. The mean numbers of reversals per hour in the *B. bacteriovorus* Δ*bd3100* strain (5.8) was significantly higher than the wild type HD100 (2.5). The complementation of *B. bacteriovorus* Δ*bd3100* with pK18*bd3100* brought gliding reversals back to wildtype levels thus restoring more sustained unidirectional runs of gliding motility on the 1% agarose CaHEPES surface.

6.4.4.3. The percentage of *B. bacteriovorus Δbd3100* attack phase cells that can demonstrate movement via gliding motility is comparable to wild type cells

The above study of the gliding ability of the *⊿bd3100* strain shows gliding motility is altered from WT gliding. However by quick visual observation it can be seen that a high percentage of *⊿bd3100* attack phase cells still display surface motility. Previously gliding defects examined in this study have resulted in a lower percentage of gliding cells compared to WT (e.g *⊿bd1971* HD strain in Chapter 5) so this was examined in the *⊿bd3100* strain. Unlike the gliding defects observed in *⊿bd1971* the percentage of *⊿bd3100* attack phase cells that are able to glide was unaffected by the loss of *bd3100* and was comparable to the percentage observed gliding in HD100 Figure 6.19.

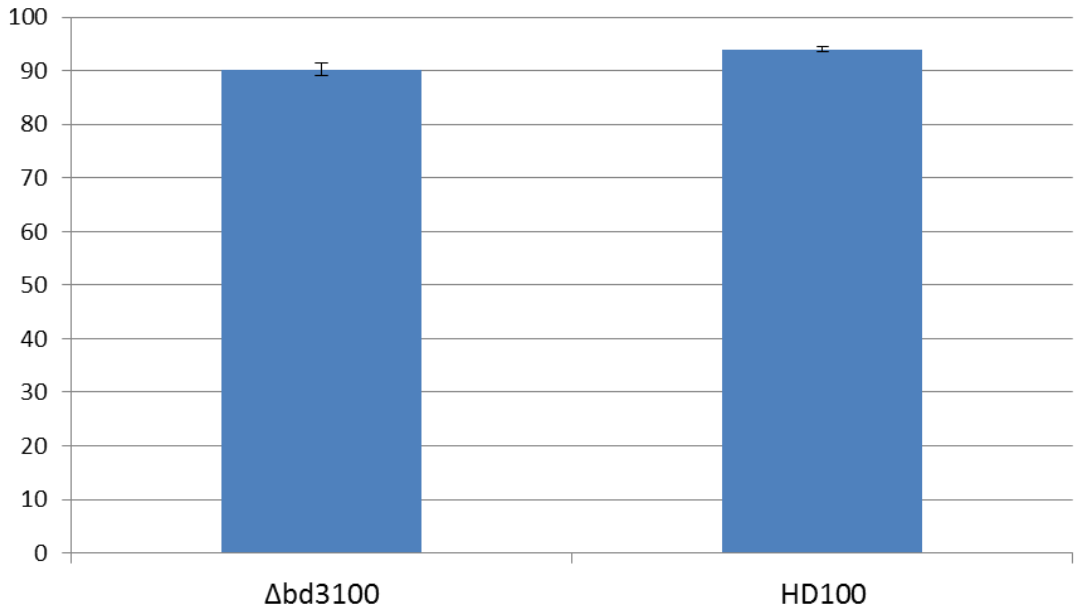

Figure 6.19 The percentage of *Δbd3100* HD attack phase cells that demonstrate gliding motility is similar to WT. The cells were applied to a 1% agarose CaHEPES surface and time-lapse microscopy was used to record cell movements for 6-8 hours. Regions were selected randomly and the number of cells that moved within the time frame was recorded. The data was obtained from three biological repeats 232 HD100 cells 264 Δ*bd3100* cells. Error bars show 95% confidence and there is no significant difference when tested with Student t test.

6.4.5. Examining the role of cellular c-di-GMP levels in Bd3100mCherry localisation

In Chapter 5 of this study I showed that the cellular c-di-GMP level influences *Bdellovibrio* gliding ability in the HD life style. The deletion studies suggest that Bd3100 is a PilZ domain protein that transduces these variations in c-di-GMP level into a molecular

output which is associated with gliding motility. The function of Bd3100 under high or low c-di-GMP environment is not yet known. To investigate if Bd3100 is affected by Bd0367 specific or global c-di-GMP the Bd3100mCherry construct was conjugated in deletion strains with low *(*Δ*bd0367* HI) and high c-di-GMP *(*Δ*bd1971* HD) to observe if the location of the Bd3100mCherry strain altered due to different cellular c-di-GMP levels, or due to the lack of DGC specific c-di-GMP.

6.4.5.1. The location of Bd3100mCherry is altered to a more diffuse localisation on expression in a low c-di-GMP cellular background (*Δbd0367*) and in the absence of interaction partner Bd0367

The Δ*bd0367* deletion strain was used to test both the effect of Bd3100 localisation in a low c-di-GMP strain and to start to examine the possibility that Bd3100 binds specifically to c-di-GMP generated by Bd0367. Unfortunately there is currently not another low c-di-GMP strain to compare the Δ*bd0367*::pK18Bd3100mCherry localisation to, as the Bd0742 deletion did not result in a decrease in extractable c-di-GMP and Bd1434 deletion could not be analysed due to its predatory nature (Hobley et al, 2012).

Previous examination of Bd3100mCherry fluorescence has been carried out in the HD attack phase cells. However the conjugation of Bd3100mCherry into the Δ*bd0367* HI strain means that the HI location of Bd3100mCherry fluorescence was examined as a control, Figure 6.20.

This showed that in HI cells the location of Bd3100mCherry does not significantly alter on surface incubation and the most common localisation is diffuse throughout the cell at 76-79%.

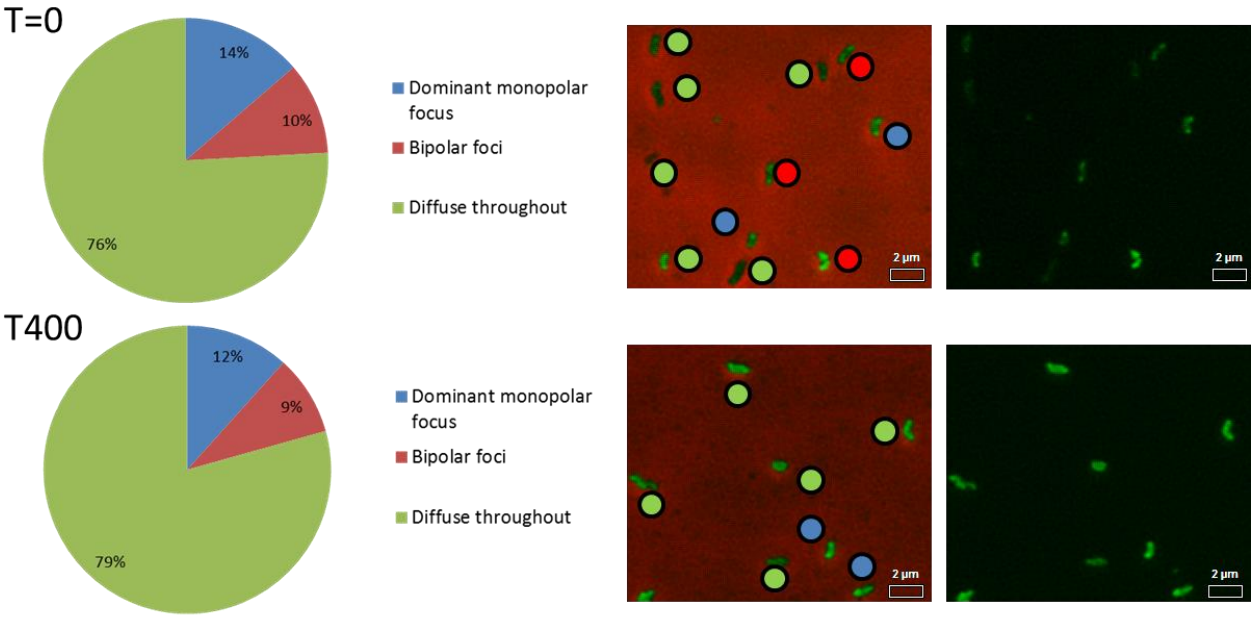

Figure 6.20 Distribution of fluorescence in Bd3100mCherry *B. bacteriovorus* WT HI strain. At time 0 min and time 400 min *B. bacteriovorus* Bd3100mCherry HI cells showed primarily a diffuse fluorescence distributed throughout the cell. To demonstrate this visually the location of fluorescence in the cell (dominant monopolar, bipolar, diffuse) is highlighted by a dot of colour next to the cell which indicates which section of the pie chart this cell is representative of. Cells were placed on a 1% agarose CaHEPES slide at room temperature and kept hydrated. These slides were imaged at time 0 and time 400. A total of 315 cell were analysed at t=0 and 300 at t=400 min, these cells were counted across 3 biological repeats.

Examination of Bd3100mCherry in Δ*bd0367* HI showed that location of Bd3100 fluorescence became more diffuse than in Bd3100mCherry HI strain. Original location of Bd3100mCherry had a throughout diffuse fluorescence in 76-79% of cells counted, Bd3100mCherry in Δ*bd0367* HI showed an increase in this localisation to 87-91% of cells with this localisation. This is an increase of over 10%. This data suggests that in a low c-di-GMP environment the location of Bd3100mCherry becomes more diffuse, and the frequency of foci decreases. However, distinct foci do still form even though less frequently in the absence of *bd0367*, which may suggest that a Bd0367 specific signal is not necessary for Bd3100mcherry localisation, and that foci formation is dependent on global c-di-GMP level.

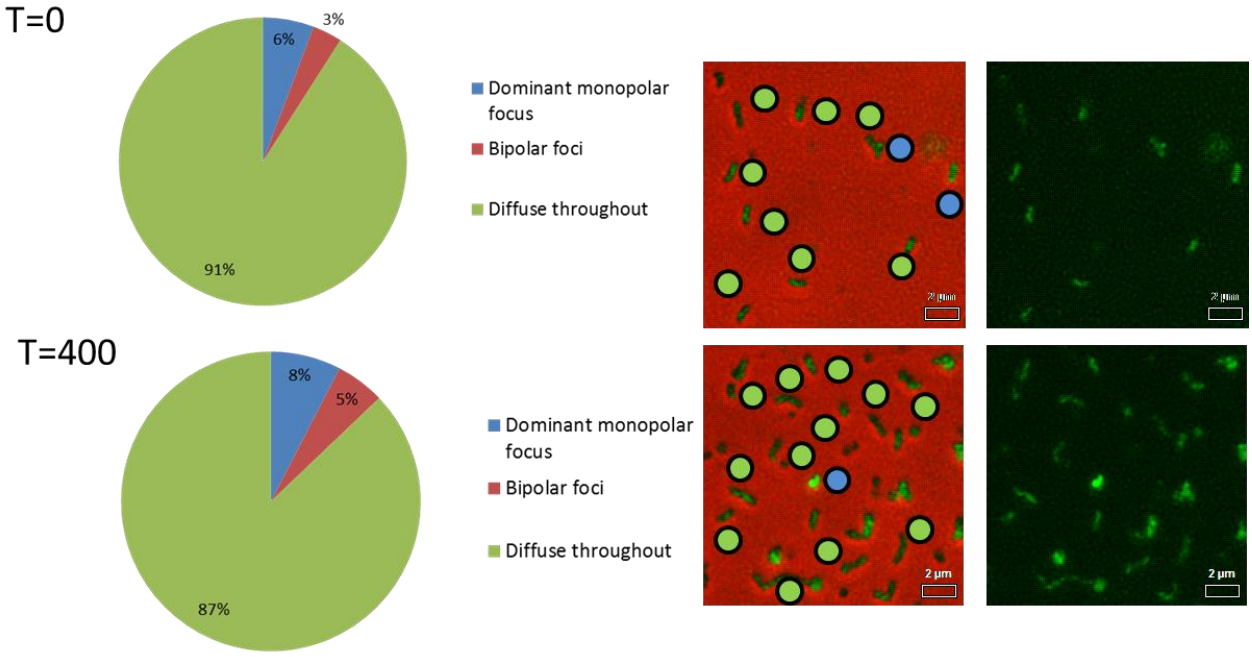

Figure 6.21 Distribution of fluorescence of Bd3100mCherry in Δ*bd0367 B. bacteriovorus* HI strain. At time 0 min and time 400 min *B. bacteriovorus* Bd3100mCherry HI cells showed primarily a diffuse fluorescence distributed throughout the cell and the frequency of foci has decreased. To demonstrate this visually the location of fluorescence in the cell (dominant monopolar, bipolar, diffuse) is highlighted by a dot of colour next to the cell which indicates which section of the pie chart this cell is representative of. Cells were placed on a 1% agarose CaHEPES slide at room temperature and kept hydrated. These slides were imaged at time 0 and time 400 min. A total of 331 cell were analysed at t=0 and 303 at t=400, these cells were counted across 3 biological repeats.

6.4.5.2. The fluorescence intensity of Bd3100mCherry decreases at T0 in Δ*bd0367* HI strain background

The mean intensity of Bd3100mCherry fluorescence was calculated in Bd3100mCherry HI strain cells and Δ*bd0367*::Bd3100mCherry HI strain cells at time 0. As these are HI cells which can vary in morphology MicrobeJ was not used as this diversity may have excluded cells from the analysis. Instead the mean fluorescent intensity of the cells was quantified by analysis in SimplePCI by calculating the net total green measurements for individual cells (see Methods 2.7.6). Interestingly this showed that the mean fluorescent intensity was significantly lower in the Δ*bd0367*::Bd3100mCherry HI strain (Figure 6.22) suggesting that in a low c-di-GMP environment cells have mean of 4.39 fold less Bd3100mCherry present in HI cells. This finding warrants further investigation.

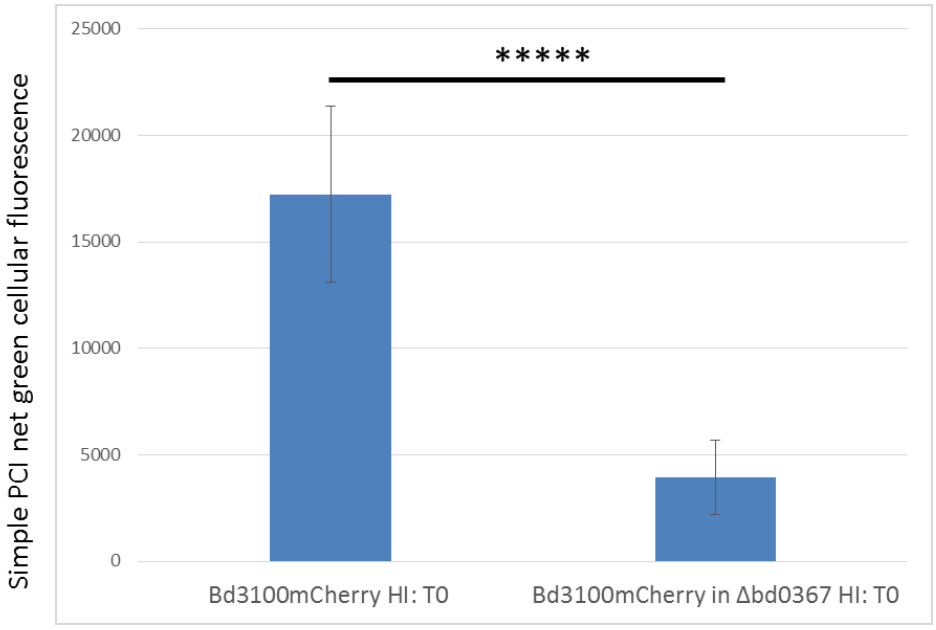

Figure 6.22 The fluorescence intensity of Bd3100mCherry is lower in *Δbd0367* strain compared to WT. This resulted in a noticeable difference in strength of cellular fluorescence. Bd3100mCherry fluorescence in the Δbd0367 low c-di-GMP background being 4.39 lower than that observed in Bd3100mCherry HI strain. 38 Bd3100mCherry HI cells and 40 Bd3100mCherry Δ*bd0367* HI cells were analysed across 3 biological repeats and the mean result is shown. The error bars show 95% confidence and the difference between the samples was found to be significant by Student t test. ***** ≤0.00001

6.4.5.3. The location of Bd0367mCherry is unaltered on expression in the Δ*bd3100* strain so Bd0367 location is unaffected by absence of interaction partner Bd3100

The Δ*bd3100* deletion strain was used to examine the possibility that the Bd3100 interaction played a role in Bd0367mCherry localisation.

Examination of Bd0367mCherry in Δ*bd3100* HD attack phase cells showed that location of Bd0367 fluorescence location was not significantly altered Figure 6.23. In Section 5.4.1.2 it was shown that Bd0367mCherry location in WT HD100 attack phase cells at T0 was 6% monopolar, 15% bipolar and 79% throughout. At T 400 the distribution was 9% monopolar, 5% bipolar and 86% throughout. Bd0367mCherry in Δ*bd3100* HD attack phase cells showed a very similar distribution to this with the difference being a 9% decrease in bipolar foci at T0, this may suggest that Bd3100 has a role in Bd0367 bi-polar localisation at T0 however I suggest that this frequency would approach WT frequency on further cell counts due to discrepancy in the population numbers counted. (Total number of Bd0367mCherry location in WT HD100 attack phase cells counted at T0 1080 vs 550 Bd0367mCherry in Δ*bd3100* HD attack phase cells). On further collection

these data may suggest that Bd0367 is not dependent on Bd3100 for its cellular localisation (as there was very small variation in mCherry distribution at T400 between the two strains) and may add to evidence that the effect seen in Section 6.4.5.1 of Bd3100 localisation being more diffuse in a Δ*bd0367* background is due to the low c-di-GMP levels and not the absence of Bd0367 protein having an effect on Bd3100 localisation.

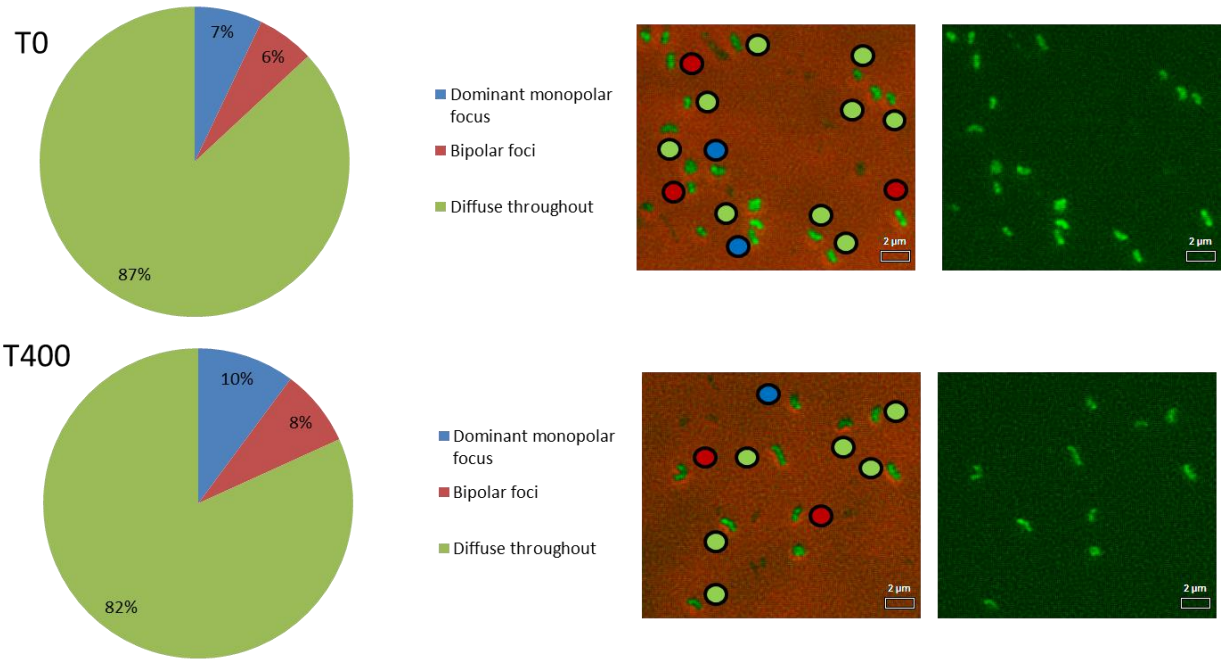

Figure 6.23 Distribution of fluorescence of Bd0367mCherry in Δ*bd3100 B. bacteriovorus* HD strain is unaltered. Location of fluorescence in cells is highlighted by a dot of that colour on the corresponding image next to the cell which indicates which section of the pie chart this cell is representative of. Cells were placed on a 1% agarose CaHEPES slide at room temperature and kept hydrated. These slides were imaged at time 0 and time 400. A total of 550 cell were analysed at t=0 and 472 at t=400, these cells were counted across 3 biological repeats.

6.4.5.4. The location of Bd3100mCherry is more monopolar on expression in high c-di-GMP cellular background, (*Δbd1971*)

The Δ*bd1971* deletion strain was used to test the effect of Bd3100 localisation in a high c-di-GMP strain. The Δ*bd1971* strain is a HD strain so these results were compared to the localisation of Bd3100mCherry in attack phase HD100. At T0 Bd3100mCherry HD cells have a distribution of 81% diffuse throughout, 14% bipolar and 4% monopolar, the Δ*bd1971*::Bd3100mCherry strain has a distribution of 74% diffuse throughout, 9% bipolar and 17% monopolar. This is a 13% increase at T0 in monopolar Bd3100mCherry

localisation in a high c-di-GMP cellular background provided by Δ*bd1971* strain, Figure 6.24.

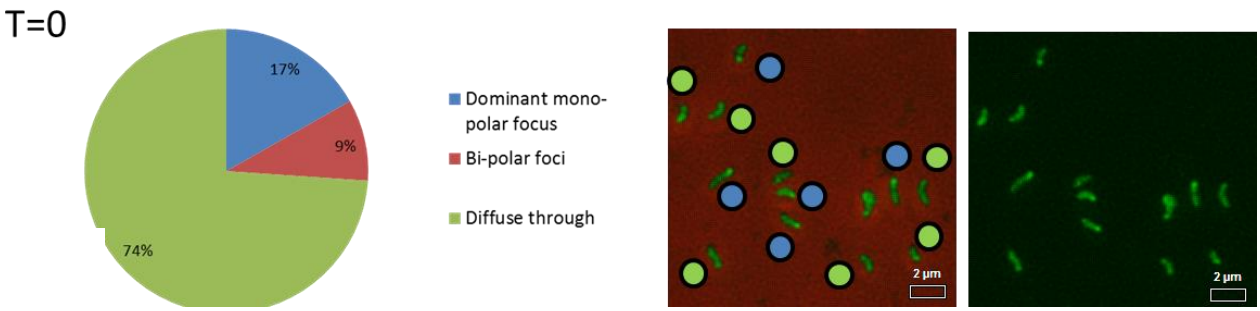

Figure 6.24 Distribution of fluorescence of Bd3100mCherry in *Δbd1971* attack phase cells. At time 0 the frequency of monopolar fluorescence had increased by 13% compared to Bd3100mCherry location in HD100. This is shown on the pie chart and cells of this description are highlighted by a dot of that colour on the corresponding image next to the cell which indicates which section of the pie chart this cell is representative of. Cells were placed on a 1% agarose CaHEPES slide. A total of 1047 cell were analysed at t=0 these cells were counted across 3 biological repeats.

6.4.5.5. The fluorescence intensity of Bd3100mCherry increases in *Δbd1971* HD strain background

The mean fluorescent intensity of Bd3100mCherry fluorescence was calculated in Bd3100mCherry HD strain cells and Δ*bd1971*::Bd3100mCherry HD strain cells at time 0. As these are HD cells MicrobeJ was used to analyse the mean fluorescent intensity of the two strains (methods 2.7.2). Interestingly this showed that the mean fluorescent intensity is significantly higher in the Δ*bd1971*::Bd3100mCherry HD strain Figure 6.25 suggesting that in a high c-di-GMP environment cells have mean of 1.276 fold more Bd3100mCherry present in HD cells. This finding agrees with the previous discovery that Bd3100mCherry was at lower levels in a low c-di-GMP strain and warrants further investigation.

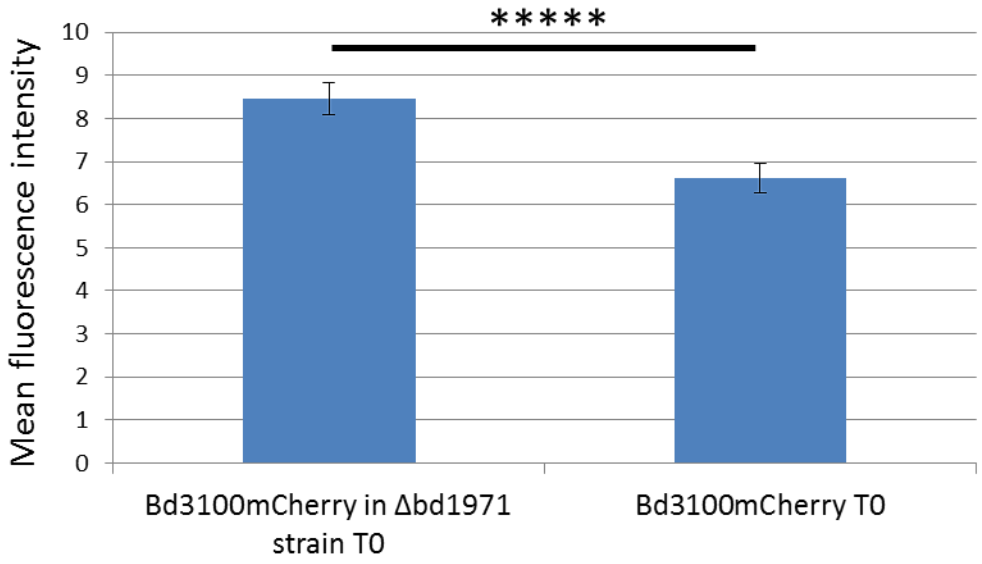

Figure 6.25 The fluorescence intensity of Bd3100mCherry is higher in *Δbd1971* strain compared to WT. This resulted in a noticeable difference in strength of cellular fluorescence. Bd3100mCherry mean fluorescence in the Δ*bd1971* high c-di-GMP background being 1.267 higher than that observed in Bd3100mCherry HD strain. A total of 450 Bd3100mCherry HD cells and 450 Bd3100mCherry Δ*bd1971* HD cells were analysed across 3 biological repeats. The error bars show 95% confidence and the difference between the samples was found to be significant by Student t test. ***** ≤0.00001

6.4.6. How does surface incubation effects two genes in the predicted functional gliding operon?

Both Bd1473 and Bd1482 are part of the most complete gliding operon in *Bdellovibrio* (Luciano et al, 2011). These genes in the operon were picked for investigation due to their potential links to Bd3100. For example Bd1473 appears to have a similar mCherry location pattern to Bd3100 with monopolar localisation increasing on surface incubation and the mCherry tag of Bd1473 caused a hyper-reversal phenotype as seen in the Bd3100 deletion strain (Milner, 2014). This suggested Bd3100 and Bd1473 may be in acting in the same pathway to regulate directionality in *Bdellovibrio* gliding. Bd1482 was chosen for examination as it is a PilZ domain protein that is present in the *Bdellovibrio* gliding operon, this suggested that a c-di-GMP input was also important for its predicted role in gliding motility. Additionally Bd1482 has a DUF4339 domain like Bd3100 which suggested they may interact with similar proteins.

6.4.6.1. Bd1473 putative gliding protein

Bd1473 does not have homology to other known gliding components but resides in a *Bdellovibrio* gliding operon and alters in fluorescent location on surface incubation (Milner, 2014). It is an uncharacterised protein with a coiled coil detected by SMART http://smart.embl.de/ and possible signal peptide.

In this study I quantify the increase of Bd1473mCherry fluorescent intensity on surface incubation, make my own examination of Bd1473mCherry localisation, and use this to observe how Bd1473mCherry localisation is effected in a Δ*bd3100* strain.

6.4.6.2. Quantification of Bd1473mCherry increase on surface incubation

In this study I carried out surface incubation assays with Bd1473mCherry, to quantify the predicted increase in fluorescence using MicrobeJ: There was a 5.39 fold increase in Bd1473mCherry fluorescence up on surface incubation. Figure 6.26.

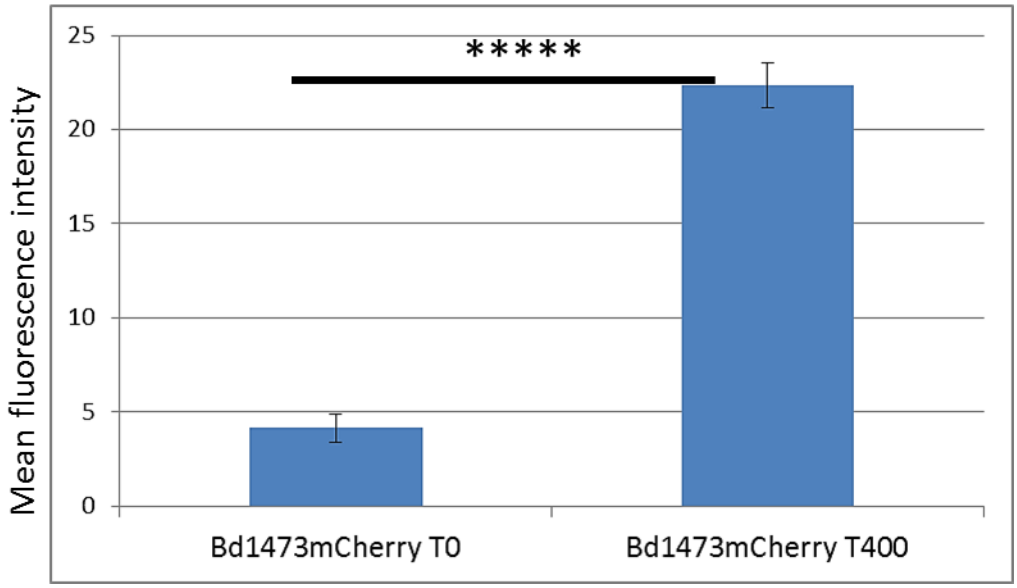

Figure 6.26 *B. bacteriovorus* Bd1473-mCherry attack phase cells show an increase of 5.39 fold fluorescence intensity when incubated on a surface. Analysis using MicrobeJ on a population of 450 cells across three biological repeat showed a significant increase in mean fluorescence intensity between the timepoints. Error bars represent 95% confidence interval. Asterisks show values of the Student t-test *****=<0.00001 .

6.4.6.3. Further examination of Bd1473mCherry location on surface incubation

The location of Bd1473mCherry at time 400 has already been documented by Dr Milner, I analysed my own images as a control to minimise any differences between my image analysis and Dr Milner. My results were very close to his with less than a 5% variation in frequencies, with Bd1473mCherry monopolar localisation increasing to 32% on surface

incubation Figure 6.27 shows the locations of Bd1473mCherry in cells upon surface incubation.

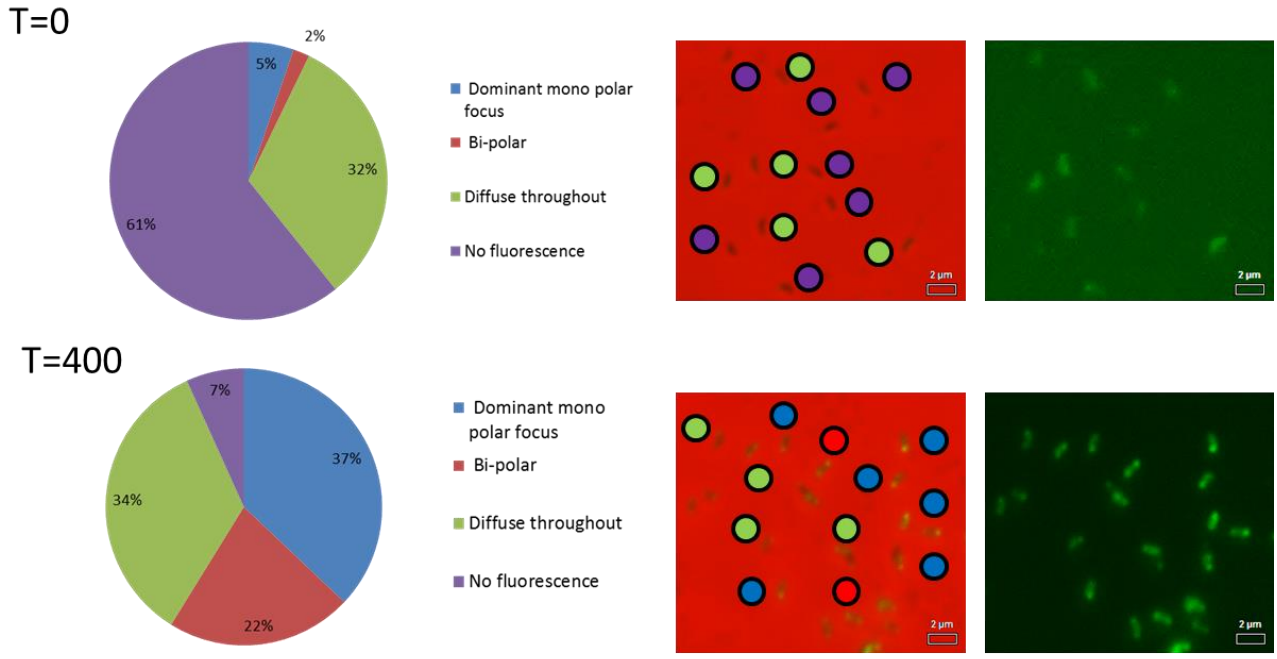

Figure 6.27 A dominant mono-polar fluorescence focus increased in frequency on surface incubation of *B. bacteriovorus* Bd1473mCherry cells. At time 0 min *B. bacteriovorus* Bd1473mCherry cells showed primarily no fluorescence, followed by a diffuse fluorescence distributed throughout the cell. This is shown on the pie chart and cells of this description are highlighted by a dot of that colour on the corresponding image next to the cell which indicates which section of the pie chart this cell is representative of. At time 400 the frequency of no fluorescence has dropped by 54%. The dominant mono-polar foci had increased by 32% on surface incubation. Cells were placed on a 1% agarose slide at room temperature and kept hydrated. These slides were imaged at time 0 and time 400. A total of 209 cell were analysed at t=0 and 340 at t=400, these cells were counted across 3 biological repeats each with 3 technical repeats.

This result is interesting as the previously studied Bd3100mCherry monopolar localisation increased by 34% on surface incubation and the Bd1473mCherry monopolar localisation increased by 32% on surface incubation.

6.4.6.4. Do Bd1473 and Bd3100 co-locate or interact within the same gliding pathway?

Bd1473mCherry and Bd3100mCherry have the same percentage increase in monopolar location on surface incubation and the reversal frequency of the Bd1473mCherry strain increases to 7.8 reversals per hr, which is comparable to the approx. 6 reversals per hour

that result from *bd3100* deletion (Milner, 2014). This suggested that these two genes may interact with each other or within the same gliding pathway. To investigate this Bd1473mCherry was expressed in the ⊿*bd3100* strain to see if Bd1473 localisation was altered. Figure 6.28.

On surface incubation Bd1473mCherry in Δ*bd3100* strain had a dominantly monopolar location, the frequency of this distribution had doubled from 37% which is observed in Bd1473mCherryHD strain to 73% in the Δ*bd3100* strain.

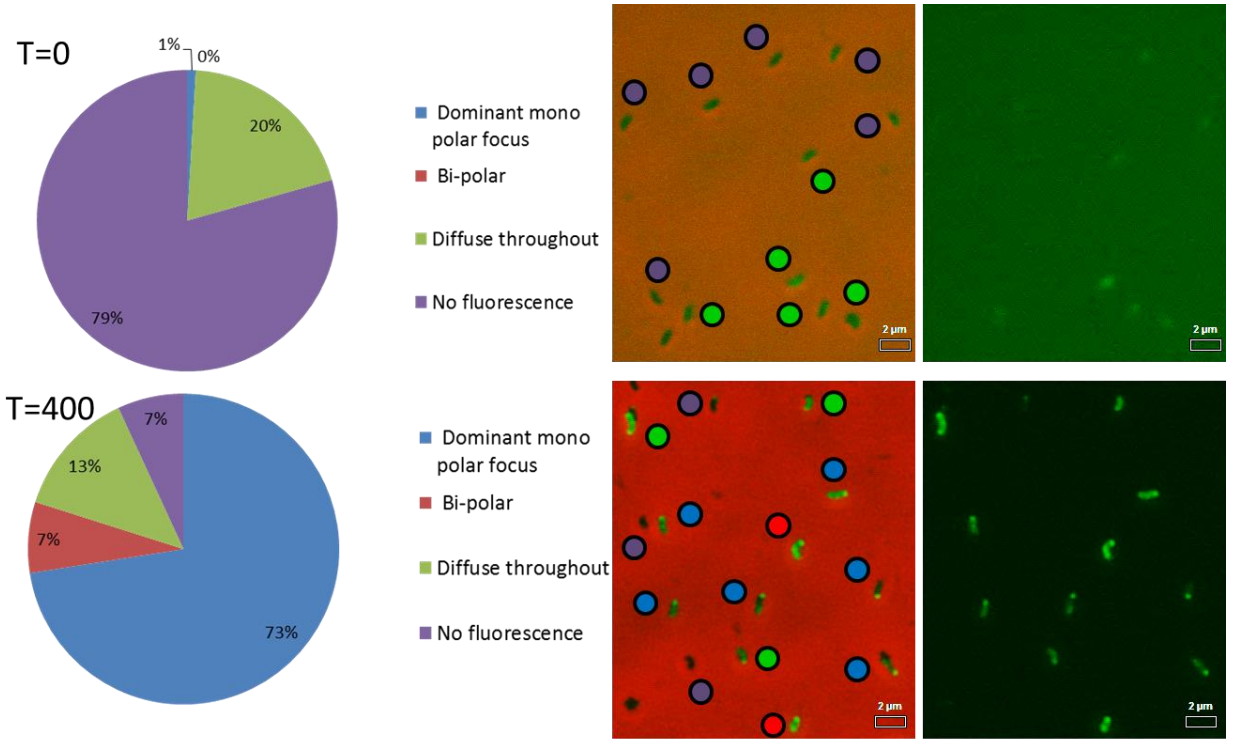

Figure 6.28 *B. bacteriovorus* Bd1473mCherry attack phase cell monopolar fluorescence doubled in frequency when expressed in *Δbd3100*. To demonstrate this visually the location of fluorescence in the cell (monopolar, bipolar diffuse or none) is highlighted by a dot of colour next to the cell which indicates which section of the pie chart this cell is representative of. At time 400 min the frequency of the dominant mono-polar foci had increased to 73% on surface incubation, this was double that observed previously. Cells were placed on a 1% agarose CaHEPES slide at room temperature and kept hydrated. These slides were imaged at time 0 and time 400. A total of 218 cell were analysed at t=0 and 393 at t=400, these cells were counted across 3 biological repeats each with 3 technical repeats.

The biological importance of this change in the frequency of Bd1473mCherry being monopolar is currently unknown but is discussed in Section 6.5.5.

6.4.7. Surface incubation effects expression of PilZ protein Bd1482mCherry

The Bd1482mCherry strain was constructed by an undergraduate student Amy Vincent this strain was originally used to observe localisation of Bd1482 throughout the lifecycle of HD *Bdellovibrio*. Bd1482 is a PilZ domain protein in one of the predicted gliding operons and is similar to Bd3100 as both comprise of a PilZ and DUF4339 domain. Due to the successful analysis of Bd3100 fluorescence on a surface Bd1482mCherry strain was investigated to examine the proteins function in gliding motility.

6.4.7.1. *B. bacteriovorus* Bd1482mCherry cells show increased fluorescence when incubated on a surface

To analyse the fluorescent intensity of 1482-mCherry between the two time points MicrobeJ was used as previously mentioned (Section 2.7.2). The strain was placed on 1% agarose CaHEPES slide which was kept hydrated at room temperature, and images were taken at time 0 and time 400 minutes. A population of 300 cells at each time point was gathered across 3 biological repeats and 2 technical repeats. This resulted in a significant difference when analysed by Student t test. This analysis showed that Bd1482mCherry intensity increased 4.64 fold on surface incubation Figure 6.29, and a typical image is shown in Figure 6.30.

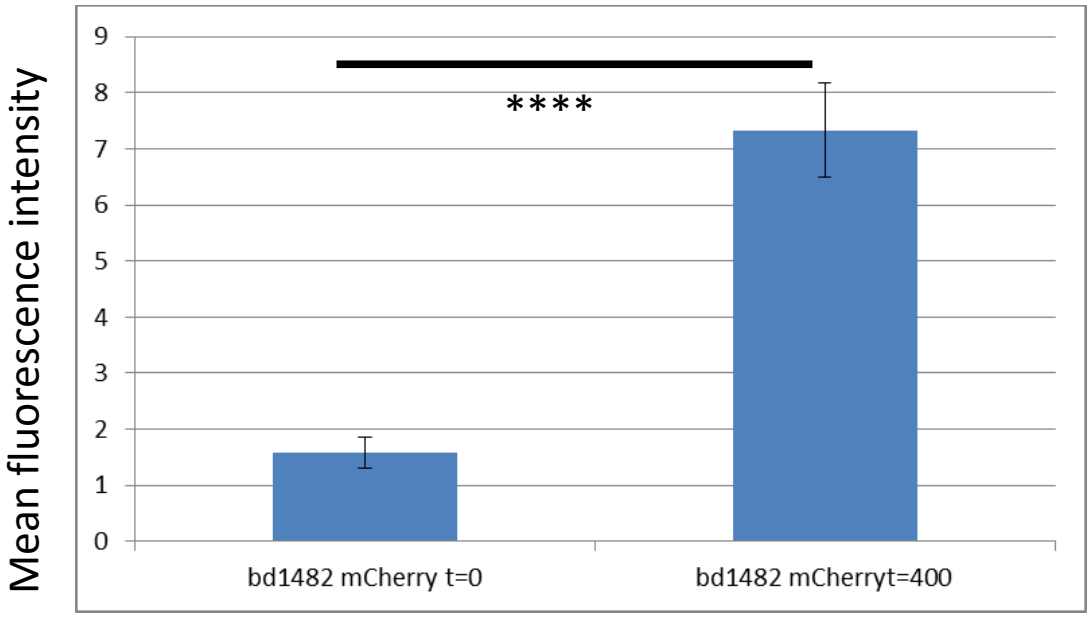

Figure 6.29 *B. bacteriovorus* Bd1482mCherry cells show an increase of 4.64 fold fluorescence intensity when incubated on a surface. Analysis using MicrobeJ on a population of 300 cells at T0 and T400 showed a significant increase in mean

fluorescence intensity between the time-points. Error bars represent 95% confidence interval. Asterisks show values of the Student t-test ****≤0.0001.

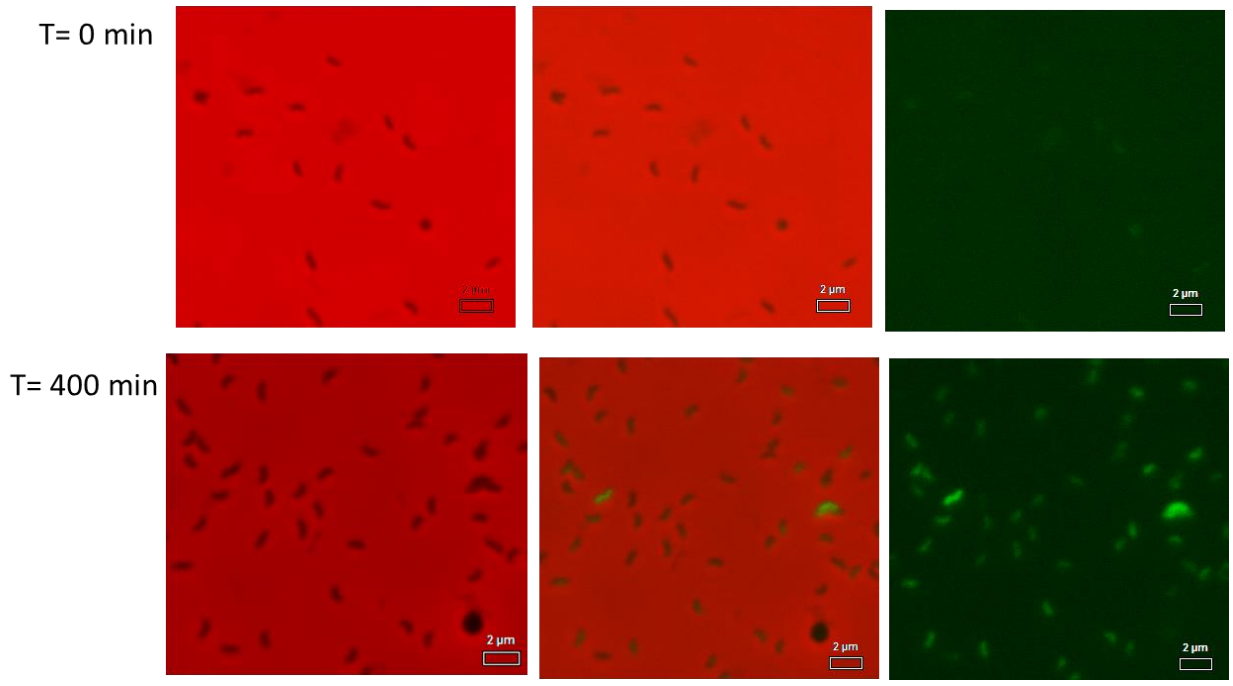

Figure 6.30 : A percentage of *B. bacteriovorus* Bd1482mCherry cells show increased fluorescence when incubated on a surface. The cells were placed on a 1% agarose CaHEPES slide and images were collected at time 0 and time 400 minutes. During this time the slide was kept consistently hydrated and at room temperature. The panel of images shows time 0 at the top and time 400 minutes bellow. The panels left to right show the bright field channel, the merged channel and the fluorescent channel. At time 0 the image shows that the cells had hardly any fluorescence. At time 400min the fluorescence had greatly increased and was located throughout the cell.

6.4.7.2. The increase of Bd1482mCherry fluorescence on a surface is not uniformly distributed in the population

During analysing the effect that surface incubation had on *B. bacteriovorus* Bd1482mCherry cells fluorescence, it was observed that the distribution of fluorescence did not alter staying diffuse throughout the cells. However the intensity of fluorescence was not consistent between surface incubated cells. Interestingly this is similar to the mCherry location data upon surface incubation that resulted for Bd1481 (also increase in 3.59 fold on surface incubation)(Milner, 2014). Over 1000 cells at each time point across 3 biological repeats each with 2 technical repeats were analysed by hand via using the 'analyse counter' function of ImageJ (Section 2.7.5). The results of this are shown in Figure 6.31, the most pronounced change is the decrease of low fluorescence (almost visible at 1 second exposure, more visible at 2 seconds exposure) to medium fluorescence

(visible at 1 second exposure), however there is also a significant increase in high fluorescence(visible at 0.5 seconds exposure) .

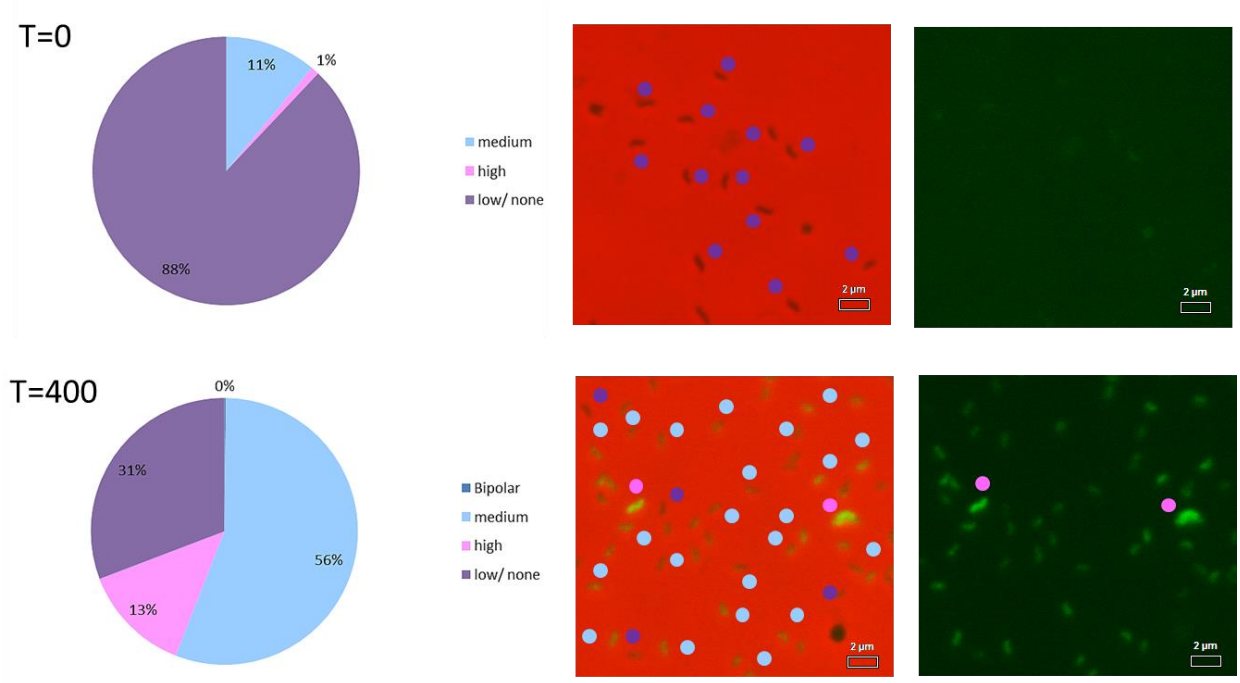

Figure 6.31 Cells exhibiting medium and high fluorescent intensity increased in frequency on surface incubation of *B. bacteriovorus* Bd1482mCherry cells. At time 0 min *B. bacteriovorus* Bd1482mCherry cells showed hardly any fluorescence. This is shown on the pie chart and cells of this description are highlighted by a dot of that colour on the corresponding image next to the cell which indicates which section of the pie chart this cell is representative of. At time 400 the frequency low fluorescence has dropped by 57%. The medium level fluorescent had increased the most on surface incubation- an increase of 45%. Cells with particularly high fluorescence also increased in frequency by 12% on surface incubation. Cells were placed on a 1% agarose CaHEPES slide at room temperature and kept hydrated. These slides were imaged at time 0 and time 400. A total of 1012 cell were analysed at t=0 and 1078 at t=400, these cells were counted across 3 biological repeats each with 3 technical repeats.

In an attempt to analyse what different cellular behaviour was occurring in the low, medium and high fluorescent cells time-lapse videos were taken. This found that only 2% of Bd1482mCherry tagged attack phase cells can glide, Figure 6.32 suggesting that the interference from the mCherry tag had a large effect on gliding motility.

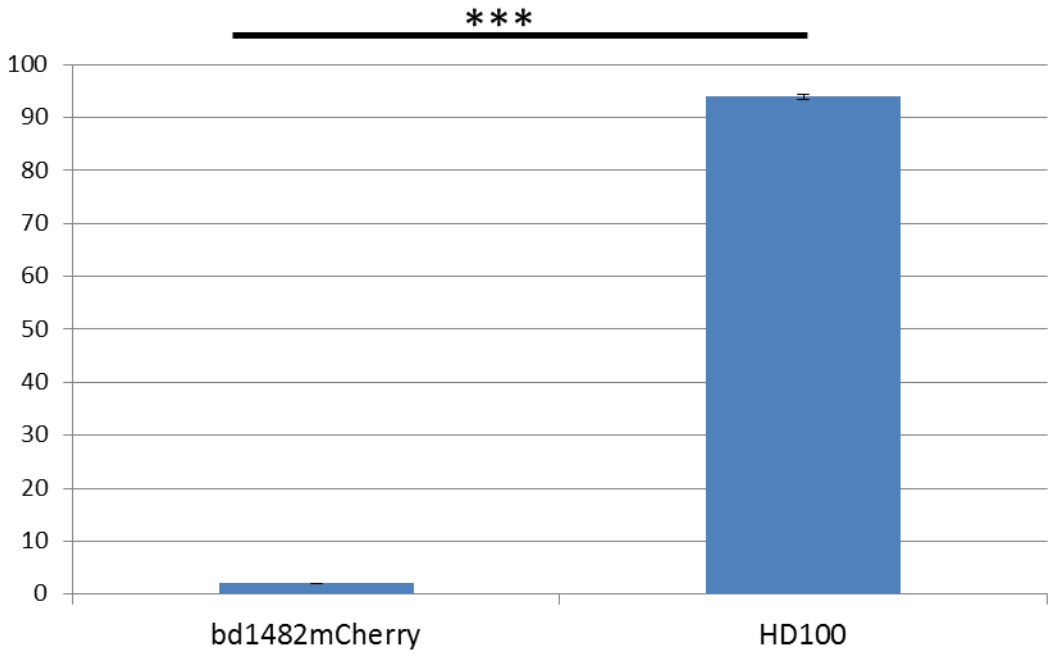

Figure 6.32 Only 2% of HD Bd1482mCherry attack phase cells glide under standard conditions compared to 94% of HD100 cells. The data are obtained from three biological repeats with the total number of cell observed for gliding or stationary being 398 Bd1482mCherry cells and 232 HD100 cells. Error bars show 95% confidence and asterisks show significant difference by Student t test ***≤0.001. A movie of this process can be located on the USB stick attached, titled 'Bd1482mCherry gliding' with a movie titled 'HD100 gliding' as a comparison, further details of these movies are found in Section 8.2.3.

~~6.4.8.~~ Investigating interactions between proteins hypothesised to be involved in gliding motility

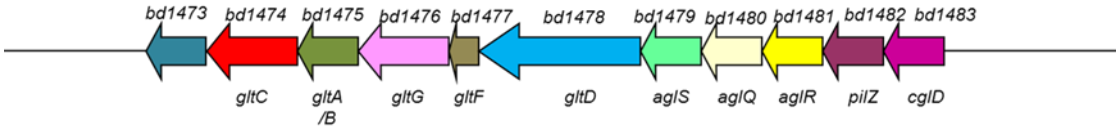

Figure 6.33 *bd1473-bd1483* gliding operon

Multiple pieces of experimental and bioinformatics data shown in this study suggest that Bd3100 and Bd1482 are involved in gliding motility. Gliding motility requires a complex of proteins to carry out the process of moving on a surface. This study hoped to identify other proteins in this 'gliding' complex via finding proteins that interacted with Bd3100. All B2H constructs of the remaining PilZ domain proteins had been constructed by the undergraduate students of 2013 which allowed the possibility of interaction studies.

It was hypothesised that the two similar PilZ domain proteins Bd3100 and Bd1482 could be performing different roles in regulating gliding motility but may interact with each other due to the link of the regulatory secondary messenger c-di-GMP. While studying the above the possibility of dimer formation was also studied. These interactions were tested by B2H and β-galactosidase assays.

6.4.8.1. The two PilZ proteins Bd3100 and Bd1482 implicated in gliding motility do not interact via B2H assay

The B2H spot plate analysis allows a qualitative assessment of the interaction between Bd3100 and Bd1482. Further testing of this interaction was carried out by β-galactosidase activity assays, these assays were used to quantify the strength of interaction between the two proteins. From these results Bd3100 and Bd1482 do not interact, they result in white spots on plates and are not significantly more than the negative in β-galactosidase assays Figure 6.34 and 6.35. These proteins were only tested with N-terminally tagged orientations which may cause steric hindrance due to the nature of the interaction; C-terminal tagging would be required to establish that Bd3100 and Bd1482 never interact.

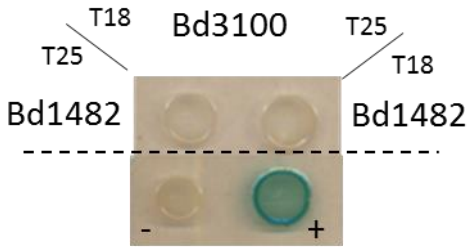

Figure 6.34: Spot plate test for interactions between PilZ domain protein Bd1482 and PilZ protein Bd3100. White spots indicate no interaction between Bd1482 and Bd3100. Results displayed are a typical representation of the results from 3 biological repeats and nine technical repeats. Positive (+) = pUT18c-zip with pKT25-zip. Negative (-) = pUT18c with pKT25.

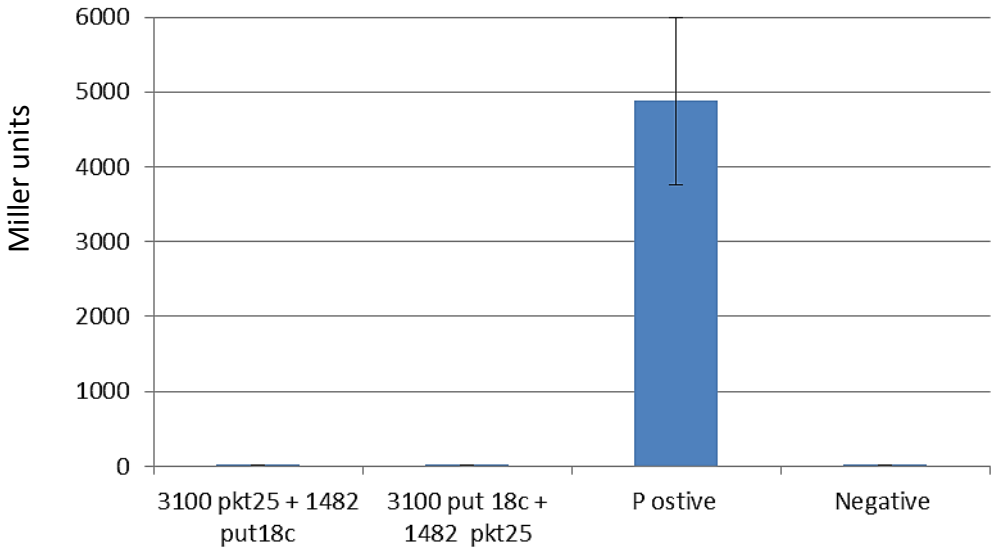

Figure 6.35: β-galactosidase activity assay testing for Bd3100 and Bd1482 show no evidence of an interaction. Error bars show standard deviation The results show the mean value from three biological repeats and comprise six technical repeats.

6.4.8.2. Bd3100 and Bd1482 do not interact as dimers by B2H analysis

From these results Bd3100 and Bd1482 do not form dimers, the test interactions resulted in white spots on plates and are not significantly more than the negative in β-galactosidase assays, Figure 6.36 and 6.37. These proteins were only tested with N-terminally tagged orientations which may cause steric hindrance due to the nature of the interaction; C-terminal tagging would be required to establish that Bd3100 and Bd1482 never form dimers.

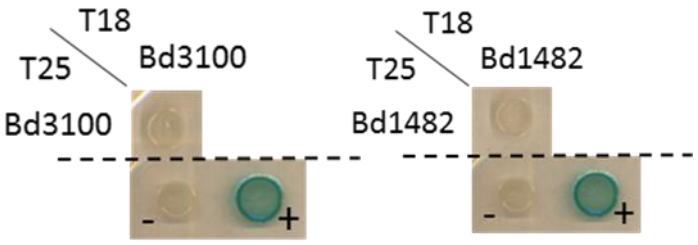

Figure 6.36 Spot plate tests for interactions between potential self-interactions in Bd3100 and Bd1482. White spots indicate no interaction between Bd1482 and Bd3100. Results displayed are a typical representation of the results from 3 biological repeats and nine technical repeats. Positive (+) = pUT18c-zip with pKT25-zip. Negative (-) = pUT18c with pKT25

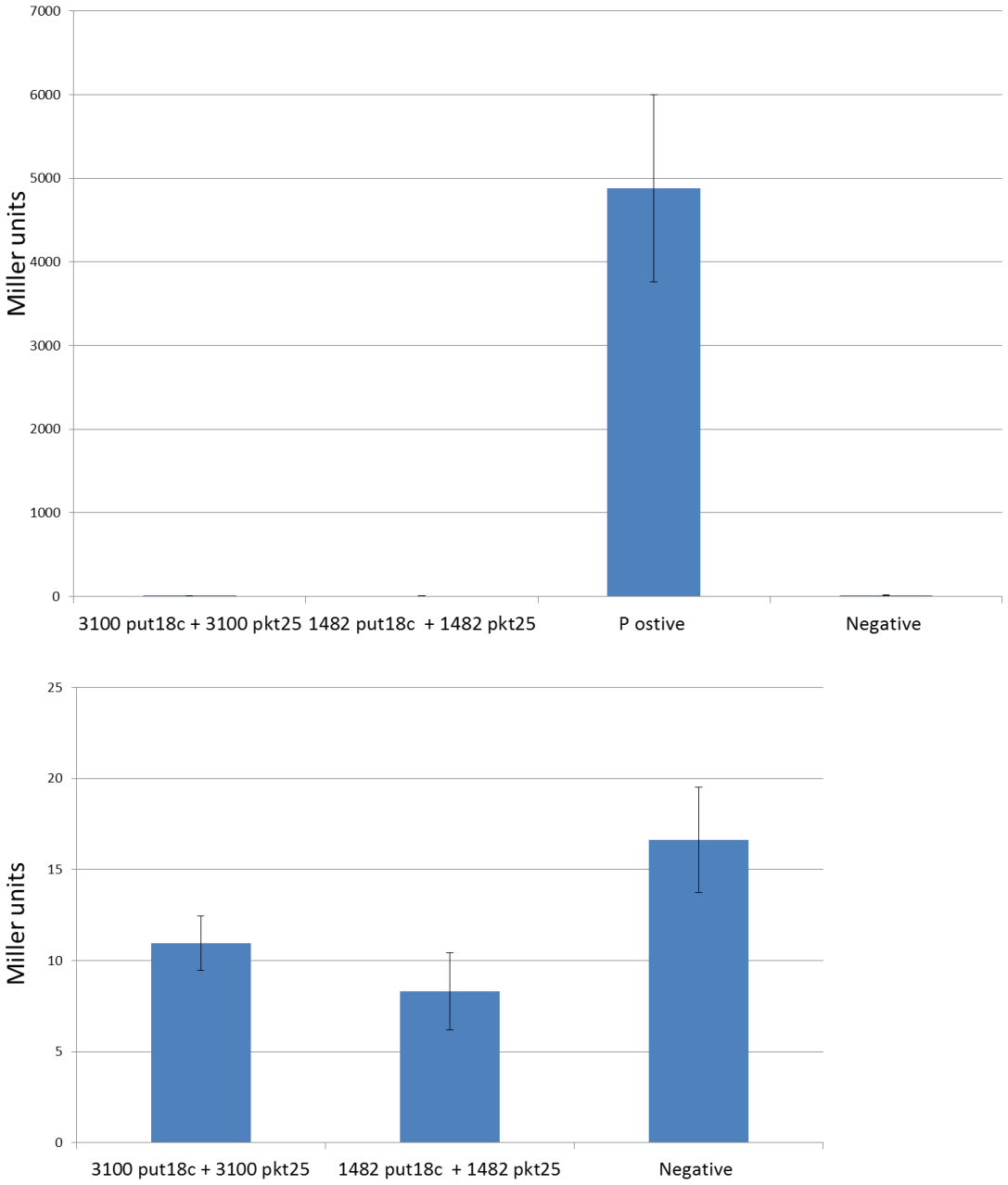

Figure 6.37: β-galactosidase activity assay for Bd3100 and Bd1482 self-interactions show no evidence of an interaction. Error bars show standard deviation. The results show the mean value from three biological repeats and comprise six technical repeats.

6.4.9. Testing for partner proteins of Bd3100 through co-purification assay

To find proteins that interact with Bd3100 *in vivo* a co-purification assay was developed. The strain used was the previously mentioned *B. bacteriovorus* Bd3100mCherry strain, this strain has mCherry fused to the C terminus of the protein, so this could be used as the bait protein (Methods 2.11). The HD strain was pelleted in attack phase as Bd3100 is expressed during this phase and large volumes were required. Once the strain was grown whole cell lysates were used. The native levels of Bd3100mCherry tagged bait protein was hoped bind to the RFP-TRAP chromo-Tek beads and allow interacting proteins bound to Bd3100 to be analysed. However the bait protein was not successfully pulled out by the beads on multiple occasions. There is however a visible band at the correct weight for mCherry (28 kDa) (Figure 6.38A) and a lower band, as these two bands were observed in the Bd3100mCherry strain and the control RomRmCherry strain (seen more clearly in Figure 6.38B the silver stained gel) it is presumed that the band at 28kDa is cleaved mCherry and that the lower band is a degradation product of mCherry rather than an interaction. This leads to the conclusion that proteases are cleaving the mCherry from the bait protein Bd3100 and control bait protein RomR. Due to lack of the bait protein Bd3100 present on the beads it was impossible to find new interacting partners of Bd3100 by this method, so it work was not continued.

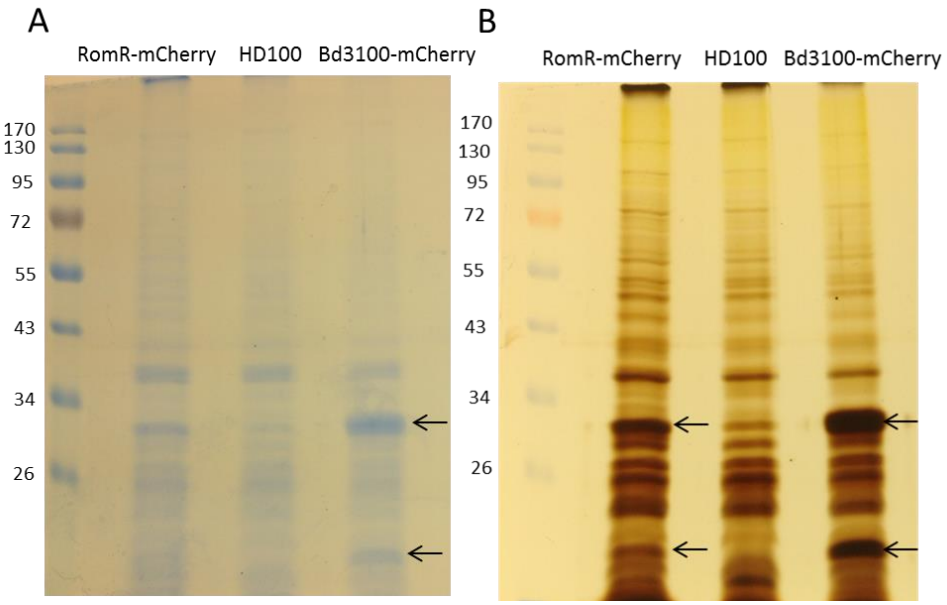

Figure 6.38 Bd3100-mCherry co-purification attempts resulted in bands of cleaved mCherry. SDS-PAGE on a 12.5% gel, with EZ-Run™ Prestained Rec Protein Ladder.

The left lane shows RomRmCherry strain used as a control, then HD100 which was a control, then Bd3100mCherry used as the test strain. The two bands that were present in Bd3100mCherry but not in HD100 were present in lower amounts in the RomR-mCherry strain (A and B). This suggested that the differences were due to the mCherry tag rather than the attached bait protein. It is expected that the protein at 28kDa is cleaved mCherry and the lower band is a putative degradation product.

6.5. Discussion

These data suggest that Bd3100 is involved in gliding motility in *Bdellovibrio* with deletion resulting in hyper reversals and delayed onset of gliding. The mechanism by which a c-di-GMP binding PilZ protein Bd3100 mediates an effect on *Bdellovibrio* gliding is unknown. However Bd3100 is part of the c-di-GMP signalling network and has been found to interact with DGC Bd0367, which is required for functional gliding suggesting the mechanism may incorporate the c-di-GMP network. Further analysis has demonstrated that the location of Bd3100 fluorescence becomes increasingly mono polar on surface incubation or when expressed in a high c-di-GMP background. This suggests that the c-di-GMP bound state of Bd3100 may be important in localisation. However it is currently unknown what the purpose of this increase of Bd3100 at the cell pole is, the possible roles for Bd3100 in c-di-GMP signalling and gliding motility are discussed below.

6.5.1. PilZ domain protein Bd3100 interacts with full length DGC protein Bd0367

The B2H interaction studies carried out between Bd3100 and Bd0367 concluded that there is reliable and repeatable spot plate evidence that Bd3100 and Bd0367 full length interact. β-galactosidase quantification data also supports this conclusion, as though the interaction strength is small it is significantly different in strength from the negative control. This weak interaction strength is not surprising as it could be speculated that the receptor protein Bd3100 would only transiently interact with the producer protein Bd0367.

Additionally it can be hypothesised that Bd3100 may only strongly bind to Bd0367 when Bd0367 itself is in a certain conformation. The conformation of Bd0367 can be altered by phosphorylation, which stimulates dimerization and c-di-GMP production. In the BTH101 *E.coli* strain we predict that Bd0367 is not phosphorylated as dimerization interaction strengths did not alter when using a Bd0367D63A construct (chapter 3).

To test if Bd3100 had a stronger interaction with the dimerized form of Bd0367 a phophomimic Bd0367 would be constructed for further B2H analysis.

Another consideration is that all B2H constructs examined are N terminally tagged, it is always possible that the tag may be causing steric hindrance and an alternatively C terminally tagged construct may have been hindered less and formed a stronger interaction.

The lack of an interaction between Bd3100 and the split domains of Bd0367 by B2H and β-galactosidase assays indicates that Bd3100 only interacts with the full length Bd0367. I had assumed that Bd3100 may preferentially bind to the DGC domain of Bd0367 in order to be in close proximity to receive c-di-GMP, however this was not the case. It could be that when Bd0367 dimerizes in production of c-di-GMP there is a better location for Bd3100 to bind to and by splitting the domains the structure of this binding location was not was preserved in either domain. This theory was supported by a recent study that showed mutations destabilising the dimerization of DGC GcbC resulted in a loss of interaction between itself and its effector LapD (degenerate EAL) by B2H (Dahlstrom et al, 2015).

The relevance of Bd3100-Bd0367 interaction *in vivo* was established by the comparing the mCherry tagged locations of Bd0367 and Bd3100 in the cell. As Bd0367 is most commonly located throughout the cell (86%) it is likely that it is available to interact with Bd3100, which is distributed throughout the cells or at the poles.

The interaction of PilZ domain protein Bd3100 with DGC Bd0367 is still the only interaction of its sort PilZ-DGC to date in *Bdellovibrio*, despite the systematic testing of multiple PilZ proteins by undergraduate students in the Sockett lab. However more of these PilZ proteins could still interact with DGC proteins as N terminal tagging or truncated constructs may account for the lack of any detectable interaction. However there is another effector protein that interacts with Bd0367, as previously mentioned in Chapter 3 the degenerate GGDEF Bd3125, but due to its preferential binding to the Bd0367 RR domain we suggest in Chapter 3 that it provides a regulatory role rather than a specific binding of the produced c-di-GMP.

The role of this physical interaction in the downstream effect of mediating gliding motility is yet to be determined however this discovery of physical interactions between producers and effectors may explain how cross talk between different c-di-GMP

signalling systems in *Bdellovibrio* is controlled and suggests a means of locally insulating signalling pathways for a particular output.

Future work should establish if Bd3100 binds specifically to c-di-GMP or if it is promiscuous and can also bind and respond to cAG produced by Bd0367. The possibility of Bd3100 binding to cAG is suggested due to the recent observation that Bd3100 interaction partner Bd0367 is a Hypr GGDEF that can produce cAG and the study by Rotem and colleagues that found Bd3100 to be a borderline candidate c-di-GMP binder as it was only >2 fold enriched 2 out of 5 times (Hallberg et al, 2016; Rotem et al, 2016). To determine the true cyclic nucleotide binding preference of Bd3100 for c-di-GMP or cAG should be investigated by microscale thermophoresis to determine the K_d or by DRaCALA (differential radial capillary action of ligand assay) in the future.

The current understanding of the Bd3100-Bd0367 interaction is summarised in Figure 6.39. It is clear that further investigation is required to determine the exact interaction site for this protein interaction and the role that c-di-GMP/cAG levels play in complex formation. These aspects could be analysed by B2H analysis via an alanine mutagenesis screen for the interaction site and by mutation of the RxxxR motif in Bd3100 to observe if the interaction can occur when c-di-GMP or cAG is no longer able to bind Bd3100.

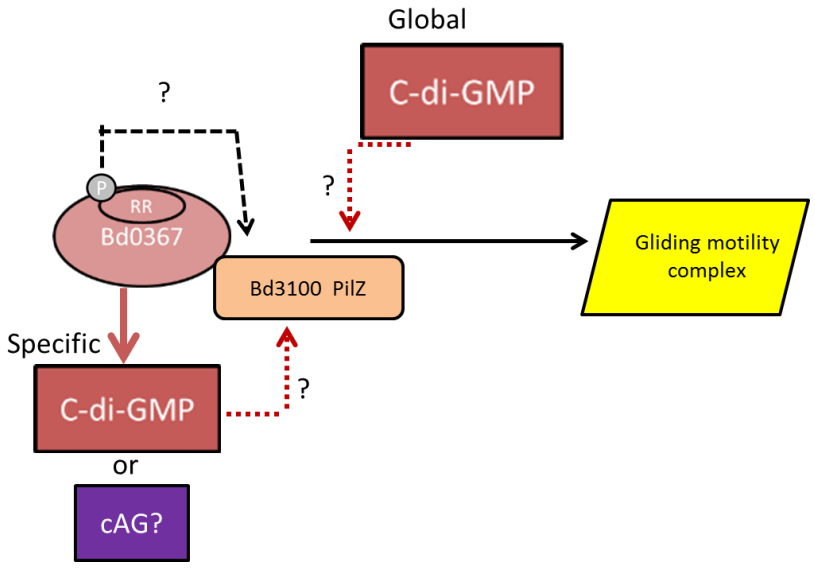

Figure 6.39 Bd0367 and Bd3100 form a transient interaction. It is unknown what factors may effect this interaction, it is possible that the interaction is strengthened or weakened by the phosphorylation and dimerization state of Bd0367. It is also possible that the interaction strength is controlled by the c-di-GMP bound state of Bd3100, the c-di-GMP/cAG that Bd3100 binds by the PilZ domain may be specific to Bd0367 or from the global c-di-GMP pool. I hypothesis that Bd3100 is activated by c-di-GMP binding

dissociates from Bd0367 to instead interact with an unknown protein in the gliding complex to regulate gliding direction.

6.5.2. No other protein interactions with Bd3100 were identified by B2H analysis

Due to success in Chapter 3 of identifying multiple interactions between c-di-GMP proteins and Bd0367 by B2H analysis a similar approach was taken with looking for other interacting partners for Bd3100.

The protein investigated was Bd1482 PilZ Duf4339 protein, this protein was chosen due to their common role in c-di-GMP signalling and similarity of domains in the case of Bd1482.

6.5.2.1. PilZ domain proteins Bd3100 and Bd1482 do not dimerize

The proteins Bd3100 and Bd1482 were tested for potential dimerization, as previous studies had shown some PilZ domain proteins can be dimers in their apo or holo forms (Ko et al, 2010). However the study also found that in some PilZ domain proteins c-di-GMP binding can trigger a structural change from a dimer to a monomer, which could have resulted in a weak or partial interaction by B2H depending on proportion of protein that was c-di-GMP bound in BTH101 cells.

The result of no dimerization of either PilZ protein by B2H spot plate analysis and β-galactosidase assay was not completely unexpected as PilZ PA4608 had been previously found to remain in monomeric form when bound or unbound to c-di-GMP (Christen et al, 2007; Habazettl et al, 2011). The different ways in which PilZ domains bind to c-di-GMP and the different results of this binding on the structure arrangements allow PilZ domains be versatile and may contribute to its evolutionary flexibility (Habazettl et al, 2011). Additionally the lack of dimerization could be due to interference caused by the N terminal tag, making constructs with the c terminal tag also could give a different result.

6.5.2.2. PilZ domain proteins Bd3100 and Bd1482 do not interact with each other

Due to the potential role of both PilZ domain proteins in gliding motility the possibly of the two interacting was investigated. They were found not to interact by B2H spot plate analysis or β-galactosidase assay; again this lack of interaction could be due to the N

terminal tagging interfering or it could be there is no interaction between these protein *in vivo*.

6.5.3. Bd3100 deletion results in slow gliding initiation and an increased in gliding reversal events

6.5.3.1. Phenotype on Bd3100 deletion

The deletion of Bd3100 resulted in an aberrant gliding phenotype in HD attack phase cells.

A similar percentage of cells compared to WT were able to glide however the Δ*bd3100* strain was found in this study to be significantly slower in initiating gliding motility taking more than 60 minutes longer than HD100 to begin gliding. This observed delay in gliding motility could suggest that part of the role of Bd3100 is to aid organisation and localisation of proteins in the gliding motility complex to be assembled into Focal Adhesion Complexes (FAC) at the leading pole.

Additionally the number of reversal events was more frequent with a mean of 5.8 reversals per hour in the Bd3100 deletion strain compared to 2.5 reversals per hour in the HD100 strain, this was a significant increase with a 2.32 fold increase in reversals on *bd3100* deletion. The increased or decreased frequency of gliding reversals has been observed in gene deletions and mutations in *Myxococcus*, commonly this phenotype is caused by the deletion of a cell pole determining factor such as MglB, MglC or RomR (Leonardy et al, 2007; McLoon et al, 2016; Zhang et al, 2012). This suggested that Bd3100 was not required for gliding motility *per se* but was required for proper regulation of reversal frequency and may act as a cell pole determining factor. Which is important for organisation of gliding complexes or FAC in enabling the cells to have sustained runs and make progressive movement. This mutant was complemented and reversal frequency was restored to WT levels, the gliding initiation start time was partially complemented.

6.5.3.2. Hypothesising the role of Bd3100 in gliding motility

The mechanism by which Bd3100 is in involved in regulating gliding onset or reversal frequency is currently unknown, however we speculate that Bd3100 mediates this control by interactions with proteins in the gliding motility complex/FAC and that these interactions occur when Bd3100 is activated by c-di-GMP binding to the PilZ domain. This would allow integration of c-di-GMP level signalling into to gliding control. Recent

experimentation by Rotem and colleagues showed that though Bd3100 is a cytoplasmic protein it was found in the membrane fraction when assaying for c-di-GMP binding proteins, this suggests to me that Bd3100 may have an unknown interaction partner in the membrane, this is promising as most of the gliding motility complex proteins are membrane bound (Rotem et al, 2016). To find out if Bd3100 interacts with a membrane bound gliding motility complex protein a large B2H screen of the ~40 gliding proteins in *Bdellovibrio* could be carried out to elucidate the partner protein that Bd3100 is regulating, starting first with those that are cytoplasmically facing (see Figure 6.40).

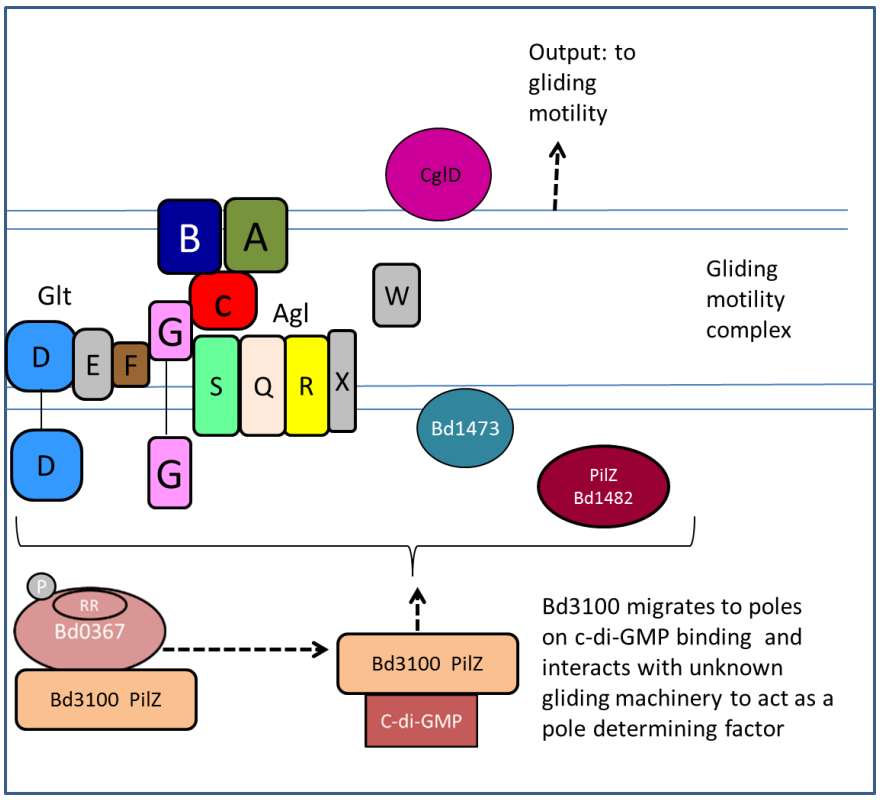

Figure 6.40 Bd3100 may form unknown interactions with the gliding motility complex at the cell pole. This diagram represents all the known gliding components in *Bdellovibrio* however it does not show the duplication of many of these proteins. The positions of these proteins are predicted cellular locations from PSORTb or by using locations of homologous *Myxococcus* proteins (Islam & Mignot, 2015; Jakobczak et al, 2015).

From our current data I predict that Bd3100 has a role in pole determination, I predict it is one of the proteins involved in defining the leading pole when cells are gliding. This is suggested as the pole determining factors are currently unknown in *Bdellovibrio* as the homologues to pole defining proteins used by *Myxococcus* have been repurposed to control predation in *Bdellovibrio*. However to properly determine this requires much

further investigation, but if correct would provide a potential alternative system to MglA, MglB, MglC and RomR in how to define the leading and lagging cell poles in gliding cells.

Model 1: Bd3100 acts as a pole determining factor that signals to the focal adhesion complexes to assemble at the leading pole

From data discussed previously in Section 6.4.2 Bd3100 interacts with Bd0367 and is possibly activated by binding to c-di-GMP or cAG specifically produced by Bd0367. The activity of Bd0367 is controlled by phosphorylation from an unknown HK in response to an unknown signal; in this model it is assumed that the signal indicates that the cell is located on a solid surface, stimulating Bd0367 DGC activity. This increase in DGC activity may increase the level of c-di-GMP bound Bd3100, this binding may mediate the increased polar localisation of Bd3100mCherry on surface incubation (discussed in Section 6.5.4). Activated Bd3100 locates to the leading cell pole by an unknown process and interacts with an unknown protein to signal that Focal Adhesion Complex assembly will take place at this particular pole (see Figure 6.41). This regulates the process of assembling the gliding motility complexes.

In the Δ*bd3100* strain the lack of Bd3100 results in a less defined cell polarity so the gliding motility complexes/FAC take time to assemble and assemble at both the leading and lagging poles, so there is no defined leading pole, the assembly of FAC at both poles results in a back and forth struggle which appears as increased gliding reversals.

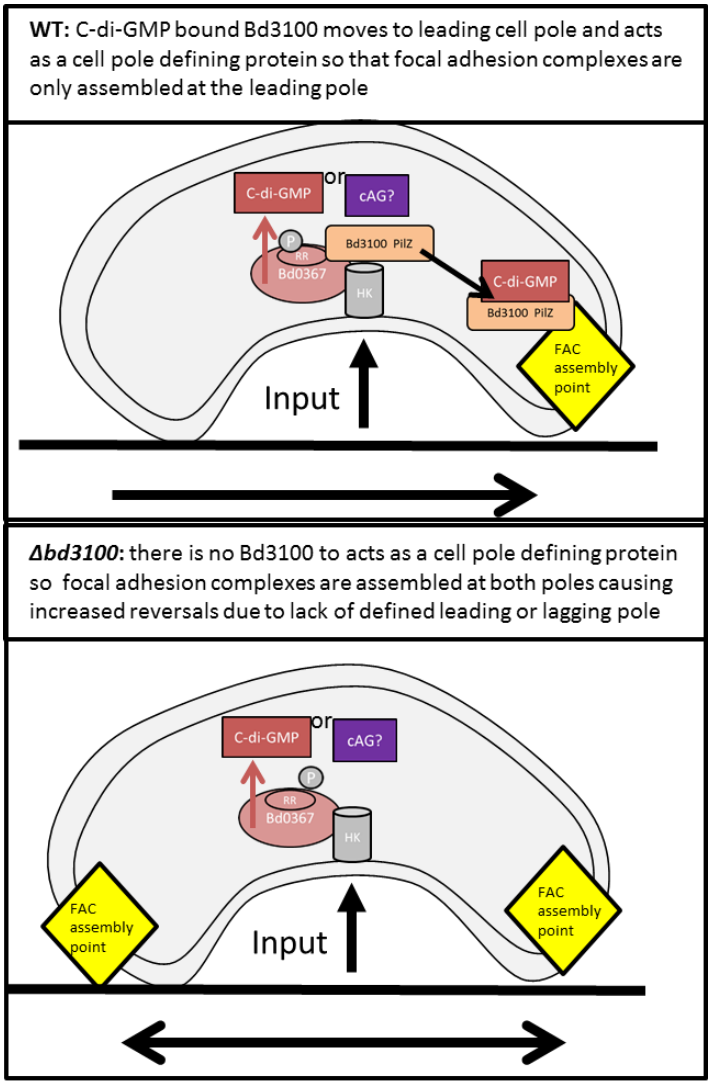

Figure 6.41 Bd3100 acts as a pole determining factor that signals to the focal adhesion complexes to assemble at the leading pole

Model 2: Bd3100 acts indirectly to exclude a protein from the leading pole that can induce FAC disassembly

In this model gliding motility complexes/FAC are located and assembled at the correct leading pole due to presence of another unknown pole determining factor: The role of Bd3100 in this model is to exclude a protein that can induce FAC disassembly specifically at the leading pole. I hypothesis that this disassembly protein is only located at the pole only upon a reversal event. In a reversal event Bd3100 moves to the new leading pole, the absence of Bd3100 allows the disassembly protein to aid in the pole reassignment by disassembling the FAC at the old leading pole, aiding in transforming this pole to the new lagging pole.

However in the Δ*bd3100* strain, the disassembly protein is not excluded from the leading pole, this means this protein can now locate to the 'leading' pole more often that it should and the proteins disassembly action reassigns the pole to the lagging pole, this increased disassembly and pole switching means increased reversal events in the Δ*bd3100* strain. See Figure 6.42.

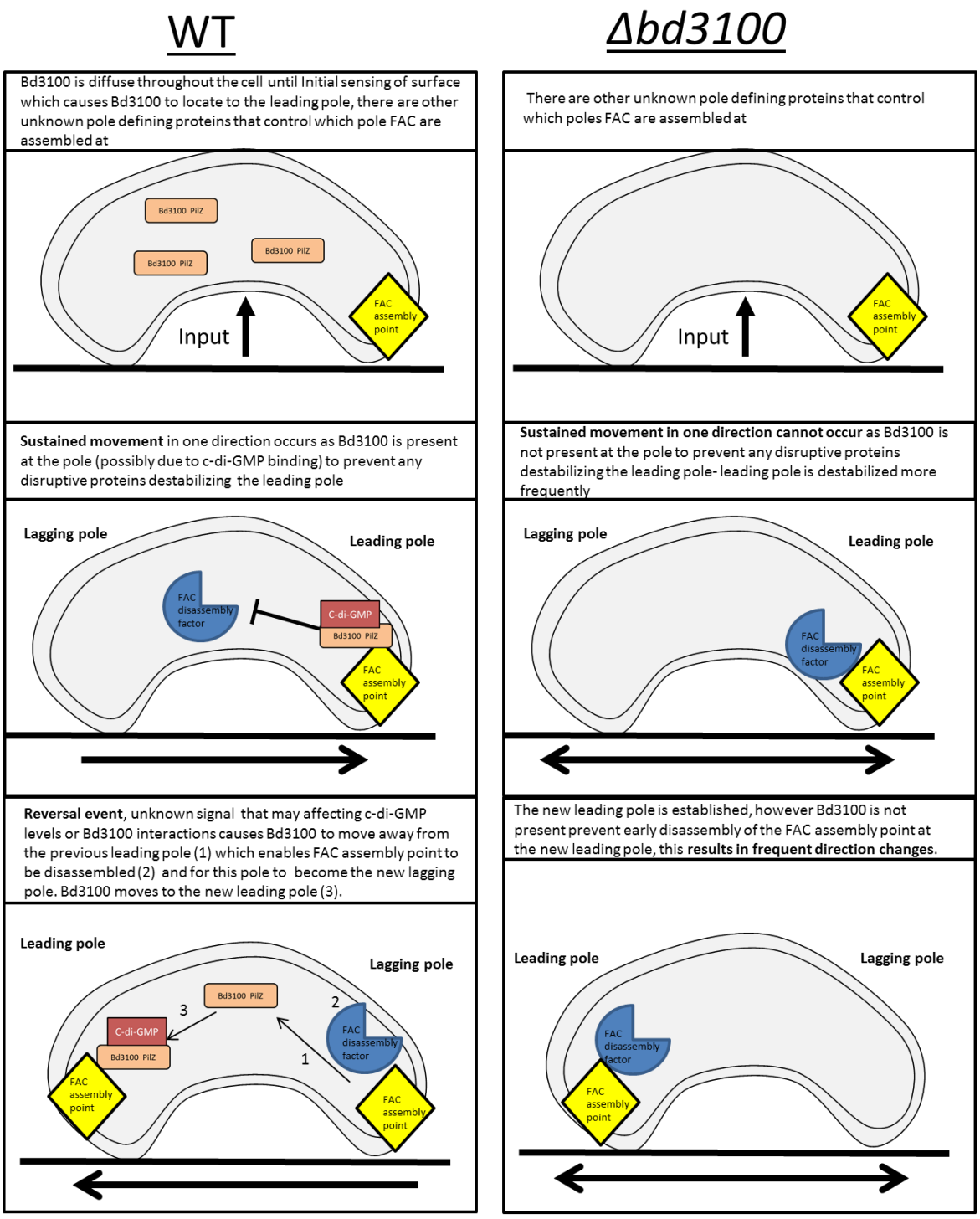

Figure 6.42 Role of Bd3100 in regulating gliding direction by exclude an unknown protein from the leading pole that can induced FAC disassembly

6.5.4. Role of Bd3100mCherry location and intensity changes

The location of Bd3100 in the cell was examined in the hope to further elucidate its function. This showed an increased fluorescence of 1.57 fold on surface incubation and a 34% increase in dominant mono polar localisation. This study also showed that without surface incubation Bd3100 fluorescence increased by 1.276 fold in a high c-di-GMP background (Δ*bd1971*) and had a 13% increase in dominant mono polar localisation compared to Bd3100mCherry at T0 in HD100. This and deletion study data suggested that Bd3100 is part of a signalling system responsible for controlling gliding motility and that this system may be integrated with the c-di-GMP network of *Bdellovibrio*.

6.5.4.1. What causes the increased frequency of dominant monopolar localisation of Bd3100mCherry?

The increase in frequency of Bd3100mCherry being located at one pole occurs on surface incubation and in a high global c-di-GMP background strain. This suggests that c-di-GMP levels may be elevated in *Bdellovibrio* cells upon surface incubation, further study through c-di-GMP extractions would be required to determine this.

I hypothesis that the location of Bd3100mCherry in the cell may be effected by the c-di-GMP bound state of the protein. So I predict c-di-GMP binding Bd3100 activates the protein to locate to the pole or to interact with an additional unknown protein which sequesters Bd3100 to the pole. To test this theory constructing a Bd3100 mCherry construct with the RxxxR site mutated should result in a localisation pattern where Bd3100 is only located diffusely through the cell if this hypothesis is correct.

The control for this experiment was Δ*bd0367* a low c-di-GMP strain, in which Bd3100mCherry is less frequently located at the pole. However Bd3100 interacts with Bd0367 so it is possible that the lack of this partner protein has caused this diffuse location. Though it was shown that Bd0367mCherry T400 location was unaffected by the absence of Bd3100, suggesting that these two proteins may not collocate or mediate each other's location, however further work is required. In future the Bd0367D63A strain should be double crossed over to remove Kan selection and allow for observation of Bd3100mCherry location when Bd0367 is present to interact with but the c-di-GMP level is low, to confirm that the c-di-GMP level is having this effect not lack of interaction partner.

However I doubt that mechanism of Bd3100 relocating to the poles is dependent on the interaction with Bd0367. If that was the case I would expect the protein complex to be delivered to pole. This would result in the percentage of Bd0367 localised at the pole to be similar to that of Bd3100mCherry which it is not (9% compared to 38%), this suggests the interaction between the two proteins is most likely transient and does not result in Bd0367 co-locating with Bd3100.

6.5.4.2. Is Bd3100mCherry located at the leading pole?

The role of Bd3100 once it is located to the pole is unknown. It is assumed that Bd3100 interacts with the gliding motility complex, however it is unknown if this interaction is occurring at the leading or lagging pole. During this study I attempted to visualise the location of Bd3100mCherry in actively gliding cells (data not shown) however this did not generate much information due to mCherry bleaching on repeat exposures. It is possible that Bd3100 recruits or excludes proteins from interact with the gliding complex, it is also possible that Bd3100 interacts directly with a protein that comprises the gliding motility complex and that this possibly alters the proteins conformation and the output of the gliding motility complex. These theories correlate with Models discussed for deletion section.

6.5.5. Investigating the role of Bd1473 in gliding motility

Bd1473 was investigated in this study as it is a novel protein in *Bdellovibrio* located in a potential gliding operon and from work by Dr Milner showed an mCherry localisation pattern similar to Bd3100 and the fact that this mCherry tag caused the strain to hyper reverse, suggested that Bd3100 may act in the same pathway as Bd1473.

The localisation of Bd1473 was altered on a surface resulting in 37% of cells having monopolar Bd1473 and the intensity of Bd1473 fluorescence also increased by 5.39 fold, suggesting that it is involved in *Bdellovibrio* gliding motility. To investigate the potential link between Bd3100 and Bd1473, Bd1473mCherry was conjugated into the Bd3100 deletion strain. On surface incubation Bd1473mCherry now had a mono polar location 73% of the time, this was a 2.15 fold increase compared its localisation in WT.

This result suggested that Bd3100 may play a role in regulating the location of Bd1473 but how or why is still unknown. However I have one hypothesis discussed below which links to model 2 discussed in the deletion section.

Model 1: Bd1473 is involved in causing the disassembly of the gliding motility complex /FAC at the old leading pole

I predict that Bd1473 is involved in causing the disassembly of the gliding motility complex at the old leading pole, in order for it to become the new lagging pole on cellular reversal events. I previously predicted that Bd3100 may act as a pole determining factor that prevents destabilizing proteins locating to the leading pole. The frequency of this predicted disassembly is increased in the absence of Bd3100, which results in the increased frequency of reversal events in the Bd3100 deletion strain see Figure 6.43. It is interesting to note that in the Bd3100 deletion strain reversal frequency increases by 2.5 fold and that the monopolar location of Bd1473mCherry increases by 2.15 fold when expressed in the Bd3100 deletion strain. Suggesting that the reason for the increased reversals may be linked to the increased prevalence of Bd1473 location at the pole.

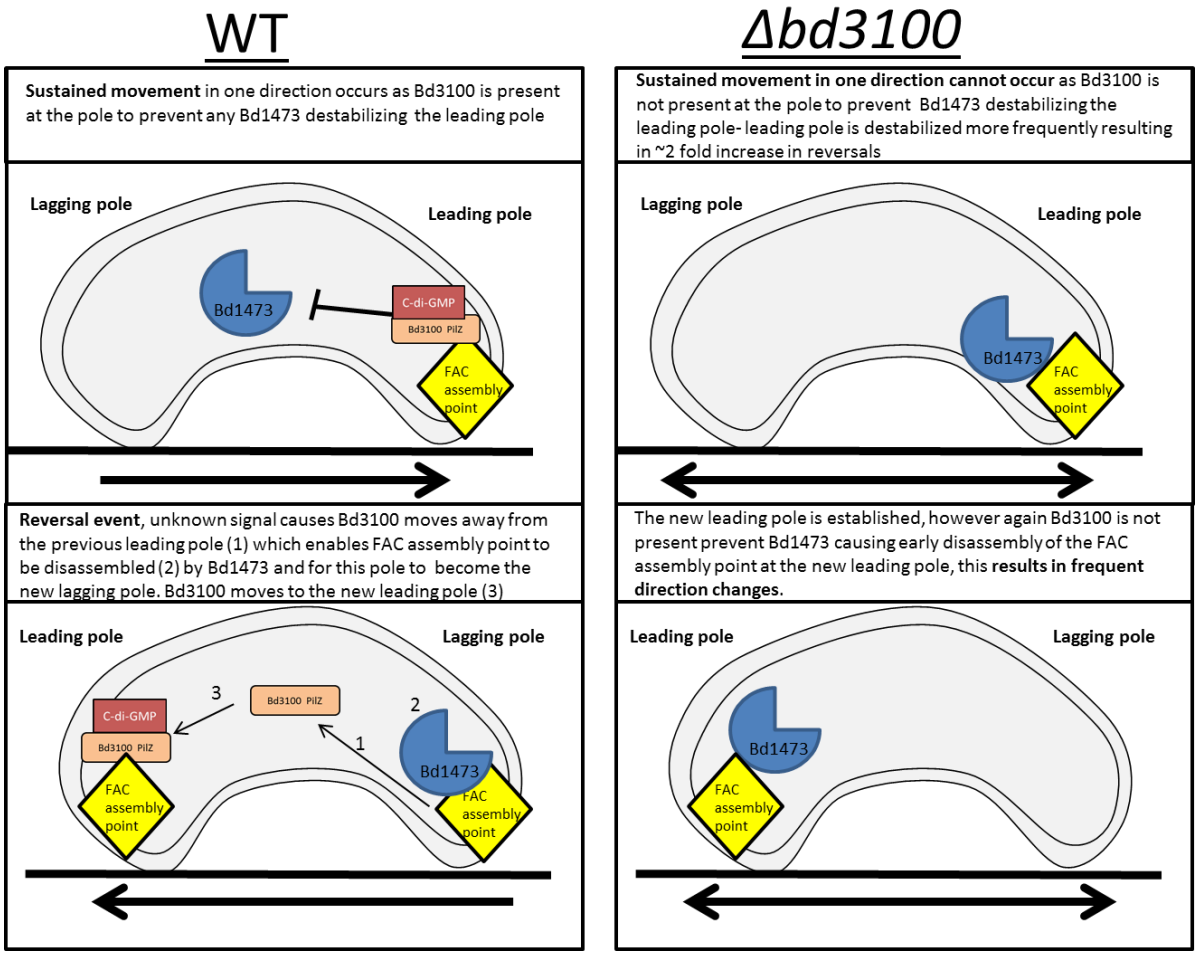

Figure 6.43 Bd1473 is involved in causing the disassembly of the gliding motility complex. This model shows the process in a WT gliding cell and in a Δ*bd3100* strain, to explain the increase in gliding reversals.

6.5.6. Fluorescent microscopy indicated that PilZ domain protein Bd1482 is involved in *Bdellovibrio* gliding motility

Bd1482 was briefly analysed in this study as it is a PilZ domain protein with Duf4339 domain like Bd3100 and shares 27.75% identity and is located in the gliding operon. These properties suggested Bd1482 was likely involved in regulating *Bdellovibrio* gliding motility.

6.5.6.1. Bd1482mCherry results in reduced gliding

The location and intensity of Bd1482mCherry on a surface was examined to assess if it was involved in gliding motility and if it had similar subcellular localisation to Bd3100. A 4.63 fold increase in fluorescent intensity occurred on surface incubation suggesting it was upregulated by surface incubation so was involved in gliding. However though Bd1482 fluorescent was always located diffusely throughout the cell the level of intensity between cells varied greatly. Time lapse microscopy was carried out to observe if there were distinct gliding patterns in the low vs high intensity Bd1482mCherry cells. However these videos showed that gliding motility was vastly reduced, with only 2% of cells observed gliding (compared to 94% that glide in WT HD100 attack phase). This suggested that functional wild type Bd1482 is crucial for gliding motility to occur in *Bdellovibrio* and that Bd1482 did not appear to act similarly or in conjunction with Bd3100.

The mechanism by which Bd1482 is involved in gliding is unknown however I have two hypotheses.

Model 1: Bd1482 is important for gliding initiation

I predict that Bd1482 may be activated by c-di-GMP binding the PilZ domain and then bind via its Duf4339 domain to an unknown gliding motility protein. I suggest that that this binding causes a conformational change that may aid in assembly and organisation of the gliding machinery and allow gliding motility to occur. I propose that in the Bd1482mCherry tagged strain the C terminal mCherry tag is creating steric hindrance that prevents the activating protein interactions at the gliding motility complex or that mCherry is hindering the correct localisation of Bd1482. This results in very rare occurrence of gliding motility.

Model 2: Bd1482 acts as a molecular brake

I predict that Bd1482 may be activated by c-di-GMP binding the PilZ domain and then bind via its Duf4339 domain to an unknown gliding motility protein. I suggest that that c-di-GMP binding causes a conformational change that enables Bd1482 to bind a protein in the motility complex and act as a molecular brake causing a conformational change in the unknown gliding protein that prevents gliding motility. The concept of a PilZ domain acting as a molecular brake has previously been predicted for PilZ domain protein YcgR in flagellar based motility as Ycrg interacts with flagellar switch complex proteins and inhibits flagella motility by reducing the efficiency of torque generation (Paul et al, 2010). I propose that in the Bd1482mCherry tagged strain the C terminal mCherry tag has altered the conformation of Bd1482 meaning that it is active and acting as a 'brake' without the signal from c-di-GMP binding, resulting in very rare occurrence of gliding motility in this strain.

To properly understand the role of Bd1482 in *Bdellovibrio* requires gene deletion and phenotyping and analysis of the affinity of Bd1482 to c-di-GMP.

6.5.7. No additional interacting partners of Bd3100 were identified

As the deletion of *bd3100* results in hyper-reversal gliding phenotype it is suspected that Bd3100 interacts with unknown gliding proteins to maintain cell polarity and sustained movement. To further understand this process of gliding we began to explore interacting partners of Bd3100. This was carried out by a native co-purification technique in which Bd3100-mCherry was the bait that bound to RFP-TRAP beads. The hope was that Bd3100 would be bound to the beads via the mCherry tag at native levels and that gentle washing would allow interaction partners to be bound to the beads through interaction with Bd3100. These interacting proteins would be investigated on SDS-PAGE and sent for protein identification. In this study we discovered no interacting partners for Bd3100. There are many reasons for this, firstly using native levels of the protein would probably not result in much bait protein, but may have resulted in more biologically relevant interaction partners. Additionally the use of the mCherry tag was considered an interesting tool to evaluate as we have many mCherry tagged proteins, however the size of the tag (28 kDa) in comparison with a His-tag shows that the mCherry tag could block potential interactions or disrupt the confirmation of the bait protein. The main problem

however was the suspected cleavage of the mCherry tag from the bait protein Bd3100, this means that not even low native levels of Bd3100 were available on the beads to pull out interacting partners. The cleavage of the mCherry tag from Bd3100 is thought to have occurred because of the high protease activity of *Bdellovibrio*. The protease activity may have been particularly high as this experiment used attack phase cells that have an arsenal of proteases present to enable predation. The protease activity may be lower in the HI stain, however the HD attack phase cells were initially used as this is the type of cells that all other fluorescent and motility analysis has been carried out in for Bd3100. Another consideration for future work on finding interacting partners for Bd3100 is its potential to binding membrane proteins so Bd3100 could have been lost in the membrane fragment if it is not examined.

6.6. Further Experiments

To progress this work further and help establish the role of Bd3100 and other proteins involved in gliding motility in *Bdellovibrio* the following experiments are recommended.

1. Make more B2H constructs. To examine the effect of a Bd0367 phosphomimic mutation has on the strength of the Bd3100-Bd0367 interaction. To locate the interaction site of this interaction pair by alanine substitution mutagenesis in B2H constructs. To mutate the Bd3100 RxxxR site to determine if the Bd3100 interaction with Bd0367 is mediated by c-di-GMP bound state. Additionally a B2H screen with Bd3100 and the cytoplasmic facing gliding motility proteins of *Bdellovibrio* could be carried out to attempt to find an additional interaction partner.
2. Examine the role of c-di-GMP binding the RxxxR site on Bd3100 by mutating this location in the Bd3100mCherry strain to establish if this mutated version can still locate to the cell pole.
3. Confirming that the diffuse location at low c-di-GMP is due to the low c-di-GMP level and not the lack of interacting partner Bd0367 by creating a silent version of the Bd0367D63A strain.
4. Biochemically characterise the binding affinity of Bd3100 for c-di-GMP/cAG by DRaCALA or microthermal calorimetry or isothermal calorimetry.
5. Attempt to develop a new microscopy method to follow the location of Bd3100mCherry in a gliding cell to determine if Bd3100 is located at the leading pole and if the rearrangement of Bd3100 to the new leading pole can be observed

after a reversal event. This could also be used to observe the location of Bd1473mCherry when a reversal event occurs. In *Myxococcus* this has been achieved by imaging cells at 30 sec intervals for 15 min. These videos were analysed by Metamorph software which can determine the position of the maximum fluorescence signal in individual cells over time allowing observation of fluorescent location shifting over time in moving cells and allows this profile to be matched with the corresponding video footage (Leonardy et al, 2010).

6. Gene deletions of Bd1473 and Bd1482 and phenotyping would aid in elucidating their function.

6.7. Chapter Conclusions

The role of c-di-GMP in *Bdellovibrio* gliding motility was expanded in this study by confirming the DGC Bd0367-Bd3100 PilZ domain interaction by B2H and fully phenotyping the effect of the Bd3100 deletion on *Bdellovibrio* gliding reversal frequency. Further study of Bd3100mCherry by fluorescent microscopy showed that the location of Bd3100 became more polar on surface incubation and was more polar when expressed in a high cellular c-di-GMP background compared to a low c-di-GMP background, suggesting the c-di-GMP bound state of Bd3100 may influence its location in the cell. However further work is needed to confirm this. How Bd3100 interacts with the gliding machinery or other accessory proteins to mediate changes in gliding motility is currently unknown however this study began to investigate this through examining proteins Bd1473 and Bd1482. The fluorescent microscopy data gathered here on these proteins suggests they are important in gliding motility as their position encoded in one of the potential gliding operons suggests and warrants further investigation.

Chapter 7. Concluding remarks

Currently there are limited publications on the role of c-di-GMP in *Bdellovibrio* and only one recent publication on the discovery of cAG production by Bd0367(Hallberg et al, 2016; Hobley et al, 2012; Karunker et al, 2013; Lovering et al, 2011; Milner et al, 2014; Rotem et al, 2016). However there is additional unpublished work that has been carried out by numerous members of the Sockett lab into c-di-GMP enzymes, protein interactions and the PilZ domain proteins of *Bdellovibrio* (Basford, 2015; Milner, 2014). This previous work allowed my study to build off these discoveries and focus specifically on the role of the Bd0367 signalling network in *Bdellovibrio*.

To investigate more fully the role of Bd0367 in *Bdellovibrio* signalling this study has touched on the regulation of c-di-GMP signalling mechanisms in *Bdellovibrio*, be this mediated by protein interactions or by phosphorylation dependent activity.

The main findings from the data shown in this thesis are discussed below and shown in Figure 7.1.

In this study new protein interaction partners were discovered by B2H and this expanded the knowledge of the Bd0367 signalling network and possible mechanisms used to control DGC activity. The study also examined the localisation of these proteins in the absence of an interaction partner or assessed altered location of proteins in high versus low cellular c-di-GMP strains using fluorescent microscopy to aid in elucidating the functions of these proteins in the signalling network.

During this study it was attempted to find the cognate HK regulating Bd0367 DGC activity with limited success through the use of B2H, deletion studies and radioactive phospho-transfer assays, with the hope that on finding the cognate HK the signal that stimulates phosphotransfer to Bd0367 could be found. This area requires further investigation.

This study confirmed that phosphorylation is required for Bd0367 to be an active DGC via mutational studies and cellular c-di-GMP extractions. It also demonstrated that loss of DGC activity through Bd0367D63A mutation appears to be important for prey cell exit, but is less important for gliding motility. Which suggests the protein interactions

formed by Bd0367 (independent of its enzymatic role) may be more important for gliding motility than the Bd0367 specific c-di-GMP generation.

This study also confirmed that Bd1971 is an active PDE and on deletion of this gene cellular c-di-GMP levels increased in both HI and HD growth conditions.

In parallel experiments this study confirmed that the Bd1971D307308A mutant strain which was predicted to inactivate the PDE active site resulted in elevated c-di-GMP levels confirming that the mutation in this region did impaired PDE activity.

This study found that both the Δ*bd1971* and the Bd1971D307308A strains resulted in impaired gliding motility suggesting that a high global level of c-di-GMP in *Bdellovibrio* cells can negatively affect motility as seen in many other bacteria.

It was also observed in the Δ*bd1971*::pK18Bd0367mCherry strain that Bd0367mCherry was present at lower levels in the rarer motile Δ*bd1971* cells in comparison to stationary cells. This suggested that the c-di-GMP levels in *Bdellovibrio* population can be heterogeneous and that an unknown mechanism was being used at high cellular c-di-GMP levels in some Δ*bd1971* motile cells to reduce the amount of Bd0367 present to presumably reduce the c-di-GMP level of the cell to enable gliding motility. The mechanism is currently unknown and could be at a transcriptional level or could possibly be mediated through active degradation of Bd0367. Further investigation into this phenomenon is needed to establish what is occurring in these particular cells.

Additionally the molecular reason for impaired gliding at high c-di-GMP levels in *Bdellovibrio* is yet to be determined and requires further study, however I have suggested it may be the result of excessive EPS production.

The investigation of the role of c-di-GMP levels and effects in *Bdellovibrio* gliding motility was expanded in this study by confirming the Bd0367-Bd3100 PilZ domain interaction by B2H and fully phenotyping the effect of the Bd3100 deletion on *Bdellovibrio* gliding motility, showing it affected gliding reversal frequency rather than gliding *per se*.

Further study of Bd3100mCherry by fluorescent microscopy showed that the location of Bd3100 became 34% more polar on surface incubation, a condition that induces gliding and was 13% more polar when expressed in a high cellular c-di-GMP background, suggesting the c-di-GMP bound state of Bd3100 may influence its location in the cell. However further work is needed to confirm this.

How Bd3100 interacts with the gliding machinery or other accessory proteins to mediate changes in gliding motility is currently unknown and would make a whole study in itself due to the ~42 genes encoding gliding apparatus, however this study began to investigate this through examining proteins Bd1473 and Bd1482 a PilZ domain in the gliding operon. The fluorescent microscopy data gathered in this study on these proteins suggests they are important in gliding motility as their position encoded from one of the potential gliding operons suggests and warrants further investigation.

This thesis did not investigate the role of Bd0367 in cAG production due to these data becoming known at a late stage in my PhD, this discovery shows there is still much more to be learnt about the *Bdellovibrio* c-di-GMP signalling system (Hallberg et al, 2016). Work into the importance of cAG production in *Bdellovibrio* is currently being investigated by Dr Lowry. It is hoped that the progress made by my study will prove valuable to a joint publication expanding the knowledge further to determine the role of Bd0367 as a bifunctional enzyme.

Overall this thesis has improved the working knowledge of c-di-GMP signalling in *Bdellovibrio*. This thesis has shown that Bd0367 is activated by phosphorylation, the importance of several protein interactions in *Bdellovibrio* signalling systems and further confirmed that c-di-GMP signalling influences gliding motility behaviour in *Bdellovibrio*.

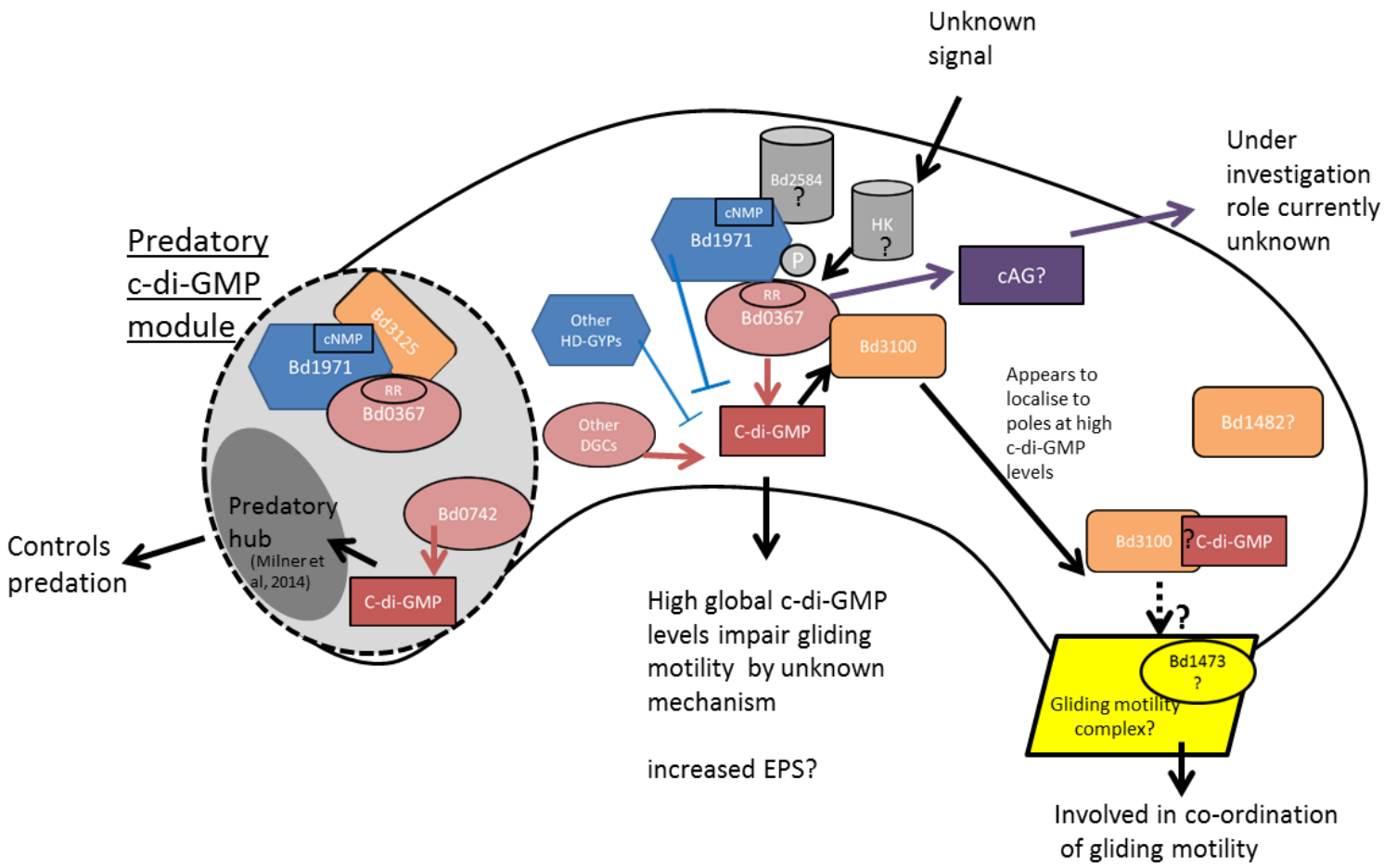

Figure 7.1 Summary of results shown in this thesis. DGC proteins are shown in red, PDE proteins are shown in blue, c-di-GMP receptor proteins are shown in orange and HK proteins are shown in grey.

Chapter 8. Appendix

8.1. Solutions

8.1.1. Buffers used for agarose gel electrophoresis

8.1.1.1. 10x TBE

108 g Tris-HCl, 55 g Boric Acid, 40 ml 0.5 M EDTA pH 8.0 (per litre).

8.1.1.2. 10x loading buffer

15% (w/v) Ficoll 400, 0.4% (w/v) Orange G dye.

8.1.1.3. 3x loading buffer

900 µl 10x loading buffer, 2.1 ml 20% (w/v) glycerol.

8.1.1.4. DNA markers

20 µl NEB DNA ladder stock (500 µg ml^{-1}), 120 µl 3x loading buffer, 160 µl TE (10 mM Tris-HCl 2 mM EDTA, pH 8.0), 100 µl 20% (w/v) glycerol. Made up to required volume with sterile distilled water

8.1.2. Buffers used for generating chemically competent E. coli

8.1.2.1. TFB1

30 mM Potassium acetate; 10 mM $CaCl_2$.$2H_2O$; 50 mM $MnCl_2$.$4H_2O$; 100 mM RbCl; 15 % (v/v) Glycerol. Adjusted to pH 5.8 prior to the addition of glycerol using 1 M acetic acid and sterilized through 0.2 µm filters.

8.1.2.2. TFB2

10 mM MOPS; 75 mM $CaCl_2$.$2H_2O$; 10 mM RbCl ; 15 % (v/v) Glycerol. Adjusted to pH 6.5 prior to the addition of glycerol using 1M KOH and sterilized through 0.2 µm filters.

8.1.3. Buffers used in β-galactosidase activity assay

8.1.3.1. Z-buffer

8.348 g Na_2HPO_4; 5.6 g $NaH_2PO_4.H_2O$; 5 ml 2M KCl; 1 ml 1M $MgS0_4$; 2.7 ml β-mercaptoethanol. Adjusted to pH 7.0 with 2M NaOH and made up to 1 litre with deionised water.

8.1.3.2. Phosphate buffer

0.85 g Na_2HPO_4; 0.55 g NaH_2PO_4.H2O. Made up to 100 ml with deionised water.

8.1.3.3. ONPG solution

4 mg ml^{-1} ONPG (ortho-nitrophenyl β-D-galactopyranoside) in 0.1 M Phosphate buffer

8.1.4. Lowry assay buffers

8.1.4.1. Solution A

2% (w/v) Na_2CO_3; 0.4% (w/v) NaOH; 0.16% (w/v) $C_4H_4O_6Na_2.2H_2O$ (sodium tartrate dihydrate); 1% (w/v) SDS. Made up to required volume with deionised water.

8.1.4.2. Solution B

4% (w/v) $CuSO_4.5H_2O$. Made up to required volume with deionised water.

8.1.5. Protein purification buffers

8.1.5.1. His tag purification and pull downs

8.1.5.2. Lysis buffer

10% glycerol, 50mM Tris pH8, 300mM NaCl, 10mM imidazole and 2mM DTT, 1mg/ml lysozyme, cOmplete mini EDTA free protease inhibitor cocktail (Roche).

8.1.5.3. Wash buffer

10% glycerol, 50mM Tris pH8, 300mM NaCl, 10mM imidazole and 2mM DTT

8.1.5.4. Elution Buffer

10% glycerol, 500mM imidazole, 150mM NaCl, 0.1mM DTT. adjusted to pH8 with HCL

8.1.5.5. Dialysis buffer

50mM Tris pH8 and 300mM NaCl

8.1.5.6. mCherry tag pull down

8.1.5.7. lysis buffer

10 mM Tris-HCl (pH 7.5), 150 mM NaCl, 1mg/ml lysozyme, cOmplete mini EDTA free protease inhibitor cocktail (Roche).

8.1.5.8. wash buffer

10 mM Tris-HCl (pH 7.5), 150 mM NaCl)

8.1.6. Buffers used in phosphotransfer experiments

8.1.6.1. Quenching solution

2xSDS EDTA loading dye, which is 10 ml 10% SDS, 2.4 ml 0.5 MEDTA, 0.5ml 1M Tris pH6.8, 5 ml 100% glycerol, 0.4 ml b-mercaptoethanol and 1.7 ml water.

8.1.6.2. 10x stock phosphotransfer buffer recipe

250mM Tris, 192 mM Glycine and 0.1% SDS.

8.2. Movie files

Movies are located on USB and have been converted to avi files at 7 frames per second.

8.2.1. Chapter 4

Bd2584 gene deletion bdelloplast exit

Bd2584 gene deletion gliding

Bd2583H389V gliding

Bd2584H389V bdelloplast exit

HD100 gliding

HD100 bdelloplast exit

8.2.2. Chapter 5

Bd0367D63A gliding cell

Bd0367D63A no bdelloplast exit

Bd0367mCherry HI bdelloplast exit and cells gliding

Bd1971 gene deletion gliding

Bd1971D307308A HD gliding

Bd1971 gene deletion with Bd0367mCherry gliding

HID13 bdelloplast exit

HID13 gliding

8.2.3. Chapter 6

Bd3100 gene deletion gliding

Bd3100 complemented gliding

Bd1482mCherry gliding

8.3. Additional figures

8.3.1. Chapter 3

8.3.1.1. RNA-seq Bd0367 start site

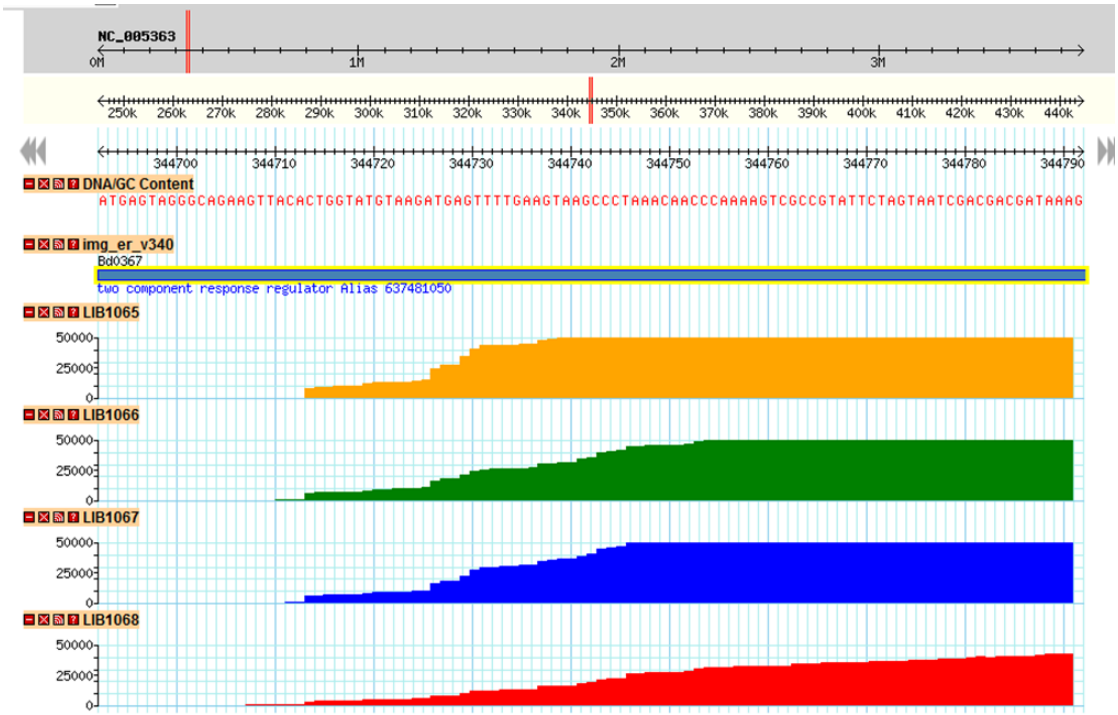

Figure 8.1 RNA-seq of *bd0367* suggests that the correct *bd0367* start site is 34 bp down from the annotated start site.

8.3.1.2. Bd0367 identified by LC-MS/MS

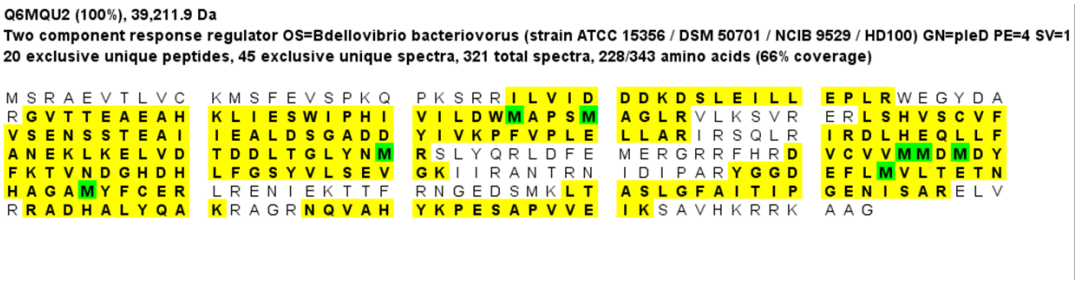

Figure 8.2 Bd0367 percentage coverage by Scaffold Software

8.3.1.3. Bd1434 identified by LC-MS/MS

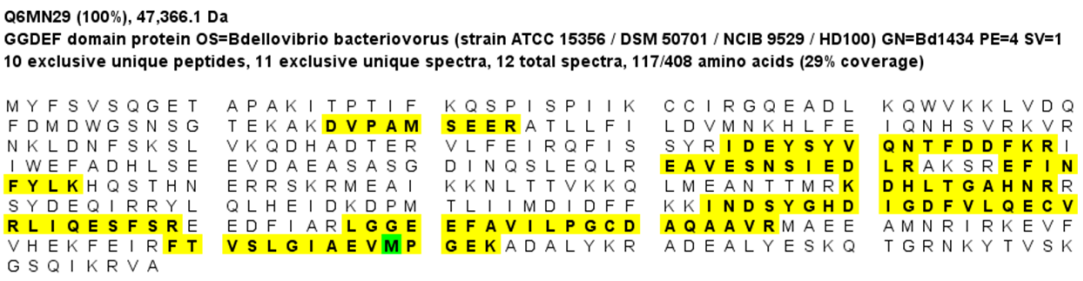

Figure 8.3 Bd1434 percentage coverage by Scaffold Software

8.3.2. Chapter 4

8.3.2.1. Bd2584 identified by LC-MS/MS

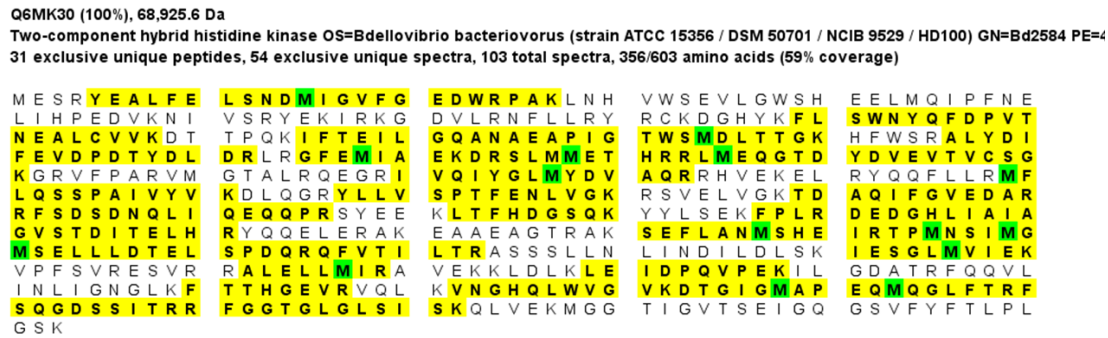

Figure 8.4 Bd2584 percentage coverage by Scaffold Software

8.3.3. Chapter 5

8.3.3.1. Prediction of Bd0367 promoter

```
> test sequence
 Length of sequence-       133
 Threshold for promoters -  0.20
 Number of predicted promoters -      1
 Promoter Pos:     72 LDF-  5.04
 -10 box at pos.     57 tcttatgat Score    63
 -35 box at pos.     38 ttaaag    Score    31

 Oligonucleotides from known TF binding sites:

 For promoter at     72:
     rpoD15:  AGGATTAA at position      34 Score -   8
     rpoD15:  CTAAATAA at position      77 Score -  12
     rpoD16:  AAATAATT at position      79 Score -  15
```

Figure 8.5 Prediction of *bd0367* promoter sequence in upstream region. The σ^{70} promoter predicted at -10 is 77 bp upstream from the RNA-seq predicted start of *bd0367* and -35 is 96 bp upstream of the RNA-seq predicted start of *bd0367*. The transcription factor binding sites are predicted below. Predicted using Softberry BPROM (Solovyev & Salamov, 2011)

8.3.3.2. Prediction of Bd0367 operon

```
 Prediction of potential genes in microbial genomes
 Time:   Tue Jan  1 00:00:00 2005
 Seq name: test sequence
 Length of sequence - 3052 bp
 Number of predicted genes - 4
 Number of transcription units - 1, operons - 1
    N      Tu/Op   Conserved  S            Start         End    Score
                   pairs(N/Pv)
    1     1 Op  1     .       +    CDS         21 -      1052   1087
    2     1 Op  2     .       +    CDS       1097 -      2134    852
    3     1 Op  3     .       +    CDS       2103 -      2801    608
    4     1 Op  4     .       +    CDS       2884 -      3052    144
Predicted protein(s):
>GENE     1       21   -      1052   1087    343 aa, chain +
MSRAEVTLVCKMSFEVSPKQPKSRRILVIDDDKDSLEILLEPLRWEGYDARGVTTEAEAH
KLIESWIPHIVILDWMAPSMAGLRVLKSVRERLSHVSCVFVSENSSTEAIIEALDSGADD
YIVKPFVPLELLARIRSQLRIRDLHEQLLFANEKLKELVDTDDLTGLYNMRSLYQRLDFE
MERGRRFHRDVCVVMMDMDYFKTVNDGHDHLFGSYVLSEVGKIIRANTRNIDIPARYGGD
EFLMVLTETNHAGAMYFCERLRENIEKTTFRNGEDSMKLTASLGFAITIPGENISARELV
RRADHALYQAKRAGRNQVAHYKPESAPVVEIKSAVHKRRKAAG
>GENE     2      1097   -      2134    852    345 aa, chain +
MQNAVSSSDKIRNRAAWVSAIASVLIFAMKVFAYRLTGSTAVLSDALESIVNVIAAIVAL
FVIRFASQPADENHPYGHGKAEYFSSAFEGGMIFFAAIMIIGEAVKALIYHEPTQQLETG
LLIVGGAALVNLALGLYLKRVGRTHQSDALKASGAHVLSDVLTTVGVMVGLGLVLLTGIQ
WLDPVIAVLVGLQLAYAGFKIVRGSLGGLMDQQDPASLEQLAEAMEKNRVPGVINIHHLR
VIRSGRFHHVDAHMVVPEYWDVSQVHAMTGDFEAAVVKDYEFDGELVFHLDPCKKSYCDS
CQVPQCPIRLQPFRQKPDFSVKSLTDDPAPTNQGTHDRSGSSQTN
>GENE     3      2103   -      2801    608    232 aa, chain +
MTDQALRRQINITKDLPNQNAYTLALNGEYAHVAFDELRAPLNKGKWRSDVFKADAAMPL
DVEVGTGNGTYFAHHAKTHSDRLLVGLELKYKPLIQSIRRAVNAGCKNAAITRFHAFNID
HLFAEGEIDNVYIHFPDPWTSPKKPKNRFVCKENLELLFRLQKPGSFINFKTDSLVYFLW
AMDEIRQSPYKIIFETQDLHNSDMKDQNFETAFEKIFLREGIKINFVRLQKI
>GENE     4      2884   -      3052    144     56 aa, chain +
MGFLLKATMTLLTLTLSLGFEQAEAAITRETDFVTPAEPMTVLRSSVVPCYGRNQA
```

Figure 8.6 Prediction that *bd0367* is at the start of an operon that include *bd0368*, *bd0370* and *bd0371* predicted by FGENESB: Bacterial Operon and Gene Prediction (Solovyev & Salamov, 2011)

8.3.4. Chapter 6

8.3.4.1. *Bdellovibrio* PilZ and DUF4339 domain protein alignment

```
CLUSTAL O(1.2.2) multiple sequence alignment


1996      -----------VNPKNWFVLTDGQVNGPFDVQEVESRVASAKE---AQIWGRGQSEWMTP
1482      ------------------------------------------------------------
3100      LCRIVRNRSIESMGKQYYLSNNGTHIGPFNLETVLKKIESQENQWTDYIYDEALGEWLML


1996      TKWRQAVK------------DSSQVAVAANEPEGLWKVRVEGKDHPPMKYSALISFLKGM
1482      ----------------------MGGVQTATNQQQWYILRGEMKYGPYEYRSLITMIQNG
3100      LEHPEFSAKLAQKPATRPSASPASLLSKLALKDKEWFILKEGNNYGPFCQLELIQMLQEK
                                       :  * :     .: *     ** :::

1996      TDYSTVDVCSDNSNVWKEIYSIPR--------IVD------DLGISRRSHPRVPMVGTLA
1482      ELYDYNFVWAAHLENWTLLGDLQEFSKDRLCRLIETKD-HIAGSFKDRKCPRVDLETPVY
3100      ALYEYDYIWHSKLPSWKRVAEVEDFSAESIRVMKDSKEADVAEIFFRRRHVRASYGASLI
            *.   :   .   *. : .:          : :         :  *   *.     :

1996      CESPKGEFSCRVISISEGGLGVN-DAQNLQIGERFKGTLT-SPNLFVTINTTCEVVYV--
1482      AHNDHNFFDGHTLSVSENGALVLLNDPLLLPGQKILLNFRTSEVNPQTFNVLCEIIRKNY
3100      VHNNKTVFRGQALEISAGGAGVLIDTPNLQPGQSLFLHFQPGDGVP-PFNAVCQIVSKQY
           .. :  *  :.:.:*  *  *  :   *  *: :   :  .      :*. *:::

1996      -GNDG------YAGLRFVGLPEEFKSSIIEYVRKFAMV------------
1482      SKQRLNVKSGLHYAVRFLSVQETGMAQLTKWTRGGVSKEETNDGILKVHE
3100      VKDSGTAVEPVKYGVKFTTLSQSARESIKNFTTKAA--------------
            :          .::*  : :    .: ::.   .
```

Figure 8.7 Clustal omega protein alignment of Bd3100, Bd1482 and Bd1996.

```
Percent Identity  Matrix - created by Clustal2.1


  1: 1996        100.00   17.65   22.32
  2: 1482         17.65  100.00   27.75
  3: 3100         22.32   27.75  100.00
```

Figure 8.8 Percentage protein identify of Bd3100, Bd1482 and Bd1996 by clustal omega.

```
CLUSTAL O(1.2.2) multiple sequence alignment


1996      ------------------------------------------------------------
3100      LCRIVRNRSIESMGKQYYLSNNGTHIGPFNLETVLKKIESQENQWTDYIYDEALGEWLML
1482      ------------------------------------------------------------


1996      ------------------------------VNPKNWFVLTDGQVNGPFDVQEVESRVASA
3100      LEHPEFSAKLAQKPATRPSASPASLLSKLALKDKEWFILKEGNNYGPFCQLELIQMLQEK
1482      ----------------------MGGVQTATNQQQWYILRGEMKYGPYEYRSLITMIQNG
                                       : ::*::*      **:   .:   : .

1996      ---KEAQIWGRGQSEWMTPTKWRQAVKDSSQVA
3100      ALYEYDYIWHSKLPSWKRVAEVEDFSAESIR--
1482      ELYDYNFVWAAHLENWTLLGDLQ----------
             .   :*     .*    . .
```

```
Percent Identity  Matrix - created by Clustal2.1


  1: 1996        100.00   22.41   14.00
  2: 3100         22.41  100.00   28.33
  3: 1482         14.00   28.33  100.00
```

Figure 8.9 Clustal omega protein alignment of N terminal region DUF4339 region of Bd3100, Bd1482 and Bd1996.

```
CLUSTAL O(1.2.2) multiple sequence alignment


1996      VNPKNWFVLTDGQVNGPFDVQEVESRVASA---KEAQIWGRGQSEWMTPTKWR
1482      ----QWYILRGEMKYGPYEYRSLITMIQNGELYDYNFVWAAHLENWTLL----
3100      ----EWFILKEGNNYGPFCQLELIQMLQEKALYEYDYIWHSKLPSWKRV----
              :*::*      **:   .:   : .    .   :*     .*
```

```
Percent Identity  Matrix - created by Clustal2.1


  1: 1996        100.00   14.29   26.19
  2: 1482         14.29  100.00   35.56
  3: 3100         26.19   35.56  100.00
```

Figure 8.10 Clustal omega protein alignment of the second DUF4339 domains of Bd3100 compared to the DUF4339 domains of Bd1482 and Bd1996.

8.4. Ladders used in this study

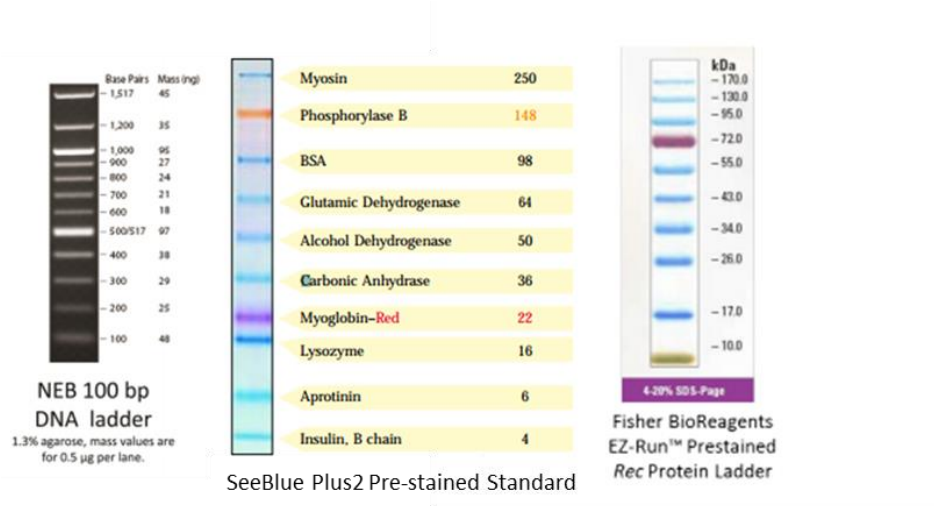

Figure 8.11 DNA ladder and protein ladders used in this study for RT-PCR and SDS-PAGE

Chapter 9. References

Abel, S., Chien, P., Wassmann, P., Schirmer, T., Kaever, V., Laub, M. T., Baker, T. A. & Jenal, U. (2011) Regulatory Cohesion of Cell Cycle and Cell Differentiation through Inter linked Phosphorylation and Second Messenger Networks. *Molecular Cell*, 43(4), 550-560.
Abram, D., Castroem.J & Chou, D. (1974) Penetration of *Bdellovibrio-bacteriovorus* into host-cells. *Journal of Bacteriology*, 118(2), 663-680.

Agrebi, R., Wartel, M., Brochier-Armanet, C. & Mignot, T. (2015) An evolutionary link between capsular biogenesis and surface motility in bacteria (vol 13, pg 318, 2015). *Nature Reviews Microbiology*, 13(6).

Ahmad, R. (2007) *Cyclic-di-GMP in the life of Bdellovibrio.*University of Nottingham.

Aldridge, P., Paul, R., Goymer, P., Rainey, P. & Jenal, U. (2003) Role of the GGDEF regulator PleD in polar development of Caulobacter crescentus. *Molecular Microbiology*, 47(6), 1695-1708.

Alm, R. A., Bodero, A. J., Free, P. D. & Mattick, J. S. (1996) Identification of a novel gene, pilZ, essential for type 4 fimbrial biogenesis in Pseudomonas aeruginosa. *Journal of Bacteriology*, 178(1), 46-53.

Amikam, D. & Galperin, M. Y. (2006) PilZ domain is part of the bacterial c-di-GMP binding protein. *Bioinformatics*, 22(1), 3-6.

Aravind, L. & Ponting, C. P. (1999) The cytoplasmic helical linker domain of receptor histidine kinase and methyl-accepting proteins is common to many prokaryotic signalling proteins. *Fems Microbiology Letters*, 176(1), 111-116.

Ashenberg, O., Keating, A. E. & Laub, M. T. (2013) Helix Bundle Loops Determine Whether Histidine Kinases Autophosphorylate in cis or in trans. *Journal of Molecular Biology*, 425(7), 1198-1209.

Baker, A. E., Diepold, A., Kuchma, S. L., Scott, J. E., Ha, D. G., Orazi, G., Armitage, J. P. & O'Toole, G. A. (2016) PilZ Domain Protein FlgZ Mediates Cyclic Di-GMP-Dependent Swarming Motility Control in Pseudomonas aeruginosa. *Journal of Bacteriology*, 198(13), 1837-1846.

Baptista, M., Depardieu, F., Reynolds, P., Courvalin, P. & Arthur, M. (1997) Mutations leading to increased levels of resistance to glycopeptide antibiotics in VanB-type enterococci. *Molecular Microbiology*, 25(1), 93-105.

Baraquet, C., Murakami, K., Parsek, M. R. & Harwood, C. S. (2012) The FleQ protein from Pseudomonas aeruginosa functions as both a repressor and an activator to control gene expression from the pel operon promoter in response to c-di-GMP. *Nucleic Acids Research*, 40(15), 7207-7218.

Barbieri, C. M. & Stock, A. M. (2008) Universally applicable methods for monitoring response regulator aspartate phosphorylation both in vitro and in vivo using Phos-tag-based reagents. *Analytical Biochemistry*, 376(1), 73-82.

Barel, G. & Jurkevitch, E. (2001) Analysis of phenotypic diversity among host-independent mutants of Bdellovibrio bacteriovorus 109J. *Archives of Microbiology*, 176(3), 211-216.

Barrick, J. E. & Breaker, R. R. (2007) The distributions, mechanisms, and structures of metabolite-binding riboswitches. *Genome Biology*, 8(11).

Basford, S. (2015) *Roles of Genes Encoding Phosphatases in Bdellovibrio bacteriovorus* University of Nottingham.

Battesti, A. & Bouveret, E. (2012) The bacterial two-hybrid system based on adenylate cyclase reconstitution in Escherichia coli. *Methods*, 58(4), 325-334.

Benach, J., Swaminathan, S. S., Tamayo, R., Handelman, S. K., Folta-Stogniew, E., Ramos, J. E., Forouhar, F., Neely, H., Seetharaman, J., Camilli, A. & Hunt, J. F. (2007) The structural basis of cyclic diguanylate signal transduction by PilZ domains. *Embo Journal*, 26(24), 5153-5166.

Bhate, M. P., Molnar, K. S., Goulian, M. & DeGrado, W. F. (2015) Signal Transduction in Histidine Kinases: Insights from New Structures. *Structure*, 23(6), 981-994.

Bilwes, A. M., Quezada, C. M., Croal, L. R., Crane, B. R. & Simon, M. I. (2001) Nucleotide binding by the histidine kinase CheA. *Nature Structural Biology*, 8(4), 353-360.
Blackhart, B. D. & Zusman, D. R. (1985) Frizzy genes of *Myxococcus-xanthus* are involved in control of frequency of reversal of gliding motility. *Proceedings of the National Academy of Sciences of the United States of America*, 82(24), 8767-8770.

Blat, Y. & Eisenbach, M. (1994) Phosphorylation-dependent binding of the chemotaxis signal molecule CheY to its phosphatase, CheZ. *Biochemistry*, 33(4), 902-906.

Bobrov, A. G., Kirillina, O., Ryjenkov, D. A., Waters, C. M., Price, P. A., Fetherston, J. D., Mack, D., Goldman, W. E., Gomelsky, M. & Perry, R. D. (2011) Systematic analysis of cyclic di-GMP signalling enzymes and their role in biofilm formation and virulence in Yersinia pestis. *Molecular Microbiology*, 79(2), 533-551.

Bordeleau, E., Fortier, L. C., Malouin, F. & Burrus, V. (2011) c-di-GMP Turn-Over in Clostridium difficile Is Controlled by a Plethora of Diguanylate Cyclases and Phosphodiesterases. *Plos Genetics*, 7(3).

Bourret, R. B. (2010) Receiver domain structure and function in response regulator proteins. *Current Opinion in Microbiology*, 13(2), 142-149.

Buelow, D. R. & Raivio, T. L. (2010) Three (and more) component regulatory systems - auxiliary regulators of bacterial histidine kinases. *Molecular Microbiology*, 75(3), 547-566.

Burchard, R. P. (1982) Trail following by gliding bacteria. *Journal of Bacteriology*, 152(1), 495-501.

Burger, L. & van Nimwegen, E. (2008) Accurate prediction of protein-protein interactions from sequence alignments using a Bayesian method. *Molecular Systems Biology*, 4.

Capeness, M. J., Lambert, C., Lovering, A. L., Till, R., Uchida, K., Chaudhuri, R., Alderwick, L. J., Lee, D. J., Swarbreck, D., Liddell, S., Aizawa, S. I. & Sockett, R. E. (2013) Activity of Bdellovibrio Hit Locus Proteins, Bd0108 and Bd0109, Links Type IVa Pilus Extrusion/Retraction Status to Prey-Independent Growth Signalling. *Plos One*, 8(11).

Capra, E. J., Perchuk, B. S., Lubin, E. A., Ashenberg, O., Skerker, J. M. & Laub, M. T. (2010) Systematic Dissection and Trajectory-Scanning Mutagenesis of the Molecular Interface That Ensures Specificity of Two-Component Signaling Pathways. *Plos Genetics*, 6(11).

Casino, P., Miguel-Romero, L. & Marina, A. (2014) Visualizing autophosphorylation in histidine kinases. *Nature Communications*, 5.

Casino, P., Rubio, V. & Marina, A. (2009) Structural Insight into Partner Specificity and Phosphoryl Transfer in Two-Component Signal Transduction. *Cell*, 139(2), 325-336.

Chan, C., Paul, R., Samoray, D., Amiot, N. C., Giese, B., Jenal, U. & Schirmer, T. (2004) Structural basis of activity and allosteric control of diguanylate cyclase. *Proceedings of the National Academy of Sciences of the United States of America*, 101(49), 17084-17089.

Chen, J.-C., Liu, J.-H., Hsu, D.-W., Shu, J.-C., Chen, C.-Y. & Chen, C.-C. (2015) Methylatable Signaling Helix Coordinated Inhibitory Receiver Domain in Sensor Kinase Modulates Environmental Stress Response in Bacillus Cereus. *Plos One*, 10(9).

Chen, L. H., Koseoglu, V. K., Guvener, Z. T., Myers-Morales, T., Reed, J. M., D'Orazio, S. E. F., Miller, K. W. & Gomelsky, M. (2014) Cyclic di-GMP-Dependent Signaling Pathways in the Pathogenic Firmicute Listeria monocytogenes. *Plos Pathogens*, 10(8).

Chou, S. H. & Galperin, M. Y. (2016) Diversity of Cyclic Di-GMP-Binding Proteins and Mechanisms. *Journal of Bacteriology*, 198(1), 32-46.

Christen, B., Christen, M., Paul, R., Schmid, F., Folcher, M., Jenoe, P., Meuwly, M. & Jenal, U. (2006) Allosteric control of cyclic di-GMP signaling. *Journal of Biological Chemistry*, 281(42), 32015-32024.

Christen, M., Christen, B., Allan, M. G., Folcher, M., Jeno, P., Grzesiek, S. & Jenal, U. (2007) DgrA is a member of a new family of cyclic diguanosine monophosphate receptors and controls flagellar motor function in Caulobacter crescentus. *Proceedings of the National Academy of Sciences of the United States of America*, 104(10), 4112-4117.

Christen, M., Christen, B., Folcher, M., Schauerte, A. & Jenal, U. (2005) Identification and characterization of a cyclic di-GMP-specific phosphodiesterase and its allosteric control by GTP. *Journal of Biological Chemistry*, 280(35), 30829-30837.

Cock, P. J. A. & Whitworth, D. E. (2007) Evolution of prokaryotic two-component system signaling pathways: Gene fusions and fissions. *Molecular Biology and Evolution*, 24(11), 2355-2357.

Cormack, R. & Somssich, I. (1997) Ultra-fast alkaline lysis plasmid extraction (UFX). BMN technical tips online.

Cotter, T. W. & Thomashow, M. F. (1992) Identification of a *Bdellovibrio-bacteriovorus* genetic-locus, hit, associated with the host-independent phenotype. *Journal of Bacteriology*, 174(19), 6018-6024.

D'Argenio, D. A., Calfee, M. W., Rainey, P. B. & Pesci, E. C. (2002) Autolysis and autoaggregation in Pseudomonas aeruginosa colony morphology mutants. *Journal of Bacteriology*, 184(23), 6481-6489.

Dahlstrom, K. M., Giglio, K. M., Collins, A. J., Sondermann, H. & O'Toole, G. A. (2015) Contribution of Physical Interactions to Signaling Specificity between a Diguanylate Cyclase and Its Effector. *Mbio*, 6(6).

De, N., Navarro, M., Raghavan, R. V. & Sondermann, H. (2009) Determinants for the Activation and Autoinhibition of the Diguanylate Cyclase Response Regulator WspR. *Journal of Molecular Biology*, 393(3), 619-633.

De, N., Pirruccello, M., Krasteva, P. V., Bae, N., Raghavan, R. V. & Sondermann, H. (2008) Phosphorylation-independent regulation of the diguanylate cyclase WspR. *Plos Biology*, 6(3), 601-617.

den Hengst, C. D., Tran, N. T., Bibb, M. J., Chandra, G., Leskiw, B. K. & Buttner, M. J. (2010) Genes essential for morphological development and antibiotic production in Streptomyces coelicolor are targets of BldD during vegetative growth. *Molecular Microbiology*, 78(2), 361-379.

Ducret, A., Quardokus, E. M. & Brun, Y. V. (2016) MicrobeJ, a tool for high throughput bacterial cell detection and quantitative analysis. *Nature Microbiology*, 1, 16077.

Dutta, R., Yoshida, T. & Inouye, M. (2000) The critical role of the conserved Thr(247) residue in the functioning of the osmosensor EnvZ, a histidine kinase/phosphatase, in Escherichia coli. *Journal of Biological Chemistry*, 275(49), 38645-38653.

Evans, K. J., Lambert, C. & Sockett, R. E. (2007) Predation by Bdellovibrio bacteriovorus HD100 requires type IV pili (vol 189, pg 4850, 2007). *Journal of Bacteriology*, 189(17), 6507-6507.

Fenton, A. K., Kanna, M., Woods, R. D., Aizawa, S. I. & Sockett, R. E. (2010) Shadowing the Actions of a Predator: Backlit Fluorescent Microscopy Reveals Synchronous Nonbinary Septation of Predatory Bdellovibrio inside Prey and Exit through Discrete Bdelloplast Pores. *Journal of Bacteriology*, 192(24), 6329-6335.

Fiedler, U. & Weiss, V. (1995) A common switch in activation of the response regulators NtrC and PhoB- phosphorylation induces dimerization of the receiver modules. *Embo Journal*, 14(15), 3696-3705.

Flemming, H. C., Neu, T. R. & Wozniak, D. J. (2007) The EPS matrix: The "House of Biofilm cells". *Journal of Bacteriology*, 189(22), 7945-7947.

Fong, J. C. N. & Yildiz, F. H. (2008) Interplay between cyclic AMP-Cyclic AMP receptor protein and cyclic di-GMP signaling in Vibrio cholerae biofilm formation. *Journal of Bacteriology*, 190(20), 6646-6659.

Forst, S., Delgado, J. & Inouye, M. (1989) Phosphorylation of ompr by the osmosensor EnvZ modulates expression of the OmpF and OmpC genes in E*scherichia-coli*. *Proceedings of the National Academy of Sciences of the United States of America*, 86(16), 6052-6056.

Fung, R. (2008) *Roles of GGDEF and EAL genes in Bdellovibrio bacteriovorus* University of Nottingham.

Galperin, M. Y. (2005) A census of membrane-bound and intracellular signal transduction proteins in bacteria: Bacterial IQ, extroverts and introverts. *Bmc Microbiology*, 5.

Galperin, M. Y. (2006) Structural classification of bacterial response regulators: Diversity of output domains and domain combinations. *Journal of Bacteriology*, 188(12), 4169-4182.

Galperin, M. Y. (2010) Diversity of structure and function of response regulator output domains. *Current Opinion in Microbiology*, 13(2), 150-159.

Galperin, M. Y., Natale, D. A., Aravind, L. & Koonin, E. V. (1999) A specialized version of the HD hydrolase domain implicated in signal transduction. *Journal of Molecular Microbiology and Biotechnology*, 1(2), 303-305.

Galperin, M. Y., Nikolskaya, A. N. & Koonin, E. V. (2001) Novel domains of the prokaryotic two-component signal transduction systems. *Fems Microbiology Letters*, 203(1), 11-21.

Gao, R. & Stock, A. M. (2009) Biological Insights from Structures of Two-Component Proteins. *Annual Review of Microbiology*, 63, 133-154.

Gentner, M., Allan, M. G., Zaehringer, F., Schirmer, T. & Grzesiek, S. (2012) Oligomer Formation of the Bacterial Second Messenger c-di-GMP: Reaction Rates and Equilibrium Constants Indicate a Monomeric State at Physiological Concentrations. *Journal of the American Chemical Society*, 134(2), 1019-1029.

Gibson, D. G., Young, L., Chuang, R. Y., Venter, J. C., Hutchison, C. A. & Smith, H. O. (2009) Enzymatic assembly of DNA molecules up to several hundred kilobases. *Nature Methods*, 6(5), 343-U41.

Goldberg, S. D., Clinthorne, G. D., Goulian, M. & DeGrado, W. F. (2010) Transmembrane polar interactions are required for signaling in the Escherichia coli

sensor kinase PhoQ. *Proceedings of the National Academy of Sciences of the United States of America*, 107(18), 8141-8146.

Goudreau, P. N., Lee, P. J. & Stock, A. M. (1998) Stabilization of the phospho-aspartyl residue in a two-component signal transduction system in Thermotoga maritima. *Biochemistry*, 37(41), 14575-14584.

Grebe, T. W. & Stock, J. B. (1999) The histidine protein kinase superfamily. *Advances in Microbial Physiology*, 41, 139-227.

Groban, E. S., Clarke, E. J., Salis, H. M., Miller, S. M. & Voigt, C. A. (2009) Kinetic Buffering of Cross Talk between Bacterial Two-Component Sensors. *Journal of Molecular Biology*, 390(3), 380-393.

Gu, W., Kofler, M., Antes, I., Freund, C. & Helms, V. (2005) Alternative binding modes of proline-rich peptides binding to the GYF domain. *Biochemistry*, 44(17), 6404-6415.

Guo, X. P., Ren, G. X., Zhu, H., Mao, X. J. & Sun, Y. C. (2015) Differential regulation of the hmsCDE operon in Yersinia pestis and Yersinia pseudotuberculosis by the Rcs phosphorelay system. *Scientific Reports*, 5.

Guzzo, C. R., Dunger, G., Salinas, R. K. & Farah, C. S. (2013) Structure of the PilZ-FimX(EAL)-c-di-GMP Complex Responsible for the Regulation of Bacterial Type IV Pilus Biogenesis. *Journal of Molecular Biology*, 425(12), 2174-2197.

Guzzo, M., Agrebi, R., Espinosa, L., Baronian, G., Molle, V., Mauriello, E. M. F., Brochier-Armanet, C. & Mignot, T. (2015) Evolution and Design Governing Signal Precision and Amplification in a Bacterial Chemosensory Pathway. *Plos Genetics*, 11(8).

Ha, D. G., Richman, M. E. & O'Toole, G. A. (2014) Deletion Mutant Library for Investigation of Functional Outputs of Cyclic Diguanylate Metabolism in Pseudomonas aeruginosa PA14. *Applied and Environmental Microbiology*, 80(11), 3384-3393.

Habazettl, J., Allan, M. G., Jenal, U. & Grzesiek, S. (2011) Solution Structure of the PilZ Domain Protein PA4608 Complex with Cyclic di-GMP Identifies Charge Clustering as Molecular Readout. *Journal of Biological Chemistry*, 286(16), 14304-14314.

Hallberg, Z. F., Wang, X. C., Wright, T. A., Nan, B., Ad, O., Yeo, J. & Hammond, M. C. (2016) Hybrid promiscuous (Hypr) GGDEF enzymes produce cyclic AMP-GMP (3 ', 3 '-cGAMP). *Proceedings of the National Academy of Sciences of the United States of America*, 113(7), 1790-1795.

Hanahan, D. (1983) Studies on transformation of *Escherichia-coli* with plasmids. *Journal of Molecular Biology*, 166(4), 557-580.

Harrington, B. J. & Hageage, G. J. (2003) Calcofluor white: A review of its uses and application's in clinical mycology and parasitology. *Laboratory Medicine*, 34(5), 361-367.

Hecht, G. B. & Newton, A. (1995) Identification of a novel response regulator required for the swarmer-to-stalked-cell transition in *Caulobacter-crescentus*. *Journal of Bacteriology*, 177(21), 6223-6229.

Hengge, R. (2009) Principles of c-di-GMP signalling in bacteria. *Nature Reviews Microbiology*, 7(4), 263-273.

Hespell, R. B., Miozzari, G. F. & Rittenberg, S. C. (1975) Ribonucleic-acid destruction and synthesis during intraperiplasmic growth of Bdellovibrio-bacteriovorus. *Journal of Bacteriology*, 123(2), 481-491.

Hess, J. F., Bourret, R. B. & Simon, M. I. (1991) Phosphorylation assays for proteins of the two-component regulatory system controlling chemotaxis in Escherichia coli. *Methods in enzymology*, 200, 188-204.

Hess, J. F., Oosawa, K., Kaplan, N. & Simon, M. I. (1988) phosphorylation of 3 proteins in the signaling pathway of bacterial chemotaxis. *Cell*, 53(1), 79-87.

Hickman, J. W. & Harwood, C. S. (2008) Identification of FleQ from Pseudomonas aeruginosa as a c-di-GMP-responsive transcription factor. *Molecular Microbiology*, 69(2), 376-389.

Hickman, J. W., Tifrea, D. F. & Harwood, C. S. (2005) A chemosensory system that regulates biofilm formation through modulation of cyclic diguanylate levels. *Proceedings of the National Academy of Sciences of the United States of America*, 102(40), 14422-14427.

Hiller, K., Grote, A., Scheer, M., Munch, R. & Jahn, D. (2004) PrediSi: prediction of signal peptides and their cleavage positions. *Nucleic Acids Research*, 32, W375-W379.

Hobley, L., Fung, R. K. Y., Lambert, C., Harris, M. A. T. S., Dabhi, J. M., King, S. S., Basford, S. M., Uchida, K., Till, R., Ahmad, R., Aizawa, S.-I., Gomelsky, M. & Sockett, R. E. (2012) Discrete Cyclic di-GMP-Dependent Control of Bacterial Predation versus Axenic Growth in Bdellovibrio bacteriovorus. *Plos Pathogens*, 8(2).

Hoch, J. A. (2000) Two-component and phosphorelay signal transduction. *Current Opinion in Microbiology*, 3(2), 165-170.

Hoch, J. A. & Silhavy, T. J. (1995) Two-component signal transduction. *Two-component signal transduction*, xvi+488p-xvi+488p.

Huangyutitham, V., Guevener, Z. T. & Harwood, C. S. (2013) Subcellular Clustering of the Phosphorylated WspR Response Regulator Protein Stimulates Its Diguanylate Cyclase Activity. *Mbio*, 4(3).

Huynh, T. N., Chen, L.-L. & Stewart, V. (2015) Sensor-response regulator interactions in a cross-regulated signal transduction network. *Microbiology-Sgm*, 161, 1504-1515.

Huynh, T. N. & Stewart, V. (2011) Negative control in two-component signal transduction by transmitter phosphatase activity. *Molecular Microbiology*, 82(2), 275-286.

Inclan, Y. F., Laurent, S. & Zusman, D. R. (2008) The receiver domain of FrzE, a CheA-CheY fusion protein, regulates the CheA histidine kinase activity and downstream signalling to the A- and S-motility systems of Myxococcus xanthus. *Molecular Microbiology*, 68(5), 1328-1339.

Islam, S. T. & Mignot, T. (2015) The mysterious nature of bacterial surface (gliding) motility: A focal adhesion-based mechanism in Myxococcus xanthus. *Seminars in Cell & Developmental Biology*, 46, 143-154.

Jakobczak, B., Keilberg, D., Wuichet, K. & Sogaard-Andersen, L. (2015) Contact- and Protein Transfer-Dependent Stimulation of Assembly of the Gliding Motility Machinery in Myxococcus xanthus. *Plos Genetics*, 11(7).

Jarrell, K. F. & McBride, M. J. (2008) The surprisingly diverse ways that prokaryotes move. *Nature Reviews Microbiology*, 6(6), 466-476.

Jenal, U. (2004) Cyclic di-guanosine-monophosphate comes of age: a novel secondary messenger involved in modulating cell surface structures in bacteria? *Current Opinion in Microbiology*, 7(2), 185-191.

Jencks, W. P. (1980) The utilization of binding energy in coupled vectorial processes. *Advances in enzymology and related areas of molecular biology*, 51, 75-106.

Jervis, A. J. & Green, J. (2007) In vivo demonstration of FNR dimers in response to lower O-2 availability. *Journal of Bacteriology*, 189(7), 2930-2932.

Jurkevitch, E., Minz, D., Ramati, B. & Barel, G. (2000) Prey range characterization, ribotyping, and diversity of soil and rhizosphere Bdellovibrio spp. isolated on phytopathogenic bacteria. *Applied and Environmental Microbiology*, 66(6), 2365-2371.

Kaimer, C. & Zusman, D. R. (2013) Phosphorylation-dependent localization of the response regulator FrzZ signals cell reversals in Myxococcus xanthus. *Molecular Microbiology*, 88(4), 740-753.

Kaimer, C. & Zusman, D. R. (2016) Regulation of cell reversal frequency in Myxococcus xanthus requires the balanced activity of CheY-like domains in FrzE and FrzZ. *Molecular Microbiology*, 100(2), 379-395.

Karimova, G., Dautin, N. & Ladant, D. (2005) Interaction network among Escherichia coli membrane proteins involved in cell division as revealed by bacterial two-hybrid analysis. *Journal of Bacteriology*, 187(7), 2233-2243.

Karimova, G., Pidoux, J., Ullmann, A. & Ladant, D. (1998) A bacterial two-hybrid system based on a reconstituted signal transduction pathway. *Proceedings of the National Academy of Sciences of the United States of America*, 95(10), 5752-5756.

Karimova, G., Ullmann, A. & Ladant, D. (2001) Protein-protein interaction between Bacillus stearothermophilus tyrosyl-tRNA synthetase subdomains revealed by a bacterial two-hybrid system. *Journal of Molecular Microbiology and Biotechnology*, 3(1), 73-82.

Karunker, I., Rotem, O., Dori-Bachash, M., Jurkevitch, E. & Sorek, R. (2013) A Global Transcriptional Switch between the Attack and Growth Forms of Bdellovibrio bacteriovorus. *Plos One*, 8(4).

Keilberg, D., Wuichet, K., Drescher, F. & Sogaard-Andersen, L. (2012) A Response Regulator Interfaces between the Frz Chemosensory System and the MglA/MglB GTPase/GAP Module to Regulate Polarity in Myxococcus xanthus. *Plos Genetics*, 8(9).

Kellenberger, C. A., Wilson, S. C., Sales-Lee, J. & Hammond, M. C. (2013) RNA-Based Fluorescent Biosensors for Live Cell Imaging of Second Messengers Cyclic di-GMP and Cyclic AMP-GMP. *Journal of the American Chemical Society*, 135(13), 4906-4909.

Kellogg, S. L. & Kristich, C. J. (2016) Functional Dissection of the CroRS Two-Component System Required for Resistance to Cell Wall Stressors in Enterococcus faecalis. *Journal of Bacteriology*, 198(8), 1326-1336.

Kim, D. & Forst, S. (2001) Genomic analysis of the histidine kinase family in bacteria and archaea. *Microbiology-Sgm*, 147, 1197-1212.

Ko, J., Ryu, K.-S., Kim, H., Shin, J.-S., Lee, J.-O., Cheong, C. & Choi, B.-S. (2010) Structure of PP4397 Reveals the Molecular Basis for Different c-di-GMP Binding Modes by Pilz Domain Proteins. *Journal of Molecular Biology*, 398(1), 97-110.

Koretke, K. K., Lupas, A. N., Warren, P. V., Rosenberg, M. & Brown, J. R. (2000) Evolution of two-component signal transduction. *Molecular Biology and Evolution*, 17(12), 1956-1970.

Krell, T., Lacal, J., Busch, A., Silva-Jimenez, H., Guazzaroni, M.-E. & Luis Ramos, J. (2010) Bacterial Sensor Kinases: Diversity in the Recognition of Environmental Signals. *Annual Review of Microbiology, Vol 64, 2010*, 64, 539-559.

Kuchma, S. L., Delalez, N. J., Filkins, L. M., Snavely, E. A., Armitage, J. P. & O'Toole, G. A. (2015) Cyclic Di-GMP-Mediated Repression of Swarming Motility by Pseudomonas aeruginosa PA14 Requires the MotAB Stator. *Journal of Bacteriology*, 197(3), 420-430.

Lambert, C., Chang, C. Y., Capeness, M. J. & Sockett, R. E. (2010a) The First Bite-Profiling the Predatosome in the Bacterial Pathogen Bdellovibrio. *Plos One*, 5(1).

Lambert, C., Fenton, A. K., Hobley, L. & Sockett, R. E. (2011) Predatory Bdellovibrio Bacteria Use Gliding Motility To Scout for Prey on Surfaces. *Journal of Bacteriology*, 193(12), 3139-3141.

Lambert, C., Ivanov, P. & Sockett, R. E. (2010b) A Transcriptional "Scream" Early Response of E. coli Prey to Predatory Invasion by Bdellovibrio. *Current Microbiology*, 60(6), 419-427.

Lambert, C. & Sockett, R. E. (2013) Nucleases in Bdellovibrio bacteriovorus contribute towards efficient self-biofilm formation and eradication of preformed prey biofilms. *Fems Microbiology Letters*, 340(2), 109-116.

Laub, M. T. & Goulian, M. (2007) Specificity in two-component signal transduction pathways. *Annual Review of Genetics*, 41, 121-145.

Lee, E. R., Baker, J. L., Weinberg, Z., Sudarsan, N. & Breaker, R. R. (2010) An Allosteric Self-Splicing Ribozyme Triggered by a Bacterial Second Messenger. *Science*, 329(5993), 845-848.

Leonardy, S., Freymark, G., Hebener, S., Ellehauge, E. & Sogaard-Andersen, L. (2007) Coupling of protein localization and cell movements by a dynamically localized response regulator in Myxococcus xanthus. *Embo Journal*, 26(21), 4433-4444.

Leonardy, S., Miertzschke, M., Bulyha, I., Sperling, E., Wittinghofer, A. & Sogaard-Andersen, L. (2010) Regulation of dynamic polarity switching in bacteria by a Ras-like G-protein and its cognate GAP. *Embo Journal*, 29(14), 2276-2289.

Lerner, T. R., Lovering, A. L., Bui, N. K., Uchida, K., Aizawa, S. I., Vollmer, W. & Sockett, R. E. (2012) Specialized Peptidoglycan Hydrolases Sculpt the Intra-bacterial Niche of Predatory Bdellovibrio and Increase Population Fitness. *Plos Pathogens*, 8(2).

Levet-Paulo, M., Lazzaroni, J. C., Gilbert, C., Atlan, D., Doublet, P. & Vianney, A. (2011) The Atypical Two-component Sensor Kinase Lpl0330 from Legionella pneumophila Controls the Bifunctional Diguanylate Cyclase-Phosphodiesterase Lpl0329 to Modulate Bis-(3 '-5 ')-cyclic Dimeric GMP Synthesis. *Journal of Biological Chemistry*, 286(36), 31136-31144.

Li, T.-N., Chin, K.-H., Fung, K.-M., Yang, M.-T., Wang, A. H. J. & Chou, S.-H. (2011) A Novel Tetrameric PilZ Domain Structure from Xanthomonads. *Plos One*, 6(7).

Li, Y. N., Bustamante, V. H., Lux, R., Zusman, D. & Shi, W. Y. (2005) Divergent regulatory pathways control A and S motility in Myxococcus xanthus through FrzE, a CheA-CheY fusion protein. *Journal of Bacteriology*, 187(5), 1716-1723.

Lindenberg, S., Klauck, G., Pesavento, C., Klauck, E. & Hengge, R. (2013) The EAL domain protein YciR acts as a trigger enzyme in a c-di-GMP signalling cascade in E. coli biofilm control. *Embo Journal*, 32(14), 2001-2014.

Lori, C., Ozaki, S., Steiner, S., Bohm, R., Abel, S., Dubey, B. N., Schirmer, T., Hiller, S. & Jenal, U. (2015) Cyclic di-GMP acts as a cell cycle oscillator to drive chromosome replication. *Nature*, 523(7559), 236-U278.

Lovering, A. L., Capeness, M. J., Lambert, C., Hobley, L. & Sockett, R. E. (2011) The Structure of an Unconventional HD-GYP Protein from Bdellovibrio Reveals the Roles of Conserved Residues in this Class of Cyclic-di-GMP Phosphodiesterases. *Mbio*, 2(5).

Luciano, J., Agrebi, R., Le Gall, A. V., Wartel, M., Fiegna, F., Ducret, A., Brochier-Armanet, C. & Mignot, T. (2011) Emergence and Modular Evolution of a Novel Motility Machinery in Bacteria. *Plos Genetics*, 7(9).

Lukat, G. S., McCleary, W. R., Stock, A. M. & Stock, J. B. (1992) Phosphorylation of bacterial response regulator proteins by low-molecular-weight phospho-donors. *Proceedings of the National Academy of Sciences of the United States of America*, 89(2), 718-722.

Lukat G. S. & Rodgers, K. R. (1997) Characterization of ferrous FixL nitric oxide adducts by resonance Raman spectroscopy. *Biochemistry*, 36(14), 4178-4187.

Marchler-Bauer, A., Derbyshire, M. K., Gonzales, N. R., Lu, S. N., Chitsaz, F., Geer, L. Y., Geer, R. C., He, J., Gwadz, M., Hurwitz, D. I., Lanczycki, C. J., Lu, F., Marchler, G.

H., Song, J. S., Thanki, N., Wang, Z. X., Yamashita, R. A., Zhang, D. C., Zheng, C. J. & Bryant, S. H. (2015) CDD: NCBI's conserved domain database. *Nucleic Acids Research*, 43(D1), D222-D226.

Marianayagam, N. J., Sunde, M. & Matthews, J. M. (2004) The power of two: protein dimerization in biology. *Trends in Biochemical Sciences*, 29(11), 618-625.

Marina, A., Mott, C., Auyzenberg, A., Hendrickson, W. A. & Waldburger, C. D. (2001) Structural and mutational analysis of the PhoQ histidine kinase catalytic domain. Insight into the reaction mechanism. *Journal of Biological Chemistry*, 276(44), 41182-41190.

Markwell, M. A. K., Haas, S. M., Bieber, L. L. & Tolbert, N. E. (1978) Modification of Lowry procedure to simplify protein determination in membrane and lipoprotein samples. *Analytical Biochemistry*, 87(1), 206-210.

Matsuyama, B. Y., Krasteva, P. V., Baraquet, C., Harwood, C. S., Sondermann, H. & Navarro, M. (2016) Mechanistic insights into c-di-GMP-dependent control of the biofilm regulator FleQ from Pseudomonas aeruginosa. *Proceedings of the National Academy of Sciences of the United States of America*, 113(2), E209-E218.

McCarter, L. L. & Gomelsky, M. (2015) Fifty Ways To Inhibit Motility via Cyclic Di-GMP: the Emerging Pseudomonas aeruginosa Swarming Story. *Journal of Bacteriology*, 197(3), 406-409.

McLoon, A. L., Wuichet, K., Haesler, M., Keilberg, D., Szadkowski, D. & Sogaard-Andersen, L. (2016) MglC, a Paralog of Myxococcus xanthus GTPase-Activating Protein MglB, Plays a Divergent Role in Motility Regulation. *Journal of Bacteriology*, 198(3), 510-520.

Medina, A. A. & Kadouri, D. E. (2009) Biofilm formation of Bdellovibrio bacteriovorus host-independent derivatives. *Research in Microbiology*, 160(3), 224-231.

Medina, A. A., Shanks, R. M. & Kadouri, D. E. (2008) Isolating Genes Involved in Predator-Prey Interactions Using Host Independent Derivatives of Bdellovibrio bacteriovorus 109J. *Abstracts of the General Meeting of the American Society for Microbiology*, 108, 326-326.

Merighi, M., Lee, V. T., Hyodo, M., Hayakawa, Y. & Lory, S. (2007) The second messenger bis-(3 '-5 ')-cyclic-GMP and its PilZ domain-containing receptor Alg44 are required for alginate biosynthesis in Pseudomonas aeruginosa. *Molecular Microbiology*, 65(4), 876-895.

Merril, C. R., Switzer, R. C. & Vankeuren, M. L. (1979) Trace polypeptides in cellular-extracts and human-body fluids detected by 2-dimensional electrophoresis and a highly sensitive silver stain. *Proceedings of the National Academy of Sciences of the United States of America*, 76(9), 4335-4339.

Mignot, T., Shaevitz, J. W., Hartzell, P. L. & Zusman, D. R. (2007) Evidence that focal adhesion complexes power bacterial gliding motility. *Science*, 315(5813), 853-856.

Miller, J. H. (1992) *A short course in bacterial genetics: a laboratory manual and handbook for Escherichia coli and related bacteria* Cold Spring Harbor Laboratory Press

Milner, D. S. (2014) *Regulatory genetics of cell morphology, motility and polarity in Bdellovibrio bacteriovorus*University of Nottingham.

Milner, D. S., Till, R., Cadby, I., Lovering, A. L., Basford, S. M., Saxon, E. B., Liddell, S., Williams, L. E. & Sockett, R. E. (2014) Ras GTPase-Like Protein MglA, a Controller of Bacterial Social-Motility in Myxobacteria, Has Evolved to Control Bacterial Predation by Bdellovibrio. *Plos Genetics*, 10(4).

Miyatake, H., Kanai, M., Adachi, S., Nakamura, H., Tamura, K., Tanida, H., Tsuchiya, T., Iizuka, T. & Shiro, Y. (1999) Dynamic light-scattering and preliminary crystallographic studies of the sensor domain of the haem-based oxygen sensor FixL from Rhizobium meliloti. *Acta Crystallographica Section D-Biological Crystallography*, 55, 1215-1218.

Morgan, J. L. W., McNamara, J. T. & Zimmer, J. (2014) Mechanism of activation of bacterial cellulose synthase by cyclic di-GMP. *Nature Structural & Molecular Biology*, 21(5), 489-+.

Munoz-Dorado, J., Marcos-Torres, F. J., Garcia-Bravo, E., Moraleda-Munoz, A. & Perez, J. (2016) Myxobacteria: Moving, Killing, Feeding, and Surviving Together. *Frontiers in Microbiology*, 7.

Najnin, T., Siddiqui, K. S., Taha, Elkaid, N., Kornfeld, G., Curmi, P. M. G. & Cavicchioli, R. (2016) Characterization of a temperature-responsive two component regulatory system from the Antarctic archaeon, Methanococcoides burtonii. *Scientific Reports*, 6.

Nan, B., Bandaria, J. N., Moghtaderi, A., Sun, I.-H., Yildiz, A. & Zusman, D. R. (2013) Flagella stator homologs function as motors for myxobacterial gliding motility by moving in helical trajectories. *Proceedings of the National Academy of Sciences of the United States of America*, 110(16), E1508-E1513.

Nan, B., Mauriello, E. M. F., Sun, I.-H., Wong, A. & Zusman, D. R. (2010) A multi-protein complex from Myxococcus xanthus required for bacterial gliding motility. *Molecular Microbiology*, 76(6), 1539-1554.

Nan, B. Y., Chen, J., Neu, J. C., Berry, R. M., Oster, G. & Zusman, D. R. (2011) Myxobacteria gliding motility requires cytoskeleton rotation powered by proton motive force. *Proceedings of the National Academy of Sciences of the United States of America*, 108(6), 2498-2503.

Nan, B. Y., McBride, M. J., Chen, J., Zusman, D. R. & Oster, G. (2014) Bacteria that Glide with Helical Tracks. *Current Biology*, 24(4), R169-R173.

Nan, B. Y. & Zusman, D. R. (2016) Novel mechanisms power bacterial gliding motility. *Molecular Microbiology*, 101(2), 186-193.

Newell, P. D., Boyd, C. D., Sondermann, H. & O'Toole, G. A. (2011) A c-di-GMP Effector System Controls Cell Adhesion by Inside-Out Signaling and Surface Protein Cleavage. *Plos Biology*, 9(2).

Newell, P. D., Monds, R. D. & O'Toole, G. A. (2009) LapD is a bis-(3 ',5 ')-cyclic dimeric GMP-binding protein that regulates surface attachment by Pseudomonas fluorescens

Pf0-1. *Proceedings of the National Academy of Sciences of the United States of America*, 106(9), 3461-3466.

Newman, J. R. S. & Keating, A. E. (2003) Comprehensive identification of human bZIP interactions with coiled-coil arrays. *Science*, 300(5628), 2097-2101.

Ohta, N. & Newton, A. (2003) The core dimerization domains of histidine kinases contain recognition specificity for the cognate response regulator. *Journal of Bacteriology*, 185(15), 4424-4431.

Pathak, D. T. & Wall, D. (2012) Identification of the cglC, cglD, cglE, and cglF Genes and Their Role in Cell Contact-Dependent Gliding Motility in Myxococcus xanthus. *Journal of Bacteriology*, 194(8), 1940-1949.

Paul, K., Nieto, V., Carlquist, W. C., Blair, D. F. & Harshey, R. M. (2010) The c-di-GMP Binding Protein YcgR Controls Flagellar Motor Direction and Speed to Affect Chemotaxis by a "Backstop Brake" Mechanism. *Molecular Cell*, 38(1), 128-139.

Paul, R., Abel, S., Wassmann, P., Beck, A., Heerklotz, H. & Jenal, U. (2007) Activation of the diguanylate cyclase PleD by phosphorylation-mediated dimerization. *Journal of Biological Chemistry*, 282(40), 29170-29177.

Paul, R., Weiser, S., Amiot, N. C., Chan, C., Schirmer, T., Giese, B. & Jenal, U. (2004) Cell cycle-dependent dynamic localization of a bacterial response regulator with a novel di-guanylate cyclase output domain. *Genes & Development*, 18(6), 715-727.

Pazy, Y., Wollish, A. C., Thomas, S. A., Miller, P. J., Collins, E. J., Bourret, R. B. & Silversmith, R. E. (2009) Matching Biochemical Reaction Kinetics to the Timescales of Life: Structural Determinants That Influence the Autodephosphorylation Rate of Response Regulator Proteins. *Journal of Molecular Biology*, 392(5), 1205-1220.

Petersen, T. N., Brunak, S., von Heijne, G. & Nielsen, H. (2011) SignalP 4.0: discriminating signal peptides from transmembrane regions. *Nature Methods*, 8(10), 785-786.

Petters, T., Zhang, X., Nesper, J., Treuner-Lange, A., Gomez-Santos, N., Hoppert, M., Jenal, U. & Sogaard-Andersen, L. (2012) The orphan histidine protein kinase SgmT is a c-di-GMP receptor and regulates composition of the extracellular matrix together with the orphan DNA binding response regulator DigR in Myxococcus xanthus. *Molecular Microbiology*, 84(1), 147-165.

Porter, S. L., Wadhams, G. H. & Armitage, J. P. (2007) In vivo and in vitro analysis of the Rhodobacter sphaeroides chemotaxis signaling complexes. *Two-Component Signaling Systems, Pt B*, 423, 392-+.

Posas, F., Takekawa, M. & Saito, H. (1998) Signal transduction by MAP kinase cascades in budding yeast. *Current Opinion in Microbiology*, 1(2), 175-182.

Pratt, J. T., Tamayo, R., Tischler, A. D. & Camilli, A. (2007) PilZ domain proteins bind cyclic diguanylate and regulate diverse processes in Vibrio cholerae. *Journal of Biological Chemistry*, 282(17), 12860-12870.

Pultz, I. S., Christen, M., Kulasekara, H. D., Kennard, A., Kulasekara, B. & Miller, S. I. (2012) The response threshold of Salmonella PilZ domain proteins is determined by their binding affinities for c-di-GMP. *Molecular Microbiology*, 86(6), 1424-1440.

Raivio, T. L. & Silhavy, T. J. (1997) Transduction of envelope stress in Escherichia coli by the Cpx two-component system. *Journal of Bacteriology*, 179(24), 7724-7733.

Rendulic, S., Jagtap, P., Rosinus, A., Eppinger, M., Baar, C., Lanz, C., Keller, H., Lambert, C., Evans, K. J., Goesmann, A., Meyer, F., Sockett, R. E. & Schuster, S. C. (2004) A predator unmasked: Life cycle of Bdellovibrio bacteriovorus from a genomic perspective. *Science*, 303(5658), 689-692.

Rittenberg, S. C. & Hespell, R. B. (1975) Energy efficiency of intraperiplasmic growth of *Bdellovibrio-bacteriovorus*. *Journal of Bacteriology*, 121(3), 1158-1165.

Rogers, M., Ekaterinaki, N., Nimmo, E. & Sherratt, D. (1986) Analysis of TN7 transposition. *Molecular and General Genetics*, 205(3), 550-556.

Romling, U., Galperin, M. Y. & Gomelsky, M. (2013) Cyclic di-GMP: the First 25 Years of a Universal Bacterial Second Messenger. *Microbiology and Molecular Biology Reviews*, 77(1), 1-52.

Romling, U., Gomelsky, M. & Galperin, M. Y. (2005) C-di-GMP: the dawning of a novel bacterial signalling system. *Molecular Microbiology*, 57(3), 629-639.

Roschanski, N., Klages, S., Reinhardt, R., Linscheid, M. & Strauch, E. (2011) Identification of Genes Essential for Prey-Independent Growth of Bdellovibrio bacteriovorus HD100. *Journal of Bacteriology*, 193(7), 1745-1756.

Ross, P., Aloni, Y., Weinhouse, H., Michaeli, D., Weinbergerohana, P., Mayer, R. & Benziman, M. (1986) Control of cellulose synthesis in *Acetobacter-xylinum* - a unique guanyl oligonucleotide is the immediate activator of the cellulose synthase. *Carbohydrate Research*, 149(1), 101-117.

Ross, P., Weinhouse, H., Aloni, Y., Michaeli, D., Weinbergerohana, P., Mayer, R., Braun, S., Devroom, E., Vandermarel, G. A., Vanboom, J. H. & Benziman, M. (1987) Regulation of cellulose synthesis in *Acetobacter-xylinum* by cyclic diguanylic acid. *Nature*, 325(6101), 279-281.

Rotem, O., Nesper, J., Borovok, I., Gorovits, R., Kolot, M., Pasternak, Z., Shin, I., Glatter, T., Pietrokovski, S., Jenal, U. & Jurkevitch, E. (2016) An Extended Cyclic Di-GMP Network in the Predatory Bacterium Bdellovibrio bacteriovorus. *Journal of Bacteriology*, 198(1), 127-137.

Ryan, R. P. & Dow, J. M. (2010) Cell-cell signal dependent dynamic interactions between HD-GYP and GGDEF domain proteins mediate virulence in Xanthomonas campestris. *Virulence*, 1(5), 404-408.

Ryan, R. P., Fouhy, Y., Lucey, J. F., Crossman, L. C., Spiro, S., He, Y. W., Zhang, L. H., Heeb, S., Camara, M., Williams, P. & Dow, J. M. (2006) Cell-cell signaling in Xanthomonas campestris involves an HD-GYP domain protein that functions in cyclic

di-GMP turnover. *Proceedings of the National Academy of Sciences of the United States of America*, 103(17), 6712-6717.

Ryan, R. P., McCarthy, Y., Kiely, P. A., O'Connor, R., Farah, C. S., Armitage, J. P. & Dow, J. M. (2012) Dynamic complex formation between HD-GYP, GGDEF and PilZ domain proteins regulates motility in Xanthomonas campestris. *Molecular Microbiology*, 86(3), 557-567.

Ryjenkov, D. A., Simm, R., Romling, U. & Gomelsky, M. (2006) The PilZ domain is a receptor for the second messenger c-di-GMP - The PilZ domain protein YcgR controls motility in enterobacteria. *Journal of Biological Chemistry*, 281(41), 30310-30314.

Ryjenkov, D. A., Tarutina, M., Moskvin, O. V. & Gomelsky, M. (2005) Cyclic diguanylate is a ubiquitous signaling molecule in bacteria: Insights into biochemistry of the GGDEF protein domain. *Journal of Bacteriology*, 187(5), 1792-1798.

S.c, R. & Shilo, M. (1970) Early host damage in infection cycle of *Bdellovibrio-bacteriovorus*. *Journal of Bacteriology*, 102(1), 149-&.

Sanders, D. A., Gillececastro, B. L., Stock, A. M., Burlingame, A. L. & Koshland, D. E. (1989) Identification of the site of phosphorylation of the chemotaxis response regulator protein, CheY. *Journal of Biological Chemistry*, 264(36), 21770-21778.

Schafer, A., Tauch, A., Jager, W., Kalinowski, J., Thierbach, G. & Puhler, A. (1994) Small mobilizable multipurpose cloning vectors derived from the *Escherichia-coli* plasmids pk18 and pk19 - selection of defined deletions in the chromosome of *Corynebacterium-glutamicum*. *Gene*, 145(1), 69-73.

Scharf, B. E. (2010) Summary of useful methods for two-component system research. *Current Opinion in Microbiology*, 13(2), 246-252.

Schirmer, T. & Jenal, U. (2009) Structural and mechanistic determinants of c-di-GMP signalling. *Nature Reviews Microbiology*, 7(10), 724-735.

Schmidt, A. J., Ryjenkov, D. A. & Gomelsky, M. (2005) The ubiquitous protein domain EAL is a cyclic diguanylate-specific phosphodiesterase: Enzymatically active and inactive EAL domains. *Journal of Bacteriology*, 187(14), 4774-4781.

Seidler, R. J. & Starr, M. P. (1969) Isolation and characterization of host-independent B*dellovibrios*. *Journal of Bacteriology*, 100(2), 769-&.

Shikuma, N. J., Fong, J. C. N., Odell, L. S., Perchuk, B. S., Laub, M. T. & Yildiz, F. H. (2009) Overexpression of VpsS, a Hybrid Sensor Kinase, Enhances Biofilm Formation in Vibrio cholerae. *Journal of Bacteriology*, 191(16), 5147-5158.

Shikuma, N. J., Fong, J. C. N. & Yildiz, F. H. (2012) Cellular Levels and Binding of c-di-GMP Control Subcellular Localization and Activity of the Vibrio cholerae Transcriptional Regulator VpsT. *Plos Pathogens*, 8(5).

Shilo, M. (1969) Morphological and physiological aspects of the interaction of Bdellovibrio with host bacteria. *Current topics in microbiology and immunology*, 50, 174-204.

Simm, R., Morr, M., Kader, A., Nimtz, M. & Romling, U. (2004) GGDEF and EAL domains inversely regulate cyclic di-GMP levels and transition from sessility to motility. *Molecular Microbiology*, 53(4), 1123-1134.

Simms, S. A., Keane, M. G. & Stock, J. (1985) Multiple forms of the CheB methylesterase in bacterial chemosensing. *Journal of Biological Chemistry*, 260(18), 161-168.

Simon, R., Priefer, U. & Puhler, A. (1983) A broad host range mobilization system for in vivo genetic-engineering - transposon mutagenesis in Gram-negative bacteria. *Bio-Technology*, 1(9), 784-791.

Skerker, J. M., Perchuk, B. S., Siryaporn, A., Lubin, E. A., Ashenberg, O., Goulian, M. & Laub, M. T. (2008) Rewiring the specificity of two-component signal transduction systems. *Cell*, 133(6), 1043-1054.

Skerker, J. M., Prasol, M. S., Perchuk, B. S., Biondi, E. G. & Laub, M. T. (2005) Two-component signal transduction pathways regulating growth and cell cycle progression in a bacterium: A system-level analysis. *Plos Biology*, 3(10), 1770-1788.

Skotnicka, D., Petters, T., Heering, J., Hoppert, M., Kaever, V. & Sogaard-Andersen, L. (2016a) Cyclic Di-GMP Regulates Type IV Pilus-Dependent Motility in Myxococcus xanthus. *Journal of Bacteriology*, 198(1), 77-90.

Skotnicka, D., Smaldone, G. T., Petters, T., Trampari, E., Liang, J., Kaever, V., Malone, J. G., Singer, M. & Sogaard-Andersen, L. (2016b) y A Minimal Threshold of c-di-GMP Is Essential for Fruiting Body Formation and Sporulation in Myxococcus xanthus. *Plos Genetics*, 12(5).

Slater, H., Alvarez-Morales, A., Barber, C. E., Daniels, M. J. & Dow, J. M. (2000) A two-component system involving an HD-GYP domain protein links cell-cell signalling to pathogenicity gene expression in Xanthomonas campestris. *Molecular Microbiology*, 38(5), 986-1003.

Sockett, R. E. & Lambert, C. (2004) Bdellovibrio as therapeutic agents: a predatory renaissance? *Nature Reviews Microbiology*, 2(8), 669-675.

Solovyev, V. & Salamov, A. (2011) Automatic Annotation of Microbial Genomes and Metagenomic Sequences. In Metagenomics and its Applications in Agriculture, Biomedicine and Environmental Studies.

Spangler, C., Bohm, A., Jenal, U., Seifert, R. & Kaever, V. (2010) A liquid chromatography-coupled tandem mass spectrometry method for quantitation of cyclic di-guanosine monophosphate. *Journal of Microbiological Methods*, 81(3), 226-231.

Spormann, A. M. & Kaiser, A. D. (1995) Gliding movements in *Myxococcus-xanthus*. *Journal of Bacteriology*, 177(20), 5846-5852.

Srivastava, D., Harris, R. C. & Waters, C. M. (2011) Integration of Cyclic di-GMP and Quorum Sensing in the Control of vpsT and aphA in Vibrio cholerae. *Journal of Bacteriology*, 193(22), 6331-6341.

Steiner, S., Lori, C., Boehm, A. & Jenal, U. (2013) Allosteric activation of exopolysaccharide synthesis through cyclic di-GMP-stimulated protein-protein interaction. *Embo Journal*, 32(3), 354-368.

Stewart, R. C. (2010) Protein histidine kinases: assembly of active sites and their regulation in signaling pathways. *Current Opinion in Microbiology*, 13(2), 133-141.

Stites, W. E. (1997) Protein-protein interactions: Interface structure, binding thermodynamics, and mutational analysis. *Chemical Reviews*, 97(5), 1233-1250.

Stock, A. M., Robinson, V. L. & Goudreau, P. N. (2000) Two-component signal transduction. *Annual Review of Biochemistry*, 69, 183-215.

Stolp, H. & Petzold, H. (1962) 'Untersuchungen uber einen obligat parasitischen Mikroorganismus mit lytischer aktivitat fur pseudomonas bakterien'. Phytopathogishe Zeithschrift.

Stolp, H. & Starr, M. P. (1963) *Bdellovibrio bacteriovorus* gen. et sp. n., a predatory, ectoparasitic, and bacteriolytic microorganism. *Antonie Van Leeuwenhoek Journal of Microbiology and Serology*, 29(3), 217-&.

Straley, S. C. & Conti, S. F. (1977) Chemotaxis by *Bdellovibrio-bacteriovorus* toward prey. *Journal of Bacteriology*, 132(2), 628-640.

Sudarsan, N., Lee, E. R., Weinberg, Z., Moy, R. H., Kim, J. N., Link, K. H. & Breaker, R. R. (2008) Riboswitches in eubacteria sense the second messenger cyclic di-GMP. *Science*, 321(5887), 411-413.

Sun, M., Wartel, M., Cascales, E., Shaevitz, J. W. & Mignot, T. (2011) Motor-driven intracellular transport powers bacterial gliding motility. *Proceedings of the National Academy of Sciences of the United States of America*, 108(18), 7559-7564.

Taboada, B., Ciria, R., Martinez-Guerrero, C. E. & Merino, E. (2012) ProOpDB: Prokaryotic Operon DataBase. *Nucleic Acids Research*, 40(D1), D627-D631.

Tal, R., Wong, H. C., Calhoon, R., Gelfand, D., Fear, A. L., Volman, G., Mayer, R., Ross, P., Amikam, D., Weinhouse, H., Cohen, A., Sapir, S., Ohana, P. & Benziman, M. (1998) Three cdg operons control cellular turnover of cyclic di-GMP in Acetobacter xylinum: Genetic organization and occurrence of conserved domains in isoenzymes. *Journal of Bacteriology*, 180(17), 4416-4425.

Tamayo, R., Pratt, J. T. & Camilli, A. (2007) Roles of cyclic diguanylate in the regulation of bacterial pathogenesis. *Annual Review of Microbiology*, 61, 131-148.

Tao, J., Li, C., Luo, C. & He, C. (2014) RavA/RavR two-component system regulates Xanthomonas campestris pathogenesis and c-di-GMP turnover. *Fems Microbiology Letters*, 358(1), 81-90.

Tarutina, M., Ryjenkov, D. A. & Gomelsky, M. (2006) An unorthodox bacteriophytochrome from Rhodobacter sphaeroides involved in turnover of the second messenger c-di-GMP. *Journal of Biological Chemistry*, 281(46), 34751-34758.

Taylor, A. J. (2013) *The role of Bd3100 in Bdellovibrio bacteriovorus* University of Nottingham.

Thomashow, M. F. & Rittenberg, S. C. (1978) Intraperiplasmic growth of *Bdellovibrio-bacteriovorus* 109j - solubilization of *Escherichia-coli* peptidoglycan. *Journal of Bacteriology*, 135(3), 998-1007.

Tischler, A. D. & Camilli, A. (2005) Cyclic diguanylate regulates Vibrio cholerae virulence gene expression. *Infection and Immunity*, 73(9), 5873-5882.

Tschauner, K., Hornschemeyer, P., Muller, V. S. & Hunke, S. (2014) Dynamic Interaction between the CpxA Sensor Kinase and the Periplasmic Accessory Protein CpxP Mediates Signal Recognition in E-coli. *Plos One*, 9(9).

Tschowri, N., Schumacher, M. A., Schlimpert, S., Chinnam, N. B., Findlay, K. C., Brennan, R. G. & Buttner, M. J. (2014) Tetrameric c-di-GMP Mediates Effective Transcription Factor Dimerization to Control Streptomyces Development. *Cell*, 158(5), 1136-1147.

Tsirigos, K. D., Peters, C., Shu, N., Kall, L. & Elofsson, A. (2015) The TOPCONS web server for consensus prediction of membrane protein topology and signal peptides. *Nucleic Acids Research*, 43(W1), W401-W407.

Ulrich, L. E. & Zhulin, I. B. (2010) The MiST2 database: a comprehensive genomics resource on microbial signal transduction. *Nucleic Acids Research*, 38, D401-D407.

Wassmann, P., Chan, C., Paul, R., Beck, A., Heerklotz, H., Jenal, U. & Schirmer, T. (2007) Structure of BeF3--modified response regulator PleD: Implications for diguanylate cyclase activation, catalysis, and feedback inhibition. *Structure*, 15(8), 915-927.

Weigt, M., White, R. A., Szurmant, H., Hoch, J. A. & Hwa, T. (2009) Identification of direct residue contacts in protein-protein interaction by message passing. *Proceedings of the National Academy of Sciences of the United States of America*, 106(1), 67-72.

Weinhouse, H., Sapir, S., Amikam, D., Shilo, Y., Volman, G., Ohana, P. & Benziman, M. (1997) c-di-GMP-binding protein, a new factor regulating cellulose synthesis in Acetobacter xylinum. *Febs Letters*, 416(2), 207-211.

Weiss, V., Claveriemartin, F. & Magasanik, B. (1992) Phosphorylation of nitrogen regulator-i of *Escherichia-coli* induces strong cooperative binding to DNA essential for activation of transcription. *Proceedings of the National Academy of Sciences of the United States of America*, 89(11), 5088-5092.

White, M. (2012) *The roles of Bd2421 and Bd2325 in Bdellovibrio bacteriovorus.* University of Nottingham.

White, R. A., Szurmant, H., Hoch, J. A. & Hwa, T. (2007) Features of protein-protein interactions in two-component signaling deduced from genomic libraries. *Two-Component Signaling Systems, Pt A*, 422, 75-+.

Willett, J. W. & Kirby, J. R. (2012) Genetic and Biochemical Dissection of a HisKA Domain Identifies Residues Required Exclusively for Kinase and Phosphatase Activities. *Plos Genetics*, 8(11).

Willett, J. W., Tiwari, N., Mueller, S., Hummels, K. R., Houtman, J. C. D., Fuentes, E. J. & Kirby, J. R. (2013) Specificity Residues Determine Binding Affinity for Two-Component Signal Transduction Systems. *Mbio*, 4(6).

Wolanin, P. M., Thomason, P. A. & Stock, J. B. (2002) Histidine protein kinases: key signal transducers outside the animal kingdom. *Genome biology*, 3(10).

Wu, Y., Li, Q. & Chen, X.-Z. (2007) Detecting protein-protein interactions by far western blotting. *Nature Protocols*, 2(12), 3278-3284.

Yamamoto, K., Hirao, K., Oshima, T., Aiba, H., Utsumi, R. & Ishihama, A. (2005) Functional characterization in vitro of all two-component signal transduction systems from Escherichia coli. *Journal of Biological Chemistry*, 280(2), 1448-1456.

Yanischperron, C., Vieira, J. & Messing, J. (1985) Improved M13 phage cloning vectors and host strains - nucleotide-sequences of the m13mp18 and puc19 vectors. *Gene*, 33(1), 103-119.

Yu, N. Y., Wagner, J. R., Laird, M. R., Melli, G., Rey, S., Lo, R., Dao, P., Sahinalp, S. C., Ester, M., Foster, L. J. & Brinkman, F. S. L. (2010) PSORTb 3.0: improved protein subcellular localization prediction with refined localization subcategories and predictive capabilities for all prokaryotes. *Bioinformatics*, 26(13), 1608-1615.

Zapf, J., Madhusudan, Grimshaw, C. E., Hoch, J. A., Varughese, K. I. & Whiteley, J. M. (1998) Source of response regulator autophosphatase activity: The critical role of a residue adjacent to the SpoOF autophosphorylation active site. *Biochemistry*, 37(21), 7725-7732.

Zhang, X. Y. Z., Goemaere, E. L., Seddiki, N., Celia, H., Gavioli, M., Cascales, E. & Lloubes, R. (2011) Mapping the Interactions between Escherichia coli TolQ Transmembrane Segments. *Journal of Biological Chemistry*, 286(13), 11756-11764.

Zhang, Y., Franco, M., Ducret, A. & Mignot, T. (2010) A Bacterial Ras-Like Small GTP-Binding Protein and Its Cognate GAP Establish a Dynamic Spatial Polarity Axis to Control Directed Motility. *Plos Biology*, 8(7).

Zhang, Y., Guzzo, M., Ducret, A., Li, Y. Z. & Mignot, T. (2012) A Dynamic Response Regulator Protein Modulates G-Protein-Dependent Polarity in the Bacterium Myxococcus xanthus. *Plos Genetics*, 8(8).

Zhu, Y., Qin, L., Yoshida, T. & Inouye, M. (2000) Phosphatase activity of histidine kinase EnvZ without kinase catalytic domain. *Proceedings of the National Academy of Sciences of the United States of America*, 97(14), 7808-7813.

Zhulin, I. B. & Taylor, B. L. (1999) Correlation of PAS domains with electron transport-associated proteins in completely sequenced microbial genomes (vol 29, pg 1522, 1998). *Molecular Microbiology*, 31(2), 741-741.

Zorraquino, V., Garcia, B., Latasa, C., Echeverz, M., Toledo-Arana, A., Valle, J., Lasa, I. & Solano, C. (2013) Coordinated Cyclic-Di-GMP Repression of Salmonella Motility through YcgR and Cellulose. *Journal of Bacteriology*, 195(3), 417-428.